Quantitative proteomic and metabolomic characterization of glucose transporter mutant promastigotes of *Leishmania mexicana*

Snezhana Nikolova Akpunarlieva

Submitted in fulfillment of the requirement for the Degree of Doctor of Philosophy

August 2015

University of Glasgow

Institute of Infection, Immunity and Inflammation

Declaration

I hereby declare that this thesis has been written by myself. I declare that this thesis has not been submitted in any previous application for a higher degree. I declare that the research in this thesis is the result of my own original work, with exception of the GC-MS sample analysis and quantitation performed by Dr. Stefan Weidt and NMR sample analysis and quantitation performed by Marc Biran and Dr. Frederic Bringaud. I declare that all sources of information have been specifically acknowledged by means of references.

Dedication

Посвещавам докторската си теза на моите родители.

I dedicate my PhD thesis to my parents.

Abstract

Parasitic protozoa of the genus *Leishmania* possess a highly adaptable metabolic system which ensures their survival in two significantly contrasting in terms of metabolism hosts. A critical component of leishmanial metabolic machinery is the central carbon metabolism which encompasses a major fraction of metabolites and constitutively expressed enzymes whose localization, function, and manner of regulation in response to changes in nutrient levels in the different host niches, however, remain unclear. In a quest to elucidate how the *Leishmania* parasites overcome conditions with diminished levels of the primary nutrient D-glucose, a null-mutant cell line that was deprived of the ability to acquire the hexose by genetic ablation of three related glucose transporters was created. As previously shown, the glucose transport deficiency in the null-mutant *Leishmania mexicana* (*Δlmgt*) is associated with reduced growth of the promastigote form in an axenic culture and the sand fly vector, no detectable utilization of the sugars D-glucose, D-fructose, D-mannose, D-galactose, and D-ribose, reduced biosynthesis of sugar-containing glycoconjugates and virulence factors, increased sensitivity to nutrient starvation, elevated temperatures, and oxidative stress, and dramatically reduced levels of growth and parasitemia of the amastigote form in an axenic culture and macrophages. Considering all phenotypic characteristics observed previously, the main aims of this study were to determine whether the *Δlmgt* promastigotes use alternative carbon and energy sources, to investigate which pathways are altered as a result of possible utilization of alternative carbon sources, and to illustrate, as comprehensively as possible, the molecular events behind the changes in the central carbon metabolism in the *Δlmgt* promastigotes. For that purpose, a number of proteomic and metabolomic techniques were applied to identify and quantify modulations in protein and metabolite abundance in the *Δlmgt* promastigotes. The results revealed that the main energy and carbon sources for the *Δlmgt* promastigotes appear to be amino acids, with the tricarboxylic acid cycle playing a central role in amino acid catabolism. Furthermore, glycolysis/gluconeogenesis, pentose phosphate pathway, mannose metabolism, purine salvage pathway, and β-oxidation of fatty acids were also among the pathways affected by the glucose transporter incapacity of the *Δlmgt* promastigotes. Glycolysis/gluconeogenesis was shown to operate in a gluconeogenic mode and to be used for the synthesis of hexose phosphates. The oxidative phase of the pentose phosphate pathway and the glutathione metabolism were found to be down-regulated in the *Δlmgt* promastigotes, which is believed to be

the main reason behind the increased sensitivity of these parasites to oxidative stress. Mannose metabolism, which provides activated substrates for the synthesis of the variety of leishmanial secreted and membrane-bound glycoconjugates and the carbohydrate reserve material and virulence factor mannogen, was also down-regulated and that finding corroborated with the previous observation of reduced glycoconjugate and mannogen synthesis in the *Δlmgt* promastigotes. Pyrimidine metabolism was not significantly modulated but the purine salvage pathway was down-regulated in the *Δlmgt* promastigotes. Nonetheless, the *Δlmgt* promastigotes appear to salvage ribose from nucleotide degradation and recycle it for the synthesis of new nucleotides. β-Oxidation of fatty acids was also decreased in the *Δlmgt* promastigotes, suggesting that lipids are not a major source of energy for these cells. Altogether, the data showed that the *Δlmgt* promastigotes i/ decrease high energy-consuming processes such as DNA, RNA, and protein synthesis, ii/ rely heavily on amino acid catabolism via the tricarboxylic acid cycle for energy generation, iii/ use alternative carbon sources for the production of biosynthetic precursors, iv/ have reduced capabilities to synthesize key metabolites such as sugar phosphates and sugar-containing macromolecules, and v/ are characterised with impaired regeneration of the antioxidant defence system and decreased production of virulence factors which appear to determine the susceptibility of these organisms to oxidative stress.

Table of contents

List of figures

List of tables

List of abbreviations

α-K - α-ketoglutarate

1D - one dimensional

2D - two dimensional

2-DE - two-dimensional gel electrophoresis

2D-DIGE - two dimensional difference gel electrophoresis

2PG - 2-phosphoglycerate

3'-NT/NU - 3'-nucleotidase/nuclease

3PG - 3-phosphoglycerate

6PDH - 6-phosphogluconate dehydrogenase

6PGl - 6-phosphogluconolactone

6PGIs - 6-phosphogluconolactonase

AAA - L-2-aminoadipic acid pathway

AAP - amino acid permease

Ac-CoA - acetyl-CoA

ACN - acetonitrile

ACP - acyl carrier protein

AdoMet/SAM - S-adenosyl-L-methionine

AdoMetDC/SAMD - S-adenosyl-L-methionine decarboxylase

ADP - adenosine 5-diphosphate

Ala - alanine

ALDH - aldehyde dehydrogenase

AMP - adenosine 5-monophosphate

APRT - adenine phosphoribosyltransferase

Ara - arabinose

Arg - arginine

ARG - arginase

ASCT - acetate:succinate CoA transferase

Asn - asparagine

Asp - aspartate

ATP - adenosine 5-triphosphate

cAMP - cyclic adenosine 5-monophosphate

CBS - cystathionine β-synthase

cGMP - cyclic guanosine 5-monophosphate

CoA - coenzyme A

CDP - cytidine diphosphate

CI - chemical ionization

CID - collision-induced dissociation

Cit - citrate

CP - syteine proteinase

CS - cysteine synthase

CSE - cystathione γ-lyase

CTP - cytidine triphosphate

Cys - cysteine

dAdoMet - decarboxylated S-adenosyl-L-methionine

DAP - diaminopimelate pathway

L-DAP - L,L-2,6-diaminopimelate

m-DPA - *meso*-diaminopimelate

DHAP - dihydroxyacetone phosphate

DHAPAT - dihydroxyacetone phosphate acetyltrnasferase

DNA - deoxyribonucleic acid

Dol-P-Man - dolicholphosphate-mannose

DPMS - dolicholphosphate-mannose synthase

DS - dialysed serum

E4P - erythrose 4-phosphate

EI - electron ionization

ELO - elongase

ENT - equilibrative nucleoside transporter

ERETIC - electronic reference to access *in vivo* concentrations

ESI - electrospray ionization

ETC - electron transport chain

ETF-QO - electron transfer flavoprotein:ubiquinone oxidoreductase

F1P - fructose 1-phosphate

F1,6P - fructose 1,6-bisphosphate

F6P - fructose 6-phosphate

FA - fatty acid

FAD - flavin adenine dinucleotide

FAE - fatty acid elongation

FASI - fatty acid synthesis type I

FASII - fatty acid synthesis type II

FASP - filter aided sample preparation

FBPase - fructose 1,6-bisphosphatase

FDR - false discovery rates

FH - fumarate hydratase

FrA - formic acid

FRD - fumarate reductase

Fru - fructose

FT-ICR - Fourier transform ion cyclotron resonance

G3P - glycerol 3-phosphate

G3PAT - glycerol 3-phosphate acetyltransferase

G3PDH - glycerol 3-phosphate dehydrogenase

G6P - glucose 6-phosphate

G6PDH - 6-phosphate dehydrogenase

Gln 6P - gluconate 6-phosphate

GALE - UDP-glc 4'-epimerase

GAP - glyceraldehyde 3-phosphate

GAPDH - glyceraldehyde 3-phosphate dehydrogenase

GC - gas chromatography

GCS - glycine cleavage system

GDH - glutamate dehydrogenase

GDP - guanosine 5-diphosphate

GDP-Man - GDP-mannose

GDPMP - GDP-mannose pyrophosphorylase

GIPL - glycosylinositol-phospholipid

GK - glycerol kinase

Glc - glucose

Gln - glutamine

Glu - glutamate

Gly - glycine

GMP - guanosine 5-monophosphate

GO - gene ontology

GPI - glycosylphosphatidylinositol

GPx-II - type II tryparedoxin peroxidase

GSH - glutathione

GT - glucose transporter

GTP - guanosine 5-triphosphate

HCD - higher-energy collision dissociation

HGPRT - hypoxanthine-guanine phosphoribosyltransferase

HILIC - hydrophylic interaction chromatography

HMG-CoA - 3-hydroxy-3-methylglutaryl coenzyme A

HMT - homocysteine S-methyltransferase
HOMEM - modified hemoflagelated media
HPLC - high-performance liquid chromatography
HXK - hexokinase
iFBS - heat-inactivated fetal bovine serum
IMP - inosine 5-monophosphate
IPC - inositol phosphorylceramide
KEGG - Kyoto encyclopedia of genes and genomes
LC - liquid chromatography
Leu - leucine
LPG - lipophosphoglycan
Lys - lysine
M1P - mannose 1-phosphate
M6P - mannose 6-phosphate
Mal - malate
Man - mannose
MAPK - mitogen-activated protein kinases
Met - methionine
MetE - 5-methyltetrahydropteroyltriglutamate--homocysteine methyltransferase
MD - Mascot Distiller
MDH - malate dehydrogenases
mPPG - membrane proteophosphoglycan
MQ - MaxQuant
mRNA - messenger ribonucleic acid
MS - mass spectrometry
MTA - 5-methylthioadenosine
MUFA - monounsaturated fatty acid
MWCO - molecular weight cut-off
myo-I - *myo*-inosito
myo-I 1P - *myo*-inositol 1-phosphate
NAD - nicotinamide adenine dinucleotide
NADP - nicotinamide adenine dinucleotide phosphate
ND - NADH dehydrogenase
NMR - nuclear magnetic resonance
NTP - nucleoside triphosphate
OAA - oxaloacetate
ODC - ornithine decarboxilase

PAGE - polyacrylamide gel electrophoresis
PBS - phosphate buffer saline
PC - phosphatidilcholine
PCA - Principal component analysis
PCR - polymerase chain reaction
PE - phosphatidylethanolamine
PEP - phosphoenolpyruvate
PEPCK - phosphoenolpyruvate carboxykinase
PG - phosphatidylglycerol
PGK - phosphoglycerate kinase
PGP - phosphatidylglycerophosphate
pHILIC - polymeric hydrophilic interaction chromatography
PI - phosphatidylinositol
PInh - protease inhibitor
PLP - pyridoxal 5-phosphate
PM - peritrophic membrane
PMI - phosphomannose isomerase
PMM - phosphomannomutase
PPDK - pyruvate phosphatedikinase
PPG - proteophosphoglycan
PPP - pentose phosphate pathway
Pro - proline
PS - phosphatidylserine
PTM - posttranslational modification
PUFA - polyunsaturated fatty acid
Pyr - pyruvate
R5P - ribose 5-phosphate
Ru 5P - ribulose 5-phosphate
RNA - ribonucleic acid
Rol - ribitol
RPC - reverse-phase liquid chromatography
RT - room temperature
S7P - sedoheptulose 7-phosphate
sAP - secreted acid phosphatase
SCL - succinyl-CoA ligase
SDH - succinate dehydrogenase
SDS - sodium dodecyl sulphate

Ser - serine

SHMT - serine hydroxymethyltransferase

SILAC - stable isotope labelling by amino acids in cell culture

SQS - squalene synthase

SRM - selective reaction monitoring

STD - serine/threonine dehydratase

Suc-CoA - succinyl-CoA

Sucr - sucrose

TAO - trypanosome alternative oxidase

TCA cycle - tricarboxylic acid cycle

THF - tetrahydrofolate

Thr - threonine

TOF - time-of-fight

TPP - thiamine pyrophosphate

TR - trypanothione reductase

tRNA - transfer RNA

TXN - tryparedoxin

TXNPx - tryparedoxin peroxidase

Tyr - tyrosine

UDP - uridine 5-diphosphate

UDP-Gal - uridine 5-diphosphate -galactose

UMP - uridine 5-monophaosphate

UTP - uridine 5-triphaosphate

Xl 5P - xylulose 5-phosphate

Xl - xylose

Xll - xylulose

Xol - xylitol

XPRT - xanthine phosphoribosyltransferase

Acknowledgements

First, and most importantly, I would like to thank my parents. Without your financial and moral help I would not have withstood the challenge of perusing a PhD degree in a foreign country. Thank you for your support.

Първо и най-важно, бих искала да благодаря на моите родители. Без Вашата финансова и морална помощ не бих могла да уча за докторант в чужбина. Благодаря за Вашате подкрепа.

Second, I would like to thank my supervisors Dr. Richard Burchmore and Dr. Karl Burgess for the help during my PhD. I would especially like to thank Katharina Johnston who shared my everyday troubles and helped me in and outside the university and, most importantly, helped me in moments when there was no one else to help me. I would also like to thank Dr. Stefan Weidt for providing invaluable help with sample analysis and software access, Dr. Fiona Achcar for the help with mzMatch-ISO, Marc Biran and Dr. Frederic Bringaud from the University of Bordeaux for the help with NMR, and Dr. Sara Zanivan from the Beatson Institute at the Garscube campus for the help with MaxQuant.

I would like to thank Angela Woolton, the administrator, and the PIs and colleagues involved in the DTC in Cell & Proteomic Technologies program.

I would like to thank my colleagues from level 5 and level 6 of the Institute of Infection, Immunity and Inflammation and the Glasgow Polyomics Facility.

Finally, I would like to thank my father's wine for lightening my mood while writing.

CHAPTER I. Introduction

I.1. Genus *Leishmania*

Order Kinetoplastida represents a medically important group of protozoa that have been subjects of considerable scientific interest for many decades. Considered to have evolved and diverged from a single common ancestor quite early in the evolution of eukaryotes (Sogin *et al.*, 1989; Stevens, 2008), the order comprises unicellular flagellated organisms possessing a number of unique features, including a presence of a kinetoplast (Jensen and Englund, 2012), glycosomes (Opperdoes and Borst, 1977), antigenic variation of surface glycoproteins (Bridgen *et al.*, 1976), bent DNA helices (Marini *et al.*, 1982), contracting telomeric deoxyribonucleic acid (DNA) repeats (Bernards *et al.*, 1983), and highly complex forms of nuclear DNA transcription (Johnson *et al.*, 1987), messenger ribonucleic acid (mRNA) trans-splicing (Boothroyd and Cross, 1982; Walder *et al.*, 1986) and mitochondrial RNA editing (Benne *et al.*, 1986). From an ecological and medical perspective, Trypanosomatina, one of the two suborders belonging to the order, comprises nine genera of obligatory parasites infecting virtually all classes of vertebrates, as well as some invertebrates and plants (Wallace, 1966; Vickerman, 1994; Svobodova *et al.*, 2007; Vickerman, 2009). Of particular importance to humans are two of the genera, *Trypanosoma* and *Leishmania*.

I.1.1. Leishmaniasis

The first scientifically significant information about *Leishmania* dates back to the beginning of 20th century when Leishman and Donovan described the species now known as *Leishmania donovani*. Subsequently, Ross classified the species in a separate genus, genus *Leishmania* (Ross, 1903). Currently, approximately 30 different species of *Leishmania* are known to exist. About 21 species infect humans (Shaw, 1994) and cause the spectrum of clinical diseases collectively referred to as leishmaniasis. The disease occurs in three main forms: cutaneous, mucocutaneous, and visceral. Cutaneous leishmaniasis is caused mainly by *L. major, L. tropica,* and *L. mexicana*. It is the most common type of leishmaniasis and is characterised by localized open or closed skin lesions that can sometimes spread over the entire body and cause Diffused/Disseminated cutaneous leishmaniasis. Mucocutaneous leishmaniasis, caused by the *L. braziliensis* complex, leads to disfiguring destruction of the mucous membranes of the nose, mouth, and throat cavities.

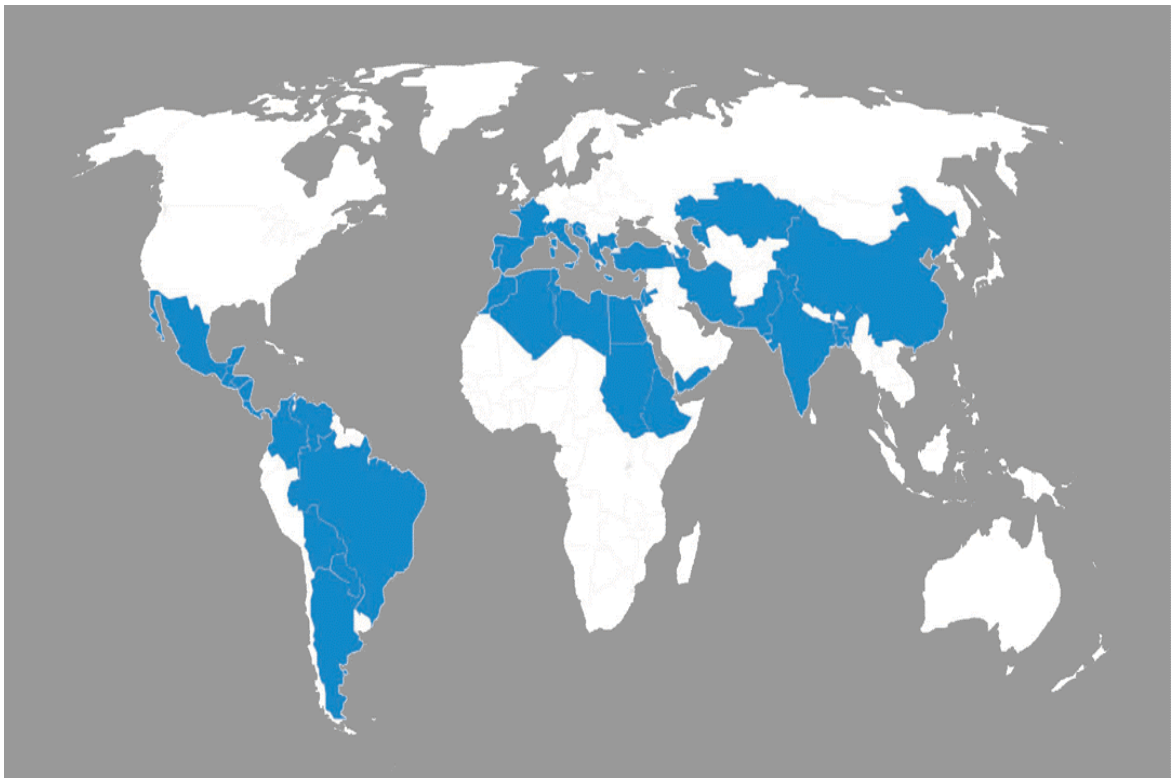

Figure I-1. Areas at risk of infection with cutaneous and visceral leishmaniasis.
Credit: WHO

Visceral leishmaniasis, caused by *L. donovani* and *L. infantum*, results in anaemia, weight loss, swelling of the spleen and liver, and death if left untreated. Typical methods for detection of leishmaniasis include microbiological and molecular-based tests. Microscopic examination of stained tissues, from skin lesions or from bone marrow, is the classical way for detection of the *Leishmania* parasites. *In vitro* culturing and inoculation of animals are other conventional methods for parasite detection. Species determination can be achieved by isoenzyme, immunologic, and PCR analyses (Herwaldt, 1999).

Successful vaccination is believed to be one of the main strategies for control of leishmaniasis. Many vaccines have been investigated on animals but none has proved effective in field tests (Kedzierski *et al.*, 2006). In the first decades after the establishment of the genus *Leishmania*, whole killed organisms had been used as first generation vaccines for prophylactic purposes (Modabber, 2010). Some of the vaccines for prophylaxis, however, showed higher efficacy in treatment and were consequently used as therapeutic vaccines. As a first generation vaccines are used also live attenuated parasites. Contrary to leishmanization, which involves inoculation with live and virulent *Leishmania*, the live attenuated parasites are infectious but not pathogenic (Nagill and Kaur, 2011). The vaccinated with this type

of vaccine subject thus develops infection similar to the natural but asymptomatic. Reversion to virulence or reappearance of the infection in immune-suppressed subjects is still an existing concern with the live attenuated vaccines (Nagill and Kaur, 2011). As second generation vaccines, which are usually comprised of a recombinant protein or poly-protein products of DNA cloning, have been tested a plethora of molecules, including gp63, gp46 (PSA-2), the *Leishmania* homologue for receptors of activated C kinase (LACK), hydrophilic acylated surface proteins (HASP), and a number of cysteine proteases (Kedzierski, 2011). The only second generation vaccine in clinical development is the LEISH_F1 + MPL_SE vaccine which is comprised of three recombinant LEISH_F1 antigens and adjuvant monophosphoryl lipid and squalene in stable emulsion (Modabber, 2010). Third generation anti-leishmanial vaccines, which consist of naked DNA, were developed as safer alternatives of the second generation vaccines. Due to a low immunogenicity, a number of strategies have been applied to increase the protective strength of the vaccines, including the use of a mixture of different conserved antigens (Rezvan and Moafi. 2015).

Current treatment of leishmaniasis involves the use of a number of antileishmanial drugs which, however, are characterized with variable effectiveness and/or high toxicity, require long treatment, and lead to serious adverse effects. Nonetheless, rational combination of drugs can be used to overcome some of these disadvantages. Leading drugs in antileishmanial therapy include pentavalent antimonials, amphotericin B, miltefosine, paromomycin, and pentamidine (de Menezes *et al.*, 2015). Alternative treatment can also involve the use of controlled release systems such as the liposomal formulation of amphotericin B, AmBisome (de Menezes *et al.*, 2015) which specifically targeting patients with HIV-*Leishmania* co-infections. For many years, however, the ongoing strategy for the development of new treatment for leishmaniasis has been the investigation of the biology of *Leishmania* and their host with the main goal of identifying potential drug targets.

I.1.2. *Leishmania* life cycle

Leishmania have a digenetic life-cycle that involves alternation between two distinct forms - an extracellular slender and motile promastigote form (Figure I-2, A) and an obligate intracellular rounded and non-motile amastigote form (Figure I-2, B), and transmission between two hosts - sand flies of the genera *Phlebotomus* and *Lutzomyia* (Killick-Kendrick, 1999) and mammalian macrophages (Herwaldt, 1999).

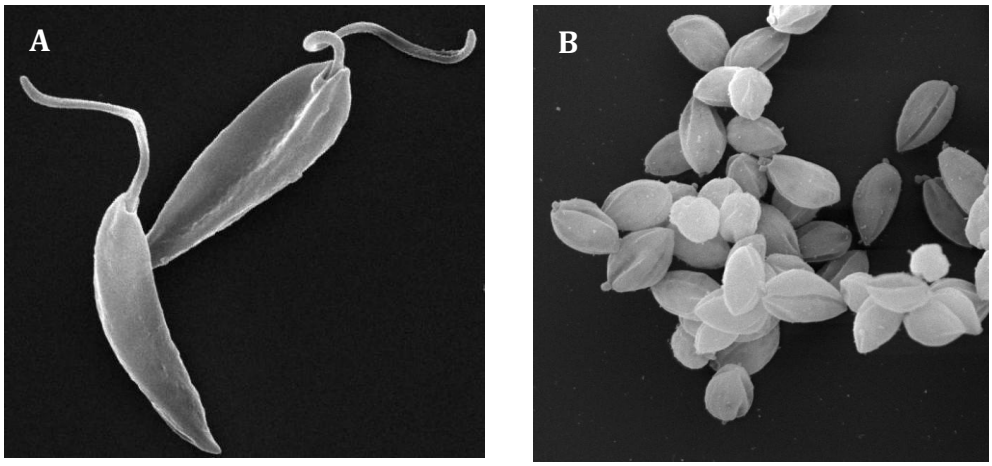

Figure I-2. Morphological forms of *Leishmania*. Scanning electron micrographs of promastigotes (A) and amastigotes (B) of *Leishmania mexicana,* WHO strain MNYC/ BZ/62/M379.

Credit: Eva Gluenz

The insect stage is initiated when a female sand fly acquires a blood meal from an infected mammalian host and ingests amastigote-containing macrophages (Figure I-3). Ingested blood is transported to the gut of the fly, where it is enclosed in a type I peritrophic membrane (PM). Subsequently, the amastigotes differentiate into procyclic promastigotes, which start proliferating intensively and differentiate into nectomonad promastigotes. Nectomonads leave the PM-encased blood meal, attach themselves to the epithelial cells of the lumen and slowly start migrating towards the front part of the gut (Figure 3). While migrating, the nectomonads differentiate into leptomonad promastigotes, which multiply intensively and colonise the stomodeal valve of the fly. Present in the valve, in a matter of days, become two promastigote forms, haptomonads and metacyclics. The metacyclics migrate towards the proboscis of the insect and are inoculated into a mammalian host when the parasitized sandfly takes a further blood meal. In the mammal, the metacyclic promastigotes are quickly phagocytosed by macrophages and other mononuclear blood cells, where they differentiate into amastigotes. The amastigotes proliferate, rupture the infected macrophage and spread to other macrophages. When a sand fly takes a blood meal from the infected mammal, the cycle is continued (Figure 3) (Kamhawi, 2006; Dostalova and Volf, 2012). The life-cycle of *Leishmania* is therefore a series of complicated alterations between several morphological forms that represent adaptations to changes in the environmental conditions the parasites encounter in the two hosts. Each environment, whether a new host or a different compartment in the same host, is characterised by a certain number of stimuli that trigger specific morphological, physiological and biochemical changes in the parasites.

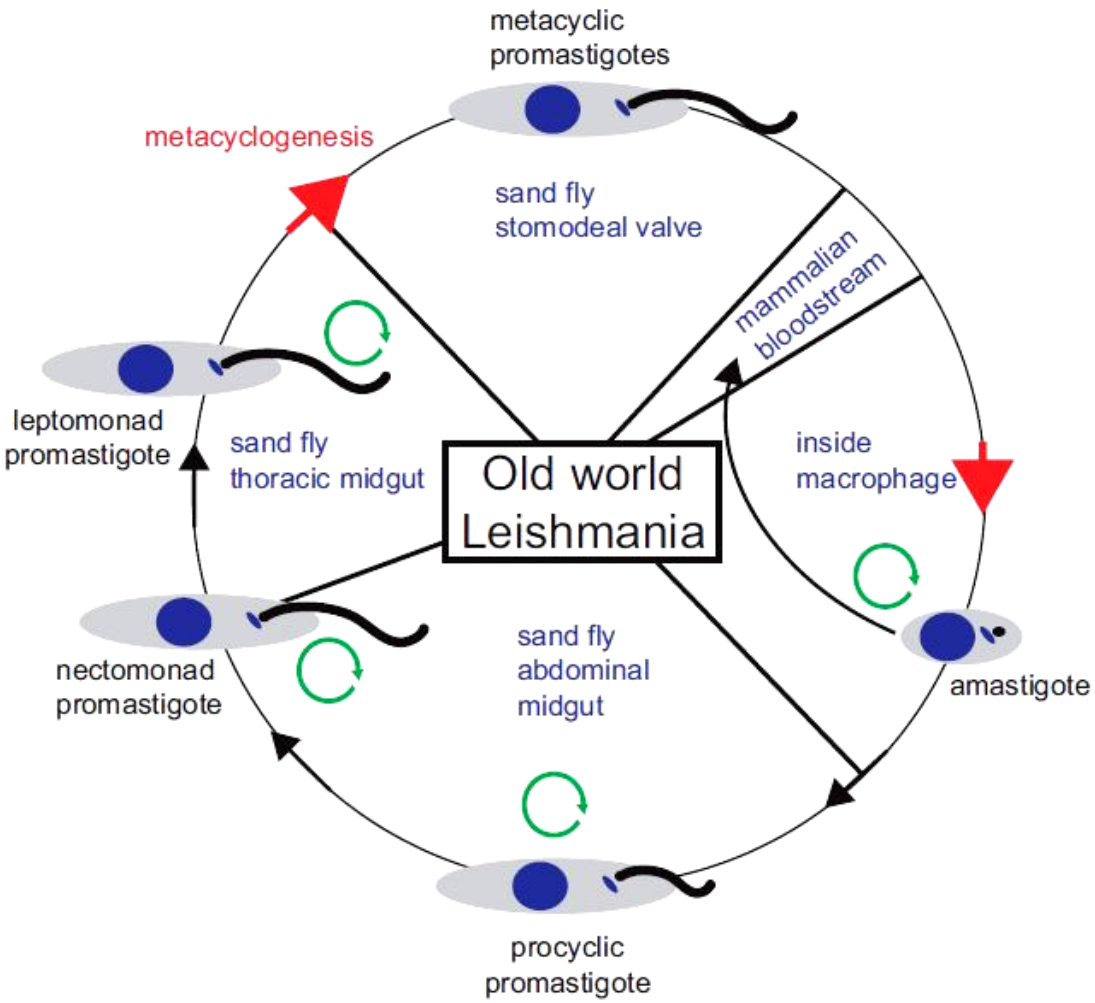

Figure I-3. *Leishmania* life cycle.

Credit: Kramer, 2012

Among the number of differences existing between the insect and mammalian host, temperature and pH are two well-known differentiation stimuli for *Leishmania*. The alimentary tract of the insect is characterised by pH ranging from acidic to slightly alkaline (Zilberstein and Shapira, 1994; Gontijo *et al.*, 1998) and temperatures between 22°C and 28°C (Zilberstein and Shapira, 1994).The parasitophorous vacuoles of the mammalian macrophages, where the amastigotes develop, are characterised by acidic pH and temperatures between 31°C and 37°C (Zilberstein and Shapira, 1994). Thus, when transmitted from the fly's alimentary track to the mammalian's macrophages, the promastigotes experience elevated temperature and decreased pH. While a reduction in pH from neutral to acidic is necessary for the induction of metacyclogenesis in the *Leishmania* promastigotes (Bates and Tetly, 1993), an increase in the temperature alone is enough to induce promastigote to amastigote differentiation in some species of *Leishmania* (Zilberstein and Shapira, 1994; Saar *et al.*, 1998).

I.1.3. Nutrient availability in the *Leishmania* hosts

I.1.3.1. Nutrient availability in the insect vector

Another critical adaptation affecting *Leishmania* propagation and infection is the spectrum of environmental niche-specific changes in the parasite metabolism resulting from the different nutrient availability in the two hosts. In the insect vector, the early promastigote forms are believed to utilize the nutrients in the PM-enclosed blood meal which contains mainly proteins, glucose, amino acids, fatty acids, phospholipids, vitamins and minerals. In addition to the blood, the flies take meals of honeydew excreted by insects of the families Aphidae and Coccidae and sap from a number of plants (Molyneux *et al.*, 1991; Schlein and Jacobson, 1999). Since Aphidae and Coccidae also feed on plant sap, the sugar composition of the honeydew mirrors that of the sap to a certain extent. The honeydew, however, contains a broader spectrum of sugars ranging from phloem sugars (sucrose, maltose, glucose and fructose) to disaccharides (trehalose and trehalulose) and trisaccharides (melezitose and erlose) synthesized by the insects (Wackers, 2005). It is suggested that *Leishmania* utilize these sugars by secreting glycosidases and disaccharide splitting enzymes to pre-digest the di- and trisaccharides to monosaccharides before taking them up (Gontijo *et al.*, 1996; Jacobson *et al.*, 2001; Blum and Opperdoes, 1994). Known glycosidase activities exhibited by *Leishmania* include endoglucanase (cellulase), cellobiohydrolase (exo-glucanase), α-amylase, α-glucosidase, sucrase (β-D-fructofuranoside fructo-hydrolase), chitinase and *N*-acetyl-β-D-glucosaminidase activity (Table I-1) (Jacobson *et al.*, 2001). The resulting monosaccharides, such as glucose, fructose and *N*-acetylglucosamine, are easily taken up by the *Leishmania* parasites (Rodriguez-Contreras *et al.*, 2007; Nadered *et al.*, 2010).

Species	Chitinase	Cellulase	α-Aamylase	α-Glucosidase	Sucrase
Leishmania major	+	+	+	+	+
Leishmania donovani	+	+	0	+	+
Leishmania infantum	+		±	+	+
Leishmania topica	+		0	0	+
Leishmania mexicana	+				+
Leishmania braziliensis	+	+		+	+

Table I-1. Glycosidase activities in *Leishmania*. + - enzyme activity; ±- low enzyme activity; 0 – no enzyme activity detected; blank space – not known.
Credit: Jacobson *et al.*, 2001

Glycosidase	Reaction
Cellulase	Cellulose + H_2O <=> Cellulose + Cellobiose
α-Amylase	Starch <=> Maltodextrin + Maltose
α-Glucosidase	Maltose + H_2O <=> 2 α -D-glucose
Sucrase	Sucrose + H_2O <=> D-fructose + D-glucose
Chitinase	Chitin + H_2O <=> N-Acetyl-D-glucosamine + Chitin

Table I-2. Reactions catalysed by the *Leishmania* glycosidases.

In addition to sugars, the honeydew is believed to also contain relatively high levels of amino acids (Sandstrom and Moran, 2001; Crafts-Brandner, 2002). The most abundant amino acids in the honeydew are L-glutamine, L-glutamate, L-asparagine, L-aspartate and L-serine (Byrne and Miller, 1990; Sandstrom and Moran, 2001; Crafts-Brandner, 2002). L-Proline and L-glutamine, additionally, are found in considerable amounts in most insects' hemolymph (Taylor, 1998). Characteristic amino acids, such as β-alanine and taurine, can also be found in the hemolymph (Kanost, 2009).

I.1.3.2. Nutrient availability in the macrophages

When transmitted to the mammalian host, the promastigote forms of *Leishmania* undergo receptor-mediated internalization by macrophages and develop into amastigote forms in the macrophage parasitophorous vacuoles (Ueno and Wilson, 2012). The latter are phagolysosome-like membrane structures characterised by highly acidic content rich in hydrolytic enzymes such as acid phosphatases, trimetaphosphatases A and B, β-glucuronidases, and cathepsins B, D, H and L (Antoine *et al.*, 1998). The hydrolytic activity of the phagolysosome, together with the potential to fuse with other endosomal vesicles, may lead to generation within, and delivery to, the vacuole of a variety of low-molecular-weight metabolites and macromolecules, such as amino acids, peptides, sugars, lipids, nucleosides and phosphates resulting from the degradation of proteins, proteoglycans, glycoproteins, glycans, RNA and DNA (Burchmore and Barrett, 2001). It was shown that the uptake of metabolites such as D-glucose, L-proline, nucleosides, and polyamines by the amastigotes is optimal at acidic pH supporting the idea that the nutrient transport system of the amastigote forms is adapted to operate optimally in an acidic environment such as that of the parasitophorous vacuoles (Burchmore and Barrett, 2001).

I.1.4. *Leishmania* metabolism

In addition to the nutrient preferences of *Leishmania*, important for our project are the metabolic specificities of these parasites which will be introduced herein.

I.1.4.1. Amino acid metabolism

Amino acids are important nutrients for *Leishmania* promastigotes and amastigotes. Apart for protein synthesis, amino acids are required in osmoregulation, energy metabolism and differentiation. Despite their importance, *Leishmania* is not able to synthesize a number of proteinogenic amino acids. In particular, *Leishmania* lack the enzymes for *de novo* synthesis of the aromatic amino acids L-phenylalanine, L-tryptophan and L-tyrosine, the branched-chain amino acids L-isoleucine, L-leucine and L-valine, and L-arginine, L-histidine and L-lysine. The parasites therefore must acquire them from the host environment.

Alanine (Ala). L-Alanine is the main constituent of the free amino acid pool in both promastigotes and amastigotes (Simon *et al.*, 1983; Mallinson and Coombs, 1989). It can be taken up exogenously via transporter(s) (Inbar *et al.*, 2013) or synthesized intracellularly from pyruvate (Pyr) by a cytosolic alanine aminotransferase, which catalyzes the reverse deamination of L-alanine to pyruvate as well (Figure I-4). L-Alanine plays a key role in osmoregulation (Darling *et al.*, 1990; Burrows and Blum, 1991) and is one of the main end products of glucose metabolism in *Leishmania* (Darling *et al.*, 1987).

Aspartate (Asp) and asparagine (Asn). L-Aspartate is synthesized from oxaloacetate by a mitochondrial aspartate aminotransferase (Figure I-4). L-Asparagine can be converted to L-aspartate by a cytoplasmic L-asparagine I-like protein and L-aspartate can be converted to L-asparagine via an ammonia- and glutamine-dependent asparagine synthetase A (Manhas *et al.*, 2014). Conversely, L-aspartate can be transaminated to oxaloacetate by a mitochondrial aspartate aminotransferase and fed into the tricarboxylic acid cycle (TCA cycle). Additionally, L-aspartate can also be converted to fumarate by adenylosuccinate synthase, adenylosuccinate lyase and adenosine 5'-monophosphate (AMP)-deaminase (Opperdoes and Michels, 2008).

Arginine (Arg). The enzyme arginine succinate lyase, which is involved in the urea cycle, is absent in *Leishmania* (Berriman *et al.*, 2005).

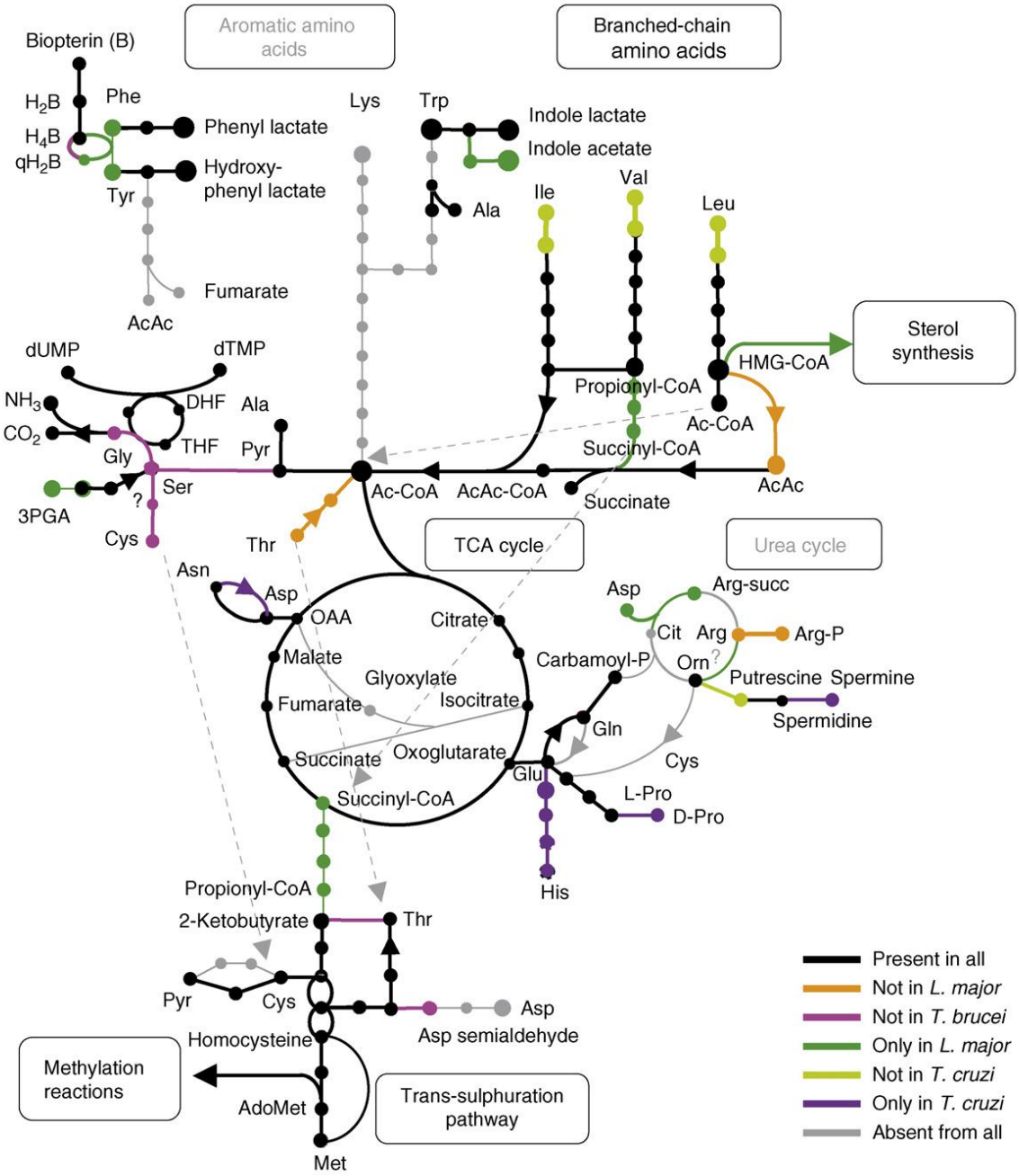

Figure I-4. Amino acid metabolism in trypanosomatids. Presented here are the pathways for amino acid biosynthesis in trypanosomatids. Indicated with question marks are the enzymes for which no unambiguous gene identification could be made. Abbreviations: AcAc - acetoacetate, AdoMet - S-adenosyl-L-methionine, B - biopterin, Cit - citrulline, DHF- dihydrofolate, HMGCoA - hydroxymethylglutaryl CoA, OAA - oxaloacetic acid, Orn - ornithine, PGA - phosphoglyceric acid, qH2B - quinoid form of dihydrobiopterin, THF - tetrahydrofolate.

Credit: Opperdoes and Coombs, 2007

Thus, the parasites are not able to synthesize L-arginine and have to salvage it from the host milieu. The L-arginine, taken up by a high affinity, high specificity arginine permease designated AAP3 (Shaked-Mishan *et al.*, 2006), can be used in protein synthesis, for energy storage, or for polyamine synthesis. In the glycosomes, which are membrane-bound peroxisome-like organelles compartmentalizing a variety of metabolic activities in trypanosomatids parasites (Parsons, 2004), L-arginine can be converted to phosphoarginine, a high-energy phosphagen (Colasante *et al.*, 2006), or to L-ornithine (Figure I-4) (Roberts *et al.*, 2004). L-Ornithine is involved in polyamine biosynthesis, important for cell growth and proliferation, and trypanothione synthesis, which has a key role in maintenance of redox homeostasis in *Leishmania* (Colotti and Ilari, 2010). Interestingly, the parasites are able to synthesize putrescine and spermidine via a cytosolic ornithine decarboxilase (ODC) and a spermidine synthase, respectively (Jiang *et al.*, 1999), but lack the enzymes (except for agmatinase) for the synthesis of putrescine from L-arginine, of L-orthinine from L-glutamate, and of spermine (Jiang *et al.*, 1999; Roberts *et al.*, 2004). Additionally, the parasites cannot convert spermine to spermidine or spermidine to putsrescine.

Cysteine (Cys). L-Cysteine can be synthesized *de novo* from L-serine via a cysteine acetyltransferase and a cysteine synthase (CS) or from L-homocysteine through the reverse *trans*-sulfuration pathways involving cystathionine β-synthase and cystathione γ-lyase (CSE) (Williams *et al.*, 2009). L-Cysteine can be converted to pyruvate (Figure I-4) or used for the synthesis of glutathione and proteins. Due to its ability to form disulfide bonds, L-cysteine plays a main role in protein folding and protein structure maintenance.

Glutamate (Glu). L-Glutamate is another proteinogenic amino acid. It can be produced from α-ketoglutarate (2-oxoglutarate) by a mitochondrial nicotinamide adenine dinucleotide (NAD)-dependent or a putative cytosolic nicotinamide adenine dinucleotide phosphate (NADP)-dependent glutamate dehydrogenase (Figure I-4) (Mottram and Coombs, 1985), or by transamination reactions. L-Glutamate is also involved in pathways of nitrogen and redox metabolism. It can also be converted to L-glutamine (Gln) via a glutamine synthetase (Figure I-4) (Opperdoes and Michels, 2008). L-Glutamine is used in several biosynthetic pathways.

Glycine (Gly). Glycine is a small amino acid. It can be reversibly oxido-decarboxylated to L-serine by serine hydroxymethyltransferase (SHMT) and tetrahydrofolate (THF)-

dependent glycine cleavage system (GCS). L-Serine can then be converted to pyruvate by the serine/threonine dehydratase (STD) (Figure I-4) (Opperdoes and Coombs, 2007; Muller and Papadopoulou, 2010). GCS, along with the serine hydroxymethyl-transferase which converts L-threonine into L-serine, is part of the folic acid biosynthesis pathway whose operation leads to the formation of one-carbon units used for the biosynthesis of pyrimidines, purines and L-methionine (Muller and Papadopoulou, 2010).

Leucine (Leu). L-Leucine is one of the branch-chain amino acids for which *Leishmania* parasites are auxotrophic. No leishmanial L-leucine transport system has been characterised to date. In the cytosol, L-leucine can be transaminated by a branched-chain amino acid aminotransferase to 2-ketoisocaproate and further oxidized to 3-hydroxy-3-methylglutaryl coenzyme A (HMG-CoA) in the mitochondrion by a short/branched-chain acyl-CoA dehydrogenase, a carboxylase and a hydratase (Opperdoes and Michels, 2008). HMG-CoA is then directed to the isoprenoid synthetic pathway where it is incorporated into sterols (Figure I-4) (Ginger *et al.*, 2000; Ginger *et al.*, 2001).

Lysine (Lys). Leishmania do not have the capacity to synthesize L-lysine *de novo*. They take it up from the host environment by a highly specific plasma membrane AAP7 transporter (Inbar *et al.*, 2012). Enzymes for L-lysine degradation are not present in *Leishmania* (Figure I-4) (Berriman *et al.*, 2005).

Methionine (Met). Leishmania take up L-methionine by a low specificity saturable, temperature- and energy-dependent transport system (Mukkada and Simon, 1977). Along with L-cysteine, L-methionine is one of the two sulphur-containing proteinogenic amino acids. L-Methionine residues, similar to cysteine residues, are easily oxidized to L-methionine sulfoxide which can then be reduced back to L-methionine. This reversible oxidation of methionine was suggested to be a regulatory post-translational modification for protein activation and inactivation (Drazic and Winter, 2014). In addition to protein synthesis, in the *Leishmania* cytosol, L-methionine can be converted to 2-oxobutanoate and transported to the mitochondrion where, through a series of reactions, can be degraded to succinyl-CoA, an intermediate of the TCA cycle. L-Methionine can also be converted to S-adenosyl-L-methionine (AdoMet) by S-adenosylmethionine synthetase (Figure I-4). AdoMet can be further decarboxylated by S-adenosylmethionine decarboxylase and used for

polyamine synthesis (Colotti and Ilari, 2011), or it can be used as a methyl donor in various methylation reactions.

Proline (Pro). As shown by Zilberstein and colleagues, *Leishmania* take up L-proline by at least three transport systems, two promastigote systems and one amastigote system (Mazareb *et al.*, 1999). Further to protein synthesis, L-proline can be used as a source of energy by being oxidized by a mitochondrial Δ^1-pyrroline-5-carboxylate dehydrogenase and a pyrroline-5-carboxylate synthetase to L-glutamate (Figure I-4) (Opperdoes and Michels, 2008). The L-glutamate thus produced can be deaminated and fuelled into the TCA cycle.

Serine (Ser). The first enzyme in the L-serine biosynthetic pathway, 3-phosphoglycerate dehydrogenase, is present in the *Leishmania* genome (Figure I-4) (Opperdoes and Coombs, 2007). A BlastP search also detected a possible phosphoserine phosphatase homologue, which is the second enzyme in the L-serine biosynthesis. L-Serine is implicated in protein synthesis but it is also an important precursor in phosphatidylserine and sphingolipid biosynthesis.

Threonine (Thr). L-Threonine can also used as an energy source. It can be degraded to glycine and acetate with the concomitant production of adenosine 5'-triphosphate (ATP). L-Threonine can be converted to glycine in two ways. In the first, L-threonine is converted by SHMT in a THF-dependent manner to glycine. In the second, SHMT cuts the Cα-Cβ bond of L-threonine to generate glycine (Opperdoes and Coombs, 2007; Muller and Papadopoulou, 2010). Alternatively, serine/threonine dehydratase (STD) can also convert L-threonine to 2-ketobutyrate which can be oxidized to succinyl-CoA.

Tyrosine (Tyr). Leishmania have a putative phenylalanine-4-hydroxylase that can convert L-phenylalanine to L-tyrosine (Opperdoes and Michels, 2008). L-Tyrosine, in turn, is most likely converted to 4-hydroxyphenylpyruvate by an aminotransferase which is then probably reduced by an aromatic hydroxyacid dehydrogenase. Le Blanq and Lanham first showed that an aminotransferase able to transaminate L-aspartate, L-tyrosine, L-tryptophan and L-alanine operates in crude extracts of *L. donovani*, *L. tropica* and *L. major* (Le Blancq and Lanham, 1984). Later, a *L. mexicana* promastigote broad substrate specificity aminotransferase, that can transaminate L-aspartate, aromatic acids, L-leucine and L-methionine, was purified (Vernal *et al.*, 1998) and the gene encoding it cloned and sequenced (Vernal *et al.*, 2003). Expression in *E. coli* and

further characterisation showed that the enzyme is closely related to the Iα subfamily of aminotransferases. In 2014, Larraga and colleagues elucidated the crystal structure of *L. infantum* tyrosine aminotransferase and showed that the enzyme is cytoplasmic, belonging to the Iγ subfamily, involved in L-tyrosine metabolism and expressed at higher rate in amastigotes (Moreno *et al.*, 2014a, b).

I.1.4.2. Carbohydrate metabolism

As presented in **I.1.3.1.**, it was shown that *Leishmania* secret glycosidases, disaccharide splitting enzymes and β-glucuronidases to digest the more complex sugars present in the insect gut to simple sugars which the parasites then take up via a number of transporters. Once internalized, the sugars can either be further hydrolysed, like sucrose which is broken-down to glucose and fructose by an intracellular sucrase (Singh and Mandal, 2011), or transported to the glycosomes where they are catabolized. *Leishmania* have several genes encoding sugar kinases that carry a glycosomal targeting signal. In addition to hexokinases, involved in glucose catabolism via the Embden-Meyerhof-Parnas glycolytic pathway, *Leishmania* have several other kinases, such as ribulokinase and xylulokinase, which indicates that other sugars can also be metabolized in the glycosomes (Opperdoes and Coombs, 2007).

Glycolysis. Glycosomes compartmentalize the first six to seven glycolytic enzymes, namely hexokinase, glucose 6-phosphate isomerase, phosphofructokinase, fructose 1,6-bisphosphate aldolase, triosephosphate isomerase, glyceraldehyde 3-phosphate dehydrogenase and phosphoglycerate kinase (Hart and Opperdoes, 1984), that convert glucose to 3-phosphoglycerate. The last glycolytic steps occur in the cytosole and lead to the production of pyruvate, the end product of glycolysis (Figure I-5). The first stage of glycolysis is characterized by consumption of ATP and NAD^+ while the last results in the generation of energy. The consumption of ATP and NAD^+ in the glycosomes would result in imbalance in the energy and redox state of the organelle. The ATP and NAD^+/NADH, however, is maintained by the glycosomal succinate fermentation in which phosphoenolpyruvate (PEP) is converted to succinate (Saunders *et al.*, 2011).

Pentose phosphate pathway. In addition to glycolysis, a portion of the D-glucose entering the glycosomes is diverted toward the PPP pathway and used for the synthesis of ribose 5-phosphate (R5P) and generation of NADPH (Maugeri *et al.*,

2003). Generally, the pathway has two stages. In the oxidative stage, glucose 6-phosphate (G6P) is oxidized to ribulose 5-phosphate (Ru5P) and CO_2, with the simultaneous generation of NADPH (2 molecules of NADPH per molecule of G6P). In the non-oxidative stage, Ru5P is converted to the glycolytic intermediates glyceraldehyde 3-phosphate (GAP), fructose 6-phosphate (F6P), and G6P. The R5P produced during the PPP is used in nucleotide biosynthesis (Maugeri *et al.*, 2003).

Glycosomal succinate fermentation. Glycosomal succinate fermentation results in the two-step reduction of PEP to succinate, which is excreted by the *Leishmania* cells (Rainey and MacKenzie, 1991), and the generation of ATP and NAD^+ (1 molecule of ATP and 2 molecules of NAD^+ for each PEP molecule) (Figure I-5). The glycosomal succinate fermentation additionally leads to the generation of C4 dicarboxilyc acids which are used for anaplerotic reactions in the TCA cycle (Saunders *et al.*, 2011).

Tricarboxylic acid cycle (TCA cycle). The end product of glycolysis, pyruvate, can be transaminated to alanine by a cytosolic alanine aminotransferase, which can be subsequently excreted by the cells (Rainey and MacKenzie, 1991), or imported in the mitochondrion where it is converted to acetyl-CoA by mitochondrial acetate:succinate CoA transferase (ASCT) and succinyl-CoA synthetase (Van Hellemond *et al.*, 1998). Acetyl-CoA then can enter the TCA cycle or be converted to acetate, which can also be excreted from the cells (Rainey and MacKenzie, 1991). Through the TCA cycle, acetyl-CoA is further metabolized to a series of intermediates (Figure I-5), with the concomitant generation of ATP and NADH. The latter is used by the electron transport chain, localized in the inner mitochondrial membrane, for the production of more energy.

Mannogen metabolism. In *Leishmania*, the excess of hexoses phosphates can be stored in the form of storage material called mannogen (previously designated as mannan) (Ralton *et al.*, 2003). Mannogen includes a family of short-chain oligosaccharides composed of β-1,2-linked mannose residues. Mannogen *de novo* synthesis starts with the formation of a mannose-α-1,4-cyclic phosphate primer from mannose 1-phosphate (M1P) (Sernee *et al.*, 2006) (Figure I-5). The primer is elongated with at least three more β-1,2-linked mannoses, then dephosphorylated and made ready for further elongation with more mannose residues originating from guanosine 5'-diphosphate (GDP)-mannose.

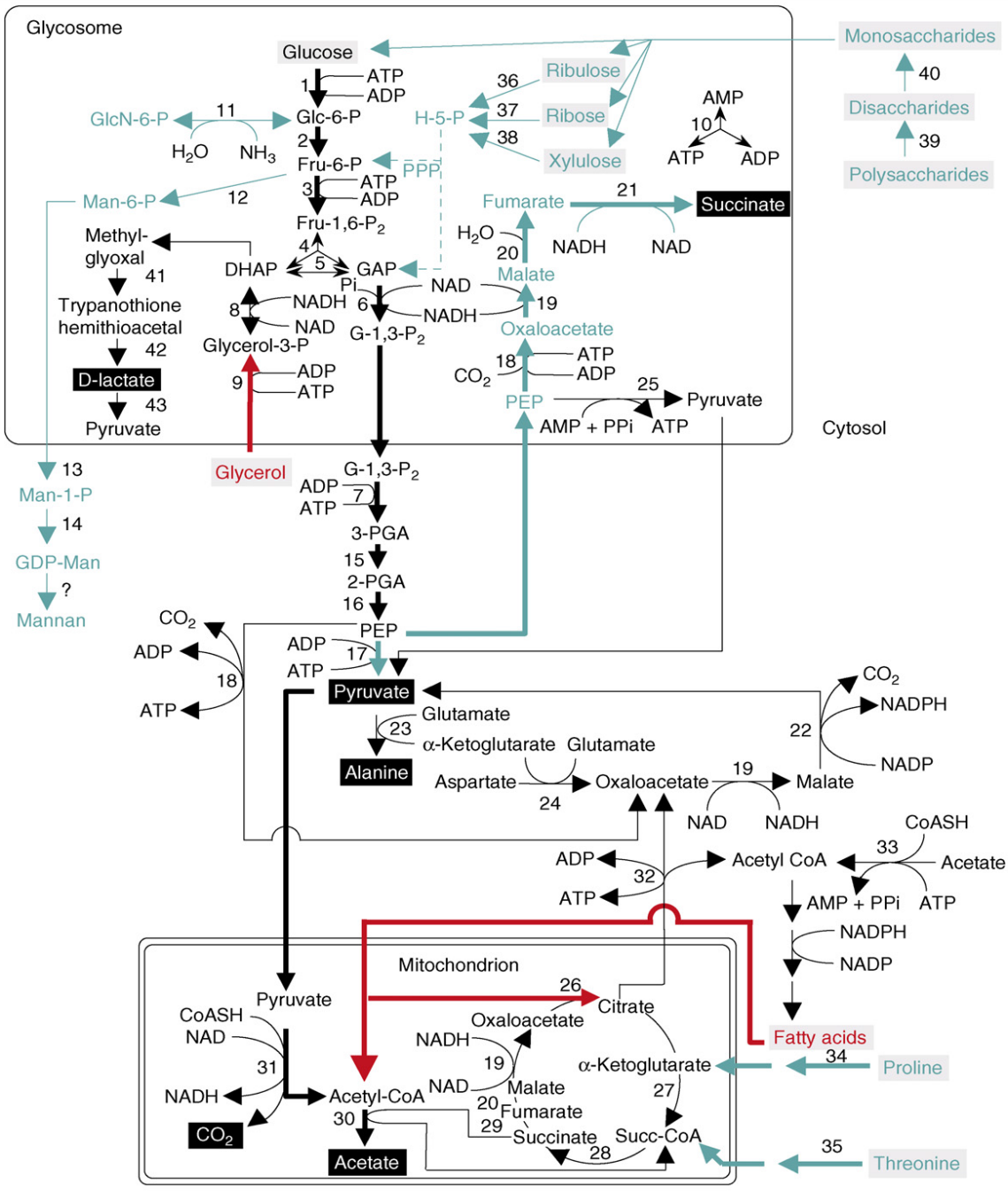

Figure I-5. Central metabolic pathways in *Leishmania*. Presented here are the central metabolic pathways taking place in the glycosomes, mitochondrion and cytosol of *Leishmania*. Included are the substrates (in grey, boxed), intermediates and end products (in black, boxed) of Glycolysis, Indicated with thick arrows are the major metabolite fluxes. The pathways in blue are believed to be more important in promastigotes while the ones in red are believed to be more important in the amastigote. Abbreviations: Fru - fructose, GAP - glyceraldehyde 3 phosphate, Glc - glucose, H-5-P - hexose 5-phosphate, Man - mannose, PEP - phosphoenolpyruvate, PGA - phosphoglyceric acid, PPP - pentose-phosphate pathway. Enzymes: 1 - hexokinase, 2 - glucose 6-phosphate isomerise, 3 - phosphofructokinase, 4 - fructose 1,6-bisphosphate aldolase, 5 - triosephosphate isomerise, 6 - glyceraldehyde 3-phosphate dehydrogenase, 7 - phosphoglycerate kinase, 8 - glycerol 3-phosphate dehydrogenase, 9 - glycerol kinase, 10 - adenylate kinase, 11 - glucosamine 6-phosphate deaminase, 12 - mannose 6-phosphate isomerise, 13 - phosphomannomutase, 14 - GDP-mannose pyrophosphorylase, 15 - phosphoglycerate mutase, 16 - enolase, 17 - pyruvate kinase, 18 - phosphoenolpyruvate carboxykinase, 19 - malate dehydrogenase, 20 - fumarate hydratase, 21 - NADH-dependent fumarate reductase, 22 - malic enzyme, 23 - alanine aminotransferase, 24 - aspartate aminotransferase, 25 - pyruvate phosphate dikinase, 26 - citrate synthase, 27 - 2-ketoglutarate dehydrogenase, 28 - succinyl-CoA ligase, 29 - succinate dehydrogenase, 30 - acetate–succinate CoA transferase, 31 - pyruvate dehydrogenase, 32 - citrate lyase, 33 - acetyl-CoA synthetase, 34 - proline oxidation pathway, 35 - threonine oxidation pathway, 36 - ribulokinase, 37 - ribokinase, 38 - xylulokinase, 39 - amylase-like protein, 40 - sucrase-like protein.

Credit: Opperdoes and Coombs, 2007

The mannogen oligosaccharides are long about 5-40 residues and accumulate to milimolar concentrations in the cytosol. Mannogen is stored by both promastigotes and amastigotes. In amastigotes, mannogen was shown to be important for parasite virulence (Sernee *et al.*, 2006).

I.1.4.3. Energy metabolism

The electron transport chain of *Leishmania* comprises of complex I (NADH dehydrogenase), complex II (succinate dehydrogenase), complex III (cytochrome *bc* oxidoreductase) and cytochrome *c* - complex IV (cytochrome oxidase). The complex chain functions by oxidizing electron donors, such as NADH and succinate produced in the TCA cycle, and generating a transmembrane electrochemical gradient. The gradient is used by the F_0F_1-ATP synthase to generate ATP by oxidative phosphorylation (Besteiro *et al.*, 2005).

I.1.4.4. Lipid metabolism

I.1.4.4.1. Fatty acid biosynthesis

Two pathways for fatty acid synthesis are believed to operate in *Leishmania*, *de novo* fatty acid synthesis type II (FASII) and fatty acid elongation (FAE) (Ramakrishnan *et al.*, 2013). Both pathways rely on consecutive addition of two carbon (C2) units to a growing carboxylic chain. The difference between the two pathways is that the growing chain is held by a carrier, more specifically, an acyl carrier protein (ACP) in the case of FASII, or a primer, in the case of FAE.

Usually, the FASII synthase is comprised of several different individual components, in contrast to the FASI system which is a single multimeric complex (Figure I-6). The FASII synthesis involves an ACP, to which the synthesized fatty acid (FA) is linked, a carbon source, which is malonyl-CoA, and acetyl-CoA carboxylase, ketoacyl reductase, dehydratase and enoyl reductase. The synthesis starts with the production of malonyl-CoA from two molecules of acetyl-CoA by the ACC. Generated malonyl-CoA is decarboxylatively condensated to the ACP to start a two carbon chain. The two carbons are then successively reduced by a ketoacyl reductase, a dehydratase and an enoyl reductase (Figure I-6, D). Further elongation of the chain occurs via condensation with another molecule of malonyl-CoA (Ramakrishnan *et al.*, 2013).

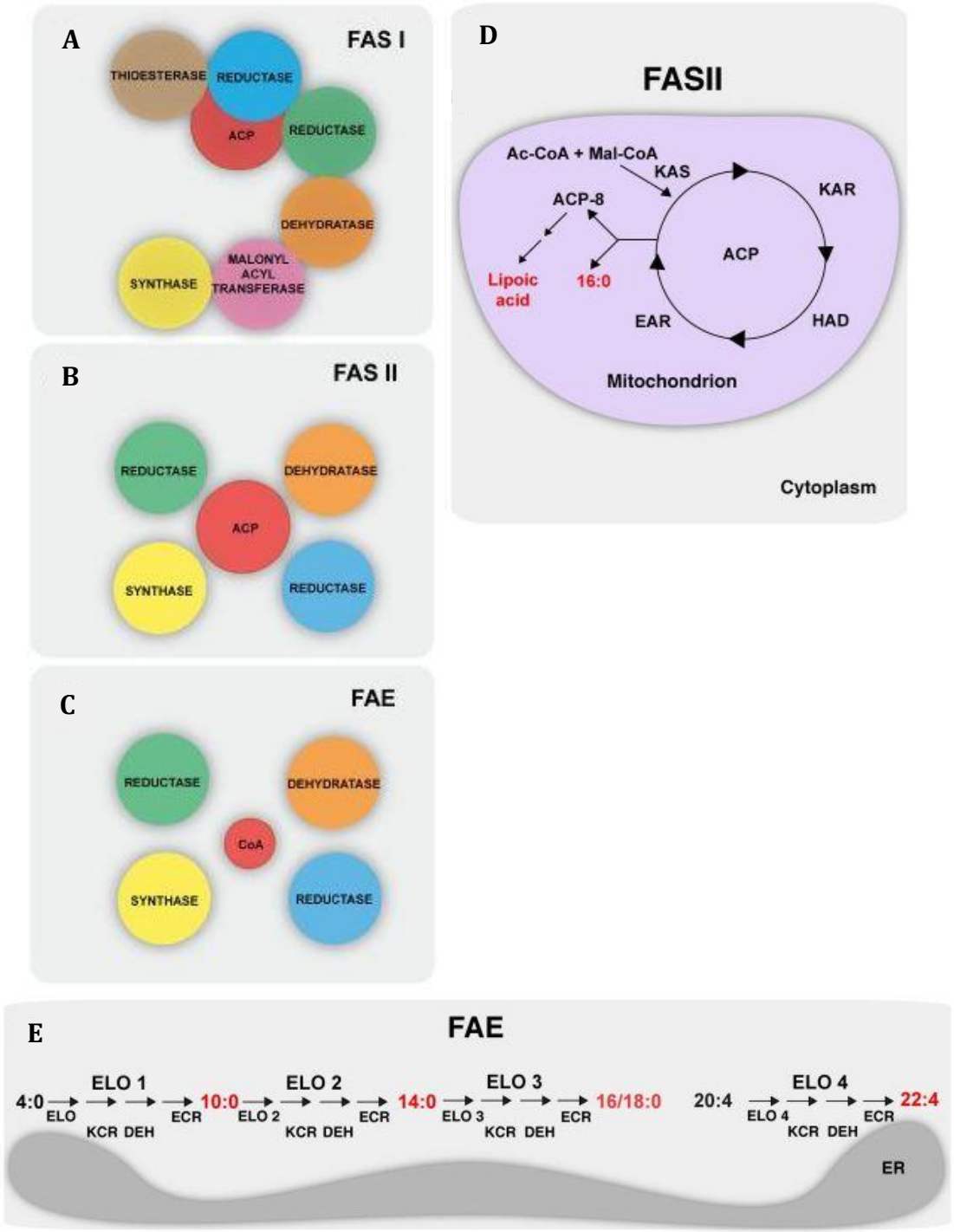

Figure I-6. Fatty acid biosynthesis. (A) Fatty acid synthase type I. (B) Fatty acid synthase type II. (C) Fatty acid elongation. (D) Saturated fatty acid biosynthesis via the fatty acid synthesis type II (FASII) pathway. (E) Saturated fatty acid biosynthesis via fatty acid elongation (FAE) pathways. Presented here are the enzyme complexes and pathways involved in saturated fatty acid biosynthesis. Abbreviations: Ac-CoA - acetyl-CoA, Mal-CoA - malonyl-CoA, KAS -ketoacyl-ACP synthase, KAR - ketoacyl-ACP reductase, HAD - hydroxyacyl-ACP dehydratase, EAR - enoyl-ACP reductase, ELO - elongase, KCR - ketoacyl-CoA reductase, DEH - acyl-CoA dehydratase, ECR -enoyl-CoA reductase.

Credit: Ramakrishnan *et al.*, 2013

To date, FAE has not been fully characterized in *Leishmania*. Some information regarding this pathway is available from studies in *T. brucei*, *T. cruzi* and *L. major*, and genome comparison between *Leishmania* and *Trypanosoma*. Observed in *T. brucei* was that four genes encode potential elongases (ELOs) of which three may be involved in FA synthesis (Lee *et al.*, 2006). The authors used a cell-free system comprised of membranes as the source of enzymes for FA synthesis, butyryl-CoA as the C4 primer and malonyl-CoA as the C2 donor, and showed that in wild-type membrane C4-CoA is efficiently elongated mostly to C14. Additionally, to investigate the role of the four ELOs, generated were also four ELO mutants, that is *Δelo1-4*. The ELO1 was shown to mainly elongate chains from C4 to C10, which results in the conversion of the primer butyryl-CoA to decanoyl-CoA; ELO2 elongates from C10 to C14, thus converting decanoyl-CoA to myristoyl-CoA; and ELO3 elongates from C14 to C18, which leads to formation of steroyl-CoA from myristoyl-CoA (Figure I-6, E). C8 to C18 long FAs, both saturated and unsaturated, were observed in *Leishmania* as well, suggesting the operation of similar ELOs (Lee *et al.*, 2006). However, the genome of *L. major* contains 12 tandemly linked homologous genes, instead of 4 ELO genes, which could be the reason why longer FA chains are observed in these parasites. ELO4 elongates the unsaturated long-chain FA arachidonate.

In addition to saturated FAs, *Leishmania* are able to synthesize unsaturated FAs as well. Unsaturated FAs are products of desaturase activities over saturated FAs. The unsaturated FAs are divided into monounsaturated (MUFA) and polyunsaturated (PUFA) FAs. The PUFA synthesis in *Leishmania* involves a stearoyl-CoA desaturase, two ELOs, that is Δ6, which is specific for C18, and Δ5, which is specific for C20 PUFAs, and five desaturases, namely Δ12, Δ6, Δ5, Δ4, and ω3 (Tripodi *et al.*, 2006; Livore *et al.*, 2006; Uttaro, 2006). Thus, the *Leishmania* parasites, most probably using the stearate (octadecanoic acid) (C18:0) generated in the FAE pathway as a precursor, are able to synthesize C22 PUFAs and linoleic acid.

I.1.4.4.2. Glycerolipid synthesis

The initial steps of glycerolipid biosynthesis occur in the glycosome. There glycerol 3-phosphate (G3P) can be produced by reduction of dihydroxyacetone phosphate (DHAP) by a glycosomal glycerol 3-phosphate dehydrogenase (G3PDH) or by glycerol phosphorylation by a glycosomal glycerol kinase (GK).

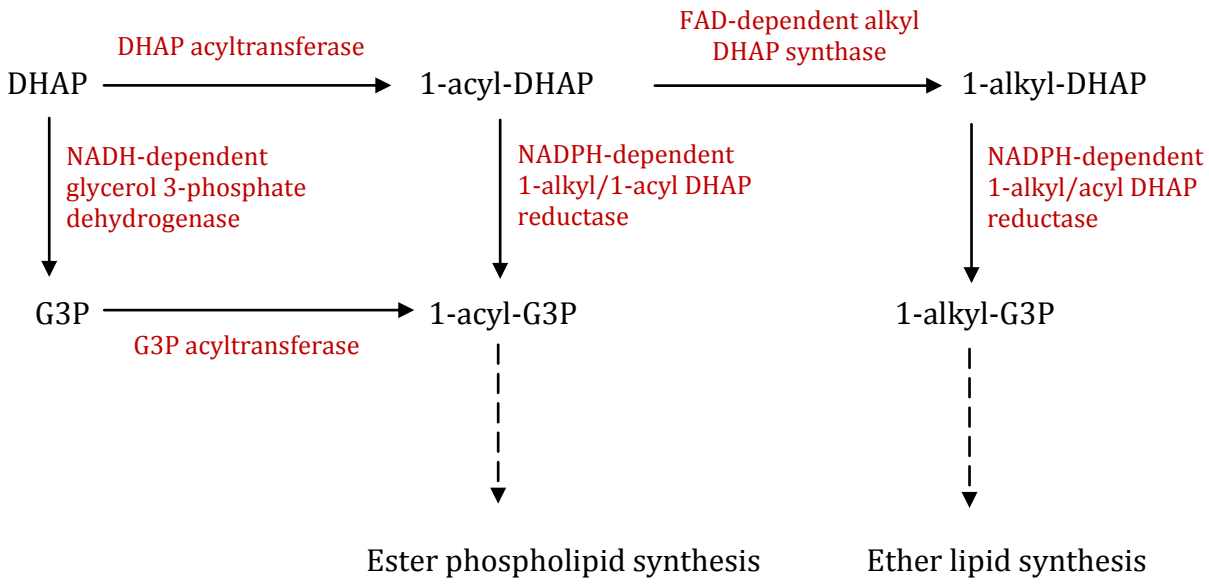

Figure I-7. Glycerolipid biosynthesis in *Leishmania*. Presented here is the pathway for generation of precursors for ether and ester phospholipid biosynthesis. Abbreviations: DHAP - dihydroxyacetone phosphate, G3P - glycerol 3-phosphate.

DHAP or G3P are then acylated by the transfer of an acyl group from a fatty acyl-CoA by a DHAP acetyltrnasferase (DHAPAT) and G3P acetyltransferase (G3PAT), respectively (Hajra and Bishop, 1982). The resulting 1-acyl-DHAP is converted to 1-alkyl-DHAP by a flavin adenine dinucleotide (FAD)-dependent alkyl DHAP synthase (Figure I-7). 1-Alkyl-DHAP is then reduced to 1-alkyl-G3P by an NADPH-dependent 1-alkyl/acyl-DHAP reductase. Additionally, 1-acyl- DHAP can be reduced to 1-acyl-G3P by an NADPH-dependent 1-alkyl/1-acyl-DHAP reductase. While 1-alkyl-G3P is a precursor for ether phospholipid biosynthesis, 1-acyl-G3P is used for ester synthesis (Zufferey and Mamoun, 2006).

I.1.4.4.3. Phospholipid synthesis

Synthesis of phosphatidilcholine and phosphatidylethanolamines. Phosphatidil-cholines (PCs) and phosphatidylethanolamines (PEs) are synthesized via the Kennedy pathway (Kennedy and Weiss, 1956; Ramakrishnan *et al.*, 2013). The first step of the pathway involves the phosphorylation of choline and ethanolamine by a choline/ethanolamine kinase (Gibellini *et al.*, 2008), followed by activation to cytidine 5'-diphosphate (CDP)-choline and CDP-ethanolamine by a choline-phosphate cytidylyltransferase and ethanolaminephosphate cytidylyltransferase, respectively (Figure I-8). The CDP-choline and CDP-ethanolamine are then transferred to diacyl glycerol (or respective ether-type glycerol species) by choline/ethanolamine

phosphotransferase to produce phosphatidylcholine and phosphatidylethanolamine, respectively (Figure I-8) (Signorell *et al.*, 2008). Potential genes encoding the enzymes involved in the Kennedy pathways in *Leishmania* have been identified and annotated but have not been characterized (Ramakrishnan *et al.*, 2013). An alternative way for PC generation by methylation of PE via PE *N*-methyltransferase is believed to operate in *Leishmania* since the organisms contain candidate genes for PE *N*-methyltransferases (Lykidis, 2007). Similarly, PEs can be formed by decarboxylation of phosphatidylserines (PS) and, though *Leishmania* possess candidate genes encoding PS decarboxylases, no experimental evidence exist to prove their functions. Finally, PE can be generated from sphingolipid degradation via a sphingosine1-phosphate lyase, a pathway whose central function in *Leishmania* is to provide PEs.

Synthesis of phosphatidylserines. Phosphatidylserines can be synthesized via two pathways. The first pathway involves head group exchange with PC and PE under the action of PS synthase 1 and 2, respectively (Figure I-8). In the second pathway, PSs are synthesized from serine and CDP-diacyl glycerol via a prokaryotic type PS synthase (Vance and Tasseva, 2012). PSs are membrane components and are involved in targeting and cell signalling.

Synthesis of phosphatidylinositol. Phosphatidylinositols (PIs) contain the cyclic polyalcohol *myo*-inositol which is formed from glucose. The phosphorylated glucose molecule, G6P, is first converted to *myo*-inositol 3-phosphate by an inositol 3-phsophate synthase and then dephosphorylated to *myo*-inositol by inositol 3-phosphate monophosphatase (Figure I-8). *myo*-Inosytol, in the final step of PI synthesis, is merged with CDP-diacylglycerol by a PI synthase (Michell, 2008). PI then can be used for the synthesis of a variety of important PI-containing phospholipids, including glycosylphosphatidylinositols (GPIs), involved in parasite:host interactions between *Leishmania* and the two hosts.

Synthesis of phosphatidylglycerol and cardiolipins. The initial step of phosphatidyl-glycerols and cardiolipins synthesis represents the activation of phosphatidic acid by cytidine 5'-triphosphate (CTP) to form CDP-diacylglycerol (Figure I-8) (Schlame, 2008). Next, phosphatidylglycerophosphate (PGP) is produced by transferring of a phosphatidyl group from CDP-diacylglycerol to G3P by PGP synthase and dephosphorylated to phosphatidylglycerol by PGP phosphatase.

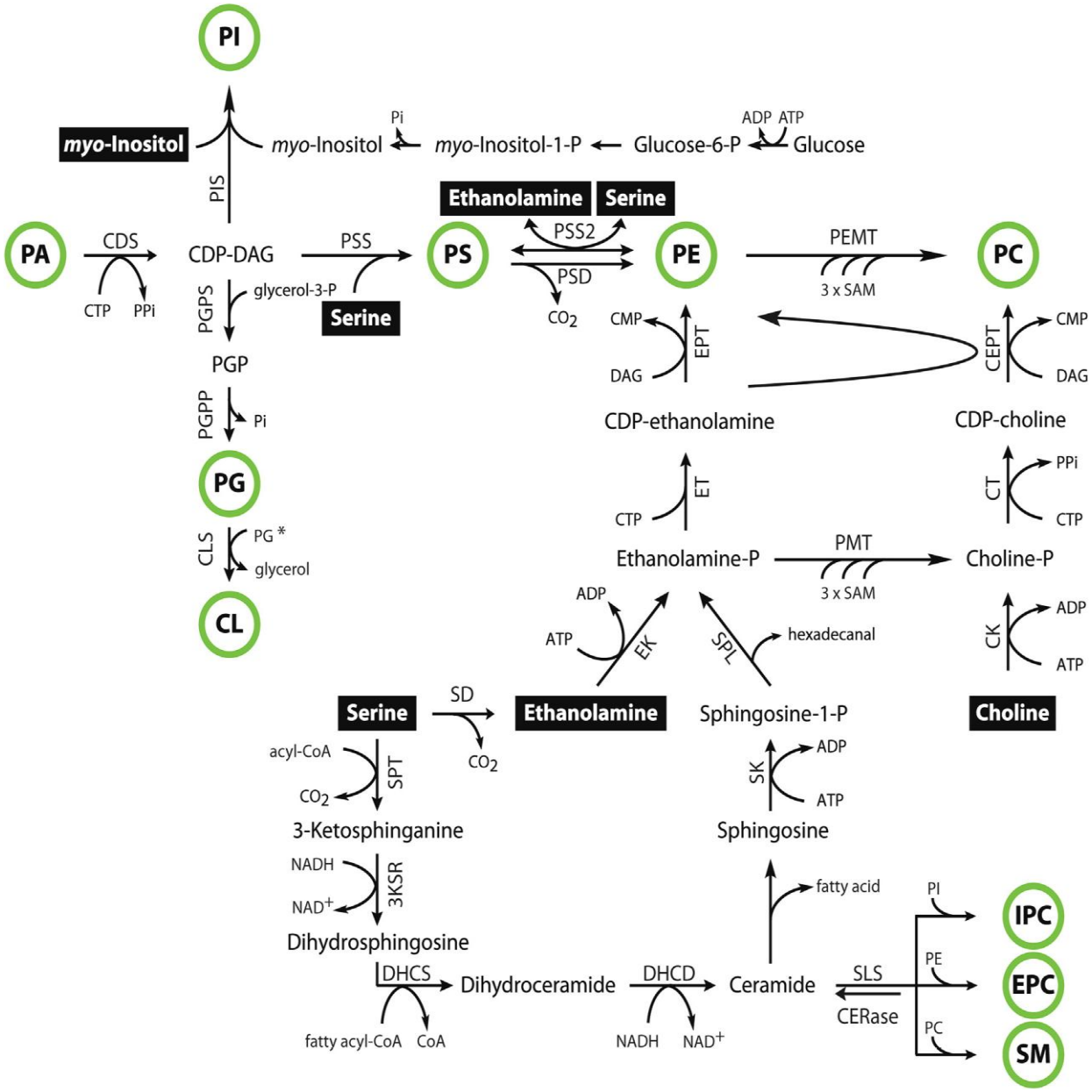

Figure I-8. Phospholipid biosynthesis in *Leishmania*. Nutrients that are taken up from the environment are indicated with black boxes. Major phospholipid classes are indicated with green circles. Abbreviations: 3KSR - 3-ketosphinganine reductase, CDS - cytidine diphosphate diacylglycerol synthase, CEPT - choline/ethanolamine phosphotransferase, CK - choline kinase, CLS - cardiolipin synthase, CT - choline-phosphate cytidylyltransferase, DAG - diacylglycerol, DHCD - dihydroceramide desaturase, DHCS - dihydroceramide synthase, EK - ethanolamine kinase, PMT - phosphoethanolamine N-methyltransferase, EPT - ethanolamine phosphotransferase, ET - ethanolamine-phosphate cytidylyltransferase, PEMT - PE N-methyltransferase, PGPP - PGP phosphatase, PGPS - PGP synthase, PIS - PI synthase, PSD - PS decarboxylase, PSS/PSS2 - PS synthase/PS synthase-2, SAM - S-adenosyl-L-methionine, SD - serine decarboxylase, SLS - sphingolipid synthase, SPL - sphingosine-1-phosphate lyase, SPT - serine palmitoyltransferase.

Credit: Ramakrishnan *et al.*, 2013

Cardiolipin is formed by transferring of another phosphatidyl group to phosphatidyl-glycerol. Knock-down of PGP synthase and knock-out of cardiolipin synthase revealed that phosphatidylglycerols and cardiolipins are essential for *Leishmania* promastigote and amastigote survival (Serricchio and Butikofer, 2012a; b).

I.1.4.4.4. Sphingolipid synthesis

Sphingophospholipid biosynthesis starts with the transfer of a palmitoyl group onto serine by serine palmitoyltransferase which leads to the formation of 3-ketosphinganine. The latter is then reduced to dihydrosphingosine by 3-ketosphinganine reductase and subsequently acylated to dihydroceramide by ceramide synthase. Dihydroceramide is converted to ceramide which is transferred from the endoplasmic reticulum (Mullen *et al.*, 2012) to the Goldgi apparatus. There, several sphingolipid synthases transfer polar head groups from glycerophospholipids to ceramides, thus generating sphingophospholipids. Particularly, inositol phosphorylceramide (IPC) synthases transfer phosphoinositol from PI and ethanolamine phosphorylceramide synthases transfer phosphoethanolamine from PE (Tafesse *et al.*, 2006). Sphingolipids were shown to be used mainly for ethanolamine phosphate generation for glycerophospholipid synthesis (Zhang *et al.*, 2007).

I.1.4.4.5. Sterol biosynthesis

Leishmania are not able to synthesize cholesterol so they take it up from the insect and mammalian host via Na^+-independent high affinity and high specificity transporter(s) operating optimally at pH 7.5-8 (Zufferey and Mamoun, 2002). Instead, *Leishmania* synthesize C24-alkylated, ergostane-based sterols (Goad *et al.*, 1984). Sterol biosynthesis pathway starts with the synthesis of isopentenyl pyrophosphate from HMG-CoA generated during leucine degradation (Ginger *et al.*, 2000). Through the mevalonate pathway, HMG-CoA is consequently converted to mevalonate, mevalonate 5-phosphate and mevalonate 5-pyrophosphate under the action of a HMG-CoA reductase, a mevalonate kinase and phosphomevalonate kinase-likeprotein. A diphosphomevalonate decarboxylase then converts mevalonate 5-pyrophsophate to isopentenyl pyrophosphate. The latter is condensed with dimethylallyl pyrophosphate to form squalene which is cyclizated into lanosterol. Finally, lanosterol is converted into ergosterol (Xu *et al.*, 2014). The last stage of ergosterol synthesis does not occur in mammals which is why the enzymes involved in it, such as the C14a-sterol demethylase and the S-adenosyl-L-methionine: C24-D-

sterol methyltransferase, are drug targets of considerable interest (Pomel *et al.*, 2015).

I.1.4.4.6. β-Oxidation of fatty acids

A comprehensive genome comparison between *T. brucei*, *T. cruzi* and *L. major* revealed that *Leishmania* should be able to oxidize fatty acids via β-oxidation (Berriman *et al.*, 2005). An unusual feature of the fatty acid β-oxidation in trypanosomatids is that it probably occurs in two organelles, the glycosomes and mitochondria, instead of the mitochondrion only as it is in mammals. How the two organelles contribute to the pathway, however, is still unknown. The pathway results in the oxidation of different chain-length fatty acids to acetyl-CoA, NADH and $FADH_2$. Acetyl-CoA can be fed into the TCA cycle (Saunders *et al.*, 2014) while NADH and FAD_2 can be further oxidized and the released electrons used by the electron transport chain to generate ATP. Four different chain-length fatty acyl-CoA dehydrogenases are present in the *Leishmania* genome (Opperdoes and Michels, 2008). Three of the acyl-CoA dehydrogenases have mitochondrial targeting signals. Bifunctional enzymes and thiolases are also predicted to be present in the glycosomes and the mitochondrion. *Leishmania* are predicted to oxidize also unsaturated fatty acids judging by the presence of genes encoding a 3,2-trans-enoyl-CoA isomerise and 2,4-dienoyl-CoA reductase in the genome of *L. major* (Opperdoes and Michels, 2008).

I.1.4.5. Nucleotide metabolism

Leishmania lack the enzymes for *de novo* synthesis of purines and have to acquire them from the insect and mammalian hosts (Opperdoes and Michels, 2008). To salvage these essential nutrients, *Leishmania* express developmentally regulated plasma membrane and secreted nucleotidase/nucleases and purine nucleoside/ nucleobase transporters (Figure I-9) (Sopwith *et al.*, 2002; Landfear *et al.*, 2004; Joshi and Dwyer, 2007). The nucleotidase/nucleases hydrolyse and dephosphorylate, where needed, exogenous polynucleotides, nucleotide monophosphates and nucleaic acids and produce suitable for transporting substrates for the purine transporters NT1, NT2, NT3, and NT4 (Aronow *et al.*, 1987; Vasudevan *et al.*, 1998; Carter *et al.*, 2000; Al-Salabi *et al.*, 2003; Sanchez *et al.*, 2004; Ortiz *et al.*, 2007).

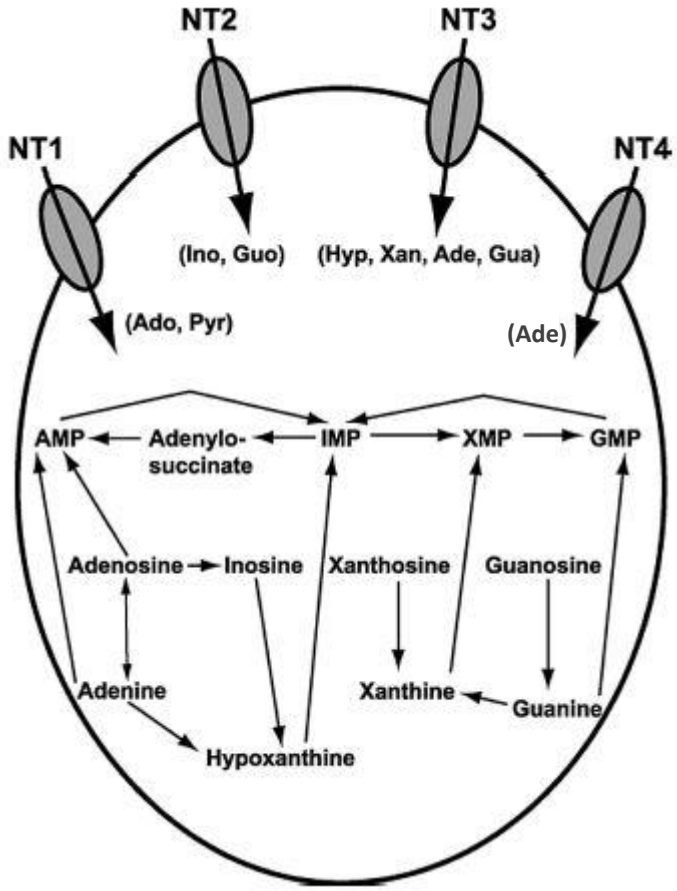

Figure I-9. Purine salvage pathway in *Leishmania* promastigotes. Presented here are the purine nucleoside/nucleobase transporters (NTs) and purine biosynthesis pathways in *Leishmania* promastigotes. Abbreviations: Ado - adenosine, Pyr - pyrimidine nucleosides, Ino - inosine, Guo - guanosine, Hyp - hypoxanthine, Xan -xanthine, Ade - adenine, Gua - guanine.

Credit: Landfear *et al.*, 2004

When imported, purine nucleosides and nucleobases are converted to nucleotides by three phosphoribosyltransferases (PRTs), a cytosolic adenine PRT (APRT) and the glycosomal xanthine PRT (XPRT) and hypoxanthine-guanine PRT (HGPRT) (Boitz and Ullman, 2006 a, b). The nucleotides are then used by the parasites for the synthesis of DNA and RNA.

Leishmania, as other trypanosomatids, are able to synthesize pyrimidines *de novo*. Precursors for the pyrimidine synthesis are L-glutamine, bicarbonate and L-aspartate which, upon the action of carbamoylphosphate synthase, aspartate carbamoyltransferase and dihydroorotase are converted to dihydroorotate. The latter is then oxidized by a cytosolic dihydroorotate dehydrogenase to orotate which is translocated to the glycosomes. There, the bifunctional orotidine 5-phsohphate decarboxylase/orotate phosphorybosyltransferase converts orotate to uridine 5-monophaosphate (UMP) (Opperdoes and Michels, 2008).

I.1.4.6. Metabolism of cofactors and vitamins

Not much is known about cofactor and vitamin metabolism in *Leishmania*. It has been established, based on studies of culture media, that *Leishmania* parasites are auxotrophic for biotin, biopterin, folate, pantothenate, pyridoxine, riboflavin, nicotin, and heme (Steiger and Steiger, 1976; Merlen *et al.*, 1999). Similar to many other cofactors and vitamins, none of the genes involved in folate/biopterin biosynthesis are present in the parasites (Opperdoes and Michels, 2008). Instead, 12 genes encoding folate/biopterin transporters are found in the parasite genome. The folate/biopterin transporter genes *BT1* of *L. donovani* and *L. tarentolae* and *FT1* and *FT5* of *L. infantume* have already been characterized (Lemley *et al.*, 1999; Kundig *et al.*, 1999; Richard *et al.*, 2002; Richard *et al.*, 2004). After it is imported, folate has to be activated to THF. Activation of folate can occur via two different enzymes, the bifunctional dihydrofolate reductase-thymidylate synthase and pteridine reductase 1 (Beverly *et al.*, 1986; Cunningham and Beverley, 2001). THF then can be used in one-carbon metabolism (see **I.1.4.1.**, *Glycine*), as well as catabolism, glycine and L-serine interconversions and L-methionine and thymidylate biosynthesis (Ouellette *et al.*, 2002).

Contrary to the complete lack of genes for folate/biopterin byosynthesis, some genes involved in the final steps of the synthesis of a number of cofactors and vitamins are present in the *Leishmania* genome. For instance, the last three enzymes involved in

the synthesis of heme from succinyl-CoA, namely coproporphyrinogen III oxidase, protoporphyrinogen oxidase and ferrochelatase, and the last two enzymes of CoA synthesis, phosphopantetheine adenylyl transferase and dephospho-CoA kinase, most of which, similar to other genes in *Leishmania*, were most probably gained by lateral transfer from bacteria (Berriman *et al.*, 2005).

I.1.5. Glucose transporter null mutant *Leishmania mexicana*

Glucose is a primary nutrient supplying many heterotrophic organisms with energy and building blocks for the synthesis of many different biomolecules. For *Leishmania*, glucose is a major energy and carbon source which the parasites compete for with the invertebrate and vertebrate hosts. Exogenous glucose is taken up by *L. mexicana* promastigotes and amastigotes via three membrane transporters, GT1, GT2 and GT3, which have discrete substrate affinities, sub-cellular localization and life cycle regulated expression (Burchmore and Landfear, 1998). Genomic and transcriptomic analyses revealed that the *GT* genes are closely related and transcribed at similar levels throughout the leishmanial life cycle. However, *GT1* and *GT3* are constitutively expressed in both life cycle stages of *Leishmania* while *GT2* is ~15-fold up-regulated in the promastigote forms. Structural analysis confirmed that the three permeases have 90% homology as they differed from one another mainly at their NH_2 and COOH terminal domains. Fluorescence microscopy showed that GT1 is localized mainly in the flagellum while GT2 and GT3 are located on the surface membrane (Burchmore *et al.*, 2003). Transport assays eventually revealed that the GT permeases are the main glucose transporter in *L. mexicana*.

Further function characterization of the three permeases involved the deletion of the *GT* locus and generation of a null mutant cell line, *Δlmgt*, which was shown to have a characteristic phenotype (Burchmore *et al.*, 2003; Rodriguez-Contreras and Landfear, 2006; Rodriguez-Contreras *et al.*, 2007; Feng *et al.*, 2011). The *Δlmgt* promastigotes:

- are not able to transport the hexoses D-glucose, D-fructose, D-mannose and D-galactose;
- are not able to grow in the presence of D-glucose, D-fructose, D-mannose or D-galactose when provided as sole carbohydrate sources;

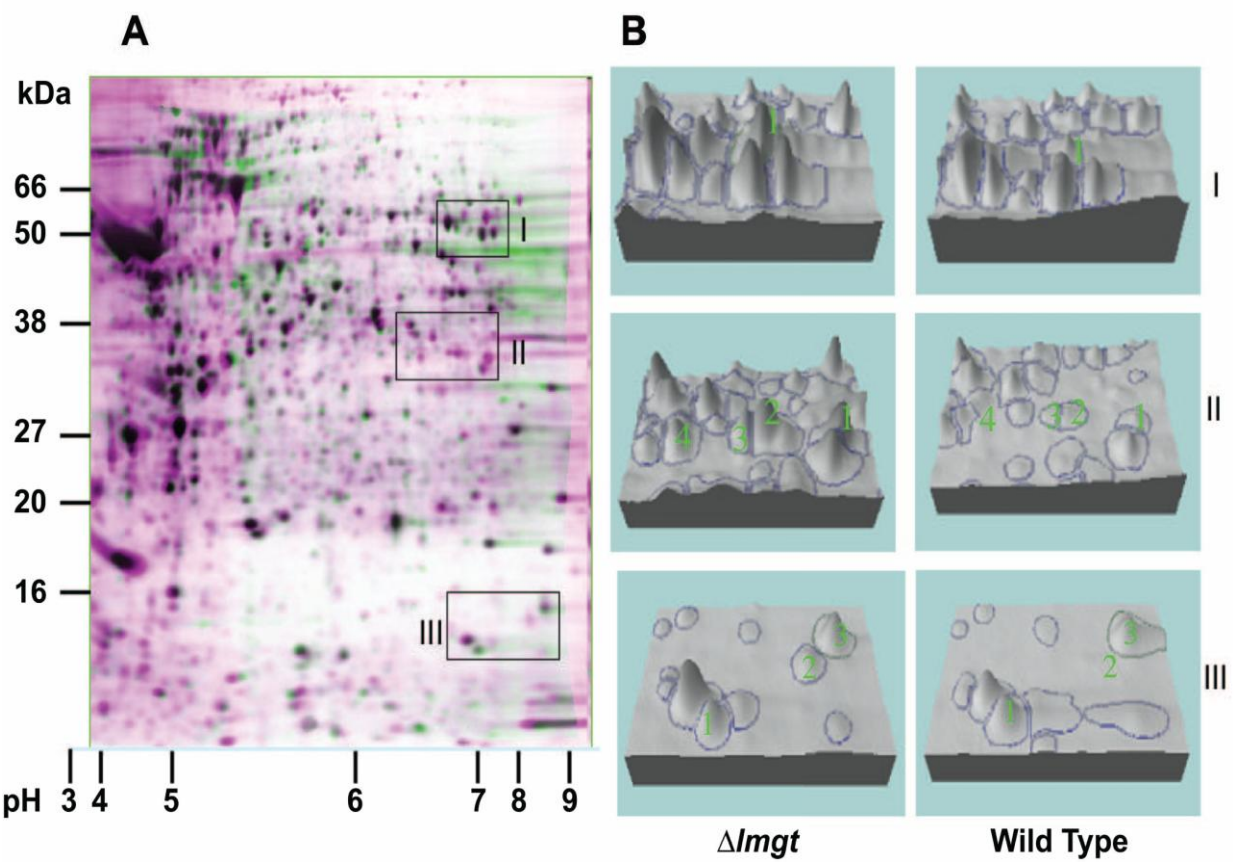

Figure I-10. Two-dimensional gel electrophoresis of wild type (green) and Δ*lmgt* (violet) promastigotes. (A) Electronic image of 2DE of wild type and Δ*lmgt* promastigotes. (B) Topographic images of three gel regions. Box I: spot 1 – mitochondrial aldehyde dehydrogenase; Box II: spot 1 – D-lactate dehydrogenase and ribokinase, spot 2 – ribokinase, spot 4 – mitochondrial aldehyde dehydrogenase; Box III: spot 1, nucleoside diphosphate kinase, spot 2 – mitochondrial aldehyde dehydrogenase, spot 3 – cyclophilin.

Credit: Feng *et al.*, 2011

- grow more slow and to a lower cell density compared with the wild type promastigotes, even in the presence of D-glucose and an alternative energy source such as L-proline in the culture medium;
- are more susceptible to oxidative stress compared with the wild type promastigotes;
- are sensitive to nutrient starvation and alkaline pH;
- are still able to synthesize the glycoconjugates lipophosphoglycan (LPG), proteophosphoglycan (PPG), small neutral glycosylinositol-phospholipids (GIPLs), gp63, and secreted acid phosphatase (sAP) at reduce rate;
- are still able to synthesize the storage carbohydrate mannogen, albeit at reduced level;

- are able to incorporate [^{14}C]-alanine, [^{14}C]-aspartate, [^{14}C]-acetate and [^{14}C]-glycerol into mannogen presumably via gluconeogenesis;
- have different protein profile compared with the wild type promastigotes (Figure I-10);
- are characterized with significantly up-regulation of ribokinase, hexokinase and two isomers of a mitochondrial aldehyde dehydrogenase;
- reproduce less rapidly in the insect vector *Lutzomyia longipalpis* compared with the wild type promastigotes;
- develop into metacyclic forms less efficiently;
- are not viable as axenic amastigote.

In 2009, Landfear and colleagues published another work on the *Δlmgt* cell line where they described the isolation of suppressor mutants of the *Δlmgt* null line. A genomic analysis showed that the suppressor mutants have amplified and overexpressed a low affinity hexose transporter designated GT4 (previously known as D2). A phenotypic analysis also revealed that the suppressor mutants were able to:

- restore growth rate to that of wild type promastigotes grown in glucose-replete media;
- restore to a certain extent their ability to proliferate within macrophages;
- partially restore their ability to infect macrophages;
- restore their ability to take up hexoses;
- restore resistance to oxidative stress;
- restore resistance to high temperatures;
- store mannogen at increased rate compared with the wild type promastigotes.

The prior phenotypic characterization of the *Δlmgt* promastigotes thus revealed that the deletion of the glucose transporters in *L. mexicana* is associated with significant metabolic changes. We have applied global proteomic and metabolomic profiling approaches such as stable isotope labelling by amino acids in cell culture (SILAC) and mass spectrometry-based untargeted and targeted metabolomics to investigate the metabolic changes in the *Δlmgt* promastigotes. The approaches used in this project are introduced herein.

I.2. Proteomics

High-paced and high-throughput genome sequence analysis and instrument, method, and bioinformatic tool development have provided fruitful environment for the blooming of modern -omics technologies. Omics approaches, including genomics, transcriptomics, proteomics, metabolomics, etc., aim to comprehensively elucidate the flow of information from gene to protein product and from a pathway to a system.

Constant advances in large-scale sequencing have resulted in the generation of an increasing number of fully or partially sequenced genomes from a variety of organisms. Each genome can be used as a database from which further information can be derived. The genome, however, can be considered as a static system. The proteome, which comprises all proteins encoded by a genome, and metabolome, which encompasses the low molecular weight compounds of a biological system, are extremely dynamic units, strongly depending on the organism's physiology and surrounding environment. Considering that, a main goal of modern proteomics is to identify and quantify all, or as many as possible, of the proteins associated with a particular state of an organism or a cell type evoked by a specific environment, chemical treatment, or altered cell phenotype. Detection of proteome changes involves the implementation of adequate methodologies for sample preparation and sensitive and accurate tools for sample and data analysis. Thus, constant development of new or improvement of the existing methodologies is extremely valuable for more comprehensive and sophisticated proteomic investigations. For instance, until recently, two-dimensional gel electrophoresis (2-DE) was the standard proteomic technique used for detection of changes in protein expression. 2-DE, however, requires subsequent targeted protein identification. The search for alternative methods allowing simultaneous accurate identification and quantitation resulted in combining 2-DE with mass spectrometry (MS) (Gorg *et al.*, 2004), an

analytical tool that can determine the type and amount of a molecule, whether it is a protein or a chemical compound for example. Thus, MS is able to generate quantitative in addition to structural information, which is why many of the current experimental platforms are MS-based. In terms of scope, an increasing number of quantitative studies focus not on the whole but on more discrete fractions of cellular proteome in order to identify and quantify a set of targeted proteins. One of the most widely applied techniques for targeted quantitative proteomics is selected reaction monitoring (SRM), also called multiple reaction monitoring (MRM). SRM is performed on triple quadrupole (QQQ) mass spectrometers in which a precursor ion with a specific *m/z* value is selected in the first quadrupole, fragmented in the second, and then the product ion selected in the third quadrupole. Thus, the main use of SRM is to overcome, though only to a certain extent, some of the disadvantages of discovery (or shotgun) proteomics with regard to reliable quantification of multiple proteins and proteins of low abundance in a high-throughput manner (Boja and Rodriguez, 2012). SRM has only recently been applied in peptide and protein quantification while it has been routinely used in clinical diagnostic and pharmaceutical industry for quantification of metabolites, drugs, hormones, etc. for many years (Boja and Rodriguez, 2012).

The quantitative but global and untargeted nature of the proteomic analysis in this study did not require the use of targeted approaches such as SRM. Instead, to investigate the *Leishmania* proteome as thoroughly as possible, we included a prefractionation step with digitonin prior to the MS analysis. Prefractionation is used to increase the protein coverage, and in particular, to enrich low abundant proteins, and is usually performed by electrophoretic, chromatographic, or gradient centrifugation techniques (Foucher *et al.*, 2006). Alternative methods also include depletion of the highly abundant proteins, immunoprecipitation, or precipitation with chemical compounds such as ammonium sulfate and digitonin (Righetti *et al.*, 2005; Foucher *et al.*, 2006). Digitonin is a detergent which binds and precipitates sterols present in membranes thus causing the intracellular or intraorganellar protein content to leak out through pores. A recently developed method exploited the intrinsic feature of digitonin to form pores and using increasing concentrations of the detergent, starting from micromolar and gradually increasing to milimolar concentrations, was able to enrich cytoplasmic and organellar proteins of *Leishmania* in sequential fractions (Foucher *et al.*, 2006). We adopted this method and used it to

increase the scope of protein identification by fractionating the proteome of wild type and *Δlmgt* promastigotes into five sub-cellular fractions. According to Foucher *et al.*, 2006, the first two fractions, resulting from using low concentrations of digitonin to damage the plasma membrane, were predicted to be enriched in plasma membrane and cytosolic proteins, the third and fourth fractions, resulting from using higher concentrations of digitonin to damage the intracellular/organellar membranes, were supposed to be enriched in organellar proteins, and the last fraction comprised of digitonin-insoluble proteins. Further to identification, however, we aimed to also compare and quantify the abundance of the proteins in each fraction which required the use of a quantitative labelling method subsequently to the digitonin-based fractionation. Based on the type of information provided by the quantitative methods, quantification can be divided into relative or absolute. A method for generation of relative quantitative information is label-free quantitation. Label-free methods do not require the use of a stable isotope containing compound to label proteins and are thus simpler, more straightforward, and more economic. Common to all label-free methods is the need for strict control of the experimental conditions, lack of fractionation, and, if possible, automated sample preparation. The quantitation in label-free is based on precursor signal intensity or on spectral counting. The former type of label-free quantitation relies on simple counting of the number of fragment-ion spectra acquired for any given peptide while the later type of quantitation involves the measurement of the peak area (or signal intensity) of a peptide precursor ion. Although in some cases label-free approaches yield higher proteome coverage, the accuracy of the quantitative information lacks compared to that obtained from stable isotope labelling experiments. Thus, stable isotope-based approaches are more suitable for detection of subtle proteome changes and correspondingly, more and more studies, in search for precise quantitation, rely on stable isotopes such as ^{3}H, ^{13}C, ^{15}N and ^{18}O to chemically or metabolically label proteins (Ong and Mann, 2005). Stable heavy isotopes enable discrimination between labelled and unlabelled proteins and calculation of a stable isotope ratio gives quantitative information regarding the abundance of one or the other type of protein. Thus, the stable isotope techniques allow comprehensive investigation of complex protein mixtures and can provide relative as well as absolute quantitative information.

Two stable isotope labelling techniques, namely the metabolic stable isotope labelling by amino acids in cell culture and the chemical stable isotope dimethyl labelling were used in this project.

I.2.1. Stable isotope labelling by amino acids in cell culture

Stable isotope labelling by amino acids in cell culture (SILAC) is one of the novel quantitative proteomic techniques that were introduced in the previous decade. It was developed by Mann and colleagues and described for the first time in 2002 (Ong *et al.*, 2002). In their original study, the authors used deuterated L-leucine to investigate changes in the protein expression during muscle cell differentiation. SILAC, however, can be applied to every type of cells that can be cultured. Additionally, besides deuterated L-leucine, a heavy version of every proteinogenic amino acid can be used in SILAC. With time, L-arginine and L-lysine, usually enriched in carbon and nitrogen, were established as the most popular amino acids for SILAC labelling. SILAC relies on metabolic incorporation of unlabelled (or light) and heavy isotope amino acids obtained by the cells from the SILAC culture media (Figure I-11). When two cell populations are cultured in light and heavy SILAC media they incorporate the unlabelled or heavy-labelled amino acids into the synthesized new proteins. Thus, after a minimum of five or six cell divisions the respective amino acids should be completely replaced with the light and heavy amino acids. The cell cultures can then be combined and subjected to protein digested with a protease, usually trypsin which cuts after arginine and lysine. The resulting light- and heavy-labelled peptides will have different mass and will be easily distinguishable by a mass spectrometer. The MS spectra will contain intensity information regarding the distinct pairs of light (Figure I-11, black dot) and heavy (Figure I-11, red star) peptide species. Comparison of the signal intensities of the identical peptides will determine the change in abundance of the protein.

To date, five studies have applied SILAC to *Trypanosoma* and four to *Leishmania*. Four of the five SILAC studies with trypanosomes quantified ~30% of the total proteome (Gunasekera *et al.*, 2012; Urbaniak *et al.*, 2012; Urbaniak *et al.*, 2013; Guther *et al.*, 2014). Two of the studies investigated proteome remodelling during differentiation. The other two studies focused on the phosphoproteome and glycoproteome of *T. brucei* but were still able to obtain quantitative data for more than 3,000 proteins.

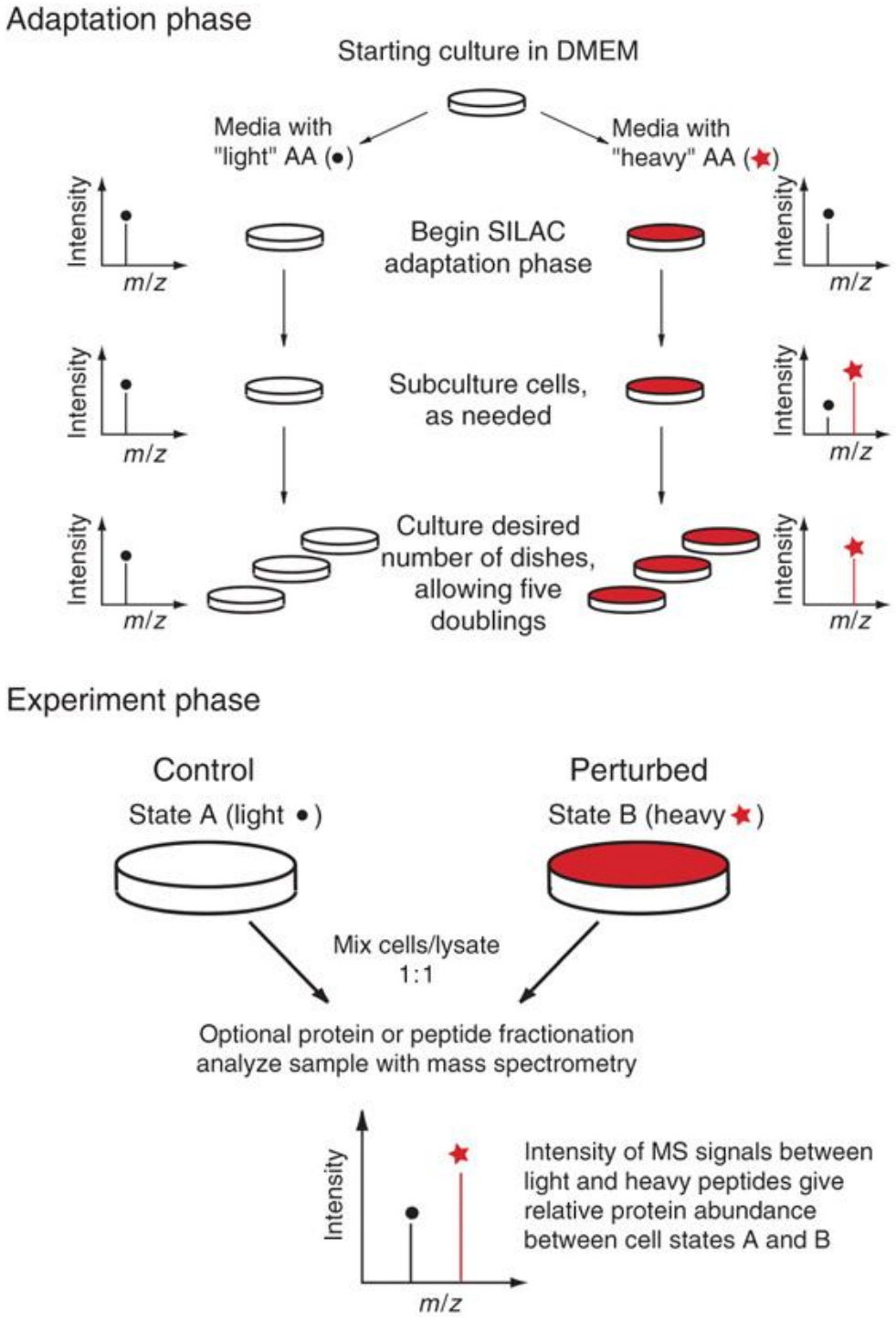

Figure I-11. Conventional stable isotope labelling by amino acids in cell culture workflow. Presented here is an elaborate schematic representation of a SILAC workflow consisting of an adaptation phase, during which cells are grown in light and heavy SILAC media until they fully incorporate the respective light and heavy amino acids, and an experimental phase, during which the two cell populations are differentially treated, inducing changes in the proteome. The labelled cells are then pooled together, lysed and analysed by MS.

Credit: Ong and Mann, 2007

Three of the four SILAC studies with *Leishmania* investigated drug resistance while the fourth studied the *L. donovani* secretome (Chawla *et al.*, 2011; Brotherton *et al.*, 2013; Brotherton *et al.*, 2014; Silverman *et al.*, 2008). In contrast to the SILAC studies with trypanosomes, those performed with *Leishmania* generated quantitative data for only between 50 and 150 proteins. This huge difference in the number of quantified proteins indicates that the SILAC approach may be biased toward high-abundance proteins and may only be good for measuring large changes in protein expression in *Leishmania*. Despite the much lower number of proteins quantified in *Leishmania*, many metabolic enzymes involved in central energy pathways such as glycolysis and TCA cycle were found significantly modulated in the tested parasites. That suited our aims and SILAC was applied, in parallel with stable isotope dimethyl labelling, to probe the *L. mexicana* proteome.

I.2.2. Stable isotope dimethyl labelling

Stable isotope dimethyl labelling was introduced in 2003 by Chen and colleagues (Hsu *et al.*, 2003). By contrast to the metabolic SILAC labelling, dimethyl labelling relies on chemical reductive amination of all primary amines (the N-terminus and ε-amino groups of L-lysine residues). The primary amine first interacts with formaldehyde which leads to the formation of a Schiff base that is rapidly reduced by sodium cyanoborohydride to form secondary amines. The latter react with another formaldehyde unit to form dimethylamino group (Hsu *et al.*, 2003). Stable isotope dimethyl labelling does not require growing of the cells/tissue/ organism of interest in specialized media/environment. When the protein samples are generated, they are subjected to protease digestion and then the resulting peptide samples are dimethyl labelled. Triplex dimethyl labelling can be achieved with formaldehyde and sodium cyanoborohydride as light labels, deuterated formaldehyde and sodium cyanoborohydride as intermediate labels and deuterated and ^{13}C-labelled formaldehyde and sodium cyanoborodeuteride as heavy labels (Figure 12, A). This labelling generates a mass increase of 28 Da, 32 Da and 36 Da in the light-, intermediate- and heavy-labelled peptides, respectively. That corresponds to a 4Da difference between the light, intermediate and heavy peaks (Figure I-12, B). Differentially labelled peptide samples are subsequently combined and analyzed by MS/MS.

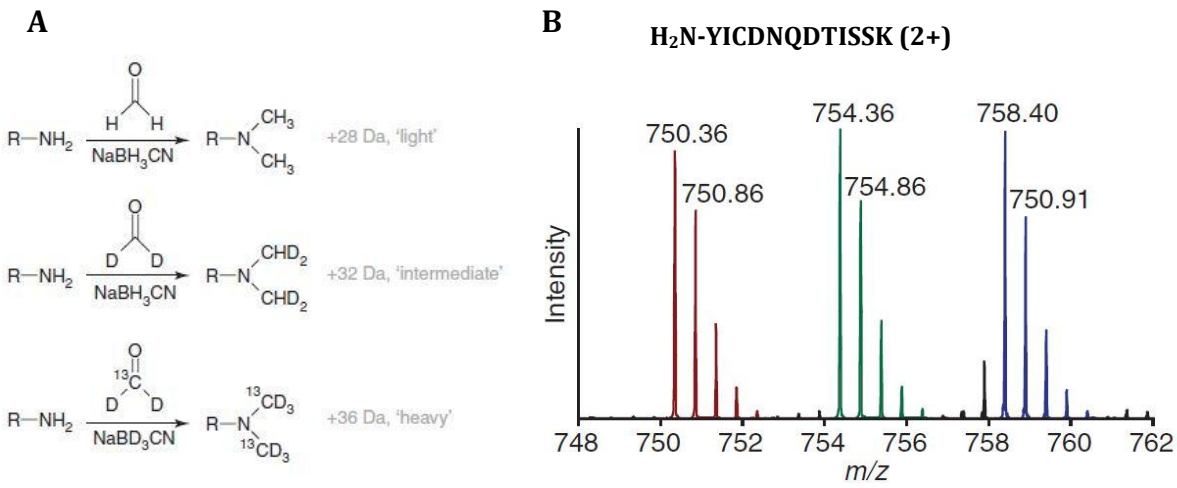

Figure I-12. Triplex stable isotope dimethyl labelling. (A) Stable isotope dimethyl labelling reactions with formaldehyde and sodium cyanoborohydride as the light labels, deuterated formaldehyde and sodium cyanoborohydride as the intermediate labels, and deuterated and ^{13}C-labelled formaldehyde and sodium cyanoborodeuteride as the heavy labels. (B) Representative peaks of light-, intermediate- and heavy-labelled species of the dimethyl labelled BSA **YICDNQDTISSK** peptide.
Credit: Boersema *et al.*, 2009

Since stable isotope dimethyl labelling occurs at the peptide level, and not at the protein level as the SILAC labelling does, the sample preparation is prone to introduction of more technical errors which could result in possible sample loss and variability. SILAC allows sample combination at the protein level which in theory should provide more precise and reproducible quantitative results. However, compared to SILAC, dimethyl labelling is considerably less expensive. Additionally, while SILAC is restricted to cells grown in culture, dimethyl labelling is applicable to any type of samples. Both labelling techniques are straightforward, robust and highly efficient. However, our experience with *L. mexicana* wild type and *Δlmgt* promastigotes revealed that SILAC depends on the metabolic specificities of the species of interest and may not be as efficient as predicted to be.

To date, no study has applied stable isotope dimethyl labelling for investigation of the *Leishmania* proteome.

I.3. Metabolomics

Contemporary metabolomics aims at investigating the metabolome comprised of all low molecular weight compounds, and more specifically, the non-genetically encoded substrates and products of enzymatic reactions or spontaneous conversions, of a biological system. The metabolome includes amino acids, organic acids, nucleotides, lipids, cofactors, vitamins, etc. These metabolites are very diverse and can spread over a wide range of concentrations. Metabolomics can provide qualitative

and quantitative information regarding metabolite structure, function, concentration and transformation paths, and can thus be used for the investigation of complex compound mixtures. The information generated can then be used to evaluate metabolites and map metabolite trafficking through metabolic networks and to pinpoint differences in phenotypes resulting from environmental influences, disease or genotype changes so that eventually a certain metabolome can be attributed to a certain phenotype. Currently, performing a comprehensive metabolomic analysis involves the implementation of several techniques. MS-based approaches are used to perform large-scale accurate quantitative analyses. However, they are still not capable to measure all compounds, even though a number of different methodologies, that include specific sample preparation and chromatographic separation prior to the MS analysis, have been developed.

Careful sample preparation is essential in metabolomics. Recently, Likic and colleagues described a method where a quick quenching of cell cultures to about 0°C, followed by cold chloroform/methanol/water extraction of metabolites was used to capture a snapshot of the *L. mexicana* cell metabolism (de Souza *et al.,* 2006). Besides cold chloroform/methanol/water extraction, methanol extraction at -40°C, hot ethanol extraction and rapid filtration have also been applied in metabolomic investigations (de Koning and van Dam, 1992; Kamleh *et al.,* 2008; Ebikeme *et al.,* 2010). In our study, we have applied a slightly different cold chloroform/ methanol/water extraction to that applied by Likic, followed by either liquid chromatography (LC) (described in **I.3.1.**), for investigation of whole cell lysates and lipids, or gas chromatography (GC) (described in **I.3.2.**), for investigation of sugars, from the wild type and *Δlmgt* promastigotes. Besides mass spectrometry, we have also used nuclear magnetic resonance (described in **I.3.3.**) to elucidate carbon utilization by the *Δlmgt* promastigotes.

I.3.1. Liquid chromatography - mass spectrometry

High-performance liquid chromatography (HPLC) is one of the most common types of chromatography used currently in the metabolomic research field. In HPLC, the solvent (or the mobile phase) passes through a chromatographic column (the stationary phase) under pressure. The separation takes place in the column and involves interaction of the analytes with matrix inside the column. For how long a compound will interact with the stationary phase and thus be retained by it depends on the chemical nature of the compound and on the chemistries of the stationary

phase and of the solvent. The HPLC systems applied most frequently for metabolomic investigations are reverse-phase liquid chromatography (RPC) and hydrophylic interaction chromatography (HILIC). Reverse-phase chromatography is preferentially used for separation of lipophilic compounds and in our project it was used for untargeted lipidomic analysis of the wild type and *Δlmgt* promastigotes while hydrophylic interaction chromatography is suitable for separation of polar and charged metabolites and it was applied for global untargeted metabolomic analysis of the two types of cells (Lu *et al.*, 2008; Watson, 2010). The separation, either by RPC or HILIC, was then followed by electrospray ionization (ESI) operating in alternating positive and negative mode so that both positive and negative ions are generated. After the ionization, our lipid samples were subjected to two fragmentation methods, namely collision-induced dissociation (CID) and higher-energy collision dissociation (HCD), and directed to an Orbitrap mass spectrometer while the untargeted metabolomic samples were directly analyzed by the Orbitrap.

I.3.2. Gas chromatography - mass spectrometry

Gas chromatography coupled to mass spectrometry (GC-MS) can be considered as one of the main techniques that lays behind the development of contemporary metabolomics. GC provides reproducibility and the highest resolution among the chromatographic techniques. When applied to complex mixtures, one of the most common types of GC, capillary GC, can result in the separation of hundreds of compounds.

As the name suggests it, the mobile phase in GC is gas while the stationary phase is solid. The analyzed compounds also have to be volatile or made volatile via derivatization. After the separation, the gas molecules are directed to an ionization unit, where electron ionization (EI) or chemical ionization (CI) occurs, which is then followed by a mass spectrometry analysis by a low resolution mass analyzer, such as quadrupole, or a high resolution mass spectrometer, such as time-of-fight (TOF) or Fourier transform ion cyclotron resonance (FT-ICR). A number of sugars and sugar phosphates that were known or presumed to be present in the *L. mexicana* wild type and glucose transporter null mutant promastigotes were analyzed. The derivatization of the sugars and sugar phosphates included methoxyamination and silylation (as described in **II.6.3.**). Then the silylated sugars were separated on a Trace GC Ultra gas chromatograph and analyzed on a quadrupole ion trap (ITQ) 900 mass spectrometer.

Method	Use	Advantages	Disadvantages	Reference
NMR spectrometry				
Proton solution NMR (also known as ^{1}H-NMR)	Analyses high energy and phospholipid metabolism to quantify amino acids, carbohydrates, fatty acids, lipids and phospholipids.	- Non-invasive - Solution - High precision - High temporal resolution - Low per-experiment cost - Minimal sample preparation required - Average analytical time of ten minutes - Non-destructive - Quantitative	- Less sensitive than mass spectrometry	
^{31}P-NMR	Quantifies high energy phosphates (e.g. ATP, phosphocreatine), phospholipid precursors and sugar phosphates.			
^{13}C-NMR	Quantifies metabolic fluxes of 13C-labelled precursors (e.g. 13C-labelled glucose fluxes through glycolysis), the TCA cycle, the pentose-phosphate cycle and de novo fatty acid synthesis			
HR-MAS ^{1}H-NMR	*In vitro* tissue applications			
Mass spectrometry (MS)				
LC-MS GC-MS	Full spectrum analysis of solutions with multiple metabolites	- High sensitivity and specificity - Full spectrum analysis - Current gold standard for analyzing solutions	- Derivatization/chemical modification needed - Destructive to sample - Not fully quantitative without appropriate standards	

Table I-3. Comparison between nuclear magnetic resonance and mass spectrometry. Presented here in the form of a table are the advantages and disadvantages if NMR and MS.

Credit: Roberts *et al.*, 2011

Apart for separation of sugars, GC has been extensively used for analysis of other metabolites of the central carbon metabolism such as organic acids, lipids, amino acids, nucleotides and etc. (Saunders *et al.*, 2011; Saunders *et al.*, 2014).

I.3.3. Nuclear magnetic resonance

Nuclear magnetic resonance (NMR) possesses a number of unique advantages over MS (Table I-3) and has been extensively used for metabolomic analyses. It requires minimal sample preparation, it is robust, non-destructive and rapid and it provides high-resolution, quantitative, reproducible and rich structural information. One of the main disadvantages of NMR, however, is the low sensitivity. Because of that, often the samples have to be at least several micrograms. An intrinsic quality of NMR is its ability to detect the spin properties of the atomic nuclei in a magnetic field. The NMR active nuclei include ^{1}H, ^{31}P, ^{13}C and ^{15}N. ^{1}H 1D Fourier-transform NMR, which is the simplest and fastest type of NMR, is routinely used to investigate urine samples or cell extracts (Bingol and Bruschweiler, 2014). More complex mixtures,

however, require longer time for analysis and/or higher-dimentional NMR. ^{1}H-, ^{13}C- and ^{31}P-NMR have been employed in a number of studies investigating for example the glucose and proline metabolism of trypanosomes, the phosphometabolome of trypanosomes, the changes in the metabolism of aconitase-deficient trypnosoma cell line and the changes in the urine and plasma of mice infected with trypanosomes (Mackenzie *et al.,* 1982; Mackenzie *et al.,* 1983; Besteiro *et al.,* 2002; Coustou *et al.,* 2003; Coustou *et al.,* 2005; Coustou *et al.,* 2006; Coustou *etal.,* 2008; Riviere *et al.,* 2009; Moreno *et al.,* 2000; Wang *et al.,* 2008; Ebikeme *et al.,* 2010; van Weelden *et al.,* 2003; Lamour *et al.,* 2005). ^{1}H-, ^{13}C- and ^{31}P-NMR were also used to elucidate the lipid profile of *L. donovani* promastigotes, to analyze the phosphometabolome of *L. major* and to investigate the involvement of leucine in sterol biosynthesis, (Adosraku *et al.,* 1993; Moreno *et al.,* 2000; Ginger *et al.,* 2001). In our metabolomic study, ^{1}H 1D NMR was used to investigate the utilization and metabolization of several enriched and non-enriched carbon sources, including D-glucose, L-proline, L-threonine and glycerol. Additionally, NMR was combined to LC-MS which helped us perform an isotope tracing analysis and elucidate the fate of the mentioned carbon sources in the wild type and *Δlmgt* promastigotes.

I.4. Aims

Phenotypically, the *Δlmgt* promastigotes were shown to differ considerably from the wild type cells of *Leishmania mexicana*. Distinguishable features of the mutant strain were altered mRNA and protein expression, reduced cell size, growth, and metacyclogenic capability, increased sensitivity to nutrient starvation, elevated temperatures, and oxidative stress, and inability to utilize hexoses as carbon and energy sources, yet, ability, even at a reduced rate, to synthesize glycoconjugates and mannogen involved in pathogenicity. To be able to synthesize hexose-containing macromolecules such as glycoconjugates and mannogen, however, the *Δlmgt* promastigotes have to switch to using carbon sources other than sugars, and to modulate their metabolism for optimal use of the alternative carbon sources for catabolic and anabolic purposes. To test this hypothesis, we set our aims to:

- investigate whether the *Δlmgt* promastigotes use alternative energy and carbon sources and whether amino acids and lipids represent such

- determine which catabolic and anabolic pathways are altered as a result of possible utilization of alternative carbon and energy sources by the *Δlmgt* promastigotes

- represent, in a global and quantitative manner, the metabolomic changes in central carbon metabolism in the *Δlmgt* promastigotes.

CHAPTER II. Materials and methods

II.1. Global proteomic characterization of *Δlmgt* promastigotes by stable isotope labelling by amino acids in cell culture

II.1.1. Serum dialysis

Heat-inactivated fetal bovine serum (iFBS) (Life Technologies) was dialyzed using SnakeSkin Dialysis Tubing, 3.5K molecular weight cut-off (MWCO) (Thermo Scientific) against 1x phosphate buffer saline (PBS) at 4°C for 24 hours.

II.1.2. Cell culturing

Adaptation phase

Wild type and *Δlmgt* promastigotes were grown in triplicate cultures at 27°C in RPMI 1640 media (Life Technologies) supplemented with 10% iFBS (PAA Laboratories) and were adapted to RPMI 1640 media with 10% dialyzed serum (DS) (Figure II-1) for two passages and four changes of the fresh medium. Each sub-culture was initiated at cell density of 1.0 x 10^6 cells mL^{-1} by sub-passaging early-log phase cells in fresh medium.

Experimental phase

Adapted early-log phase promastigotes were sub-passaged and grown for six consequence passages in triplicate cultures at 27°C in light and heavy RPMI 1640 media (Thermo Scientific). Wild type promastigotes were grown in light medium containing L-Lysine-2HCl and 10% DS. *Δlmgt* promastigotes were grown in heavy medium containing 6-^{13}C-L-Lysine-2HCl and 10% DS. Each sub-culture was initiated at cell density of 1.0 x 10^6 cells mL^{-1} by sub-passaging mid-log phase cells in fresh medium.

II.1.3. Protein extraction

Mid-log phase light- and heavy-labelled wild type and *Δlmgt* promastigotes were harvested by centrifugation at 1,000 x *g* for 10 minutes at 4°C, washed twice with 1x cold PBS, re-suspended in SDT lysis buffer (4% (w/v) sodium dodecyl sulphate (SDS) (Sigma-Aldrich), 100 mM (w/v) Tris base (Thermo Scientific) /hydrochloric acid (HCl) (pH 7.6), 0.1 M (w/v) dithiothreitol (Melford) containing cOmplete Protease Inhibitor (PInh) Cocktail (Roche) and lysed by 3 brief cycles of sonication with Soniprep 150 (MSE).

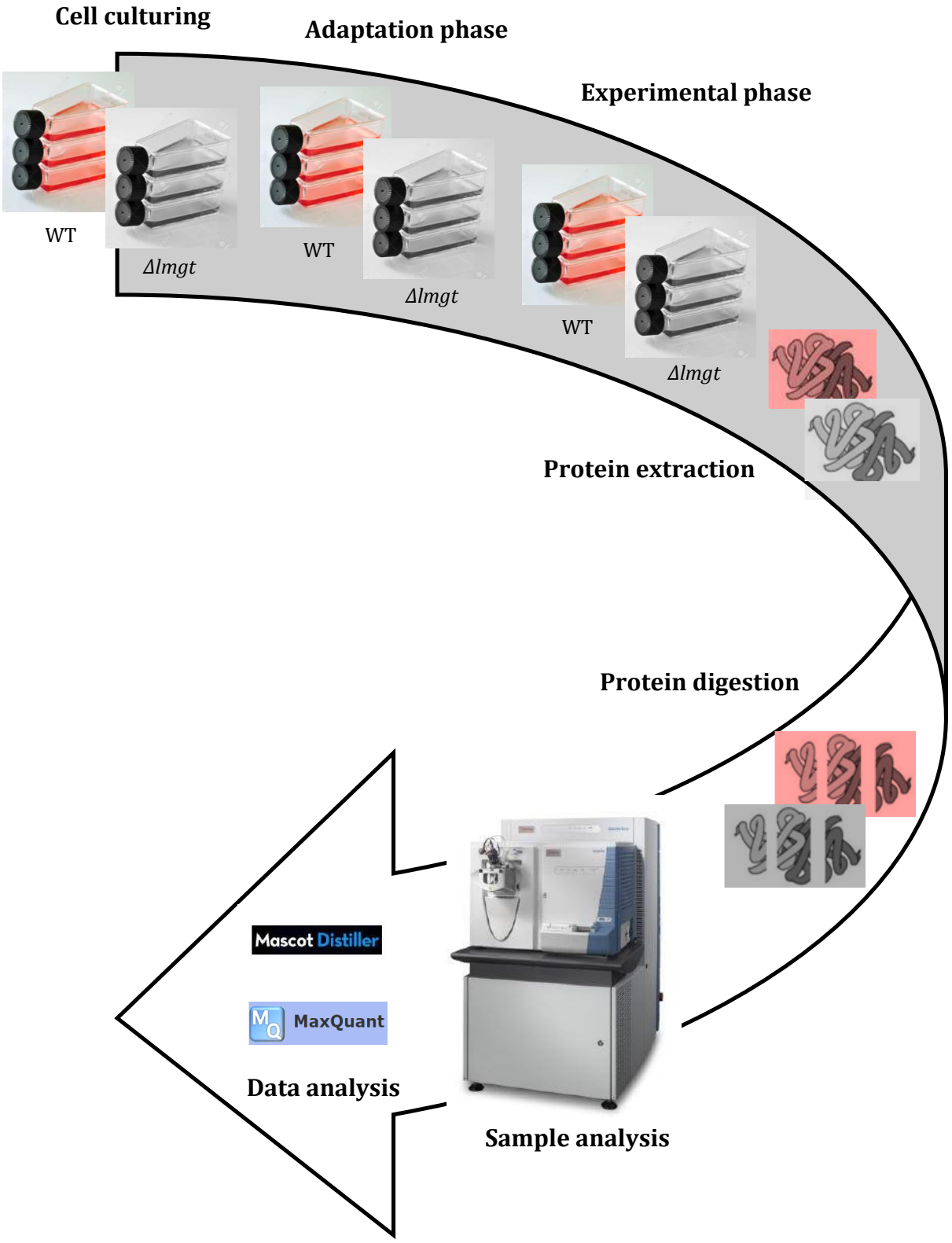

Figure II-1. Stable isotope labelling by amino acids in cell culture workflow. Cell culturing – wild type and *Δlmgt* promastigotes (biological replicates, n=3) were cultured in HOMEM with 10% iFBS. Adaptation phase - wild type and *Δlmgt* promastigotes were adapted to RPMI 1640 with 10% 3.5Da MWCO dialyzed iFBS for four passages. Experimental phase - wild type and *Δlmgt* promastigotes were grown in light and heavy SILAC media for six passages. Protein extraction – light- and heavy-labelled proteins from wild type and *Δlmgt* promastigotes, respectively, were extracted and acetone precipitated. Protein digestion – equal amounts of light- and heavy-labelled proteins were combined (1:1) and digested according to the Filter aided sample preparation (FASP) protocol (Wisniewski *et al.*, 2009). Sample analysis – peptide samples were analyzed by 1 dimensional high-performance liquid chromatography (HPLC) coupled to tandem mass spectrometry (MS/MS). Data analysis – MS data were analyzed by Mascot Distiller and MaxQuant. WT - wild type promastigotes, *Δlmgt* - *Δlmgt* promastigotes, MWCO – molecular weight cut-off.

II.1.4. Acetone precipitation

Cell lysates were mixed with cold 100% acetone (1:4), incubated overnight at -20°C, wash twice with cold 80% acetone by centrifugation at 10,000 x *g* for 10 minutes at 4°C and re-suspended in SDT buffer.

II.1.5. Estimation of protein concentration

Protein concentration of each sample was determined by protein assay (Bio-Rad) according to the manufacturer's instructions.

II.1.6. Protein digestion

50 µg of light- and heavy-labelled protein were combined and subjected to digestion with MS Grade trypsin and LysC (Promega) according to the Filter aided sample preparation (FASP) protocol (Wisniewski *et al.*, 2009). Digested samples were dried using vacuum Contentrator 5301 (Eppendorf).

II.1.7. Analysis by LC-MS/MS

Peptide samples were loaded on an Acclaim PepMap 100 C18 µ-Precolumn cartridge (5 mM x 300 µM ID, 5 µM, 100Å) (Thermo Scientific), washed for 7 minutes with 0.1% trifluoroacetic acid (TFA) (Sigma-Aldrich) and 2% acetonitrile (ACN) (Thermo Scientific) at a flow rate of 30 µL/min, then separated through an Acclaim PepMap 100 C18 Column (150 mM x 75 µM ID, 3 µM, 100Å) (Thermo Scientific). The gradient, at a flow rate of 300 ηL/min, was 4-40% 80% ACN in 0.08% formic acid (FrA) (Sigma-Aldrich) over 80 minutes, then 40-100% 80% ACN in 0.08% FrA over 40 minutes. Peptide ions were detected by Orbitrap Elite mass spectrometer (Thermo Scientific). The precursor scan (*m/z* 400-2000) was set to trigger data dependent MS/MS acquisition of the 20 most intense ions. The exclusion duration was set to 12 seconds.

II.1.8. Data analysis

II.1.8.1. Data analysis by Mascot Distiller

Raw MS/MS data were analyzed by Mascot Distiller (Version 2.5.1.0) (Matrix Sciences) using the Mascot search engine (http://www.matrixscience.com/search intro.html) against *Leishmania mexicana* FASTA database generated by TriTrypDB (Aslett *et al.*, 2010) on 30/06/2012 (8250 sequences; 5180460 residues). Carbamidomethyl (C) was set as a fixed modification while Oxidation (M) was set as a

variable modification. The peptide and fragment mass tolerances were set to ± 0.3 Da. 2 missed cleavages were allowed. Quantitation method was SILAC K+6 (MD). The reported ratio was light over heavy (L/H), with a coefficient of 1.0. Protein significance was calculated by Mascot Distiller via the following comparison equation:

$$\left|x - \mu\right| \leq t^* \frac{s}{\sqrt{N}}$$

where N is the number of peptide ratios, s is the standard deviation, x the mean of the peptide ratios (s and x calculated in log space), μ is a ratio with a true value of 0 in log space, and t is Student's t test for $N-1$ degrees of freedom and a two-sided confidence level of 95%. Significantly modulated are the proteins that are different from unit, that is 1.

II.1.8.2. Data analysis by MaxQuant

To determine the labelling efficiency of the SILAC experiment, the raw SILAC data were analyzed with MaxQuant (Cox and Mann, 2008; Cox and Mann, 2009). First, the *Leishmania mexicana* FASTA file containing 8392 canonical and isoform sequences was downloaded from UniProt (www.uniprot.org/) and configured in an appropriate for the MaxQuant programme format by the AndromedaConfig software (Cox *et al.*, 2011). Using the Andromeda search engine, MaxQuant analyzed the raw data applying the following setting: heavy-labelled – Lys6, variable modifications – Acetlyl (protein N-term) and Oxidation (M), variable modification – Carbamidomethylation (C) and a maximum of 2 missed cleavages. The proteinGroups.txt file generated by MaxQuant was used by Perseus (http://www.perseus-framework.org/) to eliminate the falsely discovered proteins and perform quantitation. The reported ratio was heavy over light (H/L).

II.1.8.3. Estimation of labelling efficiency

Generated by MaxQuant was a peptide.txt output file. The file was used by the R software to calculate the level of incorporation of heavy L-lysine into proteins by the equation: incorporation: (1 – 1/ratio H/L+1). The incorporation efficiency was estimated based on the median of the distribution obtained by plotting the incorporation of all quantified peptides. Indicated in the plot with 0 is the 0% incorporation while 100 means 100% incorporation.

II.2. Global proteomic characterization of *Δlmgt* promastigotes by stable isotope dimethyl labelling

II.2.1. Cell culturing

Wild type and *Δlmgt* promastigotes were grown at 27°C in modified hemoflagelated media, HOMEM (Berens *et al.*, 1976), supplemented with 10% iFBS (Figure II-2). Each sub-culture was initiated at cell density of 1.0 x 10^6 cells mL^{-1} by sub-passaging mid-log phase cells in fresh medium.

II.2.2. Sub-cellular fractionation

Sub-cellular fractionation was performed according to a previously described method (Foucher *et al.*, 2006). Briefly, mid-log phase wild type and *Δlmgt* promastigotes were harvested by centrifugation at 1,000 x *g* for 10 minutes at 4°C, washed twice with HEPES-sodium chloride (Thermo Scientific) and re-suspended in 1 mL of re-suspension buffer [75 mM Tris base (VWR International)/hydrochloric acid (pH 7.4), 145 mM sodium chloride (VWR International) and 11mM potassium chloride (VWR International)] containing PInh. 500 µL of the wild type and *Δlmgt* suspensions were incubated with 20 µM digitonin (Sigma-Aldrich) for 5 minutes at room temperature (RT) and mixed with 200 µL of 300 mM sucrose (Thermo Scientific). Centrifugation at 8,000 x *g* for 5 minutes at 4°C generated supernatants that represented wild type and *Δlmgt* fraction I. The remaining pellets were re-suspended in 500 µL of re-suspension buffer and treated in the same way described above but using 200 µM digitonin to generation fraction II. Fractions III and IV were generated using 1 mM and 10 mM digitonin, respectively. Fraction V was generated by re-suspending fraction IV pellets in 600 µL of re-suspension buffer.

II.2.3. Acetone precipitation

Generated fractions were precipitated as described in **II.1.4**.

II.2.4. Estimation of protein concentration

Protein concentration of each sample was determined by protein assay (Bio-Rad) according to the manufacturer's instructions.

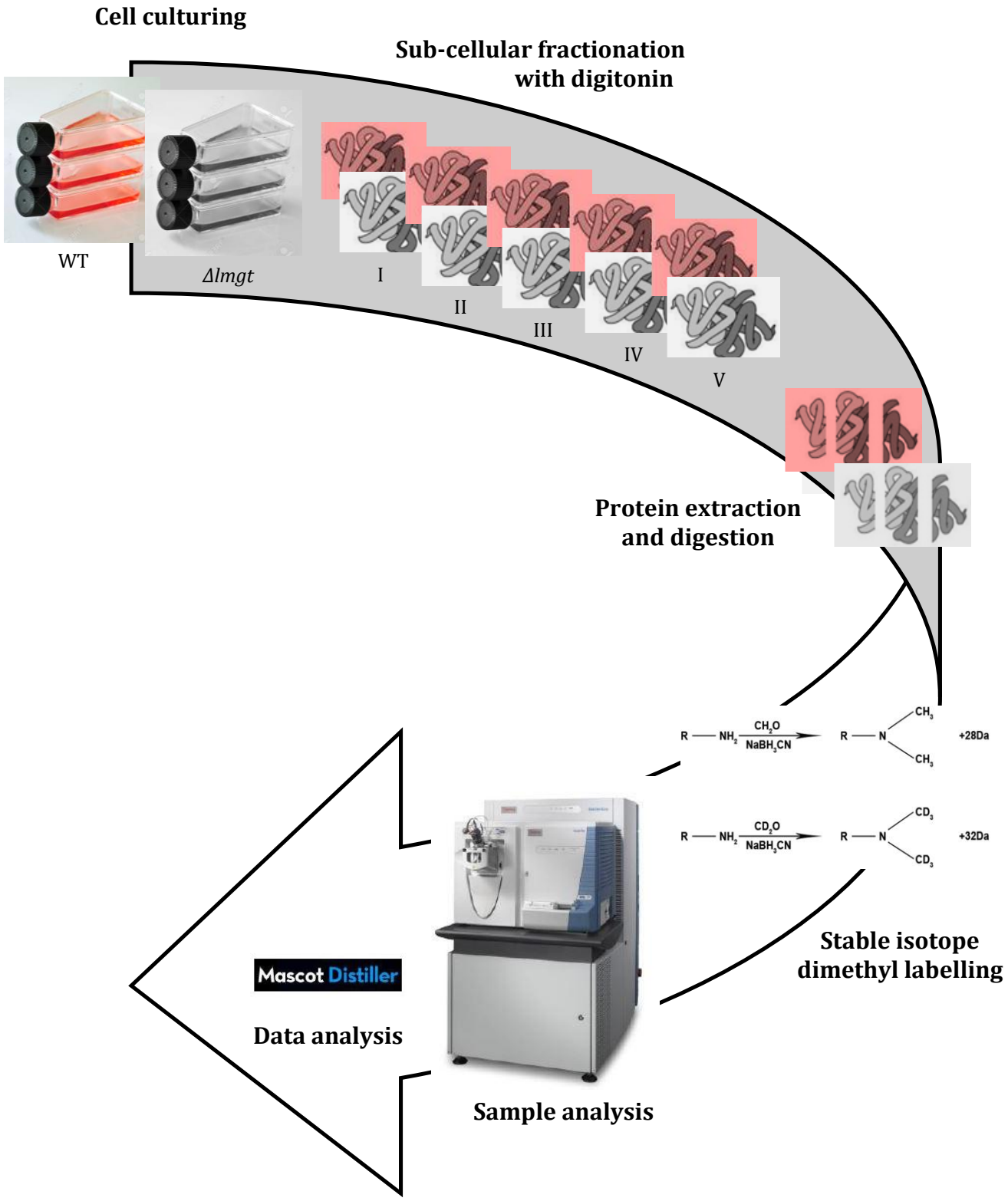

Figure II-2. Stable isotope dimethyl labelling workflow. Cell culturing – wild type and *Δlmgt* promastigotes (biological replicates, n=3) were cultured in HOMEM with 10% iFBS. Sub-cellular fractionation - 20 µM, 200 µM, 1mM, and 10 mM of digitonin were used to generate five sub-cellular fractions: two cytosolic, two organellar and one containing digitonin-insoluble material. Protein extraction - proteins from each fraction were extracted and acetone precipitated. Protein digestion – equal amounts of proteins were digested according to the Filter aided sample preparation (FASP) protocol (Wisniewski *et al.*, 2009) and stable isotope dimethyl labelled. Sample analysis – light and heavy peptide samples were combined (1:1) and analyzed by 1 dimensional high-performance liquid chromatography (HPLC) coupled to tandem mass spectrometry (MS/MS). Data analysis – MS data were analyzed by Mascot Distiller. WT - wild type promastigotes, *Δlmgt* - *Δlmgt* promastigotes, I – fraction I, II – fraction II, III- fraction III, IV – fraction IV, and V – fraction V.

II.2.5. SDS-PAGE

10 µg of protein were mixed with 1x Laemmli sample buffer (Bio-Rad) (1:1), heated to 95°C for 3 minutes in a Thermo mixer comfort (Eppendorf) and loaded on 4-20% Mini-PROTEAN TGX pre-cast gels. Gels were run in a Mini-PROTEAN Tetra Cell electrophoresis system (Bio-Rad) with 1x Tris/Glycine/SDS buffer (Bio-Rad). Electrophoresis was performed according to the manufacturer's instructions. SDS-PAGE gels were stained by incubation in fixing solution [40% (v/v) ethanol VWR International, 10% (v/v) glacial acetic acid (Sigma-Aldrich)] for 1-2 hours, followed by incubation in staining solution [10% (w/v) ammonium sulfate (VWR International), 1% (w/w) orthophosphoric acid (Thermo Scientific), 0.1% (w/v) Coomassie Brilliant Blue G-250 (Sigma-Aldrich), 25% methanol (v/v) (Sigma-Aldrich)]. Gels were destained with distilled water.

II.2.6. Protein digestion

25 µg of protein were subjected to digestion according to the FASP protocol. Digested samples were dried using vacuum Contentrator 5301 (Eppendorf).

II.2.7. Stable isotope dimethyl labelling

Peptide samples were reconstituted with 90 µL of 100 mM sodium acetate (VWR International). Wild type samples were light-labelled with 10 µL of 4% formaldehyde and 10 µL of 1 M sodium cianoborohydride for 5 minutes at RT. *Δlmgt* samples were heavy-labelled with 10 µL of 4% deuterated formaldehyde and 10 µL of 1M sodium cianoborohydride for 1 hour at RT. The labelling reaction was quenched with 10 µL of 4% ammonium hydroxide. The labelled samples were desalted according to FASP and dried in Concentrator 5301.

II.2.8. Analysis by LC-MS/MS

Labelled peptide samples were analyzed as described in **II.1.7.**

II.2.9. Data analysis

Raw MS/MS data were analyzed by Mascot Distiller (Version 2.5.1.0) (Matrix Sciences) using the Mascot search engine (http://www.matrixscience.com/search intro.html) against *Leishmania mexicana* FASTA database generated by TriTrypDB on 30/06/2012 (8250 sequences; 5180460 residues). The quantitation method was Dimethylation (MD). Carbamidomethyl (C) was set as a fixed modification. Oxidation

(M) was set as a variable modification. The peptide and fragment mass tolerances were set to ± 0.3 Da. 2 missed cleavages were allowed. The report ratio was light over heavy (L/H), with a coefficient of 1.0.

II.3. Global metabolomic characterization of *Δlmgt* promastigotes

II.3.1. Cell culturing

Wild type and *Δlmgt* promastigotes were grown in triplicate cultures at 27°C in HOMEM supplemented with 10% iFBS. Each sub-culture was initiated at cell density of 1.0 x 10^6 cells mL^{-1} by sub-passaging mid-log phase cells in fresh medium.

II.3.2. Chloroform/methanol/water extraction

Metabolite extraction was performed according to a previously described method (de Souza *et al.,* 2006). Briefly, wild type and *Δlmgt* promastigote cultures containing 3.0 x 10^8 cells in total were quickly quenched to 4°C by immersion in dry ice/ethanol bath. The cooled-down cells were harvested and washed twice with 10 mL of 1x PBS by centrifugation at 1,000 x *g* for 10 minutes at 4°C. Washed cell pellets and 10 µL of spent media were subjected to a chloroform (Thermo Scientific)/methanol/water (1:3:1, v/v/v) extraction by shaking the mixtures for 1.5 hours at 4°C.

II.3.3. Analysis by LC-MS

Metabolite extracts were separated on a ZIC-pHILIC column (SeQuant). The gradient, at a flow rate of 300 µL/min, was 80-20% 80% ACN in 0.08% FrA over 30 minutes, 5% 80% ACN in 0.08% FrA over 10 minutes, and 80% 80% ACN in 0.08% FrA over 6 minutes. The spray voltage, capillary temperature and maximum spray current were 3.5-4.5 kV, 275°C and 100, respectively. Samples were analyzed on an Orbitrap Exactive mass spectrometer (Thermo Scientific) operating in alternating positive and negative modes with a mass range of 70-1400 amu.

II.3.4. Data analysis

Raw MS data were analyzed with IDEOM using the default parameters (Creek *et al.,* 2012). Metabolite identification was based on accurate mass and predicted retention time. Retention times of 239 compounds were verified against unambiguous standard mixes.

II.4. Global metabolomic characterization of SILAC-labelled *Δlmgt* promastigotes

2.0 x 10^8 SILAC-labelled wild type and *Δlmgt* promastigotes, grown as described in **II.1.2.,** were subjected to global metabolomic analysis as described in **II.3.**

II.5. Targeted glycomic characterization of *Δlmgt* promastigotes

II.5.1. Cell culturing

Wild type and *Δlmgt* promastigotes were grown as described in **II.2.1.**.

II.5.2. Chloroform/methanol/water extraction

3.0 x 10^8 promastigotes were subjected to a chloroform/methanol/water extraction as described in **II.3.2.**

II.5.3. Derivatization

100 µL of the extracted samples were transferred into 9 mm screw cap borosilicate glass 1.5 mL tapered vials (VWR). 1 nmol of ^{13}C-D-glucose was added to each aliquoted sample. Samples were dried in a ReactiVap (Thermo Scientific), with a gentle nitrogen stream at 60°C for 30 minutes. 10 µL of 40 mg/mL (w/v) methoxyamine (Sigma-Aldrich)-HCL in pyridine (Sigma-Aldrich) was added to each dried vial, vortexed for 30 seconds and incubated at 60°C for 120 minutes. Following the methoximation step, 90 µL of N-Methyl-N-(trimethylsilyl) trifluoroacetamide (MSTFA) (Thermo Scientific) plus 1% trimethylchlorosilane (Thermo Scientific) were added, followed by a further 30 seconds of vortexing. Silylation was performed by incubation at 80°C for a further 120 minutes.

II.5.4. Analysis by GC/MS

1 µL of derivatized sample was injected into a Split/Splitless injector at 200°C using a 1 in 10 split flow using a Trace GC Ultra gas chromatograph (Thermo Scientific). Helium carrier gas at a flow rate of 1 mL/min was used for separation on a TraceGOLD TG-5MS GC column, 30 m length × 0.25 mm inner diameter × 0.25 µm film thickness (Thermo Scientific). The initial oven temperature was held at 40°C for 1 minute, followed by an initial gradient of 33°C/min ramp to 155°C. Separation of sugars was performed using a gradient of 10°C/min from 155°C to 330°C with a 1 minute final temperature hold at 330°C. Eluting peaks were transferred through an

auxiliary transfer temperature of 250°C into an ITQ 900 mass spectrometer (Thermo Scientific). The electron impact ionisation was set to 70 eV energy while the emission current was 250 µA with an ion source of 250°C. A filament delay of 6 minutes was used to prevent excess reagents from being ionised. Enhanced selectivity and sensitivity was achieved using selective reaction monitoring (SRM) determined from pure chemical standards for quantitation of metabolites. Fragment ions were isolated using a 2 *m/z* window and excited using collision-induced dissociation (CID). Selected MS2 fragment ion was detected using 6 *m/z* window.

II.5.5. Data analysis

Peak detection and quantitation of samples were processed using Xcalibur software (Thermo Scientific). Calibration curves were calculated using serial dilution of pure standard mixtures with a fixed addition of 1 nmol of ^{13}C-D-glucose. A 7-point calibration curve was then calculated for each compound and this was used to calculate the amount of detected metabolite in the extracted samples.

II.6. Stable isotope tracing analysis

II.6.1. Cell culturing

Mid-log phase wild type and *Δlmgt* promastigotes (biological replicates, n=3) were incubated for 48 hours at 27°C in RPMI 1640 media supplemented with 10% iFBS and 11 mM ^{13}C-D-glucose instead of D-glucose. The cells were then harvested and washed twice with 10 mL of 1x PBS by centrifugation at 1,000 x *g* for 10 minutes at RT.

II.6.2. Chloroform/methanol/water extraction

3.0 x 10^8 wild type and *Δlmgt* promastigotes were subjected to a chloroform/ methanol/water extraction as described in **II.3.2.**

II.6.3. Analysis by LC-MS

Samples were analyzed as described in **II.3.3.**

II.6.4. Data analysis

As previously described by Barrett and colleagues, the raw MS data were analyzed with the R-based IDEOM software using the default parameters (Creek *et al.*, 2012). Metabolite identification was based on accurate mass and predicted retention time. Retention times of 239 compounds were verified against unambiguous standard

mixes. The generated by IDEOM .mzXML files were used by the mzMatch-ISO software as described by Chokkathukalam *et al.*, 2013.

II.7. Nuclear magnetic resonance

II.7.1. Cell culturing

Wild type and *Δlmgt* promastigotes were grown as described in **II.2.1.**

II.7.2. Incubation with carbon sources

2.0 x 10^8 wild type and *Δlmgt* promastigotes were harvested and washed with 10 mL of 1x PBS by centrifugation at 1,000 x *g* for 10 minutes at RT, re-suspended in 5 mL of 1x PBS containing 4 mM non-enriched (^{12}C) and enriched (^{13}C) carbon sources in the following combinations:

- PBS
- ^{13}C-D-glucose
- ^{12}C-L-proline + ^{13}C-D-glucose
- ^{12}C-D-glucose + ^{13}C-L-proline
- ^{13}C-L-proline
- ^{12}C-L-threonine + ^{13}C-D-glucose
- ^{12}C-D-gllucose + ^{13}C-L-threonine
- ^{13}C-L-threonine
- ^{12}C-glyerol
- ^{12}C-glyerol + ^{13}C-D-glucose

The cells were incubated with the carbon sources for 6 hours at 27°C. Cell viability was checked microscopically on every hour. After 6 hours of incubation, the cell suspensions were centrifuged at 1000 x *g* for 10 minutes at 4°C to collect the spent incubation medium. An aliquot of 500 µL of each supernatant was taken for ^{1}H-NMR analysis. The suspensions were then vortexed to break the cell pellets and subjected to a metabolite extraction as described in **II.3.2.**

II.7.3. Sample and data analyses

The sample and data analyses were performed as described by Bringaud and colleagues (Millerioux *et al.*, 2012; Millerioux *et al.*, 2013). Briefly, 50 µL of maleate solution in D_2O (20 mM) were added to each sample (500 µL) as an internal standard. The samples (550 µL) were then loaded to a 125.77 MHz Bruker DPX500 spectrometer equipped with a 5-mm broadband probe head. The acquisition conditions were 90° flip angle, 5,000 Hz spectral width, 32 K memory size and 9.3 seconds total recycle time. The relaxation delay was 6 seconds for a nearly complete longitudinal relaxation. The ^{1}H-NMR spectrum measurements were taken at 25°C, with 256 scans and scan time of approximately 40 minutes. The spectra were recorded with an electronic reference to access *in vivo* concentrations (ERETIC) method. The reference was placed at 0.2 ppm to avoid superposition on sample resonances. The resonance spectra of ^{12}C-succinate at 2.35 ppm, ^{12}C-pyruvate at 2.32 ppm, ^{12}C-lactate at 1.29 ppm, ^{12}C-acetate at 1.85 ppm, ^{12}C-alanine at 1.40 ppm, ^{13}C-succinate at 2.47 and 2.22 ppm, ^{13}C-pyruvate at 2.44 and 2.18 ppm, ^{13}C-lactate at 1.39 and 1.16 ppm, ^{13}C-acetate at 2.00 and 1.73 ppm and ^{13}C-alanine at 1.53 and 1.29 ppm were integrated and the results were expressed relative to ERETIC peak integration.

CHAPTER III. Quantitative characterization of carbohydrate metabolism of *Δlmgt* promastigotes by stable isotope dimethyl labelling and global metabolomics

Leishmania are digenetic organisms involved in parasitism in insects and mammals. The insect sand fly vectors harbor the promastigote forms while the amastigote forms develop in the mammalian macrophages. The initial transformation of the amastigotes into promastigotes occurs when infected macrophages or free amastigotes are ingested by the insect during blood feeding (Kamhawi, 2006). Further in the promastigote development, the digested blood meal is followed by sugar-rich meals consisting of honeydew and plant sap (Schlein and Jacobson, 1999). The insect diet thus subjects the promastigotes to various carbon sources. Common to both types of meals, however, is the presence of sugars. The more complex sugars seem to be pre-digested by the combined action of glycosidases secreted by both the *Leishmania* cells and the sand fly vectors (Jacobson *et al.*, 2001). The resulting monosaccharides, such as D-glucose and other hexoses, are easily taken up by the *Leishmania* promastigotes (Rodriguez-Contreras *et al.*, 2007). The transport of D-glucose in *Leishmania* has been studied biochemically by a number of groups (Schaeffer *et al.*, 1974; Zilberstein and Dwyer, 1984; Burchmore and Hart, 1995). Further information about the utilization of this important nutrient by the *Leishmania* parasites was gained by the genetic characterization of several putative glucose/hexose transporter genes, namely *Pro1* of *L. enriettii* and *L. donovani*, *D2* of *L. donovani*, and *GT1, GT2, GT3* and *GT4* of *L. mexicana* (Cairns *et al.*, 1989; Langford *et al.*, 1992; Bringaud *et al.*, 1998; Burchmore and Landfear, 1998; Feng *et al.*, 2009). In addition to hexoses, *Leishmania* are also able to transport *myo*-inositol (Drew *et al.*, 1995; Klamo *et al.*, 1996), D-ribose (Pastakia and Dwyer, 1987; Maugeri *et al.*, 2003; Naula *et al.*, 2010) and sucrose (Singh and Mandal, 2011).

D-Glucose is catabolised by *Leishmania* via the Embden-Meyerhof-Parnas glycolytic pathway, TCA cycle, glycosomal succinate fermentation and the interconnected respiratory chain and oxidative phosphorylation (Saunders *et al.*, 2010). The above mentioned pathways were thoroughly investigated to identify and quantify the proteomic and metabolic changes in the carbohydrate metabolism in the promastigote parasites of *Leishmania mexicana* that were devoid of hexose transport activity and were thus not able to utilize hexoses, such as D-glucose, D-fructose, D-mannose and D-galactose, pentoses, such as D-ribose, and amino sugars, such as

glucosamine and N-acetylglucosamine, as carbon and energy sources (Burchmore *et al.*, 2003; Rodriguez-Contreras *et al.*, 2007; Naula *et al.*, 2010; Naderer *et al.*, 2010; Feng *et al.*, 2013). A metabolic comparison between the wild type and the *Δlmgt* promastigotes showed that glycolysis, gluconeogenesis, and the synthesis of hexose-containing macromolecules, including lipophosphoglycan (LPG), proteophosphoglycan (PPG), gp63 and mannogen, were among the affected by the deletion of the three glucose transporters metabolic pathways in the *Δlmgt* promastigotes (Rodriguez-Contreras and Landfear, 2006). That was corroborated by the following proteomics analysis which revealed that the glucose transporter mutation was associated with differential regulation of a number of proteins, some of which were metabolic enzymes (Feng *et al.*, 2011). All discoveries revealed to that point directed our focus at investigating the carbon metabolism of the *Δlmgt* promastigotes from proteomic and metabolomic perspective. For that purpose, we have employed a number of quantitative approaches for investigation of the changes in the *Δlmgt* proteome and metabolome. The approaches included the relatively quantitative stable isotope dimethyl labelling, which shed light on the protein and enzyme dynamic in the *Δlmgt* promastigotes, the relatively quantitative untargeted metabolomic LC-MS analysis and the absolutely quantitative glycomic GC-MS and NMR analyses, which elucidates important features of the *Δlmgt* metabolome, and the stable isotope tracing analysis, which mapped the central carbon metabolism in the *Leishmania* parasites. Integration of all omic data allowed comprehensive investigation of the *Δlmgt* promastigotes and provided in-depth information about the *Δlmgt* cell metabolism. An emphasis in this chapter is placed on the changes in the carbohydrate metabolism of the *Δlmgt* promastigotes. The energy, amino acid, nucleotide and lipid metabolism is presented in the chapter IV.

III.1. Results

III.1.1. Global quantitative proteomic characterization of carbohydrate metabolism of *Δlmgt* promastigotes

III.1.1.1. Confirmation of the glucose transporter null mutation in *Δlmgt* promastigotes

Conventional polymerase chain reaction (PCR) was used for confirmation of the glucose transporter null mutation in the genome of the *Δlmgt* promastigote cell line of *Leishmania mexicana*. For this purpose, genomic DNA obtained from wild type and *Δlmgt* promastigotes was used to amplify the three glucose transporters (GTs) *Lm*GT1, *Lm*GT2, and *Lm*GT3. The amplification results showed that PCR products of 650 base pairs (bp), 498 bp, and 491 bp corresponding to *Lm*GT1, *Lm*GT2 and *Lm*GT3, respectively, were present in the wild type promastigotes (Figure III-1, lanes 2, 3, and 4, respectively). The three glucose transporter genes were not detected in the *Δlmgt* promastigotes (Figure III-1, lanes 5, 6, and 7, respectively).

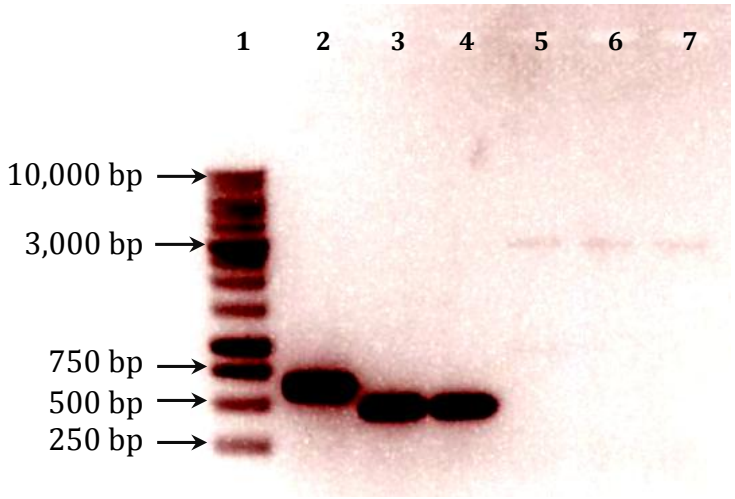

Figure III-1. Confirmation of the null mutation in the glucose transporter locus of *Δlmgt* promastigotes by PCR. DNA extracted from wild type and *Δlmgt* promastigotes was used as template for PCR amplification of GT1, GT2, and GT3. Amplification products were separated by electrophoresis on 1% TAE agarose gel and stained with SYBR Safe DNA Gel Stain. Lane 1: Molecular weight marker (250-10,000 base pairs). Lane 2: Amplification product of 650 bp corresponding to *Lm*GT1 in wild type promastigotes. Lane 3: Amplification product of 498 bp corresponding to *Lm*GT2 in wild type promastigotes. Lane 4: Amplification product of 491 bp corresponding to *Lm*GT3 in wild type promastigotes. Lane 5: Amplification product of ~3,000 bp in *Δlmgt* promastigotes. Lane 6: Amplification product of ~3,000 bp. Lane 7: Amplification product of ~3,000 bp.

III.1.1.2. Quantitative proteomic characterization of carbohydrate metabolism of *Δlmgt* promastigotes by sub-cellular fractionation with digitonin and stable isotope dimethyl labelling

To perform a comprehensive quantitative proteomic comparison between the wild type and *Δlmgt* promastigotes, we subjected the two cell lines to sub-cellular fractionation with digitonin, followed by stable isotope dimethyl labelling, analysis of the labelled samples by one dimensional (1D) high-performance liquid chromatography (HPLC) coupled to electrospray ionization and Orbitrap-based tandem mass spectrometry (ESI-MS/MS), and data analysis by Mascot Distiller (MD) (Figure II-2). The digitonin-based fractionation was not chosen as a method for enrichment of a certain cellular component but as a mean to increase the protein coverage. The prefractionation resulted in the generation of five sub-cellular fractions per cell line. Based on published work (Foucher *et al.*, 2006), the first two fractions were predicted to be enriched in plasma membrane and cytosolic proteins, the third and fourth fractions enriched in organellar proteins, and the last fraction comprised of digitonin-insoluble proteins. The five fractions were run on a 1D sodium dodecyl sulfate polyacrylamide gel electrophoresis (SDS-PAGE) to get a general overview of the protein distribution among the fractions (Figure III-2). The *Δlmgt* cytosolic fraction II and organellar fraction III showed high similarity and seemed to contain more proteins compared to the other three fractions. In general, however, all five fractions had different protein profile (Figure III-2).

The stable isotope dimethyl labelling involved light-labelling of the wild type peptide samples while the *Δlmgt* peptide samples were heavy-labelled. The corresponding samples of each fraction were combined prior to the MS analysis and the MS data were analyzed with Mascot Distiller (MD). The Mascot search showed that virtually all peptides were dimethyl-labelled (see Figure III-3 for an example). Using the automatic decoy database search of the Mascot search engine, which applies algorithms for constructing decoy sequences described by Wang and colleagues (Wang *et al.*, 2009), calculated were two protein false discovery rates (FDR) for each fraction: an identity FDR (iFDR), with a significance threshold of 0.05 ($p<0.05$), and a homology and identity FDR (i/hFDR), with a homology threshold of 5%. The idFDR and h/idFDR of each fraction are specified in Table III-1. Of the identified proteins, considered for further analysis were those with a protein score equal or above 100 and a minimum of 2 matched peptides. Of the quantified proteins, considered as significantly modulated were the proteins with a fold-change equal or above 2.

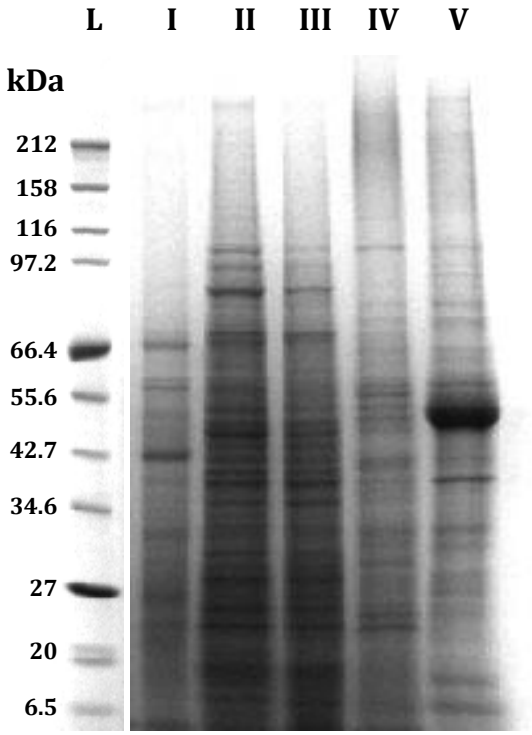

Figure III-2. SDS-PAGE of the *Δlmgt* promastigote proteome prefractionated with digitonin. *Δlmgt* promastigotes were consecutively treated with 20 μM, 200 μM, 1mM, and 10 mM of digitonin to generate five sub-cellular fractions: two cytosolic fractions - fraction I and II; two organellar fractions - fraction III and IV; and one containing digitonin-insoluble material - fraction V. The proteins of each fraction were extracted and subjected to 1D SDS-PAGE analysis with 4-20% gel and the gel was stained with Coomassie brilliant blue. Abbreviations: L – ladder, I – fraction I, II – fraction II, III- fraction III, IV – fraction IV, and V – fraction V.

1. LmxM.14.1160 Mass: 46743 Score: 2443 Matches: 118(56) Sequences: 20(15) emPAI: 3.70
| organism=Leishmania_mexicana | product=enolase | location=LmxM.14:494585-495874(+) | length=429

Query	Score	Unique	Peptide
1322	44	U	R.YCGAGCMQAVK.N [Dimethyl] + Dimethyl (K); Dimethyl (N-term)
1420	(36)	U	R.YCGAGCMQAVK.N [Dimethyl:2H(4)] + Dimethyl:2H(4) (K); Dimethyl:2H(4) (N-term)
2492	(49)	U	K.NVNEILAPALVGK.D [Dimethyl] + Dimethyl (K); Dimethyl (N-term)
2592	50	U	K.NVNEILAPALVGK.D [Dimethyl:2H(4)] + Dimethyl:2H(4) (K); Dimethyl:2H(4) (N-term)
3448	9	U	R.LPVPCFNVINGGK.H [Dimethyl] + Dimethyl (K); Dimethyl (N-term)
3547	(8)	U	R.LPVPCFNVINGGK.H [Dimethyl:2H(4)] + Dimethyl:2H(4) (K); Dimethyl:2H(4) (N-term)
4532	(17)	U	K.LGANAILGCSMAISK.A [Dimethyl] + Dimethyl (K); Dimethyl (N-term)
4533	(22)	U	K.LGANAILGCSMAISK.A [Dimethyl] + Dimethyl (K); Dimethyl (N-term)
4620	(27)	U	K.LGANAILGCSMAISK.A [Dimethyl:2H(4)] + Dimethyl:2H(4) (K); Dimethyl:2H(4) (N-term)
4641	(69)	U	K.INQIGTISESIAAAK.L [Dimethyl] + Dimethyl (K); Dimethyl (N-term)
4642	(31)	U	K.INQIGTISESIAAAK.L [Dimethyl] + Dimethyl (K); Dimethyl (N-term)
4643	(84)	U	K.INQIGTISESIAAAK.L [Dimethyl] + Dimethyl (K); Dimethyl (N-term)
4724	(36)	U	K.INQIGTISESIAAAK.L [Dimethyl:2H(4)] + Dimethyl:2H(4) (K); Dimethyl:2H(4) (N-term)
4725	118	U	K.INQIGTISESIAAAK.L [Dimethyl:2H(4)] + Dimethyl:2H(4) (K); Dimethyl:2H(4) (N-term)
4775	34	U	K.LGANAILGCSMAISK.A [Dimethyl:2H(4)] + Oxidation (M); Dimethyl:2H(4) (K); Dimethyl:2H(4) (N-term)
5481	(25)	U	R.AQIVGDDLTVTNVER.V [Dimethyl] + Dimethyl (N-term)
5482	(7)	U	R.AQIVGDDLTVTNVER.V [Dimethyl] + Dimethyl (N-term)
5484	(71)	U	R.AQIVGDDLTVTNVER.V [Dimethyl] + Dimethyl (N-term)
5528	(39)	U	R.AQIVGDDLTVTNVER.V [Dimethyl:2H(4)] + Dimethyl:2H(4) (N-term)
5529	(20)	U	R.AQIVGDDLTVTNVER.V [Dimethyl:2H(4)] + Dimethyl:2H(4) (N-term)
5530	105	U	R.AQIVGDDLTVTNVER.V [Dimethyl:2H(4)] + Dimethyl:2H(4) (N-term)
7095	34	U	R.IEEEIGSAAAYGFPGWA.- [Dimethyl:2H(4)] + Dimethyl:2H(4) (N-term)
7145	(36)	U	K.HIDEPLPILMEAIEK.A [Dimethyl] + Dimethyl (K); Dimethyl (N-term)
7146	(0)	U	K.HIDEPLPILMEAIEK.A [Dimethyl] + Dimethyl (K); Dimethyl (N-term)
7147	(45)	U	K.HIDEPLPILMEAIEK.A [Dimethyl] + Dimethyl (K); Dimethyl (N-term)
7148	(24)	U	K.HIDEPLPILMEAIEK.A [Dimethyl] + Dimethyl (K); Dimethyl (N-term)
7149	(16)	U	K.HIDEPLPILMEAIEK.A [Dimethyl] + Dimethyl (K); Dimethyl (N-term)
7150	(8)	U	K.HIDEPLPILMEAIEK.A [Dimethyl] + Dimethyl (K); Dimethyl (N-term)

Figure III-3. Partial peptide summary of enolase identified as protein hit #1 in fraction I of the *Δlmgt* promastigotes. Reported are: the accession number of enolase: LmxM.14.1160, the expected protein mass: 46743 kDa, the overall protein score: 2443, the number of MS/MS spectra matchs to the protein: 118, the number of sequences matched to the protein: 20, the query, the peptide score, the unique peptides, the peptide sequence, and the peptide modifications.

Fraction	Identified proteins	idFDR	h/idFDR	Modulated proteins	Up-regulated proteins	Down-regulated proteins
I	621	0.26 %	1.23 %	23	10	13
II	654	0.22 %	1.11 %	27	13	14
III	812	0.13 %	1.16 %	149	0	149
IV	301	0.25 %	3.12 %,	19	18	1
V	711	0.37 %	1.43 %	32	27	5

Table III-1. Number of identified and significantly modulated proteins in the *Δlmgt* promastigotes fractionated with digitonin. Wild type and *Δlmgt* promastigotes were consecutively treated with 20 μM, 200 μM, 1mM, and 10 mM of digitonin to generate five sub-cellular fractions: two cytosolic, two organellar and one containing digitonin-insoluble material. The fraction proteins were extracted, digested with trypsin, Stable isotope dimethyl labelled and analyzed by 1D HPLC-ESI-MS/MS. The data were analyzed with Mascot Distiller.

The results indicated that a similar number of proteins were identified and found significantly modulated in the two cytosolic fractions, namely 621 and 654 and 23 and 27, respectively (Table III-1). The first organellar fraction was characterized with the highest number of identified and significantly modulated proteins among the five fractions, that is 812 and 149, respectively, while the second organellar fraction had the lowest number of identified and significantly modulated proteins, 301 and 19, respectively (Table III-1). Identified in the digitonin-insoluble fraction were 711 proteins in total while significantly modulated were 32. Unique in fraction I were 6 proteins, in fraction II were 8 proteins, in fraction III were 128 proteins, in fraction IV were 16 proteins, and in fraction V were 21 proteins again (Figure III-4). In general, proteins that were found in the first three fractions were not observed in the fourth and fifth fractions. Similarly, proteins of fraction IV and V were not found in the first three fractions.

221 proteins in total, or 2.65% of the predicted *Leishmania* proteome, were found significantly modulated in the *Δlmgt* promastigotes (Table III-1). Of them, 49 proteins were up-regulated, 151 were down-regulated and 10 proteins were present in several isoforms, some of which were up-regulated while others were down-regulated (Supplemental table III-1). Evident from the protein distribution according to Light/Heavy ratio was that each fraction had a unique profile (Figure III-5).

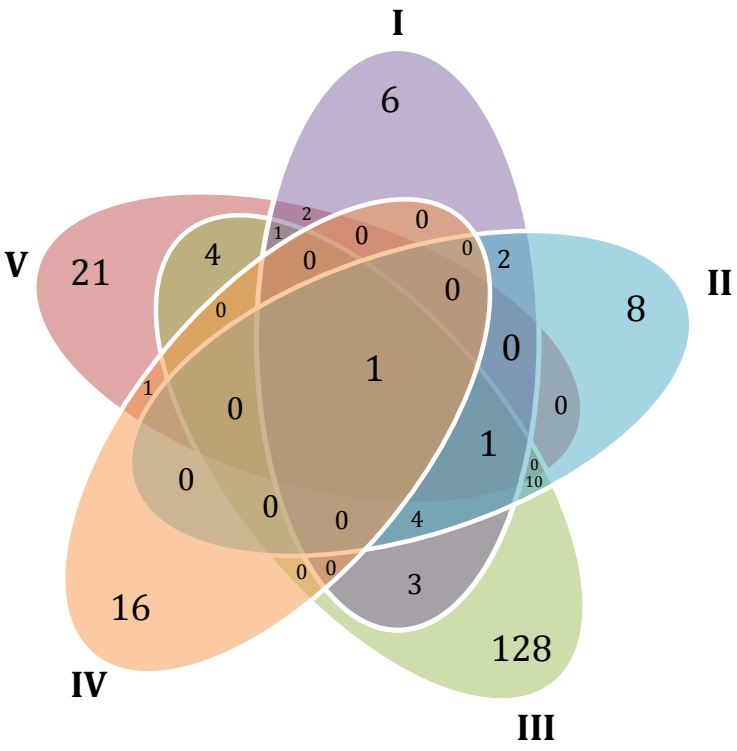

Figure III-4. Distribution of the significantly modulated proteins between the *Δlmgt* promastigote fractions. Presented are the number of unique and shared significantly modulated proteins between the *Δlmgt* promastigote fractions. I – fraction I, II – fraction II, III- fraction III, IV – fraction IV, and V – fraction V.

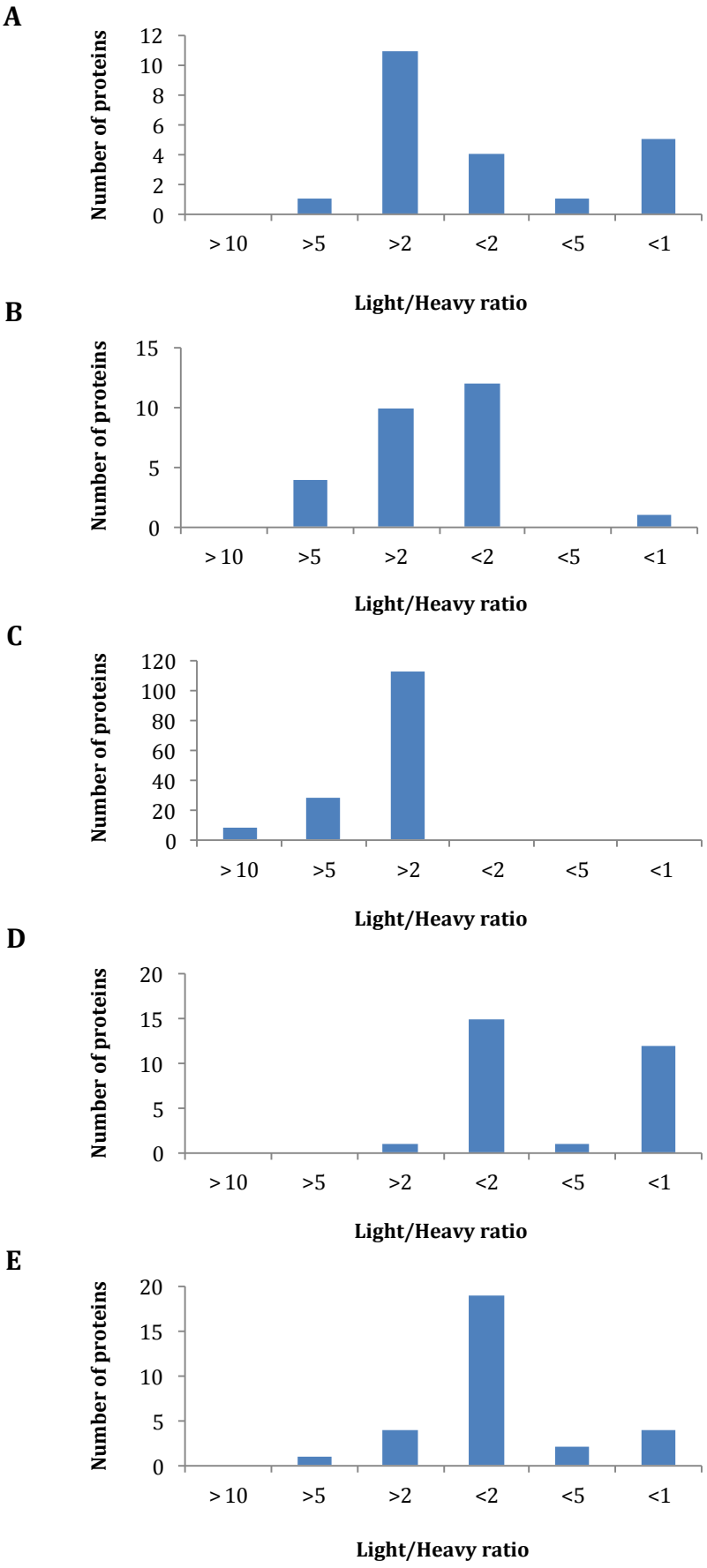

Figure III-5. Distribution of the significantly modulated proteins in the *Δlmgt* promastigote fractions according to Light/Heavy ratio. Distribution profile of fraction I (A), fraction II (B), fraction III (C), fraction IV (D) and fraction V (E). >10 - number of proteins with a Light/Heavy ratio equal or above 10; >5 - number of proteins with a Light/Heavy ratio equal or above 5; >2 - number of proteins with a Light/Heavy ratio equal or above 2; <10 - number of proteins with a Light/Heavy ratio below 10; <5 - number of proteins with a Light/Heavy ratio below -5; <2 - number of proteins with a Light/Heavy ratio below -2.

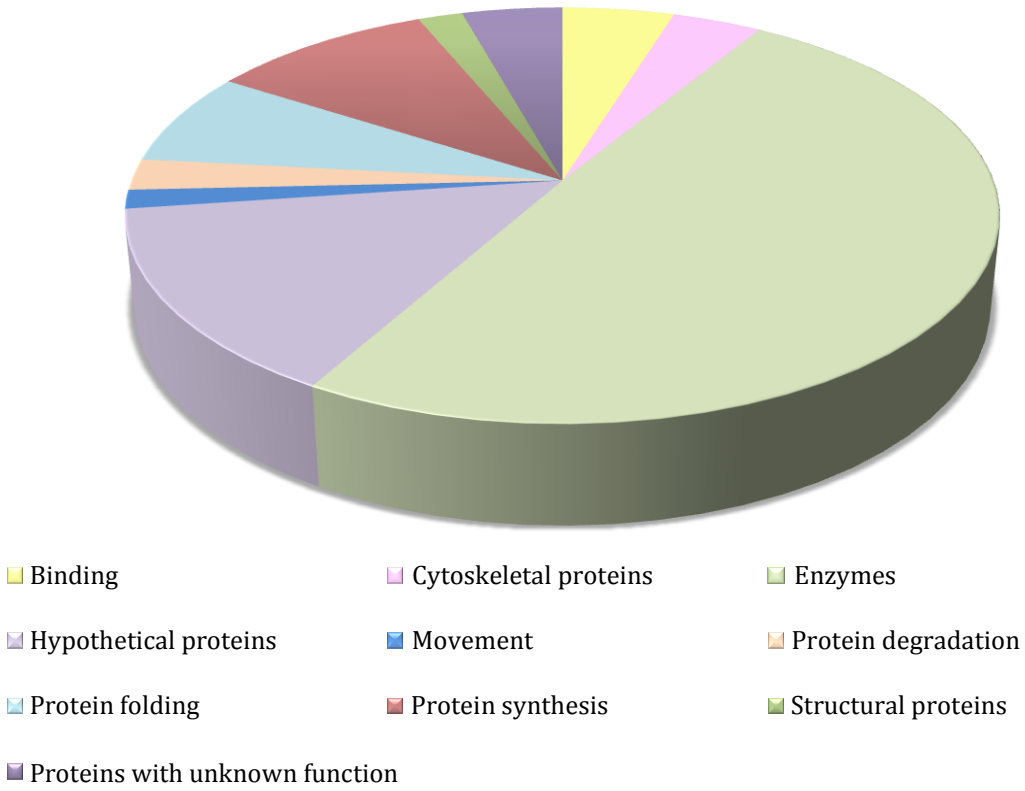

Figure III-6. Pie chart illustrating the types of significantly modulated proteins in the *Δlmgt* promastigotes. Proteins were identified and quantified with Mascot Distiller. Protein categorization is based on gene ontology (GO) terms.

Based on Gene Ontology (GO) terms, the significantly modulated proteins were grouped in 10 categories: binding proteins, cytoskeletal proteins, enzymes, hypothetical proteins, structural proteins, proteins with unknown function and proteins involved in movement, protein degradation, protein folding and protein synthesis (Figure III-6). Nearly half of the modulated proteins in the *Δlmgt* promastigotes were enzymes (Figure III-6). In turn, half of the enzymes were metabolic enzymes involved in amino acid, carbohydrate, energy, lipid and nucleotide metabolism, metabolism of vitamins and cofactors and metabolism of terpenoids and polyketides (Supplemental table III-1). Enzymes and other proteins involved in protein synthesis included ribosomal proteins of the small (40S) and large (60S) subunit, helicases, initiation factors, elongation factors and proteins participating in post-translational modifications (PTMs). The proteolytic proteins included proteasome proteins and other peptidases, such as aminopeptidases, calpaine-like cysteine peptidases and metallopeptidases. The proteins involved in protein folding included heat shock proteins of different size, T-complex proteins and chaperones.

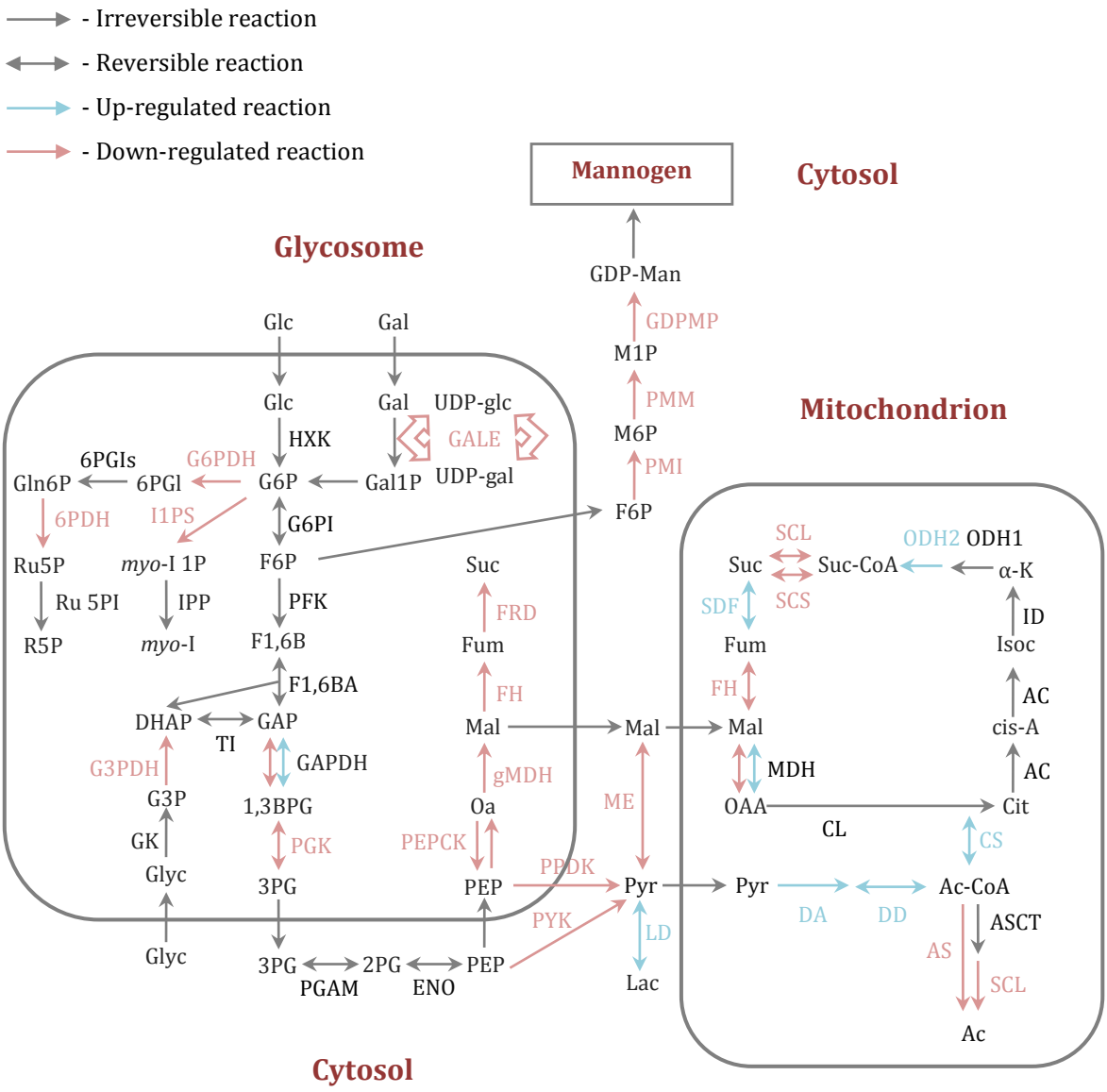

Figure III-7. Schematic representation of the proteomic changes in carbohydrate metabolism in the *Δlmgt* promastigotes. Specified with pink arrows are the down-regulated enzymes while specified with light blue arrows are the up-regulated enzymes. Abbreviations: Glc - glucose, G6P - glucose 6-phosphate, F6P - fructose 6-phosphate, F1,6B - fructose 1,6-bisphosphate, GAP - glyceraldehyde 3-phosphate, DHAP - dihydroxyacetone phosphate, G3P - glycerol 3-phosphate, Gly - glycerol, 1,3BPG - 1,3-bisphosphoglycerate, 3PG - 3-phosphoglycerate, 2PG - 2-phosphoglycerate, PEP - phosphoenolpyruvate, Pyr - pyruvate, Lac - lactate, 6PGl- 6-phosphogluconolactone, Gln6P – gluconate 6-phosphate, Ru5P – ribulose 5-phosphate, R5P – ribose 5-phosphate, *myo*-I 1P - *myo*-inositol 1-phosphate, *myo*-I - *myo*-inositol, Gal - galactose, Gal1P - galactose 1-phosphate, UDP-glc - uridine diphosphate glucose, UDP-gal - uridine diphsophate galactose, M6P - mannose 6-phosphate, M1P - mannose 1-phosphate, GDP-Man - guanosine 5'-diphosphate mannose, OAA - oxaloacetate, Cit - citrate, *cis*-A - *cis*-aconitate, Isoc - isocitrate, α-K - α-ketoglutarate, Suc-CoA - succinyl-CoA, Suc - succinate, Fum - fumarate, Mal - malate, Ac-CoA - acetyl-CoA, Ac - acetate, HXK - hexokinase, G6PI - glucose 6-phosphate isomerase, PFK - 6-phospho-1-fructokinase, F1,6BA - fructose 1,6-bisphosphate aldolase, TI – triosephosphate isomerase, GAPDH - glyceraldehyde 3-phosphate dehydrogenase, PGK - phosphoglycerate kinase, PGAM - phosphoglycerate mutase, ENO - enolase, PYK - pyruvate kinase, PPDK - pyruvate phosphate dikinase, GK - glycerol kinase, G3PDH - glycerol 3-phosphate dehydrogenase, LD - lactate dehydrogenase, DA - dihydrolipoamide acetyltransferase, DD - dihydrolipoamide dehydrogenase, PEPCK - phosphoenolpyruvate carboxikinase, GALE - uridine 5'-diphopshate glucose 4'-epimerase, PMI - phosphomannose isomerase, PMM - phosphomannomutase, GDPMP - guanosine 5'-diphosphate mannose pyrophosphorylase, G6PDH - glucose 6-phophate dehydrogenase, 6PGls - 6-phosphogluconolactonase, 6PDH - 6-phosphogluconate dehydrogenase, Ru5PI - ribulose 5-phosphate isomerase, I1PS - inositol 1-phosphate synthase, IPP - inositolphosphate phosphatase, CL - citrate lyase, CS - citrate synthase, AC - aconitase, ID - isocitrate dehydrogenase, ODH1 - 2-oxoglutarate dehydrogenase E1 component, ODH2 - 2-oxoglutarate dehydrogenase E2 component, SCL - succinyl-CoA ligase, SCS - succinyl-CoA synthetase, SDF - succinate dehydrogenase flavoprotein, FH - fumarate hydratase, FRD - fumarate reductase, MDH - malate dehydrogenase, gMDH - glycosomal malate dehydrogenase, ME - malic enzyme AS - acetyl-CoA synthetase, AL - acetyl-CoA ligase.

The binding proteins, along with many other proteins, were involved in ion, cofactor, NAD, GTP, ADP and ATP, RNA and DNA binding. The cytoskeletal proteins were mainly proteins involved in microtubule-based movement such as actin, tubulin, dynein heavy chain, kinesin and a number of flagellar proteins (Supplemental table III-1).

Enzymes of carbohydrate metabolism

Significantly modulated in the *Δlmgt* promastigotes were enzymes of glycolysis/gluconeogenesis, pentose phosphate pathway (PPP pathway), pyruvate metabolism, glycosomal succinate fermentation, tricarboxylic acid cycle (TCA cycle), fructose and mannose metabolism, and inositol phosphate metabolism (Figure III-8; Supplemental table III-1). The majority of the enzymes were detected in one fraction. A glycosomal glyceraldehyde 3-phosphate dehydrogenase and a malate dehydrogenase, however, were detected in two fractions and were down-regulated in one of the fractions but up-regulated in the other (Figure III-7; Supplemental table III-1). A malic enzyme, involved in pyruvate metabolism, a glycosomal malate dehydrogenase of the glycosomal succinate fermentation, a fumarate hydratase of the glycosomal succinate fermentation and the TCA cycle, an uridine 5'-diphosphate (UDP)-glucose 4'-epimerase of the fructose and mannose metabolism, a succinyl-CoA:3-ketoacid-CoA transferase (mitochondrial precursor), involved in synthesis and degradation of ketone bodies, and glycerol-3-phosphate dehydrogenase, linking glycerolipid metabolism with the gluconeogenesis, were significantly (>5-fold) down-regulated in the *Δlmgt* promastigotes (Supplemental table III-1).

III.1.2. Global metabolomic characterization of carbohydrate metabolism of *Δlmgt* promastigotes

III.1.2.1. Untargeted metabolomic analysis of *Δlmgt* promastigotes by LC-MS

A major objective of this work was the global and untargeted metabolomic analysis of the wild type and *Δlmgt* promastigotes. The relative quantitative comparison between the two cell lines was performed using a previously described method for metabolite extraction (biological replicates, n=3) (de Souza *et al.,* 2006), 1D polymeric hydrophilic interaction chromatography (pHILIC)-HPLC ESI-MS as an analytical platform and the R-based IDEOM software as a data analysis tool (Creek *et al.*, 2012).

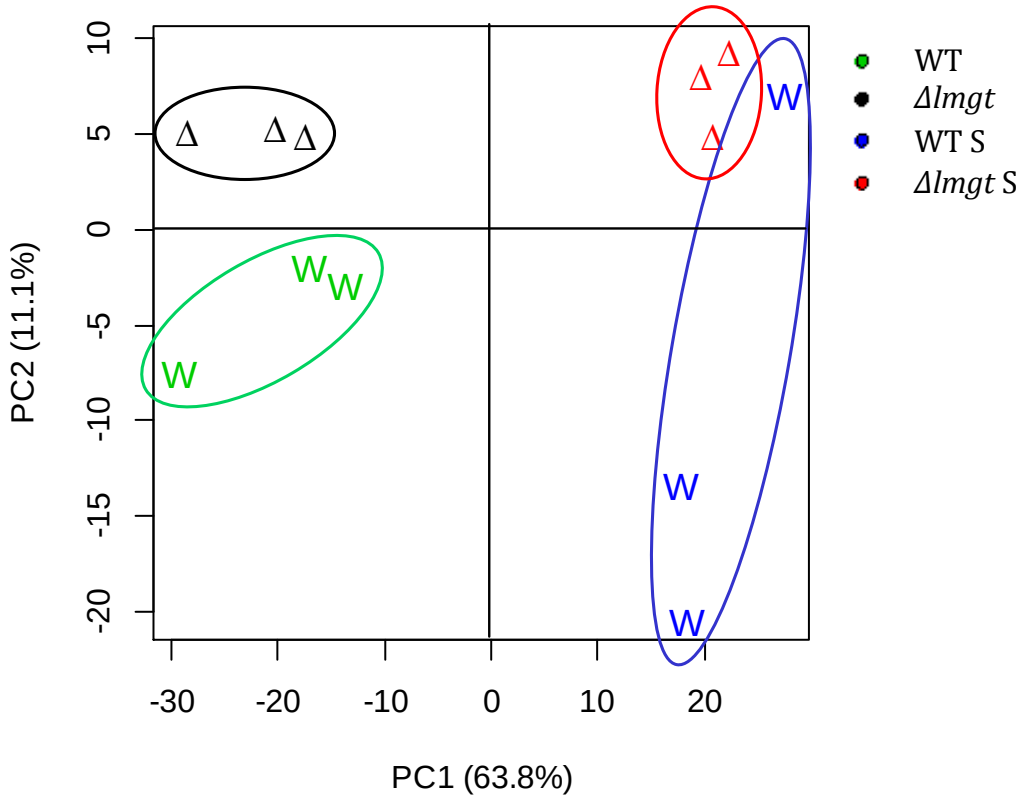

Figure III-8. Scoreplot of the Principal component analysis performed on the wild type and *Δlmgt* promastigote and spent medium metabolomic samples. Wild type and *Δlmgt* promastigotes were grown in HOMEM media supplemented with 10% serum (biological replicates, n=3) and subjected to cold chloroform/methanol/water metabolite extraction. The metabolomic samples were analyzed with 1D ZIC-pHILIC-HPLC ESI-MS and the data were analyzed with IDEOM. WT - wild type promastigotes, *Δlmgt* - *Δlmgt* promastigotes, S - spent media.

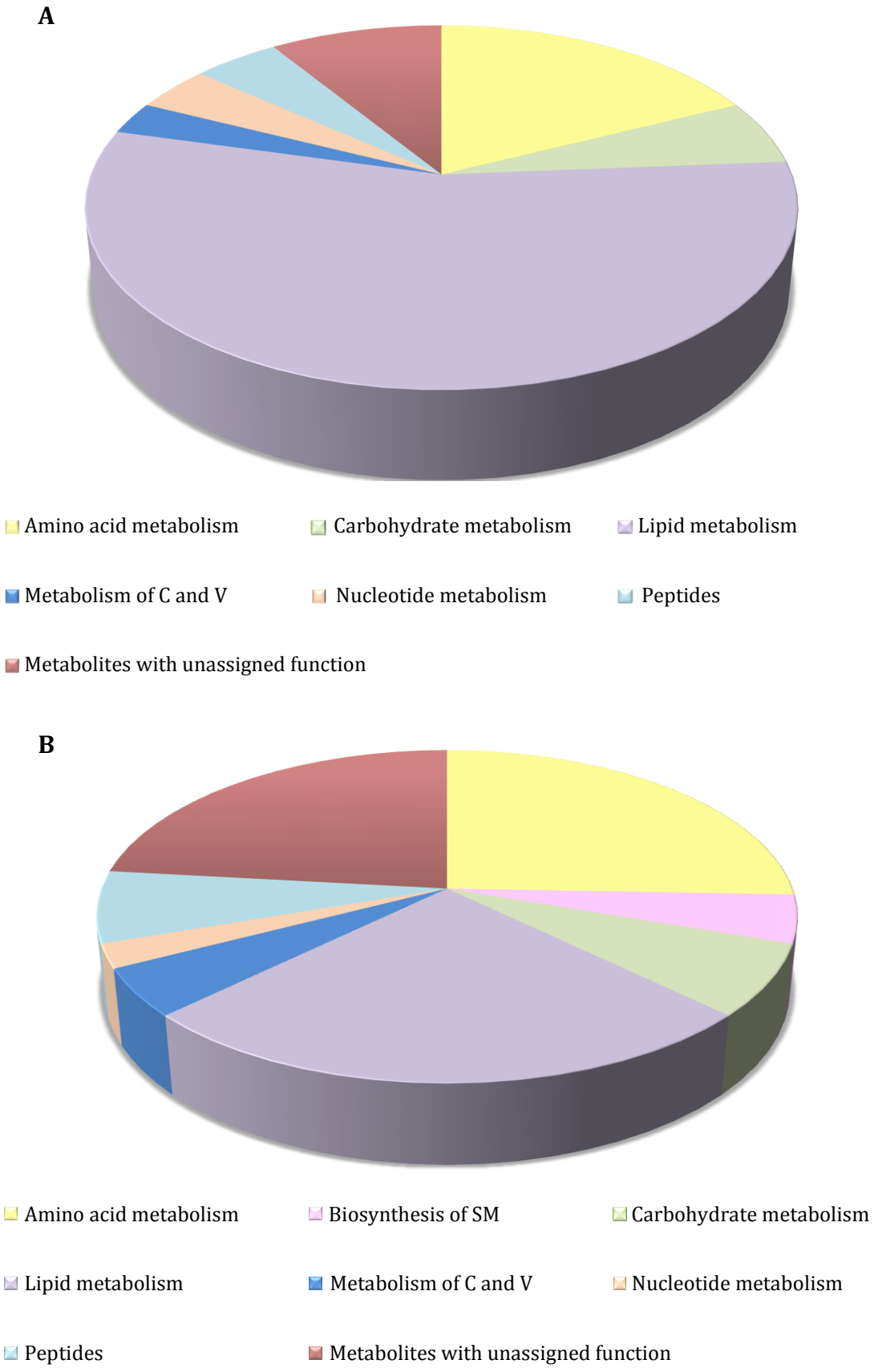

Figure III-9. Pie charts illustrating the types of significantly modulated metabolites in the *Δlmgt* promastigotes (A) and spent media (B). Abbreviations: C - cofactors, V - vitamins, SM - secondary metabolites.

Putative metabolite	Isomers	Map	Pathway	WT	*Δlmgt*
[FA trihydroxy(4:0)] 2,2,4-trihydroxy-butanoic acid	3	Lipids: Fatty Acyls	Fatty Acids and Conjugates	ND	**50.03***
Phosphodimethyl-ethanolamine	8	Lipid Metabolism	Glycerophospholipid metabolism	ND	**19.87***
Phenylpyruvate	13	Amino Acid Metabolism	Phenylalanine metabolism Phenylalanine, tyrosine and tryptophan biosynthesis	1.00	**17.32**
Glycerol	1	Carbohydrate Metabolism	Galactose metabolism Glycerolipid metabolism	1.00	**14.38**
2-Amino-3-carboxymuconate semialdehyde	1	Amino Acid Metabolism	Tryptophan metabolism	1.00	**13.55**
Nicotinate	4	Metabolism of Cofactors and Vitamins	Nicotinate and nicotinamide metabolism Alkaloid biosynthesis II	1.00	**9.21**
Ethanolamine phosphate	2	Lipid Metabolism	Glycerophospholipid metabolism Sphingolipid metabolism	1.00	**9.14**
3-(4-Hydroxyphenyl) pyruvate	11	Amino Acid Metabolism	Tyrosine metabolism Phenylalanine, tyrosine and tryptophan biosynthesis Alkaloid biosynthesis I	1.00	**7.87**
[FA hydroxy(14:0)] 3,11-dihydroxy-tetradecanoic acid	1	Lipids: Fatty Acyls	Fatty Acids and Conjugates	ND	**7.84***
Pentanoate	9	Lipids: Fatty Acyls	Fatty Acids and Conjugates	1.00	**7.41**
Butanoic acid	8	Carbohydrate Metabolism	Butanoate metabolism	1.00	**5.49**

Table III-2. Significantly increased metabolites in the *Δlmgt* promastigotes. Specified in yellow are metabolites involved in Metabolism of cofactors and vitamins, in green, metabolites involved in Lipid metabolism, in blue, metabolites involved in Amino acid metabolism, and in pink, metabolites involved in Carbohydrate metabolism. Specified in yellow are the metabolites matched to authentic standards. Metabolites with unassigned function are not included.
* - Metabolite detected in the *Δlmgt* test samples and not detected (ND) in the wild type control samples are denoted by the control group having ND as a descriptor. The value in the *Δlmgt* column is the average intensity of the compound in the *Δlmgt* samples.

Putative metabolite	Isomers	Map	Pathway	WT	*Δlmgt*
L-Glutamate	14	Amino Acid Metabolism	Arginine and proline metabolism	1.00	**0.32**
L-Aspartate	4	Amino Acid Metabolism	Alanine and aspartate metabolism	1.00	**0.31**
PA(34:1)	19	Lipids: Glycerophospholipids	Glycerophosphates	1.00	**0.30**
PC(30:1)	29	Lipids: Glycerophospholipids	Glycerophosphocholines	1.00	**0.28**
PI(34:2)	21	Lipids: Glycerophospholipids	Glycerophosphoinositols	1.00	**0.27**
PE(30:0)	30	Lipids: Glycerophospholipids	Glycerophosphoethanolamines	1.00	**0.25**
PE(32:0)	29	Lipids: Glycerophospholipids	Glycerophosphoethanolamines	1.00	**0.25**
PA(32:2)	12	Lipids: Glycerophospholipids	Glycerophosphates	1.00	**0.25**
[GP (16:0/18:0)] 1-hexadecanoyl-2-(9Z-octadecenoyl)-sn-glycero-3-phospho-(1'-myo-inositol-3'-phosphate)	5	Lipids: Glycerophospholipids	Glycerophosphoinositol monophosphates	1.00	**0.25**
[PC (14:0)] 1-tetradecanoyl-sn-glycero-3-phosphocholine	4	Lipids: Glycerophospholipids	Glycerophosphocholines	1.00	**0.24**
L-Alanine	9	Amino Acid Metabolism	Alanine and aspartate metabolism	1.00	**0.22**
PC(30:0)	32	Lipids: Glycerophospholipids	Glycerophosphocholines	1.00	**0.22**
Lactose 6-phosphate	5	Carbohydrate Metabolism	Galactose metabolism	1.00	**0.22**
PE(15:0/18:3(6Z,9Z,12Z))	14	Lipids: Glycerophospholipids	Glycerophosphoethanolamines	1.00	**0.21**
PC(30:2)	20	Lipids: Glycerophospholipids	Glycerophosphocholines	1.00	**0.19**
Glutathione	3	Amino Acid Metabolism	Glutamate metabolism Cysteine metabolism Glutathione metabolism	1.00	**0.15**
PC(28:0)	31	Lipids: Glycerophospholipids	Glycerophosphocholines	1.00	**0.14**
Succinate	7	Carbohydrate Metabolism	TCA cycle Oxidative phosphorylation	1.00	**0.11**
[SP amino,dimethyl(18:0)] 2-amino-14,16-dimethyloctadecan-3-ol	1	Lipids: Sphingolipids	Sphingoid bases	1.00	**0.07**
[SP] 1-deoxy-sphinganine	1	Lipids: Sphingolipids	Sphingoid bases	1.00	**0.05**

Table III-3. Significantly decreased metabolites in the *Δlmgt* promastigotes. Specified in green are metabolites involved in Lipid metabolism, in blue, metabolites involved in Amino acid metabolism, and in pink, metabolites involved in Carbohydrate metabolism. Specified in yellow are the metabolites matched to authentic standards. Metabolites with unassigned function are not included.

Putative metabolite	Isomers	Map	Pathway	WT	*Δlmgt*
Orotate	2	Nucleotide Metabolism	Pyrimidine metabolism	1.00	**0.48**
Nonadecanoic acid	25	Lipids: Fatty Acyls	Fatty Acids and Conjugates	1.00	**0.47**
[FA (17:0)] heptadecanoic acid	30	Lipids: Fatty Acyls	Fatty Acids and Conjugates	1.00	**0.44**
L-Proline	4	Amino Acid Metabolism	Arginine and proline metabolism	1.00	**0.37**
[FA (18:1)] 9Z-octadecenoic acid	57	Lipids: Fatty Acyls	Fatty acid biosynthesis Biosynthesis of unsaturated fatty acids	1.00	**0.34**
L-Alanine	9	Amino Acid Metabolism	Alanine and aspartate metabolism Cysteine metabolism D-Alanine metabolism	1.00	**0.30**
Succinate	7	Carbohydrate Metabolism	TCA cycle Oxidative phosphorylation Glutamate metabolism Alanine and aspartate metabolism Glycosomal succinate fermentation	1.00	**0.12**

Table III-4. Significantly decreased metabolites in the *Δlmgt* promastigote spent media. Specified in blue are metabolites involved in Amino acid metabolism, in pink, metabolits involved in Carbohydrate metabolism, in green, metabolites involved in Lipid metabolism, and in bright pink, metabolites involved in Nucleotide metabolism. Specified in yellow are the metabolites matched to authentic standards. Specified in red are the metabolites with more than one isomeric peak. Metabolites with unassigned function are not included.

Using the Principal component analysis, IDEOM calculated the variability between the wild type and *Δlmgt* cell and spent medium samples (Figure III-8). The analysis showed distinct grouping of the wild type and *Δlmgt* samples. 799 metabolites in total were identified in the untargeted analysis, of which 79 showed statistically significant differences (with $p<0.05$) and a fold-change equal or above 2 in the promastigotes and 43 in the spent media (Supplemental table III-2). 11 of the cell metabolites and 6 of the excreted metabolites were identified against authentic standards. The rest of the metabolites were putatively identified.

Three big categories of metabolites were represented in the promastigotes and these included metabolites of lipid and amino acid metabolism and metabolites with unassigned function (Figure III-9, A). Noteworthy, nearly half of the significantly modulated cell metabolites were lipids. In the spent media, amino acids, lipids and metabolites with an unassigned function again comprised the three big categories of modulated metabolites (Figure III-9, B). Compared to the wild type promastigotes and spent media, 37 of the *Δlmgt* cell metabolites and 35 of the excreted metabolites were increased while 42 and 8, respectively, were decreased (Supplemental table III-2). In the *Δlmgt* promastigotes, increased was glycerol and butanoate were highly (>10-fold) and significantly (>5-fold) increased, respectively (Table III-2). while succinate, an intermediate of the TCA cycle, was highly decreased (Tables III-2 and III-3). The putatively identified deoxyribose was decreased in the cells but increased in the spent media which showed that the pentose was excreted by the *Δlmgt* promastigotes (Supplemental table III-3). Succinate, again, was significantly decreased in the *Δlmgt* spent media (Table III-4).

III.1.2.2. Targeted glycomic analysis of *Δlmgt* promastigotes by GC-MS

A main feature of the *Δlmgt* promastigotes is the inability to take up the hexoses D-glucose, D-fructose, D-mannose and D-galactose and the pentose D-ribose (Rodriguez-Contreras *et al.*, 2007; Naula *et al.*, 2010). It was shown, however, that the *Δlmgt* cells were still able to synthesize important hexose-containing macromolecules, such as glycoconjugates and glycoproteins (Rodriguez-Contreras and Landfear, 2006). This prompted us to investigate the glycome of the *Δlmgt* promastigotes by targeted gas chromatography (GC)-MS.

Name	Mean±SD		
	HOMEM + 10 % iFBS nM	WT nM	*Δlmgt* nM
D-Glucose	261 ± 94	**0.94** ± 0.06	**12** ± 4
D-Glucose 6-phosphate	NF	**615** ± 38	**150** ± 19
D-Fructose 6-phosphate	NF	**1000** ± 500	**369** ± 154 **
D-Fructose 1,6-bisphosphate	617 ± 15 **	**647** ± 15 **	NF
Glyceraldehyde 3-phosphate	NF	NF	NF
Dihydroxyacetone phosphate	NF	**1700** ± 600	NF
2-phosphoglycerate	301 ± 172	**4300** ± 2500	**4200** ± 1900
Phosphoenolpyruvate	35 ± 0.0 *	**7700** ± 5900	**7100** ± 3500
D-Fructose	0.24 ± 0.06	**0.007** ± 0.006	**0.35** ± 0.13
D-Fructose-1-phosphate	NF	**211** ± 0.0 *	NF
D-Mannose	0.78 ± 0.05	NF	NF
D-Mannose 6-phosphate	NF	NF	NF
D-Sorbitol	1.2 ± 0.3	**5.5** ± 1.1	**66** ± 27
D-Mannitol	0.27 ± 0.14	NF	NF
L-Rhamnose	NF	NF	NF
Fucose	NF	NF	NF
D-Galactose	NF	NF	NF
Galactitol	NF	NF	NF
Raffinose	NF	NF	NF
Lactose	NF	NF	NF
Gluconate 6-phosphate	0.54 ± 0.014 **	**507** ± 155	**398** ± 0.00 *
Ribulose 5-phosphate	NF	**521** ± 174	NF
D-Ribose 5-phosphate	NF	**1500** ± 600	**521** ± 260 **
D-Ribose	0.06 ± 0.001 **	**0.087** ± 0.0 *	**0.28** ± 0.013
2-Deoxyribose	NF	NF	NF
Erythrose 4-phosphate	1000 ± 500	NF	**3400** ± 2000
Sedoheptulose 7-phosphate	NF	**276** ± 4.8	**62** ± 27 *
D-Xylose	NF	NF	NF
D-Xylulose	0.009 ± 0.001	NF	NF
Xylitol	0.026 ± 0.013	**0.45** ± 0.11	**0.35** ± 0.17
D-Arabinose	0.007 ± 0.0	**0.46** ± 0.25	**0.07** ± 0.05 **
Ribitol	0.04 ± 0.013	**0.56** ± 0.3	**1.4** ± 0.0 *
***myo*-Inositol**	4.3 ± 0.2	**133** ± 39	**350** ± 139
***myo* -Inositol-1-phosphate**	NF	**0.042** ± 0.02	**0.150** ± 0.65
Sucrose	0.027 ± 0.002	**0.03** ± 0.02	**0.093** ± 0.052
Maltose	NF	NF	NF
D-Threose	0.2 ± 0.0 *	**0.82** ± 0.35 **	**1.1** ± 0.00 *
D-Erythrose	NF	NF	NF
2-deoxy-D-glucose	NF	NF	NF

Table III-5. Glycomic comparison between wild type and *Δlmgt* promastigotes. Wild type and *Δlmgt* promastigotes were grown in HOMEM media supplemented with 10% serum (biological replicates, n=3) and subjected to cold chloroform/methanol/water metabolite extraction. The metabolomic samples were analyzed with 1D GC-MS and the data were analyzed with Xcalibur. Specified in pink are sugars and sugar phosphates involved in glycolysis/gluconeogenesis, in blue, sugars and sugar phosphates involved in fructose and mannose metabolism, in green, sugars and sugar phosphates involved in galactose metabolism, in violet, sugars and sugar phosphates involved in pentose phosphate pathway, in yellow, sugars and sugar phosphates involved in pentose and glucuronate interconversions, in orange, sugars and sugar phosphates involved in inositol phosphate metabolism, in grey, sugars involved in and in white, sugars involved in starch and sucrose metabolism, and sugars not involved in pathways. All values are in nanomoles/10^8 cells. NF - not found.

No asterisk - a mean of three values, * - a mean of two values, ** - individual value.

Name	Mean±SD		
	HOMEM + 10 % iFBS nM	WT nM	*Δlmgt* nM
D-Glucose	261 ± 94	**122** ± 22	**211** ± 17
D-Glucose 6-phosphate	NF	NF	NF
D-Fructose 6-phosphate	NF	**4** ± 0.0 *	NF
D-Fructose 1,6-biphosphate	617 ± 15 **	NF	NF
Glyceraldehyde 3-phosphate	NF	NF	NF
Dihydroxyacetone phosphate	NF	NF	NF
2-phosphoglycerate	301 ± 172	**392** ± 0.0 *	**156** ± 0.0 *
Phosphoenolpyruvate	35 ± 0.0 *	NF	NF
D-Fructose	0.24 ± 0.06	**0.22** ± 0.02	**0.19** ± 0.005
D-Fructose-1-phosphate	NF	NF	NF
D-Mannose	0.78 ± 0.05	**0.72** ± 0.02	**0.72** ± 0.02
D-Mannose 6-phosphate	NF	NF	NF
D-Sorbitol	1.2 ± 0.3	**1** ± 0.11	**0.99** ± 0.05
D-Mannitol	0.27 ± 0.14	**0.24** ± 0.0 *	**0.17** ± 0.003
L-Rhamnose	NF	NF	NF
Fucose	NF	NF	NF
D-Galactose	NF	NF	NF
Galactitol	NF	NF	NF
Raffinose	NF	NF	NF
Lactose	NF	NF	NF
Gluconate 6-phosphate	0.54 ± 0.014 **	**1.4** ± 0.4 **	NF
Ribulose 5-phosphate	NF	NF	NF
D-Ribose 5-phosphate	NF	NF	NF
D-Ribose	0.06 ± 0.001 **	**0.14** ± 0.001	**0.1** ± 0.006
2-Deoxyribose	NF	NF	NF
Erythrose 4-phosphate	1000 ± 500	**1100** ± 100	**750** ± 100
Sedoheptulose 7-phosphate	NF	NF	NF
D-Xylose	NF	NF	NF
D-Xylulose	0.009 ± 0.001	**0.046** ± 0.013	**0.033** ± 0.0 **
Xylitol	0.026 ± 0.013	**0.049** ± 0.003 **	**0.013** ± 0.006 **
D-Arabinose	0.007 ± 0.0	**0.017** ± 0.003	**0.009** ± 0.005
Ribitol	0.04 ± 0.013	**0.05** ± 0.0 **	**0.03** ± 0.001
***myo*-Inositol**	4.3 ± 0.2	**5.2** ± 0.5	**3** ± 0.1
***myo* -Inositol-1-phosphate**	NF	**185** ± 73	**108** ± 27
Sucrose	0.027 ± 0.002	**0.055** ± 0.035	**0.01** ± 0.002
Maltose	NF	NF	NF
D-Threose	0.2 ± 0.0 *	NF	NF
D-Erythrose	NF	NF	NF
2-deoxy-D-glucose	NF	NF	NF

Table III-6. Glycomic comparison between wild type and *Δlmgt* promastigote spent media. Specified in pink are sugars and sugar phosphates involved in glycolysis/gluconeogenesis, in blue, sugars and sugar phosphates involved in fructose and mannose metabolism, in green, sugars and sugar phosphates involved in galactose metabolism, in violet, sugars and sugar phosphates involved in pentose phosphate pathway, in yellow, sugars and sugar phosphates involved in pentose and glucuronate interconversions, in orange, sugars and sugar phosphates involved in inositol phosphate metabolism, in grey, sugars involved in and in white, sugars involved in starch and sucrose metabolism, and sugars not involved in pathways. All values are in nanomoles/10^8 cells. NF - not found.

No asterisk - a mean of three values, * - a mean of two values, ** - individual value.

Analyzed were the fresh media (HOMEM supplemented with 10% iFBS), the wild type and *Δlmgt* promastigotes and the wild type and *Δlmgt* promastigote spent media (biological replicates, n=3). 39 sugars were used as authentic standards: 8 participating in glycolysis/gluconeogenesis, 8 in fructose and mannose metabolism, 4 in galactose metabolism, 7 in PPP pathway, 5 in pentose and glucuronate interconversions, 2 in inositol phosphate metabolism, 2 in starch and sucrose metabolism and 3 belonging to no pathway (Tables III-5 and III-6). 18 sugars were detected in the fresh media, 22 in the wild type promastigotes, 19 in the *Δlmgt* promastigotes, 17 in the wild type spent media and 15 in the *Δlmgt* spent media.

Glycolysis/gluconeogenesis

D-Glucose was the metabolite with the lowest concentration among the detected glycolytic/gluconeogenic intermediates in both the wild type and *Δlmgt* promastigotes (Table III-5; Figure III-10). Importantly, the level of D-glucose in the *Δlmgt* promastigotes was higher compared to its level in the wild type promastigotes. Glucose 6-phosphate (G6P) and fructose 6-phosphate (F6P), however, had considerably lower concentrations. Glyceraldehyde 3-phosphate (GAP), fructose 1,6-bisphosphate (F1,6P) and dihydroxyacetone phosphate (DHAP) were not detected in the *Δlmgt* promastigotes or spent mdia (Tables III-5 and III-6). 2-Phosphoglycerate (2PG) and phosphoenolpyruvate (PEP) had high concentrations similar to those in the wild type promastigotes (Figure III-10).

Pentose phosphate pathway

A considerable amount of G6P appears to be directed toward the PPP pathway judging by the concentrations of gluconate 6-phosphate (Gln6P) in the wild type and *Δlmgt* promastigotes (Table III-5; Figure III-10). Gln6P, ribose 5-phosphate (R5P) and sedoheptulose 7-phosphate (S7P) were decreased while D-ribose was increased in the *Δlmgt* promastigotes (Table III-5). Contrary to the wild type promastigotes, erythrose 4-phosphate (E4P) was detected at relatively high concentration in the *Δlmgt* promastigotes (Figure III-10).

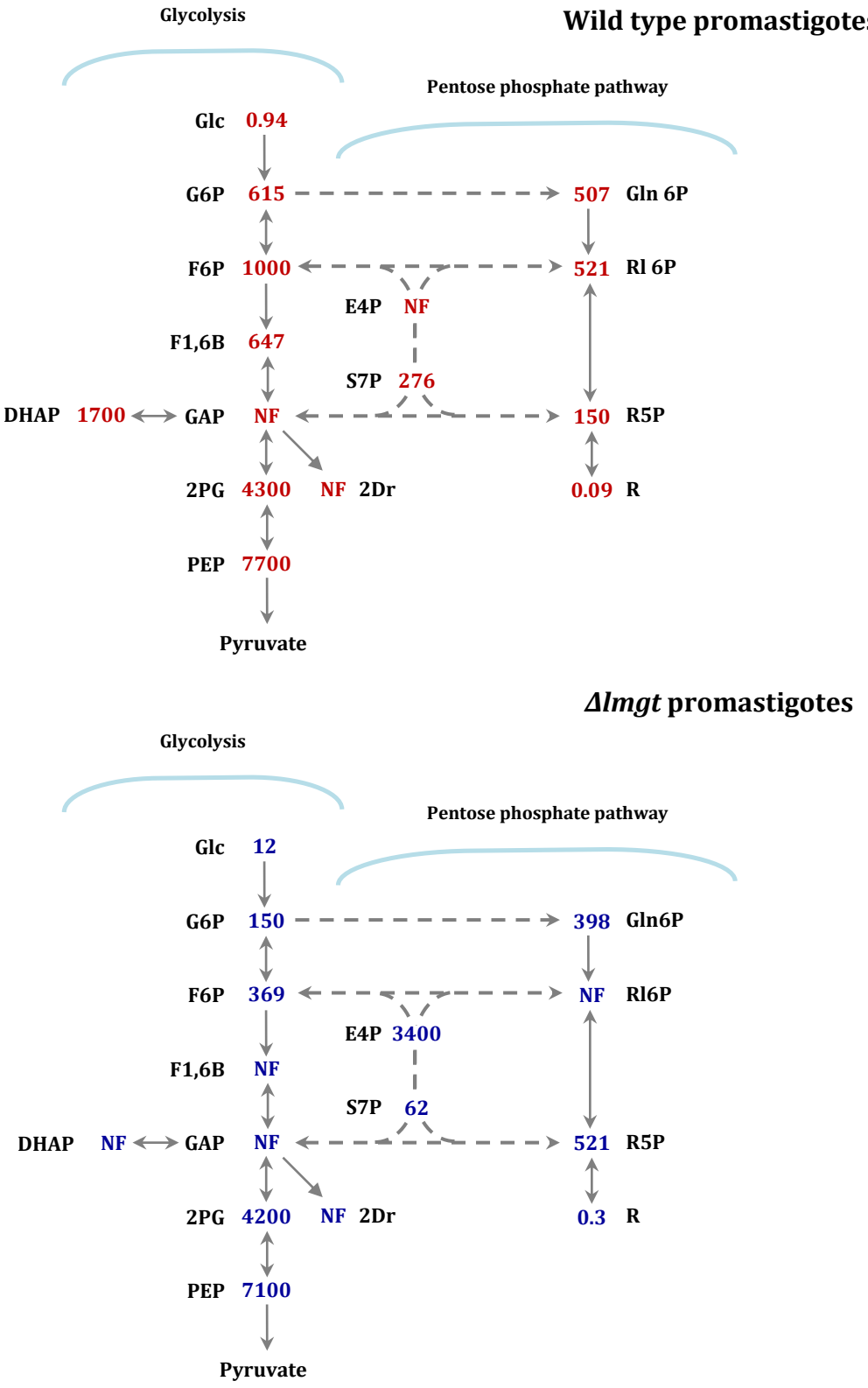

Figure III-10. Quantitative glycomic map of glycolysis/gluconeogenesis and pentose phosphate pathway in the wild type (top) and *Δlmgt* (bottom) promastigotes. Specified in red/blue is the average value of the respective metabolite in nanomoles/10^8 cells. Dashed lines indicate an indirect connection. Abbreviations: Glc - glucose, G6P - glucose 6-phosphate, F6P - fructose 6-phosphate, F1,6B - fructose 1,6-bisphophate, GAP - glyceraldehyde 3-phosphate, DHAP - dihydroxyacetone phosphate, 2PG - 2-phosphoglycerate, PEP - phosphoenolpyruvate, Gln6P - gluconate 6-phosphate, Rl5P - ribulose 5-phosphate, R5P - ribose 5-phosphate R - ribose, E4P - erythrose 4-phosphate, S7P - sedoheptulose 7-phosphate, 2Dr - 2-deoxyribose, NF - not found.
Adapted from KEGG.

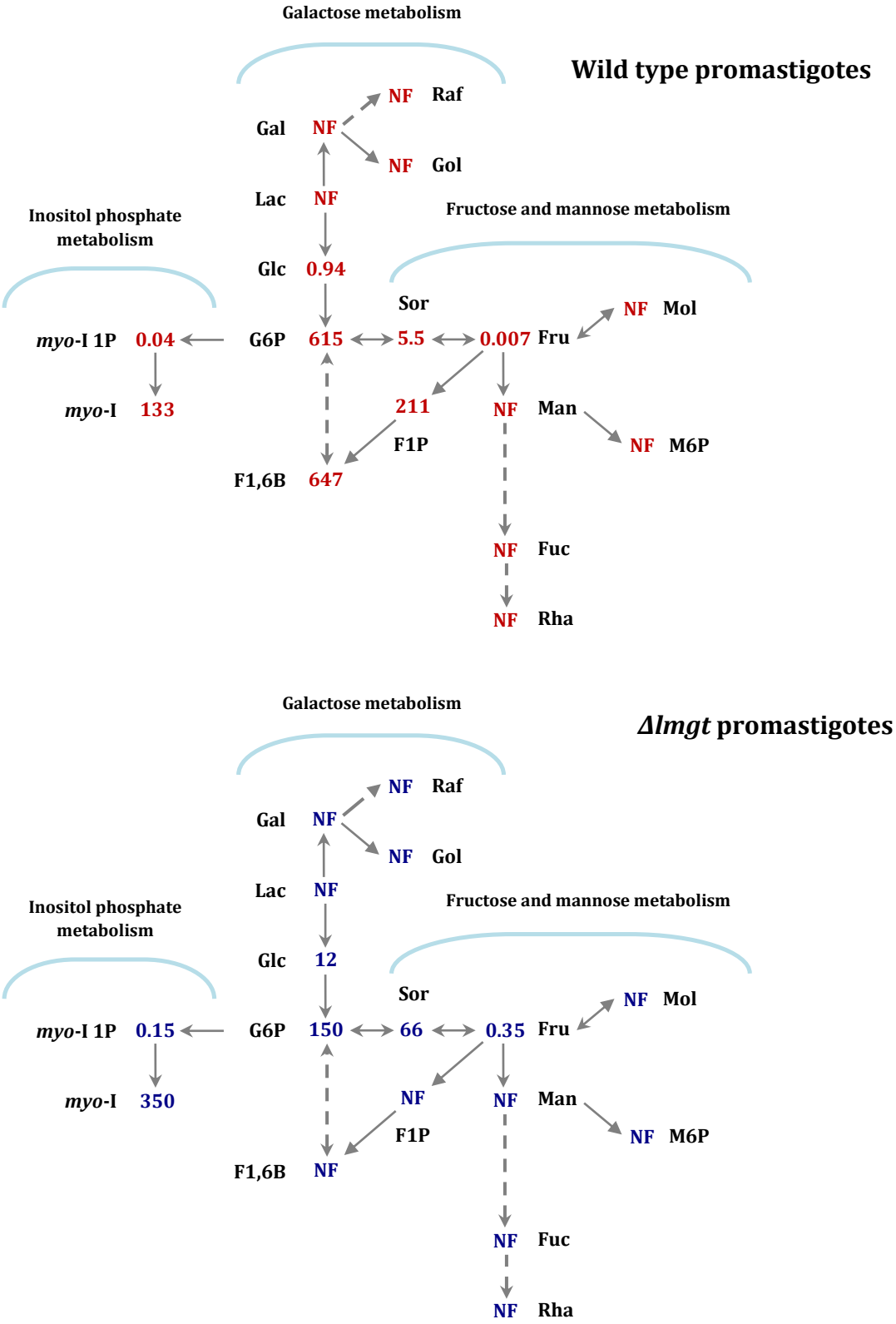

Figure III-11. Quantitative glycomic map of inositol phosphate metabolism, galactose metabolism and fructose and mannose metabolism in the wild type (top) and *Δlmgt* (bottom) promastigotes. Specified in red/blue is the average value of the respective metabolite in nanomoles/10^8 cells. Dashed lines indicate an indirect connection. Abbreviations: Glc - glucose, G6P - glucose 6-phosphate, F1,6B - fructose 1,6-bisphophate, Fru - fructose, F1P - fructose 1-phosphate, Man - mannose, M6P - mannose 6-phosphate, Sor - sorbitol, Mol - mannitol, Rha - rhamnose, Fuc - fucose, Gal - galactose, Gol - galactitol, Lac - lactose, Raf - raffinose, *myo*-I - *myo*-inositol, *myo*-I 1P - *myo*-inositol 1-phosphate, NF - not found.
Adapted from KEGG.

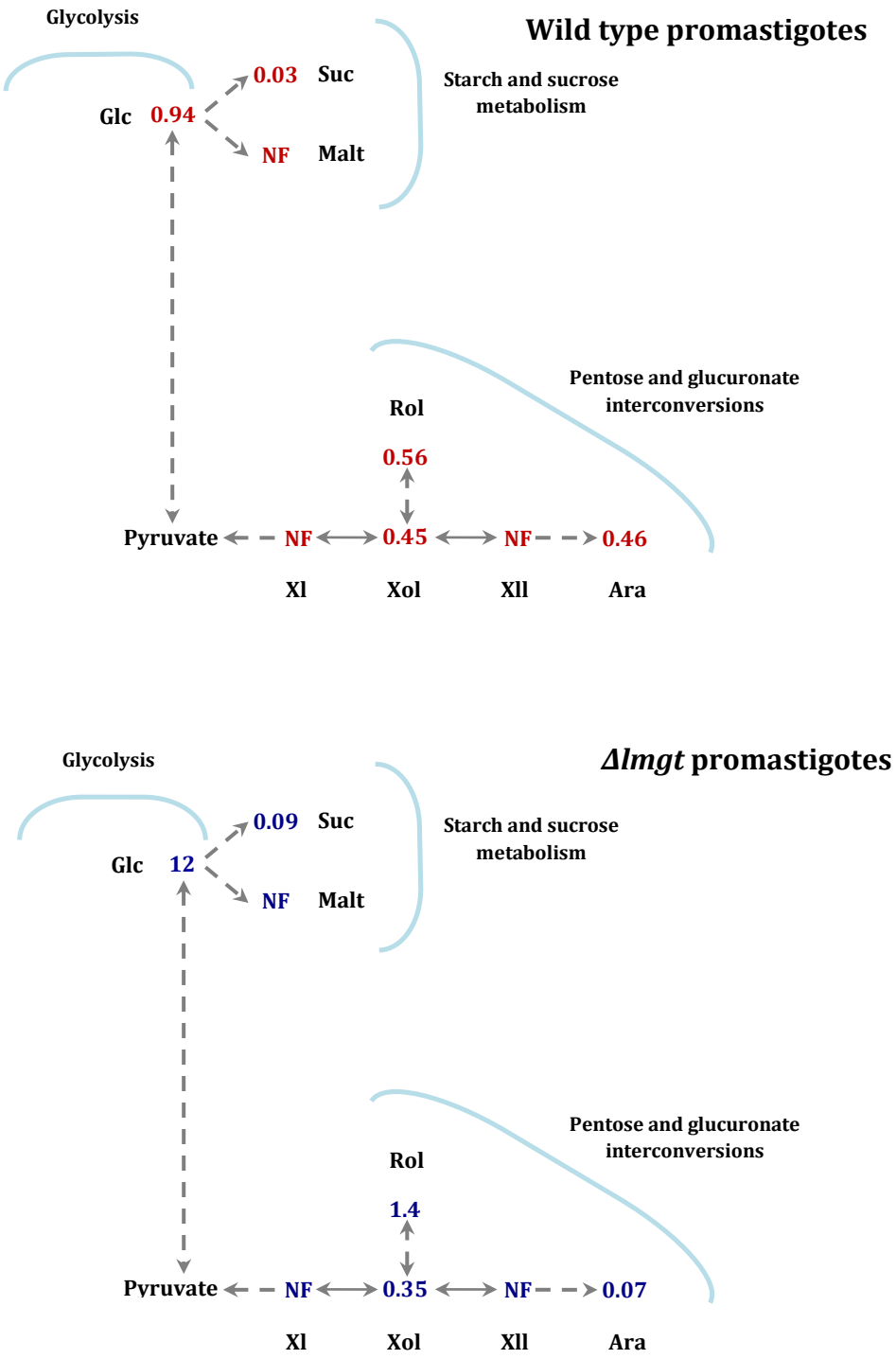

Figure III-12. Quantitative glycomic map of starch and sucrose metabolism and pentose and glucuronate interconversions in the wild type (top) and *Δlmgt* (bottom) promastigotes. Specified in red/blue is the average value of the respective metabolite in nanomoles/10^8 cells. Dashed lines indicate an indirect connection. Abbreviations: Glc - glucose, Xl - xylose, Xll - xylulose, Xol - xylitol, Ara - arabinose, Rol - ribitol, Sucr - sucrose, Malt - maltose, NF - not found.
Adapted from KEGG.

Inositol phosphate metabolism, galactose metabolism and fructose and mannose metabolism

Small amounts of *myo*-inosito (*myo*-I) and *myo*-inositol 1-phosphate (*myo*-I 1P) were found in the wild type promastigotes (Figure III-11). In the *Δlmgt* cells, the two compounds were present at slightly higher concentrations (Figure III-11). Similar to D-glucose, the level of D-fructose (Fru) was higher in the *Δlmgt* promastigotes. F1,6BP and fructose 1-phosphate (F1P) were not present in the *Δlmgt* promastigotes. D-Mannose (Man) was not detected. Also, none of the sugars of galactose metabolism were detected in the wild type and *Δlmgt* promastigotes.

Starch and sucrose metabolism and pentose and glucuronate interconversions

Sucrose (Sucr) was present at a higher level in the *Δlmgt* promastigotes (Figure III-12). Xylose (Xl) and xylulose (Xll), from the pentose and glucuronate interconversions, were not detected but xylitol (Xol), arabinose (Ara) and ribitol (Rol) were found at more or less similar levels in the wild type and *Δlmgt* promastigotes.

III.1.2.3. Metabolomic analysis of *Δlmgt* promastigotes by NMR and LC-MS

As part of our metabolic characterization of the *Δlmgt* promastigotes, we performed 1D proton (^{1}H) nuclear magnetic resonance (NMR) to investigate the carbon utilisation by the wild type and *Δlmgt* promastigotes. As a complementary analysis, the two types of promastigotes were further subjected to 1D pHILIC HPLC-ESI-MS and stable isotope tracing with mzMatch-ISO (Chokkathukalam *et al.*, 2013). For the NMR analysis, the two cell lines (biological replicates, n=3) were incubated for 6 hours in PBS with 4 mM non-enriched (**^{12}C**) and enriched (**^{13}C**) carbon sources in the follow combinations:

- PBS [Condition 1 (**C1**)]
- ^{13}C-D-glucose [condition 2 (**C2**; ***glc**)]
- ^{12}C-L-proline + ^{13}C-D-glucose [condition 3 (**C3**; **pro+*glc**)]
- ^{12}C-D-glucose + ^{13}C-L-proline [condition 4 (**C4**; **glc+*pro**)]

- ^{13}C-L-proline [condition 5 (**C5**; ***pro**)]
- ^{12}C-L-threonine + ^{13}C-D-glucose [condition 6 (**C6**; **thr+*glc**)]
- ^{12}C-D-glucose + ^{13}C-L-threonine [condition 7 (**C7**; **glc+*thr**)]
- ^{13}C-L-threonine [condition 8 (**C8**; ***thr**)]
- ^{12}C-glycerol [condition 9 (**C9**; **glr**)]
- ^{12}C-glycerol + ^{13}C-D-glucose [condition 10 (**C10**; **glr+*glc**)].

III.1.2.3.1. Metabolomic analysis of *Δlmgt* promastigotes by NMR

Condition 1, **C1**, revealed that the short incubation without external carbon sources resulted in the excretion of ^{12}C-acetate and ^{12}C-succinate by the wild type and *Δlmgt* promastigotes, originating most probably from the intracellular reserve material mannogen (Ralton *et al.*, 2003) (Table III-7; Supplemental figure III-1). The *Δlmgt* promastigotes excreted less ^{12}C-acetate and only a small amount of ^{12}C-succinate (Table III-8; Supplemental figure III-1). When D-glucose was supplied as a sole carbon source in condition 2, ***glc**, the wild type promastigotes excreted less ^{12}C-acetate and ^{12}C-succinate and more ^{13}C-acetate and ^{13}C-succinate (Table III-7; Figure III-13; Supplemental figure III-2). The *Δlmgt* promastigotes excreted similar amounts of ^{12}C-acetate and ^{12}C-succinate as the ones observed in condition 1. The addition of L-proline towards D-glucose in conditions 3 and 4, **pro+*glc** and **glc+*pro**, resulted in the excretion of less ^{13}C-acetate and ^{13}C-succinate from D-glucose but more from L-proline by the wild type promastigotes (Table III-8; Figure III-13; Supplemental figures III-3 and III-4). Under condition **glc+*pro** the wild type promastigotes excreted also ^{13}C-pyruvate (Table III-7; Figure III-13). The *Δlmgt* promastigotes excreted similar amounts of ^{12}C-acetate and ^{12}C-succinate as those observed in conditions **C1** and ***glc** again. Contrary to the previous two conditions where L-proline and D-glucose were provided together, the results from condition 5, ***pro**, showed that L-proline alone is a less energogenic substrate for the wild type promastigotes (Table III-7; Supplemental figure III-5).

* - ^{13}C-labelled compound

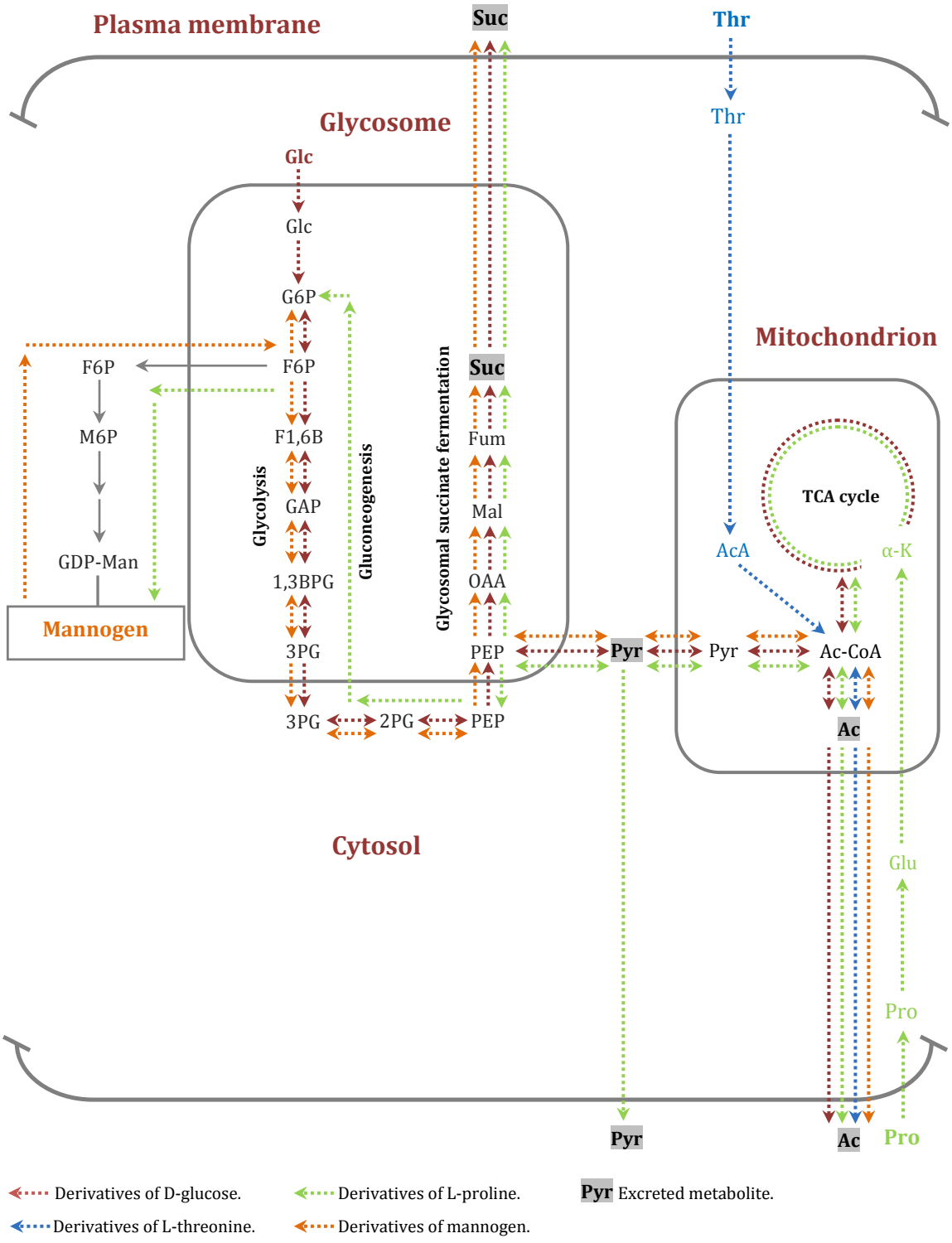

Figure III-13. Schematic representation of carbon source utilization by *Leishmania mexicana* promastigotes. Abbreviations: Glc - glucose, G6P - glucose 6-phosphate, F6P - fructose 6-phosphate, F1,6B - fructose 1,6-bisphosphate, GAP - glyceraldehyde 3-phosphate, 1,3BPG - 1,3-bisphosphoglycerate, 3PG - 3-phosphoglycerate, 2PG - 2-phosphoglycerate, PEP - phosphoenolpyruvate, Pyr - pyruvate, OAA - oxaloacetate, α-K - α-ketoglutarate, Suc-CoA - succinyl-CoA, L-Thr - L-threonine, AcA - acetoaldehyde, Mal - malate, Fum - fumarate, Suc - succinate, Aa-CoA - acetoacetyl-CoA, Ac-CoA - acetyl-CoA, Ac - acetate.

	^{13}C-Succinate	^{12}C-Succinate	^{13}C-Pyruvate	^{13}C-Acetate	^{12}C-Acetate	Total (^{13}C)	Total (^{12}C)
	Mean±SD	**Mean±SD**	**Mean±SD**	**Mean±SD**	**Mean±SD**	**Mean±SD**	**Mean±SD**
C1	-	7.3±2.4	-	-	49.7±5.2	-	57.0±6.5
C2	13.8±2.1	4.8±1.8	-	206.1±26.5	45.2±4.4	219.9±28.2	50.0±5.0
C3	8.1±0.6	<5	-	209.0±49.0	<45	217.1±49.2	<50
C4	21.6±0.5	<5	5.1±3.3	244.3±53.1	<45	271.0±56.0	<50
C5	-	<5	-	-	<45	-	<50
C6	-	-	-	121.5±7.7	47.2±7.5	121.5±7.7	47.2±7.5
C7	-	8.3±4.5	-	13.5±4.5	126.1±30.2* 47.2±7.5	13.5±4.5	126.1±30.2* 47.2±7.5
C8	-	-	-	13.6±5.8	29.6±4.0	13.6±5.8	29.6±4.0
C9	-	-	-	-	24.7±8.7	-	24.7±8.7
C10	-	-	-	126.9±5.9	41.5±1.2	126.9±5.9	41.5±1.2

Table III-7. Non-enriched (^{12}C) and enriched (^{13}C) metabolic end products excreted by the *Leishmania mexicana* wild type promastigotes. Wild type promastigotes (biological replicates, n=3) were incubated for 6 hours in PBS with 4 mM of the following non-enriched and enriched carbon sources: no carbon sources - condition 1 (**C1**), ^{13}C-D-glucose - condition 2 (**C2**), ^{12}C-L-proline and ^{13}C-D-glucose – condition 3 (**C3**), ^{12}C-D-glucose and ^{13}C-L-proline – condition 4 (**C4**), ^{13}C-L-proline – condition 5 (**C5**), ^{12}C-L-threonine and ^{13}C-D-glucose – condition 6 (**C6**), ^{12}C-D-glucose and ^{13}C-L-threonine – condition 7 (**C7**), ^{13}C-L-threonine – condition 8 (**C8**), ^{12}C-glycerol – condition 9 (**C9**), and ^{12}C-glycerol and ^{13}C-D-glucose – condition 10 (**C10**), and analyzed by ^{1}H-NMR. All values are in nmoles/hour/10^8 cells.

* - originating from D-glucose

	^{13}C-Succinate	^{12}C-Succinate	^{13}C-Pyruvate	^{13}C-Acetate	^{12}C-Acetate	Total (^{13}C)	Total (^{12}C)
	Mean±SD	**Mean±SD**	**Mean±SD**	**Mean±SD**	**Mean±SD**	**Mean±SD**	**Mean±SD**
C1	-	<3	-	-	15.5±3.0	-	<18
C2	-	<3	-	-	13.5±6.2	-	<18
C3	-	<3	-	-	<15	-	<18
C4	-	<3	-	-	<15	-	<18
C5	-	<3	-	-	<15	-	<18
C6	-	-	-	-	45.8±20.5** 15.1	-	45.8±20.5** 15.1
C7	-	-	-	32.4±1.0	51.1±4.0	32.4±1.0	51.1±4.0
C8	-	-	-	30.8±9.6	17.5±3.8	30.8±9.6	17.5±3.8
C9	-	-	-	-	12.7±0.7	-	12.7±0.7
C10	-	-	-	-	15.6±0.5	-	15.6±0.5

Table III-8. Non-enriched (^{12}C) and enriched (^{13}C) metabolic end products excreted by the *Δlmgt* promastigotes. *Δlmgt* promastigotes (biological replicates, n=3) were incubated for 6 hours in PBS with 4 mM of the following non-enriched and enriched carbon sources: no carbon sources - condition 1 (**C1**), ^{13}C-D-glucose - condition 2 (**C2**), ^{12}C-L-proline and ^{13}C-D-glucose – condition 3 (**C3**), ^{12}C-D-glucose and ^{13}C-L-proline – condition 4 (**C4**), ^{13}C-L-proline – condition 5 (**C5**), ^{12}C-L-threonine and ^{13}C-D-glucose – condition 6 (**C6**), ^{12}C-D-glucose and ^{13}C-L-threonine – condition 7 (**C7**), ^{13}C-L-threonine – condition 8 (**C8**), ^{12}C-glycerol – condition 9 (**C9**), and ^{12}C-glycerol and ^{13}C-D-glucose – condition 10 (**C10**), and analyzed by ^{1}H-NMR. All values are in nmoles/hour/10^8 cells.

** - originating from L-threonine

When labelled D-glucose was provided in combination with unlabelled L-threonine in condition 6, **thr+*glc**, the wild type promastigotes excreted the same amount of ^{12}C-acetate from mannogen as in the previous conditions but twice as less ^{13}C-acetate from D-glucose (Table III-7; Supplemental figure III-6). The *Δlmgt* promastigotes, on the other hand, excreted two types of ^{12}C-acetate: one originating from mannogen, the amount of which was the same as in the previous conditions, and one produced from L-threonine, which was 3 times more (Table III-8; Figure III-13; Supplemental figure III-6). Switching the labelling of D-glucose and L-proline in condition 7, **glc+*thr**, revealed that the wild type promastigotes produced the same amounts of ^{12}C-acetate and ^{12}C-succinate from mannogen, approximately 3 times more ^{12}C-acetate from ^{12}C-D-glucose and a small amout of ^{13}C-acetate from ^{13}C-L-threonine (Table III-7; Supplemental figure III-7). That showed that the wild type promastigotes preferentially utilized D-glucose when L-threonine was the alternative carbon source. When the heavy-labelled variant of the amino acid was provided as a sole carbon source in condition 8, ***thr**, the wild type promastigotes excreted the same small amount of heavy-labelled acetate as that observed in the previous condition but approximately twice as less acetate originating from mannogen compared to all previous conditions (Table III-7; Supplemental figure III-8). That indicated that L-threonine is still an important carbon source for the promastigotes. For the *Δlmgt* promastigotes, L-threonine appear to be a primary source for acetate judging by the higher levels of acetate in all three conditions with L-threonine (Table III-7; Supplemental figures III-6, III-7 and III-8). In the penultimate condition, condition 9, **glr**, where glycerol was provided as a sole carbon source, the two types of promastigotes excreted ^{12}C-acetate only (Tables III-7 and III-8; Supplemental figure III-9). Finally, in the last condition, **glr+*glc**, where glycerol was combined with ^{13}C-D-glucose, the wild type promastigotes excreted the same amounts of ^{12}C-acetate from mannogen and ^{13}C-acetate from D-glucose as those observed in condition 6 while the *Δlmgt* promastigotes excreted the same amount of ^{12}C-acetate as that in the previous conditions, except for those with L-threonine (Table III-8; Supplemental figure III-10).

III.1.2.3.2. Metabolomic analysis of carbohydrate metabolism of *Δlmgt* promastigotes by LC-MS and stable isotope tracing analysis

We have taken advantage of the heavy isotope nature of some of the carbon sources used in the NMR analysis and subjected the two lines of *Leishmania*

promastigotes grown for 6 hours under the 10 NMR conditions to a stable isotope tracing analysis. With regard to this analysis, however, two points have to be clarified. First, a similar to condition 2 (***glc**) analysis was performed beforhand and it involved incubation of the wild type and *Δlmgt* promastigotes in defined media supplemented with serum and ^{13}C-D-glucose for 48 hours. This condition was designated condition 0 (**C0**; ***glc0**) and helped us pinpoint metabolic differences between nutrient-replete (condition 0) and nutrient-restricted conditions (the NMR conditions). Second, the stable isotope tracing analysis is not quantitative. As said before, it was used to elucidate the metabolic fate of the carbon sources in the wild type and *Δlmgt* promastigotes.

The data were analyzed with IDEOM and mzMatch-ISO (Creek *et al.*, 2012; Chokkathukalam *et al.*, 2013). The PCA analysis, performed with IDEOM, revealed distinct separation between the wild type and *Δlmgt* C1-C5 cell and spent medium samples (Figure III-14). The C6-C10 wild type cell samples were also separated from the *Δlmgt* samples (Figure III-15). The C6-C10 *Δlmgt* cell samples, additionally, were separated into two groups indicating that the *Δlmgt* promastigotes incubated with ^{12}C-glycerol (C9) and ^{12}C-glycerol + ^{13}C-glucose (C10) had distinct metabolic phenotype (Figure III-15, A). The C6-C10 spent medium samples showed hardly any separation between each other (Figure III-15, B). A certain pattern, however, was still observed. The wild type C6 (**thr+*glc**) samples were grouped separately from the rest of the samples. The *Δlmgt* C6, C7 and C8 samples (with L-threonine) were clustered together with the wild type C7 and C8 samples while the *Δlmgt* C9 and C10 samples (with glycerol) were grouped with the wild type C9 and C10 samples (Figure III-15, B).

15 pathways of carbohydrate metabolism were investigated with mzMatch-ISO. All necessary information regarding metabolites and pathways was extracted from the Kyoto Encyclopedia of Genes and Genomes (KEGG) pathway database and MetaCyc. The pathways were used as reference pathways only. Analysis of 13 of the 15 carbohydrate pathways gave inconclusive information. One to maximum 4 metabolites of butanoate metabolism, C5-branched dibasic acid metabolism, glyoxylate and dicarboxylate metabolism and propanoate metabolism were detected.

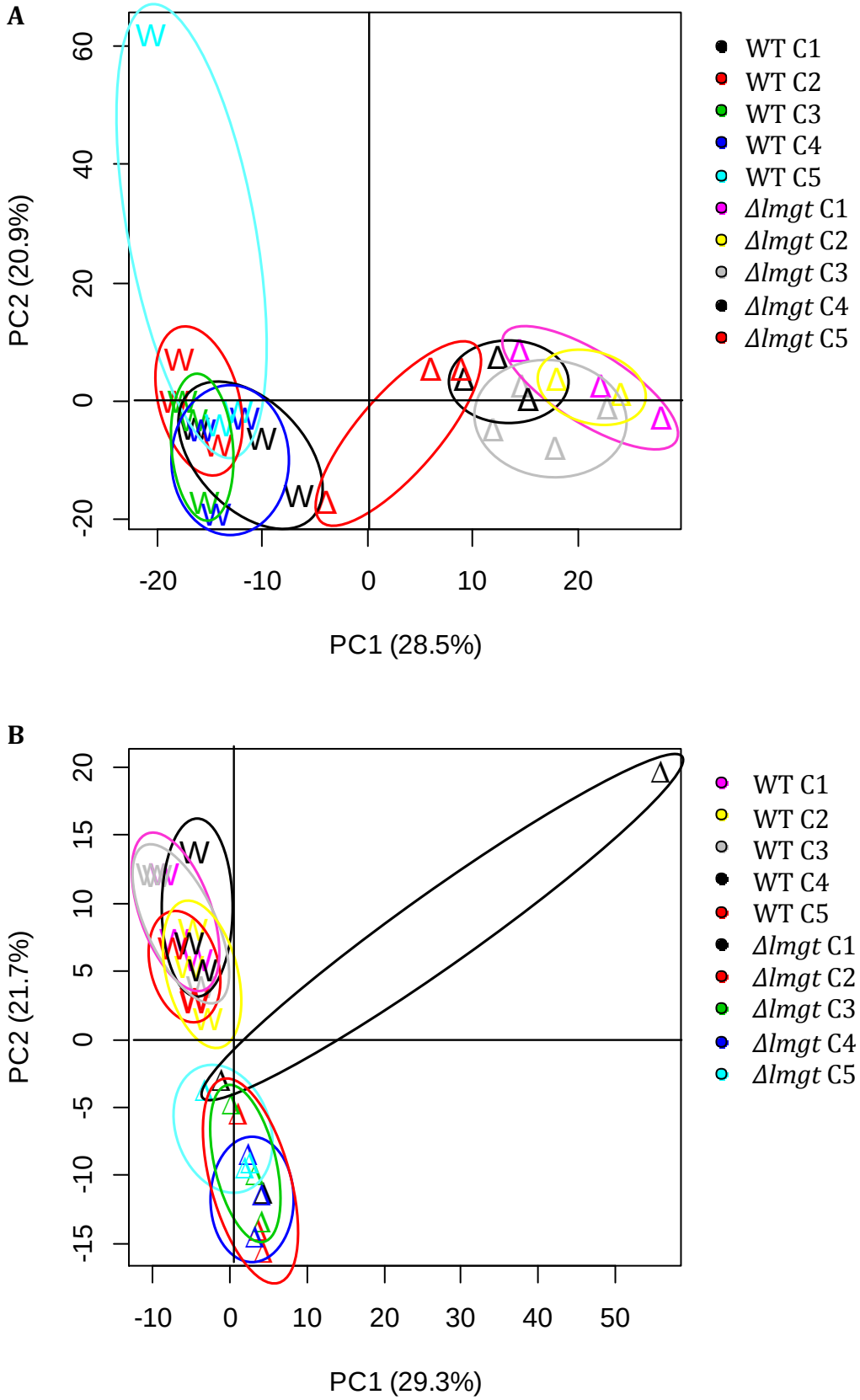

Figure III-14. Scoreplots of the Principal component analysis performed on the wild type and *Δlmgt* promastigote (A) and spent medium (B) metabolomic samples generated after incubation under conditions C1, C2, C3, C4 and C5. Wild type and *Δlmgt* promastigotes (biological replicates, n=3) were incubated for 6 hours in PBS (condition 1, C1), in PBS with ^{13}C-D-glucose (condition 2, C2), in PBS with ^{12}C-L-proline + ^{13}C-D-glucose (condition 3, C3), in PBS with ^{12}C-D-glucose + ^{13}C-L-proline (condition 4, C4) and in PBS with ^{13}C-L-proline (condition 5, C5), and subjected to cold chloroform/methanol/water metabolite extraction. The samples were analyzed by 1D pHILIC HPLC-ESI-MS and the data were analyzed with IDEOM. WT - wild type promastigotes, *Δlmgt* - *Δlmgt* promastigotes.

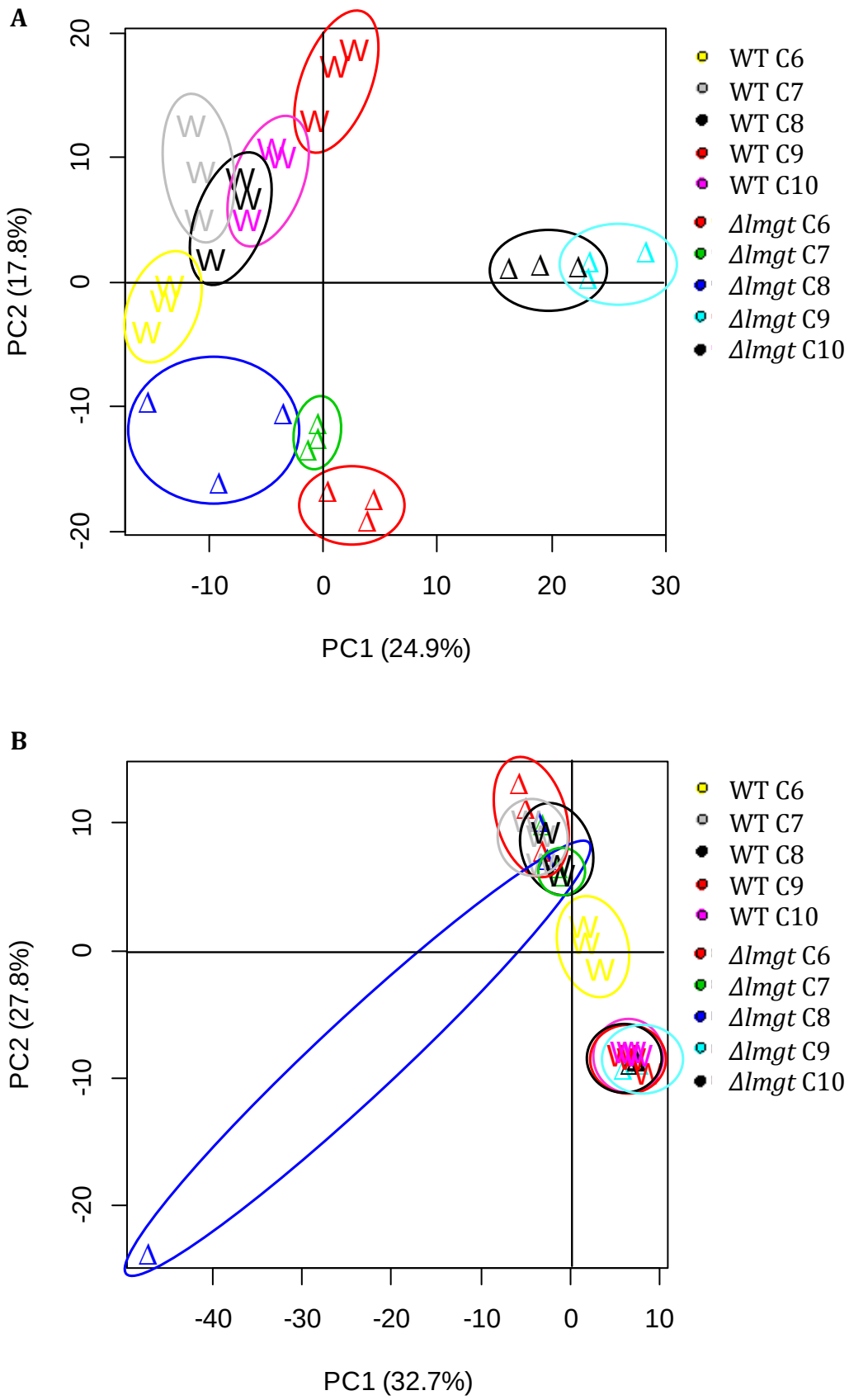

Figure III-15. Scoreplots of the Principal component analysis performed on the wild type and *Δlmgt* promastigote (A) and spent medium (B) metabolomic samples generated after incubation under conditions C6, C7, C8, C9 and C10. Wild type and *Δlmgt* promastigotes (biological replicates, n=3) were incubated for 6 hours in PBS with ^{12}C-L-threonine + ^{13}C-D-glucose (condition 6, C6), in PBS with ^{12}C-D-glucose + ^{13}C-L-threonine (condition 7, C7), in PBS with ^{12}C-L-proline and ^{13}C-L-threonine (condition 8, C8), in PBS with ^{12}C-glycerol (condition 9, C9) and in PBS with ^{12}C-glycerol + ^{13}C-D-glucose (condition 10, C10), and subjected to cold chloroform/methanol/water metabolite extraction. The samples were analyzed by 1D pHILIC HPLC-ESI-MS and the data were analyzed with IDEOM. WT - wild type promastigotes, *Δlmgt* - *Δlmgt* promastigotes.

For instance, itaconate was the only one of the C5-branched dibasic acid metabolism intermediates that was authentically identified and labelled in the wild type promastigotes. Similarly, 3-hydroxybutanoate, 2-hydroxyglutarate and butanoate were the only intermediates of butanoate metabolism that were detected. The first two metabolites were authentically identified and universally labelled in the wild type promastigotes while butanoate was unlabelled. This shows that our data are incomplete and do not allow further interpretation. Moreover, many intermediates of amino sugar and nucleotide sugar metabolism, ascorbate and alderate metabolism, fructose and mannose metabolism, galactose metabolism, glycolysis/ gluconeogenesis, inositol phosphate metabolism, pentose phosphate pathway, pentose and glucuronate interconversions, pyruvate metabolism and starch and sucrose metbaolism are isomers of each and their identification remained unconfirmed. Nevertheless, we could say that UDP-hexoses, GDP-hexoses, N-acetyl-D-hexosamine 1/6-phosphates, UDP-N-acetyl-D-hexoseamines, hexoses, hexose phosphates, pentoses and pentose phosphates are among the labelled metabolites in the wild type promastigotes incubated with D-glucose. Additionally, oligosaccharides such as cellotriose, cellotetraose, cellopentaose and cellohexaose were also identified as labelled in the wild type promastigotes incubated with D-glucose but only putatively.

Glycolysis/gluconeogenesis

The first stage of D-glucose catabolism in *Leishmania* occurs via glycolysis which is partially compartmentalized in the glycosomes (Hart and Opperdoes, 1984). Corroborating with a previous study on *L. mexicana* promastigotes (Saunders *et al.*, 2011), all detected glycolytic/gluconeogenic intermediates were labelled in condition ***glc0** wild type promastigotes (Figure III-16). D-Glucose was authentically identified in conditions ***glc**, **pro+*glc**, **thr+*glc** and **glr+*glc** wild type promastigotes. G6P, F6P, 2PG, 3PG and PEP were authentically identified in all conditions whereas glyceraldehyde 3-phosphate/dihydroxyacetone phosphate was putatively identified. All of the listed glycolytic/gluconeogenic intermediates were universally labelled in conditions ***glc0**, ***glu**, **pro+*glc**, ***pro**, **thr+*glc** and **glr+*glc** wild type promastigotes and in conditions **glc+*pro** and ***pro** *Δlmgt* promastigotes. Pyruvate was also putatively identified and was universally labelled in conditions ***glc**, **pro+*glu**, **thr+*glu** and **glr+*glu** wild type promastigotes and in conditions **glc+*pro** and ***pro** *Δlmgt* promastigotes.

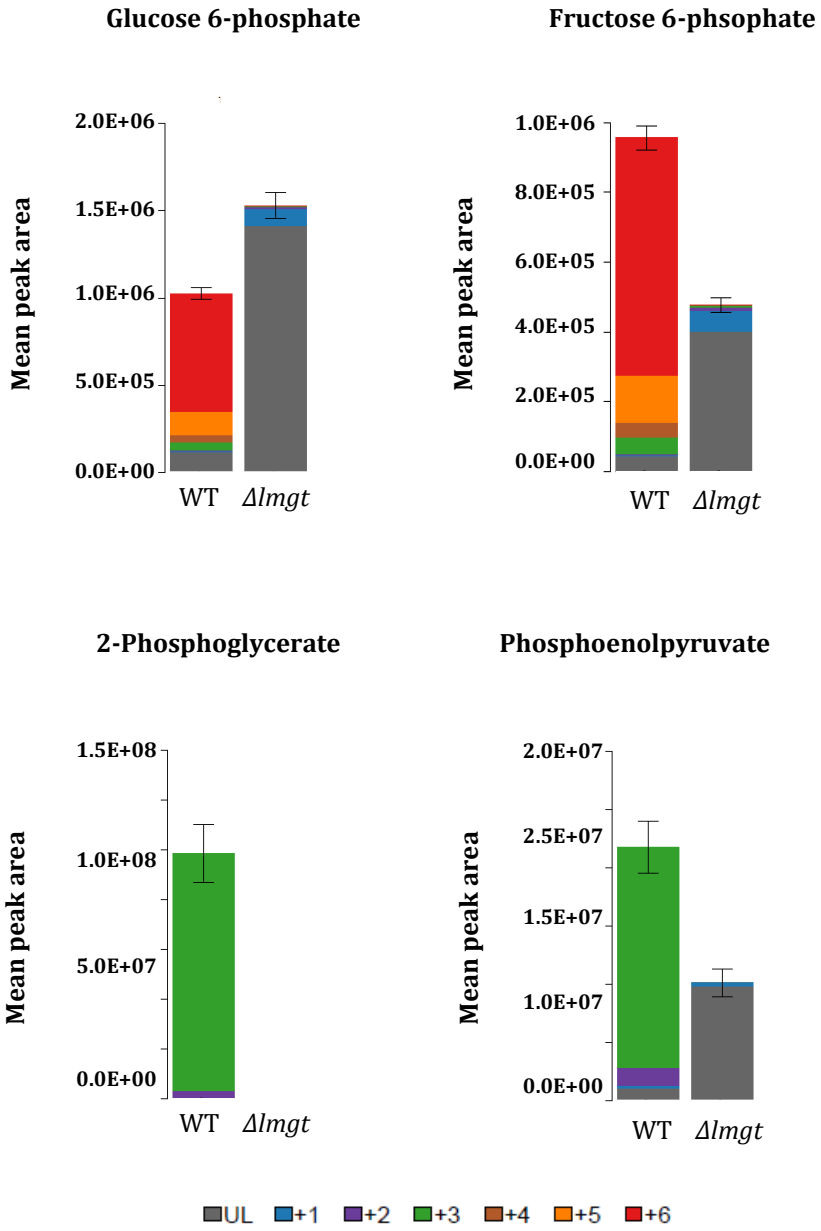

Figure III-16. Labelling pattern of glucose 6-phosphate, fructose 6-phosphate, 2-phosphoglycerate and phosphoenolpyruvate in wild type and *Δlmgt* promastigotes incubated with ^{13}C-D-glucose. Abbreviations: UL- Unlabelled carbon, +1 - 1-^{13}C-labelled carbon, +2 - 2-^{13}C-labelled carbon, +3 - 3-^{13}C-labelled carbon, +4 - 4-^{13}C-labelled carbon, +5 - 5-^{13}C-labelled carbon, +6 - 6-^{13}C-labelled carbon, WT – wild type promastigotes, *Δlmgt* - *Δlmgt* promastigotes.

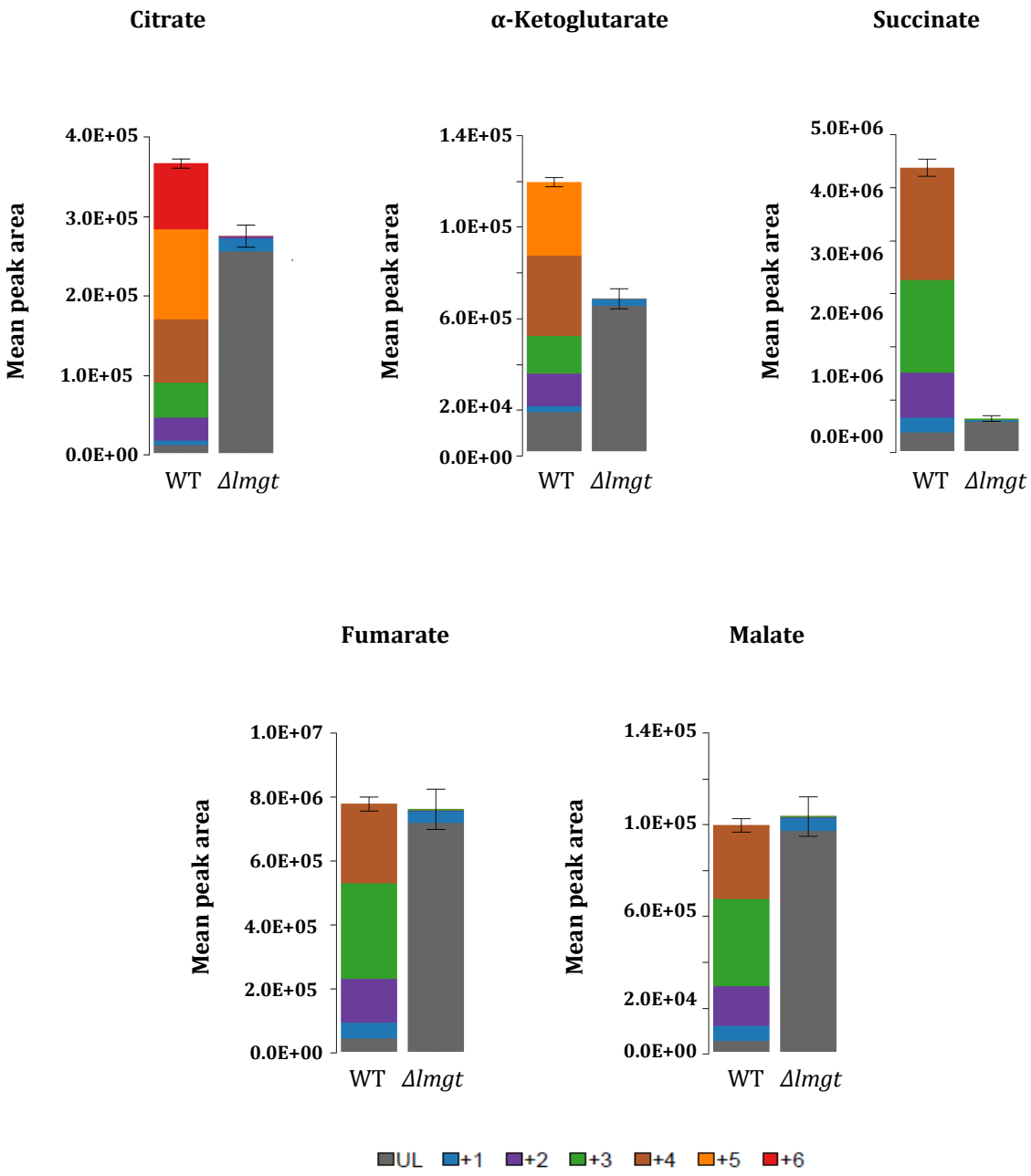

Figure III-17. Labelling pattern of citrate, α-ketoglutarate, succinate, fumarate and malate in wild type and *Δlmgt* promastigotes incubated with ^{13}C-D-glucose. Abbreviations: UL- Unlabelled carbon, +1 - 1-^{13}C-labelled carbon, +2 - 2-^{13}C-labelled carbon, +3 - 3-^{13}C-labelled carbon, +4 - 4-^{13}C-labelled carbon, +5 - 5-^{13}C-labelled carbon, +6 - 6-^{13}C-labelled carbon, WT – wild type promastigotes, *Δlmgt* - *Δlmgt* promastigotes.

Tricarboxylic acid cycle

The second stage of D-glucose catabolism in *Leishmania* involves the mitochondrially operating tricarboxylic acid cycle (TCA cycle) which is linked to the final component of the cellular respiratory machinery, the electron transport chain (see Chapter IV). The cycle consists of eight steps and involves nine intermediates. Authentically identified and universally labelled in condition ***glc0** wild type promastigotes were citrate, α-ketoglutarate, succinate, fumarate and malate (Figure III-17). Citrate, malate, succinate and fumarate were authentically identified and universally labelled also in conditions ***glc**, **pro+*glc** and ***pro** wild type promastigotes and in conditions **glc+*pro** and ***pro** *Δlmgt* promastigotes. Malate, succinate and fumarate were labelled also in conditions **thr+*glc** and **glr+*glc** wild type promastigotes. *cis*-Aconitate was authentically identified and found universally labelled in conditions ***glc** and **pro+*glc** wild type promastigotes and in conditions **glc+*pro** and ***pro** *Δlmgt* promastigotes.

The third stage of D-glucose catabolism involves reoxidation of reduced coenzymes such as NADH and $FADH_2$ generated in glycolysis and TCA cycle by the electron transport chain for the production of energy in the form of ATP (see Chapter IV). The role of D-glucose, however, is not limited to an energy source. D-Glucose is an important source for anabolic precursors, such as nucleotides, amino acids and lipids, which are involved in macromolecular synthesis. For instance, the phosphorylated form of D-glucose, glucose 6-phosphate, is catabolized in the pentose phosphate pathway for the synthesis of ribose 5-phosphate (R5P). R5P is a precursor for nucleotides (Maugeri *et al.*, 2003) which are the building blocks of DNA and RNA. Fructose 6-phosphate can be used for the synthesis of GDP-mannose which is the main mannose donor for glycoconjugate and mannogen biosynthesis (Ilg *et al.*, 1999; Ralton *et al.*, 2003). Dihydroxyacetone phosphate is involved in ether-lipid biosynthesis (Heise and Opperdoes, 1997) whereas pyruvate can be converted to acetyl-CoA which is a fatty acid precursor. Ether lipids and fatty acids are precursors for phospholipids and triacylglycerols which are major structural lipids in cell membrane. Pyruvate, oxaloacetate and α-ketoglutarate are sources of L-alanine, L-aspartate and L-asparagine, and L-glutamate and L-glutamine, respectively (Opperdoes and Michels, 2008) (see Chapter IV), all of which are involved in protein synthesis.

III.2. Discussion

A number of recent studies have aimed at comprehensive identification and quantitation of new and known proteins and metabolites in order to elucidate new aspects of trypanosomatid metabolism. Some proteomic and metabolomic studies have focused on global and comparative profiling of the trypanosomatid development (Drummelsmith *et al.*, 2003; Rosenzweig *et al.*, 2008a). Other studies have been interested in more specific components of the proteome and metabolome, such as the phosphoproteome (Urbaniak *et al.*, 2013), the glycoproteome (Guther *et al.*, 2014) or central carbon metabolism (Saunders *et al.*, 2011).

With regard to proteomics, the aim of this study was to develop a gel-free methodology for global quantitative comparison between *L. mexicana* wild type and *Δlmgt* promastigotes. The methodology involved prefractionation of the wild type and *Δlmgt* promastigote proteomes with digitonin and consecutive analysis of the resulting fractions by mass spectrometry (MS). The digitonin fractionation was developed by Oullette and colleagues in 2006 and was successfully used for comparative proteomic analysis of *L. infantum* promastigotes and amastigotes (Foucher *et al.*, 2006). The method involves the use of increasing amounts of digitonin, which precipitates sterols and forms pores in the plasma and organellar membranes, to successively extract cytosolic, organellar and digitonin-insoluble proteins. In our study, the 5 fractions generated with digitonin were directly analyzed by MS. Oullette and colleagues, however, used 2D gel electrophoresis to further separate the protein fractions prior to analyzing some of the gel spots by MS. The MS analysis showed that the presence of most of the proteins in a certain fraction is indicative for their localization in the cells. A comparison between our data and several other papers indicated that the same principle applied for the proteins detected in the five fractions generated in our study (Colasante *et al.*, 2006; Guther *et al.*, 2014). However, the digitonin-based fractionation was not chosen as a method for enrichment of a certain cellular component. Rather, it was used solely to increase the protein coverage. Compared to preliminary experiments where around 1% of the predicted *Leishmania* proteome was found differentially expressed in the *Δlmgt* promastigotes, the prefractionation allowed us to see more than 2 times more proteins differentially regulated in the *Δlmgt* cells. The modulated proteins included binding proteins, cytoskeletal proteins, enzymes, hypothetical proteins, structural

proteins, proteins involved in movement, protein degradation, protein folding and protein synthesis, and proteins with unknown function (Figure III-6). The largest category, that of the enzymes, comprised ~40% of all significant proteins. The majority of the significantly modulated enzymes were metabolic enzymes involved in amino acid, carbohydrate, energy, lipid and nucleotide metabolism and metabolism of terpenoids and polyketides (Supplemental table III-1). Discussed below will be all enzymes with known function that belong to metabolic pathways of the carbohydrate metabolism.

With regard to metabolomics, the aim of this study was to complement the proteomic data by investigating the central carbon metabolism of the *Δlmgt* promastigotes. Prior characterization of the *Δlmgt* promastigotes has revealed that the gene deletion of the hexose transporters is accossiated with a number of phenotypic modulations, including significant changes in pathways of carbohydrate metabolism, such as the gluconeogenesis and glycoconjugate biosynthesis (Rodriguez-Contreras and Landfear, 2006). These studies provided valuable yet partial information regarding the changes in the *Δlmgt* promastigote metabolism. So, to expand on the proteomic information gathered by us, we decided to also perform comprehensive untarget and targeted metabolomic analyses, driven by the following questions:

- are the changes in the *Δlmgt* promastigote metabolism restricted to the carbohydrate metabolism?
- are other components of carbon metabolism, including amino acid, energy, lipid and nucleotide metabolism, affected?
- are alternative carbon sources used by the *Δlmgt* promastigotes to sustain their energy needs and which are they?

Significant changes in the carbon metabolism of the *Δlmgt* promastigotes were detected. Only carbohydrate metabolism will be discussed in this chapter. Amino acid, energy, lipid and nucleotide metabolism are discussed in Chapter IV.

Carbohydrate metabolism

Glycolysis/gluconeogenesis

The continuous influx of energy is a necessity for maintaining cell growth, homeostasis, and development. In heterotrophic organisms, the flux of energy is fulfilled by the acquisition of nutrients which are biochemically converted to high energy intermediates such as ATP. A major nutrient and source of energy for many organisms is D-glucose. *L. mexicana* can acquire D-glucose from the host by the GT1, GT2, GT3, and GT4 transporters (Burchmore and Landfear, 1998; Feng *et al.*, 2009). After internalization, most of D-glucose is directed towards the glycosomes, specialized peroxisome-related organelles, where it is metabolized via glycolysis to 3-phosphoglycerate (3PG) (Hart and Opperdoes, 1984; Michels *et al.*, 2006). 3PG is then transported to the cytosol, where the last few steps of glycolysis occur, and lead to the production of pyruvate. The reverse pathway in which the end product of glycolysis, pyruvate, and a number of other metabolites such as acetate, lactate, and some glucogenic amino acids, are converted back to D-glucose is designated as gluconeogenesis. Gluconeogenesis shares most but not all of its enzymes with glycolysis. Nevertheless, some key gluconeogenic enzymes, such as fructose 1,6-bisphosphatase, were shown to also be present in the *Leishmania* glycosomes (Michels *et al.*, 2006).

Naturally, our analysis of the glucose transporter null-mutant promastigotes started with investigating the glycolytic/gluconeogenic pathway. As expected, the stable isotope tracing analysis revealed that none of the intermediates of the pathwy were heavy-labelled in the *Δlmgt* promastigotes (Figure III-18). The global untargeted metabolomic data did not reveal anything significant with respect to the pathway (Tables III-2, III-3 and III-4). The quantitative proteomic and glycomic data, however, provided valuable information regarding the way glycolysis/gluconeogenesis operates in the *Δlmgt* promastigotes. First, the glycomic data showed that D-glucose was maintained roughly at a 12 times higher level in the *Δlmgt* promastigotes in comparison with the wild type promastigotes. This observation, along with the notion that the last gluconeogenic enzyme, namely glucose 6-phosphatase which converts glucose 6-phosphate (G6P) to D-glucose, appears to be missing from *Leishmania* (Rodriguez-Contreras and Landfear, 2006), suggests that gluconeogenesis in *Leishmania*, and in the *Δlmgt* promastigotes, serves to generate G6P but not D-

glucose. Thus, taking into account that, on one hand, *Leishmania* are not able to synthesize D-glucose via gluconeogenesis and, on the other hand, that the levels of two specific sugars, namely sucrose and fructose, are also increased in the *Δlmgt* promastigotes, we assumed that the glucose transporter null-mutant promastigotes most probably use alternative sources for the production of D-glucose. Sucrose, most probably present in the serum supplementing the culture media, appears to be such source for the *Δlmgt* promastigotes. It is a disaccharide made from D-glucose and D-fructose and under the action of sucrase, it is cleaved into the two monosaccharides. *Leishmania* are capable of breaking down sucrose extracellularly, by secreting sucrase, and intracellularly (Jacobson *et al.*, 2001; Singh and Mandal, 2011). Intracellular sucrase acts upon sucrose internalized by a two component symport system that is characterised with high specificity for sucrose and high and low affinity dual kinetics (Singh and Mandal, 2011). Other sources of D-glucose, in addition to sucrose, may also be used by the *Δlmgt* promastigotes although our data did not specify any other such metabolites.

The higher level of D-glucose and up-regulated hexokinase in the *Δlmgt* promastigotes (Feng *et al.*, 2011) indicate that the hexose is used for the generation of G6P. The levels of G6P and fructose 6-phosphate (F6P), however, were 3 to 4-fold lower in the *Δlmgt* promastigotes compared with the wild type promastigotes. The two intermediates are key precursors for a number of important metabolites. G6P can be directed toward the pentose phosphate pathway (PPP) for the synthesis of ribose 5-phosphate and reducing equivalents (see Pentose phosphate pathway), while F6P can be directed toward the nucleotide sugar and mannose metabolism which, in turn, provide precursors for the synthesis of a variety of glycoconjugates and the reserve material of *Leishmania* called mannogen (see Fructose and mannose metabolism) (Maugeri *et al.*, 2003; Garami *et al.*, 2001; Ralton *et al.*, 2003). The next three intermediates, fructose 1,6-bisphosphate (F1,6B), glyceraldehyde 3-phosphate (GAP) and dihydroxyacetone phosphate (DHAP), were not detected in the wild type or *Δlmgt* promastigotes. It is possible that the three intermediates are metabolized right after synthesis and only trace quantities, below the limit of detection of the GC-MS method used in this project, are present in the cells. Three points regarding GAP are of relevance. First, glyceraldehyde 3-phosphate dehydrogenase (GAPDH) isoforms were found both up- and down-regulated in the *Δlmgt* promastigotes (Supplemental table III-1).

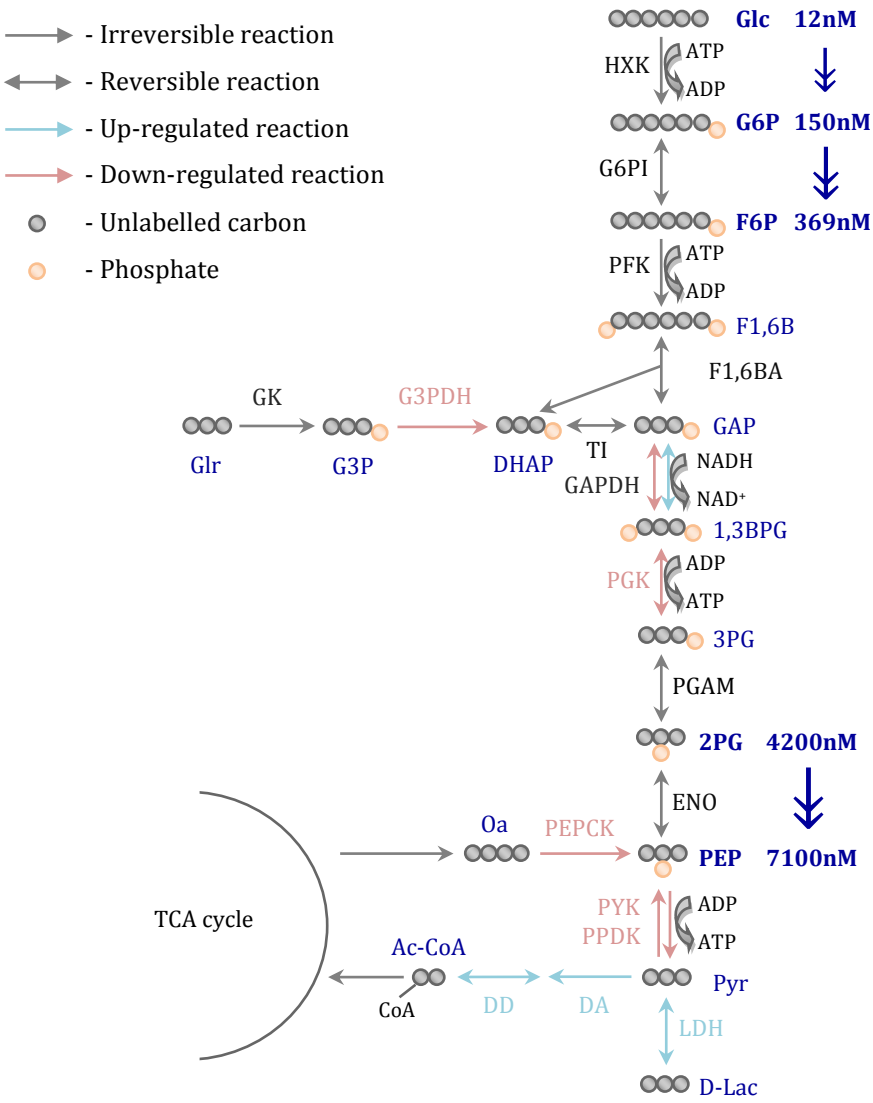

Figure III-18. Schematic representation of glycolysis/gluconeogenesis in *Δlmgt* promastigotes incubated with ^{13}C-D-glucose. Presented here are integrated quantitative proteomic, glycomic and stable isotope tracing data. Specified with light blue arrows are the up-regulated enzymes while specified with pink arrows are the down-regulated enzymes. Specified in dark blue are the glycolitic intermediates quantified by GC-MS. Indicated next to each quantified metabolite is its concentration in nanomoles (nM). Abbreviations: Glc - glucose, G6P - glucose 6-phosphate, F6P - fructose 6-phosphate, F1,6B - fructose 1,6-bisphosphate, GAP - glyceraldehyde 3-phosphate, DHAP - dihydroxyacetone phosphate, G3P - glycerol 3-phosphate, Gly - glycerol, 1,3BPG - 1,3-bisphosphoglycerate, 3PG - 3-phosphoglycerate, 2PG - 2-phosphoglycerate, PEP - phosphoenolpyruvate, Pyr - pyruvate, Glr - glycerol, G3P - glycerol 3-phosphate, Lac - lactate, Ac-CoA - acetyl-CoA, Oa - oxaloacetate, HXK - hexokinase, G6PI - glucose 6-phosphate isomerase, PFK - 6-phospho-1-fructokinase, Fru1,6BA - fructose 1,6-bisphosphate aldolase, TI - triosephosphate isomerase, GAPDH - glyceraldehyde 3-phosphate dehydrogenase, PGK - phosphoglycerate kinase, PGAM - phosphoglycerate mutase, ENO - enolase, PYK - pyruvate kinase, PPDK - pyruvate phosphate dikinase, GK - glycerol kinase, G3PDH - glycerol 3-phosphate dehydrogenase, LDH - lactate dehydrogenase, DA - dihydrolipoamide acetyltransferase, DD - dihydrolipoamide dehydrogenase, PEPCK - phosphoenolpyruvate carboxikinase, ATP - adenosine triphosphate, ADP - adenosine diphosphate, NAD - nicotinamide adenine dinucleotide.

Considering that different isoforms of glycolytic/gluconeogenic enzymes, such as enolase (Avilan *et al.*, 2011), often have kinetic properties facilitating changes in the flux in the glycolytic or gluconeogenic direction in accordance with the cellular needs, it could be hypothesized that one of the isoforms contributes to glycolysis while the other is involved in gluconeogenesis. Second, under the action of GAPDH, GAP is converted to glycerate 1,3-bisphosphate with the simultaneous reduction of NAD^+ to NADH. The generated NADH, however, has to be re-oxidised so that the glycosomal NAD^+/NADH balance is maintained. It was proposed that three pathways are involved in the maintenance of this balance in trypanosomatids: a glycosomal succinate fermentation, a glycerol 3-phosphate (G3P)/DHAP shuttle and a glycosomal glycerol production pathway (Ebikeme *et al.*, 2010). When cultured with abundance of D-glucose, the glycosomal succinate fermentation has been shown to be the primary mechanism by which *Leishmania* maintain this balance and only insignificant amount of NAD^+ is regenerated via the DHAP/glycerol 3-phsophate (G3P) shuttle (see Glycosomal succinate fermentation) (Hart and Coombs, 1982; Cazzulo *et al.*, 1985; Saunders *et al.*, 2011). Third, GAP is the point linking lipid and carbohydrate metabolism. Glycerol, an intermediate of glycerolipid metabolism, enters gluconeogenesis in *Leishmania* via glycerol kinase (GK) (Figure III-18) (Rodriguez-Contreras and Hamilton, 2014). G3P generated by GK is converted to DHAP by a glycerol 3-phosphate dehydrogenase (G3PDH) and then fuelled into gluconeogenesis. A previous study showed that ^{14}C-glycerol is incorporated in mannogen by the *Δlmgt* promastigotes which confirmed that glycerol is used as a glucogenic precursor for the synthesis of G6P (Rodriguez-Contreras and Landfear, 2006). Our proteomic analysis, however, revealed that a glycosomal/mitochondrial NAD^+-dependent G3PDH was highly (>10-fold) decreased in the *Δlmgt* promastigotes which indicates that glycerol may not be a preferred glucogenic source for the *Δlmgt* promastigotes. The highly increased level of glycerol in the mutant promastigotes (Table III-2), on the other hand, suggests that it is probably needed in glycerolipid biosynthesis.

The last intermediates of the glycolytic pathway are 1,3-bisphosphoglycerate, 3PG, 2PG, PEP, and pyruvate. *Leishmania* express two phosphoglycerate kinase (PGK) enzymes - a cytosolic PGKB and a glycosomal PGKC (Kaushik *et al.*, 2012), both of which were found down-regulated in the *Δlmgt* promastigotes. PGK catalyzes the interconversion of 1,3-bisphosphoglycerate and 3PG. The latter can then be interconverted to 2PG by phosphoglycerate mutase. In the cytosol, 2PG is converted

to PEP by the enzyme enolase (ENO) (Figure III-18), which was confirmed as down-regulated in the *Δlmgt* promastigotes by a 2D difference gel electrophoresis (2D-DIGE) analysis (in preparation). In the cytosol, PEP can either be re-imported into the glycosomes and reduced to succinate via the glycosomal succinate fermentation or irreversibly converted to pyruvate by a cytosolic pyruvate kinase (Michels *et al.*, 2006). The PEP-to-pyruvate conversion is responsible for the net glycolytic ATP production. The pyruvate kinase catalyzing the reaction, however, was found down-regulated in the *Δlmgt* promastigotes. The decreased activity of the enzyme could be associated with redirection of the majority of PEP into gluconeogenesis. Indeed, the glycomic data revealed that the levels of PEP and 2PG in the *Δlmgt* promastigotes are close to those in the wild type promastigotes (Table III-5; Figure III-10). Furthermore, the stable isotope tracing analysis revealed that pyruvate, PEP, 2PG, 3PG, and GAP/DHAP contain much more 3-^{13}C isotopomers in the wild type promastigotes incubated with ^{13}C-D-glucose whereas those in the *Δlmgt* promastigotes incubated with the glucogenic amino acid ^{13}C-L-proline contain equal amounts of 2-^{13}C and 3-^{13}C isotopomers. Similarly, in the *Δlmgt* promastigotes incubated with ^{13}C-L-proline, F6P and G6P contain more 2-^{13}C, 3-^{13}C and 4-^{13}C isotopomers resulting from gluconeogenesis while the wild type promastigotes incubated with ^{13}C-D-glucose contain more 5-^{13}C and 6-^{13}C isotopomers resulting from catabolism of D-glucose. Altogether, these data confirm that glycolysis/gluconeogesis operates in a gluconeogenic mode. Furthermore, the similar levels of PEP and 2PG in the wild type and mutant promastigotes show that the *Δlmgt* promastigotes strive to maintain a stable influx of glucogenic compounds into the pathway. At the same time, however, the enzymes G3PDH, PEPCK and PPDK which participate in the entry of glycerol, L-aspartate, and L-alanine in gluconeogenesis, respectively (Rodriguez-Contreras and Hamilton, 2014), are down-regulated in these promastigotes. Moreover, the last intermediates of gluconeogenesis, including F6P and G6P, have decreased levels in the *Δlmgt* promastigotes. Concisely, it could be concluded that both D-glucose and gluconeogenesis are used to generate G6P but that gluconeogenesis is not able to meet the requirements for glycolytic/gluconeogenic biosynthetic precursors in the *Δlmgt* promastigotes.

The data discussed above were obtained with *Δlmgt* promastigotes grown in defined media supplemented with serum. When the *Δlmgt* promastigotes were maintain in buffer (PBS) supplemented with no carbon sources or with either one or two of the

following sources - D-glucose, L-proline, L-threonine and glycerol, some variations in the pathway were observed. The stable isotope tracing revealed that the glycolytic/ gluconeogenic intermediates in the wild type promastigotes were heavy-labelled only in the conditions where ^{13}C-D-glucose was supplied as a carbon source, conditions ***glc**, **pro+*glc**, **thr+*glc** and **glr+*glc,** and in condition ***pro** where ^{13}C-L-proline was provided as a sole carbon source. Thus, as shown before (Krassner, 1969; Krassner and Flory, 1972), D-glucose and L-proline are major nutrients for the *L. mexicana* wild type promastigotes and they are able to sustain cell growth when provided as sole carbon sources or in combination with one another. In the *Δlmgt* promastigotes, the glycolytic/gluconeogenic intermediates were heavy-labelled only in the two conditions with ^{13}C-L-proline, **glc+*pro** and ***pro**, which confirmed that L-proline is among the glucogenic precursors used by the *Δlmgt* promastigotes for the synthesis of hexose phosphates (see Arginine, glutamate and proline metabolism). It must be added, however, that in contrast to the lack of labebelling in the *Δlmgt* promastigotes grown in defined media supplemented with serum and ^{13}C-D-glucose, condition ***glc0**, minor labelling of 2PG, 3PG and PEP was observed in conditions ***glc** and **pro+*glc** *Δlmgt* promastigotes. That indicates that when no nutrients other than D-glucose alone or D-glucose and L-proline are available in the environment, the *Δlmgt* promastigotes might possibly up-regulate the alternative GT4 glucose transporter (previously known as D2). Lastly, it should be noted that minor labelling was observed in some of the glycolytic/gluconeogenic intermediates in the conditions with ^{13}C-L-threonine showing that the amino acid is not preferentially fed into gluconeogenesis in the *Δlmgt* promastigotes (see Glycine, serine and threonine metabolism).

Fructose and mannose metabolism

The hexose sugars D-fructose and D-mannose are also substrates of LmGT transporters, so the *Δlmgt* promastigotes are not able to acquire these potential carbon sources (Rodriguez-Contreras *et al.*, 2007). Nevertheless, the level of D-fructose in the *Δlmgt* cells was 50 times higher compared to its level in the wild type promastigotes (Table III-5). Similar to D-glucose, D-fructose is phosphorylated before entering the intermediary metabolism by either hexokinase (Pabon *et al.*, 2007) or fructokinase.

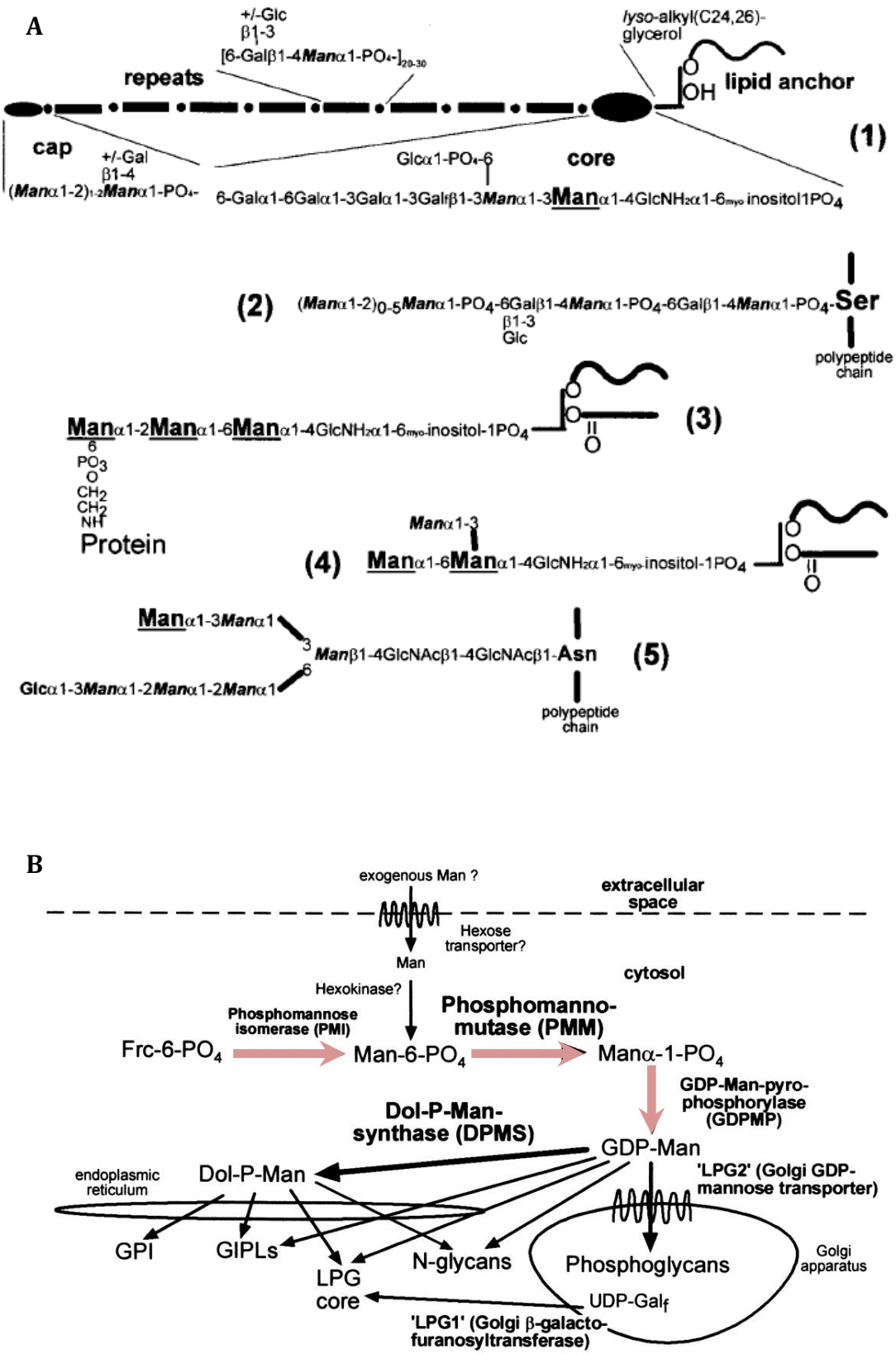

Figure III-19. Structure and synthesis of mannose-containing glycoconjugates in *Leishmania mexicana*. (A) Structure of (1) LPG, (2) PPG, (3) protein PGI anchor, (4) GIPL iM3 and (5) protein *N*-glycan. Enlarged and underlined are mannose residues donated from dolicholphosphate-mannose while those donated from GDP-mannose are italic and bolded. (B) Mannose activation pathway and biosynthesis of glycoconjugates in *Leishmania mexicana*. Specified with pink arrows are the down-regulated reactions in the *Δlmgt* promastigotes.
Credit: Garami *et al.*, 2001

D-Fructose can be phosphorylated at 1st or 6th position to produce fructose 1-phosphate (F1P) and F6P, respectively, which can be fuelled into glycolysis. The glycomic data showed that while F6P was present in the *Δlmgt* promastigotes, though approximately 3 times less compared with the wild type promastigotes, F1P was not (Table III-5). The negligible amount or absence of F1P in the *Δlmgt* promastigotes indicated that fructose is mainly phosphorylated to F6P. Another source of F6P could be D-sorbitol, originating most probably from the serum supplementing the culture media, and whose level, similar to that of D-glucose, was 12 times increased in the *Δlmgt* promastigotes (Table III-5). F6P can be converted to mannose 6-phosphate (M6P) by phosphomannose isomerase (PMI) and directed toward the mannose (Man) metabolism (Figure III-19). Phosphomannose isomerase, however, was found down-regulated in the *Δlmgt* promastigotes and Man and M6P were not detected in the wild type or *Δlmgt* promastigotes (Table III-5). Thus, from the glycomic and proteomic data, it might be assumed that the level of free Man in the wild type and *Δlmgt* promastigotes is maintained really low and that the influx of F6P into Man metabolism is decreased in the *Δlmgt* promastigotes.

Man is a building block for two main types of macromolecules in *Leishmania:* the reserve material and virulence factor called mannogen (previously known as β-mannan) (Ralton *et al.*, 2003) and a spectrum of surface associated and secreted glycoconjugates such as lipophosphoglycan (LPG), proteophosphoglycans (PPGs), glycosylphosphatidylinositol (GPI)-anchored proteins, glycoinositolphospholipids (GIPLs), and N-glycans (Turco and Descoteaux, 1992; McConville and Ferguson, 1993; Ilg *et al.*, 1999). Before being incorporated into glycoconjugates, Man has to be activated. The activation involves the conversion of M6P to mannose 1-phosphate (M1P) by phosphomannomutase (PMM), which was down-regulated in the *Δlmgt* promastigotes (Supplemental table III-1), followed by the conversion of M1P to GDP-mannose (GDP-Man) by GDP-mannose pyrophosphorylase (GDPMP), which was also found down-regulated in the *Δlmgt* promastigotes by the 2D-DIGE analysis (in preparation), and finally, the conversion of GDP-Man to dolicholphosphate-mannose (Dol-P-Man) by dolicholphosphate-mannose synthase (DPMS). The products of the pathway, GDP-Man and Dol-P-Man, are the two central activated Man donors in mannosylation reactions of the glycoconjugate biosynthesis (Figure III-19) (Garami *et al.*, 2001). Down-regulation of two of the three enzymes involved in the activation of these two metabolites renders the pathway down-regulated and the glycoconjugate

biosynthesis hindered in the *Δlmgt* promastigotes. These results corroborate with a previous study conducted with the *Δlmgt* promastigotes which investigated the synthesis of LPG, membrane PPG (mPPG), GILP, gp63 (an important leishmanial virulence factor), secreted acid phosphatase (a secreted glycoprotein enzyme), and mannogen by the *Δlmgt* promastigotes (Rodriguez-Contreras and Landfear, 2006). The study revealed that the *Δlmgt* promastigotes, first, did not use external sources for glycoconjugate biosynthesis, second, used gluconeogenesis for the synthesis of the necessary carbohydrate precursors, third, were able to properly *N*-glycosylate glycoproteins, and, fourth, were able to synthesize the glycoconjugates listed above and mannogen, although at reduced levels. Our proteomic data elucidated one significant difference with regard to gp63 though: the analysis performed by Rodriguez-Contreras and Landfear involved concentration of the membrane-bound and secreted gp63 from the *Δlmgt* promastigote culture medium and detection by Western blot, whereas our MS-based quantitative proteomic analysis was performed with promastigote cell lysate. As a result, while the previous study determined the level of gp63 in the *Δlmgt* spent media, our analysis elucidated the metalloprotease level in the promastigotes where four isoforms were found up-regulated (Supplemental table III-1). This is consistent with increased synthesis of gp63 but reduced efficiency of GPI anchor conjugation in the *Δlmgt* promastigotes. Another possibility is that gp63, as a protease, might have an additional intracellular function.

Mannogen is a cytosolic carbohydrate reserve material comprised of β-1,2-linked mannose residues (Ralton *et al.*, 2003). The synthesis of mannogen was shown to be significantly impaired in the *Δlmgt* promastigotes, suggesting that gluconeogenesis was not able to fully compensate for the inability of the glucose transporter null0mutant promastigotes to acquire exogenous hexose precursors. Our NMR data revealed that the wild type promastigotes excreted acetate and succinate originating from an intracellular carbon source, possibly mannogen, along with the acetate and succinate produced from the different exogenous carbon sources used in the experiment (see Pyruvate metabolism and Tricarboxylic acid cycle). That confirmed that some amount of the internal carbon storage material is metabolized simulatenously with the catabolism of exogenous energy and carbon sources such as amino acids (see Amino acid metabolism). The *Δlmgt* promastigotes, except for the conditions with L-threonine, which was shown to be the primary precursor for acetate (see Pyruvate metabolism and Glycine, serine and threonine metabolism),

excreted acetate and succinate originating only from the storage material (Table III-7). The levels of acetate and succinate produced, however, were reduced to less than half the levels measured in the wild type cells, consistent with reduced mannogen reserves in the *Δlmgt* cells.

Galactose metabolism

Galactose is another hexose the *Δlmgt* promastigotes cannot take up (Rodriguez-Contreras *et al.*, 2007). The proteomic data indicated that UDP-glc 4'-epimerase (GALE), which catalyzes the final step of the Leloire pathway of galactose catabolism, namely the conversion of UDP-galactose to UDP-glucose, was down-regulated in the *Δlmgt* promastigotes. Similar to GDP-Man and Dol-P-Man, which are the main Man donors in mannosylation reactions, UDP-galactose (UDP-Gal) is the main source of glucosyl units for the synthesis of the glycan core of the GPI anchors by which many glycoconjugates such as LPG, GIPLs, PPGs and proteins such as gp63 and gp46/PSA-2 are attached to the cell surface of *Leishmania* (McConville and Ferguson, 1993; Turco and Descoteaux, 1992; Ilg *et al.*, 1999). The biosynthesis of GPI anchors is a complex multistep process that takes place in the endoplasmic reticulum and involves several transporters, enzymes and enzyme complexes (Hong and Kinoshita, 2009 and the references therein). In trypanosomatids, the exact mechanism and many of the enzymes involved in the lipid remodelling, and in the GPI biosynthesis as a whole, remains elusive. Furthermore, many of them are considered to be novel. None of the GPI biosynthetic enzymes listed above was differentially expressed in the *Δlmgt* promastigotes. Additionally and unfortunately, N-acerylglucosamine was not detected in the wild type and *Δlmgt* promastigotes. It is worth saying, however, that the first enzyme of inositol synthesis, which catalyzes the conversion of G6P to *myo*-inositol-1-phosphate, was down-regulated in the *Δlmgt* promastigotes. That points out that another pathway important for the GPI biosynthesis is possibly suppressed in the *Δlmgt* promastigotes.

Glycosomal succinate fermentation

In the glycosomes, the re-imported PEP is first converted to oxaloacetate by PEPCK, which was down-regulated in the *Δlmgt* promastigotes. Then oxaloacetate is successively converted to malate, fumarate, and succinate by malate dehydrogenase (MDH), fumarate hydratase (FH), and NADH-dependent fumarate reductase (FRD), respectively. Three MDHs were found differentially expressed in the *Δlmgt*

promastigotes. A glycosomal MDH was significantly (>5-fold) down-regulated, isoforms encoded by a second MDH gene were down- and up-regulated, and a third MDH gene product was down-regulated (Supplementary table III-1). An FH was down-regulated in the second cytosolic and first organellar fractions (Supplemental table III-1). Additionally, an NADH-dependent FRD was down-regulated in the organellar fraction. It is known that *T. brucei* has a glycosomal FRD (FRDg) and two mitochondrial FRDs (FRDm1 and FRDm2) (Coustou *et al.*, 2005). FRDg is a soluble glycosomal FRD transferring electrons from cofactors such as NADH or $FADH_2$/$FMNH_2$ to fumarate while FRDm1 and FRDm2 are subunits of a mitochondrial multimeric complex involved in transferring electrons from quinol to fumarate (Coustou *et al.*, 2005). In our study, the NADH-dependent FRD was found differentially expressed in the first organellar fraction while most of the respiratory complex subunits were detected in the insoluble fraction. It could be hypothesized, therefore, that the NADH-dependent FRD is a glycosomal FRD. Thus, based on the down-regulated glycosomal MDH, FH, FRDg, and PEPCK and the decreased levels of malate and succinate in the *Δlmgt* promastigotes and spent media (see Tricarboxylic acid cycle), it can be concluded that the glycosomal succinate fermentation, which is considered as the main or sole pathway involved in maintaining the glycosomal ATP and redox balance (Saunders *et al.*, 2011), is suppressed in the *Δlmgt* promastigotes. In addition to regenerating ATP and NAD^+, the glycosomal succinate fermentation was shown to also be involved in supplying C4 dicarboxylic acids for the tricarboxylic acid cycle (TCA cycle) (Saunders *et al.*, 2011). The reduced influx of C4 dicarboxylic acids from the glycosomal succinate fermentation suggests that other carbon sources may be used by the *Δlmgt* promastigotes to replenish the TCA cycle (see Amino acid metabolism).

Pyruvate metabolism

As a major glycolytic end product, a portion of the pyruvate produced is excreted by the *Leishmania* cells (Rainey and MacKenzie, 1991). The NMR data showed that a small amount of ^{13}C-pyruvate was solely excreted when the wild type promastigotes were incubated with ^{12}C-D-glucose in combination with ^{13}C-L-proline (Table III-7). Thus, combined catabolism of D-glucose and L-proline in the wild type *L. mexicana* promastigotes leads to an increase in pyruvate production most probably resulting from increased respiratory activity (Krassner and Flory, 1972). Indeed, the amount of excreted end products by the wild type promastigotes was the highest in

the conditions with D-glucose and L-proline which suggests that oxidation of the two substrates together is more energogenic than oxidizing either one alone, oxidizing L-threonine and glycerol alone or in combination with D-glucose (Table III-7). The NMR data also showed that the *Δlmgt* promastigotes did not secrete pyruvate.

A second portion of pyruvate can be transported to the mitochondrion where it is decarboxylated to acetyl-CoA by the mitochondrial pyruvate dehydrogenase complex (PDC). The α subunit of the E1 component of the PDC was found up-regulated in the *Δlmgt* promastigotes (Figure III-18). Two other enzymes involved in the pyruvate-to-acetate conversion, dihydrolipoamide acetyltransferase and dihydrolipoamide dehydrogenase, were also up-regulated in the *Δlmgt* promastigotes (Figure III-18), thus suggesting that pyruvate is converted to acetyl-CoA at a higher rate in the *Δlmgt* promastigotes. In the mitochondrion, acetyl-CoA can be fed into the TCA cycle, which appears to be the preferred route of catabolism of acetyl-CoA in the *Δlmgt* promastigotes (see Tricarboxylic acid cycle), or converted to acetate, which is another major metabolic end product of glucose metabolism which is excreted by the *Leishmania* cells (Rainey and MacKenzie, 1991). The NMR data showed that both the wild type and *Δlmgt* promastigotes excrete acetate (Tables III-7 and III-8). The wild type promastigotes excreted ^{12}C-acetate when no exogenous carbon sources were available. When ^{13}C-D-glucose, ^{13}C-L-proline, and ^{13}C-L-threonine were supplied as exogenous carbon sources, the wild type promastigotes exceted both ^{12}C-acetate and ^{13}C-acetate (Table III-7). This confirmes that another carbon source, most probably an unlabelled intracellular reserve material such as mannogen, is utilized by the wild type promastigotes in parallel with the exogenous carbon sources. Furthermore, the data show that L-proline, L-threonine or glycerol, when supplied with D-glucose, can serve as precursors for the synthesis of acetate in the wild type promastigotes, as can D-glucose alone (Table III-7). In contrast, *Δlmgt* promastigotes excreted the same amount of ^{12}C-acetate when no carbon sources were available and when D-glucose, L-proline or glycerol were provided (Table III-8). The *Δlmgt* promastigotes, however, excreted more acetate when L-threonine was available as a carbon source. Thus, the NMR data revealed that L-threonine is an important precursor for acetyl-CoA in the *Δlmgt* promastigotes (see Glycine, serine and threonine metabolism).

A further portion of pyruvate can be reversibly transaminated to L-alanine (see Alanine, aspartate andglutamate metabolism) or converted to lactate and subsequently excreted by the *Leishmania* cells (Rainey and MacKenzie, 1991).

Leishmania excrete D-lactate but not L-lactate (Darling *et al.*, 1988). The NMR analysis did not detect D-lactate in the wild type or *Δlmgt* promastigote spent media. The proteomic data, on the other hand, showed that a D-lactate dehydrogenase-like protein, which interconverts pyruvate and D-lactate, was up-regulated in the *Δlmgt* promastigotes (Figure III-18). D-Lactate can be produced from methylglyoxal, a toxic byproduct of glycolysis, which is neutralized by the glyoxylase detoxification system of *Leishmania* (Opperdoes and Michels, 2008). The generated D-lactate can then be converted to pyruvate by the up-regulated D-lactate dehydrogenase-like protein and fed into gluconeogenesis (Figure III-18).

Pentose phosphate pathway

The main function of the pentose phosphate pathway (PPP) (also known as the hexose-monophopshate shunt) is to generate ribose 5-phosphate, used in the synthesis of nucleic acids, NADPH, used in redox reactions, and the glycolytic/gluconeogenic intermediates F6P and GAP. The pathway is divided into two phases, an oxidative phase which includes two irreversible oxidative reactions, and a non-oxidative phase that includes a series of reversible sugar-phosphate interconversions. The first two reactions of the oxidative phase, the irreversible and $NADP^+$-dependent oxidation of G6P to 6-phosphoglucono-1,5-lactone (6PG1,5l) and the conversion of the latter to 6-phosphogluconate (6PG), are catalyzed by glucose 6-phosphate dehydrogenase (G6PDH) and 6-phosphogluconolactonase (6PGIs), respectively. As observed previously in *T. brucei* (Heise and Opperdoes, 1999; Duffieux *et al.*, 2000), glucose 6-phosphate dehydrogenase was found to have dual cytosolic and organellar localization and, along with 6-phosphogluconate dehydrogenase (6PDH), to be down-regulated in the *Δlmgt* promastigotes (Figure III-20). Thus, the phase of the PPP pathway that is responsible for regeneration of NADPH seems to be down-regulated in the *Δlmgt* promastigotes. A main reason for that could be the reduced influx of G6P into the pathway. Another reason for the suppressed oxidative phase, however, could be a decreased demand for NADPH as a result of reduced glycosomal metabolism.

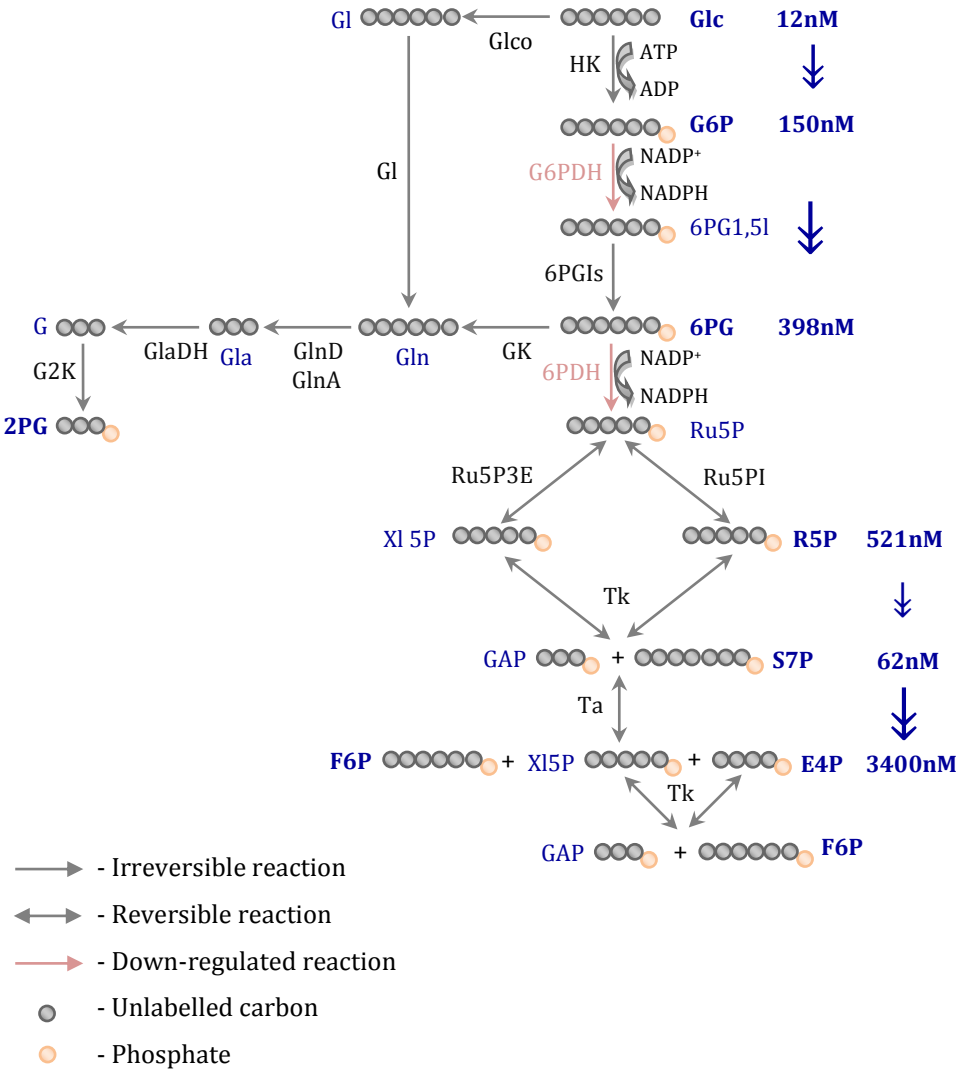

Figure III-20. Schematic representation of pentose phosphate pathway in *Δlmgt* promastigotes incubated with ^{13}C-D-glucose. Presented here are integrated quantitative proteomic, glycomic and stable isotope tracing data. Specified with pink arrows are the down-regulated enzymes. Specified in blue are the PPP intermediates quantified by GC-MS. Indicated next to each quantified metabolite is its concentration in nanomoles (nM). Abbreviations: Gl - gluconolactone, Gln - gluconate, Gla - glyceraldehyde, G - glycerate, 2PG - 2-phosphoglycerate, Glc - glucose, G6P - glucose 6-phosphate, 6PG1,5l - 6-phosphoglucono-1,5-lactone, 6PG - 6-phosphogluconate, Ru5P - ribulose 5-phosphate, Xl5P - xylulose 5-phosphate, R5P - ribose 5-phosphate, GAP - glyceraldehyde 3-phosphate, S7P - sedoheptulose 7-phosphate, F6P - fructose 6-phosphate, E4P - erythrose 4-phosphate, Glco - glucose oxidase, Gl - gluconolactonase, GK - gluconokinase, GlnD - gluconate dehydratase, GlnA - 2-deoxy-3-deoxy-gluconate aldolase, GlaDH - glyceraldehyde dehydrogenase, G2K - glycerate 2-kinase, G6PDH - glucose 6-phophate dehydrogenase, 6PGls - 6-phosphogluconolactonase, 6PDH - 6-phosphogluconate dehydrogenase, Ru 5P3E - ribulose 5-phosphate 3-epimerase, Ru5PI - ribulose 5-phosphate isomerase, Tk - transketolase, Ta - transaldolase.

The non-oxidative phase was not so easy to decipher. Similar to a previous study (Colasante *et al.*, 2006), the first enzymes of the non-oxidative phase, ribulose 5-phosphate 3-epimerase and ribulose 5-phosphate isomerase, which convert ribulose 5-phosphate (Ru5P) to xylulose 5-phosphate (Xl5P) and ribose 5-phosphate (R5P), respectively, were not detected. Ru5P, which was present in the wild type promastigotes, was absent from the *Δlmgt* promastigotes. This shows that G6P is probably not be the main source of R5P in the *Δlmgt* promastigotes. R5P itself was 3 times less in the *Δlmgt* promastigotes compared with the wild type promastigotes (Table III-5). Next, transketolase, a thiamine pyrophosphate (TPP)-dependent enzyme that transfers two-carbon units from Xl5P to either R5P or erythrose 4-phosphate (E4P) to produce GAP, and translaldolase, which interconverts sedoheptulose 7-phosphate (S7P) and GAP into F6P and E4P, were not significantly modulated in the *Δlmgt* promastigotes. Interestingly, E4P, which was not detected in the wild type promastigotes, was present at a relatively high level in the *Δlmgt* promastigotes while S7P levels were reduced (Table III-5). The decrease in S7P and increase in E4P suggests that the equilibrium of the interconversion of S7P and GAP to F6P and E4P is shifted towards the synthesis of F6P. Thus, a main function of the non-oxidative phase in the *Δlmgt* promastigotes could be to maintain the levels of F6P, while E4P is a side product accumulating in the process. Similarly, the increased level of D-ribose, along with the up-regulated ribokinase in the *Δlmgt* promastigotes (Feng *et al.*, 2011), suggests that D-ribose is used for the synthesis of R5P (Table III-5). Ribose is one of the sugars present in the honeydew the sand fly vectors of *Leishmania* feed upon (Cameron *et al.*, 1995). Two studies have characterized ribose transporters in *Leishmania*. Pastakia and Dwyer determined that a specific carrier is involved in the transport of ribose in *L. donovani* promastigotes (Pastakia and Dwyer, 1987). In the second study, Burchmore and colleagues revealed that the *L. mexicana* transporter GT2 can also transport ribose (Naula *et al.*, 2010). The second study also showed that the *Δlmgt* promastigotes are not able to take up ribose. Besides import from the environment, however, ribose can be produced by cleavaging the ribose moieties of nucleosides. In the *Δlmgt* promastigotes, one nonspecific nucleoside hydrolase, which acts on nucleosides and hydrolyses them to ribose and the respective base (see Nucleotide metabolism), was found up-regulated in the *Δlmgt* promastigotes (in preparation). Thus, the up-regulated nucleoside hydrolase and the increased level of ribose in the *Δlmgt* promastigotes indicate that ribose is recycled and most probably used as a main precursor for the production of R5P.

Tricarboxylic acid cycle

The tricarboxylic acid cycle (also known as the citric acid cycle or the Krebs cycle) is characterized with both catabolic and anabolic functions. Many catabolic pathways of carbohydrate, amino acid, and lipid metabolism lead to intermediates of the cycle and many TCA cycle intermediates are precursors for anabolic pathways. For instance, oxaloacetate (OAA) and malate (Mal) are precursors for the synthesis of G6P via gluconeogenesis, succinyl-CoA (Suc-CoA) is a precursor for the synthesis of porphyrins, α-ketoglutarate (α-K) and oxaloacetate are precursors for the synthesis of some amino acids, such as L-glutamate, L-glutamine, L-aspartate, and L-asparagine, and citrate (Cit) is a precursor for the synthesis of fatty acids. In *Leishmania*, the end product of glycolysis, pyruvate (Pyr), can be transported from the cytosol to the mitochondrion where it is converted to acetyl-CoA (Ac-CoA). Acetyl-CoA can be converted to acetate to yield ATP and then excreted by the cells (Rainey and MacKenzie, 1991), or it can be fed into the TCA cycle. In the TCA cycle, acetyl-CoA is oxidized to CO_2 with the concomitant synthesis of key intermediates, ATP, NADH, and $FADH_2$. The reduced coenzymes can then be used by the electron transport chain, localized in the inner mitochondrial membrane, for the production of more ATP (see Energy metabolism).

A recent stable isotope labelling study has provided thorough information regarding the central carbon metabolism of the *L. mexicana* promastigotes grown in media with abundant D-glucose, with a particular focus on the TCA cycle (Saunders *et al.*, 2011). The study showed that the cycle is fully functional in the *Leishmania* promastigotes. Using ^{13}C-D-glucose, we observed that all detected TCA intermediates were heavy-labelled in the wild type *L. mexicana* promastigotes (Figure III-21). Citrate was universally labelled which indicated that oxaloacetate was also universally labelled and the acetyl moiety of acetyl-CoA was 2-^{13}C-labelled, although neither of the two metabolites was detected in condition ***glc0** promastigotes. α-Ketoglutarate and succinate were also universally labelled thus demonstrating the lost of carboxylic groups in the form of CO_2. The last intermediates of the cycle, fumarate and malate, were also universally labelled (Figure III-21). α-Ketoglutarate, fumarate and oxaloacetate are precursors for the synthesis of L-glutamate and L-glutamine and L-aspartate and L-asparagine, respectively, which were also found universally labelled in the wild type promastigotes (see Arginine, glutamate and proline and Alanine and aspartate metabolism).

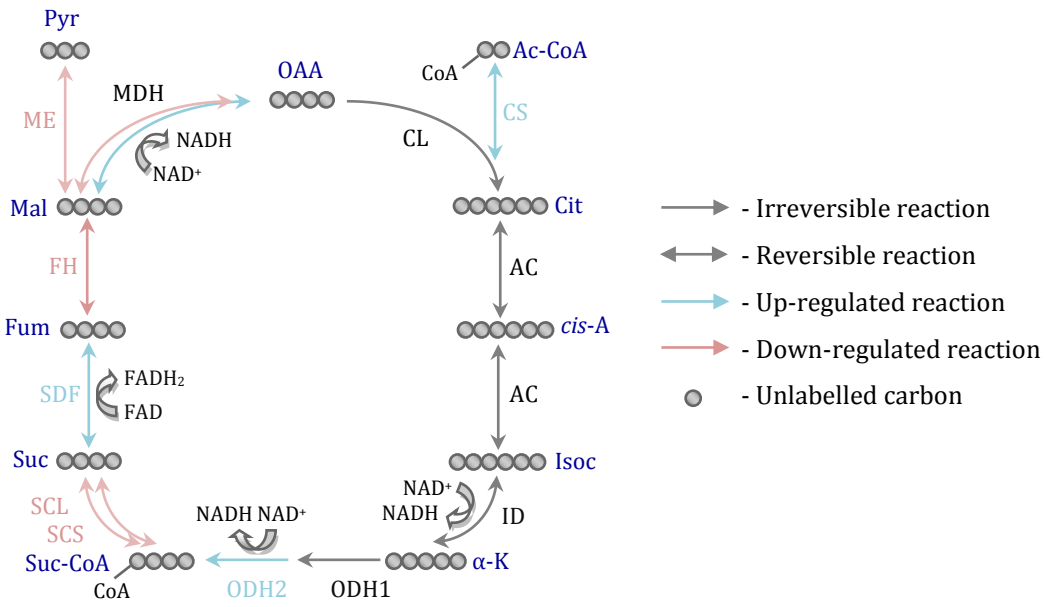

Figure III-21. Schematic representation of tricarboxylic acid cycle in *Δlmgt* promastigotes incubated with ^{13}C-D-glucose. Presented here are integrated quantitative proteomic and glycomic data. Specified with light blue arrows are the up-regulated enzymes while specified with pink arrows are the down-regulated enzymes. Abbreviations: Ac-CoA - acetyl-CoA, OAA - oxaloacetate, Cit - citrate, *cis*-A - *cis*-aconitate, Isoc - isocitrate, α-K – α-ketoglutarate, Suc-CoA - succinyl-CoA, Suc - succinate, Fum - fumarate, Mal - malate, Pyr - pyruvate, CL - citrate lyase, CS - citrate synthase, AC - aconitase, ID - isocitrate dehydrogenase, ODH1 - 2-oxoglutarate dehydrogenase E1 component, ODH2 - 2-oxoglutarate dehydrogenase E2 component, SCL - succinyl-CoA ligase, SCS - succinyl-CoA synthetase, SDF - succinate dehydrogenase flavoprotein, FH - fumarate hydratase, MDH - malate dehydrogenase, ME - malic enzyme.

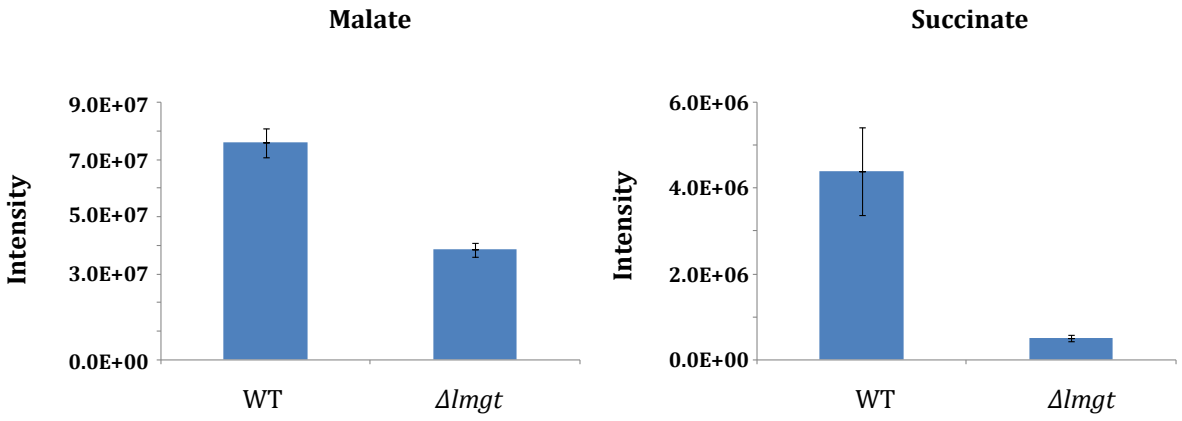

Figure III-22. Histograms of malate and succinate in the wild type and *Δlmgt* promastigotes.

In the *Δlmgt* promastigotes, the TCA intermediates were labelled only in conditions **glc+*pro** and ***pro**, in which ^{13}C-L-proline was present, and slightly labelled in conditions **glc+*thr** and ***thr**, where ^{13}C-L-threonine was provided as a carbon source. That shows that L-proline is used to replenish the TCA cycle intermediates in the *Δlmgt* promastigotes (see Arginine and proline metabolism), and only a small amount of L-threonine contributes to that (see Glycine, serine and threonine metabolism). The untargeted metabolomic data revealed that malate and succinate were decreased in the *Δlmgt* promastigotes compared with the wild type promastigotes (Figure III-22). The NMR analysis confirmed that the *Δlmgt* promastigotes excreted less succinate compared with the wild type promastigotes (Table III-8). The analysis elaborated also that:

- wild type and *Δlmgt* promastigotes excrete succinate when incubated without exogenous carbon sources, thus indicating that both cell lines rely on reserves, most probably mannogen;

- the higher amount of labelled succinate originating from ^{13}C-D-glucose, when the latter was provided as a sole carbon source, compared to the one produced from the intracellular carbon source showed that the sugar, as expected, was actively metabolized by the wild type promastiogtes when available;

- the amount of succinate produced from D-glucose decreased when L-proline was provided as an additional carbon source while the amount of succinate produced from L-proline increased; that indicated that the contribution of L-

proline to the TCA cycle anaplerosis in the wild type promastigotes is greater when both nutrients are utilized together;

- the amount of succinate excreted by the wild type promastigotes when incubated with D-glucose and L-threonine was comparable to that of the wild type promastigotes incubated with no carbon sources; that showed again that the majority of L-threonine is not fed into the TCA cycle in the wild type promastigotes;

- last, the *Δlmgt* promastigotes excreted more or less the same small amount of succinate when incubated with no carbon sources or with D-glucose and L-proline.

In conclusion, the proteomic characterization revealed that a considerable number of reactions of the TCA cycle were regulated in the *Δlmgt* promastigotes, that more than one enzyme is involved in the catalysis of some reactions, and that the pathway was up-regulated at the points of entry of acetyl-CoA and α-ketoglutarate. L-Alanine was shown to be converted to acetyl-CoA and used in the TCA cycle anaplerosis in wild type *L. mexicana* promastigotes grown under D-glucose-replete conditions (Saunders *et al.*, 2011). A number of other glucogenic and ketogenic amino acids can also be converted to acetyl-CoA and fed either in gluconeogenesis or the TCA cycle where they are used for the synthesis of G6P or oxidized for energy, respectively (see Amino acid metabolism). Lipid metabolism is also a source of acetyl-CoA. Another recent study of McConville and colleagues confirmed that fatty acids fuel the TCA cycle with acetyl-CoA (Saunders *et al.*, 2014). The analysis elaborated further that β-oxidation of fatty acids, by which acetyl-CoA is generated, is stimulated in *L. mexicana* promastigotes grown in D-glucose-restricted conditions and that acetyl-CoA is used for the synthesis of L-glutamate and L-glutamine via the TCA cycle. β-Oxidation of fatty acids in the *Δlmgt* promastigotes, however, appears to be down-regulated (see Lipid metabolism). Moreover, in the *Δlmgt* promastigotes, the cycle seems to utilize much more L-glutamate than it generates. L-Glutamate and L-proline, via L-glutamate, can enter the TCA cycle via α-ketoglutarate. The labelled TCA cycle intermediates in the conditions with heavy L-proline confirmed that the amino acid is used to replenish the TCA cycle intermediates in the *Δlmgt* promastigotes (see Arginine, glutamate and proline metabolism). Finally, in addition to L-alanine, L-aspartate, which can enter the TCA cycle via fumarate or oxaloacetate, was also

shown to be used in TCA cycle anaplerosis (Saunders *et al.*, 2011). Thus, other amino acids besides L-proline are most probably mobilized as carbon sources for the TCA cycle in the *Δlmgt* promastigotes (see Amino acid metabolism). In addition to the reactions feeding acetyl-CoA and α-ketoglutarate to the TCA cycle, the succinate-to-fumarate conversion catalyzed by succinate dehydrogenase (SDH) was also up-regulated in the *Δlmgt* promastigotes (Figure III-21). Succinate dehydrogenase is complex II of the electron transport chain that links the TCA cycle with the cellular respiration. It catalyzes the oxidation of succinate to fumarate and transfers the electrons yielded in the reaction to ubiquinone which is reduced to ubiquinol (see Energy metabolism). The significantly reduced level of succinate in the *Δlmgt* promastigote (Figure III-22) and up-regulated oxidation of succinate indicate that the TCA cycle is one of the main participants in energy generation in the *Δlmgt* promastigotes. Thus, the integrated multi-omic data depicted a quite dynamic and complicated TCA cycle with a key role in the *Δlmgt* promastigote metabolism.

III.3. Summary

The thorough analysis of carbohydrate metabolism in the glucose transporter null mutant *Leishmania* revealed that the inability of the insect form to utilize exogenous D-glucose as an energy and carbon source leads to a distinct shift in key pathways of central carbon metabolism. D-Glucose transport deficiency in the *Δlmgt* promastigotes results in utilization of alternative sugars such as sucrose which appears to be the main source of D-glucose and D-fructose for these organisms (Figure III-23). The produced D-glucose is used for the synthesis of G6P but it is not further catabolized via glycolysis. Instead, gluconeogensis is the dominant pathway which also functions toward the synthesis of G6P. Gluconeogesis, however, is still ineffective in meeting the biosynthetic requirements of the *Δlmgt* promastigotes because pathways for which G6P is the main precursor, such as inositol synthesis and the PPP pathway, have decreased activity in these organisms. Exogenous inositol and/or lipid metabolism appear to be the main source(s) for inositol while D-ribose, originating most probably from nucleotide degradation, is used, instead of G6P, for the synthesis of R5P (Figure III-23). The decreased influx of G6P in the PPP further impacts the regeneration of NADPH which is believed to be the main reason behind the high sensitivity of the *Δlmgt* promastigotes to oxidative stress.

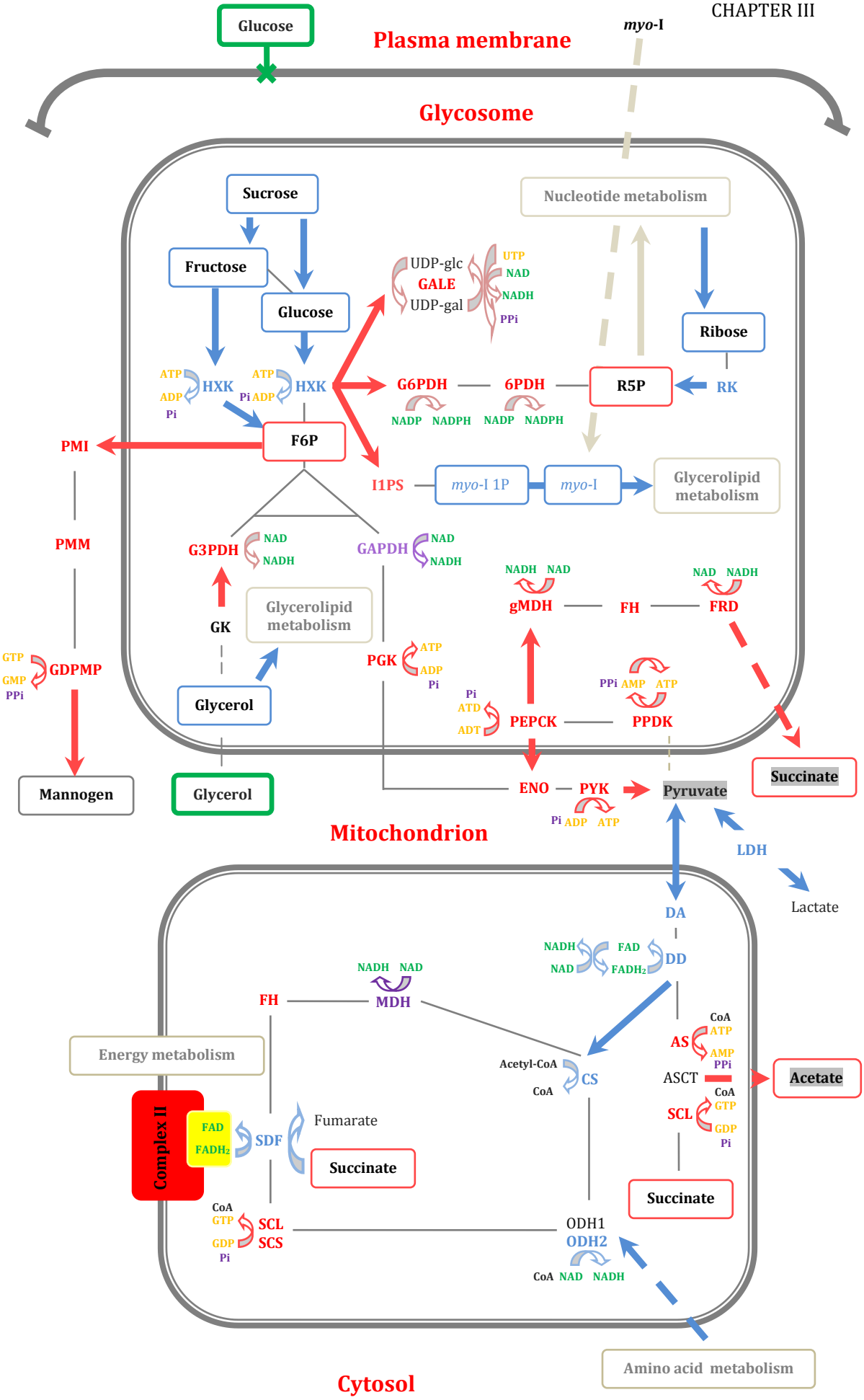

The legend is presented on page 113.

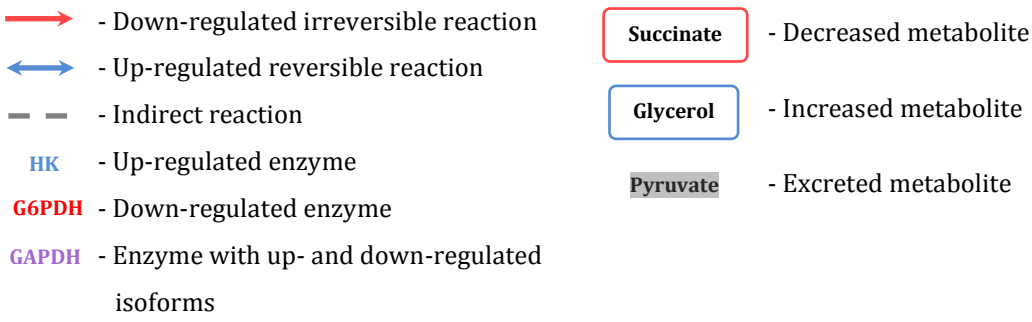

Figure III-23. Schematic representation of the changes in carbohydrate metabolism in the *Δlmgt* promastigotes. Specified with red arrows are the down-regulated enzymes while indicated in blue are the up-regulated enzymes. Abbreviations: F6P - fructose 6-phosphate, R5P – ribose 5-phosphate, *myo*-I 1P - *myo*-inositol 1-phosphate, *myo*-I - *myo*-inositol, UDP-glc - uridine 5'-diphosphate glucose, UDP-gal - uridine 5'-diphsophate galactose, AMP - adenosine 5'-monophosphate, ADP - adenosine 5'-diphosphate, ATP - adenosine 5'-triphosphate, GMP - guanosine 5'-monophosphate, GDP - guanosine 5'-diphosphate, GTP - guanosine 5'-triphosphate, NAD - nicotinamide adenine dinucleotide, NADP - nicotinamide adenine dinucleotide phosphate, FAD - flavin adenine dinucleotide, CoA - coenzyme A, Pi - inorganic phosphate, HXK - hexokinase, GAPDH - glyceraldehyde 3-phosphate dehydrogenase, PGK - phosphoglycerate kinase, ENO - enolase, PYK - pyruvate kinase, PPDK - pyruvate phosphate dikinase, GK - glycerol kinase, G3PDH - glycerol 3-phosphate dehydrogenase, DA - dihydrolipoamide acetyltransferase, DD - dihydrolipoamide dehydrogenase, PEPCK - phosphoenolpyruvate carboxikinase, GALE - uridine 5'-diphopshate glucose 4'-epimerase, G6PDH - glucose 6-phophate dehydrogenase, 6PDH - 6-phosphogluconate dehydrogenase, RK - ribokinase, I1PS - inositol 1-phosphate synthase, PMI - phosphomannose isomerase, PMM - phosphomannomutase, GDPMP - 5'-guanosine diphosphate mannose pyrophosphorylase, CS - citrate synthase, ODH1 - 2-oxoglutarate dehydrogenase E1 component, ODH2 - 2-oxoglutarate dehydrogenase E2 component, SCL - succinyl-CoA ligase, SCS - succinyl-CoA synthetase, SDF - succinate dehydrogenase flavoprotein, FH - fumarate hydratase, FRD - fumarate reductase, MDH - malate dehydrogenase, gMDH - glycosomal malate dehydrogenase, ME - malic enzyme, AS - acetyl-CoA synthetase, ASCT - acetate:succinate CoA transferase.

D-Fructose, produced from the break down of sucrose, is phosphorylated to F6P. F6P, through GDP-Man, is used for the synthesis of a variety of Man-containing macromolecules such as glycoconjugates and mannogen. The levels of certain glycoconjugates and mannogen, however, are decreased in the *Δlmgt* promastigotes which again shows that D-glucose, D-fructose, and gluconeogenesis are not able to provide enough precursors for biosynthetic purposes. Down-regulated in the *Δlmgt* promastigotes is also the glycosomal succinate fermentation. Changes in the glycosomal succinate fermentation affect the glycosomal redox/energy balance and the contribution of dicarboxylic acids to the TCA cycle. Instead of dicarboxylic acids from the glycosomal succinate fermentation, a substantial part of pyruvate and L-threopnine appear to be preferentially converted to acetyl-CoA and fed into the TCA cycle. Furthermore, amino acids such as L-alanine, L-aspartate, L-glutamate, and L-proline are also oxidize in the TCA cycle for the production of energy in the *Δlmgt* promastigotes. Altogether, our study confirmed that *Leishmania* promastigotes rely heavily on D-glucose for optimal functioning and showed that when the latter cannot be utilize as a carbon and energy source, due to a genetic ablation of the three primary glucose transports, the organisms alter their metabolism to use i/ alternative

sugars for the production of D-glucose, ii/ alternative carbon sources, such as amino acids, glycogen, and acetate, for the production of biosynthetic precursors, and iii/ alternative sources, such as amino acids, for the generation of energy. Alternative metabolism, thus, appears to be essential for *Leishmania* adaptation and survival in conditions with a varying nutrient content and fluctuating nutrient levels. Investigating the utilization of secondary (in terms of consumption) and/or less abundant nutrients such as di- and trisaccharides, glucogenic and ketogenic amino acids, and lipids as alternative carbon and energy sources, as well as elucidating the kinetics of the pathways involved in the metabolization of these sources, will shed light on the copmplexity of the central carbon metabolism and will point out essential processes as drug targets. Our data showed that one such process could be the defence against oxidative stress.

CHAPTER IV. Quantitative characterization of amino acid, energy, nucleotide and lipid metabolism of *Δlmgt* promastigotes by stable isotope dimethyl labelling and global metabolomics

Essential substrates for *Leishmania*, besides carbohydrates, include amino acids, lipids, nucleotides, cofactors, and vitamins. In the insect vector, amino acids and proteins are among the blood meal nutrients. Additionally, amino acids are abundant in the honeydew and plant sap on which the sand flies primarily feed (Sandstrom and Moran, 2001; Weibull *et al.*, 1990). In the parasitophorous vacuole of the mammalian host macrophages, a variety of low-molecular-weight metabolites, including amino acids and peptides, may be generated by the hydrolytic enzymes localized in this compartment. Moreover, it has been shown that amastigotes can up-regulate the expression of certain cysteine proteases, offering a mechanism to provide additional sources of amino acids (Besteiro *et al.*, 2007). In axenic cultures, both promastigotes and amastigotes are typically maintained in media that are rich in amino acids (Berens *et al.*, 1976). From these niches, amino acids can be taken by *Leishmania* by a large family of amino acid permeases (AAP), some of which have already been characterized. For instance, AAP3, AAP7 and AAP24 of *L. donovani* transport L-arginine, L-lysine and L-proline and L-alanine, respectively (Shaked-Mishan *et al.*, 2006; Inbar *et al.*, 2012; Inbar *et al.*, 2013). Characterized in *Leishmania* were also an L-glutamate, L-methionine and L-serine transport systems (Paes *et al.*, 2008; Mukkada and Simon, 1977; dos Santos *et al.*, 2009). The imported amino acids can enter the intracellular free amino acid pool. L-Alanine, L-ornithine, L-glutamine and glycine were shown to be the main constituents comprising the pool of free amino acids in the promastigotes, although the cells maintain most of the amino acids present at all time (Simon *et al.*, 1983; Shaked-Mishan *et al.*, 2006). Amino acids are important sources of carbon and energy, essential building blocks for protein and polyamine biosynthesis, and osmolytes (Naderer and McConville, 2008, Blum, 1996). When used as energy sources, some amino acids can be partially oxidized to pyruvate, α-ketoglutarate, succinate, fumarate, oxaloacetate and acetyl-CoA and consequently directed to gluconeogenesis for the synthesis of D-glucose or oxidized in the TCA cycle to CO_2 with the generation of ATP and NADH (Figure IV-1).

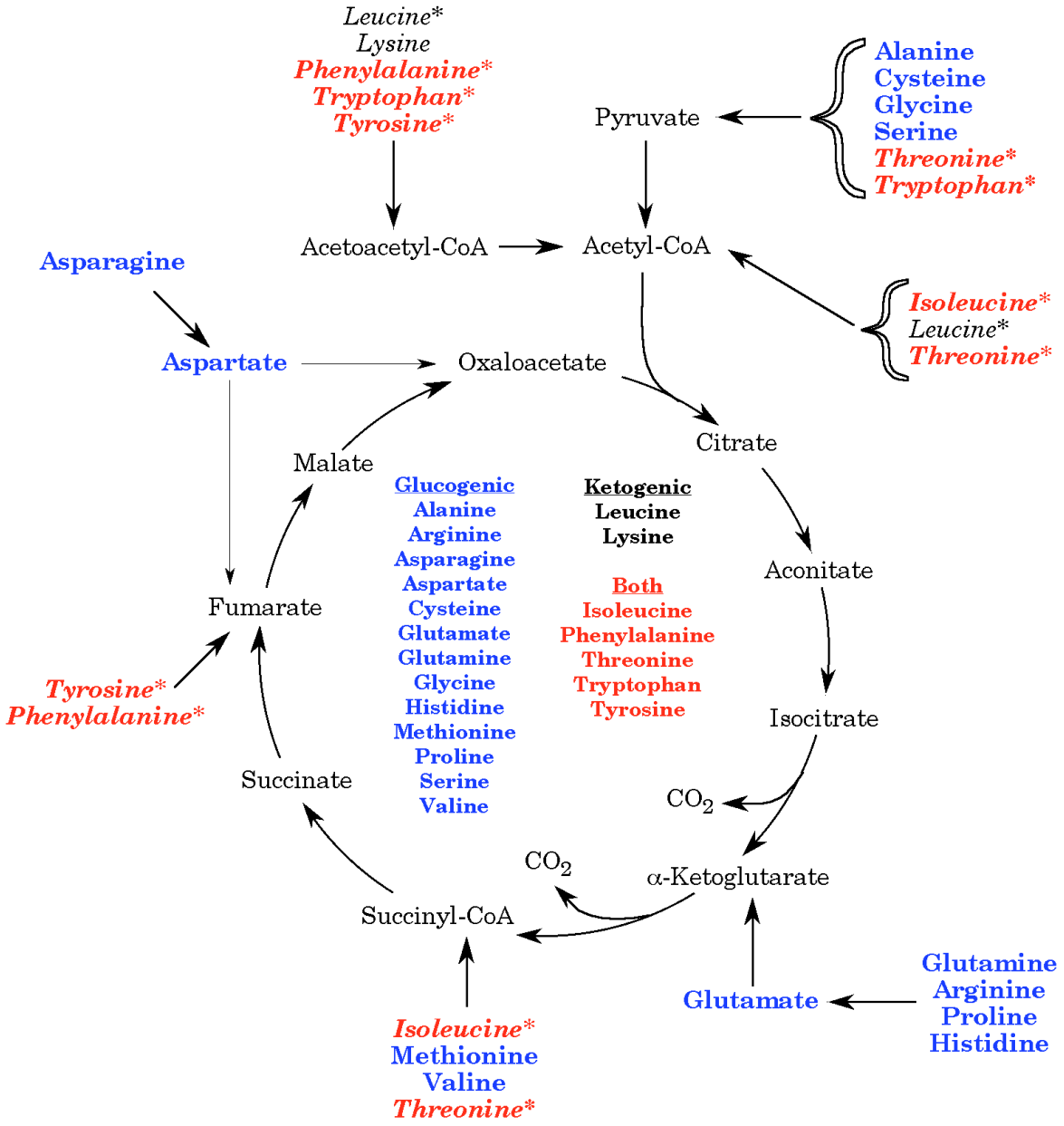

Figure IV-1. Schematic representation of amino acid catabolism.

Another class of important nutrients for *Leishmania* are lipids. Contrary to promastigotes, amastigotes develop in a sugar-poor environment where β-oxidation of fatty acids appears to be of central importance for the parasite viability (Hart and Coombs, 1982; Opperdoes and Michels, 2008). β-Oxidation of fatty acids results in the breakdown of fatty acids to acetyl-CoA, NADH and $FADH_2$. Acetyl-CoA is further oxidized in the TCA cycle while the NADH and $FADH_2$ produced are directed toward the electron transport chain for the production of ATP. Thus, besides amino acids, fatty acids could be important energy sources for *Leishmania*. In addition to energy sources, lipids are essential structural components and building blocks of a variety of glycoconjugates. Expressed on the promastigote surface are mainly lipophosphoglycan (LPG) and GPI-anchored proteins. LPG was shown to have a number of functions including the attachment of the promastigotes to the insect stomach epithelium, protection against oxidative radicals and nitric oxide upon promastigote phagocytosis, protection against lysis by the complement system, and hindrance of phagolysosome maturation (Novozhilova and Bovin, 2010 and the references therein). gp63, the major surface protein of the *Leishmania* promastigotes, on the other hand, is involved in protein hydrolysis, e.g. of protein of the extracellular matrix or the opsonizing components of the complement system, as well as receptor-mediated interactions with the host macrophages and with the complement cascade (Novozhilova and Bovin, 2010 and the references therein).

Nucleotide metabolism is also important in *Leishmania* biology. While the insect and mammalian hosts of *Leishmania* have the ability to synthesize purines *de novo*, *Leishmania* are auxotrophic for these important nutrients and must salvage them from the host environments. Two high-affinity nucleoside transporters, NT1 and NT2, which belong to the equilibrative nucleoside transporter (ENT) family, were detected through biochemical and genetic approaches in *L. donovani* promastigotes (Aronow *et al.*, 1987; Vasudevan *et al.*, 1998; Carter *et al.*, 2000). NT1 is encoded by two closely related genes, *NT1.1* and *NT1.2*, and transports adenosine and uridine. NT1.1 was suggested to transport also thymidine and cytidine while NT1.2 can also mediate the uptake of inosine and guanosine (Vasudevan *et al.*, 1998; Carter *et al.*, 2000; de Koning *et al.*, 2005). NT2 is encoded by a single gene and is involved in the transport of inosine and guanosine only (Carter *et al.*, 2000). Functioning in *L. major* are also the nucleobase transporters NBT1 (Al-Salabi *et al.*, 2003), NT3 (Sanchez *et al.*, 2004) and NT4 (Ortiz *et al.*, 2007). The NBT1 was shown to be a high-affinity permease with

specificity for adenine, hypoxanthine and the antileishmanial hypoxanthine analogue allopurinol (Al-Salabi *et al.*, 2003). Functional characterization of the *NT3* and *NT4* genes in *L. major* revealed that NT3 is the principle nucleobase transporter in promastigotes which mediates the uptake of hypoxanthine, xanthine, adenine and guanine (Sanchez *et al.*, 2004). NT4 was shown to be a low-affinity transporter of adenine at neutral pH (Ortiz *et al.*, 2007). At acidic pH, however, the NT4 transporter is activated to transport hypoxanthine, guanine, and xanthine as well (Ortiz *et al.*, 2009). Besides purine nucleoside/nucleobase transporters, implicated in the purine salvage pathway are also a number of plasma membrane and secreted nucleotidase/ nucleases, hydrolases, phosphorybosyl transferases, kinases and deaminases (Sopwith *et al.*, 2002; Landfear *et al.*, 2004; Joshi and Dwyer, 2007; Colasante *et al.*, 2006).

Contrary to purines, *Leishmania* are able to synthesize as well as take some pyrimidines from the environment. The first pyrimidine transporter of *Leishmania* was described in 2005 by de Koning and colleagues. They showed that the U1 transporter of *L. major* is a high-affinity, high-specificity uracil transporter that does not transport other pyrimidine or purine nucleobases or pyrimidine nucleosides (Papageorgiou *et al.*, 2005).

Purines and pyrimidines are essential nutrients with versatile functions in cellular metabolism. Adenosine 5'-triphosphate (ATP) is used as a universal source of energy in energy transfer processes, cyclic adenosine 5'-monophosphate (cAMP) and cyclic guanosine 5'-monophosphate (cGMP) are key second messengers, nucleotides are precursors for deoxyribonucleic acid (DNA) and ribonucleic acid (RNA) synthesis and nucleotide derivatives are important cofactors.

While chapter III elaborated on the changes in carbohydrate metabolism in the *Δlmgt* promastigotes, this chapter focuses on *Leishmania* proteins and metabolites that are involved in amino acid, energy, lipid and nucleotide metabolism. The applied proteomic and metabolomic approaches included stable isotope dimethyl labelling, untargeted LC-MS analysis and NMR analysis. The NMR analysis involved incubation of wild type and *Δlmgt* promastigotes with stable isotope labelled D-glucose, L-proline and L-threonine (see **III.1.2.3.** for details), which allowed us to perform a stable isotope tracing analysis and elucidate the preferences of the *Δlmgt* promastigotes for carbon sources.

IV.1. Results

IV.1.1. Quantitative proteomic characterization of amino acid, energy, nucleotide and lipid metabolism of *Δlmgt* promastigotes by sub-cellular fractionation with digitonin and stable isotope dimethyl labelling

The quantitative proteomic characterization of the *Δlmgt* promastigotes involved sub-cellular fractionation with digitonin coupled to stable isotope dimethyl labelling and 1D HPLC ESI-MS/MS analysis. 5 sub-cellular fractions were generated, and analysed to enhance proteomic coverage over that expected with unfractionated cell lysates (see Chapter III). A total of 217 proteins were significantly modulated when *Δlmgt* promastigotes were compared with wild type. Nearly half of the modulated proteins in the *Δlmgt* promastigotes were enzymes (Figure III-7). In turn, half of the enzymes were metabolic enzymes involved in amino acid, carbohydrate, energy, lipid and nucleotide metabolism, metabolism of vitamins and cofactors and metabolism of terpenoids and polyketides (Supplemental table III-1). Further to the enzymes of carbohydrate metabolism (see Chapter III, **III.1.1.2.**), enzymes of amino acid, energy, lipid and nucleotide metabolism were also investigated. 4 pathways and 7 enzymes of amino acid metabolism, 6 enzymes of energy metabolism, 8 enzymes of nucleotide metabolism and 3 enzymes of lipid metabolism were differentially regulated. Glutamate dehydrogenase, alanine aminotransferase and arginase were down-regulated by >10-fold, >5-fold and >2-fold, respectively (Supplemental table III-1). Enzymes of L-methinine, L-lysine and glycine metabolism were also modulated in the *Δlmgt* promastigotes (Supplemental table III-1).

The majority of the enzymes involved in energy metabolism were detected in the second fraction enriched with glycosomal and mitochondrial proteins and the fraction with digitonin-insoluble proteins. Detection of most respiratory complex subunits in the last fractions is indicative of the highly hydrophobic nature of these proteins (Maslov *et al.*, 2002). The regulated enzymes were a putative cytochrome *c* oxidase subunit V and 4 subunits of complex V: ATPase α subunit, ATPase β subunit, ATP synthase F1 subunit γ protein and ATP synthase, ε chain and most of them were up-regulated (Supplemental table III-1).

A considerable number of enzymes of nucleotide metabolism were differentially expressed in the *Δlmgt* promastigotes. In view of their importance and the inability of the *Leishmania* parasites to synthesize purines (Opperdoes and Michels, 2008), the

majority of the modulated enzymes belonged to purine salvage pathway. In turn, the majority of the enzymes of the purine metabolism, namely an adenosine kinase, an adenine phosphoribosyltransferase, a guanine deaminase, a bifuntional 3'-nucleotidase/ nuclease precursor, a nucleoside hydrolase-like protein and a xanthine phosphoribosyltransferase, were down-regulated (Supplemental table III-1) while up-regulated in the *Δlmgt* promastigotes was a nonspecific nucleoside hydrolase. Of the pyrimidine metabolism, only aspartate carbamoyltransferase was modulated.

Finally, the 3 differentially expressed enzymes of lipid metabolism were the significantly up-regulated β-ketoacyl-CoA reductase which participates in fatty acid biosynthesis, the down-regulated electron transfer flavoprotein, α polypeptide which links β-oxidation of fatty acids with cellular respiration and alkyl dihydroxyacetone-phosphate synthase which is involved in glycerolipid biosynthesis.

IV.1.2. Global metabolomic characterization of amino acid, energy, nucleotide and lipid metabolism of *Δlmgt* promastigotes

The untargeted metabolomic characterization of the *Δlmgt* promastigotes involved cold chloroform/methanol/water extraction and 1D pHILIC-HPLC ESI-MS analysis (see Chapter III, **III.1.2.**). The data revealed that 79 of the cell metabolites and 43 of the metabolites excreted by promastigotes were significantly modulated (Supplemental tables III2 and III-3). Lipids and amino acids comprised the two largest groups of the significantly modulated metabolites in the cells and the spent media. 6 metabolites of amino acid metabolism were authentically identified. The glucogenic amino acids L-alanine, L-aspartate and L-glutamate were significantly down-regulated in the *Δlmgt* promastigotes compared to the wild type promastigotes (Figure IV-2). L-Alanine and L-proline were decreased in the *Δlmgt* spent media as well (Figure IV-2). Glutathione, an important antioxidant for trypanosomatids, was also decreased in the *Δlmgt* promastigotes (Figure IV2) while phenylpyruvate was increased in the ccells but decreased in the spent media (Figure IV-3).

Lipids represented more than half of the significantly modulated metabolites in the *Δlmgt* promastigotes (Figure III-9). There were fatty acids, glycerophosphocholines, glycerophosphoethanolamines, glycerophosphoserines and sphingoid bases. Authentically identified, however, were only phosphoethanolamine and phosphocholine which were increased in the *Δlmgt* promastigotes (Figure IV-3).

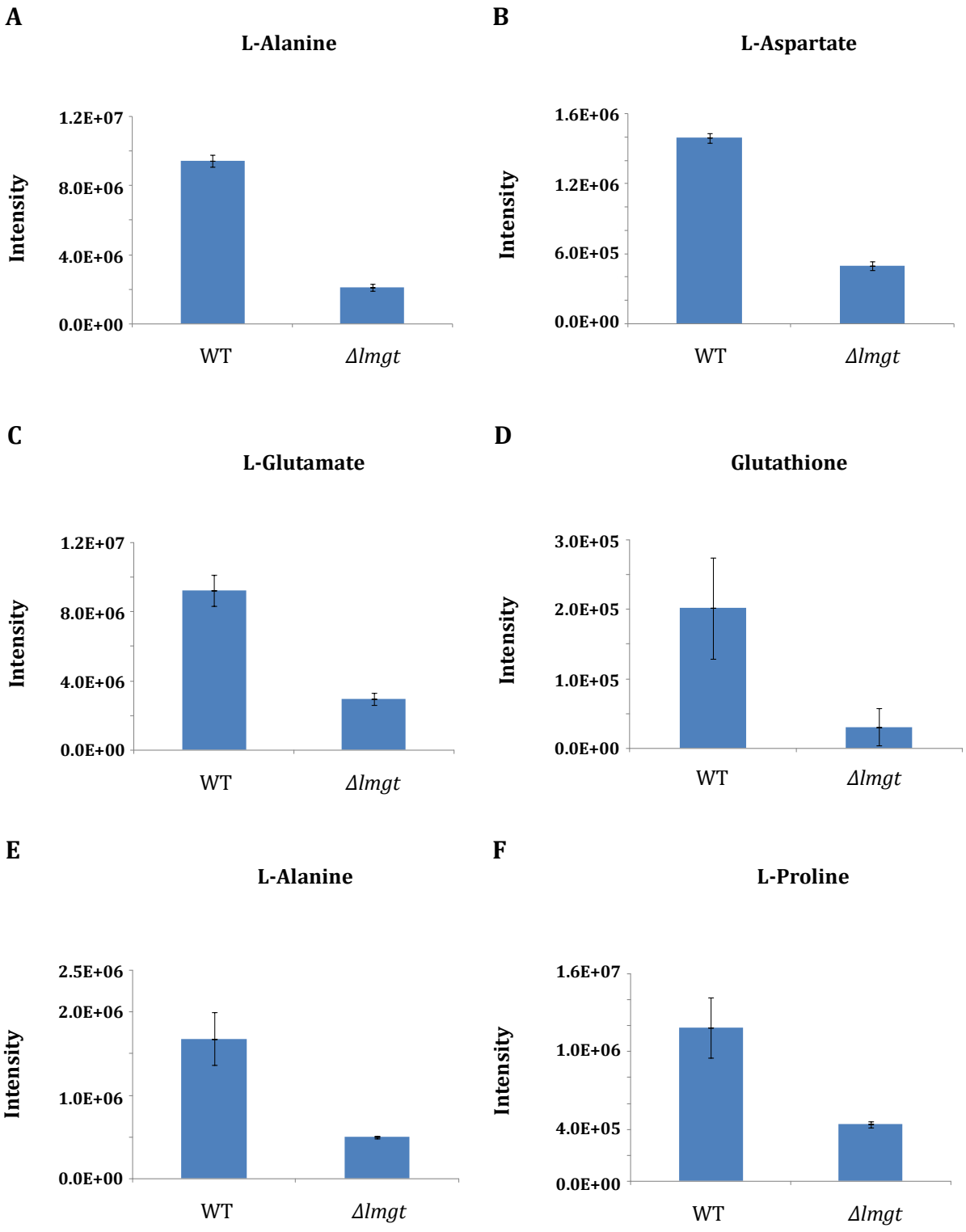

Figure IV-2. Histograms of L-alanine (A), L-aspartate (B), L-glutamate (C) and glutathione (D) in the wild type and *Δlmgt* promastigotes and of L-alanine (E) and L-proline (F) in the wild type and *Δlmgt* promastigote spent media.

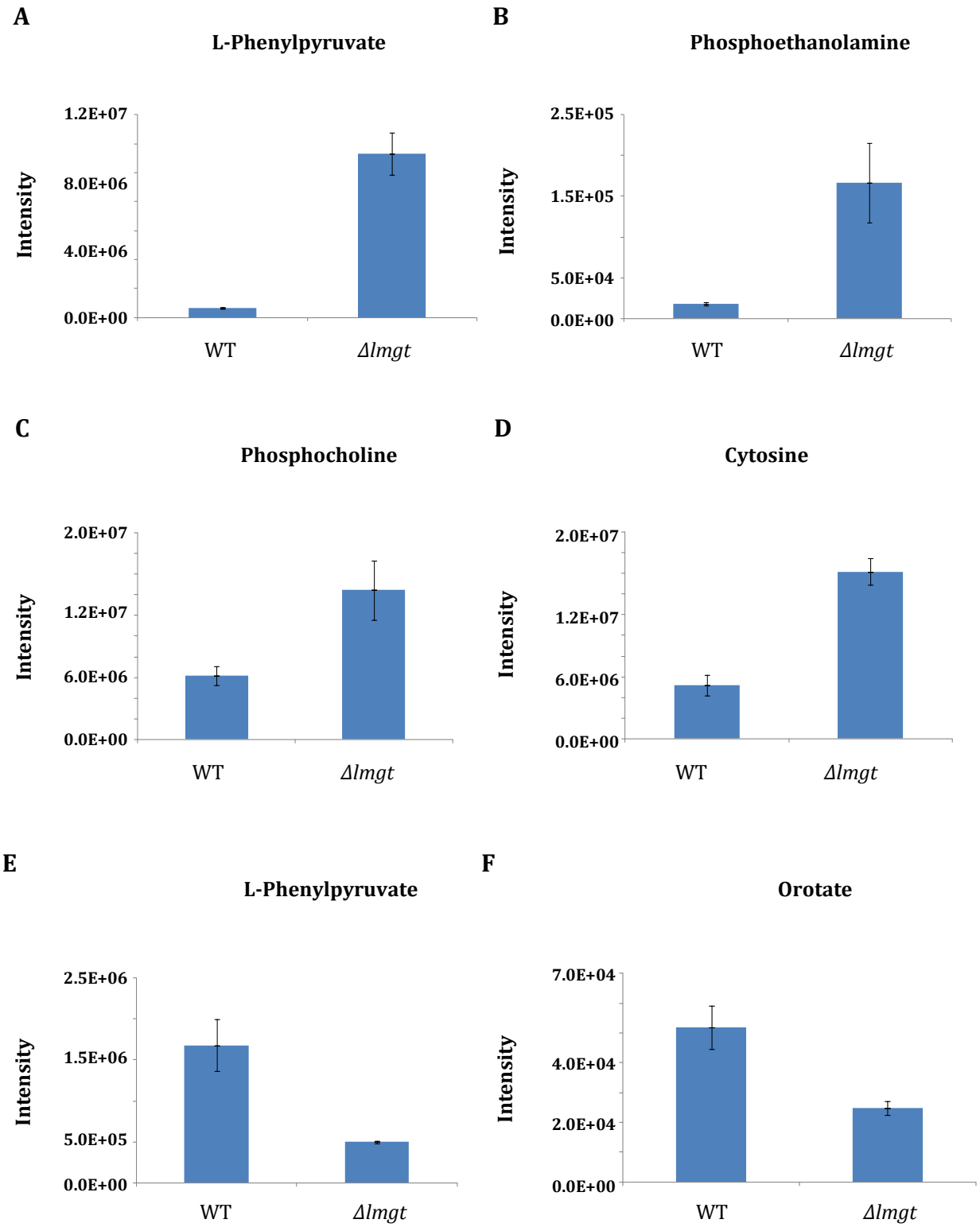

Figure IV-3. Histograms of L-phenylpyruvate (A), phosphoethanolamine (B), phosphocholine (C) and cytosine (D) in the wild type and *Δlmgt* promastigotes and of L-phenylpyruvate (E) and orotate (F) in the wild type and *Δlmgt* promastigote spent media.

Of the metabolism of cofactors and vitamins, nicotinate had significantly increased level in the *Δlmgt* promastigotes (Supplemental table III-2). Finally, of nucleotide metabolism, cytosine was slightly increased in the *Δlmgt* promastigotes while orotate was significantly decreased in the spent media (Figure IV-3).

IV.1.3. Stable isotope tracing analysis of amino acid, energy, nucleotide and lipid metabolism of *Δlmgt* promastigotes

The stable isotope tracing analysis of the *Δlmgt* promastigote carbohydrate metabolism revealed that sugars and intermediates of glycolysis/gluconeogenesis, fructose, mannose and galactose metabolism, pentose phosphate pathway, TCA cycle and other pathways were heavy-labelled only in the conditions with ^{13}C-L-proline and ^{13}C-L-threonine (see **III.1.2.3.** for details about the ten NMR conditions). ^{13}C-D-glucose was supplied in conditions ***glc0**, ***glc**, **pro+*glc**, **thr+*glc** and **glr+*glc**, ^{13}C-L-proline in conditions **glc+*pro** and ***pro** and ^{13}C-L-threonine in conditions **glc+*thr** and ***thr**. In addition to the 15 pathways of carbohydrate metabolism, 12 pathways of amino acid, lipid and nucleotide metabolism were investigated.

Amino acid metabolism

Alanine and aspartate metabolism

In addition to using exogenous L-alanine (Inbar *et al.*, 2013), *Leishmania* are able to synthesize the amino acid from pyruvate via a cytosolic alanine aminotransferase. L-Alanine, along with L-aspartate, L-asparagine and 4-aminobutanoate, was authentically identified and universally labelled in conditions ***glc0**, ***glc**, **pro+*glc**, **thr+*glc** and **glr+*glc** wild type promastigotes and in conditions **glc+*pro** and ***pro** *Δlmgt* promastigotes (Figure IV-5; Supplemental table IV-1). The universal labelling of L-alanine (Figure IV-4) indicates that pyruvate, produced from D-glucose in the wild type promastigotes and from L-proline in the *Δlmgt* promastigotes is transaminated to L-alanine. Similarly, the universal labelling of L-aspartate and L-asparagine (Figure IV-4) shows that the two amino acids are synthesized from oxaloacetate by a mitochondrial aspartate aminotransferase and asparagine synthase, respectively (Opperdoes and Michels, 2008). Putatively identified and labelled in the wild type promastigotes were also L-argininosuccinate and adenylosuccinate which means that L-aspartate may also be produced from fumarate.

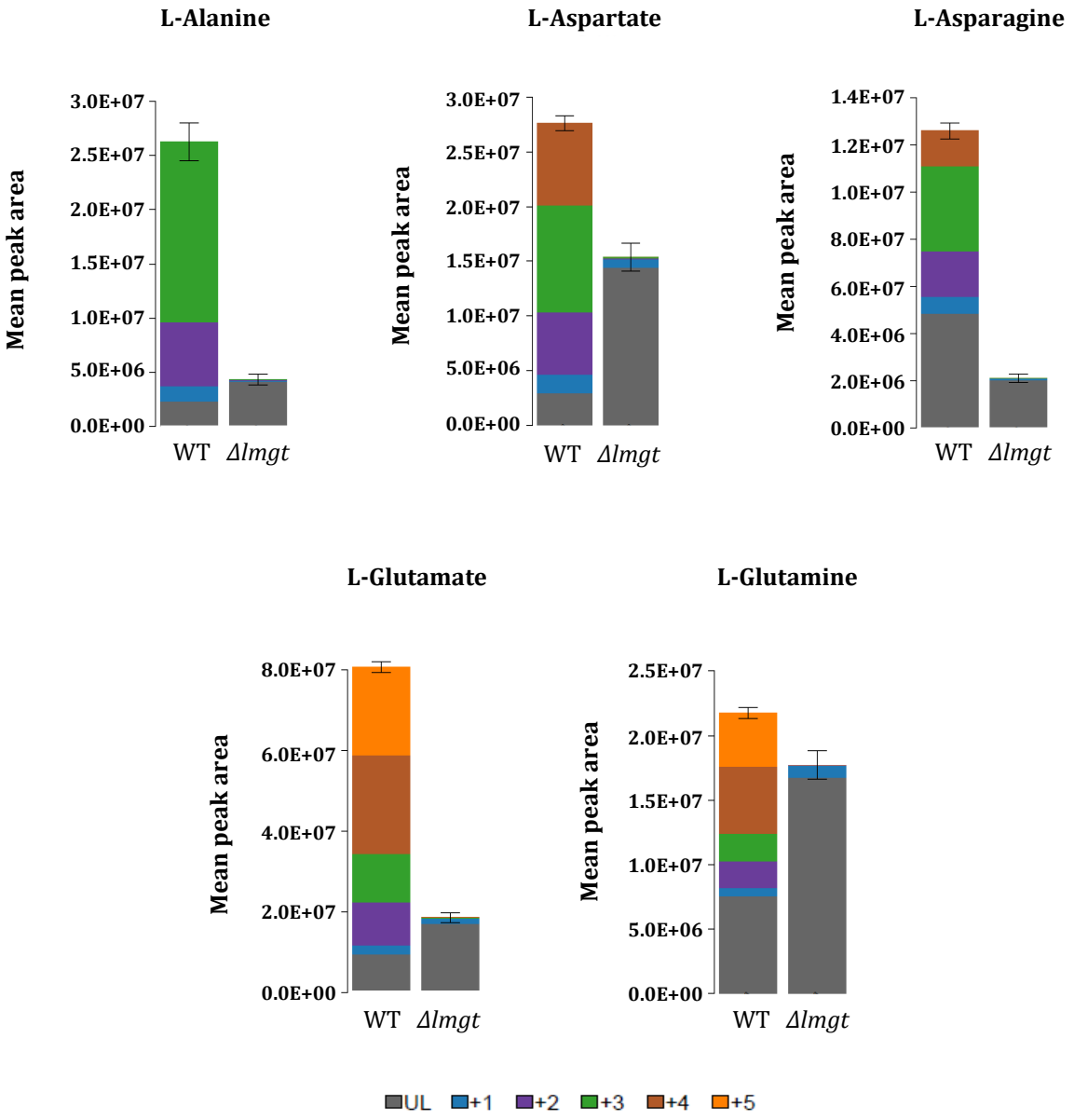

Figure IV-4. Labelling pattern of L-alanine, L-aspartate, L-asparagine, L-glutamate and L-glutamine in wild type and *Δlmgt* promastigotes incubated with ^{13}C-D-glucose. Wild type and *Δlmgt* promastigotes (biological replicates, n=3) were grown with ^{13}C-D-glucose (condition 0) and subjected to cold chloroform/methanol/water metabolite extraction. The metabolomic samples were analyzed with 1D pHILIC-HPLC ESI-MS and the data were analyzed with mzMatch-ISO. UL- Unlabelled carbon, +1 - 1-^{13}C-labelled carbon, +2 - 2-^{13}C-labelled carbon, +3 - 3-^{13}C-labelled carbon, +4 - 4-^{13}C-labelled carbon, WT – wild type promastigotes, *Δlmgt* - *Δlmgt* promastigotes.

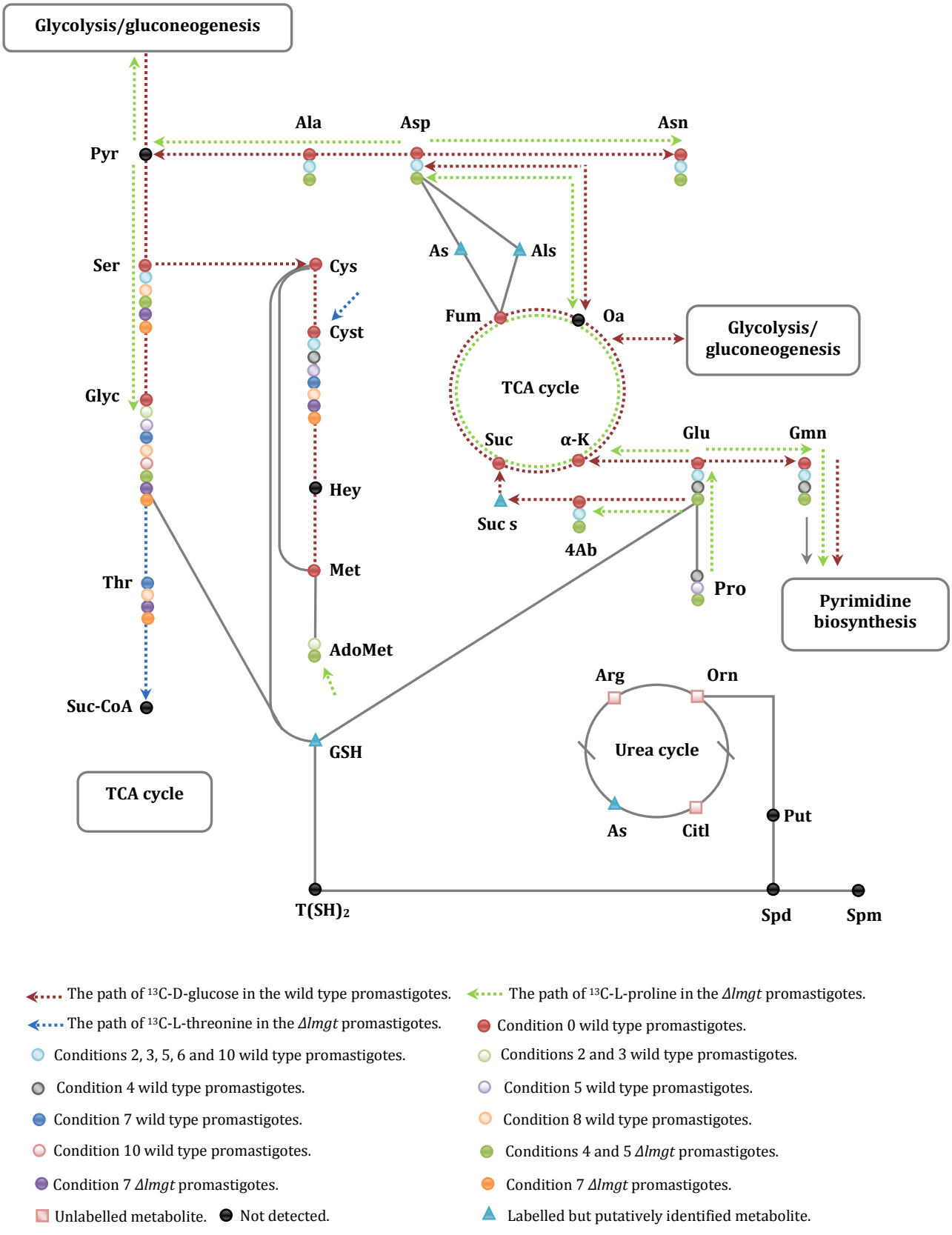

Figure IV-5. Schematic representation of amino acid metabolism in wild type and *Δlmgt* promastigotes. Abbreviations: Pyr - pyruvate, Ala - L-alanine, Asp - L-aspartate, Asn - L-asparagine, Ser - L-serine, Cys - L-cysteine, Cyst - L-cystathionine, Hey - L-homocyetine, Met - L-methionine, AdoMet - S-adenosyl-L-methionine, Glyc - glycine, Thr - L-threonine, Suc CoA - succinyl-CoA, GSH - glutathione, $T(SH)_2$ - trypanothione, Spd - spermidine, Spm - spermine, Put - putrescine, Orn - L-ornithine, Arg - L-arginine, Arg-suc - L-agrinine-succinate, Adl-suc - adenylosuccinate, Citl - L-citrulline, Pro - L-proline, 4Ab - 4-aminobutanoate, Suc s - succinate semialdehyde, Suc - succinate, α-K - α-ketoglutarate, Fum - fumaretae, Oa - oxaloacetate, Glu - L-glutamate, Gmn - L-glutamine.

In the *Δlmgt* promastigotes, L-aspartate and L-asparagine were labelled only in the conditions with ^{13}C-L-proline which underlines the significance of L-proline for the *Δlmgt* promastigotes (see Discussion).

Arginine, glutamate and proline metabolism

L-Arginine, one of the amino acids *Leishmania* are auxotrophic for, is taken up by the high affinity, high specificity L-arginine permease AAP3 (Shaked-Mishan *et al.*, 2006) while L-proline is imported by AAP24 (Inbar *et al.*, 2013). L-Arginine, along with L-citrulline and L-ornithine, was unlabelled in the wild type and *Δlmgt* promastigotes and L-proline was labelled only in the conditions where it was used as an enriched carbon source (Figure IV-5). L-Glutamate and L-glutamine were universally labelled in conditions ***glc0**, ***glc**, **pro+*glc**, **glc+*pro**, ***pro**, **thr+*glc** and **glr+*glc** wild type promastigotes and in conditions **glc+*pro** and ***pro** *Δlmgt* promastigotes (Figure IV-5; Supplemental table IV-1). That shows that L-glutamate can be synthesized either from D-glucose via α-ketoglutarate or from L-proline (see Discussion). A small amount of L-glutamate and L-glutamine was also labelled in the *Δlmgt* promastigotes incubated with ^{13}C-L-threonine.

Cysteine and methionine metabolism

Leishmania are not able to take up L-cysteine from the environment (Williams *et al.*, 2009) so they synthesize it intracellularly. The slight labelling of L-serine (see Glycine, serine and threonine metabolism) and L-cysteine indicates that a portion of L-serine is converted to L-cysteine in condition ***glc0** wild type promastigotes. Alternatively, L-cysteine can be synthesized from L-homocysteine via the reverse *trans*-sulfuration pathway (Williams *et al.*, 2009). Although L-cysteine remained unlabelled in all 10 conditions, a small amount of L-cystathionine, an intermediate in the *trans*-sulfuration pathway, was found labelled in conditions ***glc0**, ***glc**, **pro+*glc**, **glc+*pro**, ***pro**, **thr+*glc, glc+*thr**, ***thr** and **glr+*glc** wild type promastigotes and in conditions **glc+*thr** and ***thr** *Δlmgt* promastigotes. That shows that all three carbon sources used in this experiment, D-glucose, L-proline and L-threonine, can serve as precursors for the synthesis of L-cysteine. However, it appears that the synthesis of L-cysteine via the reverse *trans*-sulfuration pathway in wild type promastigotes incubated for a short period of time with a restricted number of nutrients is minimal. The amino acid was unlabelled in the *Δlmgt* promastigotes.

Consistent with the minimal labelling of L-cysteine, L-methionine was also only slightly labelled in condition 0 wild type promastigotes and it was unlabelled in all 10 conditions and in the *Δlmgt* promastigotes. L-Methionine, in the form of S-adenosyl-L-methionine (AdoMet), is a universal methyl donor in methylation reactions. AdoMet was authentically identified and found labelled in conditions ***glc** and **pro+*glc** wild type promastigotes and in conditions **glc+*pro** and ***pro** *Δlmgt* promastigotes (Figure IV-5). It must be noted, however, that the adenosine moiety of AdoMet was labelled, indicating that both D-glucose and L-proline can be precursors for purines (see Discussion).

Glutathione metabolism

Glutathione [γ-glutamyl-cysteinyl-glycine, (GSH)] is among the four major low molecular weight thiols synthesized by trypanosomatids. The compound is produced from L-glutamate, L-cysteine and glycine. Glutathione was only putatively identified and found labelled in conditions ***glc**, **pro+*glc** and ***pro** wild type promastigotes and condition **glc+*pro** and ***pro** *Δlmgt* promastigotes (Figure IV-5). In turn, glutathione, along with the polyamine spermidine, is involved in the synthesis of trypanothione, the major antioxidant of the oxidative defence system of trypanosomatids (Steenkamp, 2002). Trypanothione, unfortunately, was not detected. On the other hand, the oxidized forms of both glutathione and trypanothione, glutathione disulfide and trypanothione disulfide, respectively, were putatively identified and labelled in conditions ***glc0**, ***glc**, **pro+*glc** and ***pro** wild type promastigotes and conditions **glc+*pro** and ***pro** *Δlmgt* promastigotes. Trypanothione disulfide was additionally labelled in conditions **thr+*glc, glc+*thr**, ***thr** and **glr+*glc** wild type promastigotes.

Glycine, serine and threonine metabolism

Glycine is a small amino acid that can be produced from L-threonine and L-serine (Opperdoes and Coombs, 2007). A small amount of the authentically identified L-serine and glycine was labelled in conditions ***glc0**, ***glc**, **pro+*glc**, ***pro** and **glr+*glc** wild type promastigotes and in conditions **glc+*pro**, ***pro**, **glc+*thr** and ***thr** *Δlmgt* promastigotes (Figure IV-5). Additionally, glycine was labelled in conditions **glc+*thr** and ***thr** wild type promastigotes, which suggested that glycine is mainly a product of L-threonine degradation, while L-serine was labelled in conditions **thr+*glc** and ***thr** wild type promastigotes, which shows that L-serine can be synthesized from both D-glucose and L-threonine. L-Threonine was unlabelled in the

wild type and *Δlmgt* promastigotes except for the conditions where it was used as a heavy-labelled carbon source. Thus, our tracing data revealed that L-proline, via pyruvate and L-serine, and L-threonine are precursors for the synthesis of glycine in the *Δlmgt* promastigotes.

Nucleotide metabolism

Purine metabolism

In contrast with their hosts, *Leishmania* parasites are not able to synthesize purines *de novo*. Our tracing analysis confirmed that unlabelled nucleobases such as adenine, xanthine and hypoxanthine are taken up by condition ***glc0** wild type promastigotes. Nevertheless, nucleosides and nucleotides were also found labelled in condition ***glc0** wild type promastigotes which showed that the sugar moiety originated from ^{13}C-D-glucose. More important, however, was the observation that some nucleotides were also slightly labelled in condition ***glc0** *Δlmgt* promastigotes (Figure IV-6). Adenosine, guanosine, adenosine 5-monophosphate (AMP), inosine 5-monophosphate (IMP) and guanosine 5-monophosphate (GMP) were authentically identified. The rest of the detected purines were putatively identified.

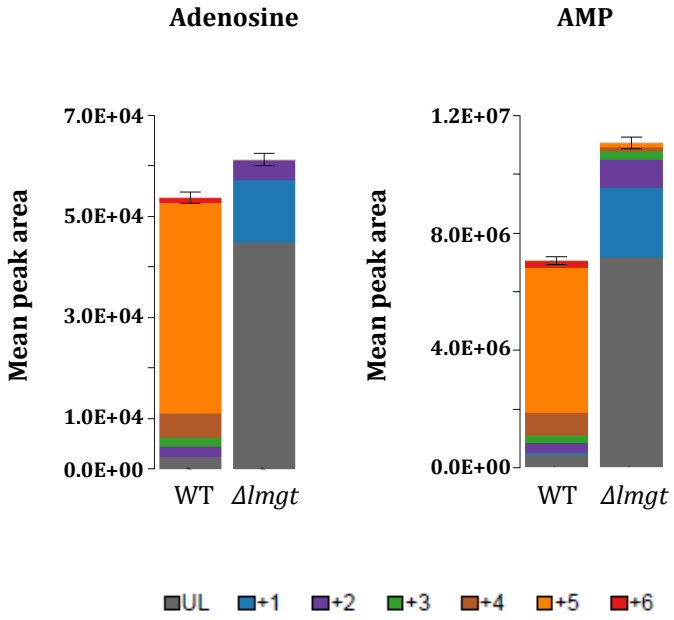

Figure IV-6. Labelling pattern of adenosine and adenosine 5'-monophosphate (AMP) in wild type and *Δlmgt* promastigotes incubated with ^{13}C-D-glucose. UL- Unlabelled carbon, +1 - 1-^{13}C-labelled carbon, +2 - 2-^{13}C-labelled carbon, +3 - 3-^{13}C-labelled carbon, +4 - 4-^{13}C-labelled carbon, +5 - 5-^{13}C-labelled carbon, +6 - 6-^{13}C-labelled carbon, WT – wild type promastigotes, *Δlmgt* - *Δlmgt* promastigotes.

AMP and the putative ADP and ATP were some of the purine intermediates that were labelled in condition ***glc0** wild and *Δlmgt* promastigotes (Figure IV-6). In addition to conditions **glc+*pro** and ***pro** *Δlmgt* promastigotes, in which the sugar moiety is synthesized from L-proline, AMP, ADP and ATP were also slightly labelled in conditions ***glc** and **pro+*glc** *Δlmgt* promastigotes. The labelling in the *Δlmgt* promastigotes in the conditions with heavy-labelled D-glucose shows, as suggested before, that the alternative GT4 glucose transporter is probably up-regulated. Additionally, the labelling shows that purines are extremely important for the *Δlmgt* promastigote biology. The labelling pattern of the rest of the purines is presented in Supplemental table IV-2.

Pyrimidine metabolism

Pyrimidines are among the metabolites *Leishmania* are able to synthesize *de novo*. Similarly to purines, some of the detected pyrimidine intermediates, such as the putative UDP and UTP, were labelled in condition ***glc0** wild type and *Δlmgt* promastigotes. The putative identification, however, requires further confirmation. Orotate, uracil and cytidine were authentically identified and labelled in conditions ***glc0**, ***glc** and **pro+*glc** wild type promastigotes and conditions **glc+*pro** and ***pro** *Δlmgt* promastigotes. That shows that L-proline is a precursor for pyrimidine synthesis in the *Δlmgt* promastigotes. Dihydrouracile and 5,6-dihydrothymine were putatively identified and found labelled in condition **thr+*glc** and **glr+*glc** wild type promastigotes. Similar to the putative UDP and UTP, further confirmation is needed.

Lipid metabolism

All lipids were putatively identified on the basis of mass measurements, without any structural analysis to resolve isomers.

Biosynthesis of fatty acids

The lipid profile of the leishmanial cell membranes has been a focus of many studies. The major lipids of *Leishmania* include choline, ethanolamine, inositol phospholipids, sterols and triglycerides and contain different length-chain fatty acids (Beach *et al.*, 1979; Wassef *et al.*, 1985). Several C16, C18, C20 and C22 fatty acids were found heavy-labelled in the wild type and *Δlmgt* promastigotes.

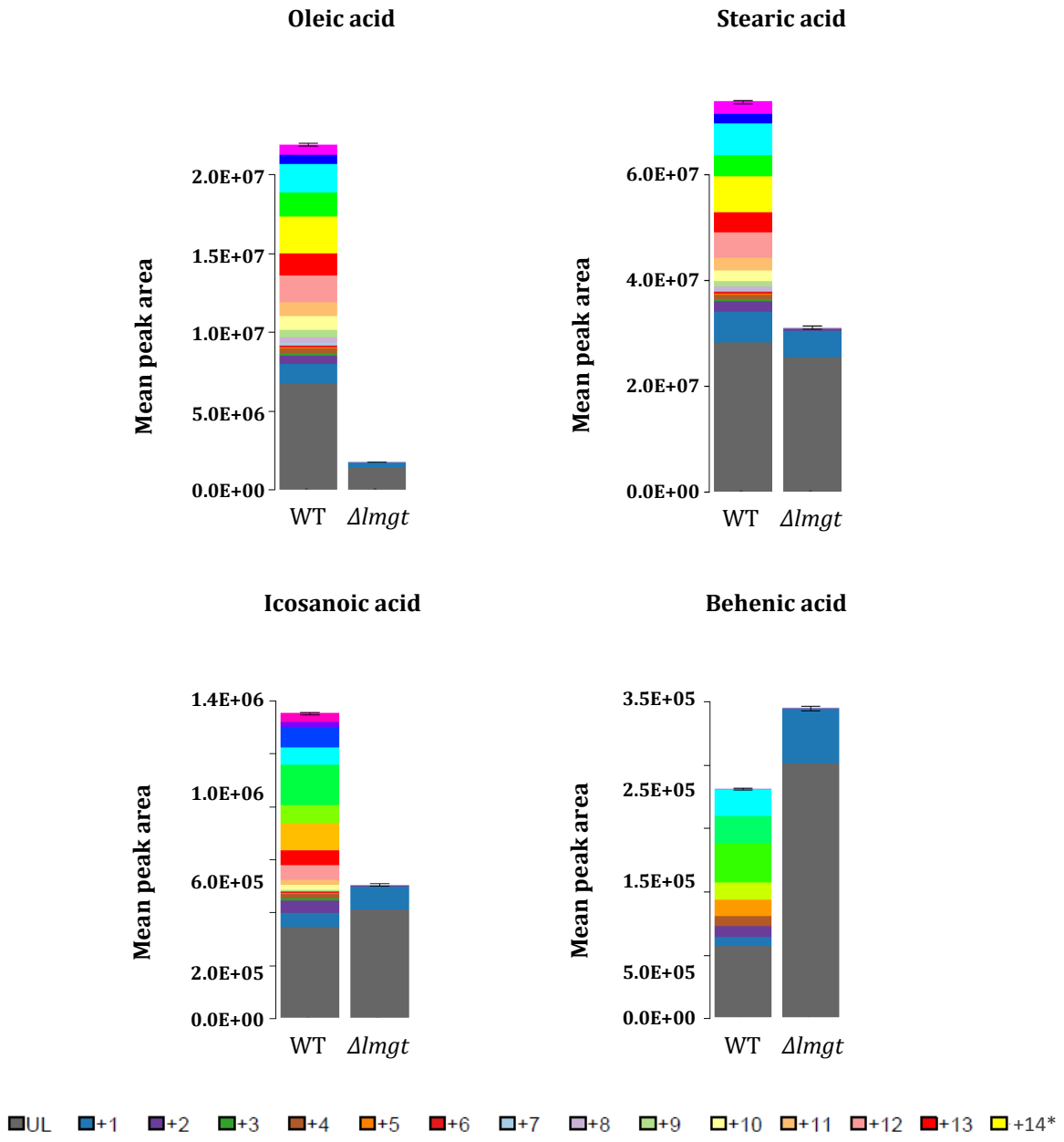

Figure IV-7. Labelling pattern of oleic acid, stearic acid, icosanoic acid and behenic acid in wild type and *Δlmgt* promastigotes incubated with ^{13}C-D-glucose. UL- Unlabelled carbon, +1 - 1-^{13}C-labelled carbon, +2 - 2-^{13}C-labelled carbon, +3 - 3-^{13}C-labelled carbon, +4 - 4-^{13}C-labelled carbon, +5 - 5-^{13}C-labelled carbon, +6 - 6-^{13}C-labelled carbon, +7 - 7-^{13}C-labelled carbon, +8 - 8-^{13}C-labelled carbon, +9 - 9-^{13}C-labelled carbon, +10 - 10-^{13}C-labelled carbon, +11 - 11-^{13}C-labelled carbon, +12 - 12-^{13}C-labelled carbon, +13 - 13-^{13}C-labelled carbon, +14 - 14-^{13}C-labelled carbon, WT – wild type promastigotes, *Δlmgt* - *Δlmgt* promastigotes. * - the colours corresponding to the type of labelling above +14 are not presented.

Oleic acid and stearic acid were universally labelled in condition ***glc0** wild type promastigotes (Figure IV-7). Labelled in the condition ***glc0** wild type promastigotes were also icosanoic acid (or arachidic acid) (Figure IV-7), behenic acid (Figure IV-7) and linoleic acid. Label incorporation in these fatty acids in the 10 NMR conditions was only minor, suggesting that fatty acid biosynthesis is decreased in the wild type promastigotes under nutrient restricted conditions. Labelled in conditions **glc+*pro** and ***pro** *Δlmgt* promastigotes were icosanoic acid, behenic acid and lignoceric acid which shows that a portion of the acetyl-CoA synthesized from L-proline is directed toward lipid synthesis in the *Δlmgt* promastigotes. Interestingly, no labelling was observed in the *Δlmgt* promastigotes incubated with L-threonine which shows that acetyl-CoA produced from this amino acid is not used in lipid synthesis.

Sphingolipid metabolism

Sphingolipids are another heterogeneous group of important membrane-anchored macromolecules that comprise about 5 - 10% of the *Leishmania* membrane lipids (Kaneshiro *et al.*, 1986). The principal building blocks of sphingolipids are long-chain bases or sphingoid bases. In yeast, the main sphingoid bases are sphinganine (dihydrosphingosine) and phytosphingosine (Dickson, 2008; Bartke and Hannun, 2009). Sphinganine can contain 16, 18 or 20 carbons while phytosphinganine can contain 18 or 20 carbons (Lester and Dickson, 2001). The two types of sphingoid bases were putatively identified and found labelled in the wild type promastigotes (Supplemental figure IV-1). Both, sphinganine and phytosphingasine were 18-^{13}C-labelled in the wild type promastigotes incubated with ^{13}C-D-glucose (Supplemental figure IV-1). In the *Δlmgt* promastigotes, the putative sphinganine was labelled only in the conditions with ^{13}C-L-threonine (Supplemental figure IV-1). That showed that a portion of L-threonine is converted to L-serine and used in sphingolipid synthesis in the *Δlmgt* promastigotes. L-serine was found labelled in the *Δlmgt* promastigotes in the conditions with ^{13}C-L-proline but sphinganine and phytosphingosine were not detected.

IV.2. Discussion

Amino acid metabolism

Alanine and aspartate metabolism

L-Alanine is present at the highest concentration in the free amino acid pool in both promastigotes and amastigotes (Simon *et al.*, 1983; Mallinson and Coombs, 1989). As an osmoregulator, L-alanine (Ala) is one of the main solutes involved in maintaining the cell volume (Vieira *et al.*, 1996). As a metabolite, L-alanine is one of the main end products of D-glucose catabolism in *Leishmania* (Darling *et al.*, 1987). As such, it is excreted by the cells (Rainey and MacKenzie, 1991). While excreted, however, L-alanine can be simultaneously taken up as a nutrient and/or osmolite from the environment via transporter(s) (Inbar *et al.*, 2013).

In D-glucose-replete conditions L-alanine and/or L-aspartate are taken up at an increased rate and needed in TCA cycle anaplerosis and synthesis of L-glutamate (Saunders *et al.*, 2011). Additionally, the two amino acids are glucogenic amino acids that can be converted to D-glucose via gluconeogenesis (Figure IV-1). An incorporation analysis performed with ^{14}C-L-alanine and ^{14}C-L-aspartate revealed that mannogen was radiolabelled when the *Δlmgt* promastigotes were incubated with either of the amino acids thus confirming that they are used in gluconeogenesis in the *Δlmgt* promastigotes (Rodriguez-Contreras and Landfear, 2006). L-Alanine, under the action of alanine aminotransferase (ALT), can be transaminated to pyruvate (via the reaction presented below) and fed into gluconeogenesis via pyruvate phosphate dikinase (PPDK) (Rodriguez-Contreras and Hamilton, 2014). Similarly, L-aspartate can be converted to oxaloacetate via a mitochondrial aspartate aminotransferase or to fumarate via the consecutive action of an adenylosuccinate synthase, an adenylosuccinate lyase and an adenosine 5-monophosphate (AMP)-deaminase, and fed into the gluconeogenesis via phosphoenolpyruvate carboxykinase (PEPCK) (Opperdoes and Michels, 2008).

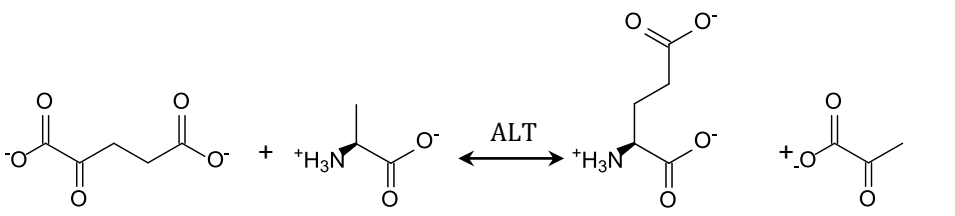

α-Ketoglutarate L-Alanine L-Glutamate Pyruvate

In the *Δlmgt* promastigotes, alanine aminotransferase and PPDK were found down-regulated (Supplemental figure III-1). Neither aspartate aminotransferase nor the enzymes of the purine-nucleotide cycle were found differentially regulated in the *Δlmgt* promastigotes. PEPCK, on the other hand, was also down-regulated (Supplemental table III-1). Considering that the levels of L-alanine and L-aspartate were significantly decreased in the *Δlmgt* promastigotes (Figure IV-2, A and C), along with the down-regulation of PPDK and PEPCK, it could be proposed that the majority of L-alanine and L-aspartate is actively directed toward the TCA cycle to be oxidized for the generation of energy and only a small amount is used in the gluconeogenesis. Up-regulation of PPDK and PEPCK would have meant that L-alanine, L-aspartate and possibly other glucogenic amino acids are used primarily as glucogenic precursors. L-Alanine and L-aspartate, although confirmed glucogenic sources for the *Δlmgt* promastigotes, appear to be used mainly as energy sources by these promastigotes.

Arginine, glutamate and proline metabolism

It was demonstrated that *L. donovani* promastigotes incorporate approximately 20% of the internalized L-arginine into proteins while the majority of it remains unused within the amino acid pool or used for polyamine and derivative synthesis (Kandpal *et al.*, 1995). An amino acid uptake assay performed with the *Δlmgt* promastigotes revealed that L-arginine is taken up at a decreased rate compared to the wild type promastigotes (Thesis: Lamasudin, 2012). The amino acid was found unlabelled in the wild type and *Δlmgt* promastigotes (Figure IV-5). Unlabelled in both cell lines were also the immediate derivatives of L-arginine, L-citruline and L-ornithine (Figure IV-5). The proteomic data specified that arginase (ARG), involved in the conversion of L-arginine to L-ornithine, was down-regulated in the *Δlmgt* promastigotes (Supplemental table III-1). L-Arginine and L-ornithine are precursors for the synthesis of polyamines which in turn are involved in the synthesis of trypanothione (Colotti and Ilari, 2011) (see Glutathione metabolism). The next enzyme of the polyamine biosynthesis, after arginase, is ornothine decarboxylase which decarboxylates L-ornithine to putrescine. The latter, together with decarboxylated S-adenosyl-L-methionine (dAdoMet), is used for the synthesis of spermidine by a spermidine synthase while spermine synthase converts spermidine to spermine (Colotti and Ilari, 2011). In condition ***glc0** wild type promastigotes, S-adenosyl-L-methionine was not detected. It was found labelled only in condition ***glc** and **pro+*glc** wild type promastigotes and condition **glc+*pro** and ***pro** *Δlmgt*

promastigotes (see Cysteine and methionine metabolism). Thus, dAdoMet was also most probably labelled in the wild type promastigotes. Unfortunately, putrescine, spermidine and spermine were not detected in the wild type or *Δlmgt* promastiogtes. Trypanothione also was not detected (see Glutathione metabolism). Thus, considering that *Leishmania* are able to take up polyamines from the environment (Basselin *et al.*, 2000), down-regulation of the initial step of the polyamine biosynthesis in the *Δlmgt* promastigotes suggests that the main use of L-arginine is protein synthesis. Another possibility is that L-arginine is converted to phosphoarginine, a high-energy phosphagen that provides fast energy supply (Colasante *et al.*, 2006). The compound, however, was not detected.

Contrary to L-alanine and L-aspartate, which are taken up and utilized at an increased rate, L-glutamate and L-glutamine are barely used as carbon sources by wild type *L. mexicana* promastigotes grown under D-glucose-replete conditions (Saunders *et al.*, 2011). The fate of the two amino acids in the *Δlmgt* promastigotes, however, appears to be different. In addition to being taken up from the environment (Paes *et al.*, 2008), L-glutamate can be generated from L-proline via a mitochondrial Δ^1-pyrroline-5-carboxylate dehydrogenase and a pyrroline-5-carboxylate synthetase, or by transamination from α-ketoglutarate (Opperdoes and Michels, 2008). L-Proline and L-glutamate were authentically identified and found unlabelled and universally labelled, respectively, in condition ***glc0** wild type promastigotes (Figure IV-6). That showed that L-glutamate was synthesized from α-ketoglutarate and not from L-proline in the wild type promastigotes. The conversion of α-ketoglutarate to L-glutamate (presented below) is catalised by the enzyme glutamate dehydrogenase (GDH). Two glutamate dehydrogenases are believed to operate in *Leishmania*, one mitochondrial NAD-dependent enzyme and one NADPH-dependent enzyme, possibly localized to the cytosol (Opperdoes and Michels, 2008).

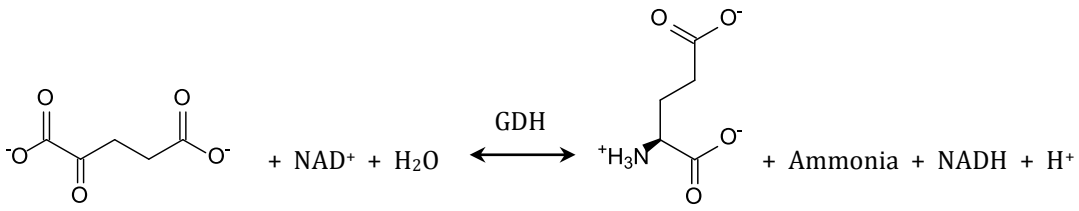

L-Glutamate α-Ketoglutarate

The proteomic data showed that a glutamate dehydrogenase, with a dual presence in the cytosolic and organellar fraction, was found highly down-regulated in the *Δlmgt* promastigotes (Supplemental table III-1). Additionally, the level of L-glutamate was decreased in the *Δlmgt* promastigotes (Table III-3). Thus, similar to a starvation study performed with *L. tropica* promastigotes (Simon *et al.*, 1983), the enzyme activity of glutamate dehydrogenase in the *Δlmgt* promastigotes appears to be significantly decreased in the direction of production of L-glutamate. That indicates that the equilibrium of the L-glutamate-to-α-ketoglutarate interconversion (shown above) would be preferentially shifted toward the synthesis of α-ketoglutarate. That suggests that the amino acids is actively fuelled into the TCA cycle via α-ketoglutarate, a suggestion supported by the up-regulation of the E2 component of the oxoglutarate dehydrogenase complex (Figure III-21), and possibly utilized as a glucogenic precursor. In addition to α-ketoglutarate, L-glutamate could also possibly be fed into the TCA cycle via 4-aminobutanoate, succinate semialdehyde and succinate, the former and the last of which were authentically identified and universally labelled while succinate semialdehyde, unfortunately, was not detected in the promastigotes.

The next amino acid of interest to the *Δlmgt* promastigotes metabolism is L-glutamine. An amino acid uptake assay revealed that L-glutamine was taken up by the *Δlmgt* promastigotes at an increased rate compared to the wild type promastigotes (Thesis: Lamasudin, 2012). The amino acid was authentically identified and found universally labelled in condition ***glc0** wild type promastigotes (Figure IV-4). That showed that L-glutamine was synthesized from L-glutamate via a glutamine synthetase. The L-glutamate-to-L-glutamine conversion plays a central role in nitrogen metabolism. Glutamine synthetase, along with a number of enzymes, including glutamate dehydrogenase (GDH), are believed to be involved in maintaining nitrogen and carbon balance (Miffin and Habash, 2002). GDH, in particular, is proposed to facilitate the recycling of the carbon incorporated into proteins back to carbon metabolism and the TCA cycle. The opposite conversion of L-glutamine to L-glutamate does not seem to occur in trypanosomatids (Opperdoes and Coombs, 2007). Thus, the amino acid cannot be used as a glucogenic precursor. In *Leishmania*, L-glutamine is a nitrogen donor (Manhas *et al.*, 2014) and is involved in *de novo* pyrimidine and amino sugar biosynthesis (Carter *et al.*, 2008; Opperdoes and Michels, 2008; Naderer *et al.*, 2008). The increased uptake of L-glutamine possibly indicates

an increased requirement for amino sugars and pyrimidine nucleotides (see Nucleotide metabolism).

Besides α-ketoglutarate and L-glutamine, authentically identified and universally labelled in the *Δlmgt* promastigotes was also N-acetyl-L-glutamate. N-Acetyl-L-glutamate can be converted to L-ornithine via N-acetyl-L-ornithine, which, as expected, was only 2-^{13}C-labelled from the acetyl moiety. N-Acetyl-L-glutamate is also involved in activation of carbamoyl phosphate synthetase in the urea cycle. The cycle, however, does not appear to be fully operational in *Leishmania*. The organisms have the initial enzymes of the cycle, namely carbamoylphosphate synthase, argininosuccinate synthase and arginase, which shows that L-arginine, L-ornithine and urea could be formed, but lack the enzymes ornithine carbamoyltransferase and argininosuccinate lyase (Opperdoes and Coombs, 2007; Opperdoes and Michels, 2008). Only arginase, as said above, was found down-regulated in the *Δlmgt* promastigotes.

The last amino acid to be discussed is L-proline. L-Proline is an abundant amino acid in the insect hemolymph which is utilized as an energy substrate during flight (Taylor, 1998). The insect forms of *Leishmania* have evolved to use L-proline as a major energy source, even in the presence of D-glucose (Bringaud *et al.*, 2006). In trypanosomes, L-proline is taken up six times more when D-glucose is not available (Lamour *et al.*, 2005). Similarly, the *Δlmgt* promastigotes were shown to consume much more L-proline compared to the wild type promastigotes (Thesis: Lamasudin, 2012). At the uptake peak, the *Δlmgt* promastigotes consumed approximately 10,000 times more L-proline in comparison with the wild type promastigotes. Additionally, compared to L-glutamine and L-serine, L-proline was taken up ten to hundreds of times more. When internalized, L-proline can be used in protein synthesis or metabolized in the central carbon metabolism. When used as an energy and carbon source, L-proline is oxidation to L-glutamate by a mitochondrial Δ^1-pyrroline-5-carboxylate dehydrogenase and a pyrroline-5-carboxylate synthetase and then fed into the TCA cycle via α-ketoglutarate (Opperdoes and Michels, 2008). It has to be emphasized that the oxidation of L-proline to L-glutamate is an important source of reducing equivalents which are directed toward oxidative phosphorylation for the generation of energy (see Energy metabolism). The isotope labelling analysis revealed that L-proline was converted to L-glutamate in the *Δlmgt* promastigotes in the conditions where ^{13}C-L-proline was provided as a carbon source. The label from

L-proline appeared in all detected TCA cycle intermediates, acetyl-CoA and all detected glycolysis/gluconeogenesis intermediates. In addition to being used in TCA cycle anaplerosis and gluconeogenesis, L-proline is implicated in stress protection, including oxidative stress, as it was proposed to function by stabilizing proteins and antioxidant enzymes, balancing the intracellular redox homeostasis (*e.g.*, the ratio of NADP/NADPH and reduced glutathione/oxidized glutathione) (see Glutathione metabolism) and promoting cell signalling (Liang *et al.*, 2013). L-Proline thus appears to be a substrate with versatile functions and of primary importance for the *lmgt* promastigotes of *L. mexicana*.

Cysteine and methionine metabolism

Neither of the two enzymes involved in the *de novo* synthesis of L-cysteine from L-serine, namely cysteine acetyltransferase and cysteine synthase (Williams *et al.*, 2009), were differentially expressed in the *Δlmgt* promastigotes which indicates that the L-serine-to-L-cysteine conversion may not be regulated at the level of protein abundance in the *Δlmgt* promastigotes. Alternatively, L-cysteine can be generated via the reverse *trans*-sulfuration pathway involving cystathionine β-synthase and cystathionine γ-lyase (Figure IV-8) (Williams *et al.*, 2009). The final step of the pathway, in which L-cystathionine, under the action of cystathionine γ-lyase (CSE), is broken down to L-cysteine, 2-oxobutanoate and ammonia, was differentially regulated in the *Δlmgt* promastigotes. Isoforms of the enzyme, however, were found both up- and down-regulated in the *Δlmgt* promastigotes (Supplemental table III-1). In particular, the down-regulated isoform was found in the organellar fraction while the up-regulated was in the digitonin-insoluble fraction. In *L. major*, both cysteine synthase and cystathionine γ-lyase were localized to the cytosol where the L-cysteine synthesis was proposed to take place (Giordana *et al.*, 2014). Considering our proteomic data, we could hypothesize that the enzyme(s) catalyzing the final stage of the reverse *trans*-sulfuration pathway may have dual localization. The conversion of L-homocysteine to L-cysteine, which in turn is involved in the synthesis of iron-sulfur clusters found in a number of enzymes, and of trypanothione (see Glutathione metabolism) (Giordana *et al.*, 2014), thus appears to be decreased in the *Δlmgt* promastigotes. The organellar activity of cystathionine γ-lyase, at the same time may be due to unrelated to L-cysteine synthesis function. In *T. cruzi*, cystathionine γ-lyase was implicated in the maintenance of the cellular redox balance (Pineyro *et al.*, 2011).

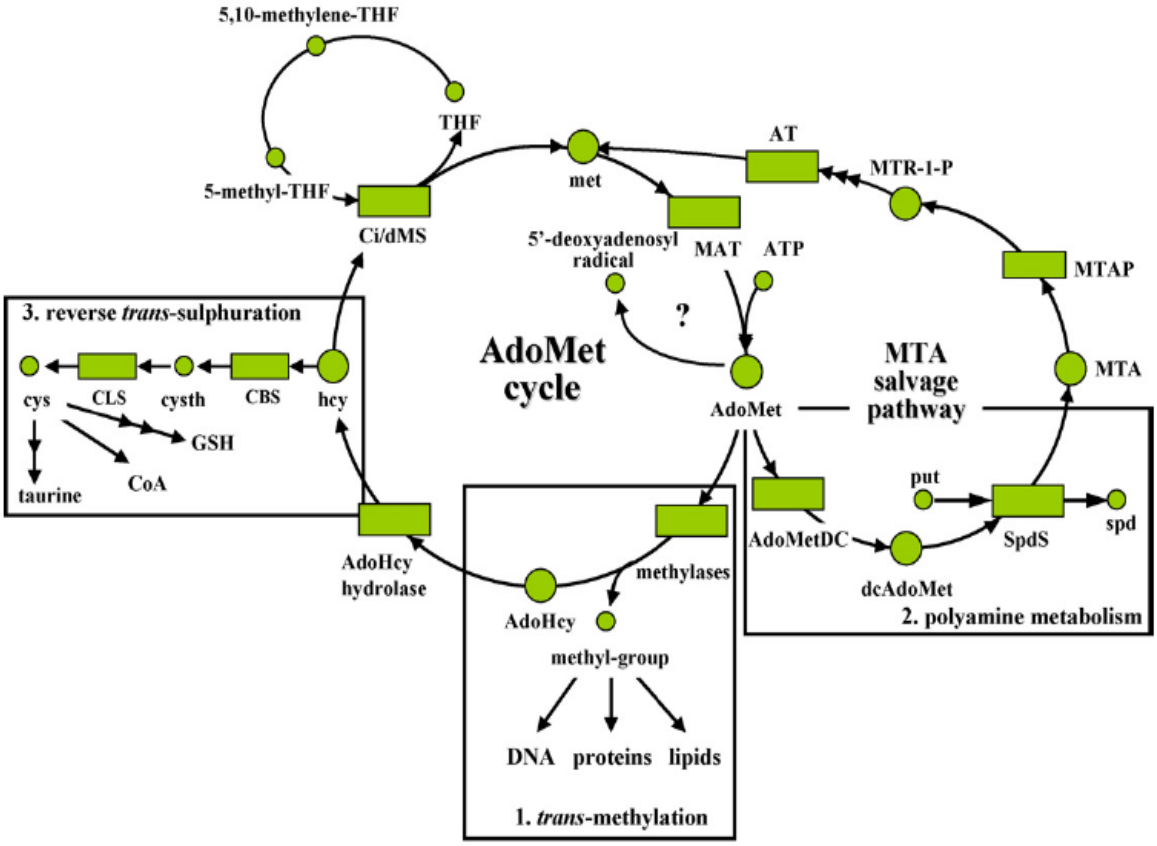

Figure IV-8. L-Methionine metabolism in trypanosomatids. Abbreviations: AdoHcy - *S*-adenosylhomocysteine, AdoMet - *S*-adenosylmethionine, cys - cysteine, cysth - cystathionine, dcAdoMet - decarboxylated *S*-adenosylmethionine, GSH - reduced glutathione, hcy - homocysteine, met - methionine, MTA - methylthioadenosine, MTR - 5′-methylthioribose, MTR-1-P - 5′-methylthioribose-1-phosphate, put - putrescine, spd - spermidine, THF - tetrahydrofolate, AdoHcy hydrolase - *S*-adenosylhomocysteine hydrolase, AdoMetDC - *S*-adenosylmethionine decarboxylase, AT - unspecific aminotransferase, CBS - cystathionine β-synthase, CdMS - cobalamin-dependent methionine synthase, CiMS - cobalamin-independent methionine synthase, CLS - cystathionine γ-liase, MAT - methionine adenosyltransferase, MTAN - methylthioadenosine nucleosidase, MTAP - methylthioadenosine phosphorylase, MTRK - 5′-methylthioribose kinase, SpdS - spermidine synthase, ODC/AdoMetDC - bifunctional ornithine decarboxylase/*S*-adenosylmethionine decarboxylase.
Credit: Reguera *et al.*, 2006

Leishmania synthesize L-methionine from L-cysteine by a methionine synthase or from L-homocysteine via a homocysteine S-methyltransferase (HMT) (Opperdoes and Coombs, 2007). Neither methionine synthase nor HMT was detected in the *Δlmgt* promastigotes. Another enzyme involved in the synthesis of L-methionine from L-homocysteine, namely 5-methyltetrahydropteroyltriglutamate--homocysteine methyltransferase (MetE), however, was down-regulated in the *Δlmgt* promastigotes. Down-regulation of cystathionine γ-lyase, involved in L-cysteine synthesis, and MetE, involved in L-methionine, would result in accumulation of L-homocysteine. The amino acid, however, was not among those observed to be significantly modulated in the *Δlmgt* promastigotes. Down-regulated was also the putative methylthioadenosine phosphorylase which catalyzes the initial step in the methionine salvage pathway, that is the reversible phosphorylation of 5-methylthioadenosine (MTA) to adenine and 5-methylthioribose 1-phosphate (Figure IV-8). This would mean that less adenine would be produced and at the same time less ATP would be engaged in the formation of MTA. MTA is a major byproduct of polyamine biosynthesis which is recycled to L-methionine via the methionine salvage pathway. The polyamine biosynthesis was presumed down-regulated in the *Δlmgt* promastigotes (see Arginine and proline metabolism) which is possibly linked to down-regulation of the methionine salvage pathway as well. Thus, two enzymes of two alternative pathways for synthesis of L-methionine are down-regulated in the *Δlmgt* promastigotes. We could therefore speculate that the more or less similar levels of L-methionine in the wild type and *Δlmgt* promastigotes are due to uptake of the amino acid from the environment by the latter (Mukkada and Simon, 1977). L-Methionine is another important sulfur-containing amino acid involved in protein synthesis and possibly also in protein activation and inactivation (Drazic and Winter, 2014). In addition to protein synthesis, L-methionine, in the form of S-adenosyl-L-methionine (AdoMet), is a methyl donor in all but one known *trans*-methylation reactions, an aminopropyl group donor in spermidine and spermine biosynthesis and a precursor for glutathione biosynthesis (Figure IV-8) (Reguera *et al.*, 2006). Additionally, AdoMet is a precursor for 5-deoxyadenosyl radicals which are involved in biological processes such as DNA precursor biosynthesis, biodegradation pathways, DNA repair and transfer RNA (tRNA) modification (Fontecave *et al.*, 2004; Lu, 2000). Thus, AdoMet may have non-metabolic function(s) but still influence the metabolism of the *Δlmgt* promastigotes.

Glutathione metabolism

Involved in the synthesis of glutathione (GSH) are the enzymes γ-glutamylcysteine synthetase, which ligates L-glutamate and L-cysteine into γ-L-glutamyl-L-cysteine, and glutathione synthase, which conjugates the product of the first reaction with glycine (Irigoin *et al.*, 2008). Glutathione is then transferred, in an ATP-dependent manner, to one of the amino acids of spermidine to form glutathionylspermidine, which is catalyzed by glutathionylspermidine synthetase. The addition of the second glutathione molecule is catalyzed by trypanothione synthase and leads to the synthesis of trypanothione (N^1,N^8-bis-(glutathionyl)-spermidine). Glutathionyl-spermidine synthetase, however, has not yet been reported for *Leishmania*, and trypanothione synthase was not detected in the promastigotes. Not detected in the wild type and *Δlmgt* promastigotes grown under any of the 10 NMR conditions were also glutathione and trypanothione. Trypanothione plays a central role in antioxidant defence system of *Leishmania* (Steenkamp, 2002). While mammalian thiol redox homeostasis is maintained by glutathione/glutathione reductase, *Leishmania* redox network relies on trypanothione/trypanothione reductase (Irigoin *et al.*, 2008). Trypanothione is maintained in the reduced form by the NADPH-dependent flavoenzyme trypanothione reductase (TR). Although the oxidative phase of the pentose phosphate pathway, the phase in which NADPH is regenerated, was down-regulated in the *Δlmgt* promastigotes (see Pentose phosphate pathway), the trypanothione reductase that was differentially regulated in these parasites was below the threshold of 2-fold-change and was thus considered as insignificantly regulated. The next enzyme of the thiol-redox system, tryparedoxin (TXN), upon which the reduced trypanothione acts, was down-regulated in the *Δlmgt* promastigotes. Tryparedoxins are electron donors involved in the reduction of peroxides by tryparedoxine peroxidase, the formation of deoxyribonucleotides by the trypanosomal ribonucleotide reductase and the conversion of dehydroascorbate to ascorbate and of glutathione disulfide to glutathione (Figure IV-9) (Irigoin *et al.*, 2008; Steenkamp, 2002 and the references therein). In addition to tryparedoxin, down-regulated in the *Δlmgt* promastigotes were a tryparedoxin peroxidase and a type II tryparedoxin peroxidase (Supplemental table III-1). As said above, both tryparedoxin and tryparedoxin peroxidase are involved in peroxide neutralization. Hydrogen peroxide (H_2O_2) was chosen as the reactive oxygen species to test the antioxidant capacity of the *Δlmgt* promastigotes.

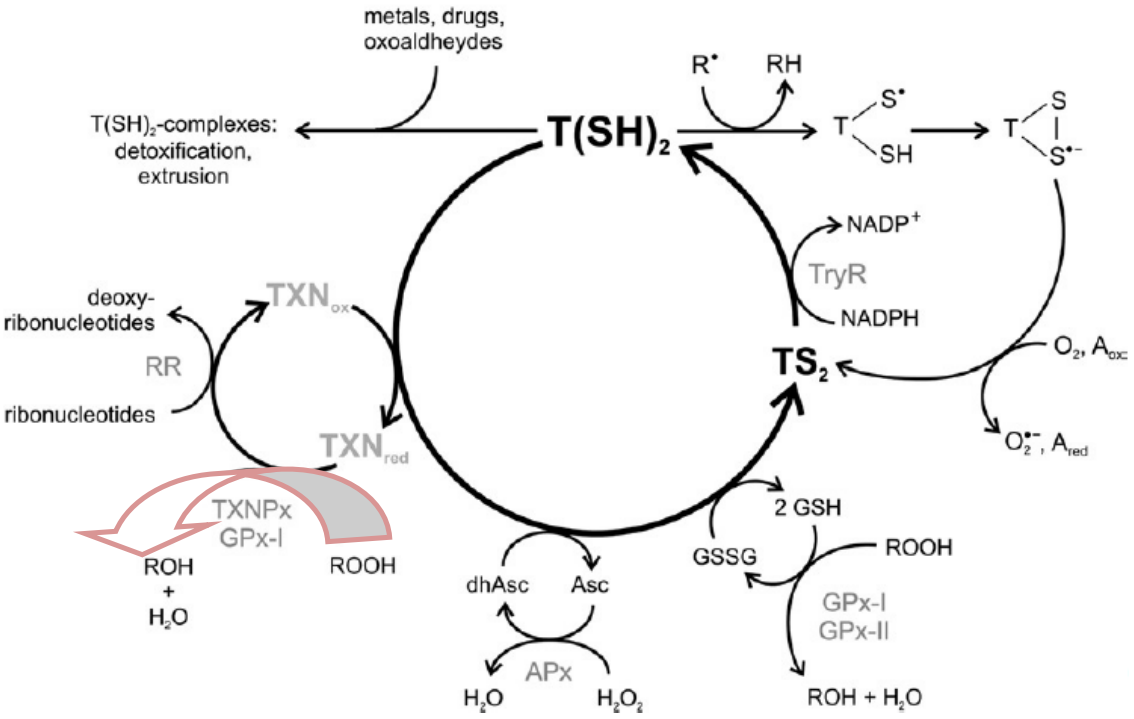

Figure IV-9. Trypanothione metabolism in *Leishmania*. Specified with a pink arrow is the down-regulated reaction in the *Δlmgt* promastigotes. Abbreviations: $T(SH)_2$ - dihydrotrypanothione, TS_2 - trypanothione disulfide, GSH - glutathione, GSSG - glutathione disulfide, TryR - trypanothione reductase, TXN - tryparedoxin, TXN_{ox} - oxidized tryparedoxin, TXN_{red} - reduced tryparedoxin, RR - ribonucleotide reductase, H_2O_2 - hydrogen peroxide, TXNPx - tryparedoxin peroxidase, GPx - glutathione peroxidase, Apx - ascorbate-dependent hemoperoxidase, dhAsc - dehydroascorbate, Asc - ascorbate, $^{\cdot}NO$ - nitric oxide, $O_2^{\cdot-}$ - superoxide radical, $R^{\cdot}$ - radical, ROOH - hydroperoxides, A - one-electron oxidant, A_{ox} - oxidised one-electron oxidant, A_{red} - reduced one-electron oxidant, GPx-I and GPx-II - glutathione peroxidase-like tryparedoxin peroxidases I and II.
Credit: Irigoin *et al.*, 2008

The *Δlmgt* promastigotes were shown to be highly sensitive to oxidative stress (Rodriguez-Contreras *et al.*, 2007) which could be accounted for by reduced generation of NADHP and decreased activity of the thiol-redox system.

Glycine, serine and threonine

The glycine cleavage system (GCS) is part of the folate biosynthesis pathway which is an important source of one-carbon units used in a number of biosynthetic pathways, such as the pyrimidine, purine and L-methionine biosynthesis. GCS is comprised of four proteins: T-protein [tetrahydrofolate (THF) requiring aminomethyltransferase, or glycine synthase], P-protein (pyridoxal phosphate containing glycine decarboxylase), L-protein (lipoamide dehydrogenase) and H-protein (lipoic acid containing carrier). Genes for all four proteins are expressed in *L. infantum* and their expression is triggered by high levels of glycine (Muller and Papadopoulou, 2010). The P-protein was not detected in the promastigotes. A putative pyridoxal kinase which reversibly phosphorylates pyridoxal to pyridoxal 5-phosphate, the coenzyme of the P-protein, however, was found down-regulated in the *Δlmgt* promastigotes (Supplemental table III-1). The H protein, considered as the core protein, was also found down-regulated in the *Δlmgt* promastigotes. Glycine was not detected in condition ***glc0** *Δlmgt* promastigotes but it was universally labelled in the conditions with heavy L-proline. This shows that the amino acid is still synthesized in the *Δlmgt* promastigotes but possibly at a decreased rate. Glycine can be synthesized from L-serine via a serine hydroxymethyltransferase (SHMT) and the tetrahydrofolate (THF)-dependent glycine cleavage system or from L-threonine by SHMT (Opperdoes and Coombs, 2007). Instead for the synthesis of glycine and the generation of one-carbon units, L-serine could be mainly directed toward the synthesis of pyruvate in the *Δlmgt* promastigotes, although our data did not provide conclusive evidence for that. The NMR data, instead, suggested that L-threonine may be the primary source of glycine in the *Δlmgt* promastigotes. L-Threonine is a major carbon source for cultured *T. brucei* procyclic forms (Cross *et al.*, 1975). It is believed to be a preferred source for production of acetate via acetyl-CoA over D-glucose (Cross *et al.*, 1975; Linstead *et al.*, 1977). In *T. brucei*, L-threonine is catabolised to acetyl-CoA and glycine via a threonine dehydrogenase and an acetyl-CoA:glycine *C*-acetltrasnferase (Linstead *et al.*, 1977). *Leishmania*, however, lacks threonine dehydrogenase (Opperdoes and Michels, 2008). Instead, the parasites can convert L-threonine to α-ketobutyrate or glycine (Figure IV-10).

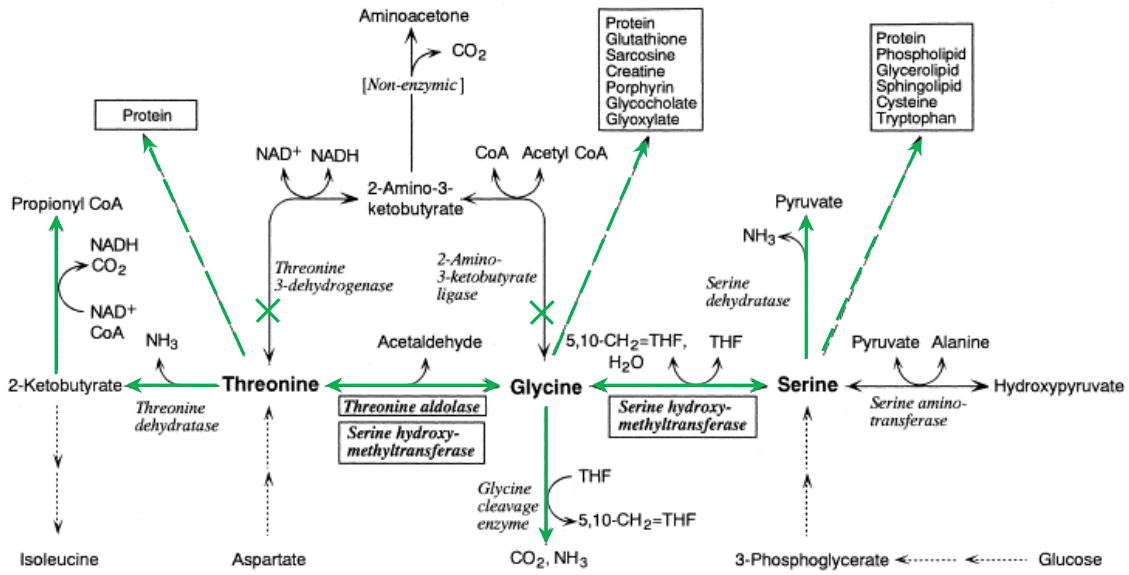

Figure IV-10. Glycine, L-serine and L-threonine metabolism. Specified with green arrows are reactions of glycine, serine and threonine metabolism occurring in *Leishmania*.
Credit: Ogawa *et al.*, 2000

L-Threonine can be converted to α-ketobutyrate by a serine/threonine dehydratase (STD) and subsequently oxidized to succinyl-CoA (Opperdoes and Coombs, 2007). Succinyl-CoA can then be converted to acetyl-CoA. Acetate can be produced from acetyl-CoA either by a cytosolic acetyl-CoA synthetase, which was found down-regulated in the *Δlmgt* promastigotes (Figure IV-11), or by a glycosomal acetate:succinate CoA transferase (ASCT) and succinyl-CoA ligase (SCL) (van Hellemond *et al.*, 1998; Riviere *et al.*, 2004). Acetate:succinate CoA transferase acts by transferring the CoA moiety of acetyl-CoA to succinate to produce acetate and succinyl-CoA. The latter can then be converted back to succinate by succinyl-CoA synthetase which results in the production of ATP (van Hellemond *et al.*, 1998). Acetate:succinate CoA transferase was not detected but succinyl-CoA ligase [GDP-forming] β-chain was found down-regulated in the *Δlmgt* promastigotes (Figure IV-11; Supplemental table III-1). A putative succinyl-CoA synthetase α subunit was also detected and it was down-regulated (Figure IV-11).

L-Threonine can be converted to glycine in two ways. In the first, L-threonine is converted in a THF-dependent manner to glycine. In the second, the Cα-Cβ bond of L-threonine are cleaved to generate glycine (Opperdoes and Coombs, 2007; Muller and Papadopoulou, 2010). The enzyme involved in both reactions is SHMT. SHMT is a pyridoxal 5-phosphate (PLP)-dependent enzyme whose primary function is to interconvert L-serine and THF to glycine and 5,10-methylene-THF.

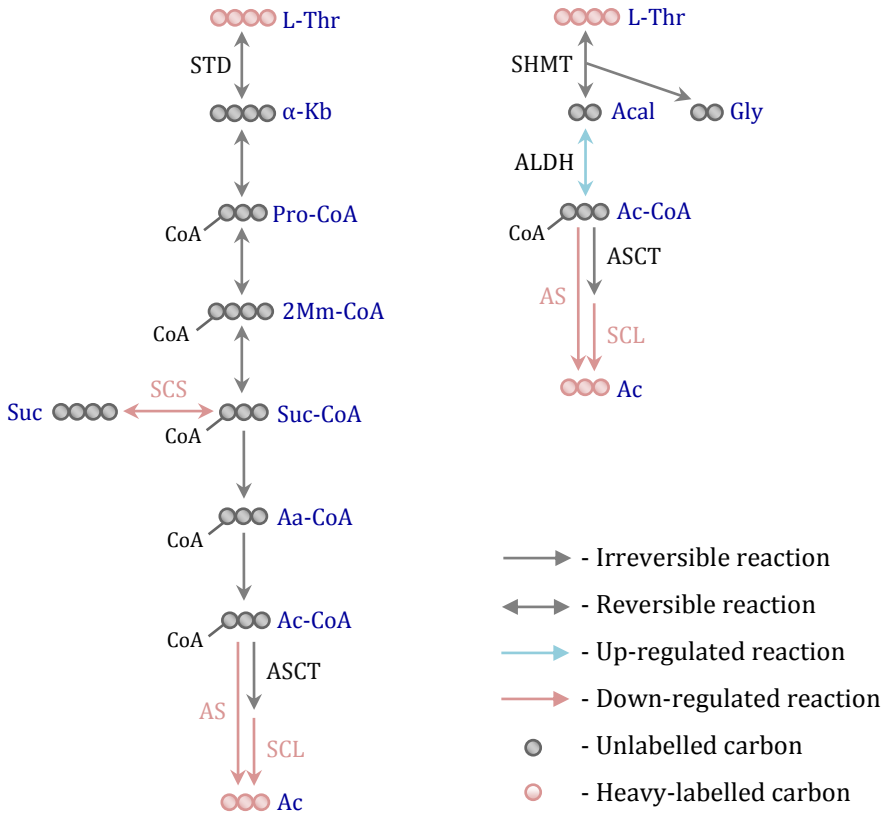

Figure IV-11. Schematic representation of L-threonine catabolism in *Δlmgt* promastigotes incubated with ^{13}C-D-glucose. Specified with light blue arrows are the up-regulated enzymes while specified with pink arrows are the down-regulated enzymes. Abbreviations: L-Thr - L-threonine, α-Kb - α-ketobutyrate, Pro-CoA - propanoyl-CoA, 2Mm-CoA - 2-methyl-malonyl-CoA, Suc-CoA - succinyl-CoA, Suc - succinate, Aa-CoA - acetoacetyl-CoA, Ac-CoA - acetyl-CoA, Ac - acetate, CoA - coenzyme A, Acal - acetladehdye, Gly - glycine, STD - serine/threonine dehydratase, AS - acetyl-CoA synthetase, ASCT - acetate:succinate CoA transferase, SCL - succinyl-CoA ligase, SCS - succinyl-CoA synthetase, SHMT - serine hydroxymethyltransferase, ALDH - aldehyde dehydrogenase.

An alternative and THF-independent aldolase activity of SHMT involves the cleavage of β-hydroxyamino acids into glycine and aldehydes (Chiba *et al.*, 2011). A transcriptomic analysis of the *Δlmgt* promastigotes revealed that SMHT mRNA was up-regulated (Feng *et al.*, 2011). Our proteomic analysis, however, showed that SHMT was insignificantly regulated in the *Δlmgt* promastigotes. The produced by SHMT aldehyde can then be converted by aldehyde dehydrogenase to acetyl-CoA. A prior DIGE analysis, complemented by an LC-MS/MS analysis, revealed that a mitochondrial aldehyde dehydrogenase (mALDH) is up-regulated in the *Δlmgt* promastigotes (Feng *et al.*, 2011). That was corroborated by the DIGE and LC-MS/MS analysis performed by us (in preparation). Thus, if we consider the up-regulated mALDH we could speculate that L-threonine is converted to acetyl-CoA primarily via SHMT in the *Δlmgt* promastigotes. Additionally, down-regulation of acetyl-CoA synthetase and succinyl-CoA ligase suggests that the conversion of acetyl-CoA to acetate is decreased in the *Δlmgt* promastigotes. Indead, the NMR analysis confirmed that the amount of acetate excreted by the *Δlmgt* promastigotes is considerably less compared to that excreted by the wild type promastigotes (Tables III-7 and III-8). This could mean that the majority of acetyl-CoA in the *Δlmgt* promastigotes is preferentially directed toward more important pathways such as the TCA cycle and lipid biosynthesis, and only a small amount is converted to acetate and excreted. Under standard culture conditions, the excretion of acetate and other partially-oxidized end products results from consumption of higher amounts of D-glucose than can be utilized by the cells (Saunders *et al.*, 2011). Excretion of less acetate and succinate shows that carbon sources such as L-proline, L-threonine and glycerol are more effectively catabolized in the *Δlmgt* promastigotes.

Energy metabolism

Mitochondria are the power stations of the cells. Located on the inner membrane, the mitochondrial electron transport chain (ETC) is involved in the generation of energy in the form of ATP. The ETC of trypanosomatids is comprised of a ubiquinone/ubiquinol pool and complex I (NADH dehydrogenase or NADH:ubiquinone reductase), complex II (succinate dehydrogenase or succinate: ubiquinone reductase), complex III (cytochrome *bc* oxidoreductase or ubiquinone: cytochrome *c* reductase) and cytochrome *c* - complex IV (cytochrome *c* oxidase) (Acestor *et al.*, 2011). The transfer of electrons begins with oxidoreductive reactions in which coenzymes such as NAD and FAD are reduced by accepting electrons. The

electrons are then donated to the ubiquinone/ubiquinol pool and consequently transferred to the final electron acceptor, oxygen. Concomitantly, the produced protons are drawn across the inner mitochondrial membrane by complexes III and IV which generates an electrochemical gradient that is used by the F_0/F_1-ATP synthase (complex V) to produce ATP by oxidative phosphorylation (Besteiro *et al.*, 2005).

A number of studies with trypanosomatids belonging to the genera *Trypanosoma*, *Leishmania*, *Crithidia* and *Burkholderia* have focused on elucidating the exact structure and composition of the respiratory complexes and revealed that the complex subunits are encoded in the nuclear and kinetoplast-mitochondrial genomes and that an unexpectedly high number of the subunits were specific for the trypanosomatids (Speijer *et al.*, 1996a, b; Horvath *et al.*, 2000a, b; Maslov *et al.*, 2002; Acestor *et al.*, 2011; Gnipova *et al.*, 2012).

Complex I (NADH dehydrogenase, ND) is the largest one among the respiratory complexes. It is involved in transferring electrons from NADH to ubiquinone. The existence of the ND complex in trypanosomatids was questioned for a long time until genomic and proteomic studies provided evidence for its presence in these parasites (Duarte and Tomas, 2014). So far, 7-8 subunits are known to be encoded in the mitochondrial genome (Acestor *et al.*, 2011; Duarte and Tomas, 2014). The ND1-ND5 subunits are found to be homologous to the human ND proteins. 3 subunits, however, are homologous to the nuclearly encoded NDUFS2/ND7, NDUFS8/ND8 and NDUFS3/ND9. Nuclearly encoded in the trypanosomatids are the core subunits NDUFV1, NDUFV2, NDUFS1 and NDUFS7. Unfortunately, no enzymes associated with complex I were detected in our study.

Complex II (succinate dehydrogenase, SDH) is the component of the electron transport chain that links the TCA cycle with the cellular respiration. It functions by oxidizing succinate to fumarate with the concomitant reduction of ubiquinone to ubiquinol. In trypanosomatids, SDH was shown to be a membrane-bound protein complex comprised of four core subunits, SDH1, SDH2, SDH3 and SDH4 (Acestor *et al.*, 2011). The two hydrophilic SDH1 and SDH2 subunits are anchored on the inner mitochondrial membrane by the two hydrophobic subunits SDH3 and SDH4. Identified in our study was a putative SDH1 subunit, also known as succinate dehydrogenase flavoprotein. It was found up-regulated in the second organellar fraction (Supplemental table III-1) supporting its localization to the inner

mitochondrial membrane. In addition to the up-regulated SDH1 subunit, the level of succinate in the *Δlmgt* promastigotes was highly decreased which illustrating the key role of the substrate in energy generation in these parasites.

Complex III (cytochrome *c* reductase) is involved in reoxidation of ubiquinol by transferring electrons to cytochrome *c*. The core of complex III in trypanosomatids is comprised of a mitochondrially encoded cytochrome *b* and the nuclearly encoded cytochrome c_1 and the Rieske iron-sulfur protein (Acestor *et al.*, 2011). It is known that cytochrome b_5 can receive electrons from NADH-cytochrome b_5 reductase and cytochrome P450 (Schenkman and Jansson, 2003). In one of our preliminary comparative proteomic experiments cytochrome P450 was found 100 times up-regulated in the *Δlmgt* promastigotes compared to the wild type cells (data not included). With regard to the other two components of the complex, a study in *T. brucei* procyclic forms revealed that RNAi silencing of cytochrome c_1 results in ablation of Rieske iron-sulfur protein and vice versa which shows strong co-dependence between the two proteins (Horovath *et al.*, 2005). Additionally, silencing of any of the subunits proved that both proteins are necessary for complex III assembly and activity. The study further elucidated that inactivation of complexes III and IV redirects, to a certain extent, the electron flow toward the trypanosome alternative oxidase (TAO). TAO, however, is presumed abcent in *Leishmania* (van Hellemond *et al.*, 1998).

Trypanosomatid cytochrome *c* - complex IV (cytochrome *c* oxidase) appears to be considerably dissimilar to that of other eukaryotic organisms (Gnipova *et al.*, 2012). The core of the complex is comprised of 3 large mitochondrially encoded subunits and 10 smaller nuclear subunits (Speijer *et al.*, 1996a; Horvath *et al.*, 2000a). Additional subunits, however, are believed to also be associated with the complex. Surprisingly, 8 of the nuclear subunits do not have homologues in other eukaryotic cells (Speijer *et al.*, 1996b). In the *Δlmgt* promastigotes, differentially regulated was a putative cytochrome *c* oxidase subunit V. It was up-regulated in the second organellar fraction (Supplemental table III-1). A putative cytochrome *c* oxidase subunit IV was also differentially regulated in the *Δlmgt* promastigotes but not significantly. In 2002 Maslov and colleagues characterized subunit IV (COIV) of *L. tarentolae* (Maslov *et al.*, 2002). They found that COIV (trCOIV) is the largest subunit of cytochrome *c* oxidase, followed by subunit V (COV). They also showed that *T. cruzi*, *T. brucei* and *L. major* have homologous genes for trCOIV and detected the trCOIV polypeptides in procyclic

forms of *T. brucei* and promastigote forms of *L. amazonensis*. Regarding the function of COIV, the authors speculated, based on the peripheral localization of trCOIV toward the membrane and potential presence of an ATP-domain, that trCOIV have a regulatory function. If we assume that both COIV and COV have similar function it could be hypothesized that the regulation of complex IV in the *Δlmgt* promastigotes is more stringent with respect to more efficient production of energy.

Complex V (F_0F_1-ATP synthase) of trypanosomatids is comprised of two component, F_0 and F_1. The F_0 component is membrane bound and is involved in proton translocation while the F_1 component is soluble and represents the catalytic core. In bacteria, F_0 is comprised of three subunits in the following ratio – $a_1b_1c_{6\text{-}12}$. In different eukaryotic cells, however, the number and type of subunits is increased and varies considerably. The F_1 component of complex V has five subunits in the following ratio – $\alpha_3\beta_3\gamma_1\delta_1\varepsilon_1$. The F_1 α and β subunits of *T. brucei* have been characterized (Brown *et al.*, 2001). The β subunit, which is the catalytic subunit of the human H^+-ATP synthase, was shown to be the largest subunit of F_1. Besides the β subunit, differentially expressed in the *Δlmgt* promastigotes were also the α, γ and ε subunits of F_1. Noteworthy, they were all up-regulated (Supplemental table III-1). Thus, up-regulation of the majority of the subunits of the catalytic component of the ATP synthase shows that the ATP generation in the *Δlmgt* promastigotes is increased. At the same time, however, the increased generation of ATP appears to remain insufficient with respect to meeting the energy requirements of these cells judging by the decreased rate of many energy-consuming biosynthetic pathways, including non-metabolic pathways such as RNA, DNA and protein synthesis (Supplemental table III-1). So far, up-regulated in the *Δlmgt* promastigotes seem to be the synthesis of D-glucose and the ATP production. The rest of the metabolic pathways are more or less down-regulated in the *Δlmgt* promastigotes. Partially down-regulated is also the TCA cycle which was shown to play a central role in energy metabolism in the *Δlmgt* promastigotes. Another complementary pathway that could contribute to energy production in the *Δlmgt* promastigotes is the β-oxidation of fatty acids which is presented below (see Lipid metabolism).

Nucleotide metabolism

Maintaining the nucleotide pool homeostasis is a fundamental factor influencing metabolic capabilities and functional viability of any given cell. Most

eukaryotic cells are able to synthesize purines and pyrimidines. *Leishmania*, however, are not able to synthesize purines *de novo* so they have to acquire them from the insect and mammalian hosts. The purine salvage pathway in *Leishmania*, or one of the salvage pathways, is proposed to involve a plasma membrane-associated bifuntional ecto-3'-nucleotidase/nuclease (ecto-3'-NT/NU) which can cleave extracellular polynucleotides and 3'-nucleotide monophosphates to nucleosides and nucleobases (Sopwith *et al.*, 2002). Detected in the *Δlmgt* promastigotes was a putative down-regulated 3'-NT/NU precursor. Down-regulation of the 3'-NT/NU precursor shows that the promastigotes may possibly use alternative mechanisms to generate nucleosides and nucleobases. It was additionally demonstrated that *Leishmania* synthesize and secrete a dithiothreitol-sensitive nuclease which can also hydrolyse extracellular polynucleotides and nucleic acids, including RNA and single- and double-stranded DNA (Joshi and Dwyer, 2007). The exogenous nucleosides and nucleobases preformed by the parasite enzymes are then imported by purine transporters. Various studies indicated that *Leishmania* are able to transport all naturally occurring nucleosides and nucleobases, including xanthine and xanthosine (Carter *et al.*, 2008). The stable isotope tracing analysis confirmed the presence of unlabelled adenine and hypoxanthine in condition ***glc0** wild type and *Δlmgt* promastigotes (Figure IV-12). No transporters, however, were found differentially expressed in the *Δlmgt* promastigotes but it is typical for such integral membrane proteins, which are of relatively low abundance, to be poorly represented in proteomic analyses. Thus, besides the decreased activity of the 3'-NT/NU precursor, no information about the purine requirements and transport in the *Δlmgt* promastigotes could be obtained from this investigation. It is not excluded, however, that a number of ecto-enzymes are co-expressed by the promastigotes in order to supply the parasites with purines.

When imported, the nucleosides and nucleobases can be metabolised via several different ways. Nucleosides can be subjected to hydrolysis in which the *N*-glycosidic bond of purine and pyrimidine ribosides is hydrolysed to produce ribose and a respective nucleobase (Miller *et al.*, 1984). A nonspecific nucleoside hydrolase was found up-regulated in the *Δlmgt* promastigotes by the 2D-DIGE analysis (in preparation) which is possibly involved in supplying the cells with higher amounts of ribose and/or nucleobases.

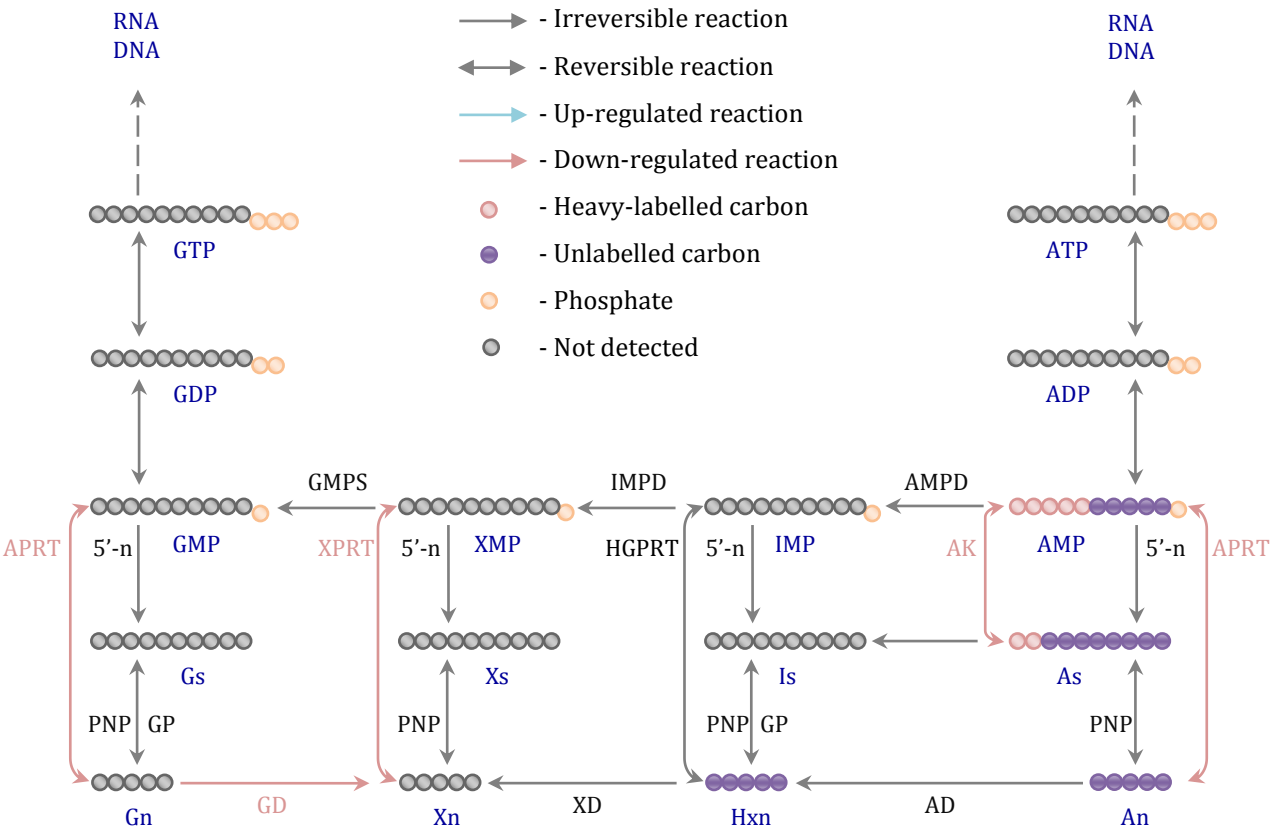

Figure IV-12. Schematic representation of purine metabolism in *Δlmgt* promastigotes incubated with ^{13}C-D-glucose. Presented here are quantitative proteomic data. Specified with light blue arrows are the up-regulated enzymes while specified with pink arrows are the down-regulated enzymes. Abbreviations: Gn - guanine, Xn - xanthine, Hxn - hypoxanthine, An - adenine, Gs - guanosine, Xs - xanthosine, Is - inosine, As - adenosine, GMP - guanine 5'-monophosphate, GDP - guanosine 5'-diphosphate, GTP - guanosine 5'-triphosphate, XMP - xanthosine 5'-monophosphate, IMP - inosine 5'-monophosphate, AMP - adenosine 5'-monophosphate, ADP - adenosine 5'-diphosphate, ATP - adenosine 5'-triphosphate, DNA - deoxyribonucleic acid, RNA - ribonucleic acid, 5'-n - 5'-nucleosidase, AK - adenosine kinase, PNP - purine-nucleoside phosphorylase, GP - guanosone phosphorylase, GD - guanine deaminases, GMPS - GMP synthase, IMPD - IMP dehydrogenase, AMPD - AMP deaminases, XD - xanthine dehydrogenase, AD - adenine deaminases, APRT - adenine phosphoribosyltransferase, HGPRT - hypoxanthine-guanine phosphoribosyltransferase, XPRT - xanthine phosphoribosyltransferase.

At the same time, a nucleoside hydrolase-like protein was down-regulated which indicated that the *Δlmgt* promastigotes are tuning their enzyme activities in order to use certain substrates for the generation of specific nucleobases. For instance, the up-regulated nonspecific nucleoside hydrolase (LmxM.18.1580) of *L. mexicana* is an ortholog/paralog to a putative inosine-guanine nucleoside hydrolase in *L. braziliensis*, *L. infantum* and *L. major* (TriTrypDB.org) and is most probably involved in inosine and guanine metabolism. The generated or imported nucleobases then can either be phosphorylated or deaminated. For instance, adenosine can be hydrolysed to adenine which can then be phosphorylated to AMP or deaminated first to hypoxanthine and then phosphorylated to IMP (Carter *et al.*, 2008). Eventually, under the action of the glycosomal adenine phosphoribosyltransferase (APRT), hypoxanthine-guanine phosphoribosyltransferase (HGPRT) and xanthine phosphoribosyltransferase (XPRT), the nucleobases adenine, guanine, hypoxanthine and xanthine can be converted to the nucleotides AMP, GMP, inosnine 5'-monophosphate (IMP) and xanthosine 5'-monophosphate (XMP), respectively (Colasante *et al.*, 2006). APRT and XPRT, involved in adenine and guanine, and xanthine metabolism, respectively (Colasante *et al.*, 2006), were down-regulated in the *Δlmgt* promastigotes. Additionally, an adenosine kinase, which reversibly phosphorylates adenosine to AMP, and a guanine deaminase, which converts guanine to xanthine, were also down-regulated. Taken together, we could say:

- that purine nucleotides are intermediates of significant importance for the *Δlmgt* promastigotes judging by the minimal heavy-labelling observed in some of them in condition ***glc0** *Δlmgt* promastigotes (see **IV.1.3.**);
- that purine salvage pathway is decreased in the *Δlmgt* promastigotes;
- that the *Δlmgt* promastigotes recycle ribose via a nonspecific nucleoside hydrolases (see Pentose phosphate pathway).

In contrast to purines, *Leishmania* are able to *de novo* synthesize pyrimidines from L-glutamine, bicarbonate and L-aspartate (Opperdoes and Michels, 2008). L-Glutamine was shown to be taken up by the *Δlmgt* promastigotes at an increased rate (Thesis: Lamasudin, 2012). The inability of *Leishmania* to convert L-glutamine into L-glutamate, and thus be used a glucogenic precursor, means that the amino acid is used for biosynthetic purposes mainly. Of the five enzymes involved in the pyrimidine

synthesis, namely carbamoylphosphate synthase, aspartate carbamoyltransferase, dihydroorotase, dihydroorotate dehydrogenase and orotidine 5'-phosphate decarboxylase/orotate phosphoribosyltransferase, only a putative aspartate carbamoyltransferase, involved in the condensation of L-aspartate and carbamoyl-phosphate into N-carbamoyl-L-aspartate, was found slightly down-regulated in the *Δlmgt* promastigotes (Supplemental table III-1). This indicates that the intial steps of the UMP synthesis are insignificantly down-regulated in the *Δlmgt* promastigotes. The slightly increased level of cytosine, a precursor for cytidine 5'-diphosphate (CDP) which is involved in phospholipid biosynthesis (see Phospholipid metabolism), thus could be accounted for uptake from the media, as it was observed in *T. cruzi* (Gutteridge and Gaborak, 1979). The minimal change in the activity of aspartate carbamoyltransferase and slightly different levels of orotate and cytosine in the *Δlmgt* promastigotes (Figure IV-3, E and F) compared to the wild type cells suggests that pyrimidine synthesis is not significantly affected by the deletion of the glucose transporters in the *L. mexicana* promastigotes.

Lipid metabolism

Fatty acid biosynthesis

D-Glucose, L-proline and L-threonine were shown to be precursors, via acetyl-CoA, for fatty acid (FA) biosynthesis in procyclic trypanosomes (Bringaud *et al.*, 2006). In *Leishmania* specifically are believed to operate two types of *de novo* FA synthesis - an unconventional FA elongation (FAE) and type II FA synthesis (FASII) (Ramakrishnan *et al.*, 2013). The synthesis starts with the conjugation of two molecules of acetyl-CoA into a molecule of malonyl-CoA (Lee *et al.*, 2006). Both pathways rely on consecutive addition of two carbon units from malonyl-CoA to a growing carboxylic chain. The difference between the two pathways is that the growing chain is held by a carrier, an acyl carrier protein (ACP) in the case of FASII and a primer in the case of FAE. The enzymes involved in the fatty acid synthesis are an acetyl-CoA carboxylase, a ketoacyl synthase, a ketoacyl reductase, a dehydratase and an enoyl-CoA reductase. Of the listed proteins, genes for an acyl carrier protein, a ketoacyl synthase and an enoyl-CoA reductase were found in the genome of *L. major* (Ramakrishnan *et al.*, 2013). Our quantitative proteomic analysis revealed that only a putative β-ketoacyl-CoA reductase (3-ketoacyl-CoA reductase) was significantly up-regulated in the *Δlmgt* promastigotes (Supplemental table III-1).

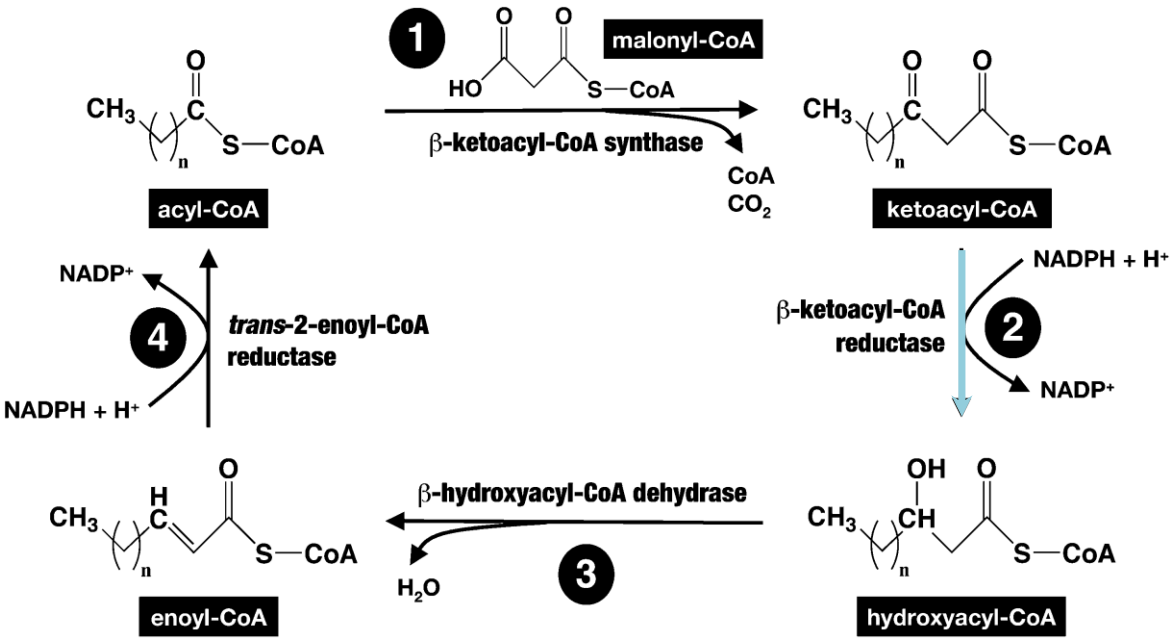

Figure IV-13. Fatty acid elongation in trypanosomes. Specified with a light blue arrow is the up-regulated reaction in the *Δlmgt* promastigotes.
Credit: Lee *et al.*, 2006

β-Ketoacyl-CoA reductase catalyses the reduction of β-ketoacyl-CoA resulting from extending the growing acyl chain with two carbons (Figure IV-13) (Lee *et al.*, 2006). The reduced β-ketoacyl-CoA is then dehydrated by a β-hydroxyacyl-CoA dehydrase and reduced again by an enoyl-CoA reductase. The four-step process yields a longer, saturated acyl-CoA. The longest fatty acid chain in trypanosomes can contain up to 18 carbons (C18) but the presence of 12 tandemly linked homologous genes for elongases (ELOs) in *L. major*, compared to the four ELOs involved in fatty acid elongation in *T. brucei*, along with the presence of C22, C24 and C26 alkyl chains in LPG and C24 and C26 alkyl chains in gp63 suggest that *Leishmania* can synthesize longer fatty acids (Ferguson *et al.*, 2009; Ramakrishnan *et al.*, 2013). The long-chain fatty acids are the main precursors for the synthesis of phospholipids, sphingolipids and ergosterols. Fatty acid biosynthesis is thus important for the synthesis of a variety of lipids that are involved in the maintenance of the cellular integrity, which in turn was shown to be important for the proper functioning of the mitochondrial electron transport chain (ETC) in *T. brucei* (Guler *et al.*, 2008). Only a single reaction of the fatty acid biosynthesis, however, was found regulated in the *Δlmgt* promastigotes, namely the second step of the fatty acid elongation. In *E. coli*, the enzyme catalyzing the second step of the FA synthesis cannot be substituted by any other enzyme (Jansen and Steinbuchel, 2014). Additionally, β-ketoacyl-CoA reductase functions at the expence of NADPH (Figure IV-13).

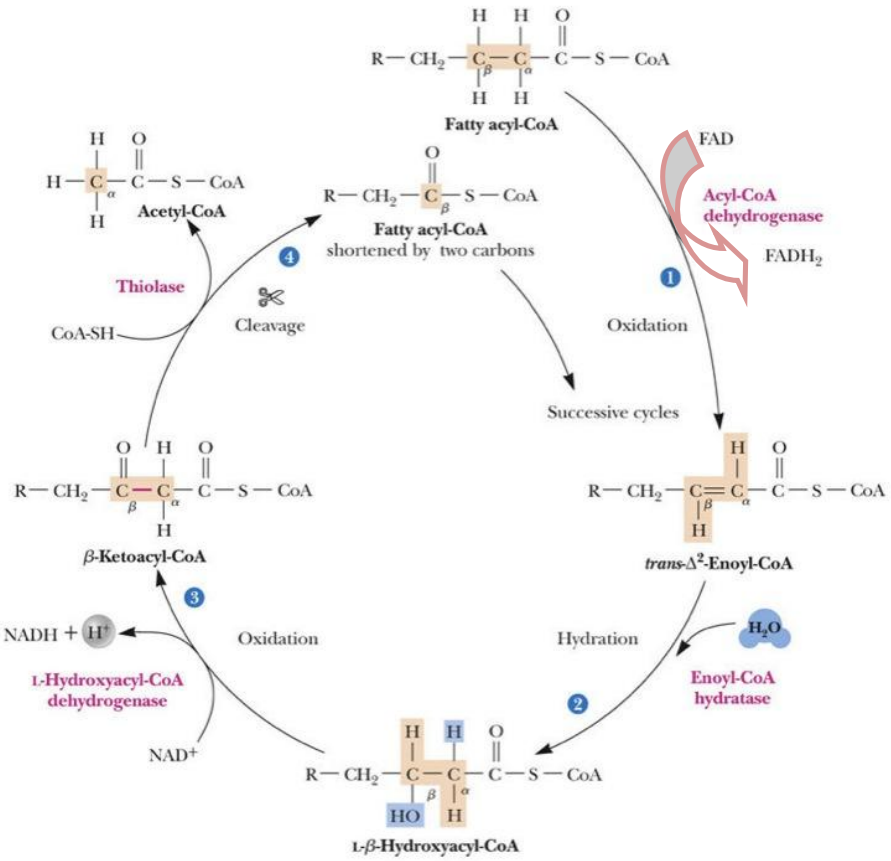

Figure IV-14. β-Oxidation of fatty acids. Specified with a pink arrow is the down-regulated reaction in the *Δlmgt* promastigotes.
Credit: oregonstate.edu

NADPH is a crucial coenzyme for many cellular processes, including defense against oxidative stress via trypanothione (see Glutathione metabolism). The level of NADPH is presumably decreased in the glycosomes of the *Δlmgt* promastigotes as a consequence of the suppressed oxidative phase of the pentose phosphate pathway which is responsible for the regeneration of NADPH (see Pentose phosphate pathway). It is not known whether the NADPH generated in the glycosomes could be directed towards redox reactions outside the glycosomes and vice versa, but it could not be excluded that other NADPH sources may also exist in the cells. The contribution of similar reactions in the maintenance of the glycosomal redox balance, however, is probably negligible. Thus, the up-regulation of β-ketoacyl-CoA reductase may suggest that the enzyme has a key role in fatty acid biosynthesis and could be linked to the up-regulated ETC in the *Δlmgt* promastigotes. Though the evidence is based on up-regulation of a single enzyme, an increase in fatty acid synthesis in the *Δlmgt* promastigotes, in addition to the increased level of glycerol in these cells (Supplemental table III-2), supports the idea that, in addition to the short-term

carbohydrate reserve material mannogen, *Leishmania* can store fatty acids in the form of triglyceride, similar to *T. cruzi* (Rogerson and Gutteridge, 1980). This energy store, however, does not appear to be immediately used by the *Δlmgt* promastigotes (see β-Oxidation of fatty acids) but it may have a function in the infectious forms of *Leishmania*, the amastigotes.

In addition to saturated fatty acids, *Leishmania* are able synthesize unsaturated fatty acids as well (Lee *et al.*, 2006). The unsaturated FAs are divided into mono-unsaturated (MUFA) and polyunsaturated (PUFA) FAs. The PUFA synthesis in *Leishmania* involves a stearoyl-CoA desaturase, two ELOs, that is Δ6, which is specific for C18 PUFAs, and Δ5, which is specific for C20 PUFAs, and five desaturases, namely Δ12, Δ6, Δ5, Δ4, and ω3 (Tripodi *et al.*, 2006; Livore *et al.*, 2006; Uttaro, 2006). *Leishmania* are thought to be able to synthesize all the PUFAs they require by using the stearate generated in the FAE pathway as a precursor. Palmitate, stearate and oleate were found universally labelled in condition ***glc0** wild type promastigotes grown under regular conditions (Figure IV-7). The labelling in conditions 2 - 10 wild type promastigotes was absent or negligible which showed that under nutrient-restricted conditions the fatty acid synthesis in the wild type promastigotes is limited. On the other hand, minor labelling was observed in some unsaturated fatty acids in conditions **glc+*pro**, ***pro**, **glc+*thr** and ***thr** *Δlmgt* promastigotes which showed that a small amount of L-proline and L-threonine are used as fatty acid precursors by the *Δlmgt* promastigotes.

β-Oxidation of fatty acids

Sugar catabolism plays a central role in energy supply for *Leishmania* promastigotes. The main pathway performing the same function in amastigotes is β-oxidation of fatty acids (Rosenzweig *et al.*, 2008a; Brotherton *et al.*, 2010). β-Oxidation of fatty acids is another pathway that takes place in the glycosomes (Hart and Opperdoes, 1984; Berriman *et al.*, 2005). It is believed, however, that the mitochondrion also plays a role in the process. How the two organelles contribute to the pathway, however, is still unknown.

β-Oxidation of fatty acids involves the oxidation of fatty acids with different chain-length to acetyl-CoA, NADH and $FADH_2$. Acetyl-CoA can be oxidized in the TCA cycle (Saunders *et al.*, 2014) while NADH and FAD_2 can be directed to the electron transport chain for the generation of ATP. Four different chain-length fatty acyl-CoA

dehydrogenases are present in the *Leishmania* genome (Opperdoes and Michels, 2008). Three of the acyl-CoA dehydrogenases have mitochondrial targeting signals. Bifunctional enzymes and thiolases are predicted to be present in the glycosomes and the mitochondrion as well. *Leishmania* are also predicted to be able to oxidize unsaturated fatty acids judging by the presence of genes encoding a 3,2-trans-enoyl-CoA isomerise and 2,4-dienoyl-CoA reductase in the genome of *L. major* (Opperdoes and Michels, 2008).

Palmitate, stearate and oleate, abundant in the serum supplementing culture media, are rapidly taken up by the *L. mexicana* amastigotes (Berman *et al.*, 1987). Additionally, it was determined that the amastigotes are able to oxidize short-, medium- and long-chain fatty acids at a comparable rate which revealed that a large amount of energy could be generated via β-oxidation of fatty acids (Berman *et al.*, 1987). Due to the inability of the *Δlmgt* promastigotes to utilize exogenous carbohydrates, it could be assumed that besides amino acids, the *Δlmgt* promastigotes would actively use fatty acids as energy sources as well. Surprisingly, our proteomic data disproved that assumption. The data revealed that the first and third steps of the β-oxidation of fatty acids, catalyzed by an acyl-CoA dehydrogenase and a short chain 3-hydroxyacyl-CoA dehydrogenase, respectively (Figure IV-19), were regulated in the *Δlmgt* promastigotes but not significantly. The only enzyme of the β-oxidation pathway that was significantly modulated in the *Δlmgt* promastigotes was a putative electron-transfer flavoprotein, α polypeptide (ETFA) which shuttles the electrons generated in the first step of the fatty acid oxidation to the membrane-bound electron transfer flavoprotein:ubiquinone oxidoreductase (ETF-QO) of the mitochondrial respiratory chain which, in turn, transfers the electrons to the ubiquinone pool. The acyl-CoA dehydrogenase and the short chain 3-hydroxyacyl-CoA dehydrogenase, included for illustrative purposes only, and the electron transfer protein were down-regulated in the *Δlmgt* promastigotes. Thus, quite surprisingly, the decreased β-oxidation of fatty acids in the *Δlmgt* promastigotes indicates that fatty acids do not appear to be energy sources for these cells. Instead, the fatty acids are probably used for the synthesis of the spectrum of phospholipids comprising the leishmanial membranes (see Phospholipid metabolism), for the synthesis of the lipid-containing molecules anchoring proteins on the plasma membrane and for the synthesis of signalling molecules, all of which required for the parasite viability and infectivity.

Phospholipid metabolism

Leishmania are able to utilize ether-lipids from the environment or synthesize them *de novo* (Opperdoes, 1984). The ether biosynthesis can occur via two pathways: the glycerol 3-phosphate (G3P) pathway or the dihydroxyacetone phosphate (DHAP) pathway. A study by Heise and Opperdoes clarified that the ether-lipid biosynthesis in *L. mexicana* occurs via the DHAP pathway (Heise and Opperdoes, 1997). In the first three steps of the pathway DHAP is successively converted to 1-acyl-DHAP, 1-alkyl-DHAP and 1-alkyl-glycerol 3-phosphate (G3P) by a DHAP acyltransferase (DHAPAT), a FAD-dependent alkyl DHAP synthase and an NADPH-dependent 1-alkyl/acyl DHAP reductase (Zufferey and Mamoun, 2006). Detected in the *Δlmgt* promastigotes was only alkyl DHAP synthase which was found to be up-regulated (Supplemental table III-1). Although the three enzymes are sequestered in the glycosomes (Zufferey and Mamoun, 2006), alkyl DHAP synthase was found present in the insoluble fraction only, suggesting a high degree of hydrophobicity. Emanating from the essential role of DHAPAT for growth, survival during stationary phase, synthesis of ether lipids and virulence in *L. major* (Al-Ani *et al.*, 2011), and the up-regulation of the alkyl DHAP synthase, we could allow ourselves to speculate again that, first, the reaction catalyzed by the alkyl DHAP synthase is the critical step in the ether-phospholipid biosynthesis in *Leishmania* and, second, that the pathway is increased in the *Δlmgt* promastigotes. Ether lipids, in the form of 1-*O*-alkyl-glycerols, are components of a variety of glycoconjugates such as LPG, GILPs and GPI-anchored proteins (McConville and Ferguson, 1993). The down-regulated synthesis of GDP-Man, Dol-P-Man and UDP-Gal, involved in the synthesis of the glycan core of the GPI anchors (see Fructose and mannose and Galactose metabolism), along with the up-regulated alkyl DHAP synthase indicates that the bulk of ether lipids is not used for GPI anchor synthesis but it is possibly directed toward the synthesis of phospholipids. Ether-lipids are especially present in phosphatidylethanolamines (PEs) and phosphatidylserines (PSs). PEs, PSs, phosphatidylcholines (PCs) and phosphatidylinositol (PIs) constitute around 60-70% of *Leishmania* lipids (Zhang and Beverly, 2009 and the references therein). PCs are the most abundant phospholipids (30-40%) while PEs and PIs together comprise about 20% of the total cellular lipids (Zhang and Beverly, 2009).

The first study on choline transport in *Leishmania* was reported by Zufferey and Mamoun in 2002. They showed that *L. major* takes up choline via a carrier-mediated and Na^+-independent process involving high affinity and high specificity

transporter(s) operating optimally at pH 7.5-8 (Zufferey and Mamoun, 2002). A year later, a study with fluorescent analogues of phosphatidylcholine (PC), phosphatidylethanolamine (PE), phosphatidylserine (PS) and sphingomyelin in *L. infantum* promastigotes revealed that PC, PE and PS are promptly taken up in a protein- and energy-dependent but temperature- and endocytosis-independent manner (Araujo-Santos *et al.*, 2003). In addition to taking up phospholipids such as PC, PE and PS, *Leishmania* are able to synthesize them. Phosphorylation of choline and ethanolamine to phosphocholine and phosphoethanolamine by a choline/ethanolamine kinase represents the first step of phospholipid biosynthesis via the Kennedy pathway (Gibellini *et al.*, 2008; Kennedy and Weiss, 1956; Ramakrishnan *et al.*, 2013). Phosphocholine and phosphoethanolamine were authentically identified and found increased in the *Δlmgt* promastigotes compared to the wild type promastigotes (Figure IV-3, C and D). Phosphocholine and phosphoethanolamine are then activated to cytidine diphosphate (CDP)-choline and CDP-ethanolamine by a cholinephosphate cytidylyltransferase and ethanolaminephosphate cytidylyltransferase, respectively. In the *Δlmgt* promastigotes, CDP-choline and CDP-ethanolamine were labelled only in the conditions with ^{13}C-L-proline, which again confirmed the important function of L-proline as a carbon source for the *Δlmgt* promastigotes. Cytosine, a precursor for CDP, was also slightly increased in the *Δlmgt* promastigotes (Figure IV-3, E).

Altogether, the metabolomic data indicate that the *Δlmgt* promastigotes still synthesize the precursors for PC and PE and that these precursors have increased levels in these cells. None of the proteins with known function modulated in the *Δlmgt* promastigotes belonged to the PC, PE, PI or PS synthesis (see Chapter I, **I.1.5.4.3.**). Although PCs and PEs are abundant glycerophospholipids in *Leishmania*, their role is not really known. PCs are possibly involved in defence against host oxidants (Zhang and Beverley, 2010). PIs are involved in the GPI anchor biosynthesis (Turco *et al.*, 1989) and could be involved also in cell signalling and membrane trafficking. PSs facilitate the entry of the *Leishmania* promastigotes into the phagolysosomes and protect the cells from degradation by the host phagocytes (Zhang and Beverley, 2010 and the references therein). It appears that phospholipid synthesis is important for the *Δlmgt* promastigotes, judging by the increased fatty acid and ether lipid biosynthesis and the increased levels of phosphocholine and phosphoethanolamine.

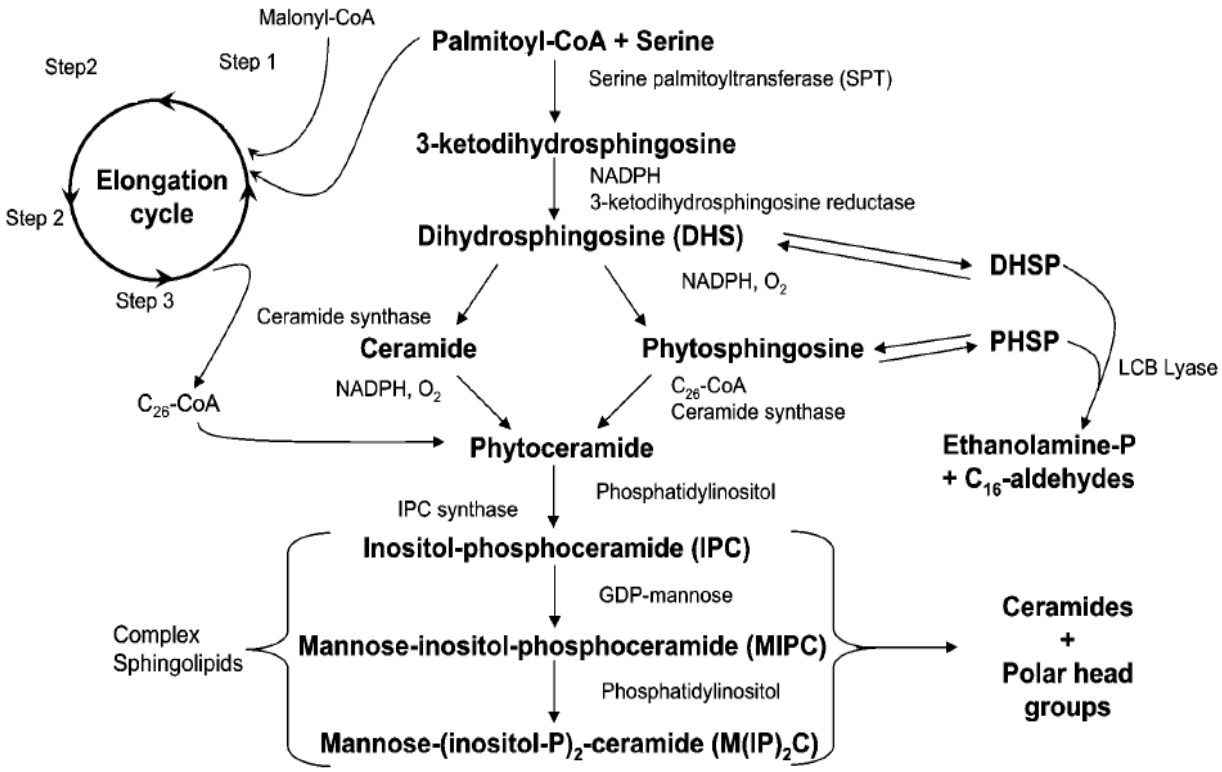

Figure IV-15. Sphingolipid biosynthesis in *Saccharomyces cerevisiae*. P - phosphate.
Credit: Dickson, 2008

It could be speculated that these macromolecules are important in maintaining the cellular integrity. Their specific role, however, is yet to be elucidated.

Sphingolipid metabolism

In addition to PC and PE, phosphocholine and phosphoethanolamine are also components of sphingomyelin. *Leishmania*, however, are not able to synthesize sphingomyelin or complex glycosphingolipids (Zhang and Beverley, 2010). Instead, they synthesize ceramides, unglycosylated inositol phosphorylceramide (IPC) and neutral glycosphingolipids (Zhang and Beverley, 2010 and the references therein). Myristoyl-CoA, which is believed to be preferentially utilized by *Leishmania* in the sphingolipid biosynthesis instead of palmitoyl-CoA (Hsu *et al.*, 2007), the first enzyme of the sphingolipid biosynthesis, the PLP-dependent serine palmitoyltransferase which catalyzes the condensation of L-serine and myristoyl-CoA/palmytoil-CoA (Figure IV-15), as well as the rest of the enzymes of the pathway, were also not detected in the *L. mexicana* promastigotes. Two studies, focused on sphingolipid biosynthesis in *Leishmania*, were also not able to detect serine palmitoyltransferase subunit 2 which suggested that the biosynthetic pathway is down-regulated in

metacyclic promastigotes and amastigotes (Zhang et al., 2003; Denny *et al.*, 2004). It was not evident from our data whether the sphingolipid synthesis was regulated in the *Δlmgt* promastigotes or not.

The other central intermediates in sphingolipid synthesis are ceramids (Figure IV-15), composed of sphingosine and a fatty acid, while the end product of the synthesis, IPC, is comprised of a ceramide linked to an insitol phosphate. In fungi and *Leishmania*, IPC is a common sphingolipid but it is not present in mammals which makes it an interesting drug target (Zhang and Beverley, 2010 and the references therein). The majority of IPC in *Leishmania* is phosphoryl inositol N-stearoylsphingosine (d18:1/18:0-IPC). The other IPC species present in these parasites is phosphoryl inositol N-stearoylhexadecesphing-4-enine (d16:1/18:0-IPC) (Zhang and Beverley, 2010). Other than that, little is known about the function of IPC. Up to date, there are no data suggesting that IPC can serve as an anchor for glycoconjugates. In general, one of the main roles of sphingolipids (of IPC mostly) is as structural components of the outer leaflet of the plasma membrane bilayer where they, along with sterols and GPI-anchored molecules, form specific sub-domains designated lipid rafts (Denny and Smith, 2004). In *Plasmodium falciparum*, another protozoan parasite that causes malaria in humans, lipid rafts are involved in parasitophorous vacuolar membrane biogenesis and trafficking of GPI-anchored proteins (Denny and Smith, 2004). It is not known yet whether lipid rafts have the same function in *Leishmania* or not. Besides structural role, sphingolipids such as sphingosine, sphingosine 1-phosphate, ceramide and ceramide 1-phosphate are involved in a number of signalling pathways including apoptosis, cell-to-cell recognition, growth and differentiation in mammalian cells (Zhang and Beverley, 2010 and the references therein). It is believed that some of these molecules may have similar signalling function in *Leishmania* as well.

IV.3. Summary

Amino acids are alternative carbon and energy sources for many organisms. The uptake of amino acids such as L-glutamine, L-proline, and L-serine is increased in the glucose transporter null-mutant *Leishmania*. At the same time, the levels of L-alanine, L-aspartate, L-asparagine, L-glutamate, L-glutamine, L-ornithine, and L-proline are decreased in these organisms. These results indicate that the rate of utilization of amino acids by the *Δlmgt* promastigotes is increased.

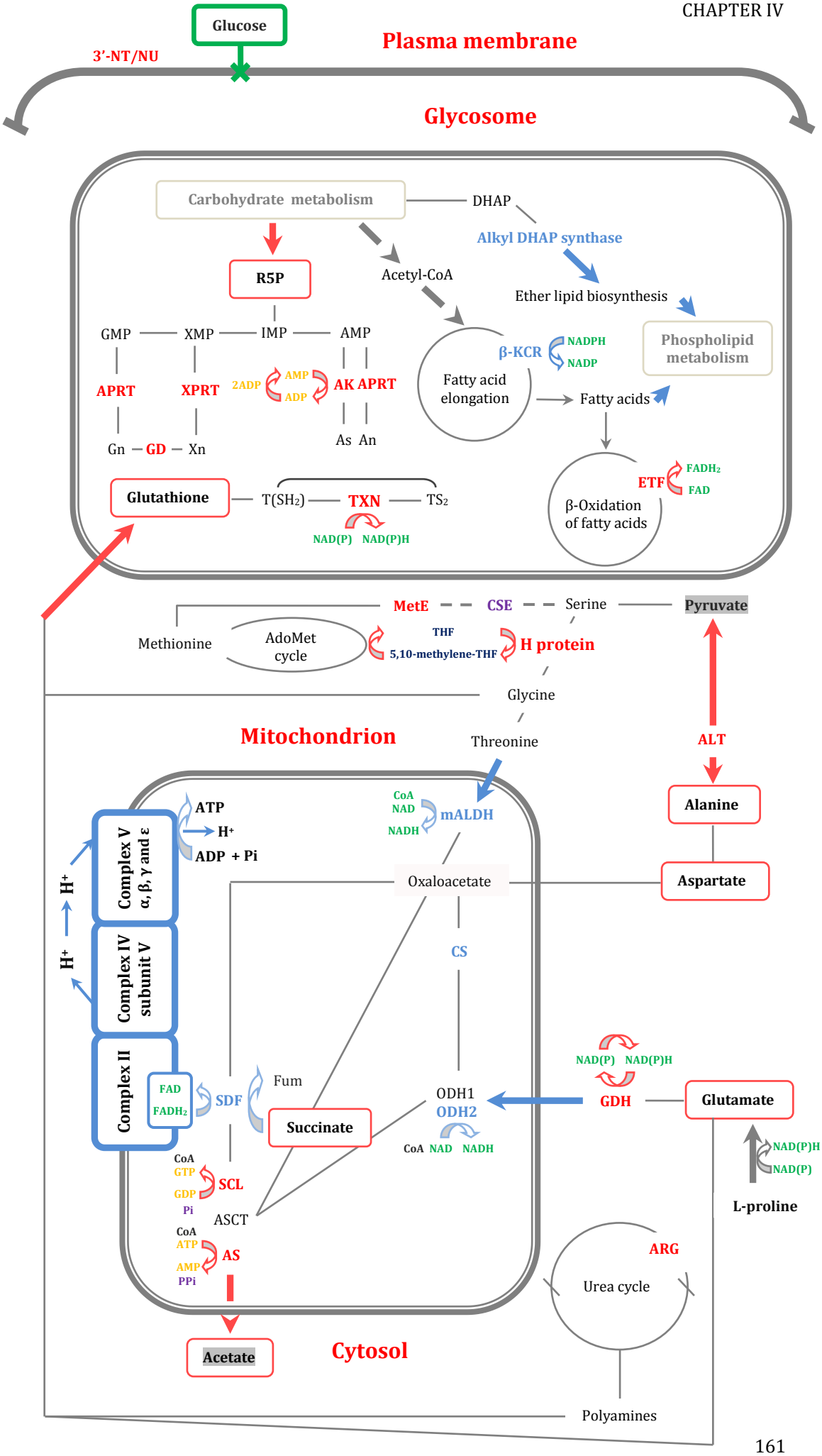
Glucose
3'-NT/NU
Plasma membrane
Glycosome
Carbohydrate metabolism
DHAP
Alkyl DHAP synthase
R5P
Acetyl-CoA
Ether lipid biosynthesis
GMP
XMP
IMP
AMP
APRT
XPRT
2ADP
AMP
ADP
AK APRT
As An
Gn
GD
Xn
β-KCR
NADPH
NADP
Fatty acid elongation
Fatty acids
Phospholipid metabolism
ETF
FADH2
FAD
β-Oxidation of fatty acids
Glutathione
T(SH2)
TXN
TS2
NAD(P)
NAD(P)H
MetE
CSE
Serine
Pyruvate
Methionine
AdoMet cycle
THF
5,10-methylene-THF
H protein
Glycine
Threonine
Mitochondrion
ALT
Alanine
Aspartate
ATP
H+
ADP + Pi
CoA
NAD
NADH
mALDH
Oxaloacetate
Complex V α, β, γ and ε
Complex IV subunit V
Complex II
CS
FAD
FADH2
SDF
Fum
Succinate
ODH1
ODH2
CoA
NAD
NADH
NAD(P)
NAD(P)H
GDH
Glutamate
NAD(P)H
NAD(P)
L-proline
CoA
GTP
GDP
Pi
SCL
ASCT
CoA
ATP
AMP
PPi
AS
ARG
Urea cycle
Acetate
Cytosol
Polyamines

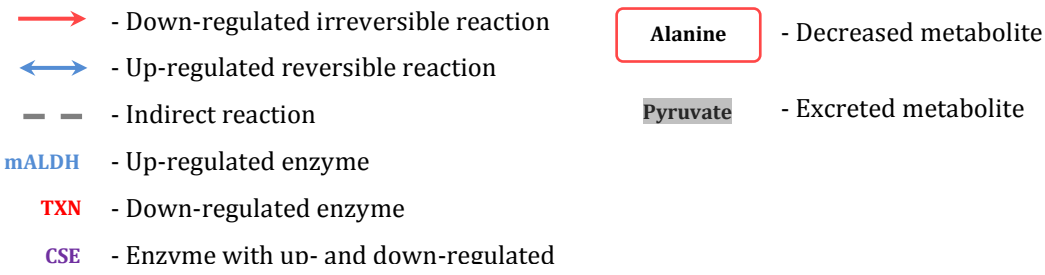

Figure IV-16. Schematic representation of the changes in amino acid, energy, nucleotide and lipid metabolism in the *Δlmgt* promastigotes. Specified with blue arrows are the up-regulated enzymes while specified with red arrows are the down-regulated enzymes. Abbreviations: R5P – ribose 5-phosphate, DHAP - dihydroxyacetone phosphate, Gn - guanine, Xn - xanthine, An - adenine, As - adenosine, XMP - xanthosine 5'-monophosphate, IMP - inosine 5'-monophosphate, AMP - adenosine 5'-monophosphate, ADP - adenosine 5'-diphosphate, ATP - adenosine 5'-triphosphate, GMP - guanosine 5'-monophosphate, GDP - guanosine 5'-diphosphate, GTP - guanosine 5'-triphosphate, $T(SH)_2$ - trypanothione, TS_2 - trypanothione disulfide, NAD - nicotinamide adenine dinucleotide, NADP - nicotinamide adenine dinucleotide phosphate, FAD - flavin adenine dinucleotide, CoA - coenzyme A, Pi - inorganic phosphate, THF - tetrahydrofolate, H^+ - proton, 3'-NT/NU - 3'-nucleotidase/nuclease, AK - adenosine kinase, GD - guanine deaminases, GMPS - GMP synthase, IMPD - IMP dehydrogenase, AMPD - AMP deaminases, XD - xanthine dehydrogenase, APRT - adenine phosphoribosyl-transferase, XPRT - xanthine phosphoribosyltransferase, β-KCR - β-ketoacyl-CoA reductase, ETF - electron-transfer flavoprotein, α polypeptide, TXN - tryparedoxin, MetE - 5-methyltetrahydropteroyltriglutamate--homocysteine methyltransferase, CSE - cystathionine γ-lyase, ALT - alanine aminotransferase, GDH - glutamate dehydrogenase, ARG - arginase, mALDH - mitochondrial aldehyde dehydrogenase, CS - citrate synthase, ODH1 - 2-oxoglutarate dehydrogenase E1 component, ODH2 - 2-oxoglutarate dehydrogenase E2 component, SCL - succinyl-CoA ligase, SCS - succinyl-CoA synthetase, SDF - succinate dehydrogenase flavoprotein, AS - acetyl-CoA synthetase, ASCT - acetate:succinate CoA transferase.

This observation is further strengthened by the up-regulation of a number of enzymes that facilitate the entry of ketogenic and glucogenic amino acids, through acetyl-CoA and α-ketoglutarate, respectively, in the TCA cycle (Figure IV-16). On the other hand, some enzymes that fuel amino acids, such as L-aspartate and L-alanine, into gluconeogenesis and the gluconeogenesis itself are down-regulated which shows that a major part of the amino acids is used by the *Δlmgt* promastigotes for energy production and only a minor part for biosynthesis. Further to that, our data illustrate that alternative amino acid pathways for energy production and biosynthesis are activated in the *Δlmgt* promastigotes. L-Arginine, for instance, may not be the only precursor for L-ornitine. L-Glutamate, through N-acetyl-L-glutamate and N-acetyl-L-ornithine, may also be a source for L-ornithine and polyamines. L-Proline, through L-glutamate or 4-aminobutanoate (GABA) and succinate, may be fed into the TCA cycle and used both as a carbon and energy source. L-Glutamine, similarly, may be fed into the TCA cycle via α-ketoglutaramate and α-ketoglutarate. L-Glutamine, furthermore, is utilized as a pyrimidine precursor by the *Leishmania* parasites. Our data showed that pyrimidine metabolism is not significantly modulated in the *Δlmgt* parasites. A significant number of enzymes of the purine salvage pathway, however, have altered expression in the *Δlmgt* promastigotes. The formation of nucleotides such AMP, GMP

and XMP is down-regulated which can affect i/ ATP synthesis, ii/ RNA and DNA synthesis, iii/ coenzyme synthesis, iv/ cyclic AMP and GMP synthesis, and v/ protein synthesis. It is evident from our proteomic data that a large number of enzymes involved in RNA and DNA synthesis and metabolism, and protein synthesis are down-regulated in the *Δlmgt* promastigotes. Taken together, the data indicate that the *Δlmgt* promastigotes reduce energy-consuming processes such as RNA, DNA, and protein synthesis, while up-regulate energy generation through the electron transport chain and oxidative phosphorylation. Finally, our lipidomic study showed minimal changes in lipid metabolism in the *Δlmgt* promastigotes. Altogether, the data revealed that the *Δlmgt* promastigotes i/ have significantly decreased thiol-redox system, ii/ have decreased amino acid biosynthetic capacity, iii/ use exogenous amino acids as main alternative energy and carbon sources, iv/ use L-threonine as a main source of acetate, v/ use L-proline as a major carbon and energy source, vi/ use the TCA cycle, electron transport chain, and oxidative phosphorylation for energy production via amino acid catabolism, and vii/ use lipids as biosynthetic precursors but not as energy sources. Our proteomic and metabolomic analysis of the *Δlmgt* promastigotes thus showed that carbohydrate, amino acid, and energy metabolism are intimately linked in *Leishmania*, as in many other organisms. At the same time, these organisms appear not to use lipids as alternative energy sources when carbohydrates are not available. Utilization of exogenous lipids is yet to be thoroughly investigated in *Lesihmania*, however. Nonetheless, our data demostrate that *Leishmania* are still considerably flexible in terms of coping with changes in nutrient availability but, at the same time, unconventional in terms of carbon preferences which could be a fruitfulll ground for drug target hunting (see Chapter VI).

CHAPTER V. Quantitative characterization of *Δlmgt* promastigotes by stable isotope labelling by amino acids in cell culture and global metabolomics

In the field of proteomics, stable isotope labelling by amino acids in cell culture (SILAC) (Ong *et al.*, 2002), combined with mass spectrometry (MS), has emerged as a promising methodology for obtaining quantitative proteomic information. The approach relies on complete metabolic incorporation of stable isotope amino acids into proteins during protein turnover. The metabolic labelling at the protein and organism level thus provides high-confidence quantitative information. Considering these advantages, SILAC was chosen as a suitable approach to fulfil one of the main objectives of this study: to identify and quantify the proteins that are differentially expressed in *Δlmgt* promastigotes.

SILAC depends upon efficient incorporation of labelled amino acids into the proteome. This requires that the biological system of interest is

- auxotrophic for the chosen labelled amino acids
- does not significantly metabolize or transaminate the chosen labelled amino acids
- is able to grow in a defined media or media supplemented with serum that has been dialyzed to deplete unlabelled amino acids.

These requirements are often overlooked in discussions of the utility of SILAC as a quantitative proteomic approach. In practice, most cells can be adapted to grow in SILAC-compatible media, but the consequences of this selection are rarely discussed. One possible adaptation is a biochemical remodeling that may result in an altered phenotype, and that may also compromise protein labelling efficiency.

SILAC has been successfully applied to trypanosomatids, yet not as extensively as it has been to mammalian cells. To date, five studies have applied SILAC to *Trypanosma* and four to *Leishmania*. Two studies investigated the proteome remodelling in *T. brucei* during differentiation from bloodstream to procyclic forms (Urbaniak *et al.*, 2012; Gunasekera *et al.*, 2012). The first study compared the long slender and procyclic forms while the second study followed the development of long slender to short stumpy forms and from short stumpy to procyclic forms. Both studies corroborated with each other on the observation that expression of the mitochondrial

proteins is higher in the procyclic forms. Later on, Urbaniak and colleagues investigated the specificities of the phosphoproteome of *T. brucei* bloodstream and procyclic forms (Urbaniak *et al.*, 2013) while a separate study focused on the mitochondrial translation elongation factor-Tu in *T. brucei* (Cristodero *et al.*, 2013). Finally, in their most recent study, Ferguson and colleagues employed SILAC to investigate the glycosome proteome of procyclic forms of *T. brucei* (Guther *et al.*, 2014). The isotope labelling technique was used in combination with epitope-tagging and magnetic bead pull-out assay which generated high-confidence data and allowed unambiguous identification of a high number of glycosomal proteins. Besides the seven glycolytic proteins, from hexokinase (HK) to phosphoglycerate kinase (PGK), the study confirmed the presence of enzymes belonging to the glycosomal glycerol 3-phosphate/dihydroxyacetone phosphate (G3P/DHAP) shuttle, β-oxidation of fatty acids, ether-lpid synthesis, isoprenoid/sterol synthesis, methylglyoxal pathway, nucleotide sugar metabolism, purine salvage pathway, pyrimidine biosynthesis, peroxide and superoxide inactivation system and a number of Pex proteins and such involved in post-translational modifications and protein folding (Guther *et al.*, 2014).

With regard to *Leishmania*, three of the four studies have used SILAC to investigate drug-resistant strains of *Leishmania*, namely a paromomycin resistant strain of *L. donovani* (Chawla *et al.*, 2011), an antimony resistant strain of *L. infantum* (Brotherton *et al.*, 2013) and an amphotericin B resistant strain of *L. infantum* (Brotherton *et al.*, 2014), while the fourth study provided thorough information about the *L. donovani* secretome (Silverman *et al.*, 2008). The subject of interest of our study, however, was *L. mexicana* in which SILAC studies have not previously been reported. Thus, we had to develop a SILAC-based strategy for the analysis of the *L. mexicana* promastigotes (Figure II-1). The development and application of a SILAC-based methodology to the *L. mexicana* wild type and *Δlmgt* promastigotes, however, proved to be challenging for a number of reasons. The labelled amino acids that are routinely employed in SILAC studies are L-lysine and L-arginine, because these are the sites at which trypsin cleaves proteins, so the tryptic peptide produced should each carry one labelled amino acid. However, it is evident from previous studies that *Leishmania* are capable of metabolising exogenously acquired L-arginine (Kandpal *et al.*, 1995; Colotti and Ilari, 2011). Thus, we elected to label parasites with L-lysine only in our experiments. Initially, we observed severly reduced growth of the wild type and *Δlmgt* promastigotes in media supplemented with dialysed serum and it was

necessary to optomise serum dialysis conditions and to adapt the promastigotes to the SILAC culture media. After successfully adapting and growing the promastigotes in the SILAC media for more than 2-3 times the recommended minimum, we analyzed the SILAC-labelled protein samples by MS. The generated data provided surprising information for both the applicability of the SILAC method to the *L. mexicana* promastigotes and for understanding L-lysine metabolism.

V.1. Results

V.1.1. Global proteomic characterization of *Δlmgt* promastigotes by stable isotope labelling by amino acids in cell culture

V.1.1.1. Growth of *Δlmgt* promastigotes in SILAC media

Growth profiles of the wild type and *Δlmgt* promastigotes (biological replicates, n=3) were investigated under regular culture conditions (as described in **II.1.**) in three media: HOMEM supplemented with 10% heat-inactivated fetal bovine serum (iFBS), RPMI 1640 supplemented with 10% iFBS, and light and heavy RPMI 1640 supplemented with 10% 3.5K molecular weight cut-off (MWCO) dialyzed iFBS (DS). In accordance with previous observations (Burchmore *et al.*, 2003), the *Δlmgt* promastigotes grew slower and to a lower cell density compared to the wild type promastigotes when cultured in HOMEM with 10% iFBS (Figure V-1). To ensure full incorporation of the isotope-labelled L-lysine, both strains were adaptated to RPMI 1640 with 10% DS for two passages before being trnasferred, at initial density of 1.0 x 10^5 cells ml^{-1}, to light and heavy RPMI 1640 with 10% DS. In the first passage, the wild type promastigotes reached a slightly higher average cell density in the light cultures compared to the heavy ones (Figures V-2, A and V-3, A). In the second passage, after an initial drop, the promastigotes showed a slight recovery in growth but started dying quickly afterwards (Figures V-2, B and V-3, B). The light and heavy *Δlmgt* promastigotes gradually died out after the initiation (Figures V-2, C and V-3, C).

To overcome the poor growth of promastigotes in the SILAC media, the initial cell density was increased from 1.0 x 10^5 cells ml^{-1} to 1.0 x 10^6 cells ml^{-1}. Additionally, to ensure proper adaptation to the DS and establish stable cultures, the wild type and *Δlmgt* promastgotes were maintained for two passages in RPMI 1640 with DS with four changes of the fresh media. In the first passage, the wild type promastigotes doubled once, presumably as a result of metabolism of residual compounds from the non-dialysed serum, while the *Δlmgt* promastigotes did not. After the initial growth of the wild type promastigotes, both cell lines entered a "shock" phase where the promastigotes stayed viable but did not multiply for a long period of time. That imposed the neccesity to supply fresh nutrients by changing the culture media. The culture media of the wild type promastigotes was changed three time for the period of slightly over a month after the initiation of the adaptation cultures whereas that of the *Δlmgt* promastigotes was changed two times. Gradually, the promastigotes exited the shock stage and started dividing slowly.

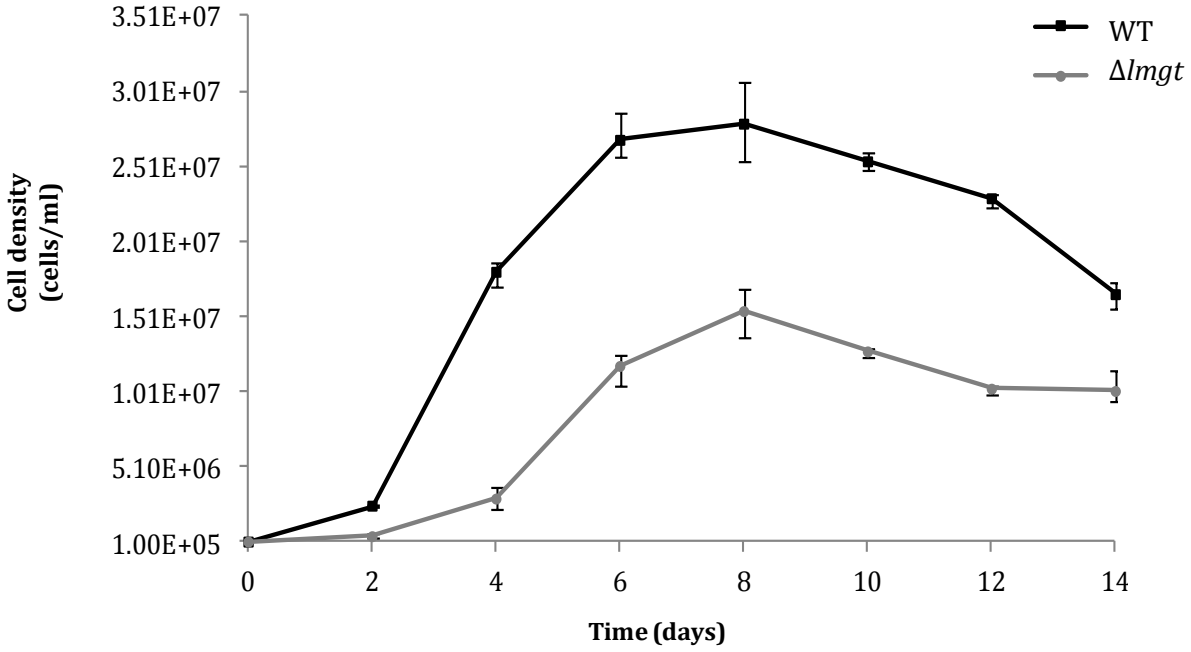

Figure V-1. Growth rate of wild type and *Δlmgt* promastigotes in HOMEM media supplemented with 10% heat-inactivated fetal bovine serum. Wild type (WT) (black line, squares) and *Δlmgt* (grey line, dots) promastigotes were grown in HOMEM media supplemented with 10% serum. Growth curve time point values are the mean values from three biological replicates. Error bars represent the standard deviation.

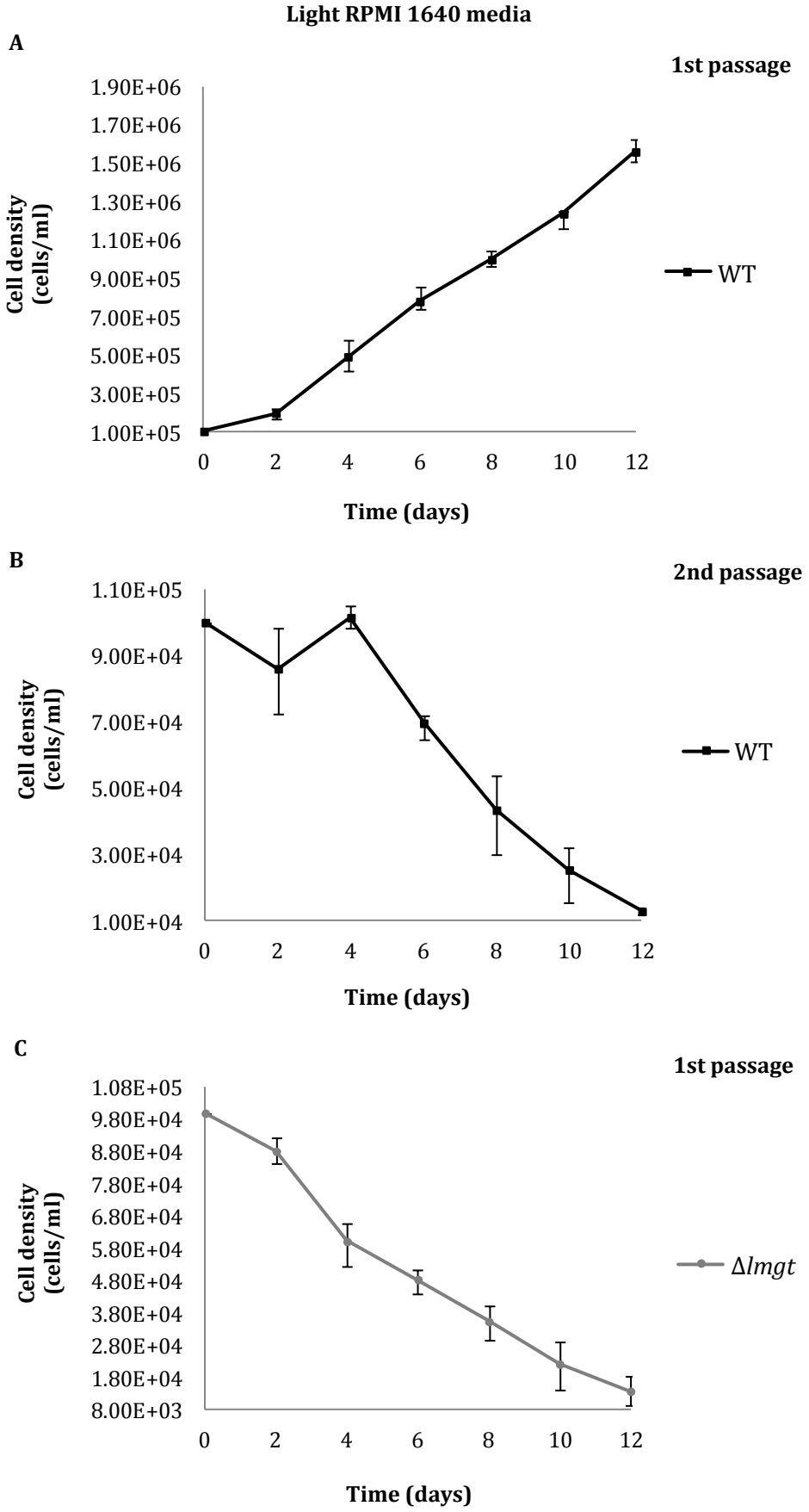

Figure V-2. Growth rate of wild type and *Δlmgt* promastigotes in light RPMI 1640 media supplemented with 10% dialyzed serum. First (A) and second (B) passage of wild type (WT) promastigotes (black line, squares) in light RPMI 1640 media supplemented with 10% 3.5K MWCO dialyzed serum. First (C) passage of *Δlmgt* promastigotes (grey line, dots) in light RPMI 1640 media supplemented with 10% 3.5K MWCO dialyzed serum. Growth curve time point values are the mean values from three biological replicates. Error bars represent the standard deviation. MWCO – molecular weight cut-off.

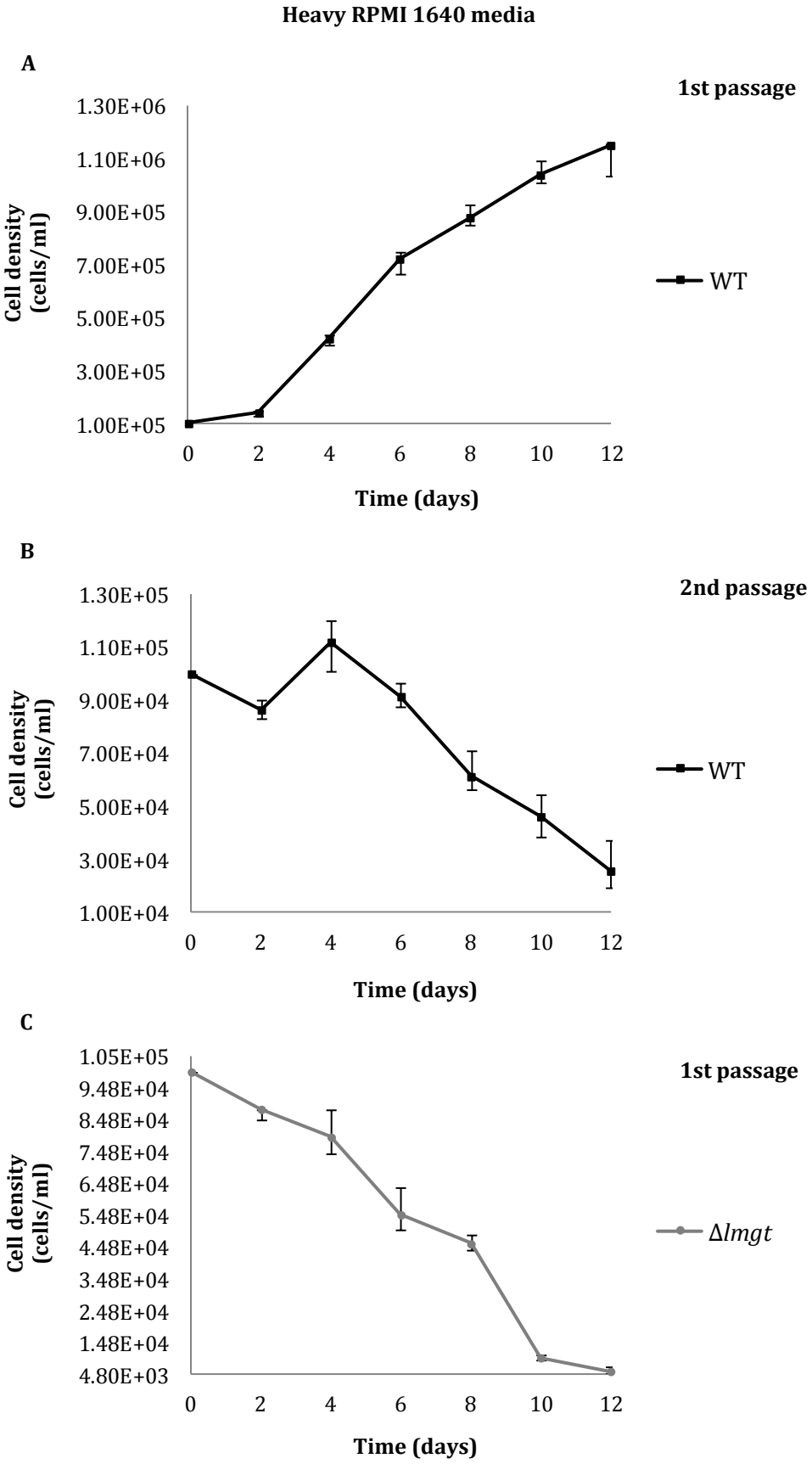

Figure V-3. Growth rate of wild type and *Δlmgt* promastigotes in heavy RPMI 1640 media supplemented with 10% dialyzed serum. First (A) and second (B) passage of wild type (WT) promastigotes (black line, squares) in heavy RPMI 1640 media supplemented with 10% 3.5K MWCO dialyzed serum. First (C) passage of *Δlmgt* promastigotes (grey line, dots) in heavy RPMI 1640 media supplemented with 10% 3.5K MWCO dialyzed serum. Growth curve time point values are the mean values from three biological replicates. Error bars represent the standard deviation. MWCO – molecular weight cut-off.

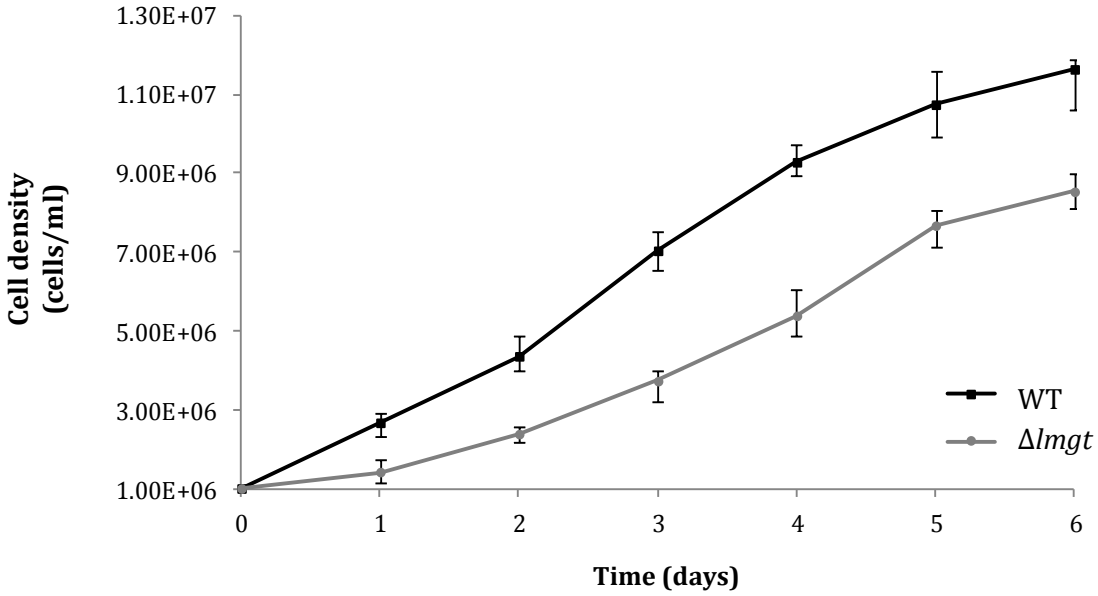

Figure V-4. Growth rate of adapted to dialyzed serum wild type and *Δlmgt* promastigotes in SILAC media. Wild type promastigotes (black line, squares) were grown in light RPMI 1640 media supplemented with 10% 3.5K MWCO dialyzed serum. *Δlmgt* promastigotes (grey line, dots) were grown in heavy RPMI 1640 media supplemented with 10% 3.5K MWCO dialyzed serum. Growth curve time point values are the mean values from three biological replicates. Error bars represent the standard deviation. MWCO – molecular weight cut-off.

Not unexpectedly, the wild type started proliferating sooner than the *Δlmgt* promastigotes. When both cell lines reached mid-log phase, the promastigotes were passaged, at initial cell density of 1.0 x 10^6 cells ml^{-1}, to fresh RPMI 1640 with DS. In the second passage, the promastigotes multiplied for another half a month, with a single change of the media. When the promastigotes reached mid-log phase again, the wild type promastigotes were transferred to light SILAC media with DS while the *Δlmgt* promastigotes were transferred to the heavy SILAC media with DS. In the SILAC media, the adapted promastigotes were cultured for six consequent passages. Between 7 and 8 days were necessary for the *Δlmgt* promastigotes to double twice in the heavy RPMI 1640 in the first three passages. Gradually, the growth rate of the *Δlmgt* promastigotes increased, reaching approximately three doublings for the period of six days in the last passage (Figure V-4). The growth rate of the wild type promastigotes increased from approximately two and a half doublings in the first passages to three and a half in the last passages (Figure V-4). Thus, the *Δlmgt* promastigotes were cultured in the SILAC media for more than twice the recommended minimum of six doublings while the wild type were cultured for more than three times.

V.1.1.2. Examination of SILAC labelling efficiency in *Leishmania mexicana* promastigotes

The incorporation efficiency of the heavy L-lysine was first investigated in the *Δlmgt* promastigotes. However, the unexpected results led to investigating the heavy L-lysine labelling efficiency in the wild type promastigotes as well.

Initially, 10 μg of heavy-labelled proteins derived from the *Δlmgt* promastigotes were subjected to digestion and analysis by 1D HPLC-ESI-MS/MS. Identified with MaxQuant (MQ) were 905, 891 and 697 proteins in sample I, II and III, respectively (Table V-1, top table). Slightly less proteins were found with Mascot Distiller (MD), i.e. 786, 760 and 625 in sample I, II and III, respectively (Table V-1, bottom table). Evident from the Mascot search was that:

- most of the peptides cut after L-arginine (R) (Figure V-5) did not contain L-lysine (K) and were therefore not used for quantitation;
- many peptides cut after L-lysine or L-lysine-containing peptides were not heavy-labelled (Figure V-5).

MaxQuant

	Identified proteins	Modulated proteins	Up-regulated proteins	Down-regulated proteins
Sample I	905	222	156	66
Sample II	891	201	187	14
Sample III	697	168	128	40

Mascot Distiller

	Identified proteins	idFDR %	h/iFDR %	Quantified proteins	Modulated proteins	Up-regulated proteins	Down-regulated proteins
Sample I	786	0.23	1.39	129	35	33	2
Sample II	760	0.20	1.62	119	43	43	0
Sample III	613	0.24	1.43	84	21	21	0

Table V-1. Identified, quantified and significantly modulated heavy-labelled proteins in the *Δlmgt* promastigotes. Heavy-labelled proteins from *Δlmgt* promastigotes (biological replicates, n=3) were digested with trypsin prior to analysis by 1D-HPLC-ESI-MS/MS. The data were analysed with MaxQuant (top table) and Mascot Distiller (bottom table).

That led to further analysis of the raw MS data, determination of the incorporation efficiency by MQ and quantitative analysis of the heavy data by MD and MQ. Analysis of the raw MS data confirmed the presence of unlabelled and heavy-labelled peptides in the heavy samples (Figure V-5), noticeably exemplified by the doubly-charged QLFNPEQLVSGK peptide of α-tubulin (LmxM.13.0280) which was found in two forms, light and heavy, with m/z of 680.3669 and 683.3763, respectively (Figure V-6). Next, we used MQ and R to estimate the labelling efficiency in the *Δlmgt* promastigotes. The analysis revealed that only half (52.1%) of the peptides were heavy labelled (Figure V-7, A). To illustrate the partial incorporation of the heavy L-lysine, we performed protein quantitation with the data from the *Δlmgt* heavy samples generated by MD and MQ. The analysis, which was performed with the same settings and parameters that are used for analysis of tcombined light/heavy samples, showed that a considerable number of proteins were significantly modulated in the heavy I, II and III (Table V-1).

1. LmxM.28.2770 Mass: 71482 Score: 2481 Matches: 74(53) Sequences: 25(22)
| organism=Leishmania_mexicana | product=heat-shock protein hsp70, putative

Query	Score	Unique	Peptide
146	(67)	U	K.DAGTISGLEVLR.I
147	72	U	K.DAGTISGLEVLR.I
276	70	U	R.LVTFFTEEFK.R [light]
297	(63)	U	R.LVTFFTEEFK.R [heavy] + Label:13C(6) (K)
378	(57)	U	K.VQSLVSDFFGGK.E [light]
385	70	U	R.FEELCGDLFR.S
387	(2)	U	K.FNDSVVQSDMK.H [light] + Oxidation (M)
410	75	U	K.VQSLVSDFFGGK.E [heavy] + Label:13C(6) (K)
411	(45)	U	K.VQSLVSDFFGGK.E [heavy] + Label:13C(6) (K)
418	44	U	K.FNDSVVQSDMK.H [heavy] + Oxidation (M); Label:13C(6) (K)
495	(70)	U	K.NGLENYAYSMK.N [light] + Oxidation (M)
498	(0)	U	K.NGLENYAYSMK.N [light] + Oxidation (M)
499	(1)	U	K.NGLENYAYSMK.N [light] + Oxidation (M)
514	70	U	K.NGLENYAYSMK.N [heavy] + Oxidation (M); Label:13C(6) (K)
519	(9)	U	K.NGLENYAYSMK.N [heavy] + Oxidation (M); Label:13C(6) (K)
599	(29)	U	R.SVHDVVLVGGSTR.I
600	92	U	R.SVHDVVLVGGSTR.I
854	(29)	U	K.GDDKPVISVQYR.G [light]
855	47	U	K.GDDKPVISVQYR.G [light]
881	(47)	U	K.GDDKPVISVQYR.G [heavy] + Label:13C(6) (K)
1066	(9)	U	R.LVTFFTEEFKR.K [light]
1067	(42)	U	R.LVTFFTEEFKR.K [light]
1097	49	U	R.LVTFFTEEFKR.K [heavy] + Label:13C(6) (K)
1098	(41)	U	R.LVTFFTEEFKR.K [heavy] + Label:13C(6) (K)
1327	(7)	U	K.ELENVCNPIMTK.M [light] + Oxidation (M)
1352	73	U	K.ELENVCNPIMTK.M [heavy] + Oxidation (M); Label:13C(6) (K)
1373	69	U	R.TTPSYVAFTDSER.L

Figure V-5. Partial peptide summary of heat shock protein 70 identified as protein hit #1 in the heavy SILAC sample I. Reported are: the accession number of enolase: LmxM.28.2770, the expected protein mass: 71482 kDa, the overall protein score: 2481, the number of MS/MS spectra match to the protein: 74, the number of sequences matched to the protein: 25, the observed peptide mass, the number of misscleavages, the peptide score, the unique peptides, the peptide sequence, and the peptide modifications.

2. LmxM.13.0280 Mass: 61058 Score: 2153 Matches: 59(43) Sequences: 16(12)
| organism=Leishmania_mexicana | product=alpha tubulin |

Query	Observed	Score	Unique	Peptide
543	658.2499	53	U	K.YMSCCLMYR.G + 2 Oxidation (M)
768	680.3665	(36)	U	R.QLFNPEQLVSGK.E [light]
769	680.3667	(63)	U	R.QLFNPEQLVSGK.E [light]
801	683.3761	66	U	R.QLFNPEQLVSGK.E [heavy] + Label:13C(6) (K)
802	683.3768	(59)	U	R.QLFNPEQLVSGK.E [heavy] + Label:13C(6) (K)

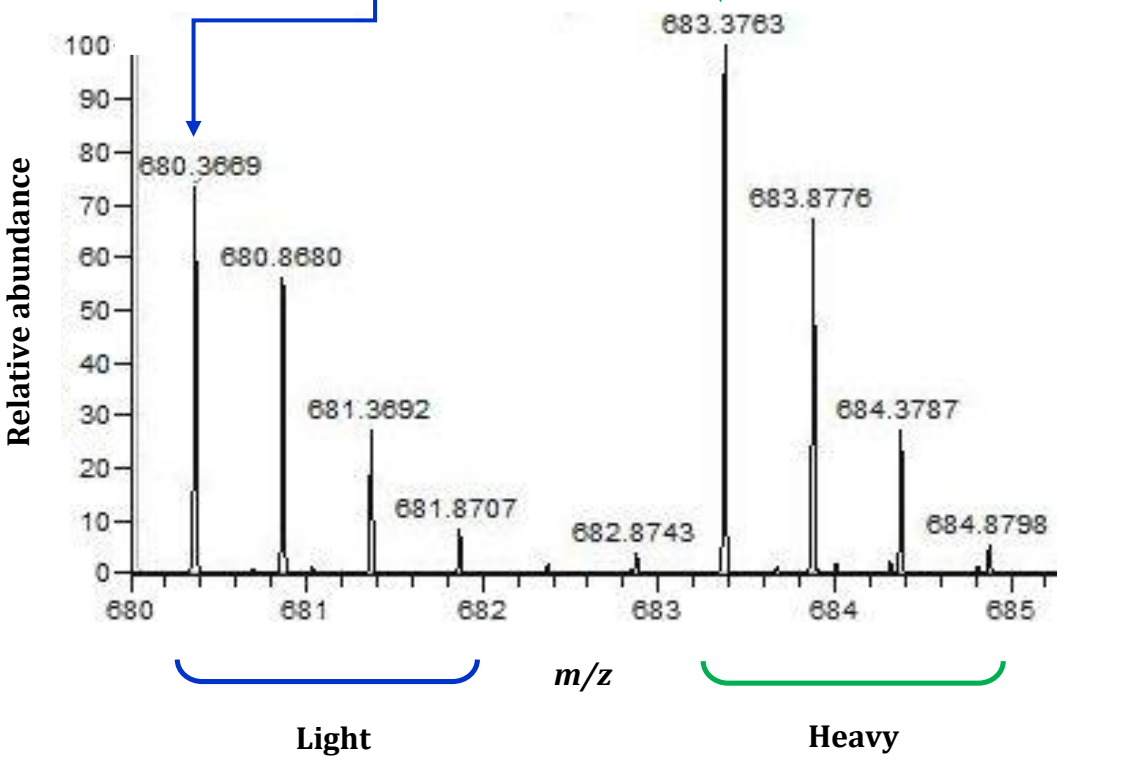

Figure V-6. Chromatogram of the doubly charged species of the peptide **QLFNPEQLVSGK** of α-tubulin in the heavy SILAC sample I. Presented here is an example of a light and a heavy form of a peptide in the heavy SILAC sample I. Reported are: the accession number of α-tubulin: LmxM.13.0280, the expected protein mass: 61058 kDa, the overall protein score: 2153, the number of MS/MS spectra match to the protein: 59, the number of sequences matched to the protein: 16, the query, the observed peptide mass, the peptide score, the unique peptides, the peptide sequence, and the peptide modifications.

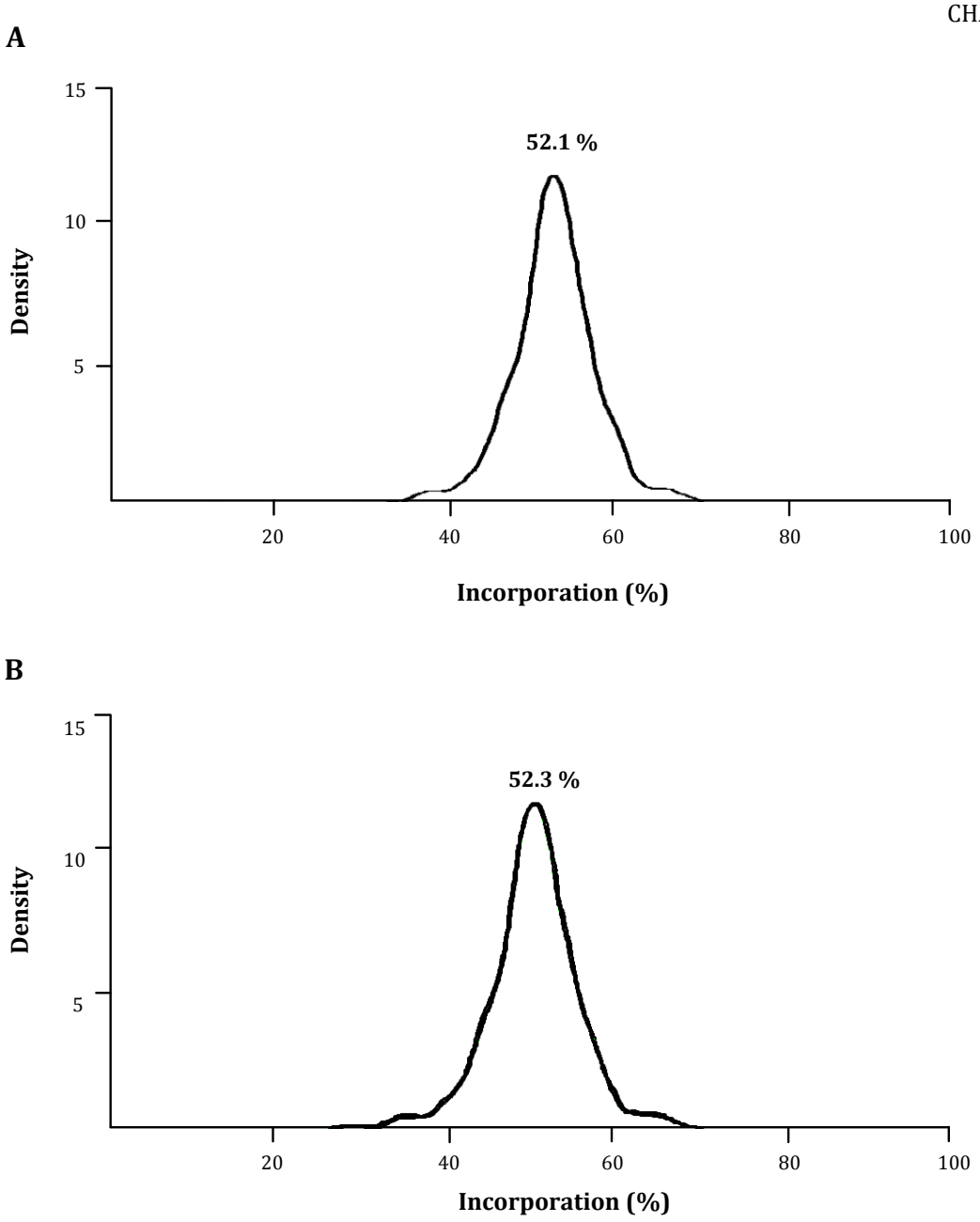

Figure V-7. SILAC labelling efficiency in the *Leishmania mexicana* promastigotes. ^{13}C-L-lysine labelling efficiency in the *Δlmgt* (A) and wild type (B) promastigotes. The *Δlmgt* and wild type promastigotes were grown in heavy SILAC media supplemented with 3.5 kDa MWCO serum. The heavy-labelled proteins were extracted and subjected to digestion with trypsin, analysis of the peptide samples by 1D-HPLC-ESI-MS/MS and analysis of the data by MaxQuant and R (as described in **II.1.8.**). The incorporation curve represents the distribution of the quantified peptides. The incorporation (in percents) was calculated according to the following equasion: peptide incorporation = 1- 1/(Ratio Heavy/Light + 1). Density is an arbitrary unit.

Except for one protein in sample I and II, which was significantly modulated (that is, had a fold-change above 2), all quantified proteins were insignificantly modulated. That again underlined the incomplete labelling efficiency in the heavy samples. Complete (>98%) labelling efficiency is a prerequisite for accurate quantitation based on isotope labelling and would be evident in detection of a minimal number of unlabelled peptides in the labelled samples. Our analysis of the heavy samples, however, showed that many peptides were unlabelled, despite maintenance of the promastigotes for many divisions in media where all L-lysine was heavy labelled. Taken together, our proteomic data (together with further metabolomic data presented in **V.1.3.**) suggested that *L. mexicana* promastigotes may not be auxotrphic for L-lysine.

To exclude the possibility that the observed partial incorporation in the *Δlmgt* promastigotes was due to metabolic adaptations resulting from deletion of D-glucose transport capacity, we grew wild type promastigotes in heavy SILAC media and estimated the labelling efficiency in the wild cell line as well. Analysis of the raw MS data revealed that many of the peptides were not labelled. Additionally, the labelling efficiency was determined to be pretty much the same as that in the *Δlmgt* promastigotes (Figure V-7, B). That confirmed that L-lysine was incorporated into proteins in the same way in the wild type and *Δlmgt* promastigotes. It also, however, raised the question of what exactly was the fate of this amino acid in the *Leishmania* promastigotes.

V.1.2. Global metabolomic characterization of SILAC-labelled *Δlmgt* promastigotes

As a metabolic labelling technique, SILAC relies on *in vivo* incorporation of exogenously supplied stable isotope amino labelled acids into proteins. To avoid the incorporation of unlabelled amino acids, SILAC requires the use of defined medium, supplemented if necessary with serum that has been dialyzed to deplete amino acids. That in turn requires the cells under investigation to be grown in different that the regular culturing conditions. As described in **V.1.1.1.**, the growth of the wild type and *Δlmgt* promastigotes was initially impaired when the promastigotes were cultured in media with dialyzed serum (Figures V-2 and V-3). Eventually, the promastigotes adapted to the dialyzed serum and grew in the SILAC media. Adaptation, however, was most probably associated with modulations in the cell metabolism.

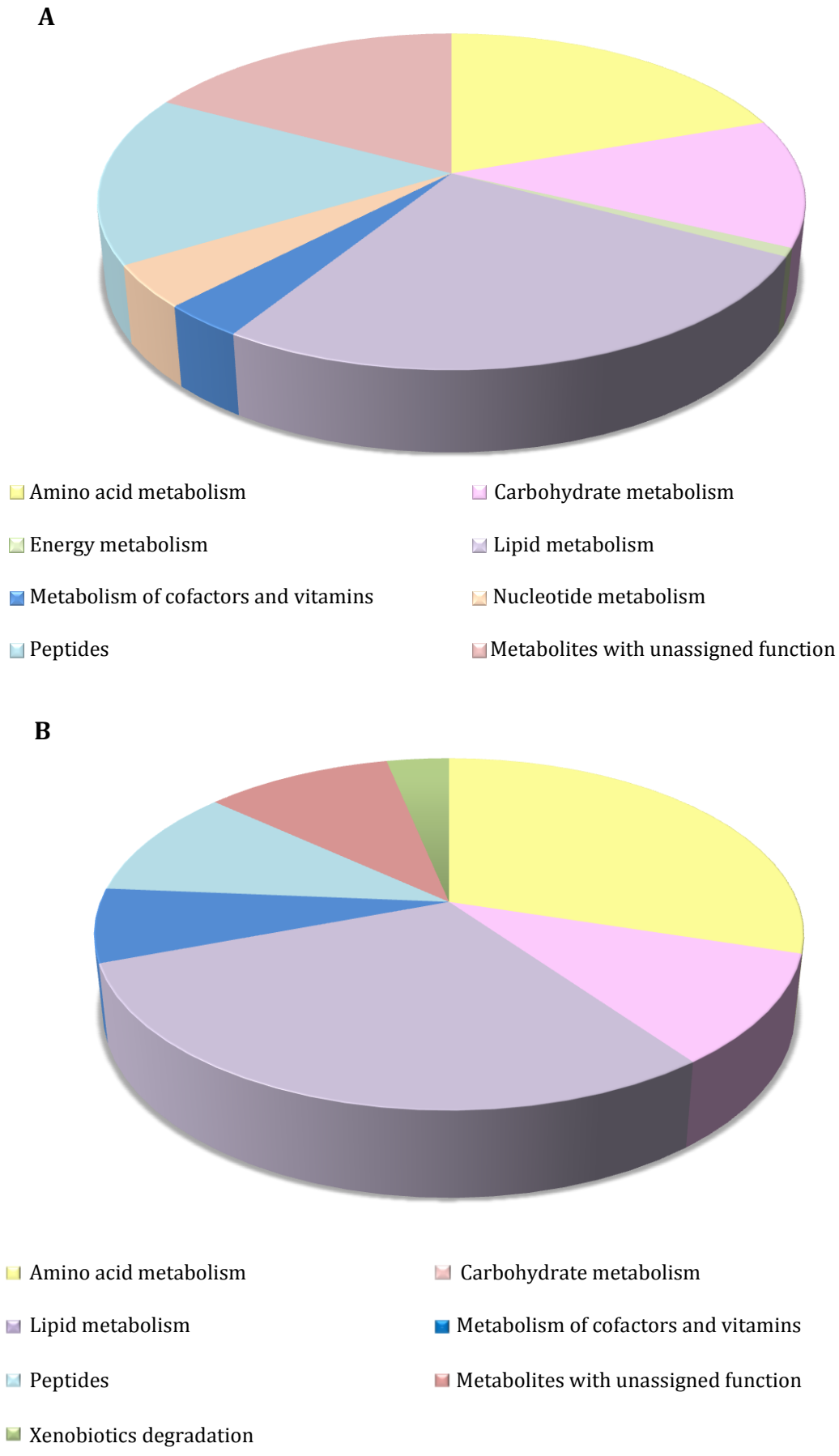

Figure V-8. Distribution of the significantly modulated metabolites in the SILAC-labelled *Δlmgt* promastigotes (A) and spent media (B). SM - secondary metabolites, C - cofactors, V – vitamins, UF – unassigned function.

Putative metabolite	Isomers	Map	Pathway	WT	*Δlmgt*
Nonaprenyl-4-hydroxybenzoate	2	Metabolism of Cofactors and Vitamins	Ubiquinone-9 biosynthesis	1.00	**20.28**
PC(18:4(6Z,9Z,12Z,15Z)/18:4(6Z,9Z,12Z,15Z))	8	Lipids: Glycerophospholipids	Glycerophosphocholines	1.00	**5.99**
[SP hydroxy(16:0)] N-(hexadecanoyl)-4S-hydroxysphinganine	1	Lipids: Sphingolipids	Ceramides	1.00	**3.53**
[PC (22:6/22:6)] 1,2-di-(4Z,7Z,10Z,13Z,16Z,19Z-docosahexaenoyl)-sn-glycero-3-phosphocholine	3	Lipids: Glycerophospholipids	Glycerophosphocholines	1.00	**3.42**
[FA methyl, hydroxy(5:0)] 3R-methyl-3,5-dihydroxy-pentanoic acid	14	Lipids: Fatty Acyls	Fatty Acids and Conjugates	1.00	**3.34**
PC(14:1(9Z)/22:6(4Z,7Z,10Z,13Z,16Z,19Z))	8	Lipids: Glycerophospholipids	Glycerophosphocholines	1.00	**3.32**
Sorbate	19	Lipids: Fatty Acyls	Fatty Acids and Conjugates	1.00	**3.24**
PE(18:3(6Z,9Z,12Z)/P-18:1(11Z))	15	Lipids: Glycerophospholipids	Glycerophosphoethanolamines	1.00	**3.18**

Table V-2. Significantly increased metabolites in the SILAC-labelled *Δlmgt* promastigotes. Specified in yellow, metabolites involved in metabolism of cofactors and vitamins, and in green, metabolites involved in lipid metabolism. Metabolites with unassigned function are not included.

Putative metabolite	Isomers	Map	Pathway	WT	*Δlmgt*
Tetradecanoic acid	23	Lipid Metabolism	Fatty acid biosynthesis	1.00	**0.20**
L-Glutamate	14	Amino Acid Metabolism	Arginine and proline metabolism Glutamate metabolism Nitrogen metabolism	1.00	**0.19**
3-Phospho-D-glycerate	3	Carbohydrate Metabolism	Glycolysis / Gluconeogenesis Glycerolipid metabolism	1.00	**0.18**
Nicotinamide	4	Metabolism of Cofactors and Vitamins	Nicotinate and nicotinamide metabolism	1.00	**0.17**
Glutathione disulfide	1	Amino Acid Metabolism	Glutamate metabolism Glutathione metabolism	1.00	**0.17**
ATP	4	Energy Metabolism	Oxidative phosphorylation Purine metabolism	1.00	**0.15**
Lys-Lys	1	Peptide(di-)	Basic peptide	1.00	**0.15**
Asp-Phe-Cys-Tyr	1	Peptide(tetra-)	Hydrophobic peptide	1.00	**0.13**
Cellohexaose	3	Carbohydrate Metabolism	Starch and sucrose metabolism	1.00	**0.12**
Cellopentaose	4	Carbohydrate Metabolism	Starch and sucrose metabolism	1.00	**0.12**
[PR] (-)-Limonene	39	Lipids: Prenols	Monoterpenoid biosynthesis Limonene and pinene degradation	1.00	**0.11**
[FA (18:3)] 13S-hydroperoxy-9Z,11E,14Z-octadecatrienoic acid	20	Lipids: Fatty Acyls	Fatty Acids and Conjugates	1.00	**0.10**
Ethanolamine phosphate	2	Lipid Metabolism	Glycerophospholipid metabolism Sphingolipid metabolism	1.00	**0.10**
Asp-Lys-Trp-Pro	3	Peptide(tetra-)	Basic peptide	1.00	**0.09**
[FA (16:0)] N-hexadecanoyl-glycine	2	Lipids: Fatty Acyls	Fatty amides	1.00	**0.08**
[PR] (+)-Longifolene	151	Lipids: Prenols	Oleoresin turpentine biosynthesis	1.00	**0.07**
Sucrose	42	Carbohydrate Metabolism	Galactose metabolism Starch and sucrose metabolism	1.00	**0.03**

Table V-3. Significantly decreased metabolites in the SILAC-labelled *Δlmgt* promastigotes. Specified in blue are metabolites involved in amino acid metabolism, in pink, metabolits involved in carbohydrate metabolism, in yellow, metabolites involved in metabolism of cofactors and vitamins, in green, metabolites involved in lipid metabolism, in brown, peptide, and in violet, metabolites involved in energy metabolisms. Specified in yellow are the metabolites matched to authentic standards.

Putative metabolite	Isomers	Map	Pathway	WT	*Δlmgt*
Cholate	82	Lipids: Sterol lipids	Bile acid biosynthesis	ND	**27.55***
SM(d16:1/18:1)	3	Lipids: Sphingolipids	Phosphosphingolipids	ND	**16.41***
Docosahexaenoicacid	11	Lipids: Fatty Acyls	Biosynthesis of unsaturated fatty acids	1.00	**9.86**
Leu-Arg	2	Peptide(di-)	Basic peptide	1.00	**8.48**
Nicotinate	4	Metabolism of Cofactors and Vitamins	Nicotinate and nicotinamide metabolism Alkaloid biosynthesis II	1.00	**7.63**
[FA (20:4)] 5Z,8Z,11Z,14Z-eicosatetraenoic acid	46	Lipids: Fatty Acyls	Fatty Acids and Conjugates	1.00	**6.31**
Glu-Gln-Gln-Tyr	1	Peptide(tetra-)	Hydrophobic peptide	1.00	**6.21**
sn-glycero-3-Phosphocholine	1	Lipid Metabolism	Glycerophospholipid metabolism Ether lipid metabolism	1.00	**6.13**
3-(4-Hydroxyphenyl) pyruvate	11	Amino Acid Metabolism	Tyrosine metabolism Phenylalanine, tyrosine and tryptophan	1.00	**3.74**

Table V-4. Significantly increased metabolites in the SILAC-labelled *Δlmgt* promastigote spent media. Specified in yellow are metabolites involved in metabolism of cofactors and vitamins, in green, metabolites involved in lipid metabolism, in blue, metabolites involved in amino acid metabolism, and in brown, peptides. Specified in yellow are the metabolites matched to authentic standards. Metabolites with unassigned function are not included.
* - Metabolite detected in the *Δlmgt* test samples and not detected (ND) in the wild type control samples are denoted by the control group having ND as a descriptor. The value in the *Δlmgt* column is the average intensity of the compound in the *Δlmgt* samples.

Putative metabolite	Isomers	Map	Pathway	WT	*Δlmgt*
Fumarate	3	Carbohydrate Metabolism	TCA cycle Oxidative phosphorylation	1.00	**0.27**
[PR] (+)-Longifolene	151	Lipids: Prenols	Oleoresin turpentine biosynthesis	1.00	**0.25**
L-Citrulline	3	Amino Acid Metabolism	Arginine and proline metabolism	1.00	**0.22**
Malate	4	Carbohydrate Metabolism	TCA cycle Glutamate metabolism Alanine and aspartate metabolism Pyruvate metabolism Glyoxylate and dicarboxylate metabolism Carbon fixation	1.00	**0.21**
Asp-Cys-Cys-Ser	2	Peptide(tetra-)	Acidic peptide	1.00	**0.21**
D-Lysine	8	Amino Acid Metabolism	Lysine degradation	1.00	**0.21**
Nicotinamide	4	Metabolism of Cofactors and Vitamins	Nicotinate and nicotinamide metabolism	1.00	**0.08**
Sucrose	42	Carbohydrate Metabolism		1.00	**0.06**

Table V-5. Significantly decreased metabolites in the SILAC-labelled *Δlmgt* promastigote spent media. Specified in blue are metabolites involved in amino acid metabolism, in pink, metabolits involved in carbohydrate metabolism, in green, metabolites involved in lipid metabolism, in yellow, metabolites involved in metabolism of cofactors and vitamins, and in brown, peptides. Specified in yellow are the metabolites matched to authentic standards. Metabolites with unassigned function are not included.

SILAC			Regular metabolomics		
Putative metabolite	WT	Δlmgt	Putative metabolite	WT	Δlmgt
L-Alanine	1.00	**0.37**	**L-Alanine**	1.00	**0.22**
L-Asparagine	1.00	**0.42**	**L-Asparagine**	1.00	**0.68**
L-Glutamate	1.00	**0.19**	**L-Glutamate**	1.00	**0.32**
Malate	1.00	**0.28**	**Malate**	1.00	**0.51**
Succinate	1.00	**0.32**	**Succinate**	1.00	**0.11**

Table V-6. Metabolic comparison between regular and SILAC-labelled *Δlmgt* promastigotes. Significantly modulated cell metabolites in the SILAC (left side) and regular (right side) global metabolomics data sets.

To compare the metabolomes of the wild type and *Δlmgt* promastigotes grown under SILAC conditions and detect possible metabolic changes, we have subjected the SILAC-labelled promastigotes to a global metabolomic analysis by 1D LC-MS/MS and analysis of the generated data with IDEOM (Creek *et al.*, 2012). 956 metabolites were identified in total. 122 metabolites were statistically significant (with $p<0.05$ and a fold-change equal or above 2) in the cells. 16 of the significant cell metabolites were identified against authentic standards. 32 metabolites were significant in the spent media. 10 of the significant spent medium metabolites were authentically identified. The rest of the metabolites were putatively identified. The cell metabolites were grouped in the 8 categories: amino acid metabolism, carbohydrate metabolism, energy metabolism, lipid metabolism, metabolism of cofactors and vitamins, nucleotide metabolism, peptides and metabolites with unassigned function (Figure V-8). The four large categories of significantly modulated metabolites in the cells were amino acids, lipids, peptides and metabolites with unassigned function (Figures V-8, A) while amino acids and lipids dominated the metabolites in the spent media (Figure V-8, B). A number of lipids were increased in the SILAC *Δlmgt* promastigotes (Table V-2). Significantly (>5- fold) decreased in the *Δlmgt* promastigotes were L-citrulline, orotate, UDP-glucose, UDP-N-acetyl-D-glucosamine, sedoheptulose 7-phosphate, glucose 6-phsophate, 3-phosphoglycerate, phosphoenolpyruvate, succinate, malate, fumarate, L-glutamate, L-threonine, L-alanine, L-asparagine, L-ornithine, ovothiol A disulfide, trypanothione disulfide, glutathione disulfide, nicotinamide, ATP, phosphoethanolamine, cellohexaose and cellopentaose (Table V-3; Supplemental

table V-1). Sucrose was 50-fold decreased in the *Δlmgt* promastigotes (Table V-3). Nicotinate and glycerol-3-phosphocholine were among the increased metabolites in the *Δlmgt* spent media (Table V-3) whereas fumarate, malate, L-citrulline and D-lysine were significantly decreased. Highly decreased in the *Δlmgt* spent media were nicotinamide and sucrose (Table V-4).

To elucidate any differences in the SILAC *Δlmgt* promastigote metabolism, we compared the regular metabolomic data described in Chapter III and Chapter IV) with the SILAC ones. The analysis revealed that metabolites of the central carbon metabolism such as L-alanine, L-asparagine, L-glutamate, malate and succinate had similar levels in the regular and SILAC promastigotes (Table V-9). Some metabolites that were not observed in the regular *Δlmgt* promastigotes were found in the SILAC *Δlmgt* promastigotes (Supplemental tables III-2 and V-1). Their absence in the regular promastigotes may indicate changes in the SILAC *Δlmgt* promastigotes metabolism. Confirmative analysis, however, are needed to deduce anything further.

V.1.3. Stable isotope tracing in SILAC-labelled *Δlmgt* promastigotes

L-Lysine is an essential amino acid for *Leishmania* (Opperdoes and Michels, 2008). The partial incorporation of the heavy lysine by the *Δlmgt* promastigotes, along with the significant lack of information regarding L-lysine metabolism in *Lesihmania*, drove us to engage novel bioinformatics tools to look in more detail into promastigote metabolism. Employing two sets of metabolomic data, derived from **SILAC**/^{13}C-L-lysine-labelled and ^{13}C-D-glucose-labelled (condition 0, ***glc0**) wild type and *Δlmgt* promastigotes, as well as the isotope data analysis software mzMatch-ISO (Chokkathukalam *et al.*, 2013), we have performed a comprehensive isotope tracing analysis among a number of pathways and L-lysine derivatives that gave a redefined overview of L-lysine metabolism in the *Leishmania* parasites. The **SILAC** labelling data revealed that the fresh light media, light-labelled wild type promastigotes and wild type spent media contain unlabelled L-lysine (grey peaks) only (Figure V-9). ^{13}C-L-Lysine (red peaks) was expectedly present only in the fresh heavy media, labelled *Δlmgt* promastigotes and *Δlmgt* spent media (Figure V-9). In consensus with the proteomics results, which indicated that only 52% of the heavy L-lysine was incorporated into proteins, the labelling trend of the ^{13}C-L-lysine revealed that approximately 55% of the total L-lysine inside the *Δlmgt* promastigotes was heavy-labelled (Figure V-10).

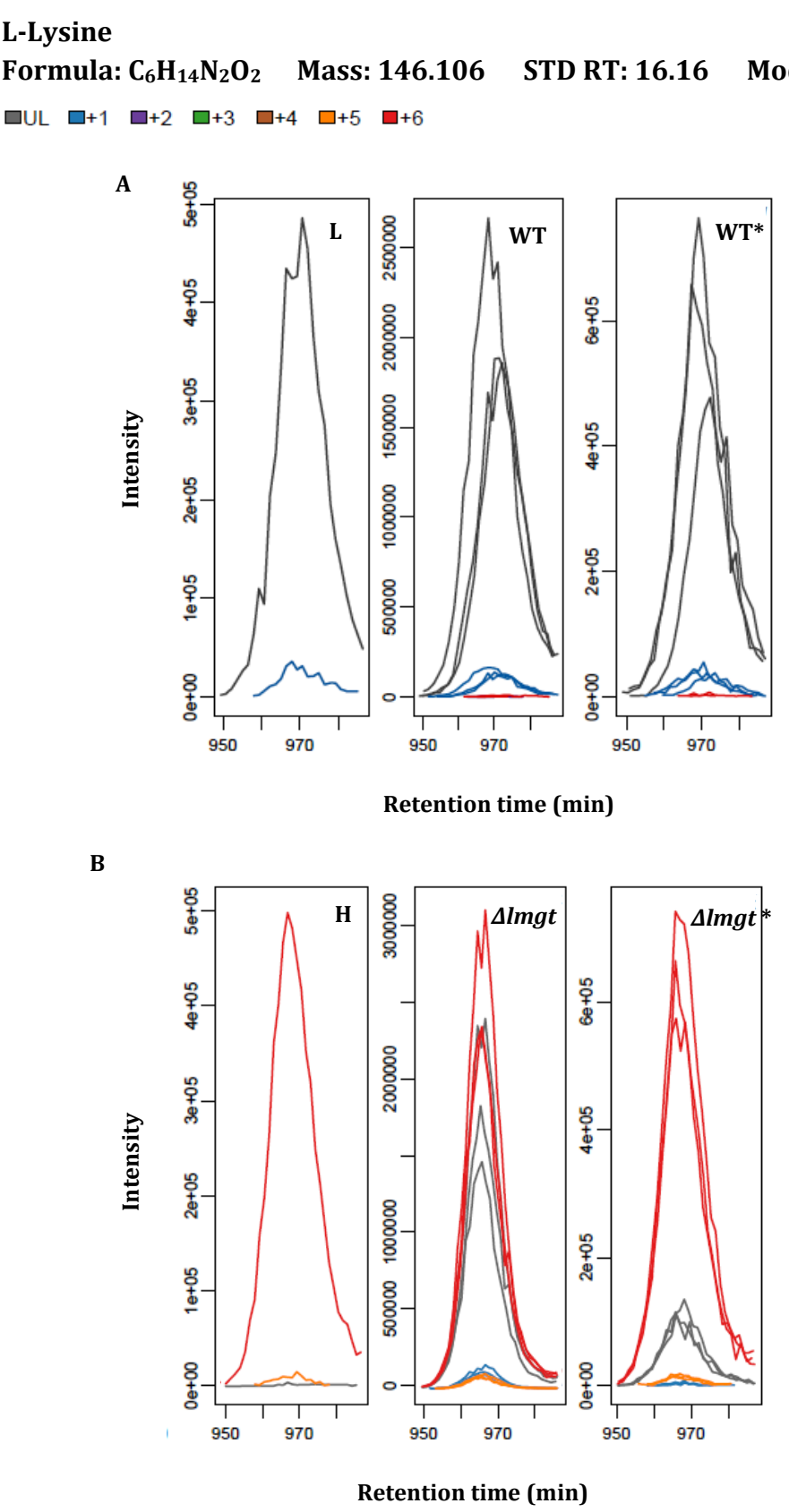

Figure V-9. Chromatograms of unlabelled (A) and ^{13}C-labelled L-lysine (B) in the fresh media, wild type and *Δlmgt* promastigotes, and wild type and *Δlmgt* spent media. The chromatograms were generated by mzMatch-ISO and illustrate the presence of unlabelled L-lysine in the light fresh media, wild type promastigotes, wild type spent media, *Δlmgt* promastigotes and *Δlmgt* spent media. ^{13}C-L-lysine was present in the heavy fresh media, *Δlmgt* promastigotes and *Δlmgt* spent media. Abbreviations: B - blank, L - fresh light media, WT – wild type promastigotes, WT* - wild type spent media, H - fresh heavy media, *Δlmgt* - *Δlmgt* promastigotes, *Δlmgt** - *Δlmgt* spent media.. UL- unlabelled carbon, +1 - 1-^{13}C-labelled carbon, +2 - 2-^{13}C-labelled carbon, +3 - 3-^{13}C-labelled carbon, +4 - 4-^{13}C-labelled carbon, +5 - 5-^{13}C-labelled carbon, +6 - 6-^{13}C-labelled carbon. STD - standard, RT - retention time, +ve - positive mode.

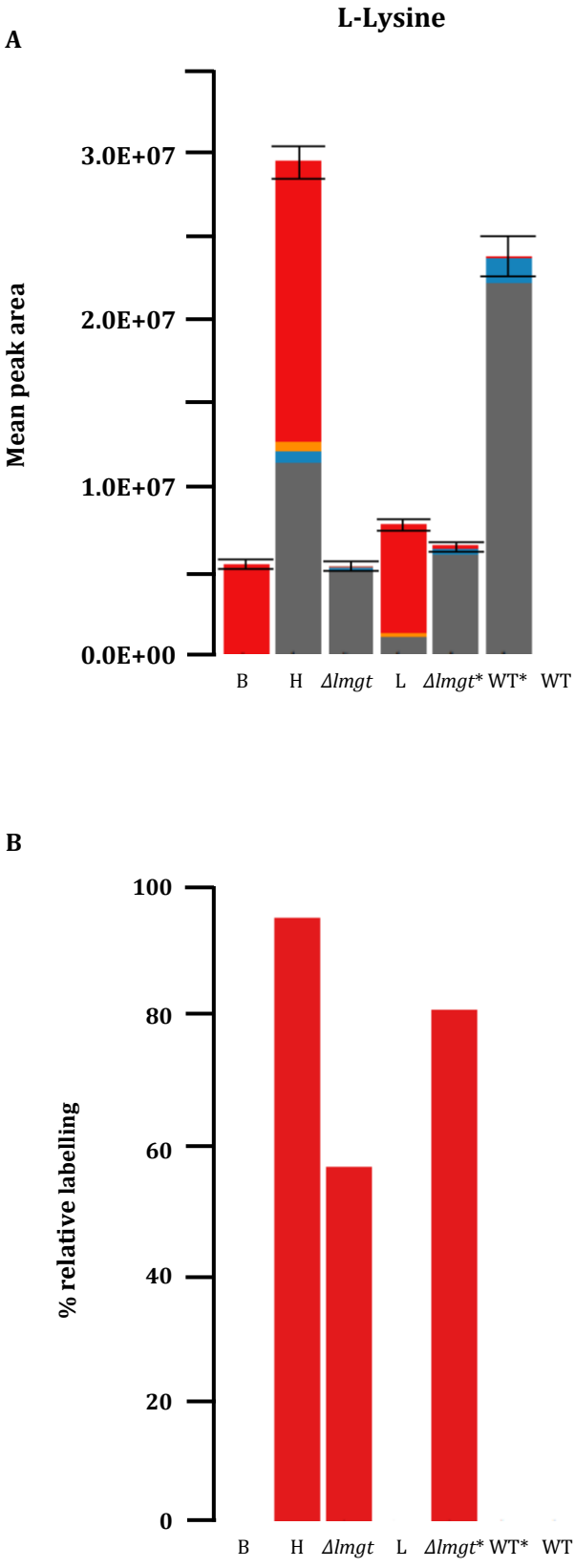

Figure V-10. Labelling pattern of L-lysine in the wild type and *Δlmgt* promastigotes. (A) Overall labelling trend of L-lysine. (B) Labelling trend of ^{13}C-L-lysine. Abbreviations: B - blank, L - fresh light media, WT – wild type promastigotes, WT* - wild type spent media, H - fresh heavy media, *Δlmgt* - *Δlmgt* promastigotes, *Δlmgt** - *Δlmgt* spent media.

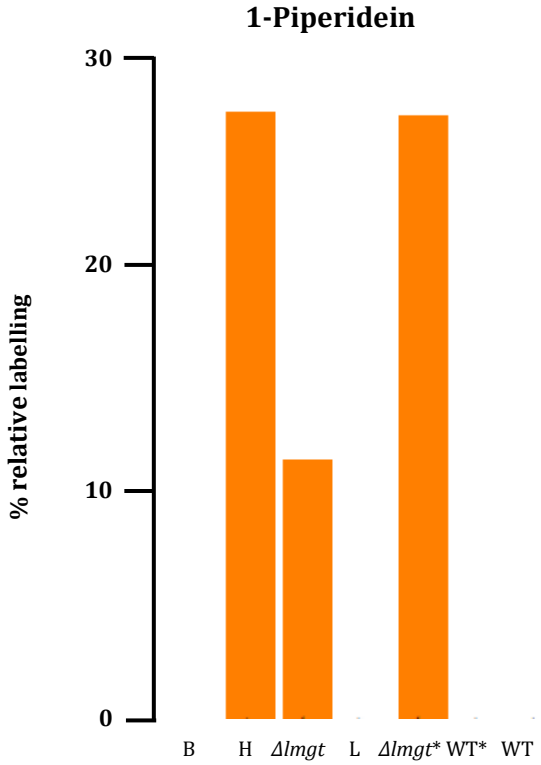

Figure IV-11. Labelling trend of 5-^{13}C-1-piperidein in the wild type and *Δlmgt* promastigotes. Abbreviations: B - blank, L - fresh light media, WT – wild type promastigotes, WT* - wild type spent media, H - fresh heavy media, *Δlmgt* - *Δlmgt* promastigotes, *Δlmgt** - *Δlmgt* spent media.

The labelling trend of the ^{13}C-L-lysine additionally showed that approximately 95% of the L-lysine in the fresh medium was heavy-labelled (Figure V-10, B). Possible impurity or degradation of the heavy L-lysine could account for the rest 5%, as evident from the presence of 5-^{13}C-labelled 1-piperidein in the fresh heavy media (Figure V-11). Since 1-piperideine is an intermediate in the L-lysine degradation via cadaverin (Supplemental figure V-1), together with the fact that the level of heavy lysine in the fresh media is approximately 95% while the level of heavy 1-piperideine is nearly 28 % in both the fresh and spent media, the latter is more likely to be a result of L-lysine degradation during the process of obtaining ^{13}C-L-lysine than a product of L-lysine degradation in the fresh media. Additionally, other than 5-^{13}C-labelled 1-piperidein, no other 5-^{13}C-labelled compounds were detected in the cells or spent media.

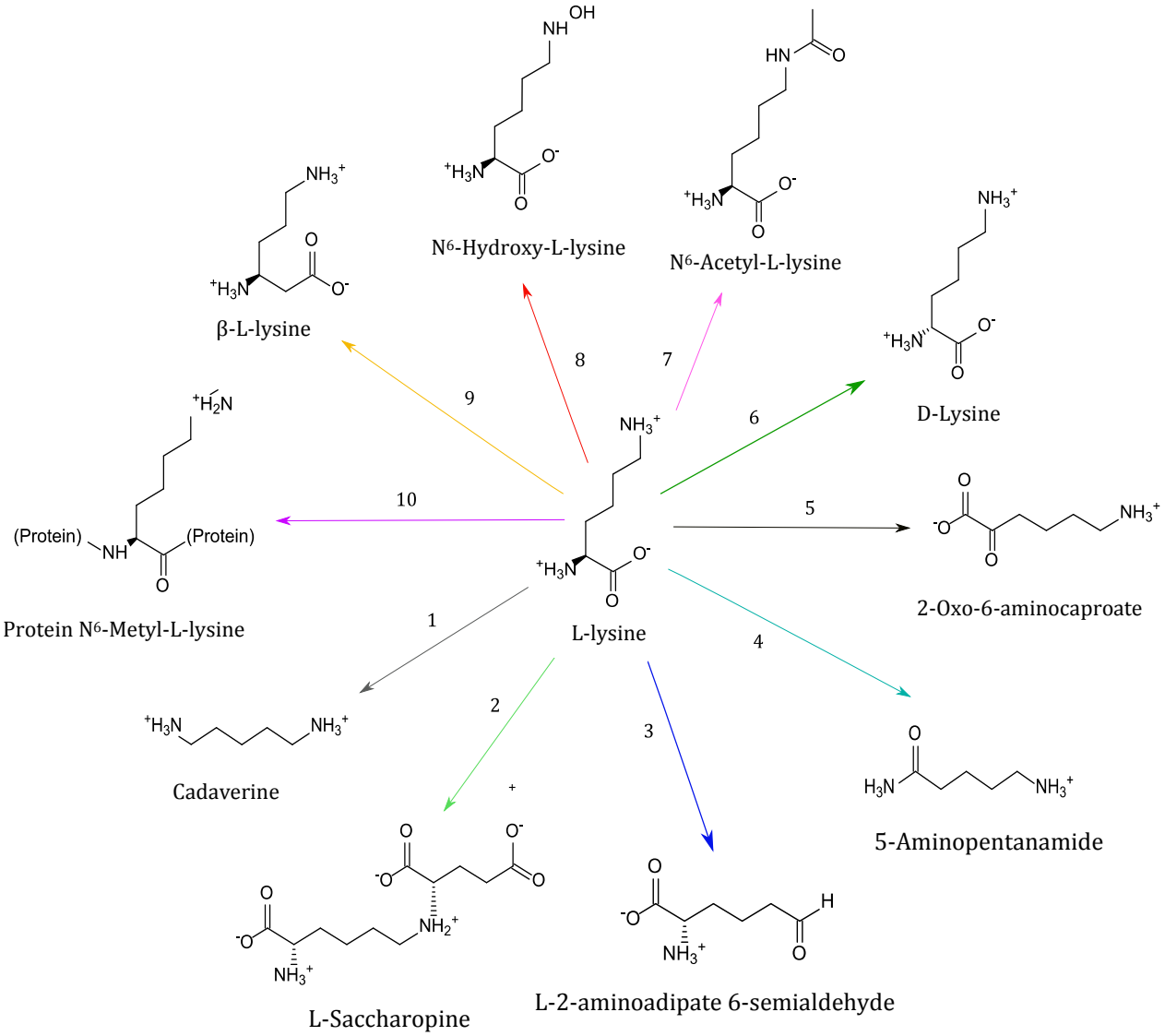

Figure V-12. Initial steps in L-lysine degradation pathways: 1 - Lysine decarboxylase (EC 4.1.1.18), 2 - Saccharopine dehydrogenase (NADP+, L-lysine forming) (EC 1.5.1.8) (Lysine-α-ketoglutarate reductase), 3 - Lysine:α-ketoglutarate ε-aminotransferase (EC 2.6.1.36), 4 - Lysine 2-monooxygenase (EC 1.13.12.2), 5 - Lysine α-oxidase (EC 1.4.3.14), 6 - Lysine racemase (EC 5.1.1.5), 7 - Lysine N⁶-acetyltransferase (EC 2.3.1.32), 8 - Lysine N⁶-hydroxylase (EC 1.14.13.59), 9 - Lysine 2,3-aminomutase (EC 5.4.3.2), 10 – Lysine N-methyltransferase (2.1.1._).
Credit: Zabriskie and Jackson, 2000

L-Lysine degradation

Nine L-lysine degradation pathways are known to exist in the living organisms so far and they occur via cadaverine, 5-aminopentanamide, L-saccharopine, Δ^1-piperideine-6-carboxylate, N^6-acetyl-L-lysine, 2-oxo-6-acetamidocaproate, D-lysine, L-β-lysine, and N^6-hydroxylysin (Figure V-12) (Zabriskie and Jackson, 2000). All nine pathways, as well as the protein-lysine degradation pathway (10) (Figure V-13, where each pathway is presented as a single vertical line with circles indicating the respective metabolites belonging to the pathway, ordered according to their place in the pathway) were investigated for isotope labelling. 8 of the 239 authentic standards used in our metabolomic experiments belonged to the L-lysine degradation pathways. Six of the standards, namely L-lysine, L-carnitine, L-2-aminoadipate, glycine, N^2-acetyl-L-lysine, 4-trimethyl-ammoniobutanoate and acetoacetate, were detected. Acetyl-CoA, however, was not. Thus, 37 of the detected metabolites were putatively identified.

The isotope tracing in the ten degradation pathways showed that:

- there was no isotope labelling in six of the L-lysine degradation pathways, i.e. pathway 1, 2, 3, 4, 8, and 9 (Figure V-13), (see Supplemental figures V-1, V-2, V-3, V-4, V-5 and V-6 for detailed representation of each individual pathway, including their labelling profile),

- three metabolites in four different pathways were ^{13}C-labelled and they included N^6-acetyl-L-lysine, involved in L-lysine degradation via N^6-acetyl-L-lysine (Figure V-14), L-pipecolate, involved in two L-lysine degradation pathways, via 2-oxo-6-aminocaproate and via D-lysine (Figures V-15 and V-16) and N^6, N^6, N^6-trimethyl-L-lysine, involved in protein lysine degradation (Figure V-17). It must be emphasized, however, that the three metabolites were putatively identified.

D-Lysine, L-β-lysine and 3,5-diaminohexanoate have the same mass and therefore the same labelling pattern as L-lysine (Figure V-13). Analysis of the raw MS data, however, confirmed the presence of L-lysine only. Investigated were also L-glutamate, α-ketoglutarate, coenzyme A (CoA), succinate and succinyl-CoA which are involved in many reactions of the L-lysine degradation pathways (Figure V-13). L-Glutamate, α-ketoglutarate and succinate were found unlabelled.

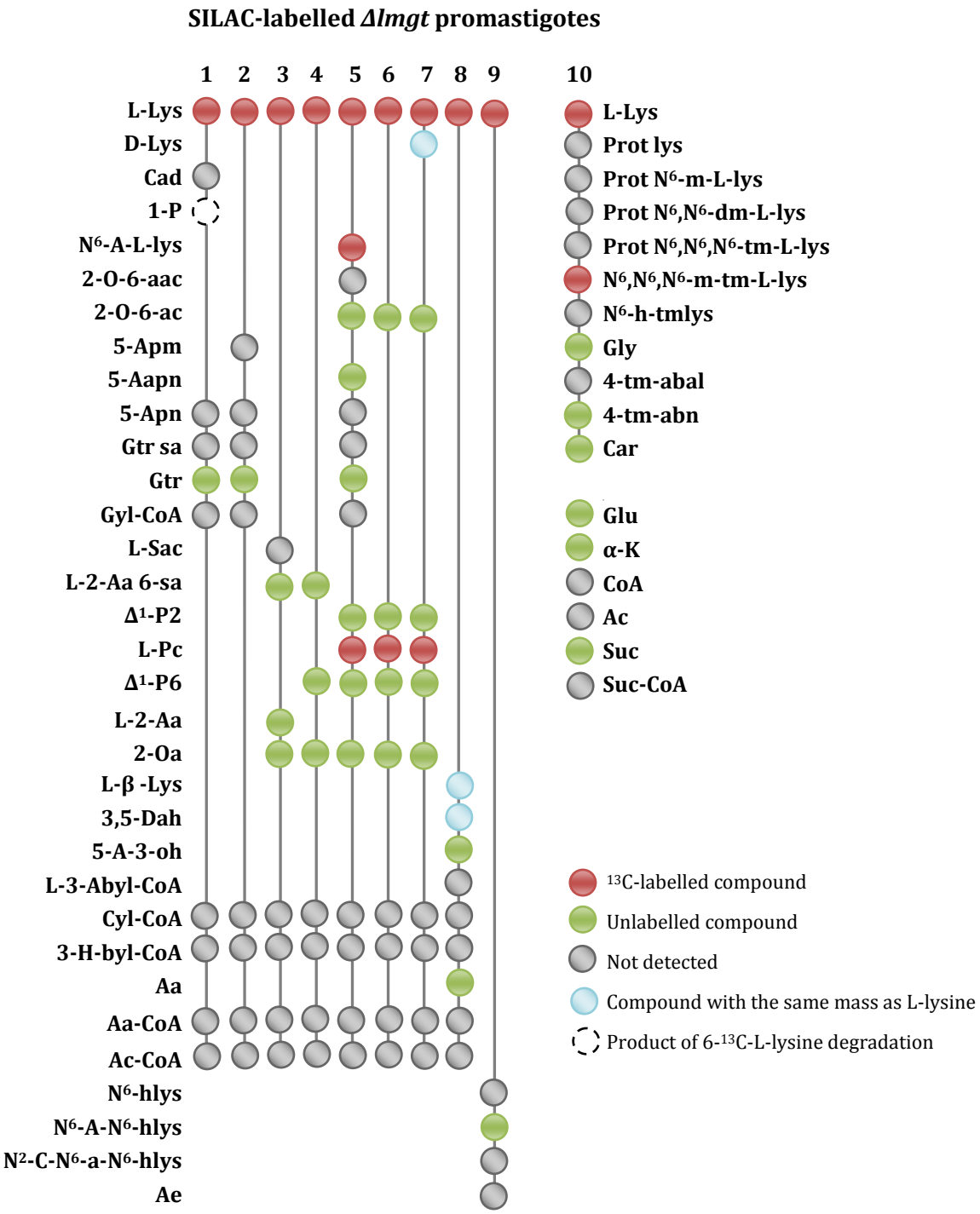

Figure V-13. Stable isotope tracing analysis of L-lysine degradation in SILAC-labelled *Δlmgt* promastigotes. Each pathway is presented as a single vertical line with circles indicating the respective metabolites belonging to the pathway, ordered according to their place in the pathway. 1- via cadaverin (Cad), 2 - via 5-aminopentanamide (5-Apm), 3 - via L-saccharopine (L-Sac), 4 - via Δ¹-piperideine-6-carboxylate (Δ¹-P6), 5 - via N⁶-acetyl-L-lysine (N⁶-A-L-lys), 6 - via 2-oxo-6-acetamido-caproate (2-O-6-aac), 7 - D-lysine (D-Lys), 8 - L-β-Lysine (L-β -Lys), 9 - via N⁶-hydroxy-lysine (N⁶-Hlys), 10 - via protein lysine (Prot lys).

Abbreviations: L-Lys - L-lysine, D-Lys - D-lysine, Cad - cadaverine, 1-P- 1-piperideine, N6-A-L-lys - N⁶-acetyl-L-lysine, 2-O-6-aac - 2-oxo-6-acetamidocaproate, 2-O-6-ac - 2-oxo-6-aminocaproate, 5-Apm - 5-aminopentanamide, 5-Aapn - 5-acetamidopentanoate, 5-Apn - 5-aminopentanoate, Gtr sa - glutarate semialdehyde, Gtr - glutarate, Gyl-CoA - glutaryl-CoA, Δ¹-P2 - Δ¹-piperideine-2-carboxylate, L-Pc - L-pipecolate, Δ¹-P6 - Δ¹-piperideine-6-carboxylate, L-Sac - L-saccharopine, L-2-Aa 6-sa - L-2-aminoadipate 6-semialdehyde, L-2-Aa - L-2-aminoadipate, 2-Oa - 2-oxoadipate, L-β -Lys - L-β-lysine, 3,5-Dah - 3,5-diaminohexanoate, 5-A-3-oh - 5-amino-3-oxohexanoate, L-3-Abyl-CoA - L-3-aminobutyryl-CoA, Cyl-CoA - crotonyl-CoA, 3-H-byl-CoA - 3-hydroxy-butanoyl-CoA, Aa - acetoacetate, Aa-CoA - acetoacetyl-CoA, Ac-CoA - acetyl-CoA, N⁶-Hlys - N⁶-hydroxylysine, N⁶-A-N⁶-hlys - N⁶-acetyl-N⁶-hydroxylysine, N²-C-N⁶-a-N⁶-hlys - N²-citryl-N⁶-acetyl-N⁶-hydroxylysine, Ae - aerobactin, Prot lys - protein lysine, Prot N⁶-m-L-lys - protein N⁶-methyl-L-lysine, Prot N⁶,N⁶-dm-L-lys - protein N⁶,N⁶-dimethyl-L-lysine, Prot N⁶,N⁶,N⁶-tm-L-lys - protein N⁶,N⁶,N⁶-trimethyl-L-lysine, N⁶,N⁶,N⁶-tm-L-lys - N⁶,N⁶,N⁶-trimethyl-L-lysine, N⁶-h-tmlys - N⁶-hydroxy-trimethyllysine, Gly - glyvine, 4-tm-abal - 4-trimethyl-ammoniobutanal, 4-tm-abn - 4-trimethyl-ammoniobutanoate, Car - L-carnitine, Glu - L-glutamate, α-K - α-ketoglutarate, CoA - coenzyme A, Ac - acetate, Suc - succinate, Suc-CoA - succinyl-CoA.

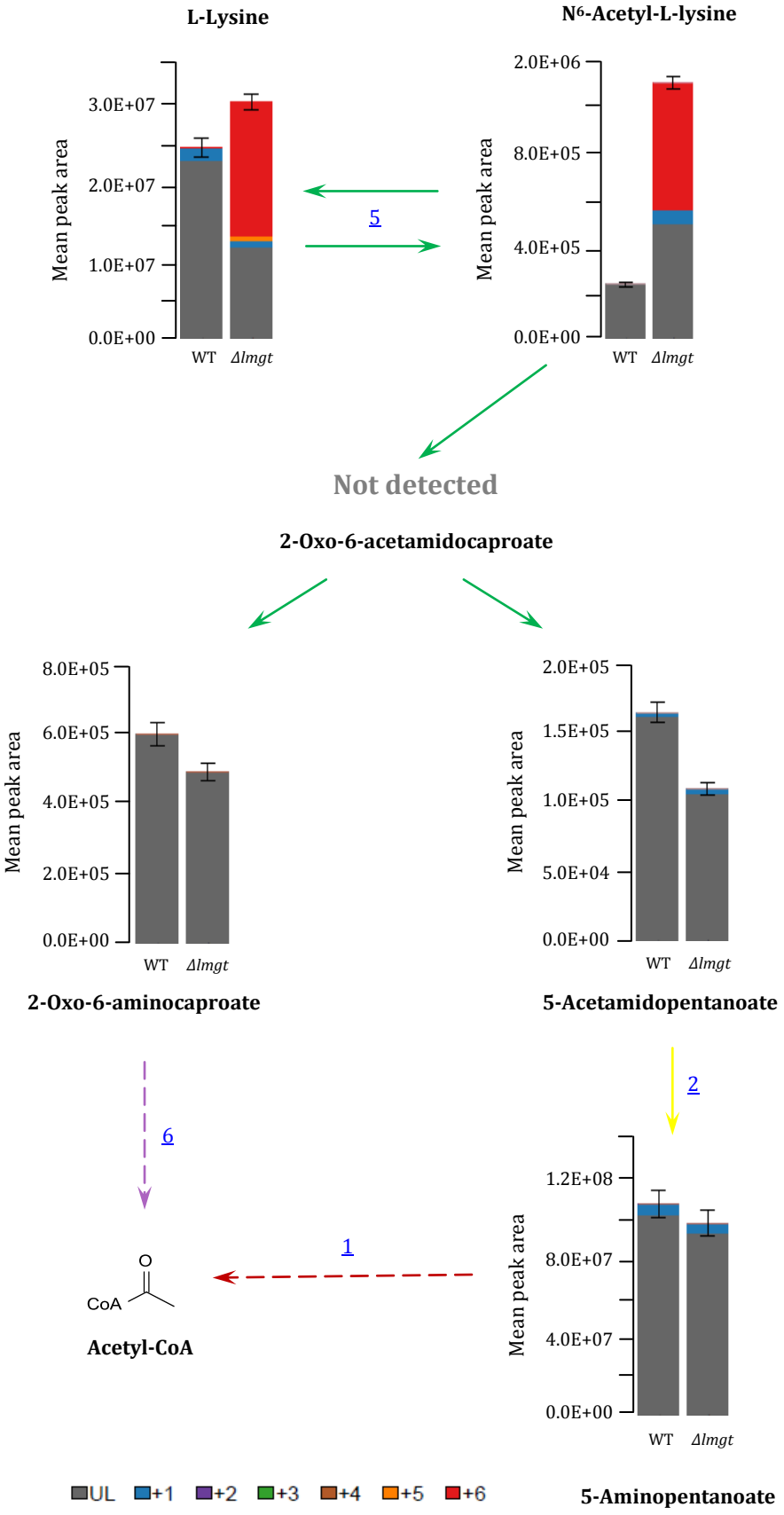

Figure V-14. Labelling profile of L-lysine degradation via N⁶-acetyl-L-lysine in the SILAC-labelled wild type and *Δlmgt* promastigotes. Abbreviations: WT – wild type promastigotes, *Δlmgt* - *Δlmgt* promastigotes, UL- unlabelled carbon, +1 - 1-^{13}C-labelled carbon, +2 - 2-^{13}C-labelled carbon, +3 - 3-^{13}C-labelled carbon, +4 - 4-^{13}C-labelled carbon, +5 - 5-^{13}C-labelled carbon, +6 - 6-^{13}C-labelled carbon. Dashed lines indicate indirect enzymatic reaction.
Adapted from KEGG and MetaCyc.

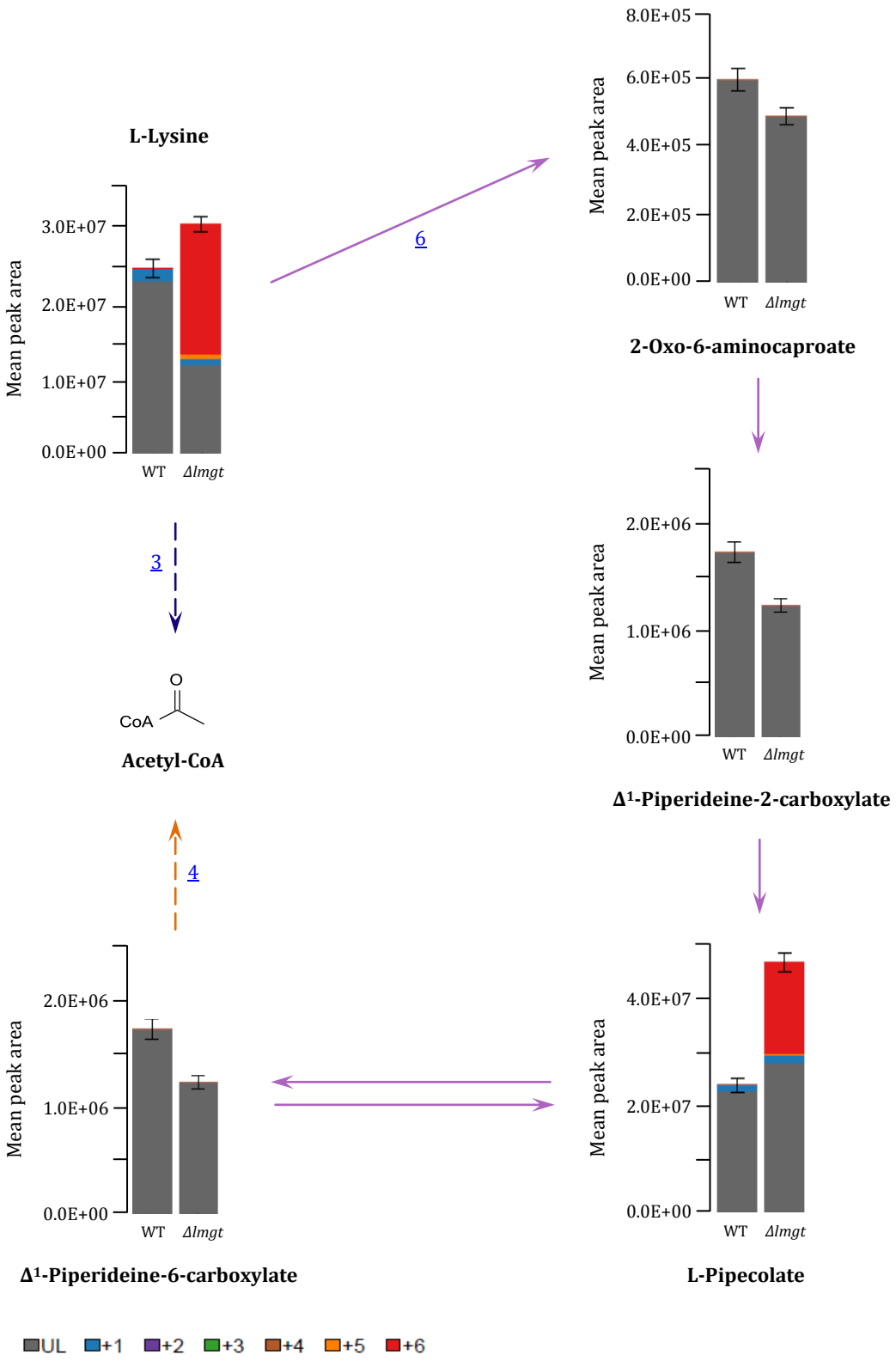

Figure V-15. Labelling profile of L-lysine degradation via 2-oxo-6-aminocaproate in the SILAC-labelled wild type and *Δlmgt* promastigotes. Abbreviations: WT – wild type promastigotes, *Δlmgt* - *Δlmgt* promastigotes, UL- unlabelled carbon, +1 - 1-^{13}C-labelled carbon, +2 - 2-^{13}C-labelled carbon, +3 - 3-^{13}C-labelled carbon, +4 - 4-^{13}C-labelled carbon, +5 - 5-^{13}C-labelled carbon, +6 - 6-^{13}C-labelled carbon. Dashed lines indicate indirect enzymatic reaction.
Adapted from KEGG and MetaCyc.

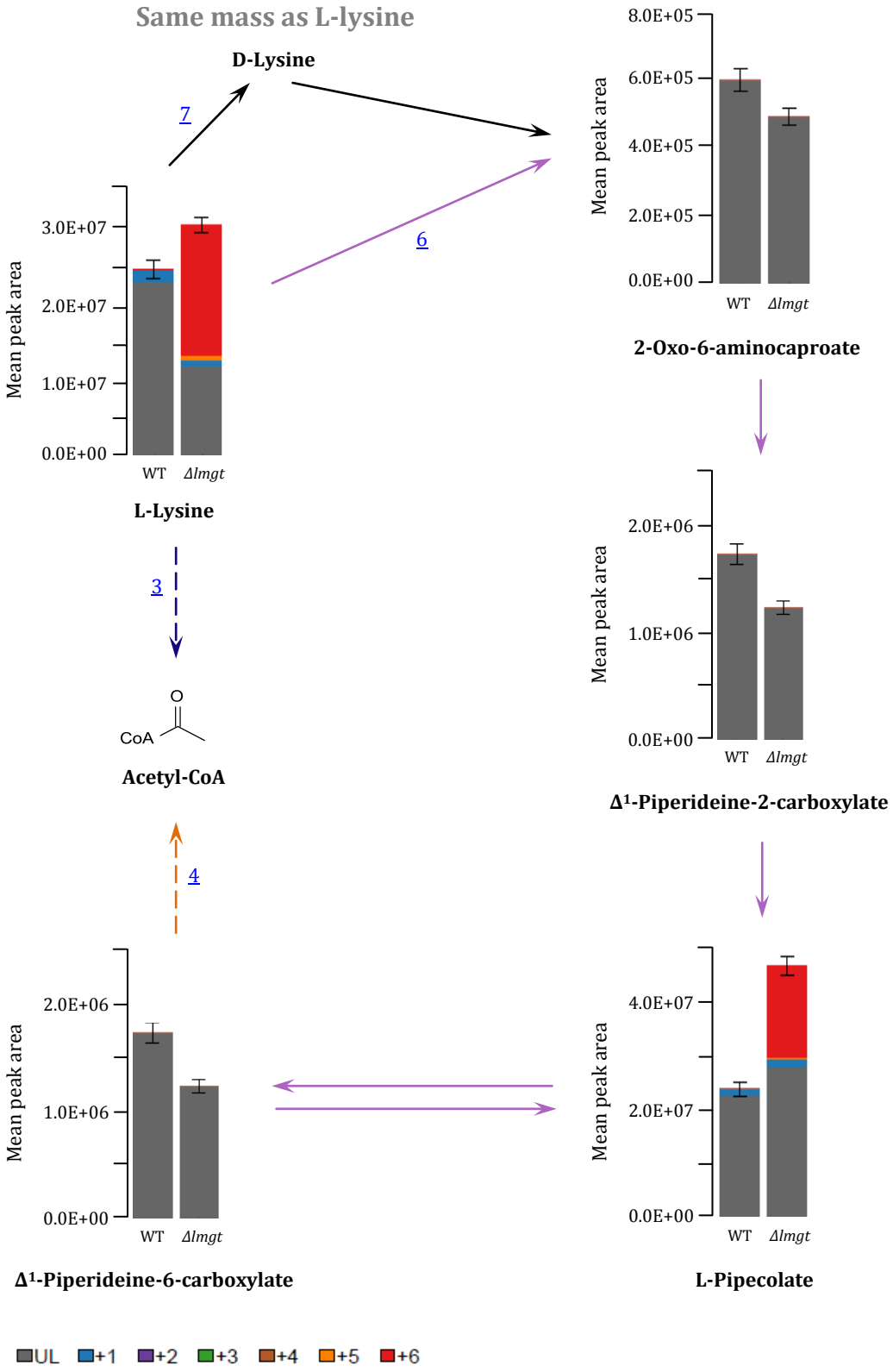

Figure V-16. Labelling profile of L-lysine degradation via D-lysine in the SILAC-labelled wild type and *Δlmgt* promastigotes. Abbreviations: WT – wild type promastigotes, *Δlmgt* - *Δlmgt* promastigotes, UL- unlabelled carbon, +1 - 1-^{13}C-labelled carbon, +2 - 2-^{13}C-labelled carbon, +3 - 3-^{13}C-labelled carbon, +4 - 4-^{13}C-labelled carbon, +5 - 5-^{13}C-labelled carbon, +6 - 6-^{13}C-labelled carbon. Dashed lines indicate indirect enzymatic reaction.
Adapted from KEGG and MetaCyc.

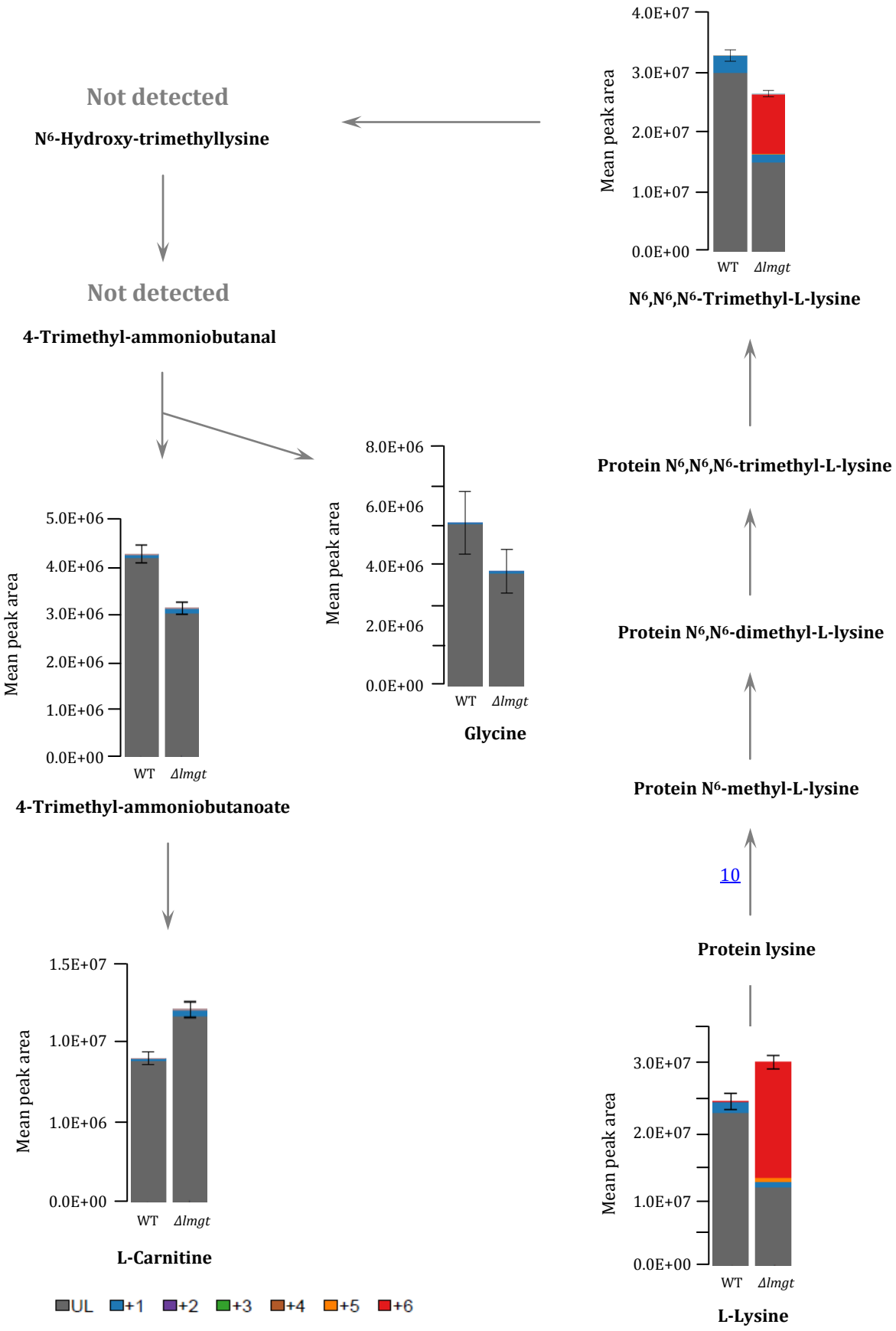

Figure V-17. Labelling profile of protein-lysine degradation in the SILAC-labelled wild type and *Δlmgt* promastigotes. Abbreviations: WT – wild type promastigotes, *Δlmgt* - *Δlmgt* promastigotes, UL- unlabelled carbon, +1 - 1-^{13}C-labelled carbon, +2 - 2-^{13}C-labelled carbon, +3 - 3-^{13}C-labelled carbon, +4 - 4-^{13}C-labelled carbon, +5 - 5-^{13}C-labelled carbon, +6 - 6-^{13}C-labelled carbon. Dashed lines indicate indirect enzymatic reaction.
Adapted from KEGG and MetaCyc.

L-Lysine biosynthesis

Two main pathways for L-lysine biosynthesis are known to exist to date and these are the diaminopimelate (DAP) and L-2-aminoadipic acid (AAA) pathways, where L-aspartate and α-ketoglutarate are used as precursors for the synthesis, respectively (Zabriskie and Jackson, 2000). Key enzymes from the L-lysine synthesis are absent in *Leishmania* and the pathway is believed not to operate in these organisms (Opperdoes and Coombs, 2007). The DAP and AAA L-lysine biosynthetic pathways, however, were also scrutinized for isotope labelled intermediates. Used for that purpose were two metabolomic data sets, the **SILAC** (^{13}C-L-lysine) and ***glc0** (^{13}C-D-glucose) sets. The **SILAC** data showed that all metabolites of the four variant DAP pathway, except for L,L-2,6-diaminopimelate (**L-DAP**) and *meso*-2,6-diaminopimelate (***m*-DAP**), were unlabelled (Figure V-18). The identification of **L-DAP** and ***m*-DAP** as ^{13}C-labelled derivatives of L-lysine, however, was accompanied with several issues. First, an authentic standard was available for ***m*-DAP** only and it was detected in the ***glc0** data but not in the **SILAC** data. Analysis of the raw ***glc0** data revealed that the unlabelled peak for ***m*-DAP** in both the wild type and *Δlmgt* promastigotes did not coincide with the authentic standard peak. A peak for 6-^{13}C-***m*-DAP** was not found either. By contrast, peaks for unlabelled and 6-^{13}C-***m*-DAP** were found in the **SILAC** samples but they had different retention times. Thus, ***m*-DAP** was only putatively identified, similar to most of the intermediate of the DAP pathway, except for L-aspartate and L-homoserine. Second, **L-DAP** and ***m*-DAP** have the same mass and are indistinguishable from one another. No other metabolite involved in the L-lysine biosynthesis or degradation has the same mass as the two metabolites. However, a search in the PubChem Compound, ChemSpider, and ChEBI databases revealed that N^6-carboxymethyl-L-lysine, methyl L-lysinate, N^6-carboxy-L-lysine, the Ala-Thre dipeptide, N,N'-Bis(2- hydroxyethyl) malonamide and diethyl methylene-biscarbamate were among the compounds with the same mass of 190.095 as **L-DAP** and ***m*-DAP**. Only the former three compounds, however, are directly related to the L-lysine metabolism. Finally, 6-^{13}C-**L-DAP** and/or 6-^{13}C-***m*-DAP**, similar to 1-piperidein, could be degradative products of ^{13}C-L-lysine. In condition ***glc0** wild type promastigotes, except L-aspartate and α-ketoglutarate, none of the detected intermediates of the DAP and AAA L-lysine biosynthetic pathways were labelled (Figure V-19).

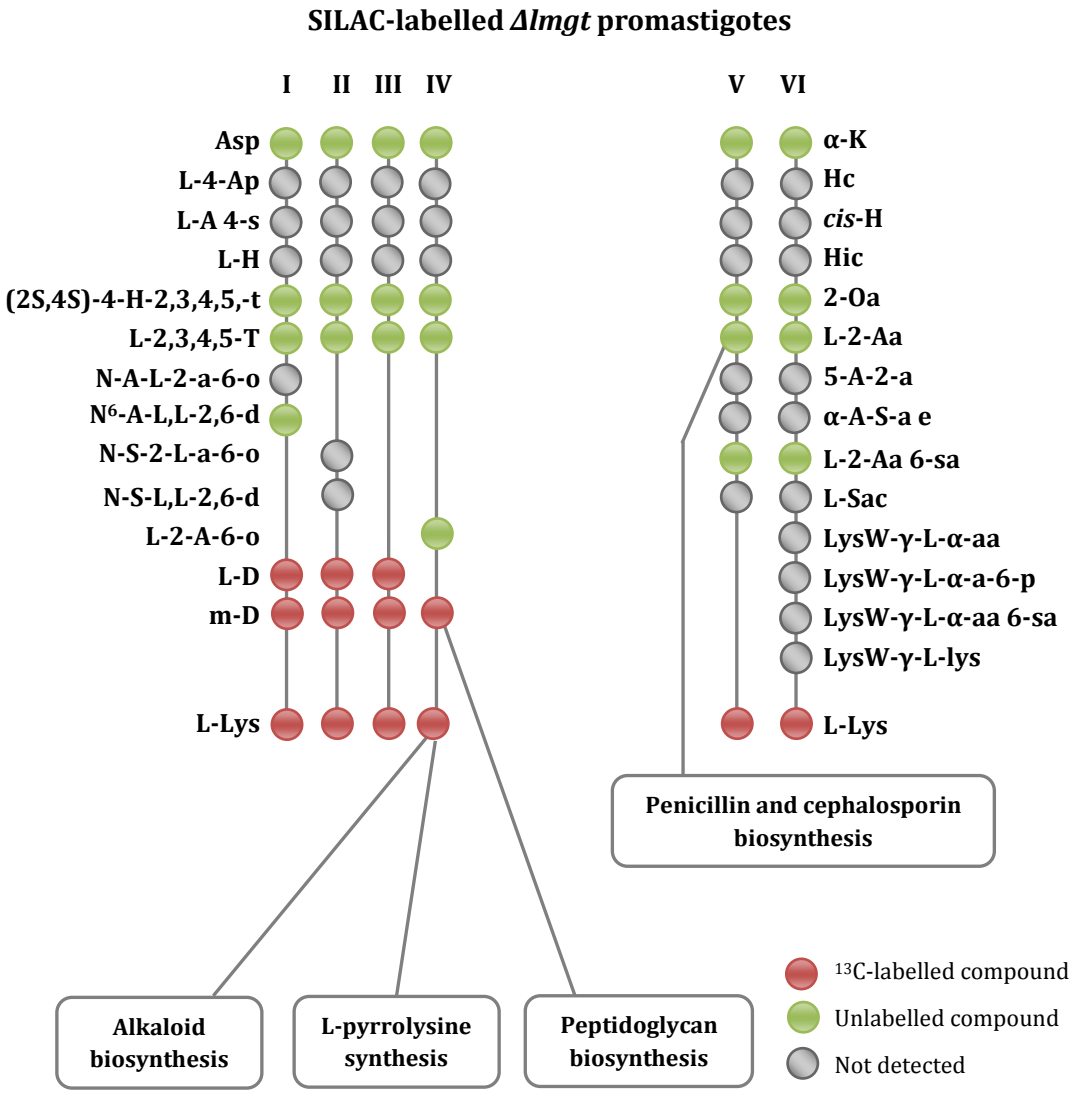

Figure V-18. Stable isotope tracing analysis of L-lysine biosynthesis in the SILAC-labelled *Δlmgt* promastigotes. Each pathway is presented as a single vertical line with circles indicating the respective metabolites belonging to the pathway, ordered according to their place in the pathway. I - diaminopimelate pathway (DAP) via N-acetyl-L-2-amino-6-oxopimelate (N-A-L-2-a-6-o), II - DAP via N-succinyl-2-L-amino-6-oxoheptanedioate (N-S-2-L-a-6-o), III - DAP via L-2-amino-6-oxopimelate (L-2-A-6-o), IV - DAP via L,L-2,6-diaminopimelate (L,L-2,6-D), V - L-2-amino adipic acid pathway (AAA) via L-saccharopine (L-Sac), VI - AAA via LysW-γ-L-lysine (LysW-γ-L-lys).

Asp - L-aspartate, L-4-Ap - L-4-aspartyl phosphate, L-A 4-s - L-aspartate 4-semialdehyde, L-H - L-homoserine, (2S,4S)-4-H-2,3,4,5,-t - (2S,4S)-4-hydroxy-2,3,4,5-tetrahydrodipicolinate, L-2,3,4,5-T - L-2,3,4,5-tetrahydrodipicolinate, N-A-L-2-a-6-o - N-acetyl-L-2-amino-6-oxopimelate, N6-A-L,L-2,6-d - N6-acetyl-L,L-2,6-diaminoheptanedioate, N-S-2-L-a-6-o - N-succinyl-2-L-amino-6-oxoheptanedioate, N-S-L,L-2,6-d - N-succinyl-L,L-2,6-diaminoheptanedioate, L-2-A-6-o - L-2-amino-6-oxopimelate, L-D - L,L-2,6-diaminopimelate, m-D - *meso*-2,6-diaminopimelate, L-Lys - L-lysine, α-K - α-ketoglutarate, Hc - homocitrate, *cis*-H - *cis*-homoaconitate, Hic - homoisocitrate, 2-Oa - 2-oxoadipate, L-2-Aa - L-2-aminoadipate, 5-A-2-a - 5-adenyl-2-aminoadipate, α-A-S-a e - α-aminoadipoyl-S-acyl enzyme, L-2-Aa 6-sa - L-2-aminoadipate 6-semialdehyde, L-Sac - L-saccharopine, LysW-γ-L-α-aa - LysW-γ-L-α-aminoadipate, LysW-γ-L-α-a-6-p - LysW-γ-L-α-aminoadipyl-6-phosphate, LysW-γ-L-α-aa 6-sa - LysW-γ-L-α-aminoadipate 6-semialdehyde, LysW-γ-L-lys - LysW-γ-L-lysine.

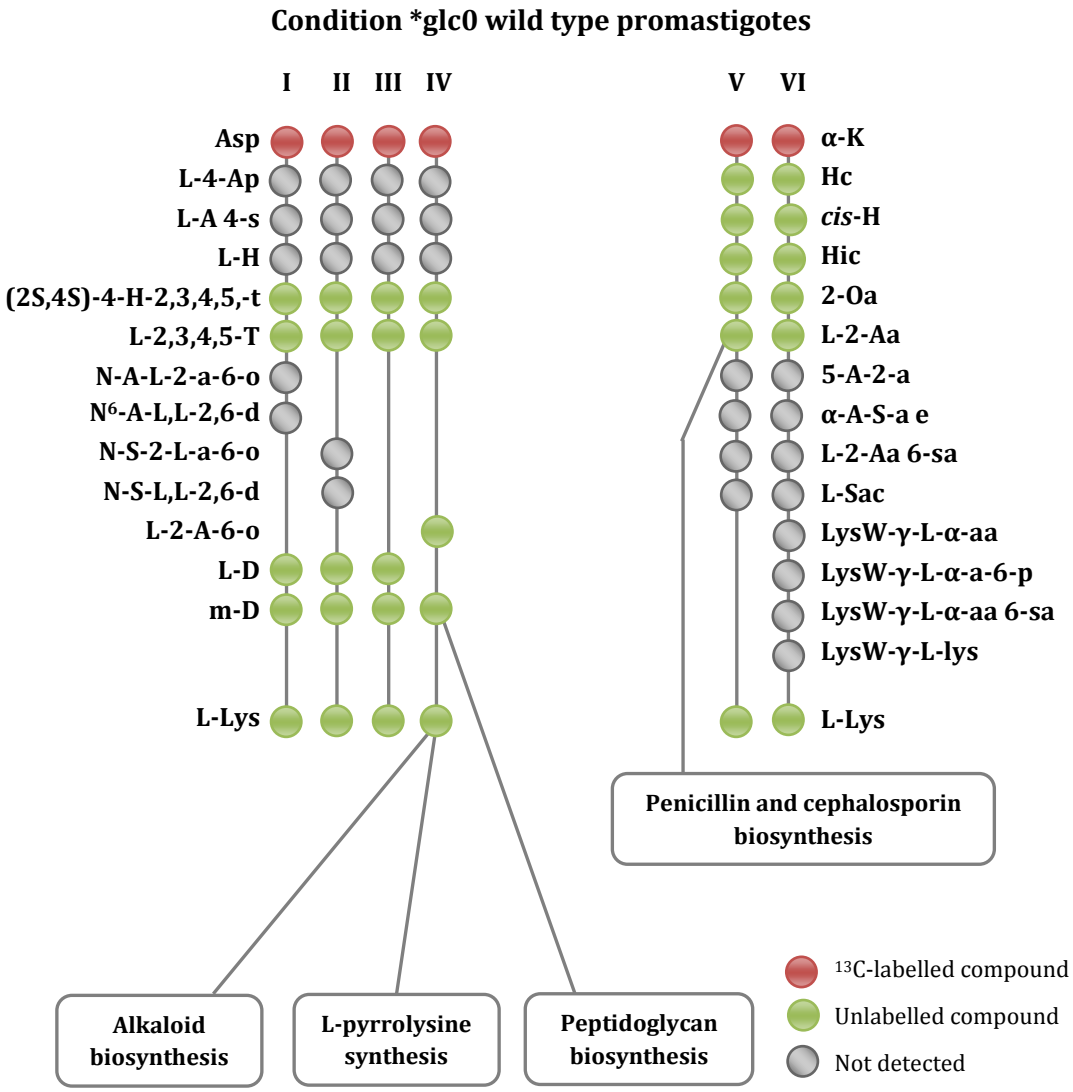

Figure V-19. Stable isotope tracing analysis of L-lysine biosynthesis in condition ***glc0** wild type promastigotes.* Each pathway is presented as a single vertical line with circles indicating the respective metabolites belonging to the pathway, ordered according to their place in the pathway. I - diaminopimelate pathway (DAP) via N-acetyl-L-2-amino-6-oxopimelate (N-A-L-2-a-6-o), II - DAP via N-succinyl-2-L-amino-6-oxoheptanedioate (N-S-2-L-a-6-o), III - DAP via L-2-amino-6-oxopimelate (L-2-A-6-o), IV - DAP via L,L-2,6-diaminopimelate (L,L-2,6-D), V - L-2-amino adipic acid pathway (AAA) via L-saccharopine (L-Sac), VI - AAA via LysW-γ-L-lysine (LysW-γ-L-lys).

Asp - L-aspartate, L-4-Ap - L-4-aspartyl phosphate, L-A 4-s - L-aspartate 4-semialdehyde, L-H - L-homoserine, (2S,4S)-4-H-2,3,4,5,-t - (2S,4S)-4-hydroxy-2,3,4,5-tetrahydrodipicolinate, L-2,3,4,5-T - L-2,3,4,5-tetrahydrodipicolinate, N-A-L-2-a-6-o - N-acetyl-L-2-amino-6-oxopimelate, N6-A-L,L-2,6-d - N6-acetyl-L,L-2,6-diaminoheptanedioate, N-S-2-L-a-6-o - N-succinyl-2-L-amino-6-oxoheptanedioate, N-S-L,L-2,6-d - N-succinyl-L,L-2,6-diaminoheptanedioate, L-2-A-6-o - L-2-amino-6-oxopimelate, L-D - L,L-2,6-diaminopimelate, m-D - *meso*-2,6-diaminopimelate, L-Lys - L-lysine, α-K - α-ketoglutarate, Hc - homocitrate, *cis*-H - *cis*-homoaconitate, Hic - homoisocitrate, 2-Oa - 2-oxoadipate, L-2-Aa - L-2-aminoadipate, 5-A-2-a - 5-adenyl-2-aminoadipate, α-A-S-a e - α-aminoadipoyl-S-acyl enzyme, L-2-Aa 6-sa - L-2-aminoadipate 6-semialdehyde, L-Sac - L-saccharopine, LysW-γ-L-α-aa - LysW-γ-L-α-aminoadipate, LysW-γ-L-α-a-6-p - LysW-γ-L-α-aminoadipyl-6-phosphate, LysW-γ-L-α-aa 6-sa - LysW-γ-L-α-aminoadipate 6-semialdehyde, LysW-γ-L-lys - LysW-γ-L-lysine.

A number of pathways directly linked to L-lysine metabolism were also investigated with mzMatch-ISO. These included alkaloid biosynthesis, L-pyrrolysine synthesis, peptidoglycan synthesis, penicillin and cephalosporin biosynthesis and fructoselysine and psicoselysine degradation. L-lysine, similar to its homologue L-ornithine, is involved in the synthesis of several groups of alkaloids, namely piperidine, quinolizidin, and indolizidine alkaloids. None of the following alkaloids: slaframine, 13 α-tigloyloxylupanine, (+)-cystine, anatalline, anapheline, piperine, sedamine and lobeline, were detected. Swainsonine, lupinine, pelletierine and pseudopelletierine were detected but they were unlabelled. All alkaloids were putatively identified. L-Lysine also serves as a precursor for the synthesis of L-pyrrolysine, an unusual proteinogenic amino acid in some methanogenic archae (Gaston *et al.*, 2011). The first step of the L-pyrrolysine synthesis is the conversion of L-lysine to 3-methyl-ornithine, a compound that has the same mass as L-lysine and is thus indistinguishable from it. Two of the next three metabolites were found unlabelled, i.e. 3-methylornithine-N^6-L-lysine and L-pyrrolysine, while 3-methylglutamyl-5-semialdehyde-N^6-lysine was not detected. The metabolites were again putatively identified. L-lysine, together with *meso*-2,6-diaminopimelate, are also important precursors in bacterial cell wall peptidoglycan synthesis (Zabriskie and Jackson, 2000). A search among the muramoyl derivatives of ***m*-DAP** in the **SILAC** and ***glc0** data sets was fruitless. Similarly, an analysis of the fructoselysine and psicoselysine degradation revealed that none of the metabolites were labelling.

Furthermore, a group of 61 L-lysine derivatives, obtained from the ChEBI database (http://www.ebi.ac.uk/chebi/) were also inspected for isotope labelling (Figure V-20). 6 of the metabolites were already investigated as part of the pathways described above, 19 were preliminary entries, 5 were manually annotated, 1 had the same mass as L-lysine and 1 was a reference compound for 3'-O-L-lysyl derivatives of any 1,2-diacyl-sn-glycero-3-phospho-1'-sn-glycerol (Supplemental tables V-3 and V-4). That left 29 metabolites for analysis. Included in the search was also the dipeptide β-alanyl-L-lysine. 11 of the 30 metabolites were detected: D-lysopine, L-homocitrulline, L-homoarginine, N^2-methyl-L-lysine, N^6-carboxymethyl-L-lysine, methyl L-lysinate, N^6-carboxy-L-lysine, psicosyl-lysine (or psicoselysine), β-alanyl-L-lysine, L-2-aminohexano-6-lactam (or L-lysine 1,6-lactam) and N^6-methyl-L-lysine, the former nine of which were unlabelled while the latter two were ^{13}C-labelled.

ChEBI Ontology

L-lysine derivative (CHEBI:25095) **is a** lysine derivative (CHEBI:53079)

1. (3*S*)-3,6-diaminohexanoic acid (CHEBI:15613) **is a** L-lysine derivative (CHEBI:25095)
2. (*Z*)-N^6-[(4*R*,5*S*)-5-(2-carboxyethyl)-4-(carboxymethyl)piperidin-3-ylidene]-L-lysine (CHEBI:41690) **is a** L-lysine derivative (CHEBI:25095)
3. 1,2-diacyl-*sn*-glycero-3-phospho-1'-(3'-*O*-L-lysyl)-*sn*-glycerol (CHEBI:29039) **is a** L-lysine derivative (CHEBI:25095)
4. 1-(L-norleucin-6-yl)pyrraline (CHEBI:59973) **is a** L-lysine derivative (CHEBI:25095)
5. 1-(L-norvalin-5-yl)pyrraline (CHEBI:60824) **is a** L-lysine derivative (CHEBI:25095)
6. 5'-(N^6-L-lysine)-L-tyrosylquinone (CHEBI:73669) **is a** L-lysine derivative (CHEBI:25095)
7. 5-glycosyloxy-L-lysine (CHEBI:21994) **is a** L-lysine derivative (CHEBI:25095)
8. *erythro*-5-phosphonooxy-L-lysine (CHEBI:16752) **is a** L-lysine derivative (CHEBI:25095)
9. *N*-hippuryl-N^6-(carboxymethyl)lysine (CHEBI:61059) **is a** L-lysine derivative (CHEBI:25095)
10. N^6-citryl-N^2-acetyl-N^2-hydroxylysine (CHEBI:63801) **is a** L-lysine derivative (CHEBI:25095)
11. N^2-(5'-guanylyl)-N^6-acetyl-L-lysine methyl ester(1−) (CHEBI:64853) **is a** L-lysine derivative (CHEBI:25095)
12. N^2-GMP-N^6-acetyl-L-lysine methyl ester (CHEBI:64856) **is a** L-lysine derivative (CHEBI:25095)
13. N^6-(5'-phosphopyridoxyl)-L-lysine (CHEBI:44759) **is a** L-lysine derivative (CHEBI:25095)
14. N^6-methyl-L-lysine (CHEBI:21756) **is a** L-lysine derivative (CHEBI:25095)
15. N^6,N^6-dimethyl-L-lysine (CHEBI:43997) **is a** L-lysine derivative (CHEBI:25095)
16. N^6-(5'-adenylyl)-L-lysine (CHEBI:21868) **is a** L-lysine derivative (CHEBI:25095)
17. N^6-(5'-guanylyl)-L-lysine (CHEBI:21869) **is a** L-lysine derivative (CHEBI:25095)
18. N^6-(pyridoxal phosphate)-L-lysine (CHEBI:21896) **is a** L-lysine derivative (CHEBI:25095)
19. N^6-[(indol-3-yl)acetyl]-L-lysine (CHEBI:17328) **is a** L-lysine derivative (CHEBI:25095)
20. N^6-acetimidoyl-L-lysine (CHEBI:63971) **is a** L-lysine derivative (CHEBI:25095)
21. N^6-acetyl-N^2-(5'-phosphopyridoxyl)-L-lysine (CHEBI:59767) **is a** L-lysine derivative (CHEBI:25095)
22. N^6-acyl-L-lysine (CHEBI:16232) **is a** L-lysine derivative (CHEBI:25095)
23. N^6-carboxy-L-lysine (CHEBI:43575) **is a** L-lysine derivative (CHEBI:25095)
24. N^6-carboxymethyl-L-lysine (CHEBI:53014) **is a** L-lysine derivative (CHEBI:25095)
25. N^6-dansyl-L-lysine (CHEBI:42024) **is a** L-lysine derivative (CHEBI:25095)
26. N^6-glycyl-L-lysine (CHEBI:21885) **is a** L-lysine derivative (CHEBI:25095)
27. N^6-methyl-L-lysine (CHEBI:17604) **is a** L-lysine derivative (CHEBI:25095)
28. D-lysopine (CHEBI:17213) **is a** L-lysine derivative (CHEBI:25095)
29. L-2-aminohexano-6-lactam (CHEBI:17342) **is a** L-lysine derivative (CHEBI:25095)
30. L-allysine (CHEBI:17917) **is a** L-lysine derivative (CHEBI:25095)
31. L-homoarginine (CHEBI:27747) **is a** L-lysine derivative (CHEBI:25095)
32. L-homocitrulline (CHEBI:17443) **is a** L-lysine derivative (CHEBI:25095)
33. L-lysine thiazolecarboxylic acid (CHEBI:21355) **is a** L-lysine derivative (CHEBI:25095)
34. L-pyrrolysine (CHEBI:21860) **is a** L-lysine derivative (CHEBI:25095)
35. L-saccharopine (CHEBI:16927) **is a** L-lysine derivative (CHEBI:25095)
36. acetyl-L-lysine (CHEBI:22193) **is a** L-lysine derivative (CHEBI:25095)
37. aerobactin (CHEBI:18157) **is a** L-lysine derivative (CHEBI:25095)
38. biocytin (CHEBI:27870) **is a** L-lysine derivative (CHEBI:25095)
39. deoxyhypusine (CHEBI:50038) **is a** L-lysine derivative (CHEBI:25095)
40. fructoselysine 6-phosphate (CHEBI:61437) **is a** L-lysine derivative (CHEBI:25095)
41. glyoxal-lysine dimer (CHEBI:59965) **is a** L-lysine derivative (CHEBI:25095)
42. heme P460-bis-L-cysteine-L-lysine (CHEBI:24481) **is a** L-lysine derivative (CHEBI:25095)
43. hydroxy-L-lysine (CHEBI:24661) **is a** L-lysine derivative (CHEBI:25095)
44. hypusine (CHEBI:21858) **is a** L-lysine derivative (CHEBI:25095)
45. indole-lysine conjugate (CHEBI:24822) **is a** L-lysine derivative (CHEBI:25095)
46. L-lysine amide (CHEBI:21353) **is a** L-lysine derivative (CHEBI:25095)
47. lysidine (CHEBI:64328) **is a** L-lysine derivative (CHEBI:25095)
48. methyl L-lysinate (CHEBI:21354) **is a** L-lysine derivative (CHEBI:25095)
49. methylglyoxal-lysine dimer (CHEBI:59963) **is a** L-lysine derivative (CHEBI:25095)
50. N6-1-carboxyethyl-L-lysine (CHEBI:21870) **is a** L-lysine derivative (CHEBI:25095)
51. N6-3,4-didehydroretinylidene-L-lysine (CHEBI:21871) **is a** L-lysine derivative (CHEBI:25095)
52. N6-formyl-L-lysine (CHEBI:21884) **is a** L-lysine derivative (CHEBI:25095)
53. N6-methyl-N6-poly(N-methyl-propylamine)-L-lysine (CHEBI:21889) **is a** L-lysine derivative (CHEBI:25095)
54. N6-mureinyl-L-lysine (CHEBI:21893) **is a** L-lysine derivative (CHEBI:25095)
55. N6-myristoyl-L-lysine (CHEBI:21894) **is a** L-lysine derivative (CHEBI:25095)
56. N6-palmitoyl-L-lysine (CHEBI:21895) **is a** L-lysine derivative (CHEBI:25095)
57. N6-pyruvic acid 2-iminyl-L-lysine (CHEBI:21897) **is a** L-lysine derivative (CHEBI:25095)
58. N6-retinylidene-L-lysine (CHEBI:21898) **is a** L-lysine derivative (CHEBI:25095)
59. N^{α}-acetyl-L-lysine methyl ester (CHEBI:64859) **is a** L-lysine derivative (CHEBI:25095)
60. Peptidyl-L-lysine (CHEBI:27424) **is a** L-lysine derivative (CHEBI:25095)
61. psicosyllysine (CHEBI:61425) **is a** L-lysine derivative (CHEBI:25095)

Figure V-20. List of L-lysine derivatives subjected to stable isotope tracing analysis.
Credits: ChEBI

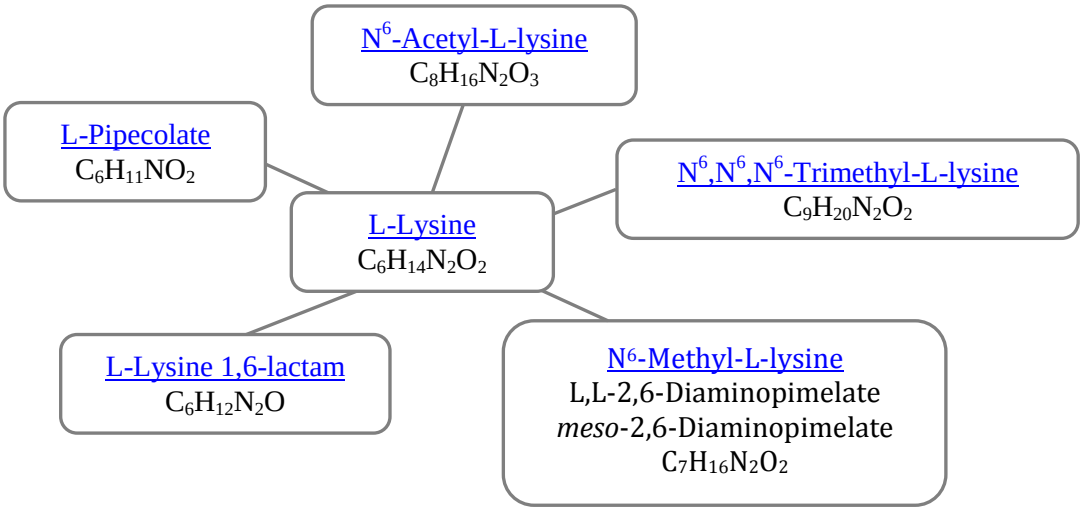

Figure V-21. Derivatives of ^{13}C-L-lysine found in the *Δlmgt* promastigotes. The metabolites are grouped based on elemental composition specified at the bottom of the rectangles.

N^2-Methyl-L-lysine has the same mass as N^6-methyl-L-lysine and was available as an authentic standard. However, the unlabelled and 6-^{13}C-lablled peaks for N^2-methyl-L-lysine did not correspond to those of the authentic standard and that indicated that the metabolite was most probably N^6-methyl-L-lysine. Additionally, N^6-methyl-L-lysine has the same mass as L-DAP and *m*-DAP. However, the unconvincing results regarding the L-D and m-D identification do not exclude N^6-methyl-L-lysine as also being labelled. The mass of L-lysine 1,6-lactam was different from that of any relevant to L-lysine metabolism compounds investigated here.

Finally, an analysis of L-alanine, L-arginine, L-asparagine, L-aspartate, L-citrulline, L-cysteine, L-cystine, L-glutamate, L-glutamine, L-histidine, L- leucine, L-methionine, L-ornithine, L-phenylalanine, L-proline, L-serine, L-threonine, L-tryptophan, L-tyrosine and L-valine, showed that none of the amino acids were heavy-labelled. Thus, the following isotopomers of ^{13}C-L-lysine were detected: L-pipecolate, N^6-acetyl-L-lysine, N^6,N^6,N^6-trimethyl-L-lysine, N^6-methyl-L-lysine and L-lysine 1,6- lactam (Figure V-21).

V.2. Discussion

V.2.1. Global quantitative proteomic characterization of *Δlmgt* promastigotes

The initial phenotypic characterization of the *Δlmgt* promastigotes by Landfear and colleagues revealed that the *Δlmgt* promastigotes grow considerably more slowly and reach lower cell density compared to the wild type promastigotes (Burchmore *et al.*, 2003). The growth profile of the *Δlmgt* promastigotes observed in this project was similar. Specifically, the growth rate of the *Δlmgt* promastigotes is approximately half that of the wild type promastigotes when cultured in the defined medium HOMEM supplemented with 10% serum (Figure V-2). The reduced growth rate of the *Δlmgt* promastigotes was one of the biggest issues with regard to one of our main aims, namely, to perform a global quantitative characterization of the *Δlmgt* promastigotes via SILAC. To apply SILAC to the wild type and *Δlmgt* promastigotes, we had to adapt the two cell lines, initially grown in media with regular serum, to media with dialyzed serum. Growing the *Δlmgt* promastigotes in media with dialyzed serum, however, proved to be problematic. While the defined media with added serum contain all necessary nutrients for the proliferation of the *Leishmania* promastigotes, media with dialyzed serum lacks low molecular weight components, some of which appear to be important for parasite growth. These may include nutrients such as sugars, other than D-glucose, amino acids, which appear to be major energy and carbon sources for the *Δlmgt* promastigotes (see Chapter IV), and other nutrients such as lipids, nucleotides, cofactors and vitamins, for many of which *Leishmania* are likely auxotrophic. Removing these components from the culture media resulted in poor growth of both the wild type and *Δlmgt* promastigotes (Figures V-3 and V-4). Concisely, the adaptation of the wild type and *Δlmgt* promastigotes was hampered, first, by the lack of important nutrients in the culturing media, second, by the period of time provided for adaptation (two passages only), and, third, by the low starting cell density. Nothing could have been changed with regard to the first problem since it is a necessity of SILAC required for the full incorporation of the isotope amino acids only. The second and third problems, however, were dealt with by extending the adaptation time to two passages with four changes of the fresh medium, which took nearly a month and a half, and increasing of the initial cell density from 1.0×10^5 cells ml^{-1} to 1.0×10^6 cells ml^{-1}, respectively. Resolving the second and third problems was based on the observation, made on multiple occasions, that the time necessary for the cell cultures to reach log phase

was longer when they were started at lower initial cell density. As a result of the prolonged time for adaptation and increased number of cells sub-passaged in fresh media, the growth of the wild type and *Δlmgt* promastigotes in the SILAC media improved which facilitated the generation of enough SILAC-labelled protein from the two cell lines. Two interesting facts became obvious from the SILAC data analysis. First, since the digestion of the labelled proteins was performed with trypsin, the resulting peptides were cut after L-arginine or L-lysine. It was observed that many peptides ending with L-arginine did not contain L-lysine and were thus not considered in the quantitation. The first important conclusion of this study, therefore, corroborates with the well known concept that more accurate quantitative information would be obtained if both L-arginine and L-lysine are used as isotope amino acids when trypsin is used as a protease. Second, the Mascot search revealed that many peptides in the heavy-labelled protein samples were actually not heavy-labelled. That led to further investigation of the labelling efficiency. It was revealed that only half (52%) of the heavy-labelled L-lysine was incorporated into proteins by both the wild type and *Δlmgt* promastigotes. With regard to L-lysine, that revealed that the amino acid, as shown before (Simon et al., 1983), was maintained in a free form in the amino acid pool and suggested that the L-lysine might have other role(s) in promastigote metabolism than just protein synthesis. With regard to the SILAC results, the partial incorporation of the heavy-lysine meant that the generated quantitative data were inaccurate because all proteins but one were found down-regulated in the *Δlmgt* promastigotes. Altogether, the proteomic data revealed that SILAC with L-lysine as a single amino acid of choice is not applicable for investigation of the *L. mexicana* proteome. Two separate analyses, with L-arginine and with both L-lysine and L-arginine, have to be performed to be clarified if the method is useful for accurate quantitative probing of the *L. mexicana* or *Leishmania* proteome in general.

V.2.2. Global metabolomic characterization of SILAC-labelled *Δlmgt* promastigotes

L-Lysine is a 6-carbon polar amino acids with a highly reactive (pKa = 10.5), positively charged ε-amino group at the end of the side chain and three methylene groups (CH_2) close to the α-amino group rendering it considerably hydrophobic. As a consequence of their high hydrophobicity, L-lysines are usually, but not exclusively, buried within the proteins with only the charged part of the side chain and the ε-amino group exposed on the outside. L-Lysines are often in the protein active or

binding sites where the ε-amino group participates in hydrogen bonding with negatively charged amino acids which is involved in protein structure stabilization and enzyme catalysis.

Among the 20 canonical amino acids, L-lysine is unusual in that it has two distinct biosynthetic pathways. In most bacteria, lower fungi and higher plants, L-lysine is synthesised from L-aspartate via the diaminopimelate pathway (DAP) (Figure V-25), while in some bacteria, yeasts and higher fungi the amino acid is synthesised via the L-2-amino adipic acid (AAA) pathway, with α-ketoglutarate serving as a precursor (Figure V-26) (Zabriskie and Jackson, 2000; Xu *et al.*, 2006).

Diaminopimelate pathway. The DAP pathway is a source for L-lysine for protein synthesis in Gram-negative bacteria and for L-lysine and *meso*-diaminopimelate for cell wall peptidoglycan biosynthesis in Gram positive bacteria. Four variants of the pathway have been identified so far: two acyl pathways going via succinyl (Figure V-25) or acetyl (Figure V-26) intermediates, one *meso*-diaminopimelate dehydrogenase pathway (Figure V-27) and one L,L-diaminopimelate aminotransferase pathway (Figure V-28) (Nachar *et al.*, 2012). The first half of all four pathways results in the synthesis of L-2,3,4,5-tetrahydrodipicolinate from L-aspartate in four consequent reactions catalysed by aspartate kinase, aspartate semialdehyde dehydrogenase, 4-hydroxy-tetrahydrodipicolinate synthase, and 4-hydroxy-tetrahydrodipicolinate reductase, respectively (Figures V-25 and V-26). The second half of the pathway leads to the conversion of L-2,3,4,5-tetrahydrodipicolinate to *meso*-diaminopimelate and is carried out in four different ways. The two acyl pathways involve four reactions once again and the enzymes 2,3,4,5-tetrahydropyridine-2,6-dicarboxylate N-acyl-transferase, N-acyl-diaminopimelate aminotransferase, acyl-diaminopimelate deacylase and acyl-diaminopimelate epimerase, respectively (Figure V-25). The other two pathways involve either oxidation or transamination of L-2,3,4,5-tetrahydrodipicolinate to *meso*-diaminopimelate in a single reaction cataslyzed by *meso*-diaminopimelate dehydrogenase and L,L-diaminopimelate aminotransferase, respectively (Figure V-26). The last half of the pathway is common to all variants again and concludes with the synthesis of L-lysine (Figures V-25 and V-26) (Nachar *et al.*, 2012).

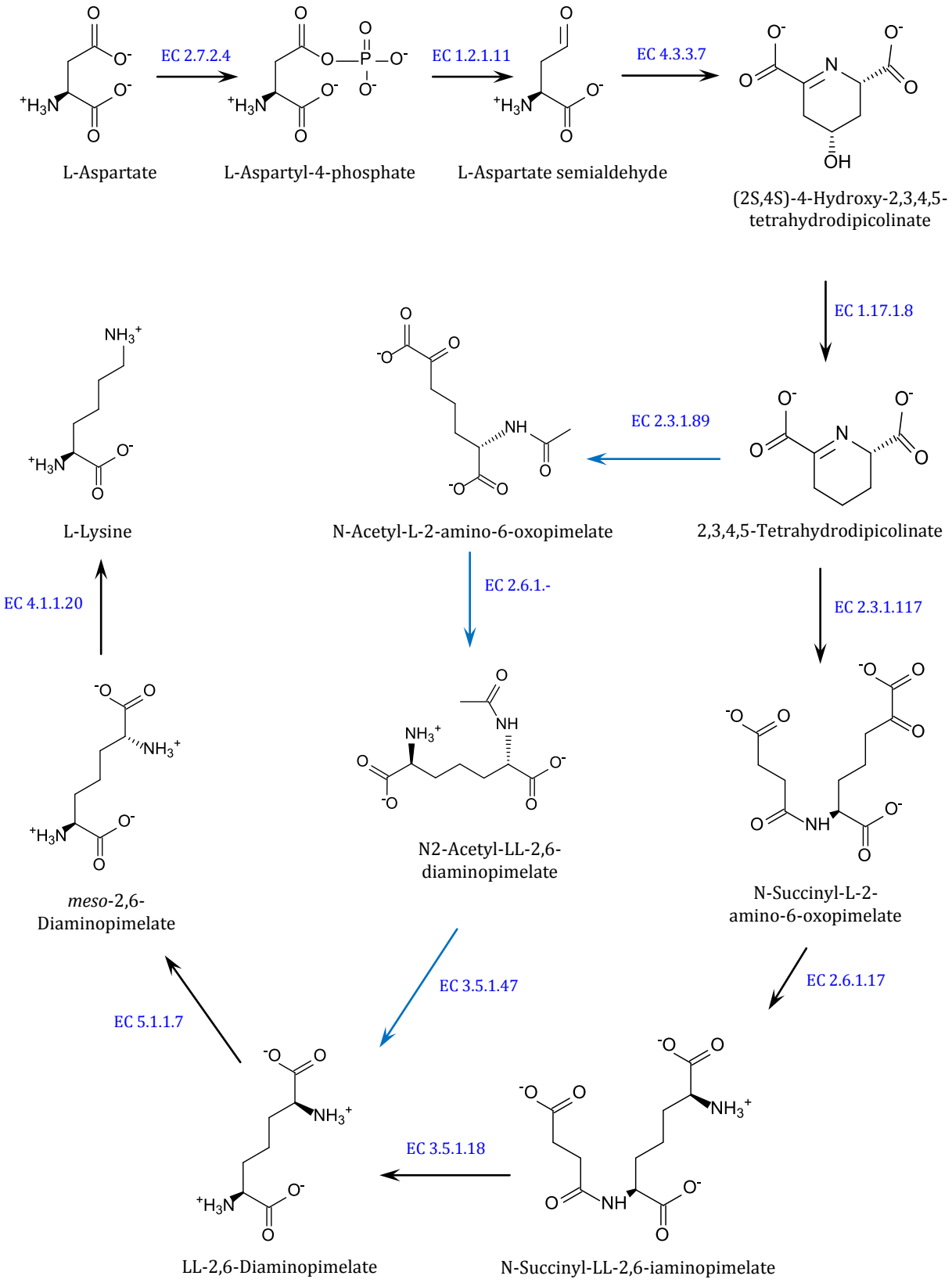

Figure V-22. Acyl diaminopimelate pathway biosynthetic pathways via succinyl (black) and acetyl (blue) intermediates. EC 2.7.2.4 - Aspartate kinase, EC 1.2.1.11 - Aspartate semialdehyde dehydrogenase, EC 4.3.3.7 - 4-hydroxy-tetrahydrodipicolinate synthase (DapA), EC 1.17.1.8 - 4-hydroxy-tetrahydrodipicolinate reductase (DapB), EC 2.3.1.117 - 2,3,4,5-tetrahydropyridine-2,6-dicarboxylate N-succinyltransferase (DapD), EC 2.6.1.17 - Succinyldiaminopimelate amino-transferase (DapC), EC 3.5.1.18 - Succinyl-diaminopimelate desuccinylase (DapE), EC 5.1.1.7 - Diaminopimelate epimerase (DapF), EC 4.1.1.20 - Diaminopimelate decarboxylase, EC 2.3.1.89 - Tetrahydrodipicolinate N-acetyltransferase (DapH, DapD), EC 2.6.1.- - Aminotransferase, EC 3.5.1.47 - N-acetyldiaminopimelate deacetylase. Adapted from KEGG and MetaCyc.

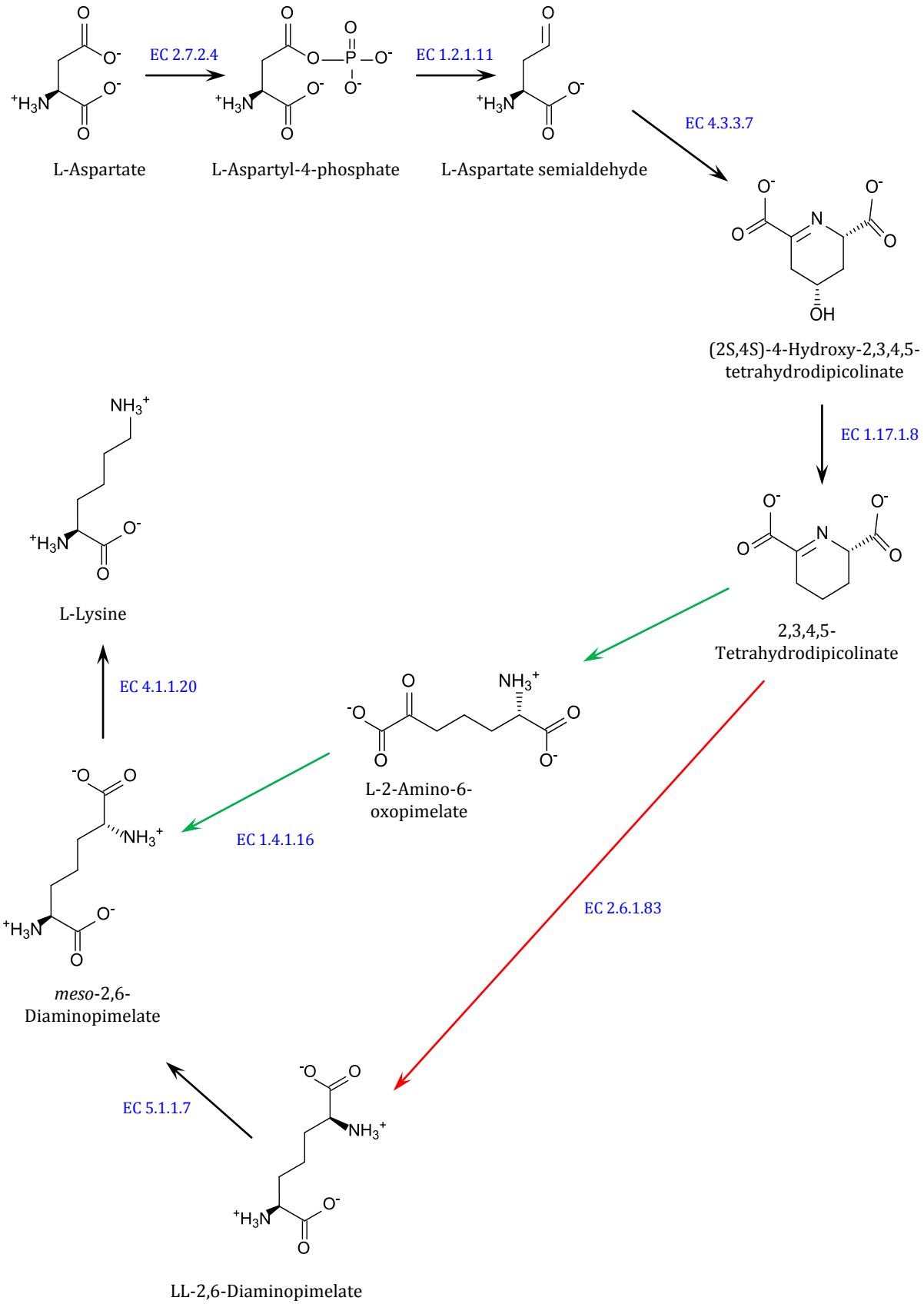

Figure V-23. *meso*-Diaminopimelate dehydrogenase (green) and LL-diaminopimelate aminotransferase (red) diaminopimelate pathway biosynthetic pathways. EC 2.7.2.4 - Aspartate kinase, EC 1.2.1.11 - Aspartate semialdehyde dehydrogenase, EC 4.3.3.7 - 4--hydroxy-tetrahydrodipicolinate synthase (DapA), EC 1.17.1.8 - 4-hydroxy-tetrahydrodipicolinate reductase (DapB), EC 2.6.1.83 - LL-diaminopimelate aminotransferase, EC 5.1.1.7 - DAP epimerase (DapF), EC 4.1.1.20 - Diaminopimelate decarboxylase. EC 2.6.1.83 - LL-diaminopimelate aminotransferase, EC 1.4.1.16 - *meso*-diamiinopimelate dehydrogenase.
Adapted from KEGG and MetaCyc.

L-2-amino adipic acid pathway. L-Lysine biosynthesis via L-2-aminoadipate is an eight-step process involving three cell compartments: nucleus, mitochondria and cytosol (Zabriskie and Jackson, 2000). The first half of the synthesis results in the generation of L-2-aminoadipate from α-ketoglutarate through several one-carbon higher homologues of the initial three tricarboxylic acids of the TCA cycle, that is, homocitrate, *cis*-homoaconitate and homoisocitrate (Figures V-27 and V-28). It starts with the condensation of α-ketoglutarate and acetyl-CoA into homocitrate by homocitrate synthase, localized to the nucleus, followed by the consequent dehydration of homocitrate to *cis*-homoaconitate and homoisocitrate by homoaconitase in the mitochondria. Homoisocitrate dehydrogenase oxidises the homoisocitrate to α-ketoadipate which then undergoes L-glutamate-dependent transamination carried out by L-2-aminoadipate transaminase to form L-2-aminoadipate (Figures V-27 and V-28). In the second half of the pathway, L-2-aminoadipate is consequently reduced to L-2-aminoadipate 6-semialdehyde and L-saccharopine by L-2-aminoadipate reductase and L-saccharopine dehydrogenase (L-glutamate-forming), respectively, before being converted to L-lysine by L-saccharopine dehydrogenase (L-lysine-forming). The second half of the pathway can occur via a protein carrier-independent or carrier-dependent way (Figures V-27 and V-28).

L. major lacks the enzymes for *de novo* synthesis of L-lysine (Opperdoes and Michels, 2008). A BLASTP search against the *L. mexicana* genome was performed to investigate whether L-lysine biosynthesis is present or absent in *L. mexicana*. The genome of *Leishmania mexicana* MHOMGT2001U1103 was derived from the TriTryp database which contains 8,500 sequences while the protein sequences of the enzymes of the L-lysine biosynthesis from five organisms, *Chlorella variabilis*, *Aspergillus fumigatus*, *Escherichia coli*, *Thermovirga lienii* and *Bacillus subtilis*, where one or two of the many variants of the DAP and the AAA pathways are present, were derived from the Kyoto encyclopedia of genes and genomes (KEGG) pathway database (http://www.kegg.jp/kegg/pathway.html). The search revealed that *L. mexicana* has a homoserine dehydrogenase, which interconvers L-aspartate 4-semialdehyde to homoserine, and a succinyl-diaminopimelate desuccinylase, involved in the interconversion of N-succinyl-LL-2,6-diaminopimelate to succinate and LL-2,6-diaminopimelate. Succinyl-diaminopimelate desuccinylase-like protein was the only enzyme of the L-lysine metabolism found differentially regulated in the *Δlmgt*

promastigotes (Supplemental table III-1). The function of the homoserine dehydrogenase and succinyl-diaminopimelate desuccinylase-like protein in *Leishmania*, however, may not be the same as the one they execute in the L-lysine biosynthesis. Thus, the proteomic data did not provide any significant information regarding the L-lysine metabolism in the *L. mexicana* promastigotes. Our metabolomic data, on the other hand, shed some light on this matter. The untargeted metabolomic profile of the *Δlmgt* promastigotes grown under SILAC conditions (**SILAC *Δlmgt* promastigotes**) was similar to that of the *Δlmgt* promastigotes grown under regular conditions (**regular *Δlmgt* promastigotes**). For instance, the levels of the glucogenic amino acids L-alanine and L-glutamate and the TCA cycle intermediates succinate and malate were decreased in the *Δlmgt* promastigotes (Table V-9). Amino acids such as L-alanine, L-glutamate and L-proline appear to be major carbon sources for the *Δlmgt* promastigotes (see chapter IV). The lack of external amino acids in the SILAC media would impair the supply of carbon and energy for the *Δlmgt* promastigotes and result in a number of defficiency which would eventually undermine the cell viability. The inability of the *Δlmgt* promastigotes to use amino acids as carbon and energy sources was probably one of the main reasons behind the poor adaptation of these cells to the media with dialyzed serum. The prolonged adaption of the *Δlmgt* promastigotes, along with the more or less similar central carbon metabolism of the SILAC *Δlmgt* promastigotes to that of the regular *Δlmgt* promastigotes, on the other hand, indicates that the cells possibly adapted to using other alternative carbon sources. For instance, fatty acids and other types of lipids are present in the serum. The absence of a glyoxylate cycle in the *Leishmania*, however, renders the parasites unable to use fatty acids as sole carbon sources for the synthesis of sugars (Opperdoes and Michels, 2008). Additionally, β-oxidation of fatty acids was down-regulated in the *Δlmgt* promastigotes (see Chapter IV). Further to that, it was demonstrated that incubation of the *Δlmgt* promastigotes in RPMI 1640 for 6 months resulted in the generation of a suppressor cell line which over-expressed the alternative hexose transporter GT4 (Feng *et al.*, 2011). The spontaneous suppression resulted in partial restoration of the hexose transport. Thus, it could be hypothesized that the shorter-term incubation of the *Δlmgt* promastigotes in the SILAC media could result in over-expression of some transporters, including GT4.

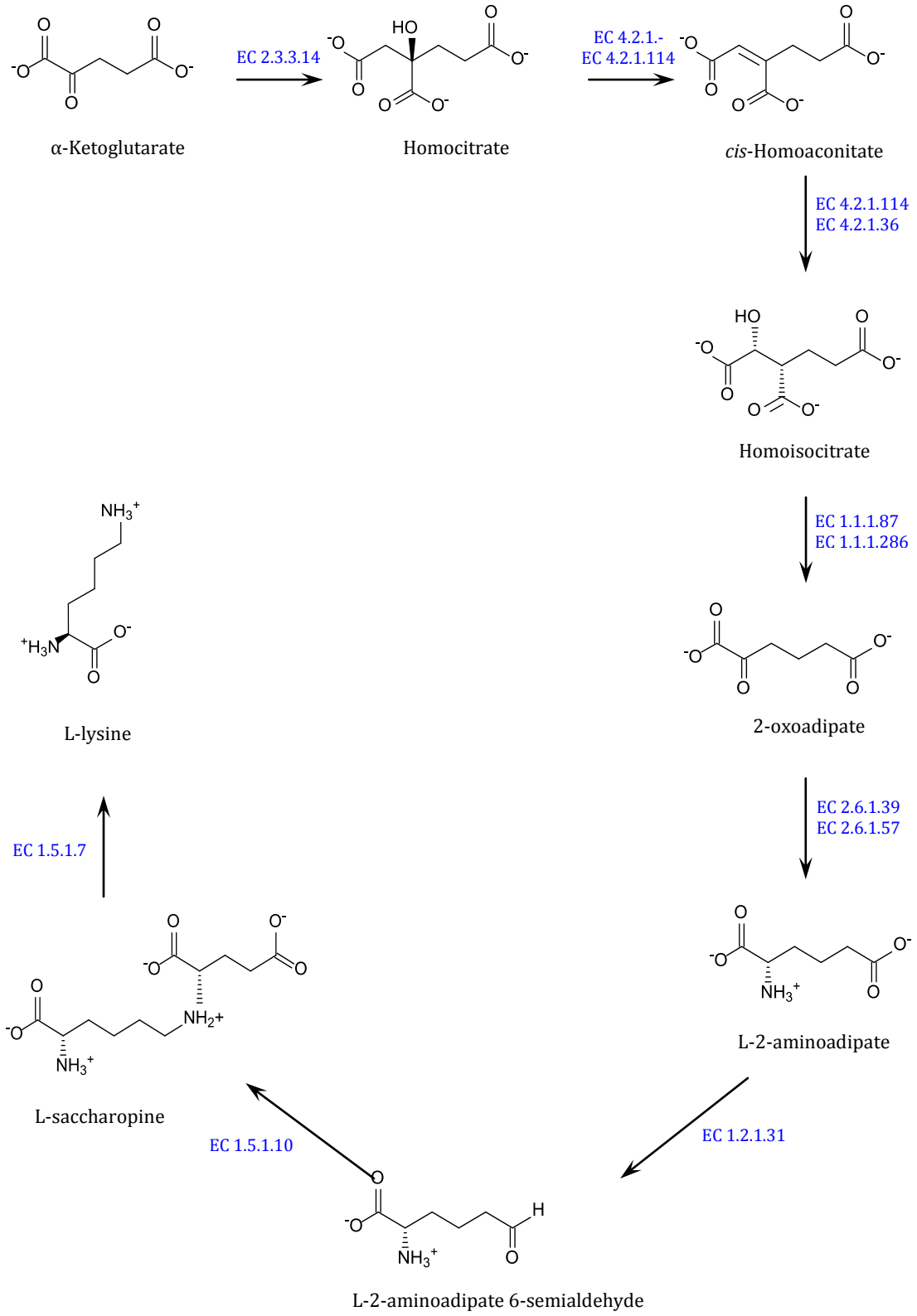

Figure V-24. Carrier-independent L-2-amino adipic acid biosynthetic pathway. EC 2.3.3.14 - Homocitrate synthase, EC 4.2.1.- - Homoaconitase, EC 4.2.1.114 - Methanogen homoaconitase, EC 4.2.1.36 - Homoaconitase, EC 1.1.1.87 - Homoisocitrate dehydrogenase, EC 1.1.1.286 - Isocitrate--homoisocitrate dehydrogenase, EC 2.6.1.39 - L-2-aminoadipate transaminase, EC 2.6.1.57 - Aromatic-amino-acid transaminase, EC 1.2.1.31 - L-2-aminoadipate-semialdehyde dehydrogenase, EC 1.5.1.10 - L-saccharopine dehydrogenase (NADP+, L-glutamate-forming), EC 1.5.1.7 - L-saccharopine dehydrogenase (NAD+, L-lysine-forming).
Adapted from KEGG and MetaCyc.

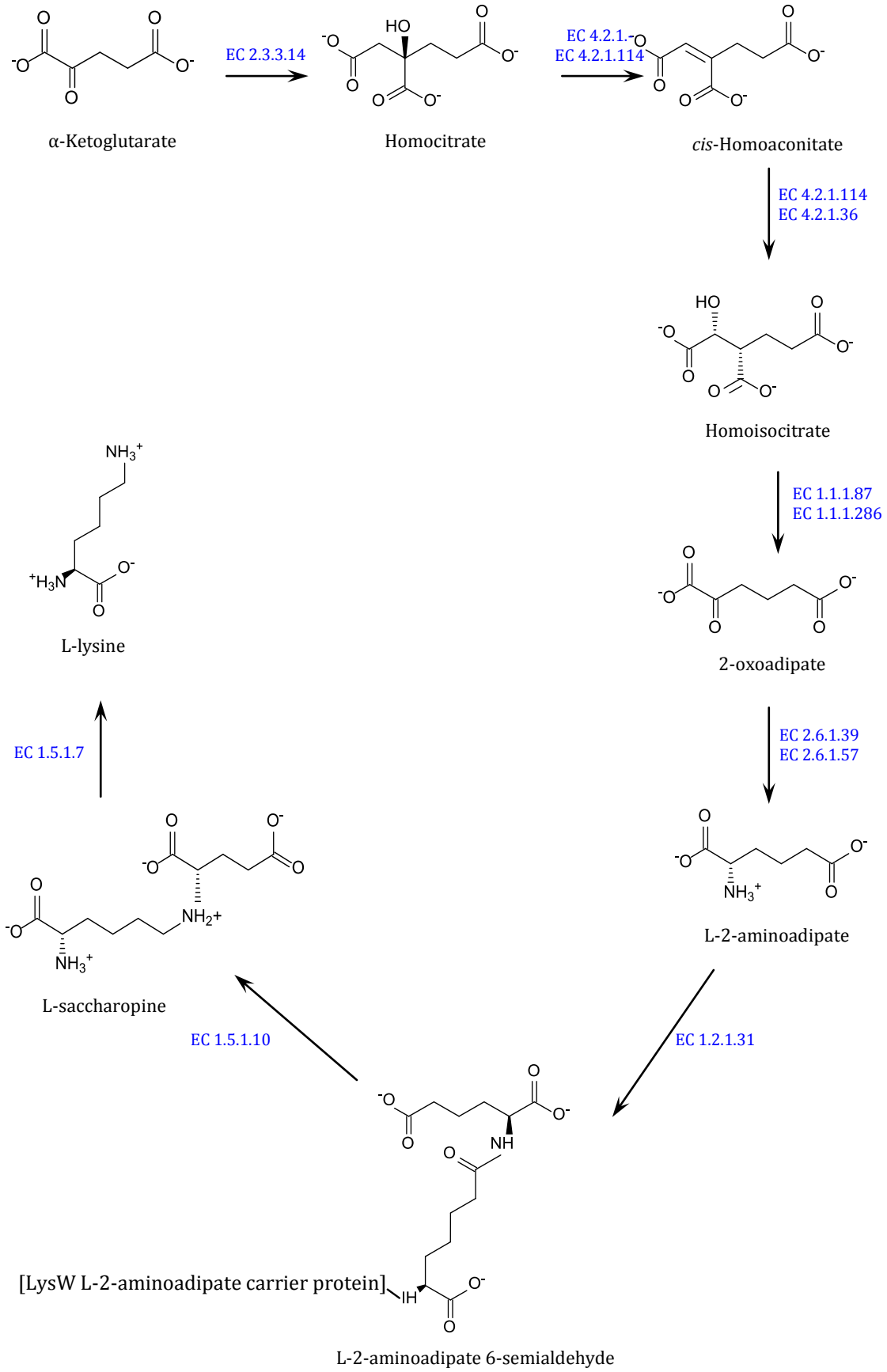

Figure V-25. Carrier-dependent L-2-amino adipic acid biosynthetic pathway. EC 2.3.3.14 - Homocitrate synthase, EC 4.2.1.- - Homoaconitase, EC 4.2.1.114 - Methanogen homoaconitase, EC 4.2.1.36 - Homoaconitase, EC 1.1.1.87 - Homoisocitrate dehydrogenase, EC 1.1.1.286 - Isocitrate--homoisocitrate dehydrogenase, EC 2.6.1.39 - L-2-aminoadipate transaminase, EC 2.6.1.57 - Aromatic-amino-acid transaminase, EC 1.2.1.31 - L-2-aminoadipate-semialdehyde dehydrogenase, EC 1.5.1.10 - L-saccharopine dehydrogenase (NADP+, L-glutamate-forming), EC 1.5.1.7 - L-saccharopine dehydrogenase (NAD+, L-lysine-forming).
Adapted from KEGG and MetaCyc.

This assumption is backed up by the observation that some of the glycolytic/gluconeogenic intermediates were negligibly labelled in condition ***glc** and **pro+*glc** *Δlmgt* promastigotes where ^{13}C-D-glucose was provided as a carbon source (see Chapter III). No labelling was observed in the *Δlmgt* promastigotes grown in the defined media supplemented with serum, condition ***glc0** *Δlmgt* promastigotes.

In addition to protein synthesis, L-Lysine can be used as an energy source. The amino acid is a ketogenic amino acid which can be converted to acetyl-CoA, fueled into the TCA cycle and catabolized for energy. Unfortunately, acetyl-CoA was not detected as a standard. No putative metabolite with the same mass was found in the *Δlmgt* promastigotes either. In addition to oxidation via the TCA cycle, we also investigated several alternative pathways for catabolism of L-lysine in the *Δlmgt* promastigotes. Up to date, known to exist in the living organisms are nine L-lysine catabolic pathways (Figure V-15) (Zabriskie and Jackson, 2000). In mammals and plants, the majority of L-lysine is catabolised via L-saccharopine (Supplemental figure V-3) (Galili *et al.*, 2001). The initial steps of the saccharopine L-lysine degradation pathway are essentially reversed analogues of the last reactions of the AAA biosynthetic pathway in fungi. Shortly, under the action of the bifunctional L-lysine:α-ketoglutarate reductase/saccharopine dehydrogenase (L-glutamate forming) L-lysine is transaminated through saccharopine to L-2-aminoadipate 6-semialdehyde and L-glutamate by transferring the lysine ε-group to α-ketoglutarate. L-2-Aminoadipate 6-semialdehyde is then converted to L-2-amino adipate by L-2-aminoadipate 6-semialdehyde dehydrogenase. In mammal, L-lysine can also be metabolised through other pathways. In rat, monkey and human brain, L-lysine is converted to L-pipecolate while in the liver and kidney, where the AAA pathways operates, L-pipecolate is a by-product formed most likely from D-lysine (Supplemental figure V-7) (Zabriskie and Jackson, 2000).

Considering all catabolic pathways described above, as well as our stable isotope tracing data, we could hypothesize that, except for protein-lysine degradation, no L-lysine biosynthesis or degradation pathways are fully functional in *Leishmania*. Some of the intermediates in the mentioned degradative pathways were not detected at all while others were putatively identified. Heavy-labelled were $N^6N^6N^6$-trimethyl-L-lysine, N^6-methyl-L-lysine, N^6-acetyl-L-lysine, L-pipecolate and L-lysine 1,6-lactam (Figures V-14, V-15, V-16 and V-17).

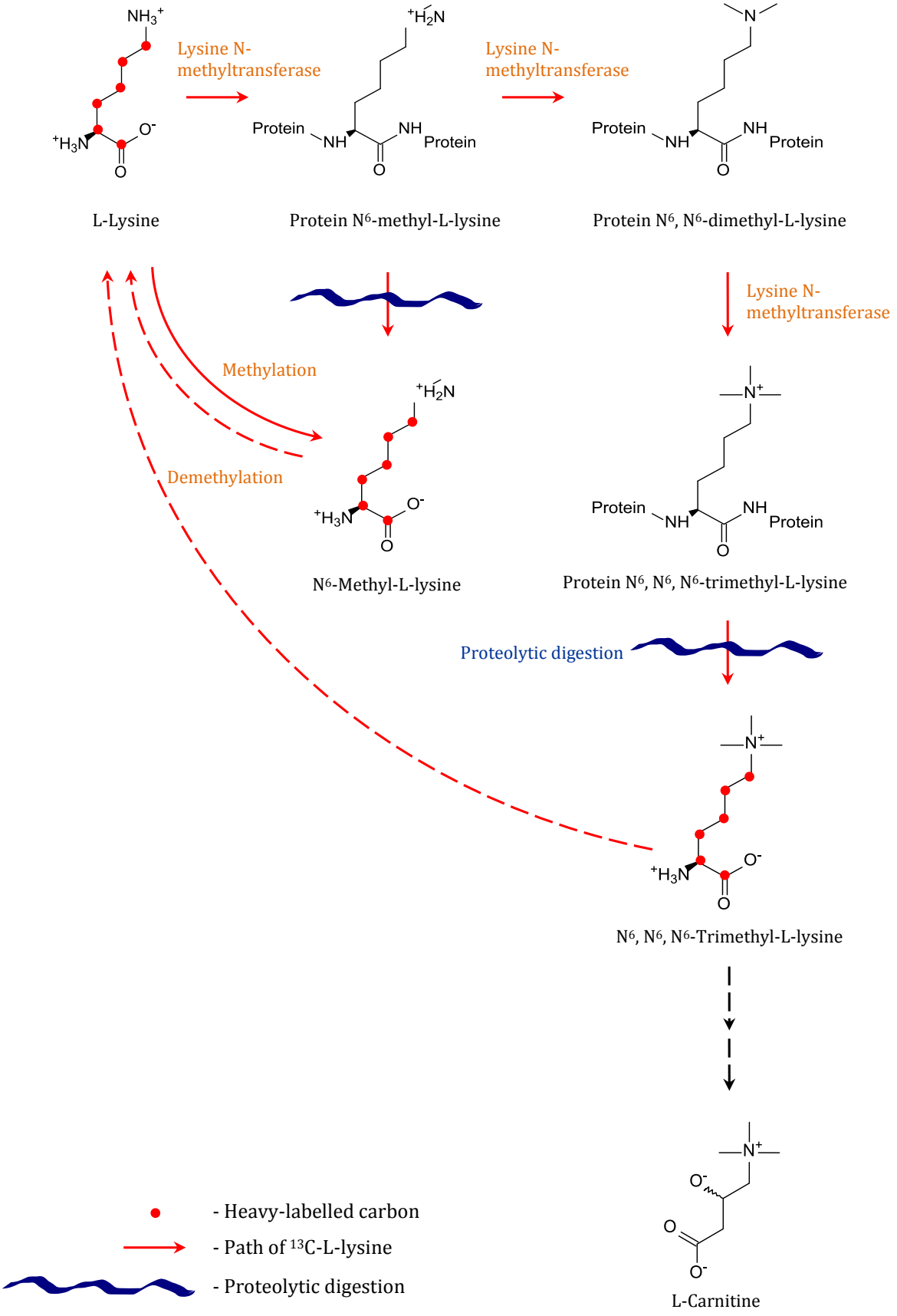

Figure V-26. Protein-lysine degradation in the SILAC-labelled *Δlmgt* promastigotes. Indicated with red dots are the heavy carbons. Indicated with red arrows are the possible routes of heavy labelling. Indicated with blue dashed line is the occurance of proteolytic digestion. Indicated with dashed black arrow is an indirect reaction.
Adapted from KEGG and MetaCyc.

The first two metabolites are involved in protein-lysine degradation, the third is involved in L-lysine degradation via N^6-acetyl-L-lysine and the forth is involved in L-lysine degradation via 2-oxo-6-aminocaproate and D-lysine. The last metabolite is an L-lysine derivative involved in a pathway-independent reaction. Protein-lysine degradation starts with triple methylation of L-lysine residues by protein-lysine methyltransferases which transfer methyl groups from S-adenosyl-L-methionine to the residues to form protein N^6-methyl-L-lysine, protein N^6,N^6-dimethyl-L-lysine and protein N^6,N^6,N^6-methyl-L-lysine, respectively (Figure V-26) (Rebouche, 1991). N^6,N^6,N^6-trimethyl-L-lysine is then released after proteolytic digestion, hydroxylated to N^6-hydroxy-L-lysine which is cleaved to 4-trimethylammoniobutanal and glycine. The aldehyde is then oxidized by an aldehyde dehydrogenase (ALDH) to 4-trimethylammoniobutanoate. The latter is hydroxylated again to L-carnitine (Rebouche, 1991). L-Carnitine, however, was not found heavy-labelled in the *Δlmgt* promastigotes. The second heavy-labelled metabolite, N^6-Methyl-L-lysine, similar to N^6,N^6,N^6-trimethyl-L-lysine, could be a product of a single methylation and proteolytic digestion or a spontaneous methylation reaction (Figure V-26). The third labelled metabolite was N^6-acetyl-L-lysine. Although it is the first compound in lysine degradation via N^6-acetyl-L-lysine, none of the other intermediates were found labelled (Supplemental figure V-5). On the other hand, acetylation is one of the most often posttranslational modifications (PTMs) of L-lysine residues. Acetylated residues could later be cleaved as a result of proteolytic digestion and released as separate compounds (Figure V-27). Genomic analysis in *L. major* revealed that *Leishmania* have methyltransferases, demethylases, acetyltransferases and deacetylases which are possibly involved in histone modifications (Ivens *et al.*, 2006; Renauld *et al.*, 2007). Modified, however, can also be nonhistone proteins such as α-tubulin for example which can be acetylated (Alonso and Serra, 2012) or p53, estrogen receptor α, nuclear factor kappa-light chain-enhancer of activated B cells, transcription factor E2F1, retinoblastoma protein and signaling transducer and activator of transcription 3 which can be methylated (Zhang *et al.*, 2012). Thus, lysine acetylation and methylation are involved in a number of cellular processes including transcription, DNA repair, splicing, chromatin remodeling, cytoskeletal dynamics, cell signalling, apoptosis, protein folding, metabolism and others (Alonso and Serra, 2012; Zhang *et al.*, 2012). It could be said that lysine acetylome and methylome are as substantial and important as the phosphoproteome.

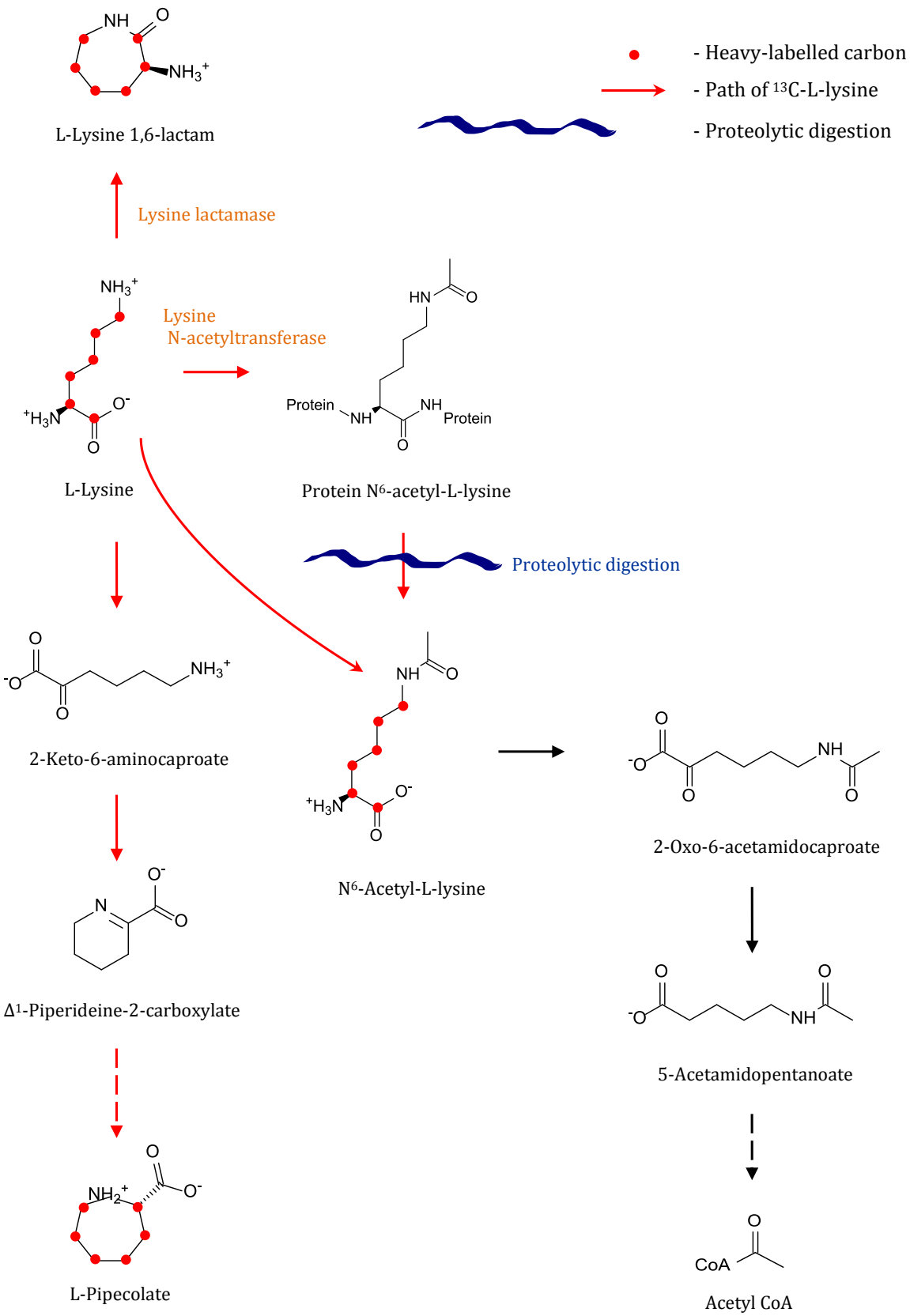

Figure V-27. L-Lysine degradation via N^6-acetyl-L-lysine and 2-oxo-6-aminocaproate in SILAC-labelled *Δlmgt* promastigotes. Indicated with red dots are the places of the heavy carbons. Indicated with red arrows are the possible routes of heavy labelling. Indicated with blue dashed line is the occurance of proteolytic digestion. Indicated with dashed black arrow is an indirect reaction.
Adapted from KEGG and MetaCyc.

Next, L-lysine 1,6-lactam is a product of L-lysine lactamase which reversibly hydrolyses L-lysine 1,6-lactam to L-lysine. Since no information about L-lysine 1,6-lactam metabolism is available, it could be hypothesized that, similar to other lactamases in bacteria, L-lysine lactamase plays a role in resistance to anti-bacterial and/or anti-leishmanial drugs. Finally, L-pipecolate is generated during L-lysine degradation via D-lysine or directly via 2-oxo-6-aminocaproate (Supplementary figures V-15 and V-16) (Zabriskie and Jackson, 2000). In addition to degradative pathways, L-pipecolate is involved in biosynthetic reactions as well. For instance, *Rhodotorula glutinis* is capable of growing on a minimal media supplemented with L-pipecolate which the aerobic red yeast uses as a nitrogen source in the synthesis of L-lysine (Zabriskie and Jackson, 2000). Since none of the other intermediates of the L-lysine degradation via 2-oxo-6-aminocaproate were heavy-labelled in the *Δlmgt* promastigotes, L-pipecolate could also be used as a nitrogen donor which possibly transfers the amine group to a more universal donor such as L-glutamate.

V.3. Summary

L-Lysine is an important proteinogenic amino acid for the *Leishmania* parasites. Our sequence similarity search confirmed that *L. mexicana* lack the enzymatic capacity to synthesize L-lysine via the diaminopimelate or L-2-amino adipic acid pathway and thus have to scavange the amino acid from the environment. Comparative information regarding the rate at which the wild type and *Δlmgt* promastigotes take up L-lysine is not available. Our metabolomic analysis, however, showed that the level of L-lysine in the two cell lines is more or less the same. These data thus show that the glucose transporter null-mutation does not affect L-lysine transport. Furthermore, the stable isotope tracing revealed that approximately 55% of the intracellular L-lysine is heavy labelled while the incorporation efficiency analysis showed that 52% of that L-lysine is used in protein synthesis in both wild type and *Δlmgt* promastigotes. Three main conclusions were made from these results: i/ 55% of the intracellular L-lysine in *Leishmania* has an exogenous origin, ii/ the majority of the exogenous L-lysine is used in protein synthesis while a small portion is used in derivative synthesis, and iii/ a source of unlabelled L-lysine provides 48% of the L-lysine for protein synthesis (and possibly the portion of L-lysine present in the free amino acid pool). Altogether, our study showed that two sources of L-lysine are present in *Leishmania*, exogenous and possibly endogenous, and that the existence of endogenous source results in ineffective labelling of the *Δlmgt* proteins

by exogenous L-lysine. The tracing study suggested that protein-lysine degradation is most probably (one of) the source(s) for endogenous L-lysine. Protein-lysine is degraded under the action of methyltransferases, then demethylated to L-lysine by demethylases, and possibly recycled back for protein synthesis and/or directed toward the free amino acid pool. Alternatively, acetyltransferases and deacetylases may also contribute toward recycling of L-lysine. Thus, degradation of protein-lysine originating from the serum supplementing the culture media or intracellular protein-lysine may be involved in maintaining the intracellular level of L-lysine and thus be a source of the remaining 48% of unlabelled L-lysine in the promastigotes. The results, additionally, implicate L-lysine in post-translational modifications. However, almost no information is available about L-lysine methylation in *Leishmania*. And finally, L-lysine is involved in derivative biosynthesis. Pathways where L-lysine is used as a precursor in other organisms, such as peptidoglycan synthesis, penicillin and cephalosporin biosynthesis, and fructoselysine and psicoselysine degradation, as well as L-lysine degradation, do not operate in *Leishmania*. Few L-lysine derivatives were found heavy labelled in the SILAC-labelled *Δlmgt* promastigotes, including L,L-2,6-diaminopimelate/*meso*-2,6-diaminopimelate, L-pipecolate, and L-lysine 1,6-lactam. Although their function in *Leishmania* is unknown, it could be hypothesized that they have roles in secondary metabolism.

The partial incorporation of exogenous L-lysine into proteins thus appears to be due to the specific metabolism of *Leishmania* and not the SILAC methodology. The latter requires the use of dialyzed serum and, contrary to the experiments with *L. infantum* and *L. donovani*, we observed that both the wild type and *Δlmgt L. mexicana* promastigotes struggled to adapt to dialyzed serum. In the *Δlmgt* promastigotes, the lack of amino acids and other essential nutrients in the dialyzed serum was adding to the stress resulting from the glucose transport deficiency. The *Δlmgt* promastigote adaptation to the dialyzed serum must have occurred through certain alterations, the nature of which was outside the scope of our investigation. Nevertheless, we could speculate that some of the alteration in terms of metabolism most probably involved over-expression of some transporters, including the glucose transporter GT4, and/or the use of alternative carbon and energy sources (other than carbohydrates and amino acids). The successful adaptation of the *Δlmgt* promastigotes was evident from the similar metabolic profile and rate of protein synthesis of these organisms to those of the wild type promastigotes. Concisely, these observations show that *Leishmania*

mexicana adapt to SILAC conditions but that the species' metabolism prevent them from being efficiently labelled by SILAC. Further investigation of this feature could lead to the development of species-specific antileishmanial compounds.

CHAPTER VI. Concluding remarks - drug targeting the *Δlmgt* promastigote metabolism

Sequencing of the genomes of several *Trypanosoma* and *Leishmania* species has allowed global comparative genomic, proteomic, and metabolomic investigations of trypanosomatid metabolism. Genomic approaches have provided information about the metabolic repertoire of trypanosomatids and have revealed that *Leishmania* contain a considerable number of genes, some of which encoding putative proteins involved in metabolism, with no homologues in other eukaryotes (Ivens *et al.*, 2005; Berriman *et al.*, 2005). Additionally, proteomic and metabolomic approaches have enhanced knowledge of *Leishmania* metabolism by comprehensive studies on promastigote and amastigote development and parasite-host relationship and have yielded a considerable amount of data that show that *Leishmania* metabolism differs from that of their hosts (Berriman *et al.*, 2005). These differences between *Leishmania* and their hosts are particularly important with respect to identifying potential drug targets and investigating the impact of antiparasitic drugs on *Leishmania* metabolism.

Promastigote metabolism is characterized with active metabolization of sugars such as D-glucose for biosynthetic and energy needs. *L. mexicana* promastigotes transport D-glucose via three high-affinity and one low-affinity transporters, namely GT1-3 and GT4, respectively (Burchmore *et al.*, 2003; Feng *et al.*, 2013). *L. mexicana* glucose transporter null mutant promastigotes, *Δlmgt* promastigotes, in which the gene locus encoding the GT1-3 transporters was deleted by targeted gene replacement, are viable which showed that D-glucose is a major but not exclusive energy and carbon source for the *Leishmania* promastigotes (Burchmore *et al.*, 2003). Phenotypic characterization of the medically relevant amastigote forms of this cell line, *Δlmgt* amastigotes, on the other hand, showed that the null mutant amastigotes cannot survive in macrophages which illustrated the central role of D-glucose in the *Leishmania* amastigotes (Burchmore *et al.*, 2003). Gene complementation of the *Δlmgt* amastigotes, furthermore, showed that GT3 alone is able to rescue *Δlmgt* amastigote growth to levels comparable with those of the wild type amastigotes which indicated that GT3 is important for amastigote survival (Burchmore *et al.*, 2003). These studies, altogether, showed that suppression of the expression of the GT gene locus, or possibly of the GT3 alone, although further confirmation is needed, has parasitocidal effect on *Leishmania* which validated GT1-3/GT3 as new drug targets.

The molecular events behind the inability of the *Δlmgt* amastigotes to proliferate in mammalian macrophages could obviously not be investigated in the non-growing *Δlmgt* amastigotes. The *Δlmgt* promastigotes, however, remain viable in axenic cultures and have been used to gain insight into the metabolic machinery of these mutants and elucidate which aspects of metabolism are affected by deletion of the GT1-3 transporters. The initial characterization revealed that the *Δlmgt* promastigote growth and biosynthetic capabilities are impaired (Burchmore *et al.*, 2003; Rodriguez-Contreras and Landfear, 2006; Rodriguez-Contreras *et al.*, 2007; Feng *et al.*, 2011). To gain more specific information, we aimed to investigate the central carbon metabolism of the *Δlmgt* promastigotes, with particular emphasis on alternative carbon source utilization. The complexity and scale of the information we were after imposed the necessity to use global quantitative proteomic and metabolomic techniques. The proteomic techniques used were SILAC and stable isotope dimethyl labelling, none of which had been applied to *L. mexicana* before. Using two stable isotope-based labelling techniques stemmed from the desire to compare quantitative proteomic data from metabolic (SILAC) and chemical (dimethyl) protein labelling. Dimethyl labelling methodology proved to be straightforward and efficient as virtually all peptides were dimethyl labelled. Dimethyl labelling, combined with digitonin prefractionation, led to quantification of a large number of enzymes of the central carbon metabolism, which was one of the main aims of this study. SILAC, on the other hand, proved time-consuming, expensive, difficult to implement to *L. mexicana*, and inefficient in isotope labelling of all proteins. As a result of the latter, no quantitative data were generated from the SILAC experiment and only the dimethyl labelling data were considered. Dimethyl labelling data helped us map the enzymatic activities in the central carbon metabolism of the *Δlmgt* promastigotes. To link enzyme activities and metabolite levels, and thus get a general overview of the changes in pathways of central carbon metabolism, we complemented quantitative proteomic with quantitative metabolomic analysis. The metabolomic techniques used were untargeted LC-MS, targeted GC-MS, and NMR analysis, each chosen for their specific advantages. The pHILIC LC-MS platform was used as a mean to quantify polar and charged metabolites such as amino and organic acids. The GC-MS platform was used to separate and quantify sugars and sugars phosphates. The NMR analysis focused on the carbon preferences of the investigated null mutant promastigotes. Lipidomic analysis of the *Δlmgt* promastigotes was also performed but it showed minimal changes in lipid metabolism in these organisms.

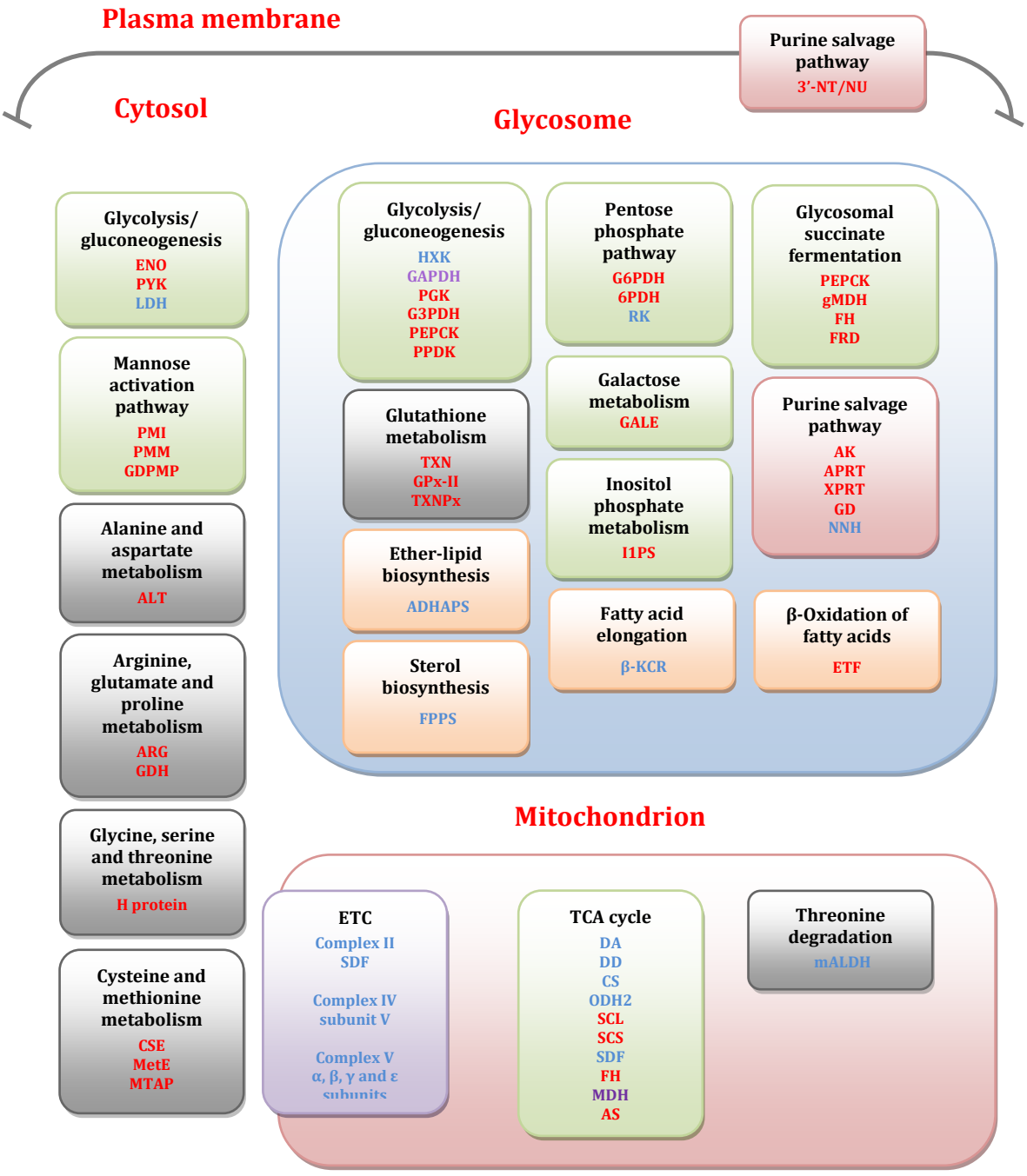

- Carbohydrate metabolism
- Amino acid metabolism
- Lipid metabolism
- Nucleotide metabolism
- Energy metabolism

HK - Up-regulated enzyme

G6PDH - Down-regulated enzyme

GAPDH Enzyme with up- and down-regulated isoforms

The legend is presented on page 220.

Figure VI-1. Regulated enzymes in the *Δlmgt* promastigotes. Abbreviations:, HXK - hexokinase, GAPDH - glyceraldehyde 3-phosphate dehydrogenase, PGK - phosphoglycerate kinase, G3PDH - glycerol 3-phosphate dehydrogenase, ENO - enolase, PYK - pyruvate kinase, PPDK - pyruvate phosphate dikinase, GK - glycerol kinase, LDH - lactate dehydrogenase, PEPCK - phosphoenolpyruvate carboxikinase, GALE - uridine diphopshate glucose 4'-epimerase, PMI - phosphomannose isomerase, PMM - phosphomannomutase, GDPMP - guanosine diphosphate pyrophosphorylase, G6PDH - glucose 6-phophate dehydrogenase, 6PDH - 6-phosphogluconate dehydrogenase, RK - ribokinase, I1PS - inositol 1-phosphate synthase, DA - dihydrolipoamide acetyltransferase, DD - dihydrolipoamide dehydrogenase, CS - citrate synthase, ODH2 - 2-oxoglutarate dehydrogenase E2 component, SCL - succinyl-CoA ligase, SCS - succinyl-CoA synthetase, SDF - succinate dehydrogenase flavoprotein, FH - fumarate hydratase, FRD - fumarate reductase, MDH - malate dehydrogenase, gMDH - glycosomal malate dehydrogenase, ME - malic enzyme AS - acetyl-CoA synthetase, 3'-NT/NU - 3'-nucleotidase/nuclease, AK - adenosine kinase, APRT - adenine phosphoribosyl-transferase, XPRT - xanthine phosphoribosyltransferase, GD - guanine deaminases, NNH - nonspecific nucleoside hydrolase, ADHAPS - alkyl dihydroxyacetone phosphate synthase, FPPS - farnesyl pyrophosphate synthase, β-KCR - β-ketoacyl-CoA reductase, ETF - electron-transfer flavoprotein, α polypeptide, TXN - tryparedoxin, GPx-II - glutathione peroxidase-like tryparedoxin peroxidases II, TXNPx - TXN-dependent peroxidase, ALT - alanine aminotransferase, ARG - arginase, GDH - glutamate dehydrogenase, MetE - 5-methyltetrahydropteroyltriglutamate--homocysteine methyltransferase, CSE - cystathionine γ-lyase, MTAP - methylthioadenosine phosphorylase, mALDH - mitochondrial aldehyde dehydrogenase, TCA - tricarboxylic acid cycle, ETC - electron transport chain.

The proteomic and metabolomic data were integrated, and elucidated a number of important, and in some cases surprising, aspects of the *Δlmgt* promastigote metabolism. The data revealed profound metabolic changes in carbohydrate, amino acid, energy, and nucleotide metabolism. First, it was determined that the inability of *Leishmania* to utilize D-glucose leads to i/ acquisition of alternative exogenous sugars, such as sucrose, for the production of D-glucose and ii/ activation of gluconeogenesis. Regarding the first observation, it could be speculated that simultaneous inhibition of D-glucose and alternative sugar transport may represent a promising antileishmanial strategy. Regarding the second observation, we concluded that D-glucose, under the action of HXK, and gluconeogenesis serve to generate G6P, a central precursor in many biosynthetic pathways. HXK, which is up-regulated in the *Δlmgt* promastigotes (Figure VI-1) (Feng *et al.*, 2011) and a validated drug target in *Leishmania* (Pabon *et al.*, 2007), thus appears to be crucial for carbohydrate anabolism in *Leishmania* and must be, respectively, a center for further inhibition investigations. Other glycolytic/gluconeogenic enzymes such as GAPDH, PPDK, and PEPCK, which exercise a considerable amount of control over the influx of intermediates in glycolysis/gluconeogenesis, are also of particular interest for the development of competitive inhibitors. GAPDH facilitates the entry of glycerol while PPDK and PEPCK participate in the entry of amino acids in gluconeogenesis (Rodriguez-Contreras and Hamilton, 2014). Indeed, the *Δlmgt* promastigotes increase the uptake of amino acids (Thesis: Lamasudin, 2012), and possibly of other glucogenic precursor such as glycerol and acetate. The gluconeogenic capacity of the *Δlmgt* promastigotes, however, is reduced and insufficient in meeting the requirements for hexose phosphates and other gluconeogenic intermediates. The

influx of G6P in the PPP is reduced and the oxidative reactions involved in regenerating NADPH, catalyzed by G6PDH and 6PDH (Figure VI-1), are down-regulated which we speculate lead to production of less NADPH in the *Δlmgt* promastigotes. Furthermore, enzymes such as ARG, TXN, TXNPx, and GPx-II, which are involved in trypanothione synthesis and metabolism, are also significantly down-regulated in the *Δlmgt* promastigotes (Figure VI-1). The cytosolic TXN1 and the mitochondrial 2-Cys peroxiredoxin (mTXNPx) of *L. infantum* have recently been validated as drug targets and the elimination of hydroperoxides by TXN/TXNPx associated with survival of *Leishmania* within macrophages and virulence (Romao *et al.*, 2009; Castro *et al.*, 2011). Taking these together, it can be postulated that i/ the high sensitivity of the glucose transporter null mutant promastigotes to oxidative stress is due to decreased ability to reduce hydroperoxides and other reactive species, and ii/ enzymes of NADPH and trypanothione synthesis, including the PPP pathway and glutathione and polyamine metabolism, represent strong candidate drug targets for antileishmanial therapy.

Two other important conclusions were drawn from our data. First, ablation of the D-glucose transport leads to down-regulation of all enzymes of glycosomal succinate fermentation and the mannose activation pathway (Figure VI-1). Considering the essential role of glycosomal succinate fermentation in maintaining the glycosomal redox and energy balance, the enzymes of the pathway, as well as proteins involved in translocation of metabolites across the glycosomal membrane and glycosomal biogenesis (peroxins, PEXs), have long been considered targets for the development of selective inhibitors (Gualdron-Lopez *et al.*, 2013 and the references therein). Similar to glycosomal succinate fermentation, our study confirmed that enzymes of glycoconjugate synthesis, in particular PMM and GDP-MP of mannose activation pathway, GALE of galactose metabolism (Figure VI-1), and arabinose metabolism, are valuable drug targets (Garami and Ilg, 2001a; Garami and Ilg, 2001b; Garami *et al.*, 2001; Stewart *et al.*, 2005; Chawla and Madhubala, 2010). Second, inhibition of D-glucose transport further interferes with the purine salvage pathway. It is known that more than one enzyme of the pathway have to be targeted for successful therapy due to the existence of several alternative purine salvage pathways in *Leishmania* (Chawla and Madhubala, 2010). One such enzyme could be ribokinase which appears to salvage ribose from nucleotide degradation for reuse in nucleotide synthesis.

Finally, our study showed that the TCA cycle has a central role in carbon and energy metabolism in *Leishmania*. When D-glucose is not available as a nutrient, amino acids such as L-proline, L-glutamate, L-glutamine, L-alanine, L-aspartate, and L-threonine are used as biosynthetic precursors in TCA cycle anaplerosis and gluconeogenesis, and as energy sources through catabolism via the TCA cycle. Lipids, most surprising, do not represent energy sources for the *Δlmgt* promastigotes. *Leishmania* rely on oxidative phosphorylation for the generation of energy in the promastigote stages and every perturbation of the electron transport chain can possibly be lethal and hence, of interest in drug development. It was recently shown, however, that *L. donovani* amastigotes are oxidative phosphorylation-independent and rely on substrate level phosphorylation for the generation of energy (Mondal *et al.*, 2014). Thus, enzymes such as PGK, PYK, PEPCK, SCS, and ASCT represent valuable drug targets.

Concisely, ablation of D-glucose transport leads to i/ import of alternative sugars for the production of D-glucose, ii/ use of amino acids as main carbon and energy sources, iii/ synthesis of hexose phosphates through gluconeogenesis, iv/ generation of energy through the TCA cycle and linked ETC and oxidative phosphorylation, v/ impaired redox balance, and vi/ overall reduction of biosynthetic capacity of *Leishmania* promastigotes.

References

Acestor, N., Zikova, A., Dalley, R.A., Anupama, A., Panigrahi, A.K., and Stuart, K.D. (2011) *Trypanosoma brucei* mitochondrial respiratome: composition and organization in procyclic form. *Mol Cell Proteomics* 10:M110 006908.

Adosraku, R. K., Anderson, M.M., Anderson, G.J., Choi, G., Croft, S.L., Yardley, V., Phillipson, J.D., and Gibbons, W.A. (1993) Proton NMR lipid profile of *Leishmania donovani* promastigotes. *Mol Biochem Parasitol* 62:251-262.

Al-Ani, G. K., Patel, N., Pirani, K.A., Zhu, T., Dhalladoo, S., and Zufferey, R. (2011) The N-terminal domain and glycosomal localization of *Leishmania initial* acyltransferase *Lm*DAT are important for lipophosphoglycan synthesis. *PLoS One* 6:e27802.

Alonso, V.L. and Serra, E.C. (2012) Lysine acetylation: elucidating the components of an emerging global signaling pathway in trypanosomes. *J Biomed Biotechnol* 2012:452934.

Al-Salabi, M.I., Wallace, L.J., and De Koning, H.P. (2003) A *Leishmania major* nucleobase transporter responsible for allopurinol uptake is a functional homolog of the *Trypanosoma brucei* H2 transporter. *Mol Pharmacol* 63:814-820.

Antoine, J.C., Prina, E., Lang, T., and Courret, N. (1998) The biogenesis and properties of the parasitophorous vacuoles that harbour *Leishmania* in murine macrophages. *Trends Microbiol* 6:392-401.

Araujo-Santos, J.M., Gamarro, F., Castanys, S., Herrmann, A., and Pomorski, T. (2003) Rapid transport of phospholipids across the plasma membrane of *Leishmania infantum*. *Biochem Biophys Res Commun* 306:250-255.

Aparicio, I.M., Marin-Menendez, A.M., Bell, A., and Engel, P.C. (2010) Susceptibility of *Plasmodium falciparum* to glutamate dehydrogenase inhibitors - a possible new antimalarial target. *Mol Biochem Parasitol* 172:152-155.

Aronow, B., Kaur, K., McCartan, K., and Ullman, B. (1987) Two high affinity nucleoside transporters in *Leishmania donovani*. *Mol Biochem Parasitol* 22:29-37.

Aslett, M., Aurrecoechea, C., Berriman, M., Brestelli, J., Brunk, B.P., Carrington, M., Depledge, D.P., Fischer, S., Gajria, B., Gao, X., Gardner, M.J., Gingle, A., Grant, G., Harb, O.S., Heiges, M., Hertz-Fowler, C., Houston, R., Innamorato, F., Iodice, J., Kissinger, J.C., Kraemer, E., Li, W., Logan, F.J., Miller, J.A., Mitra, S., Myler, P.J., Nayak, V., Pennington, C., Phan, I., Pinney, D.F., Ramasamy, G., Rogers, M.B., Roos, D.S., Ross, C., Sivam, D., Smith, D.F. , Srinivasamoorthy, G., Stoeckert, Jr, C.J., Subramanian, S., Thibodeau, R., Tivey, A., Treatman, C., Velarde, G., and Wang, H. (2010) TriTrypDB: a functional genomic resource for the Trypanosomatidae. *Nucleic Acids Res* 38:D457-D462.

Avilan, L., Gualdron-Lopez, M., Quinones, W., Gonzalez-Gonzalez, L., Hannaert, V., Michels, P.A.M., and Concepcion, J.L. (2011) Enolase: a key player in the metabolism and a probable virulence factor of trypanosomatids parasites - perspective for its use as a therapeutic target. *Enzyme Res* 2011:932549.

Baja, E.S. and Rodriguez, H. (2012) Mass spectrometry-based targeted quantitative proteomics: achieving sensitive and reproducible detection of proteins. *Proteomics* 12:1093-110.

Balana-Fouce, R., Calvo-Alvarez, E., Alvarez-Velilla, R., Prada, C.F., Perez-Pertejo, Y., and Reguera, R.M. (2012) Role of trypanosomatid's arginase in polyamine biosynthesis and pathogenesis. *Mol Biochem Parasitol* 181:85-93.

Bartke, N. and Hannun, Y. (2009) Bioactive sphingolipids: metabolism and function. *J Lipid Res* 50: S92-S96.

Basselin, M., Coombs, G.H., and Barrett, M.P. (2000) Putrescine and spermidine transport in *Leishmania*. *Mol Biochem Parasitol* 109:37-46.

Bates, P.A. and Tetley, L. (1993) *Leishmania mexicana*: induction of metacyclogenesis by cultivation of promastigotes at acidic pH. *Exp Parasitol* 76:412-423.

Beach, D.H., Holz Jr., G.G., amd Anekwe, G.E. (1979) Lipids of *Leishmania* promastigotes. *J Parasitol* 65:203-216.

Bengs, F., Scholz, A., Kuhn, D., and Wiese, M. (2005) LmxMPK9, a mitogen-activated protein kinase homologue affects flagellar length in *Leishmania mexicana*. *Mol Microbiol* 55:1606-1615.

Benne, R., van den Burg, J., Brakenhoff, J.P., Sloof, P., van Boom, J.H., and Tromp, M.C. (1986) Major transcript of the frameshifted coxII gene from trypanosome mitochondria contains four nucleotides that are not encoded in the DNA. *Cell* 46:819-826.

Berens, R.L., Brun, R., and Krassner, S.M. (1976) A simple monophasic medium for axenic culture of hemoflagellates. *J Parasitol* 62:360-365.

Bernards, A., Michels, P.A., Lincke, C.R., and Borst, P. (1983) Growth of chromosome ends in multiplying trypanosomes. *Nature* 303:592-597.

Berman, J.D., Gallalee, J.V., Best, J.M., and Hill, T. (1987) Uptake, distribution, and oxidation of fatty acids by *Leishmania mexicana* amastigotes. *J Parasitol* 73:555-560.

Berriman, M., Ghedin, E., Hertz-Fowler, C., Blandin, G., Renauld, H., Bartholomeu, D.C., Lennard, N.J., Caler, E., Hamlin, N.E., Haas, B., Bohme, U., Hannick, L., Aslett, M.A., Shallom, J., Marcello, L., Hou, L., Wickstead, B., Alsmark, U.C., Arrowsmith, C., Atkin, R.J., Barron, A.J., Bringaud, F., Brooks, K., Carrington, M., Chrevach, I., Chillingworth, T.J., Churcher, C., Clark, L.N., Corton, C.H., Cronin, A., Davies, R.M., Doggett, J., Djikeng, A., Feldbyum, T., Field, M.C., Fraser, A., Goodhead, I., Hance, Z., Harper, D., Harris, B.R., Hauser, H., Hostetler, J., Ivens, A., Jagels, K., Johnon, D., Johnson, J., Jones, K., Kerhornou, A.X., Koo, H., Larke, N., Landfear, S., Larkin, C., Leech, V., Line, A., Lord, A., Maclod, A., Mooney, P.J., Moul, S., Martin, D.M., Morgan, g.W., Mungall, K., Norbertczak, H., Ormond, D., Pai, G., Peacock, C.S., Peterson, J., Quail, M.A., Rabbinowitsch, E., Rajandream, M.A., Reitter, C., Salzberg, S.L., Sanders, M., Schobel, M., Sharp, S., Simmonds, M., Simpson, A.J., Tallon, L., Turner, C.M., Tait, A., Tivey, A.R., van Aken, S., Walker, D., Wanless, D., Wang, S., White, B., White, O., Whitehead, S., Woodward, J, Wortman, J., Adams, M.D., Embley, T.M., Gull, K., Ullu, E., Barry, J.D., Fairlamb, A.H., Opperdoes, F., Barrell, B.G., Donelson, J.E., Hall N., Fraser, C.M., Melville, S.E., and El-Sayed, N.M. (2005) The genome of the African trypanosome *Trypanosoma brucei. Science* 309:416-422.

Besteiro, S., Biran, M., Biteau, N., Coustou, V., Baltz, T., Canioni, P., and Bringaud, F. (2002) Succinate secreted by *Trypanosoma brucei* is produced by a novel and unique glycosomal enzyme, NADH-dependent fumarate reductase. *J Biol Chem* 277:38001-38012.

Besteiro, S., Barrett, M.P., Riviere, L., and Bringaud, F. (2005) Energy generation in insect stages of *Trypanosoma brucei*: metabolism in flux. *Trends Parasitol* 21, 185-191.

Besteiro, S., Williams, R.A., Coombs, G.H, and Mottram, J.C. (2007). Protein turnover and differentiation in *Leishmania*. *Int J Parasitol* 37:1063-1075.

Beverley, S.M., Ellenberger, T.E., and Cordingley, J.S. (1986) Primary structure of the gene encoding the bifunctional dihydrofolate reductase-thymidylate synthase of *Leishmania major*. *Proc Natl Acad Sci USA* 83:2584-2588.

Bingol, K. and Bruschweiler, R. (2014) Multidimensional approaches to NMR-based metabolomics. *Anal Chem* 86:47-57.

Blum, J.J. (1996) Effects of osmotic stress on metabolism, shape, and amino acid content of *Leishmania*. *Biol Cell* 87:9-16.

Blum, J.J. and Opperdoes, F.R. (1994) Secretion of sucrase by *Leishmania donovani*. *J Eukaryot Microbiol* 41:228-231.

Boitz, J.M. and Ullman, B. (2006a) A conditional mutant deficient in hypoxanthine-guanine phosphoribosyltransferase and xanthine phosphoribosyltransferase validates the purine salvage pathway of *Leishmania donovani*. *J Biol Chem* 281:16084-16089.

Boitz, J.M. and Ullman, B. (2006b) *Leishmania donovani* singly deficient in HGPRT, APRT or XPRT are viable in vitro and within mammalian macrophages. *Mol Biochem Parasitol* 148:24-30.

Boothroyd, J.C. and Cross, G.A. (1982) Transcripts coding for variant surface glycoproteins of *Trypanosoma brucei* have a short, identical exon at their 5'-end. *Gene* 20:281-289.

Bridgen, P.J., Cross, G.A.M, and Bridgen J. (1976) N-terminal amino acid sequences of variant-specific surface antigens from *Trypanosoma brucei*. *Nature* 263, 613-614.

Bringaud, F., Vedrenne, C., Cuvillier, A., Parzy, D., Baltz, D., Tetaud, E., Pays, E., Venegas, J., Merlin, G., and Baltz, T. (1998) Conserved organization of genes in trypanosomatids. *Mol Biochem Parasitol* 94:249-264.

Bringaud, F., Riviere, L., and Coustou, V. (2006) Energy metabolism of trypanosomatids: adaptation to available carbon sources. *Mol Biochem Parasitol* 149:1-9.

Brotherton, M.C., Racine, G., Foucher, A.L., Drummelsmith, J., Papadopoulou, B., and Ouellette, M. (2010) Analysis of stage-specific expression of basic proteins in *Leishmania infantum*. *J Proteome Res* 9:3842–3853.

Brotherton, M.C., Bourassa, S., Leprohon, P., Legare, D., Poirier, G.G., Droit, A., and Ouellette, M. (2013) Proteomic and genomic analyses of antimony resistant *Leishmania infantum* mutant. *PLoS One* 8:e81899.

Brotherton, M. C., Bourassa, S., Legare, D., Poirier, G.G., Droit, A., and Ouellette, M. (2014) Quantitative proteomic analysis of amphotericin B resistance in *Leishmania infantum*. *Int J Parasitol Drugs Drug Resist* 4:126-132.

Brown B., S.V., Stanislawski, A., Perry, Q.L., and Williams, N. (2001) Cloning and characterization of the subunits comprising the catalytic core of the *Trypanosoma brucei* mitochondrial ATP synthase. *Mol Biochem Parasitol* 113:289–301.

Burchmore, R.J. and Hart, D.T. (1995) Glucose transport in amastigotes and promastigotes of *Leishmania mexicana mexicana*. *Mol Biochem Parasitol* 74:77-86.

Burchmore, R.J. and Landfear, S.M. (1998) Differential regulation of multiple glucose transporter genes in *Leishmania mexicana*. *J Biol Chem* 273:29118-29126.

Burchmore, R.J. and Barrett, M.P. (2001) Life in vacuoles-nutrient acquisition by *Leishmania* amastigotes. *Int J Parasitol* 31:1311-1320.

Burchmore R.J., Rodriguez-Contreras D., McBride K., Merkel P., Barrett M.P., Modi G., Sacks D., and Landfear S.M. (2003) Genetic characterization of glucose transporter function in *Leishmania mexicana. Proc Natl Acad Sci USA* 100:3901-3906.

Burrows, C. and Blum, J.J. (1991) Effect of hyper-osmotic stress on alanine content of *Leishmania major* promastigotes. *J Protozool* 38:47-52.

Byrne, D.N. and Miller, W.B. (1990) Carbohydrate and amino acid composition of phloem sap and honeydew produced by *Bemisia tabaci*. *J Insect Physiol* 36, 433–439.

Cairns, B. R., Collard, M.W., and Landfear, S.M. (1989) Developmentally regulated gene from *Leishmania* encodes a putative membrane transport protein. *Proc Natl Acad Sci USA* 86:7682-7686.

Cameron, M.M., Pessoa, F.A., Vasconcelos, A.W., and Ward, R.D. (1995) Sugar meal sources for the phlebotomine sandfly *Lutzomyia longipalpis* in Ceara State, Brazil. *Med Vet Entomol* 9:263-272.

Carter, N.S., Drew, M.E., Sanchez, M., Vasudevan, G., Landfear, S.M., and Ullman, B. (2000) Cloning of a novel inosine-guanosine transporter gene from *Leishmania donovani* by functional rescue of a transport-deficient mutant. *J Biol Chem* 275:20935-20941.

Carter, N.S., Yates, P., Arendt, C.S., Boitz, J.M., and Ullman, B (2008) Purine and pyrimidine metabolism in *Leishmania*. In: Majumder, H.K. (ed) Drug targets in Kinetoplastid parasites. *Landes Bioscience and Springer Science+Business Media, LLC.*

Castro, H., Teixeira, F., Romao, S., Santos, M., Cruz, T., Florado, M., Appelberg, R., Oliveira, P., Ferreira-da-Silva, F., and Tomas, A.M. (2011) *Leishmania* mitochondrial peroxiredoxin plays a crucial peroxidase-unrelated role during infection: insight into its novel chaperone activity. *PLOS Pathog* 7:e1002325.

Castro, H. and Tomas, A.M. (2013) Thiol peroxidases of trypanosomatids. In: Jager,T., Koch, O., and Floche, L. (eds) Trypanosomatid diseases: molecular routes to drug discoveriy. *Wiley-Blackwell.*

Cazzulo, J.J., Franke de Cazzulo, B.M., Engel, J.C., and Cannata, J.J. (1985) End products and enzyme levels of aerobic glucose fermentation in trypanosomatids. *Mol Biochem Parasitol* 16:329-343.

Chawla, B. and Madhubala, R. (2010) Drug targets in *Leishmania*. *J Parasit Dis* 34:1-13.

Chawla, B., Jhingran, A., Panigrahi, A., Stuart, K.D., and Madhubala, R. (2011) Paromomycin affects translation and vesicle-mediated trafficking as revealed by proteomics of paromomycin-susceptible/-resistant *Leishmania donovani. PLoS One* 6:e26660.

Chen, D.Q., Kolli, B.K., Yadava, N., Lu, H.G., Gilman-Sachs, A., Peterson, D.A., and Chang, K.P. (2000) Episomal expression of specific sense and antisense mRNAs in *Leishmania amazonensis*: modulation of gp63 level in promastigotes and their infection of macrophages *in vitro*. *Infect Immun* 68:80-86.

Chiba, Y., Terada, T., Kameya, M., Shimizu, K., Arai, H., Ishii, M., and Igarashi, Y. (2011) Mechanism for folate-independent aldolase reaction catalyzed by serine hydroxymethyltransferase. FEBX J 279:504-514.

Chokkathukalam, A., Jankevics, A., Creek, D.J., Achcar, F., Barrett, M.P., and Breitling, R. (2013) mzMatch-ISO: an R tool for the annotation and relative quantification of isotope-labelled mass spectrometry data. *Bioinformatics* 29:281-283.

Colasante, C., Ellis, M., Ruppert, T., and Voncken, F. (2006) Comparative proteomics of glycosomes from bloodstream form and procyclic culture form *Trypanosoma brucei brucei*. *Proteomics* 6:3275-3293.

Colotti, G. and Ilari, A. (2011) Polyamine metabolism in *Leishmania*: from arginine to trypanothione. *Amino Acids* 40:269-285.

Comini, M.A. and Floche, L. (2013) Trypanothione-based redox metabolism of trypanosomatids. In: Jager,T., Koch, O., and Floche, L. (eds) Trypanosomatid diseases: molecular routes to drug discoveriy. *Wiley-Blackwell.*

Coustou, V., Besteiro, S., Biran, M., Diolez, P., Bouchaud, V., Voisin, P., Michels, P.A., Canioni, P., Baltz, T., and Bringaud, F. (2003) ATP generation in the *Trypanosoma brucei* procyclic form: cytosolic substrate level is essential, but not oxidative phosphorylation. *J Biol Chem* 278:49625-49635.

Coustou, V., Besteiro, S., Riviere, L., Biran, M., Biteau, N., Franconi, J.M., Boshart, M., Baltz, T., and Bringaud, F. (2005) A mitochondrial NADH-dependent fumarate reductase involved in the production of succinate excreted by procyclic *Trypanosoma brucei*. *J Biol Chem* 280:16559-16570.

Coustou, V., Biran, M., Besteiro, S., Riviere, L., Baltz, T., Franconi, J.M., and Bringaud, F. (2006) Fumarate is an essential intermediary metabolite produced by the procyclic *Trypanosoma brucei*. *J Biol Chem* 281:26832-26846.

Coustou, V., Biran, M., Breton, M., Guegan, F., Riviere, L., Plazolles, N., Nolan, D., Barrett, M.P., Franconi, J.M., and Bringaud, F. (2008) Glucose-induced remodeling of intermediary and energy metabolism in procyclic *Trypanosoma brucei*. *J Biol Chem* 283:16342-16354.

Cox, J. and Mann, M. (2008) MaxQuant enables high peptide identification rates, individualized p.p.b.-range mass accuracies and proteome-wide protein quantification. *Nat Biotechnol* 26:1367-1372.

Cox, J. and Mann, M. (2009) Computational principles of determining and improving mass precision and accuracy for proteome measurements in an Orbitrap. *J Am Soc Mass Spectrom* 20:1477-1485.

Cox, J., Neuhauser, N., Michalski, A., Scheltema, R.A., Olsen, J.V., and Mann, M. (2011) Andromeda: a peptide search engine integrated into the MaxQuant environment. *J Proteome Res* 10:1794-1805.

Crafts-Brandner, S.J. (2002) Plant nitrogen status rapidly alters amino acid metabolism and excretion in *Bemisia tabaci*. *J Insect Physiol* 48:33-41.

Creek, D.J., Jankevics, A., Burgess, K.E., Breitling, R., and Barrett, M.P. (2012) IDEOM: an Excel interface for analysis of LC-MS-based metabolomics data. *Bioinformatics* 28:1048-1049.

Cristodero, M., Mani, J., Oeljeklaus, S., Aeberhard, L., Hashimi, H., Ramrath, D.J., Lukes, J., Warscheid, B., and Schneider, A. (2013) Mitochondrial translation factors of *Trypanosoma brucei*: elongation factor-Tu has a unique subdomain that is essential for its function. *Mol Microbiol* 90:744-755.

Cross, G. A., Klein, R.A., and Linstead, D.J. (1975) Utilization of amino acids by *Trypanosoma brucei* in culture: L-threonine as a precursor for acetate. *Parasitology* 71:311-326.

Cunningham, M.L. and Beverley, S.M. (2001) Pteridine salvage throughout the *Leishmania* infectious cycle: implications for antifolate chemotherapy. *Mol Biochem Parasitol* 113:199-213.

Darling, T.N., Davis, D.G., London, R.E., and Blum, J.J. (1987) Products of *Leishmania braziliensis* glucose catabolism: release of D-lactate and, under anaerobic conditions, glycerol. *Proc Natl Acad Sci USA* 84:7129-7133.

Darling, T.N., Balber, A.E., and Blum, J.J. (1988) A comparative study of D-lactate, L-lactate and glycerol formation by four species of *Leishmania* and by *Trypanosoma lewisi* and *Trypanosoma brucei gambiense*. *Mol Biochem Parasitol* 30:253-257.

Darling, T.N., Burrows, C.M., and Blum, J.J. (1990) Rapid shape change and release of ninhydrin-positive substances by *Leishmania major* promastigotes in response to hypo-osmotic stress. *J Protozool* 37:493-499.

de Koning, W. and van Dam, K. (1992) A method for the determination of changes of glycolytic metabolites in yeast on a subsecond time scale using extraction at neutral pH. *Anal Biochem* 204:118-123.

de Koning, H.P., Bridges, D.J., and Burchmore, R.J. (2005) Purine and pyrimidine transport in pathogenic protozoa: from biology to therapy. *FEMS Microbiol Rev* 29:987-1020.

Denny, P.W., Goulding, D. Ferguson, M.A., and Smith, D.F. (2004) Sphingolipid-free *Leishmania* are defective in membrane trafficking, differentiation and infectivity. *Mol Microbiol* 52:313-327.

Denny, P.W. and Smith, D.F. (2004) Rafts and sphingolipid biosynthesis in the kinetoplastid parasitic protozoa. *Mol Microbiol* 53:725-733.

de Souza, D. P., Saunders, E.C., McConville, M.J., and Likic, V.A. (2006) Progressive peak clustering in GC-MS Metabolomic experiments applied to *Leishmania* parasites. *Bioinformatics* 22:1391-1396.

Dickson, R.C. (2008) New insights into sphingolipids metabolism and function in budding yeast. *J Lipid Res* 49:909-921.

dos Santos, M.G., Paes, L.S., Zampieri, R.A., da Silva, M.F., Silber, A.M., and Floeter-Winter, L.M. (2009) Biochemical characterization of serine transport in *Leishmania (Leishmania) amazonensis*. *Mol Biochem Parasitol* 163:107-113.

Dostalova, A. and Volf, P. (2012) *Leishmania* development in sand flies: parasite-vector interactions overview. *Parasit Vectors* 5:276.

Drazic, A. and Winter, J. (2014) The physiological role of reversible methionine oxidation. *Biochim Biophys Acta* 1844:1367-1382.

Drew, M. E., Langford, C.K., Klamo, E.M., Russell, D.G., Kavanaugh, M.P., and Landfear, S.M. (1995) Functional expression of a myo-inositol/H^+ symporter from *Leishmania donovani*. *Mol Cell Biol* 15: 5508-5515.

Dridi, L., Ahmed Ouameur, A, and Ouellette, M. (2010) High affinity S-Adenosylmethionine plasma membrane transporter of *Leishmania* is a member of the folate biopterin transporter (FBT) family. *J Biol Chem* 285:19767-19775.

Drummelsmith, J., Brochu, V., Girard, I., Messier, N., and Ouellette, M. (2003) Proteome mapping of the protozoan parasite *Leishmania* and application to the study of drug targets and resistance mechanisms. *Mol Cell Proteomics* 2:146-155.

Duarte, M. and Tomas, A.M. (2014) The mitochondrial complex I of trypanosomatids - an overview of current knowledge. *J Bioenerg Biomembr* 46:299-311.

Duffieux, F., van Roy, J., Michels, P.A., and Opperdoes, F.R. (2000) Molecular characterization of the first two enzymes of the pentose-phosphate pathway of *Trypanosoma brucei*. Glucose-6-phosphate dehydrogenase and 6-phosphoglucono-lactonase. *J Biol Chem* 275:27559-27565.

Ebikeme, C., Hubert, J., Biran, M., Gouspillou, G., Morand, P., Plazolles, N., Guegan, F., Diolez, P., Franconi, J.M., Portais, J.C., and Bringaud, F. (2010) Ablation of succinate production from glucose metabolism in the procyclic trypanosomes induces metabolic switches to the glycerol 3-phosphate/dihydroxyacetone phosphate shuttle and to proline metabolism. *J Biol Chem* 285:32312-32324.

Feng, X., Rodriguez-Contreras, D., Buffalo, C., Bouwer, H.G., Kruvand, E., Beverley, S.M., and Landfear, S.M. (2009) Amplification of an alternate transporter gene suppresses the avirulent phenotype of glucose transporter null mutants in *Leishmania mexicana*. *Mol Microbiol* 71:369-381.

Feng, X., Feistel, T., Buffalo, C., McCormack, A., Kruvand, E., Rodriguez-Contreras, D., Akopyants, N.S., Umasankar, P.K., David, L., Jardim, A., Beverley, S.M., and Landfear, S.M. (2011) Remodeling of protein and mRNA expression in *Leishmania mexicana* induced by deletion of glucose transporter genes. *Mol Biochem Parasitol* 175:39-48.

Feng, X., Rodriguez-Contreras, D., Polley, T., Lye, L.F., Scott, D., Burchmore, R.J., Beverley, S.M., and Landfear, S.M. (2013) 'Transient' genetic suppression facilitates generation of hexose transporter null mutants in *Leishmania mexicana*. *Mol Microbiol* 87:412-429.

Ferguson, M.A. (2000) Glycosylphosphatidylinositol biosynthesis validated as a drug target for African sleeping sickness. *Proc Natl Acad Sci USA* 97:10673–10675.

Ferguson, M.A.J., Kinoshita, T., and Hart, G.W. (2009) Glycosylphosphatidylinositol anchors. In: Varki, A., Cummings, R.D., Esko, J.D., Freeze, H.H., Stanley, P., Bertozzi, C.R., Hart, G.W., and Etzler, M.E. (eds) Essentials of glycobiology. *Cold Spring Harbor Laboratory Press.*

Fernandes Rodrigues, J.C., Concepcion, J.L., Rodrigues, C., Caldera, A., Urbina, J.A., and de Souza, W. (2008) *In vitro* activities of ER-119884 and E5700, two potent squalene synthase inhibitors, against *Leishmania amazonensis*: antiproliferative, biochemical, and ultrastructural effects. *Antimicrob Agents Chemother* 52:4098–4114.

Fontecave, M., Atta, M., and Mulliez, E. (2004) S-adenosylmethionine: nothing goes to waste. *Trends Biochem Sci* 29:243-249.

Foucher, A.L., Papadopoulou, B., and Ouellette, M. (2006) Prefractionation by digitonin extraction increases representation of the cytosolic and intracellular proteome of *Leishmania infantum*. *J Proteome Res* 5:1741-1750.

Galili, G., Tang, G., Zhu, X., and Gakiere, B. (2001) Lysine catabolism: a stress and development super-regulated metabolic pathway. *Curr Opin Plant Biol* 4:261-266.

Garami, A. and Ilg, T. (2001a) Disruption of mannose activation in *Leishmania mexicana*: GDP-mannose pyrophosphorylase is required for virulence, but not for viability. *EMBO J* 20:3657-3666.

Garami, A. and Ilg, T. (2001b) The role of phosphomannose isomerase in *Leishmania mexicana* glycoconjugate synthesis and virulence. *J Biol Chem* 276:6566-6575.

Garami, A., Mehlert, A., and Ilg, T. (2001) Glycosylation defects and virulence phenotypes of *Leishmania mexicana* phosphomannomutase and dolicholphosphate-mannose synthase gene deletion mutants. *Mol Cell Biol* 21:8168-8183.

Gaston, M.A., Zhang, L., Green-Church, K.B., and Krzycki, J.A. (2011) The complete biosynthesis of the genetically encoded amino acid pyrrolysine from lysine. *Nature* 471:647-650.

Gibellini, F., Hunter, W.N., and Smith, T.K. (2008) Biochemical characterization of the initial steps of the Kennedy pathway in *Trypanosoma brucei*: the ethanolamine and choline kinases. *Biochem J* 415:135-144.

Ginger, M.L., Prescott, M.C., Reynolds, D.G., Chance, M.L., and Goad, L.J. (2000) Utilization of leucine and acetate as carbon sources for sterol and fatty acid biosynthesis by Old and New World *Leishmania* species, *Endotrypanum monterogeii* and *Trypanosoma cruzi*. *Eur J Biochem* 267:2555-2566.

Ginger, M.L., Chance, M.L., Sadler, I.H., and Goad, L.J. (2001) The biosynthetic incorporation of the intact leucine skeleton into sterol by the trypanosomatid *Leishmania mexicana*. *J Biol Chem* 276:11674-11682.

Giordana, L., Mantilla, B.S., Santana, M., Silber, A.M., and Nowicki, C. (2014) Cystathionine γ-lyase, an enzyme related to the reverse transsulfuration pathway, is functional in *Leishmania* spp. *J Eukaryot Microbiol* 61:204-213.

Gnipova, A., Panicuccia, B., Paris, Z., Vernera, Z., Horvath, A., Lukesa, J., and Zikova, A. (2012) Disparate phenotypic effects from the knockdown of various *Trypanosoma brucei* cytochrome c oxidase subunits. *Mol Biochem Parasitol* 184, 90-98.

Goad, L.J., Holz, G.G., Jr., and Beach, D.H. (1984) Sterols of *Leishmania* species. Implications for biosynthesis. *Mol Biochem Parasitol* 10:161-170.

Gontijo, N.F., Melo, M.N., Riani, E.B., Almeida-Silva, S., and Mares-Guia, M.L. (1996) Glycosidases in *Leishmania* and their importance for *Leishmania* in phlebotomine sandflies with special reference to purification and characterization of a sucrase. *Exp Parasitol* 83:117-124.

Gontijo, N.F., Almeida-Silva, S., Costa, F.F., Mares-Guia, M.L., Williams, P., and Melo, M.N. (1998) *Lutzomyia longipalpis*: pH in the gut, digestive glycosidases, and some speculations upon *Leishmania* development. *Exp Parasitol* 90:212-219.

Gorg, A., Weiss, W., and Dunn, M.J. (2004) Current two-dimensional electrophoresis technology for proteomics. *Proteomics* 4:3665-3685.

Gualdron-Lopez, M., Michels, P.A.M., Quinones, W., Caceres, A.J., Avilan, L., and Concepcion, J.L. (2013) Function of glycosomes in the metabolism of trypanosomatids parasites and the promise of glycosomal proteins as drug targets. In: Jager,T., Koch, O., and Floche, L. (eds) Trypanosomatid diseases: molecular routes to drug discoveriy. *Wiley-Blackwell.*

Guler, J.L., Kriegova, E., Smith, T.K., Lukes, J., and Englund, P.T. (2008) Mitochondrial fatty acid synthesis is required for normal mitochondrial morphology and function in *Trypanosoma brucei*. *Mol Microbiol* 67:1125-1142.

Gunasekera, K., Wuthrich, D., Braga-Lagache, S., Heller, M., and Ochsenreiter, T. (2012) Proteome remodelling during development from blood to insect-form *Trypanosoma brucei* quantified by SILAC and mass spectrometry. *BMC Genomics* 13:556.

Guther, M.L., Urbaniak, M.D., Tavendale, A., Prescott, A., and Ferguson, M.A. (2014) High-confidence glycosome proteome for procyclic form *Trypanosoma brucei* by epitope-tag organelle enrichment and SILAC proteomics. *J Proteome Res* 13:2796-2806.

Gutteridge, W.E. and Gaborak, M. (1979) A re-examination of purine and pyrimidine synthesis in the three main forms of *Trypanosoma cruzi*. *Int J Biochem* 10:415-422.

Hajra, A.K. and Bishop, J.E. (1982) Glycerolipid biosynthesis in peroxisomes via the acyl dihydroxyacetone phosphate pathway. *Ann N Y Acad Sci* 386:170-182.

Hart, D.T. and Coombs, G.H. (1982) *Leishmania mexicana*: energy metabolism of amastigotes and promastigotes. *Exp Parasitol* 54:397-409.

Hart, D.T. and Opperdoes, F.R. (1984) The occurrence of glycosomes (microbodies) in the promastigote stage of four major *Leishmania* species. *Mol Biochem Parasitol* 13:159-172.

Heise, N. and Opperdoes, F.R. (1999) Purification, localisation and characterisation of glucose-6-phosphate dehydrogenase of *Trypanosoma brucei*. *Mol Biochem Parasitol* 99:21-32.

Herwaldt, B.L. (1999) Leishmaniasis. *Lancet* 354:1191-1199.

Hong, Y. and Kinoshita, T. (2009) Trypanosome glycosylphosphatidylinositol biosynthesis. *Korean J Parasitol* 47:197-204.

Horvath, A., Berry, E.A., Huang, L.S., and Maslov, D.A. (2000a) *Leishmania tarentolae*: a parallel isolation of cytochrome bc(1) and cytochrome c oxidase. *Exp Parasitol* 96:160-167.

Horvath, A., Kingan, T.G., and Maslov, D.A. (2000b) Detection of the mitochondrially encoded cytochrome c oxidase subunit I in the trypanosomatid protozoan *Leishmania tarentolae*. Evidence for translation of unedited mRNA in the kinetoplast. *J Biol Chem* 275:17160-17165.

Hsu, J.L., Huang, S.Y., Chow, N.H., and Chen, S.H. (2003) Stable isotope dimethyl labeling for quantitative proteomics. *Anal Chem* 75:6843–6852.

Hsu, F.F., Turk, J., Zhang, K., and Beverley, S. (2007) Characterization of inositol phosphorylceramides from *Leishmania major* by tandem mass spectrometry with electrospray Ionization. *J Am Soc Mass Spectrom* 18:1591-1604.

Ilg, T., Handman, E., and Stierhof, Y.D. (1999) Proteophosphoglycans from *Leishmania* promastigotes and amastigotes. *Biochem Soc Trans* 27:518-525.

Inbar, E., Canepa, G.E., Carrillo, C., Glaser, F., Suter Grotemeyer, M., Rentsch, D., Zilberstein, D., and Pereira, C.A. (2012) Lysine transporters in human trypanosomatid pathogens. *Amino Acids* 42:347-360.

Inbar, E., Schlisselberg, D., Suter Grotemeyer, M., Rentsch, D., and Zilberstein, D. (2013) A versatile proline/alanine transporter in the unicellular pathogen *Leishmania donovani* regulates amino acid homoeostasis and osmotic stress responses. *Biochem J* 449:555-566.

Irigoin, F., Cibils, L., Comini, M.A., Wilkinson, S.R., Flohe, L., and Radi, R. (2008) Insights into the redox biology of *Trypanosoma cruzi*: Trypanothione metabolism and oxidant detoxification. *Free Radic Biol Med* 45:733-742.

Ivens, A.C., Peacock, C.S., Worthey, E.A., Murphy, L., Aggarwal, G., Berriman, M., Sisk, E., Rajandream, M.A., Adlem, E., Aert R., Anupama, A., Apostolou, Z., Attipoe, P., Bason, N., Bauser, C., Beck, A., Beverley, S.M., Bianchettin, G., Borzym, K., Bothe, G., Bruschi, C.V., Collins, M., Cadag, E., Ciarloni, L., Clayton, C., Coulson, R.M., Cronin, A., Cruz, A.K., Davies, R.M., De Gaudenzi, J., Dobson, D.E., Duesterhoeft, A., Fazelina, G., Fosker, N., Frasch, A.C., Fraser, A., Fuchs, M., Gabel, C., Goble, A., Goffeau, A., Harris, D., Hertz-Fowler, C., Hilbert, H., Horn, D., Huang, Y., Klages, S., Knights, A., Kube, M., Larke, N., Litvin, L., Lord, A., Louie, T., Marra, M., Masuy, D., Matthews, K., Michaeli, S., Mottram, J.C., Müller-Auer, S., Munden, H., Nelson, S., Norbertczak, H., Oliver, K., O'Neil, S, Pentony, M., Pohl, T.M., Price, C., Purnelle, B., Quail, M.A., Rabbinowitsch, E., Reinhardt, R., Rieger, M., Rinta, J., Robben, J., Robertson, L., Ruiz, J.C., Rutter, S., Saunders, D., Schäfer, M., Schein, J., Schwartz, D.C., Seeger, K., Seyler, A., Sharp, S., Shin, H., Sivam, D., Squares, R., Squares, S., Tosato, V., Vogt, C., Volckaert, G., Wambutt, R., Warren, T., Wedler, H., Woodward, J., Zhou, S., Zimmermann, W., Smith, D.F., Blackwell, J.M., Stuart, K.D., Barrell, B., and Myler, P.J. (2005) The genome of the kinetoplastid parasite, *Leishmania major*. *Science* 309:436–442.

Jacobson, R.L., Schlein, Y., and Eisenberg, C.L. (2001) The biological function of sand fly and *Leishmania* glycosidases. *Med Microbiol Immunol* 190:51-55.

Jamdhade, M. D., Pawar, H., Chavan, S., Sathe, J., Umasankar, P. K., Mahale, K. N., Dixit, T., A. K., Madugundu, Prasad, T. S. K., Gowda, H., Pandey, A., and Patole, M. S. (2015) Comprehensive proteomics analysis of glycosomes from *Leishmania donovani*. *OMICS: J Integrative Biol* 19:157-170.

Jansen, H.J. and Steinbuchel, A. (2014) Fatty acid synthesis in *Escherichia coli* and its applications towards the production of fatty acid based biofuels. *Biotechnol Biofuels* 7:7.

Jensen, R.E. and Englund, P.T. (2012) Network news: the replication of kinetoplast DNA. *Annu Rev Microbiol* 66, 473-491.

Jiang, Y., Roberts, S.C., Jardim, A., Carter, N.S., Shih, S., Ariyanayagam, M., Fairlamb, A.H., and Ullman, B. (1999) Ornithine decarboxylase gene deletion mutants of *Leishmania donovani*. *J Biol Chem* 274:3781-3788.

Johnson, P. J., Kooter, J.M., and Borst, P. (1987) Inactivation of transcription by UV irradiation of *T. brucei* provides evidence for a multicistronic transcription unit including a VSG gene. *Cell* 51:273-281.

Joshi, M.B. and Dwyer, D.M. (2007) Molecular and functional analyses of a novel class I secretory nuclease from the human pathogen, *Leishmania donovani*. *J Biol Chem* 282:10079-10095.

Kamhawi, S. (2006) Phlebotomine sand flies and *Leishmania parasites*: friends or foes? *Trends Parasitol* 22:439-445.

Kamleh, A., Barrett, M.P., Wildridge, D., Burchmore, R.J., Scheltema, R.A., and Watson, D.G. (2008) Metabolomic profiling using Orbitrap Fourier transform mass spectrometry with hydrophilic interaction chromatography: a method with wide applicability to analysis of biomolecules. *Rapid Commun Mass Spectrom* 22:1912-1918.

Kandpal, M., Fouce, R.B., Pal, A., Guru, P.Y., and Tekwani, B.L. (1995) Kinetics and molecular characteristics of arginine transport by *Leishmania donovani* promastigotes. *Mol Biochem Parasitol* 71:193-201.

Kaneshiro, E.S., Jayasimhulu, K., and Lester, R.L. (1986) Characterization of inositol lipids from *Leishmania donovani* promastigotes: identification of an inositol sphingophospholipid. *J Lipid Res* 27:1294-1303.

Kanost, M.R. (2009) Hemolymph. In: Resh, V.H. and Carde, R.T. (eds) Encyclopedia of insects. *Elsevier.*

Kaushik, S., Krishnarjuna, B., Raghothama, S., Aggarwal, S., Raghunathana, V., and Ganjiwale, A. (2012) Theoretical and in vitro studies of a C-terminal peptide from PGKC of *Leishmania mexicana mexicana*. Mol Biochem Parasitol 185:27–35.

Kedzierski, L., Zhu, Y., and Handman, E. (2006) *Leishmania* vaccines: progress and roblems. *Parasitol* 133:S87-112.

Kennedy, E.P. and Weiss, S.B. (1956) The function of cytidine coenzymes in the biosynthesis of phospholipides. *J Biol Chem* 222:193-214.

Killick-Kendrick, R. (1999) The biology and control of phlebotomine sand flies. *Clin Dermatol* 17:279-289.

Klamo, E.M., Drew, M.E., Landfear, S.M., and Kavanaugh, M.P. (1996) Kinetics and stoichiometry of a proton/myo-inositol cotransporter. *J Biol Chem* 271:14937-14943.

Krassner, S.M. (1969) Proline metabolism in Leishmania tarentolae. *Exp Parasitol* 24:348-363.

Krassner, S.M. and Flory, B. Proline metabolism in *Leishmania donovani* promastigotes. *J Protozool* 19:682-685.

Kundig, C., Haimeur, A., Legare, D., Papadopoulou, B., and Ouellette, M. (1999). Increased transport of pteridines compensates for mutations in the high affinity folate transporter and contributes to methotrexate resistance in the protozoan parasite *Leishmania tarentolae*. *EMBO J* 18:2342-2351.

Lamasudin, D.U. (2012) *Phenotypic characterisation of glucose transporter knockout Leishmania mexicana*. University of Glasgow.

Lamour, N., Riviere, L., Coustou, V., Coombs, G.H., Barrett, M.P., and Bringaud, F. (2005) Proline metabolism in procyclic *Trypanosoma brucei* is down-regulated in the presence of glucose. *J Biol Chem* 280:11902-11910.

Landfear, S.M., Ullman, B., Carter, N.S., and Sanchez, M.A. (2004) Nucleoside and nucleobase transporters in parasitic protozoa. *Eukaryot Cell* 3:245-254.

Langford, C.K., Ewbank, S.A., Hanson, S.S., Ullman, B., and Landfear, S.M. (1992). Molecular characterization of two genes encoding members of the glucose

transporter superfamily in the parasitic protozoan *Leishmania donovani*. *Mol Biochem Parasitol* 55:51-64.

Le Blancq, S.M. and Lanham, S.M. (1984) Aspartate aminotransferase in Leishmania is a broad-spectrum transaminase. *Trans R Soc Trop Med Hyg* 78:373-375.

Lee, S.H., Stephens, J.L., Paul, K.S., and Englund, P.T. (2006) Fatty Acids synthesis by elongases in trypanosomes. *Cell* 126:691-699.

Lemley, C., Yan, S., Dole, V.S., Madhubala, R., Cunningham, M.L., Beverley, S.M., Myler, P.J., and Stuart, K.D. (1999) The *Leishmania donovani* LD1 locus gene ORFG encodes a biopterin transporter (BT1). *Mol Biochem Parasitol* 104:93-105.

Lester, R.L. and Dickson, R.C. (2001) High-performance liquid chromatography analysis of molecular species of sphingolipid-related long chain bases and long chain base phosphates in *Saccharomyces cerevisiae* after derivatization with 6-aminoquinolyl-N-hydroxysuccinimidyl carbamate. *Anal Biochem* 29:283-292.

Liang, X., Zhang, L., Natarajan, S.K., and Becker, D.F. (2013) Proline mechanisms of stress survival. *Antioxid Redox Signal* 19:998-1011.

Linstead, D.J., Klein, R.A., and Vross, G.A. (1977) Threonine catabolism in *Trypanosoma brucei*. *J Gen Microbiol* 101:243-251.

Livore, V.I., Tripodi, K.E.J, and Uttaro, A.D. (2006) Elongation of polyunsaturated fatty acids in trypanosomatids. *FEBS J* 274:264-274.

Lu, S.C. (2000) S-Adenosylmethionine. *Int J Biochem Cell Biol* 32:391-395.

Lu, W., Bennett, B.D., and Rabinowitz, J.D. (2008) Analytical strategies for LC-MS-based targeted metabolomics. *J Chromatogr B Analyt Technol Biomed Life Sci* 871:236-242.

Lykidis, A. (2007) Comparative genomics and evolution of eukaryotic phospholipid biosynthesis. *Prog Lipid Res* 46:171-199.

Mackenzie, N.E., Hall, J.E., Seed, J.R., and Scott, A.I. (1982) Carbon-13 nuclear-magnetic-resonance studies of glucose catabolism by *Trypanosoma brucei gambiense*. *Eur J Biochem* 121:657-661.

Mackenzie, N.E., Hall, J.E., Flynn, I.W., and Scott, A.I. (1983) 13C nuclear magnetic resonance studies of anaerobic glycolysis in *Trypanosoma brucei* spp. *Biosci Rep* 3:141-151.

Mallinson, D.J. and Coombs, G.H. (1989) Biochemical characteristics of the metacyclic forms of *Leishmania major* and *L. mexicana mexicana*. *Parasitology* 98:7-15.

Manhas, R., Tripathi, P., Khan, S., Sethu Lakshmi, B., Lal, S.K., Gowri, V.S., Sharma, A., and Madhubala, R. (2014) Identification and functional characterization of a novel bacterial type asparagine synthetase A: a tRNA synthetase paralog from *Leishmania donovani*. *J Biol Chem* 289:12096-12108.

Marini, J.C., Levene, S.D., Crothers, D.M., and Englund, P.T. (1982) Bent helical structure in kinetoplast DNA. *Proc Natl Acad Sci USA* 79:7664-7668.

Martin, M.B., Grimley, J.S., Lewis, J.C., Heath, III, H.T., Bailey, B.N., Kendrick, H., Yardley, V., Caldera, A., Lira, R., Urbina, J.A., Moreno, S.N.J., Docampo, R., Croft, S.L., and Oldfield, E. (2001) Bisphosphonates inhibit the growth of *Trypanosoma brucei*, *Trypanosoma cruzi*, *Leishmania donovani*, *Toxoplasma gondii*, and

Plasmodium falciparum: aa potential route to chemotherapy. *J Med Chem* 44:909-916.

Maslov, D.A., Zikova, A., Kyselova, I., and Lukes, J. (2002) A putative novel nuclear-encoded subunit of the cytochrome c oxidase complex in trypanosomatids. *Mol Biochem Parasitol* 125:113-125.

Maugeri, D.A., Cazzulo, J.J., Burchmore, R.J., Barrett, M.P., and Ogbunude, P.O. (2003) Pentose phosphate metabolism in *Leishmania mexicana*. *Mol Biochem Parasitol* 130:117-125.

Mazareb, S., Fu, Z.Y., and Zilberstein, D. (1999) Developmental regulation of proline transport in *Leishmania donovani*. *Exp Parasitol* 91:341-348.

McConville, M.J. and Ferguson, M.A. (1993) The structure, biosynthesis and function of glycosylated phosphatidylinositols in the parasitic protozoa and higher eukaryotes. *Biochem J* 294:305-324.

Merlen, T., Sereno, D., Brajon, N., Rostand, F., and Lemesre, J.L. (1999) *Leishmania* spp: completely defined medium without serum and macromolecules (CDM/LP) for the continuous *in vitro* cultivation of infective promastigote forms. *Am J Trop Med Hyg* 60:41-50.

Michell, R.H. (2008) Inositol derivatives: evolution and functions. *Nat Rev Mol Cell Biol* 9:151-161.

Michels, P.A., Bringaud, F., Herman, M., and Hannaert, V. (2006) Metabolic functions of glycosomes in trypanosomatids. *Biochim Biophys Acta* 1763:1463–77.

Miller, R.L., Sabourin, C.L., Krenitsky, T.A., Berens, R.L., and Marr, J.J. (1984) Nucleoside hydrolases from *Trypanosoma cruzi*. *J Biol Chem* 259:5073-5077.

Millerioux, Y., Morand, P., Biran, M., Mazet, M., Moreau, P., Wargnies, M., Ebikeme, C., Deramchia, K., Gales, L., Portais, J.C., Boshart, M., Franconi, J.M., and Bringaud, F. (2012) ATP synthesis-coupled and -uncoupled acetate production from acetyl-CoA by mitochondrial acetate:succinate CoA-transferase and acetyl-CoA thioesterase in *Trypanosoma*. *J Biol Chem* 287:17186-17197.

Millerioux, Y., Ebikeme, C., Biran, M., Morand, P., Bouyssou, G., Vincent, I.M., Mazet, M., Riviere, L., Franconi, J.M., Burchmore, R.J., Moreau, P., Barrett, M.P., and Bringaud, F. (2013) The threonine degradation pathway of the *Trypanosoma brucei* procyclic form: the main carbon source for lipid biosynthesis is under metabolic control. *Mol Microbiol* 90:114-129.

Molyneux, D.H., Moore, J., and Maroli, M. (1991) Sugars in sandflies. *Parassitologia* 33 Suppl:431-436.

Mondal, S., Roy, J.J., and Bera, T. (2014) Generation of adenosine tri-phosphate in *Leishmania donovani* amastigote forms. *Acta Parasitol* 59:11-16.

Moreno, B., Urbina, J.A., Oldfield, E., Bailey, B.N., Rodrigues, C.O., and Docampo, R. (2000) 31P NMR spectroscopy of *Trypanosoma brucei*, *Trypanosoma cruzi*, and *Leishmania major*. Evidence for high levels of condensed inorganic phosphates. *J Biol Chem* 275:28356-28362.

Moreno, M.A., Abramov, A., Abendroth, J., Alonso, A., Zhang, S., Alcolea, P.J., Edwards, T., Lorimer, D., Myler, P.J., and Larraga, V. (2014a) Structure of tyrosine aminotransferase from *Leishmania infantum*. *Acta Crystallogr F Struct Biol Commun* 70:583-587.

Moreno, M.A., Alonso, A., Alcolea, P.J., Abramov, A., de Lacoba, M.G., Abendroth, J., Zhang, S., Edwards, T., Lorimer, D., Myler, P.J., and Larraga, V. (2014b) Tyrosine aminotransferase from *Leishmania infantum*: A new drug target candidate. *Int J Parasitol Drugs Drug Resist* 4:347-354.

Mottram, J.C. and Coombs, G.H. (1985) *Leishmania mexicana*: subcellular distribution of enzymes in amastigotes and promastigotes. *Exp Parasitol* 59:265-274.

Mottram, J.C., Coombs, G.H., and Alexander, J. (2004) Cysteine peptidases as virulence factors of *Leishmania*. *Curr Opin Microbiol* 7:375-381.

Mukkada, A.J. and Simon, M.W. (1977) *Leishmania tropica*: uptake of methionine by promastigotes. *Exp Parasitol* 42:87-96.

Mullen, T.D., Hannun, Y.A., and Obeid, L.M. (2012) Ceramide synthases at the centre of sphingolipids metabolism and biology. *Biochem J* 441:789-802.

Muller, M. and Papadopoulou, B. (2010) Stage-specific expression of the glycine cleavage complex subunits in *Leishmania infantum*. *Mol Biochem Parasitol* 170:17-27.

Naderer, T., Ellis, M.A., Sernee, M.F., de Souza, D.P., Curtis, J., Handman, E., and McConville, M.J. (2006) Virulence of *Leishmania major* in macrophages and mice requires the gluconeogenic enzyme fructose-1,6-bisphosphatase. *Proc Natl Acad Sci USA* 103:5502–5507.

Naderer, T. and McConville, M.J. (2008) The *Leishmania*-macrophage interaction: a metabolic perspective. *Cell Microbiol* 10:301-308.

Naderer, T., Wee, E., and McConville, M.J. (2008) Role of hexosamine biosynthesis in *Leishmania* growth and virulence. *Mol Microbiol* 69:858-869.

Naderer, T., Heng, J., and McConville, M.J. (2010) Evidence that intracellular stages of *Leishmania major* utilize amino sugars as a major carbon source. *PLoS Pathogens* 6:e1001245.

Naula, C.M., Logan, F.J., Wong, P.E., Barrett, M.P., and Burchmore, R.J. (2010) A glucose transporter can mediate ribose uptake: definition of residues that confer substrate specificity in a sugar transporter. *J Biol Chem* 285:29721-29728.

Novozhilova, N.M. and Bovin, N.V. (2010) Structure, functions, and biosynthesis of glycoconjugates of *Leishmania* spp. cell surface. *Biochemistry (Mosc)* 75:686-694.

Ong, S.E., Blagoev, B., Kratchmarova, I., Kristensen, D.B., Steen, H., Pandey, A., and Mann, M. (2002) Stable isotope labelling by amino acids in cell culture. SILAC, as a simple and accurate approach to expression proteomics. *Mol Cell Proteomics* 1:376–386.

Ong, S.E. and Mann, M. (2005) Mass spectrometry-based proteomics turns quantitative. *Nat Chem Biol* 1:252-262.

Opperdoes, F.R. and Borst, P. (1977) Localization of nine glycolytic enzymes in a microbody-like organelle in *Trypanosoma brucei*: The glycosome. *FEBS Letters* 80, 360-364.

Opperdoes, F.R. (1984) Localization of the initial steps in alkoxyphospholipid biosynthesis in glycosomes (microbodies) of *Trypanosoma brucei*. *FEBS Lett* 169:35-39.

Opperdoes, F.R. and Szikora, J.P. (2006) In silico prediction of the glycosomal enzymes of *Leishmania major* and trypanosomes. *Mol Biochem Parasitol* 147:193-206.

Opperdoes, F.R. and Coombs, G.H. (2007) Metabolism of *Leishmania*: proven and predicted. *Trends Parasitol* 23:149-158.

Opperdoes, F.R. and Michels, P.A.M. (2008) The metabolic repertoire of *Leishmania* and implications for drug discovery. In: Myler, P. and Fasel, N. (eds) *Leishmania* after the genome. *Caister Academic Press*.

Ortiz, D., Sanchez, M.A., Pierce, S., Herrmann, T., Kimblin, N., Archie Bouwer, H.G., and Landfear, S.M. (2007) Molecular genetic analysis of purine nucleobase transport in *Leishmania major*. *Mol Microbiol* 64:1228-1243.

Ortiz, D., Sanchez, M.A., Koch, H.P., Larsson, H.P., and Landfear, S.M. (2009) An acid-activated nucleobase transporter from *Leishmania major*. *J Biol Chem* 284:16164-16169.

Ouellette, M., Drummelsmith, J., El-Fadili, A., Kundig, C., Richard, D., and Roy, G. (2002) Pterin transport and metabolism in *Leishmania* and related trypanosomatid parasites. *Int J Parasitol* 32:385-398.

Pabon, M.A., Caceres, A.J., Gualdron, M., Quinones, W., Avilan, L., and Concepcion, J.L. (2007) Purification and characterization of hexokinase from *Leishmania mexicana*. *Parasitol Res* 100:803-810.

Paes, L.S., Galvez Rojas, R.L., Daliry, A., Floeter-Winter, L.M., Ramirez, M.I., and Silber, A.M. (2008) Active transport of glutamate in *Leishmania (Leishmania) amazonensis*. *J Eukaryot Microbiol* 55:382-387.

Papageorgiou, I.G., Yakob, L., Al Salabi, M.I., Diallinas, G., Soteriadou, K.P., and de Koning, H.P. (2005) Identification of the first pyrimidine nucleobase transporter in Leishmania: similarities with the *Trypanosoma brucei* U1 transporter and antileishmanial activity of uracil analogues. *Parasitology* 130:275-283.

Parsons, M. (2004) Glycosomes: parasites and the divergence of peroxisomal purpose. *Mol Microbiol* 53:717-724.

Pastakia, K.B. and Dwyer, D.M. (1987) Identification and characterization of a ribose transport system in *Leishmania donovani* promastigotes. *Mol Biochem Parasitol* 26:175-181.

Pineyro, M.D., Parodi-Talice, A., Portela, M., Arias, D.G., Guerrero, S.A., and Robello, C. (2011) Molecular characterization and interactome analysis of *Trypanosoma cruzi* tryparedoxin 1. *J Proteomics* 74:1683-1692.

Pomel, S., Cojean, S., and Loiseau, P.M. (2015) Targeting sterol metabolism for the development of antileishmanials. *Trends Parasitol* 31:5-7.

Rainey, P.M. and MacKenzie, N.E. (1991) A carbon-13 nuclear magnetic resonance analysis of the products of glucose metabolism in *Leishmania pifanoi* amastigotes and promastigotes. *Mol Biochem Parasitol* 45:307-315.

Ralton, J.E., Naderer, T., Piraino, H.L., Bashtannyk, T.A., Callaghan, J.M., and McConville, M.J. (2003) Evidence that intracellular β-1-2-mannan is a virulence factor in *Leishmania* parasites. *J Biol Chem* 278:40757-407763.

Ramakrishnan, S., Serricchio, M., Striepen, B., and Butikofer, P. (2013) Lipid synthesis in protozoan parasites: a comparison between kinetoplastids and apicomplexans. *Prog Lipid Res* 52:488-512.

Rebouche, C.J. (1991) Ascorbic acid and carnitine biosynthesis. *Am J Clin Nutr* 54: 1147S-1152S.

Renauld, H., Kelly, J.M., and Horn, D. (2007) Chromosome structure and dynamics. In: Barry, D. (ed) Trypanosomes: after the genome. *Horizon Bioscience.*

Richard, D., Leprohon, P., Drummelsmith, J., and Ouellette, M. (2004) Growth phase regulation of the main folate transporter of *Leishmania infantum* and its role in methotrexate resistance. *J Biol Chem* 279:54494-54501.

Righetti, P.G., Castagna, A., Antonioli, P., and Boschetti, E. (2005) Prefractionation techniques in proteome analysis: the mining tools of the third millennium. *Electrophoresis* 26:297-319.

Riviere, L., van Weelden, S W., Glass, P., Vegh, P., Coustou, V., Biran, M., van Hellemond, J.J., Bringaud, F., Tielens, A.G., and Boshart, M. (2004) Acetyl:succinate CoA-transferase in procyclic *Trypanosoma brucei*. Gene identification and role in carbohydrate metabolism. *J Biol Chem* 279:45337-45346.

Riviere, L., Moreau, P., Allmann, S., Hahn, M., Biran, M., Plazolles, N., Franconi, J.M., Boshart, M., and Bringaud, F. (2009) Acetate produced in the mitochondrion is the essential precursor for lipid biosynthesis in procyclic trypanosomes. *Proc Natl Acad Sci USA 106*:12694-12699.

Roberts, S.C., Scott, J., Gasteier, J.E., Jiang, Y., Brooks, B., Jardim, A., Carter, N.S., Heby, O., and Ullman, B. (2002) S-Adenosylmethionine decarboxylase from *Leishmania donovani*. Molecular, genetic, and biochemical characterization of null mutants and overproducers. *J Biol Chem* 277:5902-5909.

Roberts, S.C., Tancer, M.J., Polinsky, M.R., Gibson, K.M., Heby, O., and Ullman, B. (2004) Arginase plays a pivotal role in polyamine precursor metabolism in *Leishmania*. Characterization of gene deletion mutants. *J Biol Chem* 279:23668-23678.

Rodriguez-Contreras, D. and Landfear, S.M. (2006) Metabolic changes in glucose transporter-deficient *Leishmania mexicana* and parasite virulence. *J Biol Chem* 281:20068-20076.

Rodriguez-Contreras, D., Feng, X., Keeney, K.M., Bouwer, H.G., and Landfear, S.M. (2007) Phenotypic characterization of a glucose transporter null mutant in *Leishmania mexicana*. *Mol Biochem Parasitol* 153:9-18.

Rodriguez-Contreras, D. and Hamilton, N. (2014) Gluconeogenesis in *Leishmania mexicana*: contribution of glycerol kinase, phosphoenolpyruvate carboxykinase, and pyruvate phosphate dikinase. *J Biol Chem* 289:32989-33000.

Rogerson, G.W. and Gutteridge, W.E. (1980) Catabolic metabolism in *Trypanosoma cruzi*. *Int J Parasitol* 10:131-135.

Romao, S., Castro, H., Sousa, C., Carvahlo, S., and Tomas, A.M. (2009) The cytosolic tryparedoxin of *Leishmania infantum* is essential for parasite survival. *Int J Parasitol* 36:703-711.

Rosenzweig, D., Smith, D., Opperdoes, F.R., Stern, S., Olafson, R.W., and Zilberstein D. (2008a) Retooling *Leishmania* metabolism: form sandfly gut to human macrophage. *FASEB J* 22:590-602.

Rosenzweig, D., Smith, D., Myler, P.J., Stern, S., Olafson, R.W., and Zilberstein D. (2008b) Post-translational modification of cellular proteins during *Leishmania donovani* differentiation. *Proteomics* 8:1843–1850.

Ross, R. (1903) Note on the bodies recently described by Leishman and Donovan. *Br Med J* 2:1261-1262.

Saar, Y., Ransford, A., Waldman, E., Mazareb, S., Amin-Spector, S., Plumblee, J., Turco, S.J., and Zilberstein, D. (1998) Characterization of developmentally-regulated activities in axenic amastigotes of *Leishmania donovani. Mol Biochem Parasitol* 95:9–20.

Sanchez, M.A., Tryon, R., Pierce, S., Vasudevan, G., and Landfear, S. M. (2004) Functional expression and characterization of a purine nucleobase transporter gene from *Leishmania major*. *Mol Membr Biol* 21:11-18.

Sandstrom, J.P. and Moran, N.A. (2001) Amino acid budgets in three aphid species using the same host plant. *Physiol Entomol* 26:202-211.

Saunders, E.C., de Souza, D.P., Naderer, T., Ser Nee, M.F., Ralton, J.E., Doyle, M.A., Macrae, J.I., Chambers, J.L., Heng, J., Nahid, A., Likic, V., and McConvilee, M.J. (2010) Central carbon metabolism of *Leishmania* parasites. *Parasitol* 137:1303–13.

Saunders, E.C., Ng, W.W., Chambers, J.M., Ng, M., Naderer, T., Kromer, J.O., Likic, V.A., and McConville, M.J. (2011) Isotopomer profiling of *Leishmania mexicana* promastigotes reveals important roles for succinate fermentation and aspartate uptake in tricarboxylic acid cycle (TCA) anaplerosis, glutamate synthesis, and growth. *J Biol Chem* 286:27706-17.

Saunders, E.C., Ng, W.W., Kloehn, J., Chambers, J.M., Ng, M., and McConville, M.J. (2014) Induction of a stringent metabolic response in intracellular stages of Leishmania mexicana leads to increased dependence on mitochondrial metabolism." PLoS Pathog 10(1): e1003888.

Schenkman, J.B. and Jansson, I. (2003) The many roles of cytochrome b5. *Pharmacol Ther* 97:139-152.

Schaefer III, F.W., Martin, E., and Mukkada, A.J. (1974) The glucose transporter system in *Leishmania tropica* promastigotes. *J Protozool* 21:592-596.

Schlame, M. (2008) Cardiolipin synthesis for the assembly of bacterial and mitochondrial membranes. *J Lipid Res* 49:1607-1620.

Schlein, Y. and Jacobson, R.L. (1999) Sugar meals and longevity of the sandfly *Phlebotomus papatasi* in an arid focus of *Leishmania major* in the Jordan Valley. *Med Vet Entomol* 13:65-71.

Sernee, M.F., Ralton, J.E., Dinev, Z., Khairallah, G.N., O'Hair, R.A., Williams, S.J., and McConville, M.J. (2006) *Leishmania* beta-1,2-mannan is assembled on a mannose-cyclic phosphate primer. *Proc Natl Acad Sci USA* 103:9458-9463.

Serricchio, M. and Butikofer, P. (2012) An essential bacterial-type cardiolipin synthase mediates cardiolipin formation in a eukaryote. *Proc Natl Acad Sci USA* 109:E954-961.

Serricchio, M. and Butikofer, P. (2013) Phosphatidylglycerophosphate synthase associates with a mitochondrial inner membrane complex and is essential for growth of *Trypanosoma brucei*. *Mol Microbiol* 87:569-579.

Shaked-Mishan, P., Suter-Grotemeyer, M., Yoel-Almagor, T., Holland, N., Zilberstein, D., and Rentsch, D. (2006) A novel high-affinity arginine transporter from the human parasitic protozoan *Leishmania donovani*. *Mol Microbiol* 60:30-38.

Shaw, J.J. (1994) Taxonomy of the genus *Leishmania*: present and future trends and their implications. *Mem Inst Oswaldo Cruz* 89:471-478.

Signorell, A., Rauch, M., Jelk, J., Ferguson, M.A., and Butikofer, P. (2008) Phosphatidylethanolamine in *Trypanosoma brucei* is organized in two separate pools and is synthesized exclusively by the Kennedy pathway. *J Biol Chem* 283:23636-23644.

Silverman, J.M., Chan, S.K., Robinson, D.P., Dwyer, D.M., Nandan, D., Foster, L.J., and Reiner, N.E. (2008) Proteomic analysis of the secretome of *Leishmania donovani. Genome Biology* 9:R35.

Simon, M.W., Jayasimhulu, K., and Mukkada, A.J. (1983) The free amino acid pool in *Leishmania tropica* promastigotes. *Mol Biochem Parasitol* 9:47-57.

Singh, A. and Mandal, D. (2011) A novel sucrose/H^+ symport system and an intracellular sucrase in *Leishmania donovani*. *Int J Parasitol* 41:817-826.

Sogin, M.L., Gunderson, J.H., Elwood, H.J., Alonso, R.A., and Peattie, D.A. (1989) Phylogenetic meaning of the kingdom concept: an unusual ribosomal RNA from *Giardia lamblia*. *Science* 243, 75-77.

Sopwith, W.F., Debrabant, A., Yamage, M., Dwyer, D.M., and Bates, P.A. (2002) Developmentally regulated expression of a cell surface class I nuclease in Leishmania *mexicana*. *Int J Parasitol* 32:449-459.

Sousa Silva, M., Ferreira, A.E.N., Gomes, R., Tomas, A.M., Ponces Freire, A., and Cordeiro, C. (2013) Glyoxylase enzymes in trypanosomatids. In: Jager,T., Koch, O., and Floche, L. (eds) Trypanosomatid diseases: molecular routes to drug discoveriy. *Wiley-Blackwell.*

Speijer, D., Muijsers, A.O., Dekker, H., de Haan, A., Breek, C.K., Albracht, S.P., and Benne, R. (1996a) Purification and characterization of cytochrome c oxidase from the insect trypanosomatid *Crithidia fasciculata*. *Mol Biochem Parasitol* 79:47-59.

Speijer, D., Breek, C.K., Muijsers, A.O., Groenevelt, P.X., Dekker, H., de Haan, A., and Benne, R. (1996b) The sequence of a small subunit of cytochrome c oxidase from *Crithidia fasciculata* which is homologous to mammalian subunit IV. *FEBS Lett* 381:123-126.

Steenkamp, D.J. (2002) Thiol metabolism of the trypanosomatids as potential drug targets. *IUBMB Life* 53:243-248.

Steiger, R.F. and Steiger, E. (1976) A defined medium for cultivating *Leishmania donovani* and *L. braziliensis*. *J Parasitol* 62:1010-1011.

Stevens, J.R. (2008) Kinetoplastid phylogenetics, with special reference to the evolution of parasitic trypanosomes. *Parasite* 15:226-232.

Svobodova, M., Zidkova, L., Cepicka, I., Obornik, M., Lukes, J., and Votypka, J. (2007) *Sergeia podlipaevi* gen. nov., sp. nov. (Trypanosomatidae, Kinetoplastida), a parasite of biting midges (Ceratopogonidae, Diptera). *Int J Syst Evol Microbiol* 57:423-432.

Tafesse, F.G., Ternes, P., and Holthui, J.C. (2006) The multigenic sphingomyelin synthase family. *J Biol Chem* 281:29421-29425.

Tripodi, K.E., Buttigliero, L.V., Altabe, S.G., and Uttaro, A.D. (2006) Functional characterization of front-end desaturases from trypanosomatids depicts the first polyunsaturated fatty acid biosynthetic pathway from a parasitic protozoan. *FEBS J* 273:271-280.

Tristan, C., Shahani, N., Sedlak, T.W., and Sawa, A. (2011) The diverse functions of GAPDH: views from different subcellular compartments. *Cell Signal* 23:317-323.

Turco, S.J., Orlandi, P.A., Jr., Homans, S.W., Ferguson, M.A., Dwek, R.A., and Rademacher, T.W. (1989) Structure of the phosphosaccharide-inositol core of the *Leishmania donovani* lipophosphoglycan. *J Biol Chem* 264:6711-6715.

Turco, S.J. and Descoteaux, A. (1992) The lipophosphoglycan of *Leishmania* parasites. *Annu Rev Microbiol* 46:65-94.

Tyler, G.K. (2013) Wings and flight. In. Chapman, R.F. (wrt), Simpson, S.J., and Douglas, A.E. (eds) The insects: structure and function. *Cambridge University Press.*

Ueno, N. and Wilson, M.E. (2012) Receptor-mediated phagocytosis of *Leishmania*: implications for intracellular survival. *Trends Parasitol* 28:335-344.

Urbaniak, M.D., Guther, M.L., and Ferguson, M.A. (2012) Comparative SILAC proteomic analysis of *Trypanosoma brucei* bloodstream and procyclic lifecycle stages. *PLoS One* 7:e36619.

Urbaniak, M.D., Martin, D.M., and Ferguson, M.A. (2013) Global quantitative SILAC phosphoproteomics reveals differential phosphorylation is widespread between the procyclic and bloodstream form lifecycle stages of *Trypanosoma brucei*. *J Proteome Res* 12:2233-2244.

Urbina, J.A. and Docampo, R. (2003) Specific chemotherapy of Chagas disease: controversies and advances. *Trends Parasitol* 19:495-501.

Urbina, J.A. (2009) Ergosterol biosynthesis and drug development for Chagas disease. *Mem Inst Oswaldo Cruz* 104:311-318.

Uttaro, A.D. (2006) Biosynthesis of polyunsaturated fatty acids in lower eukaryotes. *IUBMB Life* 58:563-571.

van Hellemond, J.J., Opperdoes, F.R., and Tielens, A.G. (1998) Trypanosomatidae produce acetate via a mitochondrial acetate:succinate CoA transferase. *Proc Natl Acad Sci USA* 95:3036-3041.

van Weelden, S.W., Fast, B., Vogt, A., van der Meer, P., Saas, J., van Hellemond, J.J., Tielens, A.G., and Boshart, M. (2003) Procyclic *Trypanosoma brucei* do not use Krebs cycle activity for energy generation. *J Biol Chem* 278:12854-12863.

Vance, J.E. and Tasseva, G. (2012) Formation and function of phosphatidylserine and phosphatidylethanolamine in mammalian cells. *Biochim Biophys Acta* 1831:543-554.

Vasudevan, G., Carter, N.S., Drew, M.E., Beverley, S.M., Sanchez, M.A., Seyfang, A., Ullman, B., and Landfear, S.M. (1998) Cloning of *Leishmania* nucleoside transporter genes by rescue of a transport-deficient mutant. *Proc Natl Acad Sci USA* 95:9873-9878.

Verlinde, C.L.M.J., Hannaert, V., Blonski, C., Willson, M., Périé, J.J., Fothergill-Gilmore, L.L., Opperdoes, F.R., Gelb, M.H., Hol, W.G.J., and Michels, P.A.M. (2001) Glycolysis as a target for the design of new anti-trypanosome drugs. *Drug Resist Updat* 4:50-65.

Vernal, J., Cazzulo, J.J., and Nowicki, C (1998) Isolation and partial characterization of a broad specificity aminotransferase from *Leishmania mexicana* promastigotes. *Mol Biochem Parasitol* 96:83-92.

Vernal, J., Cazzulo, J.J., and Nowicki, C (2003) Cloning and heterologous expression of a broad specificity aminotransferase of *Leishmania mexicana* promastigotes1. *FEMS Microbiol Lett* 229:217-222.

Vickerman, K. (1994) The evolutionary expansion of the trypanosomatid flagellates. *Int J Parasitol* 24:1317-1331.

Vickerman, K. (2009) "Not a very nice subject." Changing views of parasites and parasitology in the twentieth century. *Parasitology* 136:1395-1402.

Vieira, L.L., Lafuente, E., Gamarro, F., and Cabantchik, Z. (1996) An amino acid channel activated by hypotonically induced swelling of *Leishmania major* promastigotes. *Biochem J* 319:691-697.

Wackers, F.L. (2005) Suitability of (extra)-floral nectar, polen, and honeydew as insect food sources. In: Wackers, F.L., van Rijn, P.C.J., and Bruin, J. (eds) Plant-provided food for carnivorous insects: a protective mutalism and its applications. *Cambridge University Press.*

Walder, J.A., Eder, P.S., Engman, D.M., Brentano, S.T., Walder, R.Y., Knutzon, D.S., Dorfman, D.M., and Donelson, J.E. (1986) The 35-nucleotide spliced leader sequence is common to all trypanosome messenger RNA's. *Science* 233:569-571.

Wallace, F.G. (1966) The trypanosomatid parasites of insects and arachnids. *Exp Parasitol* 18:124-193.

Wang, Y., Utzinger, J., Saric, J., Li, J.V., Burckhardt, J., Dirnhofer, S., Nicholson, J.K., Singer, B.H., Brun, R., and Holmes, E. (2008) Global metabolic responses of mice to *Trypanosoma brucei brucei* infection. *Proc Natl Acad Sci USA* 105:6127-6132.

Wang, G., Wu, W.W., Zhang, Z., Masilamani, S., and Shen, R.F. (2009) Decoy methods for assessing false positives and false discovery rates in shotgun proteomics. *Anal Chem* 81:146-159.

Wassef, M.K., Fioretti, T.B., and Dwyer, D.M. (1985) Lipid analyses of isolated surface membranes of *Leishmania donovani* promastigotes. *Lipids* 20:108-115.

Watson, D.G. (2010) The potential of mass spectrometry for the global profiling of parasite metabolomes. *Parasitology* 137:1409-1423.

Weibull, J., Ronquist, F., and Brishammar, S. (1990) Free amino acid composition of leaf exudates and phloem sap: a comparative study in oats and barley. *Plant Physiol* 92:222-226.

Wiese, M. (1998) A mitogen-activate protein (MAP) kinase homologue of *Leishmania mexicana* is essential for parasite survival in the infected host. *EMBO J* 17:2619-2628.

Wiese, M., Kuhn, D., and Grunfelder, C.G. (2003) Protein kinase involved in flagellar-length control. *Eukaryot Cell* 2:769-777.

Williams, R.A., Westrop, G.D., and Coombs, G.H. (2009) Two pathways for cysteine biosynthesis in *Leishmania major*. *Biochem J* 420:451-462.

Wisniewski, J.R., Zougman, A., Nagaraj, N., and Mann, M. (2009) Universal sample preparation method for proteome analysis. *Nat Methods* 6:359-362.

Xu, H., Andi, B., Qian, J., West, A.H., and Cook, P.F. (2006) The α-aminoadipate pathway for lysine biosynthesis in fungi. *Cell Biochem Biophys* 46:43-64.

Xu, W., Hsu, F.F., Baykal, E., Huang, J., and Zhang, K. (2014) Sterol biosynthesis is required for heat resistance but not extracellular survival in leishmania. *PLoS Pathog* 10:e1004427.

Zabriskie, T.M. and Jackson, M.D. (2000) Lysine biosynthesis and metabolism in fungi. *Nat Prod Rep* 17:85-97.

Zhang, K., Pompey, J.M., Hsu, F.F., Key, P., Bandhuvula, P., Saba, J.D., Turk, J., Beverley, S.M. (2007) Redirection of sphingolipid metabolism toward de novo synthesis of ethanolamine in *Leishmania*. *EMBO J* 26:1094-1104.

Zhang, K. and Beverley, S.M. (2010) Phospholipid and sphingolipid metabolism in *Leishmania*. *Mol Biochem Parasitol* 170:55-64.

Zhang, X., Wen, H, and Shi, X. (2012) Lysine methylation: beyond histones. *Acta Biochim Biophys Sin (Shanghai)* 44:14-27.

Zilberstein, D. and Dwyer, D.M. (1984) Glucose transport in *Leishmania donovani* promastigotes. *Mol Biochem Parasitol* 12:327-336.

Zilberstein, D. and Shapira, M. (1994) The role of pH and temperature in the development of *Leishmania* parasites. *Annu Rev Microbiol* 48:449-470.

Zufferey, R. and Mamoun, C.B. (2002) Choline transport in *Leishmania major* promastigotes and its inhibition by choline and phosphocholine analogs. *Mol Biochem Parasitol* 125:127-134.

Zufferey, R. and Mamoun, C.B. (2006) *Leishmania major* expresses a single dihydroxyacetone phosphate acyltransferase localized in the glycosome, important for rapid growth and survival at high cell density and essential for virulence. *J Biol Chem* 281:7952-7959.

Appendix 1

Accession number	Protein name	Fraction				
		I	II	III	IV	V
		L/H	L/H	L/H	L/H	L/H
LmxM.26.0620	10 kDa Heat shock protein, putative			3.42		
LmxM.11.0350	14-3-3 protein, putative			4.07		
LmxM.36.3210	14-3-3 protein-like protein			3.91		
LmxM.03.0540	26S protease regulatory subunit, putative, serine peptidase, Clan SJ, family S16, putative			2.40		
LmxM.28.2420	2-Oxoglutarate dehydrogenase, E2 component, dihydrolipoamide succinyltransferase, putative					0.41
LmxM.32.1590	3-ketoacyl-CoA reductase, putative					0.19
LmxM.30.2310	3'-Nucleotidase/nuclease precursor, putative					2.20
LmxM.36.5010	40S ribosomal protein SA, putative			2.00		
LmxM.13.0570	40S ribosomal protein S12, putative			2.61		
LmxM.30.0010	5-Methyltetrahydropteroyltriglutamate—homocysteine methyltransferase, putative			3.33		
LmxM.15.1203	60S acidic ribosomal protein P2			2.67		
LmxM.29.3730	60S acidic ribosomal protein P2, putative			2.60		
LmxM.27.1380	60S acidic ribosomal subunit protein, putative			3.18		
LmxM.21.1050	60S ribosomal protein L9, putative					2.54
LmxM.04.0750	60S ribosomal protein L10, putative			2.11		
LmxM.08_29.2460	60S ribosomal protein L13, putative			6.50		
LmxM.34.3340	6-Phosphogluconate dehydrogenase, decarboxylating, putative			4.19		
LmxM.23.0710	Acetyl-CoA synthetase, putative			2.26		
LmxM.04.1230	Actin	5.5	3.48	3.83		2.05
LmxM.26.0140	Adenine phosphoribosyltransferase					6.29
LmxM.29.0880	Adenosine kinase, putative			5.00		
LmxM.12.0630	Alanine aminotransferase, putative			5.01		
LmxM.29.0120	Alkyl dihydroxyacetonephosphate synthase					0.25
LmxM.20.1550	Aminoacylase, putative, N-acyl-L-amino acid amidohydrolase, putative			3.18		
LmxM.20.1560	Aminoacylase, putative, N-acyl-L-amino acid amidohydrolase, putative			3.18		
LmxM.34.2350	Aminopeptidase P, putative			2.79		
LmxM.08_29.2240	Aminopeptidase, putative, metallo-peptidase, Clan MA(E), Family M1			2.39		
LmxM.34.1480	Arginase			2.29		
LmxM.16.0540	Aspartate carbamoyltransferase, putative			2.87		
LmxM.29.0460	Aspartyl-tRNA synthetase, putative			2.65		
LmxM.21.1770	ATP synthase F1 subunit γ protein, putative				0.32	
LmxM.29.3600	ATP synthase, ε chain, putative					0.50
LmxM.05.0510	ATPase α subunit, putative					0.39
LmxM.25.1170	ATPase β subunit, putative				0.29	0.43
LmxM.08_29.1270	ATP-dependent Clp protease subunit, heat shock protein 100 (HSP100), putative, serine peptidase, putative			26.9		
LmxM.34.0370	ATP-dependent DEAD-box RNA helicase, putative			4.51		

LmxM.34.3100	ATP-dependent RNA helicase, putative	2.3		4.91		0.40
LmxM.30.1070	Biotin/lipoate protein ligase-like protein			2.69		
LmxM.04.0010	Calcium-translocating P-type ATPase, organelle-type calcium ATPase					0.40
LmxM.20.1180	Calpain-like cysteine peptidase			3.06		0.09
LmxM.20.1185	Calpain-like cysteine peptidase, putative			3.02		0.09
LmxM.20.1310	Calpain-like cysteine peptidase, putative, calpain-like cysteine peptidase, Clan CA, family C2	3.3				
LmxM.27.0490	Calpain-like cysteine peptidase, putative, cysteine peptidase, Clan CA, family C2, putative					0.39
LmxM.13.0090	Carboxypeptidase, putative, metallo-peptidase, Clan MA(E), family 32			2.48		
LmxM.31.3270	Chaperonin α subunit, putative			3.01		
LmxM.36.2030	Chaperonin HSP60, mitochondrial precursor		0.47	2.17		
LmxM.36.2020	Chaperonin HSP60, mitochondrial precursor		0.43			
LmxM.13.1660	Chaperonin TCP20, putative			4.00		
LmxM.18.0680	Citrate synthase, putative		0.28			
LmxM.18.0670	Citrate synthase, putative		0.29			
LmxM.25.0910	Cyclophilin A			3.32		
LmxM.34.3230	Cystathione γ lyase, putative			2.13		0.17
LmxM.32.1330	Cysteine conjugate β-lyase, aminotransferase-like protein			4.33		
LmxM.19.1420	Cysteine peptidase A (CBA)			2.32		
LmxM.08_29.0820	Cysteine peptidase C (CPC), CPC cysteine peptidase, Clan CA, family C1, Cathepsin B-like			2.34		
LmxM.12.0250	Cysteinyl-tRNA synthetase, putative			4.16		
LmxM.26.1710	Cytochrome c oxidase subunit V, putative				0.38	
LmxM.36.2660	Dihydrolipoamide acetyltransferase precursor, putative					0.22
LmxM.31.3310	Dihydrolipoamide dehydrogenase, putative		0.33			
LmxM.27.2020	D-lactate dehydrogenase-like protein	0.31	0.23			0.21
LmxM.25.0980	Dynein heavy chain, putative					0.34
LmxM.28.1140	Electron-transfer-flavoprotein, α polypeptide, putative			3.56		
LmxM.17.0080	Elongation factor 1-α	2.91	2.89	8.02		
LmxM.33.0820	Elongation factor 1-β		2.35	5.06		
LmxM.09.0970	Elongation factor-1 γ			2.68		
LmxM.03.0980	Elongation initiation factor 2 α subunit, putative					0.42
LmxM.28.2310	Eukaryotic translation initiation factor, putative			2.48		
LmxM.22.1360	Farnesyl pyrophosphate synthase, putative			2.75		
LmxM.10.1190	Flagellar protofilament ribbon protein-like protein					0.23
LmxM.13.0430	Flagellar radial spoke protein, putative					0.29
LmxM.08_29.1960	Fumarate hydratase, putative			5.85		
LmxM.33.2290	G-Actin binding protein, putative, twinfilin, putative			10.40		
LmxM.33.0080	Glucose-6-phosphate dehydrogenase			4.08		
LmxM.28.2910	Glutamate dehydrogenase, putative	6.56	5.37	12.35		
LmxM.29.2980	Glyceraldehyde 3-phosphate dehydrogenase, glycosomal			3.83		0.43
LmxM.10.0510	Glycerol-3-phosphate dehydrogenase [NAD^+], glycosomal/mitochondrial			17.06		

LmxM.34.4720	Glycine cleavage system H protein, putative			2.49		
LmxM.33.0990	p-Glycoprotein	4.10				4.05
LmxM.19.0710	Glycosomal malate dehydrogenase			8.95		
LmxM.27.1805	Glycosomal phosphoenolpyruvate carboxykinase, putative			4.72		
LmxM.10.0470	GP63, leishmanolysin	0.10				
LmxM.10.0405	GP63, leishmanolysin	0.09				0.03
LmxM.10.0390	GP63, leishmanolysin	0.08	0.06			0.02
LmxM.10.0460	GP63, leishmanolysin	0.08				
LmxM.25.1420	GTP-binding protein, putative			2.71		
LmxM.08_29.0867	Guanine deaminase, putative			4.17		
LmxM.29.2460	Heat shock 70-related protein 1, mitochondrial precursor, putative		0.44	2.28		
LmxM.29.2490	Heat shock 70-related protein 1, mitochondrial precursor, putative			2.17		
LmxM.29.2550	Heat shock 70-related protein 1, mitochondrial precursor, putative			2.39		
LmxM.32.0312	Heat shock protein 83-1			2.84		
LmxM.27.2400	Heat shock protein DNAJ, putative	2.95		3.92		
LmxM.18.1370	Heat shock protein, putative			3.29		
LmxM.28.2770	Heat-shock protein hsp70, putative				2.62	
LmxM.08_29.0850	High mobility group protein homolog tdp-1, putative			6.94		
LmxM.36.6480	Histidine secretory acid phosphatase, putative	2.34				
LmxM.08_29.1720	Histone H2A, putative					0.17
LmxM.17.1220	Histone H2B					0.22
LmxM.09.1340	Histone H2B					0.25
LmxM.15.0010	Histone H4					0.26
LmxM.06.0010	Histone H4					0.25
LmxM.25.2450	Histone H4					0.24
LmxM.08_29.0320	Hypothetical protein, conserved			4.19		
LmxM.08_29.1240	Hypothetical protein, unknown function			3.17		
LmxM.08_29.1470	Hypothetical protein, conserved			3.02		
LmxM.11.1030	Hypothetical protein, conserved				0.24	
LmxM.13.0450	Hypothetical protein, conserved			6.52		
LmxM.17.0870	Hypothetical protein, conserved	3.13				
LmxM.18.0210	Hypothetical protein, conserved			2.94		
LmxM.21.0980	Hypothetical protein, conserved			2.91		
LmxM.22.0730	Hypothetical protein, conserved				0.22	
LmxM.23.1020	Hypothetical protein, unknown function				0.50	
LmxM.23.1480	Hypothetical protein, conserved			2.08		
LmxM.23.1580	Hypothetical protein, conserved			2.55		
LmxM.25.2010	Hypothetical protein, conserved			2.31		
LmxM.27.1730	Hypothetical protein, conserved	3.05				
LmxM.27.2000	Hypothetical protein, conserved			3.07		
LmxM.29.2850	Hypothetical protein, conserved		0.49			
LmxM.29.3430	Hypothetical protein, conserved			3.63		
LmxM.31.0630	Hypothetical protein, conserved			8.50		
LmxM.31.0950	Hypothetical protein, conserved			3.62		
LmxM.33.0190	Hypothetical protein, conserved			22.70		
LmxM.33.1520	Hypothetical protein, conserved	3.47	3.83	7.26		
LmxM.33.2580	Hypothetical protein, conserved			3.27		
LmxM.34.4470	Hypothetical protein, conserved		2.00			
LmxM.36.0740	Hypothetical protein, conserved			16.95		
LmxM.36.1520	Hypothetical protein, conserved, nima-related protein kinase, putative			4.66		
LmxM.36.5100	Hypothetical protein, conserved			2.61		
LmxM.36.5910	Hypothetical protein, conserved			2.87		

LmxM.36.6060	Hypothetical protein, conserved			3.18	
LmxM.36.1520	Hypothetical protein, conserved, nima-related protein kinase, putative			4.66	
LmxM.31.1820	Iron superoxide dismutase, putative			2.77	
LmxM.36.5620	Isoleucyl-tRNA synthetase, putative			2.96	
LmxM.16.1460	Kinesin, putative				0.46
LmxM.16.1470	Kinesin, putative				0.46
LmxM.27.0240	Kinetoplast-associated protein-like protein			2.17	
LmxM.33.0140	Malate dehydrogenase		0.39	2.57	
LmxM.24.0770	Malic enzyme, putative			5.18	
LmxM.05.0830	Methylthioadenosine phosphorylase, putative			2.22	
LmxM.05.0380	Microtubule-associated protein, putative				0.16
LmxM.34.1380	Mitochondrial processing peptidase, β subunit, putative, metallo-peptidase, Clan ME, Family M16				0.31
LmxM.32.1380	Mitogen activated protein kinase, putative, map kinase, putative		2.39	7.54	
LmxM.14.1360	*myo*-Inositol-1-phosphate synthase			2.59	
LmxM.34.1180	NADH-dependent fumarate reductase, putative			6.61	
LmxM.10.0210	Nucleolar protein 56, putative			2.26	
LmxM.14.0130	Nucleoside hydrolase-like protein			3.15	
LmxM.19.0440	Nucleosome assembly protein, putative			4.73	
LmxM.30.1750	Nucleosome assembly protein-like protein			5.46	
LmxM.36.4170	Oxidoreductase, putative			5.40	
LmxM.16.1430	Paraflagellar rod protein 2C	0.29	0.26		
LmxM.30.3090	Peptidase, putative, metallo-peptidase, Clan ME, Family M16			4.42	
LmxM.23.0040	Peroxidoxin,tryparedoxin peroxidase			2.22	
LmxM.20.0110	Phosphoglycerate kinase B, cytosolic			3.41	
LmxM.20.0100	Phosphoglycerate kinase C, glycosomal			3.30	
LmxM.36.1960	Phosphomannomutase, putative			3.50	
LmxM.09.0891	Polyubiquitin, putative			4.95	
LmxM.36.1600	Proteasome α 1 subunit, putative			3.18	
LmxM.34.4850	Proteasome α 1 subunit, putative			2.19	
LmxM.21.1830	Proteasome α 5 subunit, putative,20S proteasome subunit α 5, (putative)			2.35	
LmxM.31.0390	Proteasome regulatory non-ATP-ase subunit 8, putative, 26S proteasome regulatory subunit, putative			2.01	
LmxM.08_29.0120	Proteasome regulatory non-ATPase subunit, putative			3.64	
LmxM.36.6940	Protein disulfide isomerase	0.28	0.31		
LmxM.26.0660	Protein disulfide isomerase, putative			5.08	
LmxM.19.0150	Protein kinase, putative, mitogen-activated protein kinase, putative			7.73	
LmxM.07.0190	Protein phosphatase 2A, regulatory subunit B, putative,phosphotyrosyl phosphate activator protein, putative			5.25	
LmxM.29.1250	Pyridoxal kinase, putative			4.04	
LmxM.34.0020	Pyruvate kinase			2.51	
LmxM.34.0030	Pyruvate kinase, putative			2.51	
LmxM.11.1000	Pyruvate phosphate dikinase, putative			2.69	
LmxM.08_29.2160	rab-GDP dissociation inhibitor, putative	2.01		4.68	
LmxM.33.2820	Regulatory subunit of protein kinase a-like protein			2.00	
LmxM.15.0270	Replication factor A 28 kDa subunit, putative		2.92		
LmxM.15.0275	Ribonucleoprotein p18, mitochondrial precursor, putative				0.32
LmxM.08_29.1070	Ribosomal protein L1a, putative		0.47	2.47	

LmxM.21.1552	RNA helicase, putative			2.74		
LmxM.31.0750	RNA-binding protein, putative		7.97	9.84		
LmxM.25.0490	RNA-binding protein, putative, UPB1			40.00		
LmxM.11.0100	Seryl-tRNA synthetase, putative	2.31	3.23	7.77		
LmxM.14.0850	Small myristoylated protein-3, putative			4.08		
LmxM.07.0870	Splicing factor ptsr1-like protein			5.18		
LmxM.36.0070	Stress-inducible protein STI1 homolog		5.62			
LmxM.24.1630	Succinate dehydrogenase flavoprotein, putative				0.49	
LmxM.36.2950	Succinyl-CoA ligase [GDP-forming] β-chain, putative			3.94		
LmxM.25.2130	Succinyl-CoA synthetase α subunit, putative			2.96		
LmxM.32.2340	Succinyl-CoA:3-ketoacid-CoA transferase, mitochondrial precursor, putative			7.62		
LmxM.30.2020	Succinyl-diaminopimelate desuccinylase-like protein	0.22		2.53		
LmxM.04.0190	Surface antigen-like protein	0.16			0.09	
LmxM.05.1215	Surface antigen-like protein	0.07			0.05	
LmxM.21.1090	T-complex protein 1, Δ subunit, putative			3.38		
LmxM.34.3860	T-complex protein 1, η subunit, putative			2.57		
LmxM.23.1220	T-complex protein 1, γ subunit, putative			3.17		
LmxM.26.1570	Thimet oligopeptidase, putative, metallo-peptidase, Clan MA(E), Family M3			3.98		
LmxM.32.0240	Thiol-dependent reductase 1		2.29	5.66		
LmxM.29.2740	TPR domain protein, conserved			3.12		
LmxM.36.1430	Translation elongation factor 1-β, putative			5.43		
LmxM.17.1290	Translation initiation factor, putative			2.45		
LmxM.13.0280	α-Tubulin				0.20	
LmxM.08_29.1160	Tryparedoxin			2.78		
LmxM.26.0800	Type II (glutathione peroxidase-like) tryparedoxin peroxidase			16.86		
LmxM.34.3060	Ubiquitin-activating enzyme e1, putative			4.45		
LmxM.23.0550	Ubiquitin-activating enzyme e1, putative			2.49		
LmxM.32.2300	UDP-glc 4'-epimerase, putative		5.25	6.46		
LmxM.33.3670	Vacuolar ATP synthase catalytic subunit A, putative			2.66		
LmxM.23.1510	Vacuolar proton translocating ATPase subunit A, putative				0.36	
LmxM.30.1220	Vacuolar-type proton translocating pyrophosphatase 1, putative				0.39	
LmxM.29.3130	Valyl-tRNA synthetase, putative			3.11		
LmxM.21.0850	Xanthine phosphoribosyltransferase		4.50	5.47		
LmxM.01.0770	Unspecified product			2.73		
LmxM.04.0800	Unspecified product					0.20
LmxM.08.1171	Unspecified product				0.35	
LmxM.31.3650	Unspecified product			9.09		

Supplemental table III-1. Significantly modulated proteins in the *Δlmgt* promastigotes pre-fractionated with digitonin. Wild type and *Δlmgt* promastigotes was consecutively treated with 20 µM, 200 µM, 1mM, and 10 mM of digitonin to generate five sub-cellular fractions: two cytosolic, two organellar and one containing digitonin-insoluble material. The fraction proteins were extracted, digested with trypsin, stable isotope dimethyl labelled, combined and analyzed by 1D HPLC-ESI-MS/MS. The data were analyzed with Mascot Distiller. L/H - light/heavy ratio.

Mass	RT	Formula	Isomers	Putative metabolite	Confidence	Map	Pathway	WT	*Δlmgt*	*Δlmgt* t test
136.04	11.44	C4H8O5	3	**[FA trihydroxy(4:0)] 2,2,4-trihydroxy-butanoic acid**	5	Lipids: Fatty Acyls	Fatty Acids and Conjugates	**0.00**	**50.03**	0.03
169.05	16.43	C4H12NO4P	1	**Phosphodimethylethanolamine**	8	Lipid Metabolism	Glycerophospholipid metabolism	**0.00**	**19.87**	0.01
298.08	7.974	C16H14N2O2S	1	**Mefenacet**	7	0	0	**0.00**	**18.15**	0.04
164.05	4.787	C9H8O3	13	**Phenylpyruvate**	8	Amino Acid Metabolism	Phenylalanine metabolism Phenylalanine, tyrosine and tryptophan biosynthesis	1.00	**17.32**	0.01
92.047	11.46	C3H8O3	1	**Glycerol**	8	Carbohydrate Metabolism	Galactose metabolism Glycerolipid metabolism	1.00	**14.38**	0.02
185.03	17.44	C7H7NO5	1	**2-Amino-3-carboxymuconate semialdehyde**	8	Amino Acid Metabolism	Tryptophan metabolism	1.00	**13.55**	0.00
123.03	7.818	C6H5NO2	4	**Nicotinate**	10	Metabolism of Cofactors and Vitamins	Nicotinate and nicotinamide metabolism	1.00	**9.21**	0.01
141.02	18.37	C2H8NO4P	2	**Phosphoethanolamine**	10	Amino Acid Metabolism	Glycerophospholipid metabolism Sphingolipid metabolism	1.00	**9.14**	0.03
180.04	8.192	C9H8O4	11	**3-(4-Hydroxyphenyl) pyruvate**	8	Amino Acid Metabolism	Tyrosine metabolism Phenylalanine, tyrosine and tryptophan biosynthesis	1.00	**7.87**	0.01
260.2	4.032	C14H28O4	1	**[FA hydroxy(14:0)] 3,11-dihydroxy-tetradecanoic acid**	7	Lipids: Fatty Acyls	Fatty Acids and Conjugates	**0.00**	**7.84**	0.00
102.07	7.535	C5H10O2	9	**Pentanoate**	5	Lipids: Fatty Acyls	Fatty Acids and Conjugates	1.00	**7.41**	0.00
254.04	18.29	C7H14N2O4S2	1	**L-Djenkolic acid**	7	0	0	1.00	**6.72**	0.01
88.052	7.57	C4H8O2	8	**Butanoic acid**	8	Carbohydrate Metabolism	Butanoate metabolism	1.00	**5.49**	0.01
102.07	5.118	C5H10O2	9	**Ethyl propionate**	7	Lipids: Fatty Acyls	Fatty esters	1.00	**4.65**	0.00
130.06	4.783	C6H10O3	18	**Ethyl 3-oxobutanoate**	7	0	0	1.00	**4.39**	0.01
271.25	7.632	C16H33NO2	6	**[FA amino(16:0)] 2R-aminohexadecanoic acid**	7	Lipids: Fatty Acyls	Amino Fatty Acids	1.00	**4.05**	0.04
100.05	7.537	C5H8O2	18	**Tiglic acid**	5	Lipids: Fatty Acyls	Fatty Acids and Conjugates	1.00	**3.70**	0.00
131.06	16.55	C5H9NO3	14	**L-Glutamate 5-semialdehyde**	8	Amino Acid Metabolism	Arginine and proline metabolism	1.00	**3.41**	0.02
400.1	17.56	C14H20N6O4S2	1	**Ovothiol A disulfide**	5	0	0	1.00	**3.31**	0.01
111.04	12.67	C4H5N3O	1	**Cytosine**	10	Nucleotide Metabolism	Pyrimidine metabolism	1.00	**3.13**	0.00
205.07	8.079	C11H11NO3	5	**Indolelactate**	8	Amino Acid Metabolism	Tryptophan metabolism	1.00	**3.03**	0.01

200.98	19.6	C3H7NO5S2	1	**S-Sulfo-L-cysteine**	8	Amino Acid Metabolism	Cysteine metabolism	1.00	**2.93**	0.02
815.55	3.961	C47H78NO8P	17	**PE(42:8)**	5	Lipids: Glycerophospholipids	Glycerophospho-ethanolamines	1.00	**2.89**	0.04
189.04	7.647	C10H7NO3	6	**Kynurenate**	6	Amino Acid Metabolism	Tryptophan metabolism	1.00	**2.84**	0.01
132.08	5.055	C6H12O3	15	**[FA hydroxy(6:0)] 4-hydroxy-hexanoic acid**	5	Lipids: Fatty Acyls	Fatty Acids and Conjugates	1.00	**2.76**	0.00
129.08	14.17	C6H11NO2	9	**L-Pipecolate**	8	Amino Acid Metabolism	Lysine degradation	1.00	**2.41**	0.02
183.07	17.23	C5H14NO4P	1	**Choline phosphate**	10	Lipid Metabolism	Glycero phospholipid metabolism Glycine, serine and threonine metabolism	1.00	**2.35**	0.03
825.53	3.93	C48H76NO8P	3	**PC(18:4(6Z,9Z,12Z,15Z)/ 22:6(4Z,7Z,10Z,13Z, 16Z,19Z))**	7	Lipids: Glycerophospholipids	Glycerophospho-cholines	1.00	**2.34**	0.05
117.08	12.8	C5H11NO2	17	**Betaine**	10	Amino Acid Metabolism	Glycine, serine and threonine metabolism	1.00	**2.26**	0.01
118.06	7.528	C5H10O3	13	**5-Hydroxypentanoate**	5	Lipids: Fatty Acyls	Fatty Acids and Conjugates	1.00	**2.24**	0.01
126.04	13.4	C5H6N2O2	2	**Thymine**	6	Nucleotide Metabolism	Pyrimidine metabolism	1.00	**2.20**	0.02
330.26	3.722	C22H34O2	13	**[FA (22:5)] 7Z,10Z,13Z, 16Z,19Z-docosapenta enoic acid**	6	Lipids: Fatty Acyls	Biosynthesis of unsaturated fatty acids	1.00	**2.17**	0.03
328.24	3.708	C22H32O2	11	**Docosahexaenoicacid**	8	Lipids: Fatty Acyls	Biosynthesis of unsaturated fatty acids	1.00	**2.17**	0.01
145.04	12.35	C5H7NO4	2	**2-Oxoglutaramate**	8	Amino Acid Metabolism	Glutamate metabolism	1.00	**2.16**	0.00
787.61	3.881	C44H86NO8P	44	**PC(36:1)**	5	Lipids: Glycerophospholipids	Glycerophospho-cholines	1.00	**2.14**	0.01
161.07	10.74	C6H11NO4	10	**O-Acetyl-L-homoserine**	6	Amino Acid Metabolism	Methionine metabolism Sulfur metabolism	1.00	**2.13**	0.02
134.02	18.58	C4H6O5	4	**(S)-Malate**	10	Carbohydrate Metabolism	TCA cycle Glutamate metabolism Alanine and aspartate metabolism Pyruvate metabolism	1.00	**0.51**	0.00
771.61	3.873	C44H86NO7P	15	**[PC (18:1/18:0)] 1-(1Z-octadecenyl)-2-(9Z-octadecenoyl)-sn-glycero-3-phosphocholine**	5	Lipids: Glycerophospholipids	Glycerophospho-cholines	1.00	**0.49**	0.01
252.11	14.7	C19H32N6O10	3	**Asp-Lys-Asp-Gln**	7	Peptide(tetra-)	Basic peptide	1.00	**0.48**	0.03
133.04	14.31	C4H7NO4	4	**Iminodiacetate**	7	0	Nitrilotriacetate degradation	1.00	**0.48**	0.00
715.52	3.977	C39H74NO8P	27	**PE(34:2)**	5	Lipids: Glycerophospholipids	Glycerophospho-ethanolamines	1.00	**0.47**	0.00
755.55	3.977	C42H78NO8P	34	**PC(34:3)**	5	Lipids: Glycerophospholipids	Glycerophospho-cholines	1.00	**0.47**	0.00
739.52	3.865	C41H74NO8P	35	**PE(36:4)**	5	Lipids: Glycerophospholipids	Glycerophospho-ethanolamines	1.00	**0.46**	0.00

781.56	3.906	C44H80NO8P	52	**PC(36:4)**	7	Lipids: Glycerophospholipids	Glycerophospho-cholines	1.00	**0.46**	0.01
750.59	3.522	C52H78O3	2	**Nonaprenyl-4-hydroxybenzoate**	7	Metabolism of Cofactors and Vitamins	Ubiquinone-9 biosynthesis	1.00	**0.46**	0.01
523.36	4.581	C26H54NO7P	11	**[PC (18:0)] 1-octadecanoyl-sn-glycero-3-phosphocholine**	5	Lipids: Glycerophospholipids	Glycerophospho-cholines	1.00	**0.45**	0.01
729.53	4.018	C40H76NO8P	33	**PC(32:2)**	7	Lipids: Glycerophospholipids	Glycerophospho-cholines	1.00	**0.45**	0.00
521.35	4.679	C26H52NO7P	12	**1-Oleoylglycero phosphocholine**	5	0	0	1.00	**0.44**	0.01
837.55	3.58	C46H80NO10P	16	**PS(40:5)**	5	Lipids: Glycerophospholipids	Glycerophospho-serines	1.00	**0.43**	0.01
753.53	3.977	C42H76NO8P	41	**PC(34:4)**	5	Lipids: Glycerophospholipids	Glycerophospho-cholines	1.00	**0.43**	0.00
757.56	3.918	C42H80NO8P	53	**PC(34:2)**	5	Lipids: Glycerophospholipids	Glycerophospho-cholines	1.00	**0.41**	0.00
158.03	13.08	C5H6N2O4	3	**(S)-Dihydroorotate**	8	Nucleotide Metabolism	Pyrimidine metabolism	1.00	**0.41**	0.01
836.54	3.625	C43H81O13P	21	**PI(34:1)**	5	Lipids: Glycerophospholipids	Glycerophospho-inositols	1.00	**0.41**	0.01
808.51	3.693	C41H77O13P	15	**PI(32:1)**	5	Lipids: Glycerophospholipids	Glycerophospho-inositols	1.00	**0.38**	0.03
134.06	9.917	C5H10O4	8	**Deoxyribose**	8	Carbohydrate Metabolism	Pentose phosphate pathway	1.00	**0.37**	0.01
426.09	19.48	C13H22N4O8S2	2	**Asp-Cys-Cys-Ser**	5	Peptide(tetra-)	Acidic peptide	1.00	**0.36**	0.01
646.46	3.595	C35H67O8P	15	**PA(32:1)**	7	Lipids: Glycerophospholipids	Glycero phosphates	1.00	**0.36**	0.01
687.48	3.925	C37H70NO8P	20	**PE(32:2)**	5	Lipids: Glycerophospholipids	Glycerophospho-ethanolamines	1.00	**0.35**	0.00
476.16	17.49	C18H28N4O9S	2	**Asp-Met-Asp-Pro**	5	Peptide(tetra-)	Hydrophobic peptide	1.00	**0.34**	0.00
147.05	17.04	C5H9NO4	14	**L-Glutamate**	10	Amino Acid Metabolism	Arginine and proline metabolism Glutamate metabolism D-Glutamine and D-glutamate metabolism Glutathione metabolism	1.00	**0.32**	0.00
133.04	17.35	C4H7NO4	4	**L-Aspartate**	10	Amino Acid Metabolism	Alanine and aspartate metabolism Arginine and proline metabolism	1.00	**0.31**	0.00
674.49	3.592	C37H71O8P	19	**PA(34:1)**	5	Lipids: Glycerophospholipids	Glycero phosphates	1.00	**0.30**	0.00
703.52	4.047	C38H74NO8P	29	**PC(30:1)**	5	Lipids: Glycerophospholipids	Glycerophospho-cholines	1.00	**0.28**	0.00
834.53	3.659	C43H79O13P	21	**PI(34:2)**	5	Lipids: Glycerophospholipids	Glycerophospho-inositols	1.00	**0.27**	0.00
663.48	3.607	C35H70NO8P	30	**PE(30:0)**	5	Lipids: Glycerophospholipids	Glycerophospho-ethanolamines	1.00	**0.25**	0.00

691.51	3.566	C37H74NO8P	29	**PE(32:0)**	5	Lipids: Glycerophospholipids	Glycerophospho-ethanolamines	1.00	**0.25**	0.00
644.44	3.705	C35H65O8P	12	**PA(32:2)**	7	Lipids: Glycerophospholipids	Glycero phosphates	1.00	**0.25**	0.01
458.25	7.586	C43H82O16P2	5	**[GP (16:0/18:0)] 1-hexadecanoyl-2-(9Z-octadecenoyl)-sn-glycero-3-phospho-(1'-myo-inositol-3'-phosphate)**	7	Lipids: Glycerophospholipids	Glycerophospho-inositol monophosphates	1.00	**0.25**	0.01
467.3	4.932	C22H46NO7P	4	**[PC (14:0)] 1-tetradecanoyl-sn-glycero-3-phosphocholine**	5	Lipids: Glycerophospholipids	Glycerophospho-cholines	1.00	**0.24**	0.00
89.048	16.81	C3H7NO2	9	**L-Alanine**	10	Amino Acid Metabolism	Alanine and aspartate metabolism	1.00	**0.22**	0.00
705.53	4.029	C38H76NO8P	32	**PC(30:0)**	5	Lipids: Glycerophospholipids	Glycerophospho-cholines	1.00	**0.22**	0.00
422.08	18.44	C12H23O14P	5	**Lactose 6-phosphate**	8	Carbohydrate Metabolism	Galactose metabolism	1.00	**0.22**	0.01
699.48	4.063	C38H70NO8P	14	**PE(15:0/18:3(6Z, 9Z,12Z))**	5	Lipids: Glycerophospholipids	Glycerophospho-ethanolamines	1.00	**0.21**	0.02
701.5	4.031	C38H72NO8P	20	**PC(30:2)**	5	Lipids: Glycerophospholipids	Glycerophospho-cholines	1.00	**0.19**	0.01
307.08	16.85	C10H17N3O6S	3	**Glutathione**	10	Amino Acid Metabolism	Glutamate metabolism Cysteine metabolism Glutathione metabolism	1.00	**0.15**	0.04
677.5	4.06	C36H72NO8P	31	**PC(28:0)**	5	Lipids: Glycerophospholipids	Glycerophospho-cholines	1.00	**0.14**	0.00
118.03	17.64	C4H6O4	7	**Succinate**	10	Carbohydrate Metabolism	TCA cycle Oxidative phosphorylation Glutamate metabolism Alanine and aspartate metabolism	1.00	**0.11**	0.02
313.33	8.431	C20H43NO	1	**[SP amino,dimethyl (18:0)] 2-amino-14, 16-dimethyloctadecan-3-ol**	7	Lipids: Sphingolipids	Sphingoid bases	1.00	**0.07**	0.00
285.3	9.181	C18H39NO	1	**[SP] 1-deoxy-sphinganine**	7	Lipids: Sphingolipids	Sphingoid bases	1.00	**0.05**	0.00

Supplemental table III-2. Significantly modulated metabolites in the *Δlmgt* promastigotes. Wild type and *Δlmgt* promastigotes, wild type and *Δlmgt* promastigote spend media and fresh media (biological replicates, n=3) were subjected to quick quenching to 4°C, metabolite extraction with chloroform/methanol/wate (1:3:1), analysis of the extracts by 1D-pHILIC-HPLS-ESI-MS, and data analysis by IDEOM. Specified in yellow are the metabolites matched to authentic standards. Specified in red are the metabolites with more than one isomeric peak.

Mass	RT	Formula	Isomers	Putative metabolite	Confidence	Map	Pathway	WT	*Δlmgt*	*Δlmgt* t test
727.55	3.808	C41H78NO7P	16	**PE(18:1(11Z)/ P-18:1(11Z))**	7	Lipids: Glycerophospho lipids	Glycerophospho ethanolamines	**0.00**	**15.53**	0.00
164.05	4.787	C9H8O3	13	**Phenylpyruvate**	8	Amino Acid Metabolism	Phenylalanine metabolism Phenylalanine, tyrosine and tryptophan biosynthesis	**1.00**	**15.07**	0.01
222.09	4.135	C12H14O4	8	**Apiole**	5	0	0	1.00	**13.30**	0.00
123.03	7.818	C6H5NO2	4	**Nicotinate**	10	Metabolism of Cofactors and Vitamins	Nicotinate and nicotinamide metabolism Alkaloid biosynthesis	1.00	**9.73**	0.00
180.04	8.192	C9H8O4	11	**3-(4-Hydroxyphenyl) pyruvate**	8	Amino Acid Metabolism	Tyrosine metabolism Phenylalanine, tyrosine and tryptophan biosynthesis Alkaloid biosynthesis	1.00	**7.47**	0.00
170.09	4.301	C9H14O3	2	**Furfural diethyl acetal**	5	0	0	1.00	**7.21**	0.01
180.11	4.221	C11H16O2	6	**Olivetol**	5	0	0	1.00	**6.83**	0.02
226.1	7.719	C10H14N2O4	2	**Carbidopa**	5	0	0	1.00	**6.70**	0.04
341.16	5.073	C20H23NO4	6	**5,8,13,13a-Tetrahydro-columbamine**	5	Biosynthesis of Secondary Metabolites	Alkaloid biosynthesis I	1.00	**6.29**	0.02
264.1	4.148	C14H16O5	1	**1'-Acetoxyeugenol acetate**	5	0	0	1.00	**6.20**	0.02
187.12	5.135	C9H17NO3	3	**N-Heptanoylglycine**	7	0	0	1.00	**6.11**	0.02
224.14	4.25	C13H20O3	6	**[FA] Methyl jasmonate**	6	Lipids: Fatty Acyls	Octadecanoids	1.00	**5.85**	0.02
98.073	4.271	C6H10O	8	**3-Hexenal**	6	Lipids: Fatty Acyls	α-Linolenic acid metabolism	1.00	**5.62**	0.04
210.13	4.309	C12H18O3	6	**(3S,7S)-Jasmonic acid**	5	Lipids: Fatty Acyls	Octadecanoids	1.00	**5.56**	0.03
133.07	15.29	C5H11NO3	4	**1-deoxyxylono jirimycin**	7	0	0	1.00	**5.50**	0.01
168.08	4.448	C9H12O3	3	**1,3,5-trimethoxy benzene**	5	Biosynthesis of Secondary Metabolites	1,3,5-trimethoxy-benzene biosynthesis	1.00	**4.94**	0.05
133.07	7.603	C5H11NO3	4	**3-nitro-2-pentanol**	5	0	0	**0.00**	**4.33**	0.02
88.052	7.57	C4H8O2	8	**Butanoic acid**	8	Carbohydrate Metabolism	Butanoate metabolism	1.00	**4.26**	0.01
130.06	4.783	C6H10O3	18	**Ethyl 3-oxobutanoate**	7	0	0	1.00	**4.07**	0.00
102.07	7.535	C5H10O2	9	**Pentanoate**	5	Lipids: Fatty Acyls	Fatty Acids and Conjugates	1.00	**3.84**	0.03
216.15	7.56	C10H20N2O3	1	**Val-Val**	5	Peptide(di-)	Hydrophobic peptide	1.00	**3.54**	0.02
205.07	8.079	C11H11NO3	5	**Indolelactate**	8	Amino Acid Metabolism	Tryptophan metabolism	1.00	**3.52**	0.00
166.06	5.072	C9H10O3	17	**3-Methoxy-4-hydroxy phenylacetaldehyde**	8	Amino Acid Metabolism	Tyrosine metabolism	1.00	**3.26**	0.00

200.98	19.6	C3H7NO5S2	1	**S-Sulfo-L-cysteine**	8	Amino Acid Metabolism	Cysteine metabolism	1.00	**3.26**	0.00
244.09	7.563	C10H16N2O3S	1	**Biotin**	6	Metabolism of Cofactors and Vitamins	Biotin metabolism	1.00	**3.22**	0.04
100.05	7.537	C5H8O2	18	**Tiglic acid**	5	Lipids: Fatty Acyls	Fatty Acids and Conjugates	1.00	**2.69**	0.00
156.05	12.87	C6H8N2O3	4	**4-Imidazolone-5-propanoate**	6	Amino Acid Metabolism	Histidine metabolism	1.00	**2.67**	0.00
238.13	7.532	C24H36N4O6	3	**Ile-Phe-Thr-Pro**	7	Peptide(tetra-)	Hydrophobic peptide	1.00	**2.55**	0.02
102.07	5.118	C5H10O2	9	**Ethyl propionate**	7	Lipids: Fatty Acyls	Fatty esters	1.00	**2.49**	0.01
132.08	5.055	C6H12O3	15	**[FA hydroxy(6:0)] 4-hydroxy-hexanoic acid**	5	Lipids: Fatty Acyls	Fatty Acids and Conjugates	1.00	**2.49**	0.00
120.06	4.147	C8H8O	8	**Phenylacetaldehyde**	6	Amino Acid Metabolism	Phenylalanine metabolism	1.00	**2.32**	0.01
134.06	9.917	C5H10O4	8	**Deoxyribose**	8	Carbohydrate Metabolism	Pentose phosphate pathway	1.00	**2.29**	0.00
228.15	7.555	C11H20N2O3	3	**Leu-Pro**	5	Peptide(di-)	Hydrophobic peptide	1.00	**2.27**	0.04
182.06	9.909	C9H10O4	13	**3-(4-Hydroxyphenyl) lactate**	8	Amino Acid Metabolism	Tyrosine metabolism	1.00	**2.15**	0.00
161.07	10.74	C6H11NO4	10	**O-Acetyl-L-homoserine**	6	Amino Acid Metabolism	Methionine metabolism Sulfur metabolism	1.00	**2.01**	0.01
156.02	11.52	C5H4N2O4	2	**Orotate**	10	Nucleotide Metabolism	Pyrimidine metabolism	1.00	**0.48**	0.02
298.29	3.691	C19H38O2	25	**Nonadecanoicacid**	5	Lipids: Fatty Acyls	Fatty Acids and Conjugates	1.00	**0.47**	0.01
270.26	3.733	C17H34O2	30	**[FA (17:0)] heptadecanoic acid**	5	Lipids: Fatty Acyls	Fatty Acids and Conjugates	1.00	**0.44**	0.04
115.06	14.63	C5H9NO2	4	**L-Proline**	10	Amino Acid Metabolism	Arginine and proline metabolism	1.00	**0.37**	0.03
282.26	3.735	C18H34O2	57	**[FA (18:1)] 9Z-octadecenoic acid**	8	Lipids: Fatty Acyls	Fatty acid biosynthesis Biosynthesis of unsaturated fatty acids	1.00	**0.34**	0.00
89.048	16.81	C3H7NO2	9	**L-Alanine**	10	Amino Acid Metabolism	Alanine and aspartate metabolism Cysteine metabolism D-Alanine metabolism	1.00	**0.30**	0.02
81.982	17.37	H3O3P	1	**Phosphonate**	7	0	0	1.00	**0.22**	0.03
118.03	17.64	C4H6O4	7	**Succinate**	10	Carbohydrate Metabolism	TCA cycle Oxidative phosphorylation Glutamate metabolism Alanine and aspartate metabolism	1.00	**0.12**	0.02

Supplemental table III-3. Significantly modulated metabolites in the *Δlmgt* promastigote spent media. Specified in yellow are the metabolites matched to authentic standards. Specified in red are the metabolites with more than one isomeric peak.

Condition 1 – Wild type and *Δlmgt* promastigotes incubated in PBS without carbon sources

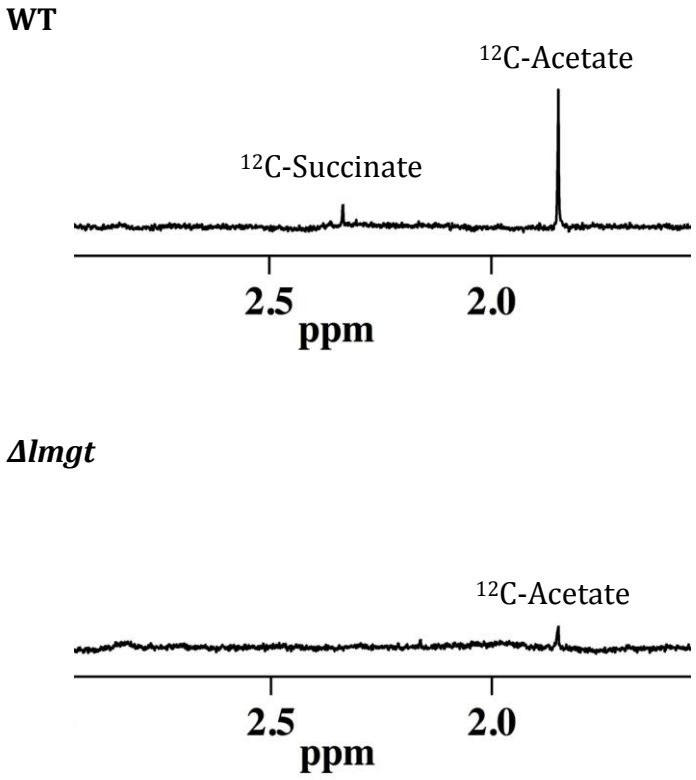

Supplemental figure III-1. ^{1}H NMR spectra of acetate nand succinate in the wild type (top spectrum) and *Δlmgt* promastigotes (bottom spectrum) incubated in PBS without carbon sources. Wild type and *Δlmgt* promastigotes (biological replicates, n=3) were incubated for 6 hours in PBS without carbon sources and analyzed by ^{1}H-NMR. The spectra are within the 1.5 – 3.0 ppm range and include the peaks of ^{12}C-acetate and ^{12}C-succinate in the wild type promastigotes (top spectrum) and of ^{12}C-acetate in the *Δlmgt* promastigotes (bottom spectrum). WT - wild type promastigotes, *Δlmgt* - *Δlmgt* promastigotes.

Condition 2 – Wild type and *Δlmgt* promastigotes incubated with ^{13}C-D-glucose

WT

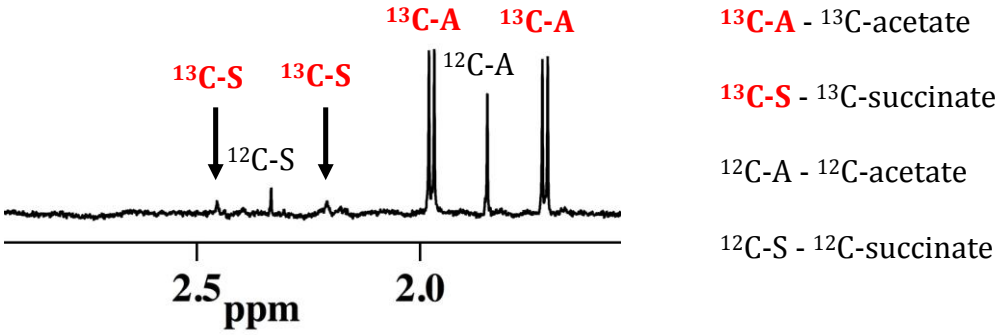

Δlmgt

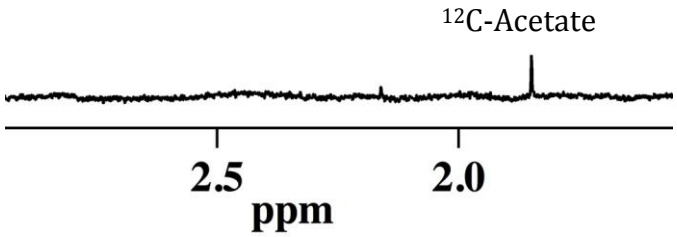

Supplemental figure III-2. ^{1}H NMR spectra of acetate and succinate in the wild type (top spectrum) and *Δlmgt* promastigotes (bottom spectrum) incubated in PBS with ^{13}C-D-glucose as a carbon source. Wild type and *Δlmgt* promastigotes (biological replicates, n=3) were incubated for 6 hours in PBS with ^{13}C-D-glucose as a carbon source and analyzed by ^{1}H-NMR. The spectra are within the 1.5 – 3.0 ppm range and include the peaks of ^{12}C-acetate, ^{13}C-acetate, ^{12}C-succinate and ^{13}C-succinate in the wild type promastigotes (top spectrum) and of ^{12}C-acetate in the *Δlmgt* promastigotes (bottom spectrum). WT - wild type promastigotes, *Δlmgt* - *Δlmgt* promastigotes.

Condition 3 – Wild type and *Δlmgt* promastigotes incubated in ^{12}C-L-proline and ^{13}C-D-glucose

WT

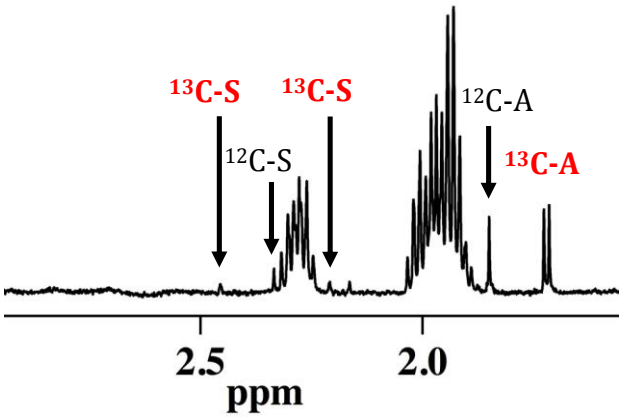

13C-A - ^{13}C-acetate

13C-S - ^{13}C-succinate

^{12}C-A - ^{12}C-acetate

^{12}C-S - ^{12}C-succinate

Δlmgt

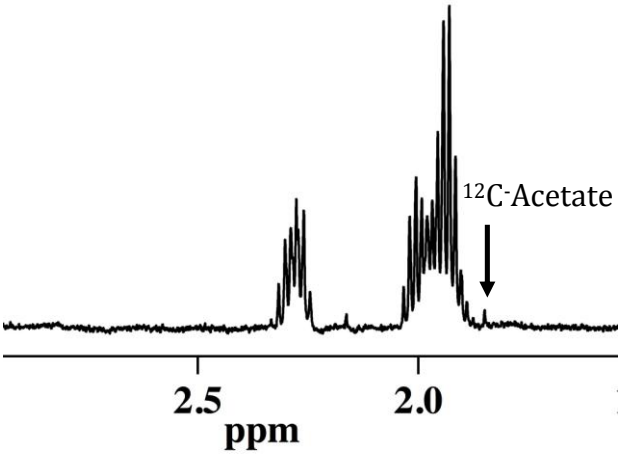

Supplemental figure III-3. ^{1}H NMR spectra of acetate and succinate in the wild type (top spectrum) and *Δlmgt* promastigotes (bottom spectrum) incubated in PBS with ^{12}C-L-proline and ^{13}C-D-glucose as carbon sources. Wild type and *Δlmgt* promastigotes (biological replicates, n=3) were incubated for 6 hours in PBS with ^{12}C-L-proline and ^{13}C-D-glucose as carbon sources and analyzed by ^{1}H-NMR. The spectra are within the 1.5 – 3.0 ppm range and include the peaks of ^{12}C-acetate, ^{13}C-acetate, ^{12}C-succinate and ^{13}C-succinate in the wild type promastigotes (top spectrum) and of ^{12}C-acetate in the *Δlmgt* promastigotes (bottom spectrum). WT - wild type promastigotes, *Δlmgt* - *Δlmgt* promastigotes.

Condition 4 – Wild type and *Δlmgt* promastigotes incubated with ^{12}C-D-glucose and ^{13}C-L-proline

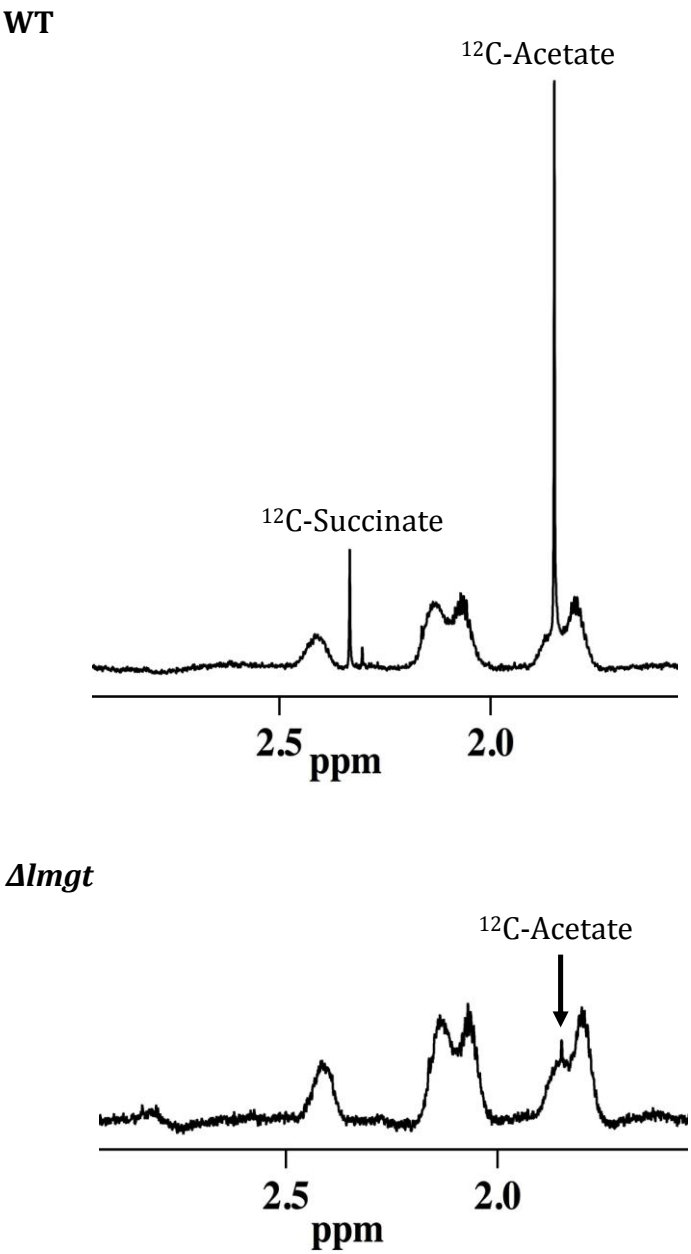

Supplemental figure III-4. ^{1}H NMR spectra of acetate and succinate in the wild type (top spectrum) and *Δlmgt* promastigotes (bottom spectrum) incubated in PBS with ^{12}C-D-glucose and ^{13}C-L-proline as carbon sources. Wild type and *Δlmgt* promastigotes (biological replicates, n=3) were incubated for 6 hours in PBS with ^{12}C-D-glucose and ^{13}C-L-proline as carbon sources and analyzed by ^{1}H-NMR. The spectra are within the 1.5 – 3.0 ppm range and include the peaks of ^{12}C-acetate and ^{12}C-succinate in the wild type promastigotes (top spectrum) and of ^{12}C-acetate in the *Δlmgt* promastigotes (bottom spectrum). WT - wild type promastigotes, *Δlmgt* - *Δlmgt* promastigotes.

Condition 5 – Wild type and *Δlmgt* promastigotes incubated with ^{13}C-L-proline

WT

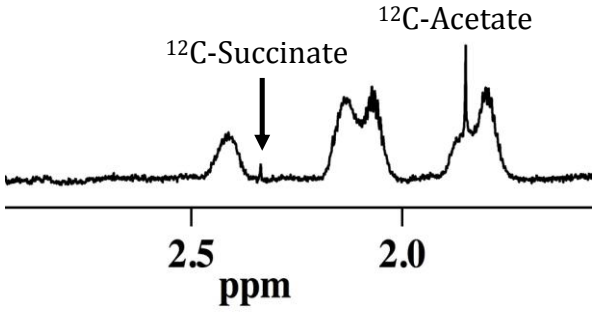

Δlmgt

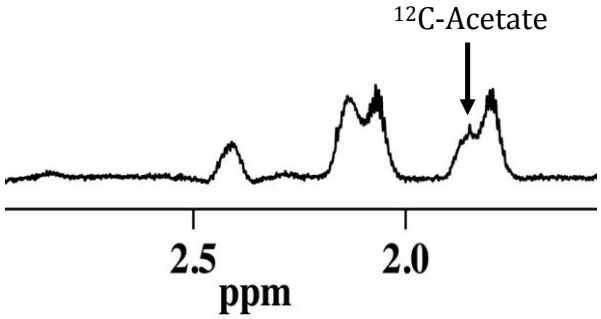

Supplemental figure III-5. ^{1}H NMR spectra of acetatate and succinate in the wild type (top spectrum) and *Δlmgt* promastigotes (bottom spectrum) incubated in PBS with ^{13}C-L-proline as a carbon source. Wild type and *Δlmgt* promastigotes (biological replicates, n=3) were incubated for 6 hours in PBS with ^{13}C-L-proline as a carbon source and analyzed by ^{1}H-NMR. The spectra are within the 1.5 – 3.0 ppm range and include the peaks of ^{12}C-acetate and ^{12}C-succinate in the wild type promastigotes (top spectrum) and of ^{12}C-acetate in the *Δlmgt* promastigotes (bottom spectrum). WT - wild type promastigotes, *Δlmgt* - *Δlmgt* promastigotes.

Condition 6 – Wild type and *Δlmgt* promastigotes incubated with ^{12}C-L-threonine and ^{13}C-D-glucose

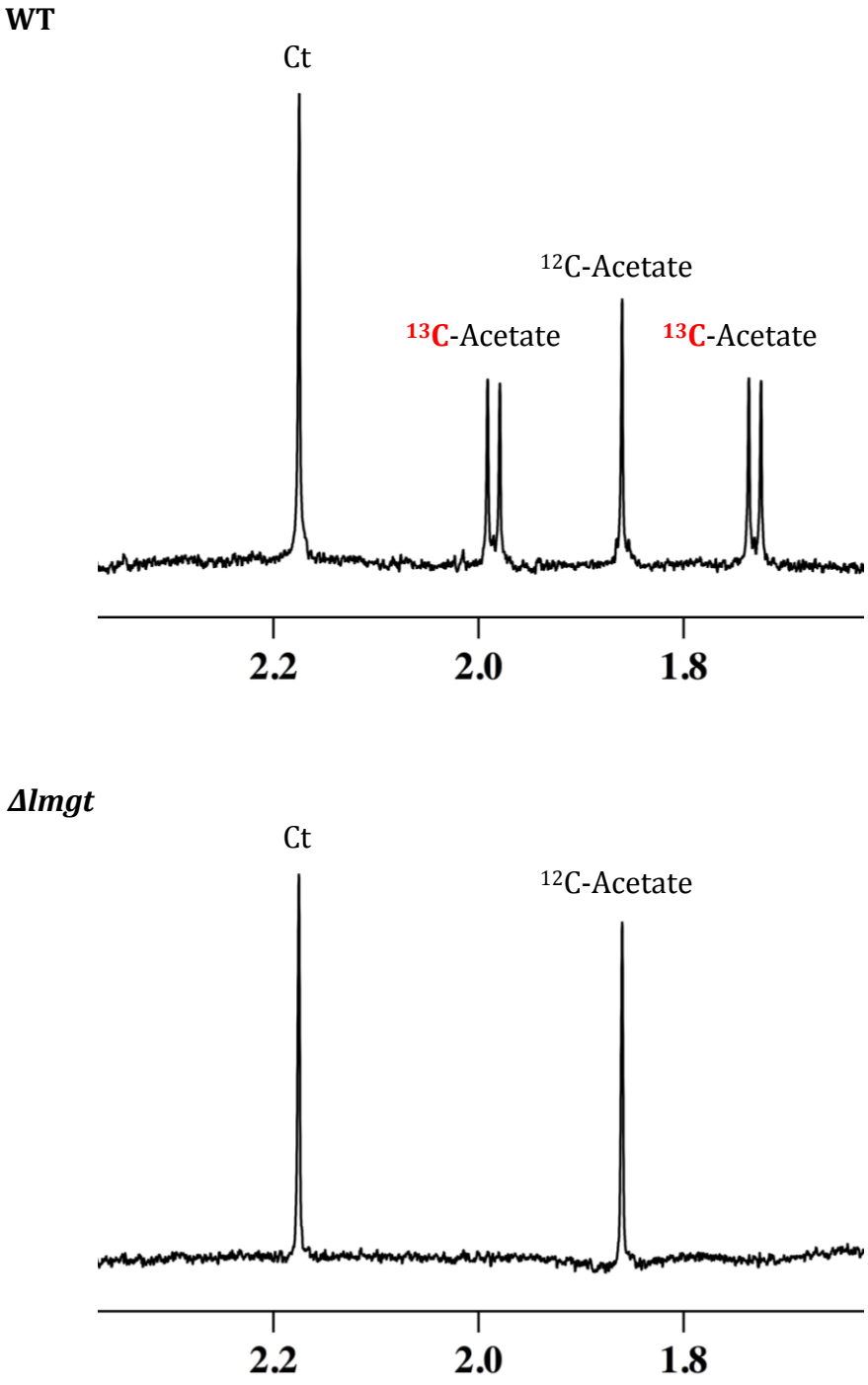

Supplemental figure III-6. ^{1}H NMR spectra of acetate and succinate in the wild type (top spectrum) and *Δlmgt* promastigotes (bottom spectrum) incubated in PBS with ^{12}C-L-threonine and ^{13}C-D-glucose carbon sources. Wild type and *Δlmgt* promastigotes (biological replicates, n=3) were incubated for 6 hours in PBS with ^{12}C-L-threonine and ^{13}C-D-glucose as carbon sources and analyzed by ^{1}H-NMR. The spectra are within the 1.6 – 2.4 ppm range and include the peaks of ^{12}C-acetate and ^{13}C-acetate in the wild type promastigotes (top spectrum) and of ^{12}C-acetate in the *Δlmgt* promastigotes (bottom spectrum). WT - wild type promastigotes, *Δlmgt* - *Δlmgt* promastigotes, Ct - contaminant.

Condition 7 – Wild type and *Δlmgt* promastigotes incubated with ^{12}C-D-glucose and ^{13}C-L-threonine

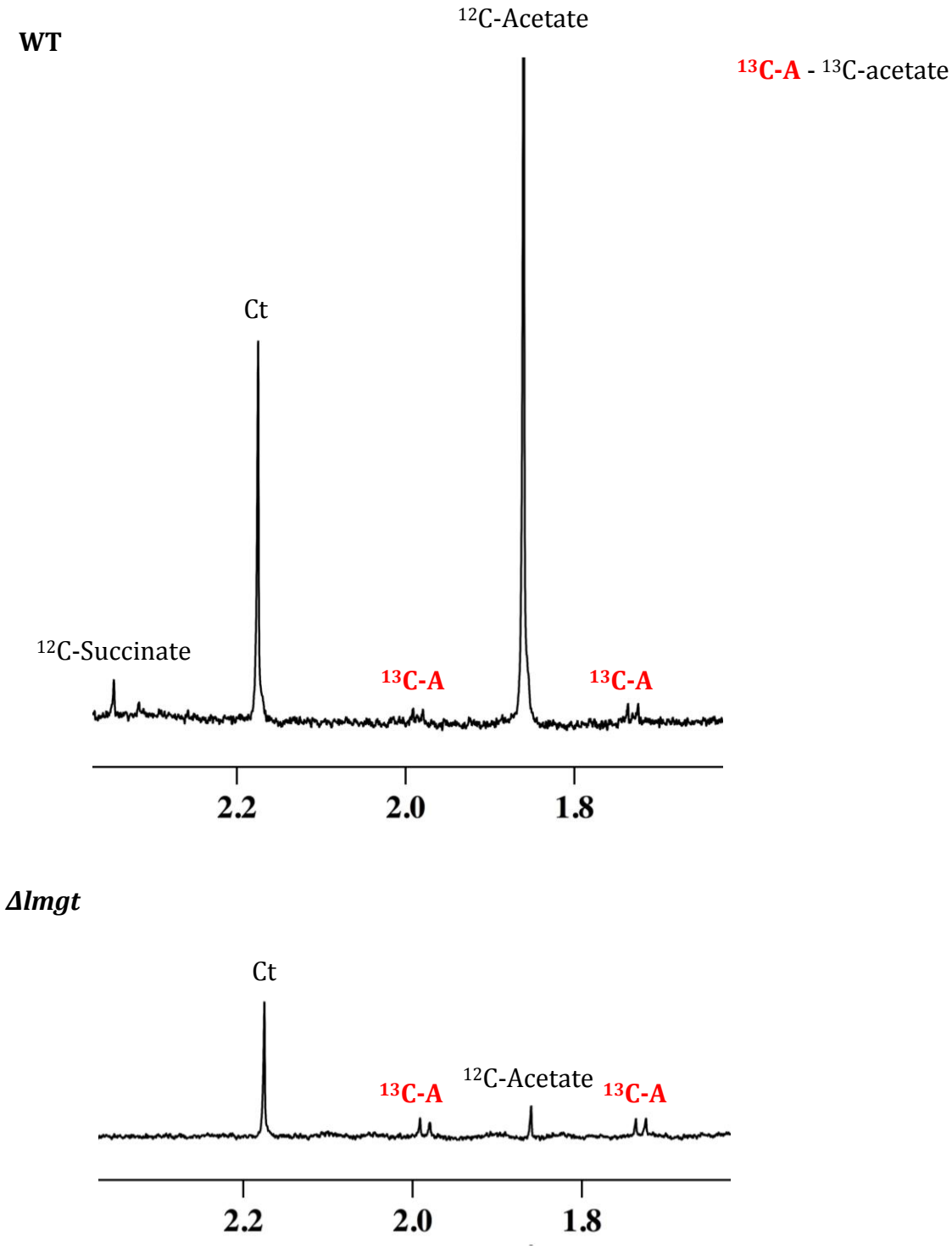

Supplemental figure III-7. ^{1}H NMR spectra of acetate and succinate in the wild type (top spectrum) and *Δlmgt* promastigotes (bottom spectrum) incubated in PBS with ^{12}C-D-glucose and ^{13}C-L-threonine as carbon sources. Wild type and *Δlmgt* promastigotes (biological replicates, n=3) were incubated for 6 hours in PBS with ^{12}C-D-glucose and ^{13}C-L-threonine as carbon sources and analyzed by ^{1}H-NMR. The spectra are within the 1.6 – 2.4 ppm range and include the peaks of ^{12}C-acetate, ^{13}C-acetate and ^{12}C-succinate in the wild type promastigotes (top spectrum) and of ^{12}C-acetate and ^{13}C-acetate in the *Δlmgt* promastigotes (bottom spectrum). WT - wild type promastigotes, *Δlmgt* - *Δlmgt* promastigotes, Ct - contaminant.

Condition 8 – Wild type and *Δlmgt* promastigotes incubated with ^{13}C-L-threonine

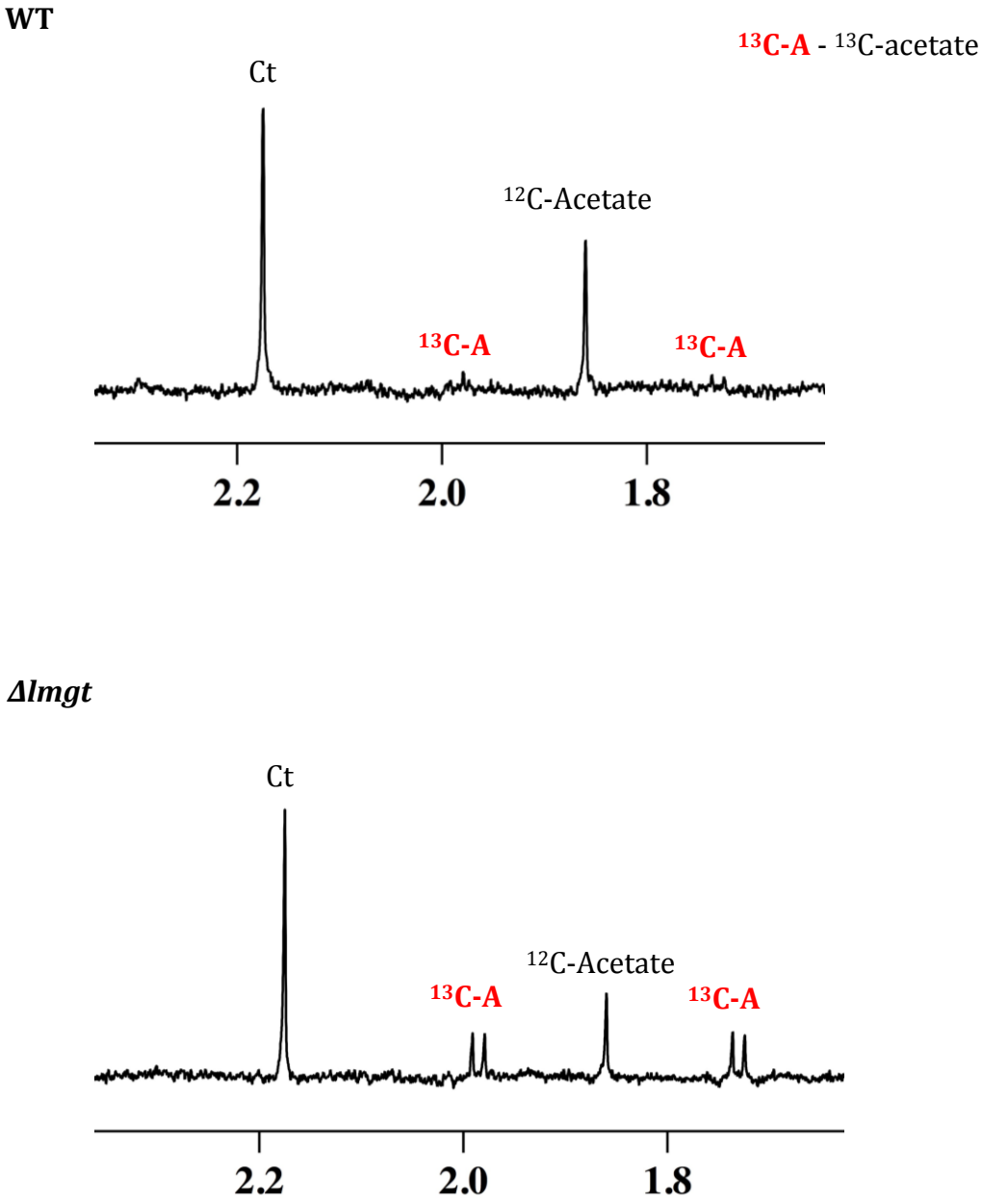

Supplemental figure III-8. ^{1}H NMR spectra of acetate and succinate in the wild type (top spectrum) and *Δlmgt* promastigotes (bottom spectrum) incubated in PBS with ^{13}C-L-threonine as a carbon source. Wild type and *Δlmgt* promastigotes (biological replicates, n=3) were incubated for 6 hours in PBS with ^{13}C-L-threonine as a carbon source and analyzed by ^{1}H-NMR. The spectra are within the 1.6 – 2.4 ppm range and include the peaks of ^{12}C-acetate and ^{13}C-acetate in the wild type promastigotes (top spectrum) and of ^{12}C-acetate and ^{13}C-acetate in the *Δlmgt* promastigotes (bottom spectra). WT - wild type promastigotes, *Δlmgt* - *Δlmgt* promastigotes, Ct - contaminant.

Condition 9 – Wild type and *Δlmgt* promastigotes incubated with ^{12}C-glycerol

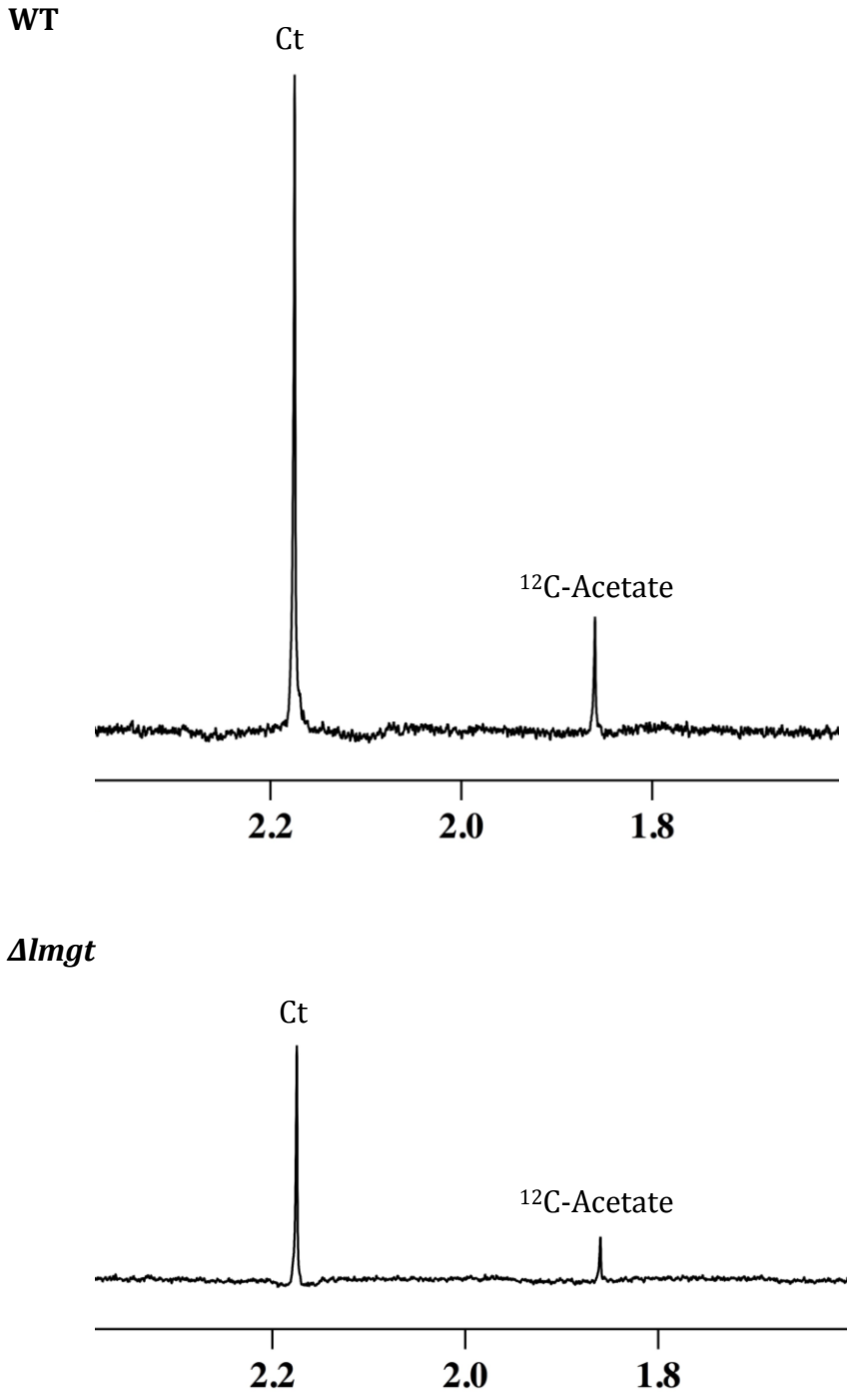

Supplemental figure III-9. ^{1}H NMR spectra of acetate and succinate in the wild type (top spectrum) and *Δlmgt* promastigotes (bottom spectrum) incubated in PBS with ^{12}C-glycerol. Wild type and *Δlmgt* promastigotes (biological replicates, n=3) were incubated for 6 hours in PBS with ^{12}C-glycerol as a carbon source and analyzed by ^{1}H-NMR. The spectra are within the 1.6 – 2.4 ppm range and include the peaks of ^{12}C-acetate in the wild type promastigotes (top spectrum) and of ^{12}C-acetate in *Δlmgt* promastigotes (bottom spectrum). WT - wild type promastigotes, *Δlmgt* - *Δlmgt* promastigotes, Ct - contaminant.

Condition 10 – Wild type and *Δlmgt* promastigotes incubated with ^{12}C-glycerol and ^{13}C-D-glucose

WT

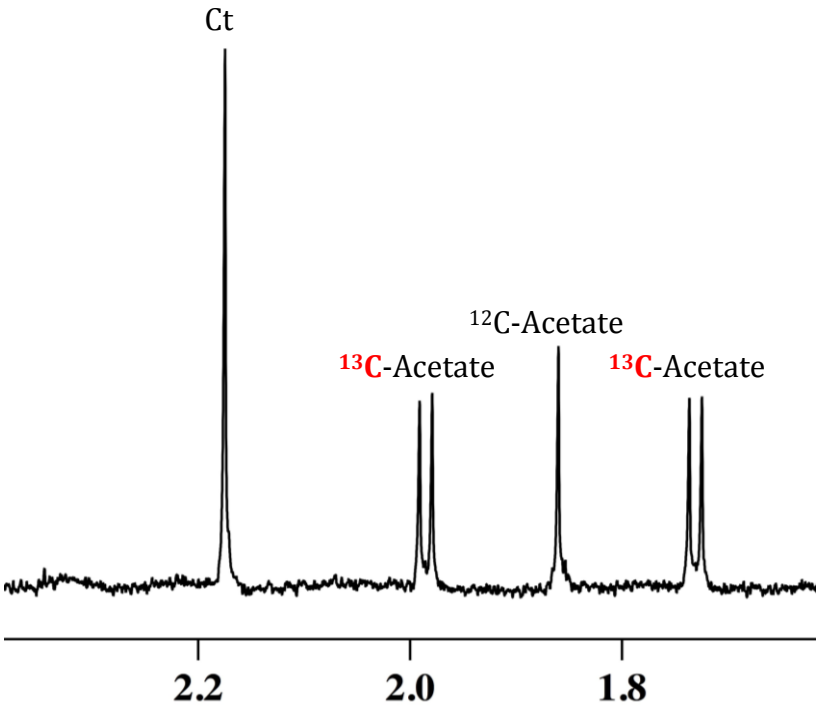

Δlmgt

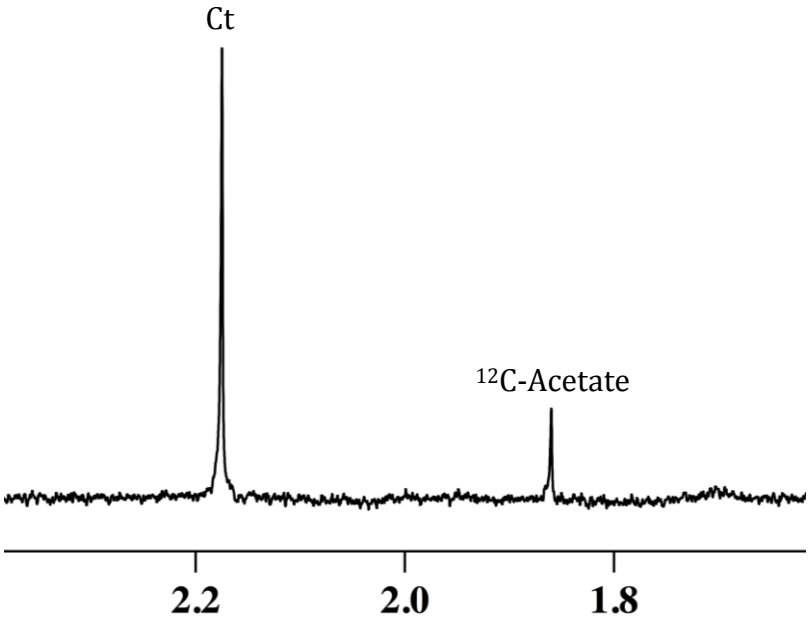

Supplemental figure III-10. ^{1}H NMR spectra of acetate and succinate in the wild type (top spectrum) and *Δlmgt* promastigotes (bottom spectrum) incubated in PBS with ^{12}C-glycerol and ^{13}C-D-glucose. Wild type and *Δlmgt* promastigotes (biological replicates, n=3) were incubated for 6 hours in PBS with ^{12}C-glycerol and ^{13}C-D-glucose as carbon sources and analyzed by ^{1}H-NMR. The spectra are within the 1.6 – 2.4 ppm range and include the peaks of ^{12}C-acetate and ^{13}C-acetate in the wild type promastigotes (top spectrum) and of ^{12}C-acetate in the *Δlmgt* promastigotes (bottom spectrum). WT - wild type promastigotes, *Δlmgt* - *Δlmgt* promastigotes, Ct - contaminant.

Appendix 2

Amino acid	Wild type promastigotes											*Δlmgt* peomastigotes										
	C0	C1	C2	C3	C4	C5	C6	C7	C8	C9	C10	C0	C1	C2	C3	C4	C5	C6	C7	C8	C9	C10
L-Alanine	+	-	+	+	-	+	+	-	-	-	+	-	-	-	-	+	+	-	-	-	-	-
L-Arginine	-	-	-	-	-	-	-	-	-	-	-	-	-	-	-	-	-	-	-	-	-	-
L-Asparagine	+	-	+	+	-	+	+	-	-	-	+	-	-	-	-	+	+	-	-	-	-	-
L-Aspartate	+	-	+	+	-	+	+	-	-	-	+	-	-	-	-	+	+	-	-	-	-	-
L-Citrulline	-	-	-	-	-	-	-	-	-	-	-	-	-	-	-	-	-	-	-	-	-	-
L-Cysteine	-	-	-	-	-	-	-	-	-	-	-	-	-	-	-	-	-	-	-	-	-	-
L-Glutamate	+	-	+	+	+	+	+	-	-	-	+	-	-	-	-	+	+	-	-	-	-	-
L-Glutamine	+	-	+	+	+	+	+	-	-	-	+	-	-	-	-	+	+	-	-	-	-	-
L-Histidine	-	-	-	-	-	-	-	-	-	-	-	-	-	-	-	-	-	-	-	-	-	-
L-Leucine	-	-	-	-	-	-	-	-	-	-	-	-	-	-	-	-	-	-	-	-	-	-
L-Lysine	-	-	-	-	-	-	-	-	-	-	-	-	-	-	-	-	-	-	-	-	-	-
Glycine	+	-	-	-	-	-	-	+	+	-	-	-	-	-	-	-	-	-	+	+	-	-
L-Methionine	+	-	-	-	-	-	-	-	-	-	-	-	-	-	-	-	-	-	-	-	-	-
L-Ornithine	-	-	-	-	-	-	-	-	-	-	-	-	-	-	-	-	-	-	-	-	-	-
L-	-	-	-	-	-	-	-	-	-	-	-	-	-	-	-	-	-	-	-	-	-	-
L-Proline	-	-	-	-	+	+	-	-	-	-	-	-	-	-	-	+	+	-	-	-	-	-
L-Serine	+	-	+	+	-	+	+	-	+	-	+	-	-	+	+	-	+	+	-	+	-	-
L-Threonine	-	-	-	-	-	-	-	+	+	-	-	-	-	-	-	-	-	-	+	+	-	-
L-Tryptophan	-	-	-	-	-	-	-	-	-	-	-	-	-	-	-	-	-	-	-	-	-	-
L-Tyrosine	-	-	-	-	-	-	-	-	-	-	-	-	-	-	-	-	-	-	-	-	-	-
L-valine	-	-	-	-	-	-	-	-	-	-	-	-	-	-	-	-	-	-	-	-	-	-

Supplemental table IV-1. Amino acids subjected to stable isotope tracing analysis. Presented here is a list of the amino acids investigated for stable isotope labelling in the wild type and *Δlmgt* promastigotes grown with ^{13}C-D-glucose for 48 hours (condition 0, C0) and the promastigotes grown under the 10 NMR conditions (C1 – C10). + - heavy-labelled, - -unlabelled.

Purine nucleotides	Wild type promastigotes										*Δlmgt* peomastigotes									
	C0	C1	C2	C3	C4	C5	C6	C7	C8	C9	C10	C0	C1	C2	C3	C4	C5	C6	C7	C8	C9	C10
Adenosine	+	N	N	N	N	N	N	N	N	N	N	N	N	N	N	N	N	N	N	N	N	N
Adenosine 5-monophosphate	+	-	+	+	-	+	+	-	-	-	+	-	-	-	-	+	+	+	-	-	-	-
Adenosine 5-diphosphate	+	-	+	+	-	+	+	-	-	-	+	-	-	-	-	+	+	+	-	-	-	-
Adenosine 5-triphosphate	+	-	+	+	-	+	+	-	-	-	+	-	-	-	-	+	+	+	-	-	-	-
Guanosine	+	N	N	N	N	N	N	N	N	N	N	N	N	N	N	N	N	N	N	N	N	N
Guanosine 5-monophosphate	+	-	+	+	-	+	+	-	-	-	+	-	-	-	-	+	+	+	-	-	-	-
Guanosine 5-monophosphate	+	-	+	+	-	+	+	-	-	-	+	-	-	-	-	+	+	+	-	-	-	-
Guanosine 5-monophosphate	+	-	+	+	-	+	+	-	-	-	+	-	-	-	-	+	+	+	-	-	-	-
Inosine 5-monophosphate	N	-	+	+	-	+	+	-	-	-	+	-	-	-	-	+	+	+	-	-	-	-

Supplemental table IV-2. Stable isotope tracing analysis of purine metabolism. Presented here is a list of the labelled purines in the wild type and *Δlmgt* promastigotes grown with ^{13}C-D-glucose for 48 hours (condition 0, C0) and the promastigotes grown under the 10 NMR conditions (C1 – C10). + - heavy-labelled, - -unlabelled, N - not detected.

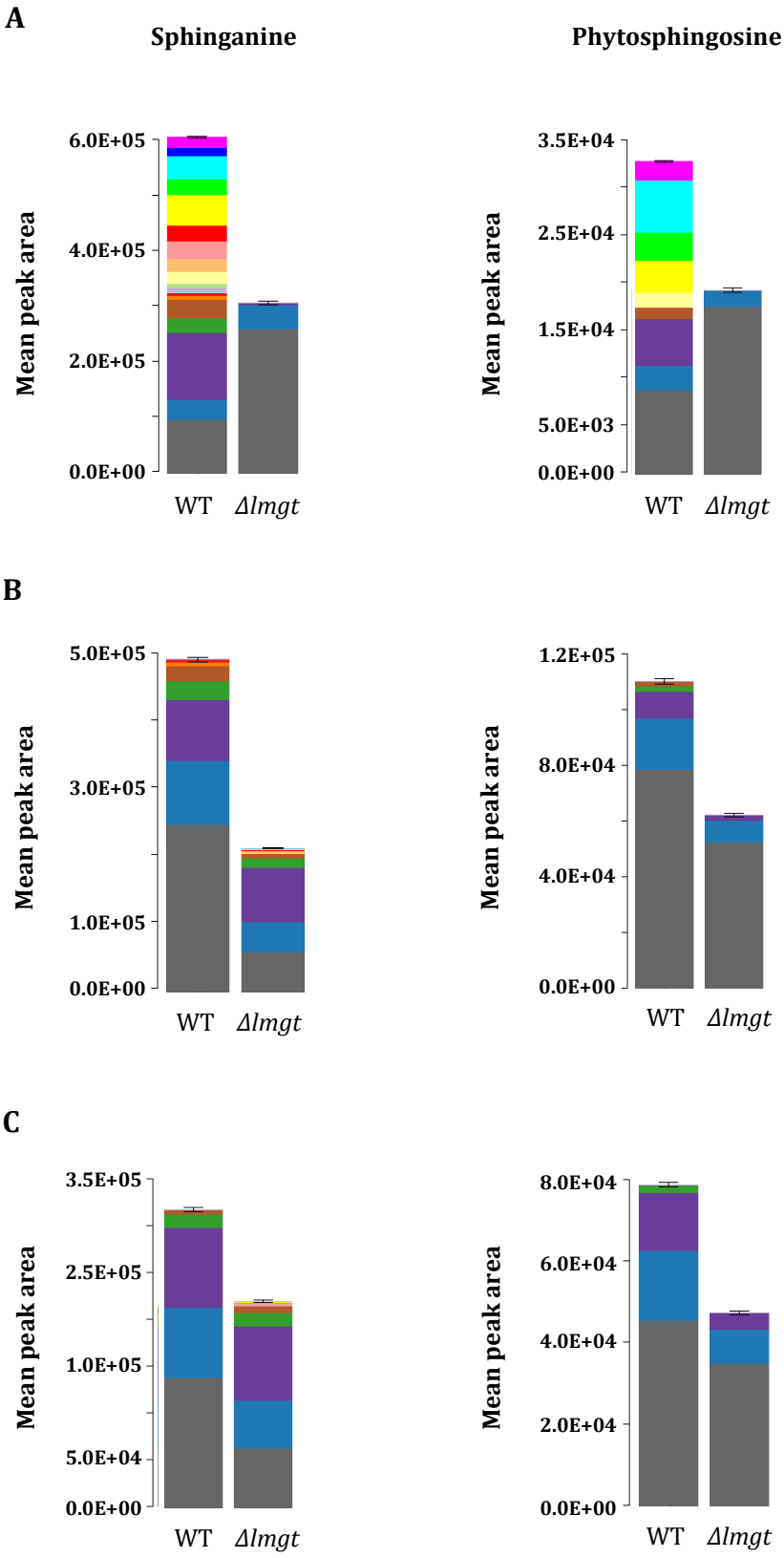

The figure continues on page 268.

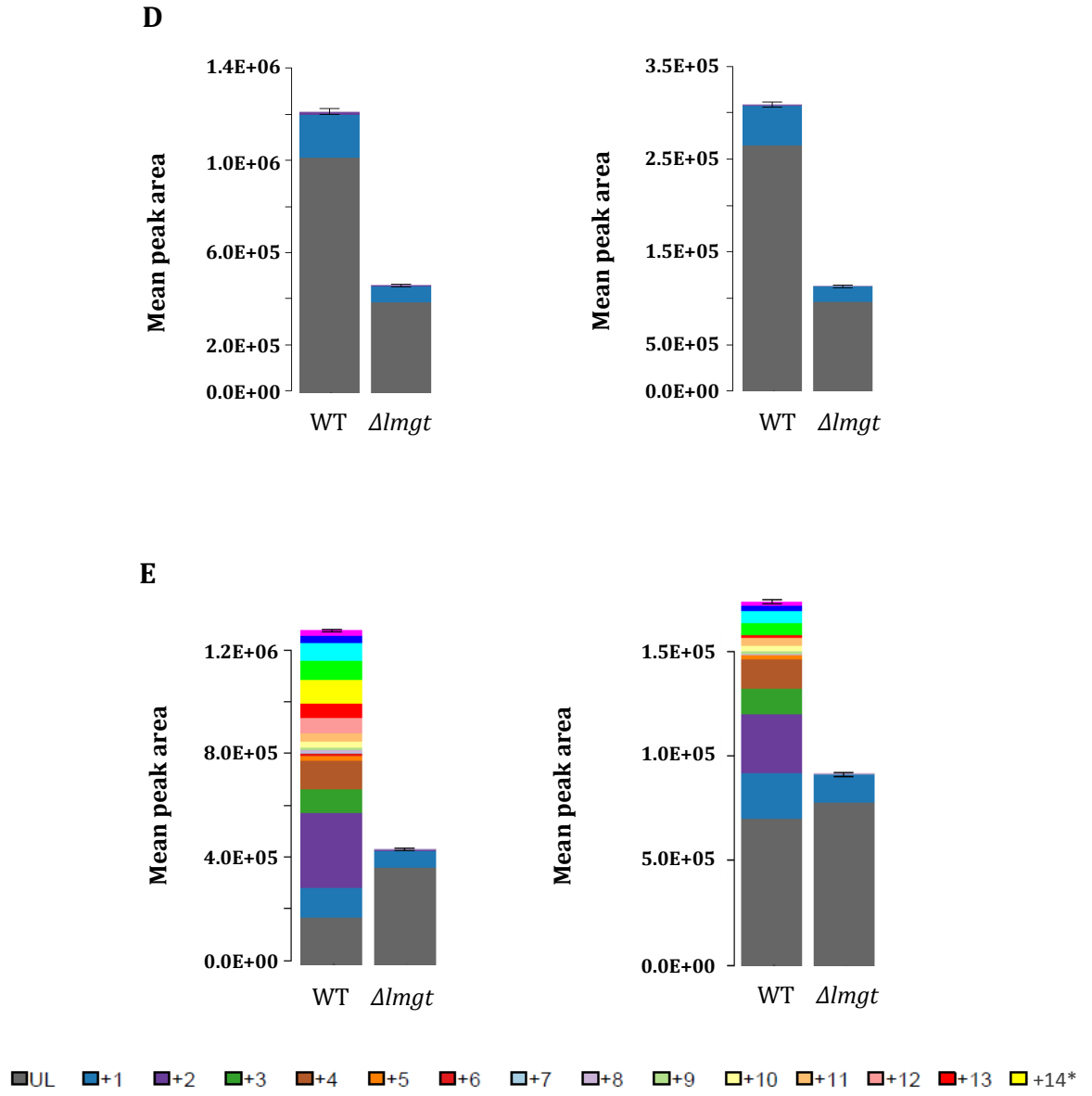

Supplemental figure IV-1. Labelling pattern of sphinganine and phytosphingosine in condition 6 (A), condition 7 (B), condition 8 (C), condition 9 (D) and condition 10 (E) wild type and *Δlmgt* promastigotes. UL- Unlabelled, +1 - 1-^{13}C-labelled, +2 - 2-^{13}C-labelled, +3 - 3-^{13}C-labelled, +4 - 4-^{13}C-labelled, +5 - 5-^{13}C-labelled, +6 - 6-^{13}C-labelled, +7 - 7-^{13}C-labelled, +8 - 8-^{13}C-labelled, +9 - 9-^{13}C-labelled, +10 - 10-^{13}C-labelled, +11 - 11-^{13}C-labelled, +12 - 12-^{13}C-labelled, +13 - 13-^{13}C-labelled, +14 - 14-^{13}C-labelled, WT – wild type promastigotes, *Δlmgt* - *Δlmgt* promastigotes. * - the colours corresponding to the type of labelling above +14 are not presented.

Appendix 3

Mass	RT	Formula	Isomers	Putative metabolite	Confidence	Map	Pathway	WT	*Δlmgt*	*Δlmgt* t test
149.11	8.9	C21H30O	1	**3-Methyl-19-nor-17alpha-pregna-1,3,5(10)-trien-17-ol**	7	0	0	**0.00**	**103.69**	0.04
750.6	3.43	C52H78O3	2	**Nonaprenyl-4-hydroxybenzoate**	7	Metabolism of Cofactors and Vitamins	Ubiquinone-9 biosynthesis	1.00	**20.28**	0.01
773.5	3.993	C44H72NO8P	8	**PC(18:4(6Z,9Z,12Z,15Z)/18:4(6Z,9Z,12Z,15Z))**	5	Lipids: Glycerophospholipids	Glycerophosphocholines	1.00	**5.99**	0.02
283.95	4.134	C6H12O4PCl3	1	**Tris(2-chloroethyl) phosphate**	5	0	0	1.00	**5.30**	0.04
555.52	3.83	C34H69NO4	1	**[SP hydroxy(16:0)] N-(hexadecanoyl)-4S-hydroxysphinganine**	5	Lipids: Sphingolipids	Ceramides	1.00	**3.53**	0.00
877.56	3.874	C52H80NO8P	3	**[PC (22:6/22:6)] 1,2-di-(4Z,7Z,10Z,13Z,16Z,19Z-docosahexaenoyl)-sn-glycero-3-phosphocholine**	5	Lipids: Glycerophospholipids	Glycerophosphocholines	1.00	**3.42**	0.00
148.07	7.284	C6H12O4	14	**[FA methyl, hydroxy(5:0)] 3R-methyl-3,5-dihydroxy-pentanoic acid**	8	Lipids: Fatty Acyls	Fatty Acids and Conjugates	1.00	**3.34**	0.05
775.52	3.964	C44H74NO8P	8	**PC(14:1(9Z)/22:6(4Z,7Z,10Z,13Z,16Z,19Z))**	5	Lipids: Glycerophospholipids	Glycerophosphocholines	1.00	**3.32**	0.01
112.05	7.477	C6H8O2	19	**Sorbate**	7	Lipids: Fatty Acyls	Fatty Acids and Conjugates	1.00	**3.24**	0.02
723.52	3.79	C41H74NO7P	15	**PE(18:3(6Z,9Z,12Z)/P-18:1(11Z))**	5	Lipids: Glycerophospholipids	Glycerophosphoethanolamines	1.00	**3.18**	0.04
825.53	3.901	C48H76NO8P	3	**PC(18:4(6Z,9Z,12Z,15Z)/22:6(4Z,7Z,10Z,13Z,16Z,19Z))**	5	Lipids: Glycerophospholipids	Glycerophosphocholines	1.00	**2.96**	0.03
139.99	10.15	C2H5O5P	2	**Acetyl phosphate**	6	Amino Acid Metabolism	Taurine and hypotaurine metabolism Pyruvate metabolism	1.00	**2.72**	0.02
96.969	10.14	[H2PO4]-	1	**Dihydrogenphosphate**	5	0	0	1.00	**2.63**	0.04
537.51	3.769	C34H67NO3	4	**[SP (16:0)] N-(hexadecanoyl)-sphing-4-enine**	5	Lipids: Sphingolipids	Ceramides	1.00	**2.52**	0.03
346.16	11.55	C12H22N6O6	1	**Asp-Gly-Arg**	7	Peptide(tri-)	Basic peptide	1.00	**2.42**	0.04
172.08	9.136	C7H12N2O3	2	**Glycylproline**	5	Peptide(di-)	Polar peptide	1.00	**0.50**	0.02
296.24	3.686	C18H32O3	40	**[FA (18:1)] 9R,10S-epoxy-12Z-octadecenoic acid**	6	Lipids: Fatty Acyls	Fatty Acids and Conjugates	1.00	**0.49**	0.03
256.24	3.612	C16H32O2	27	**Hexadecanoic acid**	6	Lipid Metabolism	Fatty acid biosynthesis Fatty acid elongation in mitochondria Fatty acid metabolism Biosynthesis of unsaturated fatty acids	1.00	**0.49**	0.03
175.1	11.1	C6H13N3O3	3	**L-Citrulline**	10	Amino Acid Metabolism	Arginine and proline metabolism	1.00	**0.49**	0.00
332.24	3.987	C21H32O3	19	**17α-Hydroxypregnenolone**	6	Lipids: Sterol lipids	C21-Steroid hormone metabolism	1.00	**0.49**	0.03

301.06	10.21	C8H16NO9P	9	**N-Acetyl-D-glucosamine 6-phosphate**	6	Amino Acid Metabolism	Glutamate metabolism Aminosugars metabolism	1.00	**0.48**	0.04
246.09	8.652	C9H14N2O6	2	**5-6-Dihydrouridine**	5	0	0	1.00	**0.48**	0.03
781.56	3.941	C44H80NO8P	52	**PC(36:4)**	7	Lipids: Glycerophospholipids	Glycerophosphocholines	1.00	**0.48**	0.05
298.25	3.782	C18H34O3	63	**2-Oxooctadecanoic acid**	5	Lipids: Fatty Acyls	Fatty Acids and Conjugates	1.00	**0.48**	0.04
174.1	10.75	C7H14N2O3	5	**N-Acetylornithine**	8	Amino Acid Metabolism	Arginine and proline metabolism	1.00	**0.47**	0.04
142.07	9.921	C6H10N2O2	1	**Ectoine**	8	Amino Acid Metabolism	Glycine, serine and threonine metabolism	1.00	**0.47**	0.05
566.05	10.84	C15H24N2O17P2	3	**UDP-glucose**	6	Carbohydrate Metabolism	Pentose and glucuronate interconversions Galactose metabolism Ascorbate and aldarate metabolism Pyrimidine metabolism Starch and sucrose metabolism Nucleotide sugars metabolism Glycerolipid metabolism	1.00	**0.47**	0.02
234.2	4.173	C16H26O	6	**[FA (16:3)] 4,6,11-hexadecatrienal**	5	Lipids: Fatty Acyls	Fatty aldehydes	1.00	**0.47**	0.04
97.016	7.054	C4H3NO2	1	**Maleimide**	5	0	0	1.00	**0.46**	0.01
130.03	10.5	C5H6O4	7	**Mesaconate**	6	Carbohydrate Metabolism	C5-Branched dibasic acid metabolism	1.00	**0.46**	0.03
275.15	10.89	C11H21N3O5	6	**L-a-glutamyl-L-Lysine**	5	Peptide(di-)	Basic peptide	1.00	**0.45**	0.03
607.08	10.17	C17H27N3O17P2	3	**UDP-N-acetyl-D-glucosamine**	6	Carbohydrate Metabolism	Aminosugars metabolism Lipopolysaccharide biosynthesis Peptidoglycan biosynthesis	1.00	**0.45**	0.02
458.34	4.19	C29H46O4	7	**[ST (2:0)] (5Z,7E)-(1S,3R)-18-acetoxy-9,10-seco-5,7,10(19)-cholestatriene-1,3-diol**	5	Lipids: Sterol lipids	Secosteroids	1.00	**0.45**	0.02
426.31	4.272	C28H42O3	9	**[ST (5:0/3:0)] (5Z,7E,22E,24E)-(1S,3R)-24a-homo-9,10-seco-5,7,10(19),22,24-cholestapentaene-1,3,25-triol**	5	Lipids: Sterol lipids	Secosteroids	1.00	**0.45**	0.04
408.3	4.153	C28H40O2	1	**4Z,7Z,10Z,13Z,16Z,19Z,22Z,25Z-octacosaoctaenoic acid**	7	Lipids: Fatty Acyls	Fatty Acids and Conjugates	1.00	**0.44**	0.03
133.07	11.11	C5H11NO3	4	**N-hydroxyvaline**	5	0	Superpathway of linamarin and lotaustralin biosynthesis	1.00	**0.44**	0.01
130.07	15.06	C5H10N2O2	4	**Casein K**	5	0	0	1.00	**0.44**	0.02
440.33	4.269	C29H44O3	11	**[ST (3:0)] (5Z,7E)-(1S,3R,11S)-11-ethynyl-9,10-seco-5,7,10(19)-cholestatriene-1,3,25-triol**	5	Lipids: Sterol lipids	Secosteroids	1.00	**0.44**	0.02
300.27	3.647	C18H36O3	27	**[FA hydroxy(18:0)] 2S-hydroxy-octadecanoic acid**	5	Lipids: Fatty Acyls	Fatty Acids and Conjugates	1.00	**0.43**	0.03

173.12	15.19	C7H15N3O2	2	**L-Indospicine**	7	0	0	1.00	**0.43**	0.01
245.15	11.17	C9H19N5O3	2	**β-Alanyl-L-arginine**	6	Amino Acid Metabolism	β-Alanine metabolism	1.00	**0.43**	0.02
113.94	14.08	H2O3S2	1	**$H_2S_2O_3$**	5	0	Sulfur metabolism	1.00	**0.42**	0.03
480.32	4.287	C24H49O7P	1	**PA(21:0/0:0)**	5	Lipids: Glycerophospholipids	Glycerophosphates	1.00	**0.42**	0.02
207.14	13.94	C20H38N4O5	8	**Ala-Leu-Leu-Val**	7	Peptide(tetra-)	Hydrophobic peptide	1.00	**0.42**	0.05
290.04	10.78	C7H15O10P	6	**D-Sedoheptulose 7-phosphate**	6	Carbohydrate Metabolism	Pentose phosphate pathway Carbon fixation	1.00	**0.42**	0.01
132.05	10.79	C4H8N2O3	6	**L-Asparagine**	8	Amino Acid Metabolism	Alanine and aspartate metabolism	1.00	**0.42**	0.01
132.09	15.04	C5H12N2O2	6	**L-Ornithine**	8	Amino Acid Metabolism	Arginine and proline metabolism D-Arginine and D-ornithine metabolism Glutathione metabolism	1.00	**0.42**	0.02
148.04	10.37	C5H8O5	18	**D-Xylonolactone**	6	Carbohydrate Metabolism	Pentose and glucuronate interconversions	1.00	**0.41**	0.03
360.64	12.7	C27H47N9O10S2	1	**Trypanothione disulfide**	8	Amino Acid Metabolism	Glutathione metabolism	1.00	**0.41**	0.01
404	11.15	C9H14N2O12P2	1	**UDP**	6	Nucleotide Metabolism	Pyrimidine metabolism Peptidoglycan biosynthesis Zeatin biosynthesis	1.00	**0.40**	0.04
159.1	15.96	C6H13N3O2	1	**Δ-Guanidinovaleric acid**	7	0	0	1.00	**0.40**	0.01
182.06	7.507	C9H10O4	13	**3-(4-Hydroxyphenyl) lactate**	8	Amino Acid Metabolism	Tyrosine metabolism	1.00	**0.40**	0.01
226.19	4.104	C14H26O2	35	**(9Z)-Tetradecenoic acid**	7	Lipids: Fatty Acyls	Fatty Acids and Conjugates	1.00	**0.40**	0.04
217.11	8.961	C8H15N3O4	3	**N-Acetyl-L-citrulline**	6	Amino Acid Metabolism	Arginine biosynthesis III	1.00	**0.40**	0.04
119.06	10.49	C4H9NO3	11	**L-Threonine**	10	Amino Acid Metabolism	Glycine, serine and threonine metabolism Valine, leucine and isoleucine biosynthesis	1.00	**0.39**	0.02
757.56	3.956	C42H80NO8P	53	**PC(34:2)**	5	Lipids: Glycerophospholipids	Glycerophosphocholines	1.00	**0.39**	0.05
183.05	7.151	C8H9NO4	6	**4-Pyridoxate**	6	Metabolism of Cofactors and Vitamins	Vitamin B6 metabolism	1.00	**0.39**	0.01
161.07	7.509	C6H11NO4	10	**O-Acetyl-L-homoserine**	8	Amino Acid Metabolism	Methionine metabolism Sulfur metabolism	1.00	**0.38**	0.04
166.06	4.769	C9H10O3	17	**3-(3-Hydroxy-phenyl)-propanoic acid**	6	Amino Acid Metabolism	Phenylalanine metabolism	1.00	**0.38**	0.04
244.11	10.17	C10H16N2O5	2	**Glu-Pro**	5	Peptide(di-)	Acidic peptide	1.00	**0.38**	0.00
192.07	9.453	C6H12N2O5	1	**Ser-Ser**	5	Peptide(di-)	Polar peptide	1.00	**0.38**	0.04
176.08	15.02	C6H12N2O4	4	**Ala-Ser**	5	Peptide(di-)	Polar peptide	1.00	**0.38**	0.01

405.14	11.36	C15H23N3O10	1	**Glu-Glu-Glu**	5	Peptide(tri-)	Acidic peptide	1.00	**0.37**	0.01
231.16	15.56	C10H21N3O3	1	**Gamma-Aminobutyryl-lysine**	7	0	0	1.00	**0.37**	0.04
89.048	10.77	C3H7NO2	9	**L-Alanine**	10	Amino Acid Metabolism	Alanine and aspartate metabolism	1.00	**0.37**	0.00
434.24	4.589	C21H39O7P	3	**LPA(0:0/18:2(9Z,12Z))**	5	Lipid Metabolism	Glycerolipid metabolism Glycerophospholipid metabolism	1.00	**0.37**	0.01
189.06	9.716	C7H11NO5	4	**N-Acetyl-L-glutamate**	10	Amino Acid Metabolism	Arginine and proline metabolism	1.00	**0.36**	0.03
327.22	4.733	C16H29N3O4	2	**Leu-Val-Pro**	5	Peptide(tri-)	Hydrophobic peptide	1.00	**0.36**	0.03
303.15	10.88	C11H21N5O5	1	**Glu-Arg**	5	Peptide(di-)	Basic peptide	1.00	**0.35**	0.04
156.02	8.203	C5H4N2O4	2	**Orotate**	8	Nucleotide Metabolism	Pyrimidine metabolism	1.00	**0.35**	0.02
260.03	11.06	C6H13O9P	46	**D-Glucose 6-phosphate**	10	Carbohydrate Metabolism	Starch and sucrose metabolism Inositol phosphate metabolism	1.00	**0.35**	0.01
145.09	10.95	C5H11N3O2	3	**4-Guanidinobutanoate**	8	Amino Acid Metabolism	Arginine and proline metabolism	1.00	**0.35**	0.00
353.23	4.639	C20H33O5	2	**13,14-Dihydro- lipoxin A4**	7	0	0	1.00	**0.34**	0.04
126.12	12.41	C7H14N2	2	**1-5-diazabicyclononane**	7	Amino Acid Metabolism	β-Alanine biosynthesis I	1.00	**0.34**	0.02
519.33	4.596	C26H50NO7P	3	**[PC (18:2)] 1-(9Z,12Z-octadecadienoyl)-sn-glycero-3-phosphocholine**	5	Lipids: Glycerophospholipids	Glycerophosphocholines	1.00	**0.34**	0.03
205.07	7.161	C11H11NO3	5	**Indolelactate**	6	Amino Acid Metabolism	Tryptophan metabolism	1.00	**0.32**	0.02
244.07	9.627	C9H12N2O6	3	**Pseudouridine**	6	Nucleotide Metabolism	Pyrimidine metabolism	1.00	**0.32**	0.03
118.03	10.41	C4H6O4	7	**Succinate**	10	Carbohydrate Metabolism	TCA cycle Oxidative phosphorylation Glutamate metabolism Alanine and aspartate metabolism	1.00	**0.32**	0.02
358.2	10.71	C14H26N6O5	1	**Pro-Ser-Arg**	5	Peptide(tri-)	Basic peptide	1.00	**0.32**	0.03
167.98	11.51	C3H5O6P	3	**Phosphoenolpyruvate**	8	Carbohydrate Metabolism	Glycolysis / Gluconeogenesis TCA cycle Pyruvate metabolism	1.00	**0.31**	0.01
210.06	7.318	C9H10N2O4	1	**N-carbamoyl-p-hydroxy-D-phenylglycine**	5	0	0	1.00	**0.31**	0.00
179.08	12.38	C7H9N5O	2	**7-Aminomethyl-7-carbaguanine**	5	0	0	1.00	**0.31**	0.01
264.15	4.519	C14H20N2O3	2	**Phe-Val**	5	Peptide(di-)	Hydrophobic peptide	1.00	**0.31**	0.01
320.2	3.931	C19H28O4	4	**Ubiquinol-2**	5	Metabolism of Cofactors and Vitamins	Oxidative phosphorylation	1.00	**0.31**	0.04
155.03	10.18	C3H10NO4P	3	**N-Methylethanolamine phosphate**	6	Lipid Metabolism	Glycerophospholipid metabolism	1.00	**0.31**	0.01

341.13	11.82	C12H23NO10	2	**Lactosamine**	8	Carbohydrate Metabolism	Aminosugars metabolism	1.00	**0.30**	0.00
250.03	4.186	C12H10O4S	1	**4,4'-Sulfonyldiphenol**	5	0	0	1.00	**0.30**	0.00
479.3	4.447	C23H46NO7P	6	**[PE (18:1)] 1-(9Z-octadecenoyl)-sn-glycero-3-phosphoethanolamine**	5	Lipids: Glycerophospholipids	Glycerophosphoethanolamines	1.00	**0.30**	0.03
226.11	10.9	C9H14N4O3	3	**Ala-His**	5	Peptide(di-)	Basic peptide	1.00	**0.30**	0.03
427.03	10.55	C10H15N5O10P2	6	**dGDP**	6	Nucleotide Metabolism	Purine metabolism	1.00	**0.30**	0.03
164.01	7.492	C5H8O4S	1	**2-mercaptoglutarate**	5	0	0	1.00	**0.30**	0.03
208.05	11.04	C6H12N2O4S	2	**Cys-Ser**	7	Peptide(di-)	Polar peptide	1.00	**0.30**	0.04
384.13	11.59	C14H24O12	1	**Acetyl-maltose**	5	0	0	1.00	**0.29**	0.01
573.09	9.021	C16H25N5O14P2	1	**GDP-3,6-dideoxy-D-galactose**	7	0	GDP-L-colitose biosynthesis	1.00	**0.28**	0.04
134.02	10.95	C4H6O5	4	**(S)-Malate**	10	Carbohydrate Metabolism	TCA cycle Glutamate metabolism Alanine and aspartate metabolism Pyruvate metabolism Carbon fixation	1.00	**0.28**	0.03
201.12	11.72	C18H34N4O6	9	**Ala-Leu-Leu-Ser**	7	Peptide(tetra-)	Hydrophobic peptide	1.00	**0.27**	0.02
116.01	10.81	C4H4O4	3	**Fumarate**	10	Carbohydrate Metabolism	TCA cycle Oxidative phosphorylation Arginine and proline metabolism Glutamate metabolism Alanine and aspartate metabolism	1.00	**0.27**	0.01
487.68	12.03	C40H53N11O18	1	**5-Methyltetrahydropteroylpentaglutamate**	7	0	0	1.00	**0.27**	0.01
174.06	8.671	C6H10N2O4	4	**N-Formimino-L-glutamate**	6	Amino Acid Metabolism	Histidine metabolism	1.00	**0.26**	0.02
252.09	7.559	C10H12N4O4	2	**Deoxyinosine**	6	Nucleotide Metabolism	Purine metabolism	1.00	**0.26**	0.02
326.16	10.9	C14H22N4O5	2	**Asn-Pro-Pro**	5	Peptide(tri-)	Polar peptide	1.00	**0.25**	0.03
400.1	10.24	C14H20N6O4S2	1	**Ovothiol A disulfide**	5	0	0	1.00	**0.23**	7.05E
166.06	7.023	C9H10O3	17	**Phenyllactate**	8	Amino Acid Metabolism	Phenylalanine metabolism	1.00	**0.23**	0.02
248.06	11.26	C8H12N2O7	2	**Asp-Asp**	5	Peptide(di-)	Acidic peptide	1.00	**0.22**	0.01
228.21	3.694	C14H28O2	23	**Tetradecanoic acid**	8	Lipid Metabolism	Fatty acid biosynthesis	1.00	**0.20**	0.04
147.05	10.15	C5H9NO4	14	**L-Glutamate**	10	Amino Acid Metabolism	Arginine and proline metabolism Glutamate metabolism D-Glutamine and D-glutamate	1.00	**0.19**	0.01

							metabolism Glutathione metabolism Nitrogen metabolism			
185.99	11.34	C3H7O7P	3	**3-Phospho-D-glycerate**	6	Carbohydrate Metabolism	Glycolysis / Gluconeogenesis Glycine, serine and threonine metabolism	1.00	**0.18**	0.03
122.05	7.183	C6H6N2O	4	**Nicotinamide**	10	Metabolism of Cofactors and Vitamins	Nicotinate and nicotinamide metabolism	1.00	**0.17**	0.01
306.08	10.98	C20H32N6O12S2	1	**Glutathione disulfide**	8	Amino Acid Metabolism	Glutamate metabolism Glutathione metabolism	1.00	**0.17**	0.00
120.09	4.116	C9H12	6	**1,2,4-Trimethylbenzene**	5	0	0	1.00	**0.16**	0.01
507	11.12	C10H16N5O13P3	4	**ATP**	6	Energy Metabolism	Oxidative phosphorylation Photosynthesis Purine metabolism	1.00	**0.15**	0.01
274.2	13.17	C12H26N4O3	1	**Lys-Lys**	7	Peptide(di-)	Basic peptide	1.00	**0.15**	0.03
546.18	11.38	C25H30N4O8S	1	**Asp-Phe-Cys-Tyr**	7	Peptide(tetra-)	Hydrophobic peptide	1.00	**0.13**	0.01
990.33	11.59	C36H62O31	3	**Cellohexaose**	8	Carbohydrate Metabolism	Starch and sucrose metabolism	1.00	**0.12**	0.00
828.28	11.48	C30H52O26	4	**Cellopentaose**	8	Carbohydrate Metabolism	Starch and sucrose metabolism	1.00	**0.12**	0.00
136.13	4.072	C10H16	39	**[PR] (-)-Limonene**	6	Lipids: Prenols	Monoterpenoid biosynthesis Limonene and pinene degradation	1.00	**0.11**	0.00
310.21	3.629	C18H30O4	20	**[FA (18:3)] 13S-hydroperoxy-9Z,11E,14Z-octadecatrienoic acid**	6	Lipids: Fatty Acyls	Fatty Acids and Conjugates	1.00	**0.10**	2.99E
141.02	10.75	C2H8NO4P	2	**Ethanolamine phosphate**	8	Amino Acid Metabolism	Glycine, serine and threonine metabolism Glycerophospholipid metabolism Sphingolipid metabolism	1.00	**0.10**	0.04
544.26	11.27	C26H36N6O7	3	**Asp-Lys-Trp-Pro**	5	Peptide(tetra-)	Basic peptide	1.00	**0.09**	0.01
313.26	4.032	C18H35NO3	2	**[FA (16:0)] N-hexadecanoyl-glycine**	5	Lipids: Fatty Acyls	Fatty amides	1.00	**0.08**	0.01
204.19	4.102	C15H24	151	**[PR] (+)-Longifolene**	8	Lipids: Prenols	Superpathway of oleoresin turpentine biosynthesis Oleoresin sesquiterpene volatiles biosynthesis	1.00	**0.07**	0.01
342.12	10.86	C12H22O11	42	**Sucrose**	10	Carbohydrate Metabolism	Galactose metabolism Starch and sucrose metabolism	1.00	**0.03**	0.01

Supplemental table V-1. Significantly modulated metabolites in the SILAC-labelled *Δlmgt* promastigotes. Specified in yellow are the metabolites matched to authentic standards. Specified in red are the metabolites with more than one isomeric peak.

Mass	RT	Formula	Isomers	Putative metabolite	Confidence	Map	Pathway	WT	*Δlmgt*	*Δlmgt* t test
135.1	9.703	C19H26O	2	**17beta-Methylestra-1,3,5(10)-trien-3-ol**	7	0	0	**0.00**	**95.21**	0.01
384.13	11.59	C14H24O12	1	**Acetyl-maltose**	5	0	0	**0.00**	**31.40**	0.01
408.29	4.754	C24H40O5	82	**Cholate**	6	Lipids: Sterol lipids	Bile acid biosynthesis	**0.00**	**27.55**	0.00
342.15	10.54	C20H22O5	2	**Phaseollidin hydrate**	5	0	0	**0.00**	**18.66**	0.04
700.55	4.178	C39H77N2O6P	3	**SM(d16:1/18:1)**	5	Lipids: Sphingolipids	Phosphosphingolipids	**0.00**	**16.41**	0.05
328.24	3.548	C22H32O2	11	**Docosahexaenoicacid**	8	Lipids: Fatty Acyls	Biosynthesis of unsaturated fatty acids	1.00	**9.86**	0.01
287.2	9.503	C12H25N5O3	2	**Leu-Arg**	5	Peptide(di-)	Basic peptide	1.00	**8.48**	0.01
123.03	7.185	C6H5NO2	4	**Nicotinate**	10	Metabolism of Cofactors and Vitamins	Nicotinate and nicotinamide metabolism Alkaloid biosynthesis II	1.00	**7.63**	0.00
304.24	3.596	C20H32O2	46	**[FA (20:4)] 5Z,8Z,11Z,14Z-eicosatetraenoic acid**	6	Lipids: Fatty Acyls	Fatty Acids and Conjugates	1.00	**6.31**	0.00
283.12	7.834	C24H34N6O10	1	**Glu-Gln-Gln-Tyr**	7	Peptide(tetra-)	Hydrophobic peptide	1.00	**6.21**	0.03
257.1	10.31	C8H20NO6P	1	**sn-glycero-3-Phosphocholine**	8	Lipid Metabolism	Glycerophospholipid metabolism Ether lipid metabolism	1.00	**6.13**	0.02
180.04	7.178	C9H8O4	11	**3-(4-Hydroxyphenyl) pyruvate**	8	Amino Acid Metabolism	Tyrosine metabolism Phenylalanine, tyrosine and tryptophan biosynthesis Alkaloid biosynthesis I	1.00	**3.74**	0.05
216.04	10.34	C5H13O7P	1	**2-C-Methyl-D-erythritol 4-phosphate**	8	Lipid Metabolism	Biosynthesis of steroids	1.00	**2.51**	0.02
129.09	17.53	C5H11N3O	3	**4-Guanidinobutanal**	8	Amino Acid Metabolism	Arginine and proline metabolism	1.00	**2.43**	0.02
204.09	9.458	C11H12N2O2	6	**L-Tryptophan**	10	Amino Acid Metabolism	Tryptophan metabolism Phenylalanine, tyrosine and tryptophan biosynthesis Indole and ipecac alkaloid biosynthesis	1.00	**2.10**	0.02
245.15	11.17	C9H19N5O3	2	**β-Alanyl-L-arginine**	6	Amino Acid Metabolism	β-Alanine metabolism	1.00	**1.95**	0.04
174.11	17.41	C6H14N4O2	2	**L-Arginine**	10	Amino Acid Metabolism	Arginine and proline metabolism D-Arginine and D-ornithine metabolism	1.00	**1.93**	0.04
133.04	10.4	C4H7NO4	4	**L-Aspartate**	8	Amino Acid Metabolism	Alanine and aspartate metabolism lycine, serine and threonine metabolism Lysine biosynthesis Arginine and proline metabolism Carbon fixation	1.00	**1.88**	0.04

165.08	8.48	C9H11NO2	7	**L-Phenylalanine**	10	Amino Acid Metabolism	Phenylalanine metabolism Phenylalanine, tyrosine and tryptophan biosynthesis Phenylpropanoid biosynthesis Alkaloid biosynthesis II	1.00	**1.72**	0.05
309.13	8.029	C14H19N3O5	3	**Ala-Gly-Tyr**	5	Peptide(tri-)	Hydrophobic peptide	1.00	**1.59**	0.03
203.13	11.53	C8H17N3O3	1	**Lys-Gly**	5	Peptide(di-)	Basic peptide	1.00	**1.58**	0.04
114.03	10.86	C5H6O3	6	**2-Hydroxy-2,4-pentadienoate**	6	Amino Acid Metabolism	Phenylalanine metabolism	1.00	**1.43**	0.05
231.11	7.107	C10H17NO5	3	**Suberylglycine**	7	0	0	1.00	**1.43**	0.04
261.14	11.38	C9H19N5O4	1	**Ser-Arg**	5	Peptide(di-)	Basic peptide	1.00	**1.40**	0.04
187.12	7.121	C9H17NO3	3	**8-Amino-7-oxononanoate**	6	Metabolism of Cofactors and Vitamins	Biotin metabolism	1.00	**1.37**	0.02
258.09	9.559	C10H14N2O6	3	**(1-Ribosylimidazole)-4-acetate**	8	Amino Acid Metabolism	Histidine metabolism	1.00	**1.37**	0.04
145.09	17.47	C5H11N3O2	3	**Fibrin**	5	0	0	1.00	**1.34**	0.03
239.9	14.08	H3O9P3	1	**Trimetaphosphate**	7	Nucleotide Metabolism	Pyrimidine metabolism	1.00	**0.94**	0.02
104.02	9.291	C2H4N2O3	1	**Urea-1-carboxylate**	6	Amino Acid Metabolism	Arginine and proline metabolism	1.00	**0.76**	0.01
182.08	10.42	C6H14O6	6	**D-Sorbitol**	6	Carbohydrate Metabolism	Fructose and mannose metabolism Galactose metabolism	1.00	**0.75**	0.03
504.17	11.55	C18H32O16	22	**Raffinose**	8	Carbohydrate Metabolism	Galactose metabolism	1.00	**0.71**	0.03
142.06	4.804	C7H10O3	6	**methoxyfuraneol (keto form)**	7	0	Furaneol biosynthesis	1.00	**0.71**	0.04
106.06	7.214	C4H10O3	1	**Diethylene glycol**	5	0	0	1.00	**0.69**	0.04
666.22	11.72	C24H42O21	14	**Stachyose**	6	Carbohydrate Metabolism	Galactose metabolism	1.00	**0.69**	0.02
294.16	4.746	C15H22N2O4	2	**Leu-Tyr**	5	Peptide(di-)	Hydrophobic peptide	1.00	**0.62**	0.04
188.15	14.96	C9H20N2O2	2	**N6,N6,N6-Trimethyl-L-lysine**	6	Amino Acid Metabolism	Lysine degradation	1.00	**0.60**	0.02
218.09	9.945	C8H14N2O5	3	**L-Ala-L-Glu**	5	Peptide(di-)	Acidic peptide	1.00	**0.59**	0.05
264.15	4.519	C14H20N2O3	2	**Phe-Val**	5	Peptide(di-)	Hydrophobic peptide	1.00	**0.58**	0.02
70.042	11.07	C4H6O	3	**3-Butyn-1-ol**	6	Carbohydrate Metabolism	Butanoate metabolism	1.00	**0.54**	0.02
182.06	7.507	C9H10O4	13	**3-(4-Hydroxyphenyl)lactate**	8	Amino Acid Metabolism	Tyrosine metabolism	1.00	**0.50**	0.02
297.05	10.13	C8H15N3O5S2	1	**L-Cysteinylglycine disulfide**	7	Peptide	0	**1.00**	**0.47**	0.02

126.03	5.065	C6H6O3	8	**Benzene-1,2,4-triol**	5.5	Xenobiotics Biodegradation and Metabolism	γ-Hexachloro-cyclohexane degradation Benzoate degradation via hydroxylation	1.00	**0.46**	0.03
130.06	4.667	C6H10O3	18	**(S)-3-Methyl-2-oxopentanoic acid**	8	Amino Acid Metabolism	Valine, leucine and isoleucine degradation and biosynthesis	1.00	**0.39**	0.00
89.048	10.77	C3H7NO2	9	**L-Alanine**	10	Amino Acid Metabolism	Alanine and aspartate metabolism D-Alanine metabolism Carbon fixation	1.00	**0.38**	0.03
310.21	3.629	C18H30O4	20	**[FA (18:3)] 13S-hydroperoxy-9Z,11E,14Z-octadecatrienoic acid**	6	Lipids: Fatty Acyls	Fatty Acids and Conjugates	1.00	**0.38**	0.02
222.07	11.29	C7H14N2O4S	4	**L-Cystathionine**	10	Amino Acid Metabolism	Glycine, serine and threonine metabolism Methionine metabolism	1.00	**0.37**	0.00
313.26	4.032	C18H35NO3	2	**[FA (16:0)] N-hexadecanoyl-glycine**	5	Lipids: Fatty Acyls	Fatty amides	1.00	**0.33**	0.01
116.01	10.81	C4H4O4	3	**Fumarate**	10	Carbohydrate Metabolism	TCA cycle Oxidative phosphorylation Arginine and proline metabolism Glutamate metabolism Alanine and aspartate metabolism Arginine and proline metabolism	1.00	**0.27**	0.01
204.19	4.102	C15H24	151	**[PR] (+)-Longifolene**	8	Lipids: Prenols	Oleoresin turpentine biosynthesis	1.00	**0.25**	0.03
175.1	11.1	C6H13N3O3	3	**L-Citrulline**	10	Amino Acid Metabolism	Arginine and proline metabolism	1.00	**0.22**	0.02
134.02	10.95	C4H6O5	4	**(S)-Malate**	10	Carbohydrate Metabolism	TCA cycle Glutamate metabolism Alanine and aspartate metabolism Pyruvate metabolism Glyoxylate and dicarboxylate metabolism	1.00	**0.21**	0.01
426.09	10.94	C13H22N4O8S2	2	**Asp-Cys-Cys-Ser**	5	Peptide(tetra-)	Acidic peptide	1.00	**0.21**	0.01
146.11	16.16	C6H14N2O2	8	**D-Lysine**	8	Amino Acid Metabolism	Lysine degradation	1.00	**0.21**	0.01
89.084	14.45	C4H11NO	1	**N-dimethyl ethanolamine**	7	0	Choline biosynthesis	1.00	**0.19**	0.02
122.05	7.183	C6H6N2O	4	**Nicotinamide**	10	Metabolism of Cofactors and Vitamins	Nicotinate and nicotinamide metabolism	1.00	**0.08**	0.01
342.12	10.86	C12H22O11	42	**Sucrose**	10	Carbohydrate Metabolism	Galactose metabolism Starch and sucrose metabolism	1.00	**0.06**	0.03

Supplemental table V-2. Significantly modulated metabolites in the SILAC-labelled *Δlmgt* spent medium. Specified in yellow are the metabolites matched to authentic standards. Specified in red are the metabolites with more than one isomeric peak.

#	Name	Formula	Infomation
1	(3*S*)-3,6-Diaminohexanoic acid	$C_6H_{14}N_2O_2$	A chiral diamino acid consisting of hexanoic acid having amino substituents at the 3- and 6-positions and (*S*)-configuration.
2	(*Z*)-N^6-[(4*R*,5*S*)-5-(2-Carboxyethyl)-4-(carboxymethyl)piperidin-3-ylidene]-L-lysine	Preliminary entry	-
3	1,2-Diacyl-*sn*-glycero-3-phospho-1'-(3'-*O*-L-lysyl)-*sn*-glycerol	$C_{14}H_{25}N_2O_{11}PR_2$	A phosphatidylglycerol that is the 3'-*O*-L-lysyl of any 1,2-diacyl-*sn*-glycero-3-phospho-1'-*sn*-glycerol.
4	1-(L-Norleucin-6-yl)pyrraline	$C_{12}H_{18}N_2O_4$	A pyrrole formed via Maillard reaction of L-lysine with glucose.
5	1-(L-Norvalin-5-yl)pyrraline	$C_{11}H_{16}N_2O_4$	A pyrrole formed via Maillard reaction of L-ornithine with glucose
6	5'-(N^6-L-Lysine)-L-tyrosylquinone	$C_{15}H_{21}N_3O_6$	An L-lysine derivative in which one of the amino hydrogens at *N*^{6}-amino is substituted by a 6-[(2*S*)-2-amino-2-carboxyethyl]-3,4-dioxocyclohexa-1,5-dien-1-yl group.
7	5-Glycosyloxy-L-lysine	-	Manually annotated
8	*erythro*-5-Phosphonooxy-L-lysine	$C_6H_{15}N_2O_6P$	The 5-phosphonooxy derivative of L-lysine having *erythro*-stereochemistry.
9	N-Hippuryl-N^6-(carboxymethyl)lysine	$C_{17}H_{23}N_3O_6$	A lysine derivative in which the α-amino nitrogen of the amino acid has entered into amide formation with hippuric acid.
11	N$^\varepsilon$-(5'-Guanylyl)-N$^\alpha$-acetyl-L-lysine methyl ester(1−)	$C_{19}H_{29}N_7O_{10}P$	An organic phosphoramidate anion obtained by removal of the proton from the phosphoramidate OH group of *N*$^\varepsilon$-(5'-guanylyl)-*N*$^\alpha$-acetyl-L-lysine methyl ester; major species at pH 7.3.
12	N$^\varepsilon$-GMP-N$^\alpha$-Acetyl-L-lysine methyl ester	$C_{19}H_{30}N_7O_{10}P$	A organic phosphoramidate that is guanosine 5'-monophosphate in which one of the hydroxy groups of the phosphate has been condensed with the side chain amino group of *N*$^\alpha$-acetyl-L-lysine methyl ester.
13	N^2-(5'-Phosphopyridoxyl)-L-lysine	$C_{14}H_{24}N_3O_7P$	An L-lysine derivative arising from reductive alkylation of the *N*^{2}-position of L-lysine by pyridoxal-5-phosphate.
14	N^2-Methyl-L-lysine	$C_7H_{16}N_2O_2$	A *N*-methyl-L-amino acid that is the *N*$^\alpha$-methyl derivative of L-lysine.
16	N^6-(5'-Adenylyl)-L-lysine	Preliminary entry	-
17	N^6-(5'-Guanylyl)-L-lysine	Preliminary entry	-
18	N^6-(Pyridoxal phosphate)-L-lysine	Preliminary entry	-
19	N^6-[(Indol-3-yl)acetyl]-L-lysine	$C_{16}H_{21}N_3O_3$	A *N*-methyl-L-amino acid that is the *N*$^\alpha$-methyl derivative of L-lysine.
20	N^6-Acetimidoyl-L-lysine	$C_8H_{17}N_3O_2$	An L-lysine derivative that is L-lysine in which one of the hydrogens attached to *N*^{6} is substituted by an acetimidoyl group.
21	N^6-Acetyl-*N*^{2}-(5'-phosphopyridoxyl)-L-lysine	$C_{16}H_{26}N_3O_8P$	An L-lysine derivative arising from reductive *N*-alkylation of *N*^{6}-acetyl-L-lysine by pyridoxal-5-phosphate.

23	N^6-Carboxy-L-lysine	$C_7H_{14}N_2O_4$	An L-lysine derivative consisting of L-lysine carrying a carboxy substituent at the N^6-position.
24	N^6-Carboxymethyl-L-lysine	$C_8H_{16}N_2O_4$	An L-lysine derivative with a carboxymethyl substituent at the N^6-position.
25	N^6-Dansyl-L-lysine	$C_{18}H_{25}N_3O_4S$	An L-lysine derivative with a dansyl group at the N^6-position.
26	N^6-Glycyl-L-lysine	$C_8H_{17}N_3O_3$	Manually annotated
27	N^6-Methyl-L-lysine	$C_7H_{16}N_2O_2$	An L-lysine derivative that is L-lysine in which one of the hydrogens attached to N^6 is substituted by a methyl group.
28	D-Lysopine	$C_9H_{18}N_2O_4$	The N^2-(*R*)-1-carboxyethyl derivative of L-lysine
29	L-2-Aminohexano-6-lactam	$C_6H_{12}N_2O$	Manually annotated
30	β-Alanyl-L-lysine	$C_9H_{19}N_3O_3$	Dipeptide

Supplemental table V-3. List of outgoing* L-lysine derivatives. * - the relationship between the ChEBI entry and its immediate related entities.
Credits: ChEBI

#	Name	Formula	Infomation
31	L-Homoarginine	$C_7H_{16}N_4O_2$	An L-lysine derivative that is the L-enantiomer of homoarginine.
32	L-Homocitrulline	$C_7H_{15}N_3O_3$	A L-lysine derivative that is L-lysine having a carbamoyl group at the N6-position.
33	L-Lysine thiazolecarboxylic acid	Preliminary entry	-
36	Acetyl-L-lysine	-	Manually annotated
38	Biocytin	$C_{16}H_{28}N_4O_4S$	A monocarboxylic acid amide that results from the formal condensation of the carboxylic acid group of biotin with the N^6-amino group ofL-lysine.
39	Deoxyhypusine	$C_{10}H_{23}N_3O_2$	An L-lysine derivative in which the N^6 of the lysine is substituted with a 4-aminobutyl group.
40	Fructoselysine 6-phosphate	$C_{12}H_{25}N_2O_{10}P$	An L-lysine derivative having a 6-phosphofructosyl group attached to the side-chain amino group.
41	Glyoxal-lysine dimer	$C_{15}H_{27}N_4O_4$	An imidazolium ion formed via cyclo-dimerisation of L-lysine and glyoxal.
42	Heme P460-bis-L-cysteine-L-lysine	Preliminary entry	-
43	Hydroxy-L-lysine	Preliminary entry	-
44	Hypusine	$C_{10}H_{23}N_3O_3$	An L-lysine derivative that is L-lysine bearing A (2*R*)-4-amino-2-hydroxybutyl substituent at position N6.
45	Indole-lysine conjugate	-	Manually annotated
46	L-lysine amide	Preliminary entry	-
47	Lysidine	$C_{15}H_{25}N_5O_6$	Cytidine in which the 2-keto group on the cytosine ring is substituted by an ε-Llysyl residue.
48	Methyl L-lysinate	$C_7H_{16}N_2O_2$	The ester formed by conjugating L-lysine with methanol.
49	Methylglyoxal-lysine dimer	$C_{16}H_{29}N_4O_4$	An imidazolium ion formed via cyclo-dimerisation of L-lysine and methylglyoxal.
50	N^6-1-Carboxyethyl-L-lysine	Preliminary entry	-
51	N^6-3,4-Didehydroretinylidene-L-lysine	Preliminary entry	-
52	N^6-Formyl-L-lysine	Preliminary entry	-
53	N^6-Methyl-N^6-poly(N-methyl-propylamine)-L-lysine	Preliminary entry	-
54	N^6-Mureinyl-L-lysine	Preliminary entry	-
56	N^6-Myristoyl-L-lysine	Preliminary entry	-
57	N^6-Palmitoyl-L-lysine	Preliminary entry	-

57	N^6-Pyruvic acid 2-iminyl-L-lysine	Preliminary entry	-
58	N^6-Retinylidene-L-lysine	Preliminary entry	-
59	N^α-Acetyl-L-lysine methyl ester	Preliminary entry	-
60	Peptidyl-L-lysine	Preliminary entry	-
61	Psicosyllysine	$C_{12}H_{24}N_2O_7$	An L-lysine derivative having a psicosyl group attached to the side-chain amino group.

Supplemental table V-4. List of incoming* L-lysine derivatives. * - the relationship between the ChEBI entry and its immediate related entities.
Credits: ChEBI

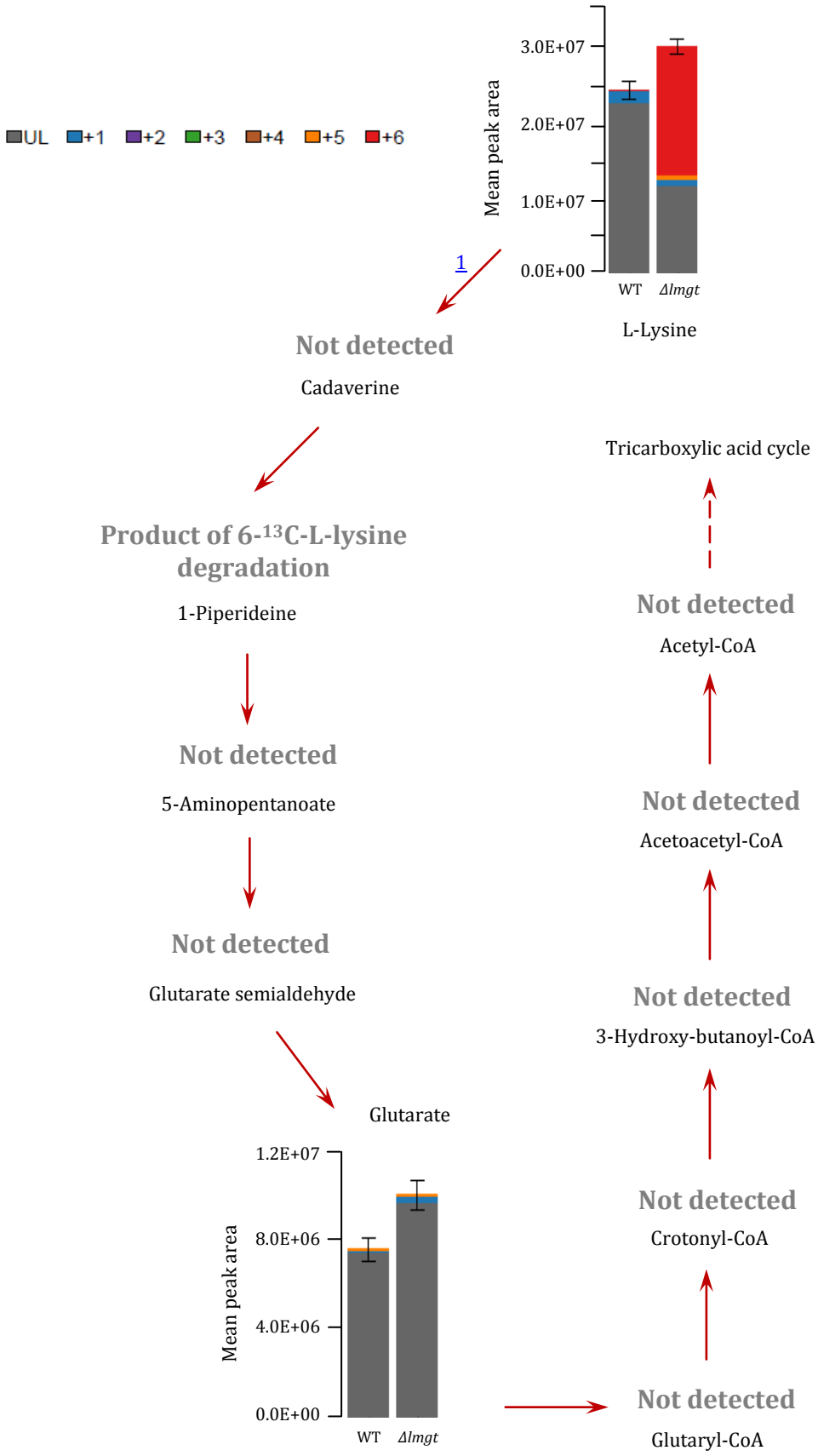

Supplemental figure V-1. Labelling profile of L-lysine degradation via cadaverine in the SILAC-labelled wild type and *Δlmgt* promastigotes. Abbreviations: WT – wild type promastigotes, *Δlmgt* - *Δlmgt* promastigotes, UL- unlabelled carbon, +1 - 1-^{13}C-labelled carbon, +2 - 2-^{13}C-labelled carbon, +3 - 3-^{13}C-labelled carbon, +4 - 4-^{13}C-labelled carbon, +5 - 5-^{13}C-labelled carbon, +6 - 6-^{13}C-labelled carbon. Dashed lines indicate indirect enzymatic reaction.
Adapted from KEGG and MetaCyc.

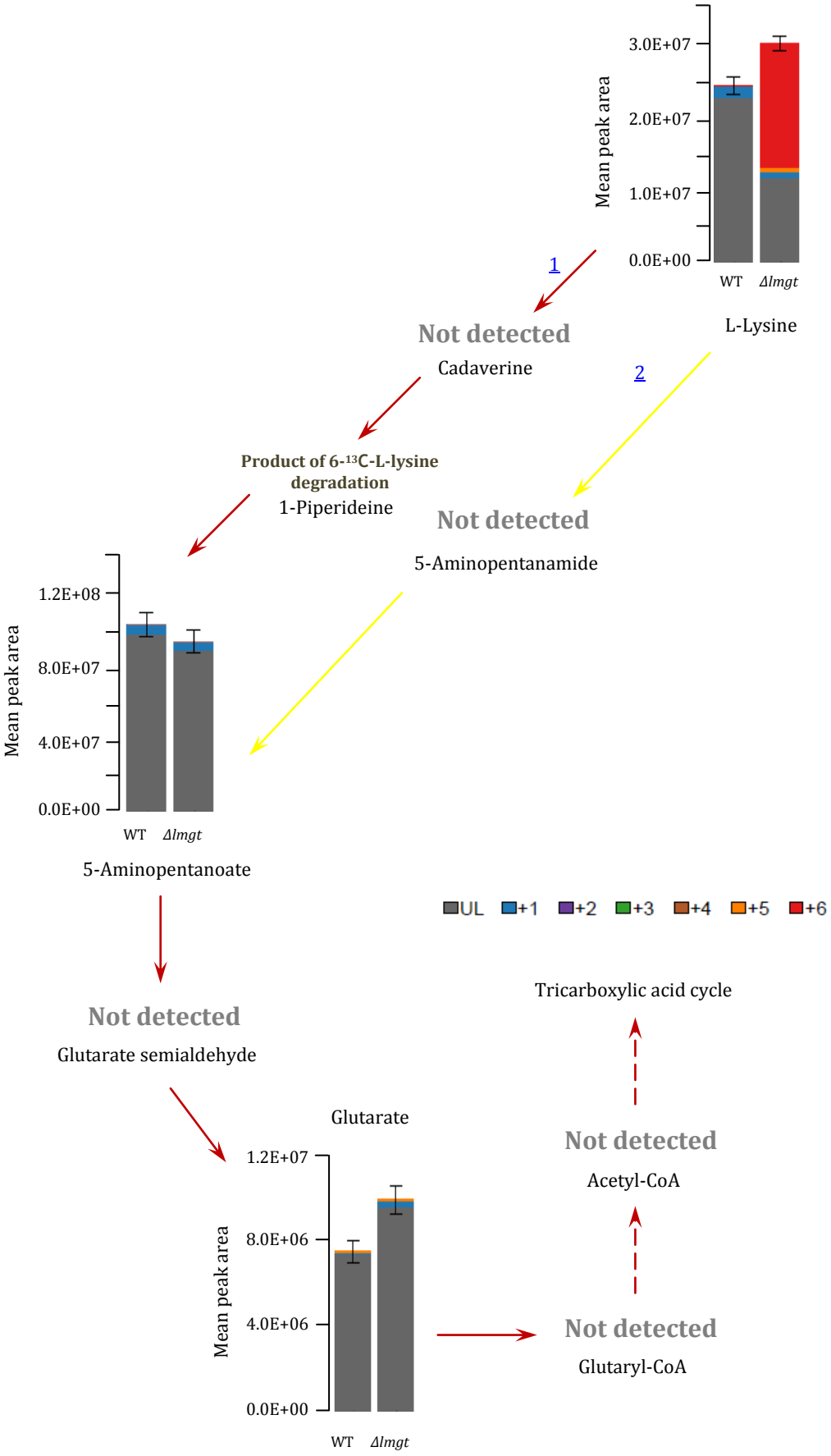

Supplemental figure V-2. Labelling profile of L-lysine degradation via 5-aminopentamide in the SILAC-labelled wild type and *Δlmgt* promastigotes.
Abbreviations: WT – wild type promastigotes, *Δlmgt* - *Δlmgt* promastigotes, UL- unlabelled carbon, +1 - 1-^{13}C-labelled carbon, +2 - 2-^{13}C-labelled carbon, +3 - 3-^{13}C-labelled carbon, +4 - 4-^{13}C-labelled carbon, +5 - 5-^{13}C-labelled carbon, +6 - 6-^{13}C-labelled carbon. Dashed lines indicate indirect enzymatic reaction.
Adapted from KEGG and MetaCyc.

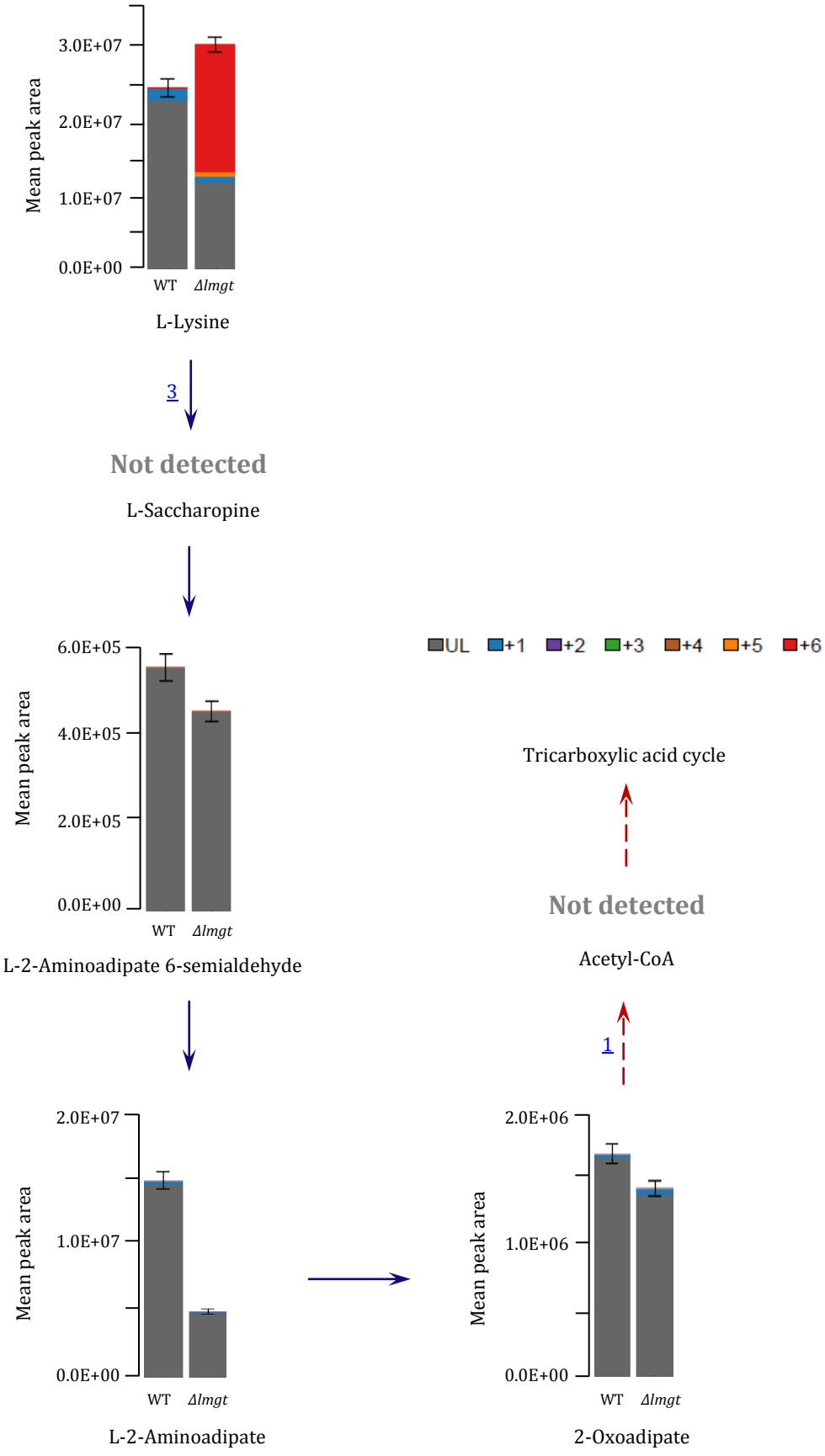

Supplemental figure V-3. Labelling profile of L-lysine degradation via L-saccharopine in the SILAC-labelled wild type and *Δlmgt* promastigotes. Abbreviations: WT – wild type promastigotes, *Δlmgt* - *Δlmgt* promastigotes, UL- unlabelled carbon, +1 - 1-^{13}C-labelled carbon, +2 - 2-^{13}C-labelled carbon, +3 - 3-^{13}C-labelled carbon, +4 - 4-^{13}C-labelled carbon, +5 - 5-^{13}C-labelled carbon, +6 - 6-^{13}C-labelled carbon. Dashed lines indicate indirect enzymatic reaction.
Adapted from KEGG and MetaCyc.

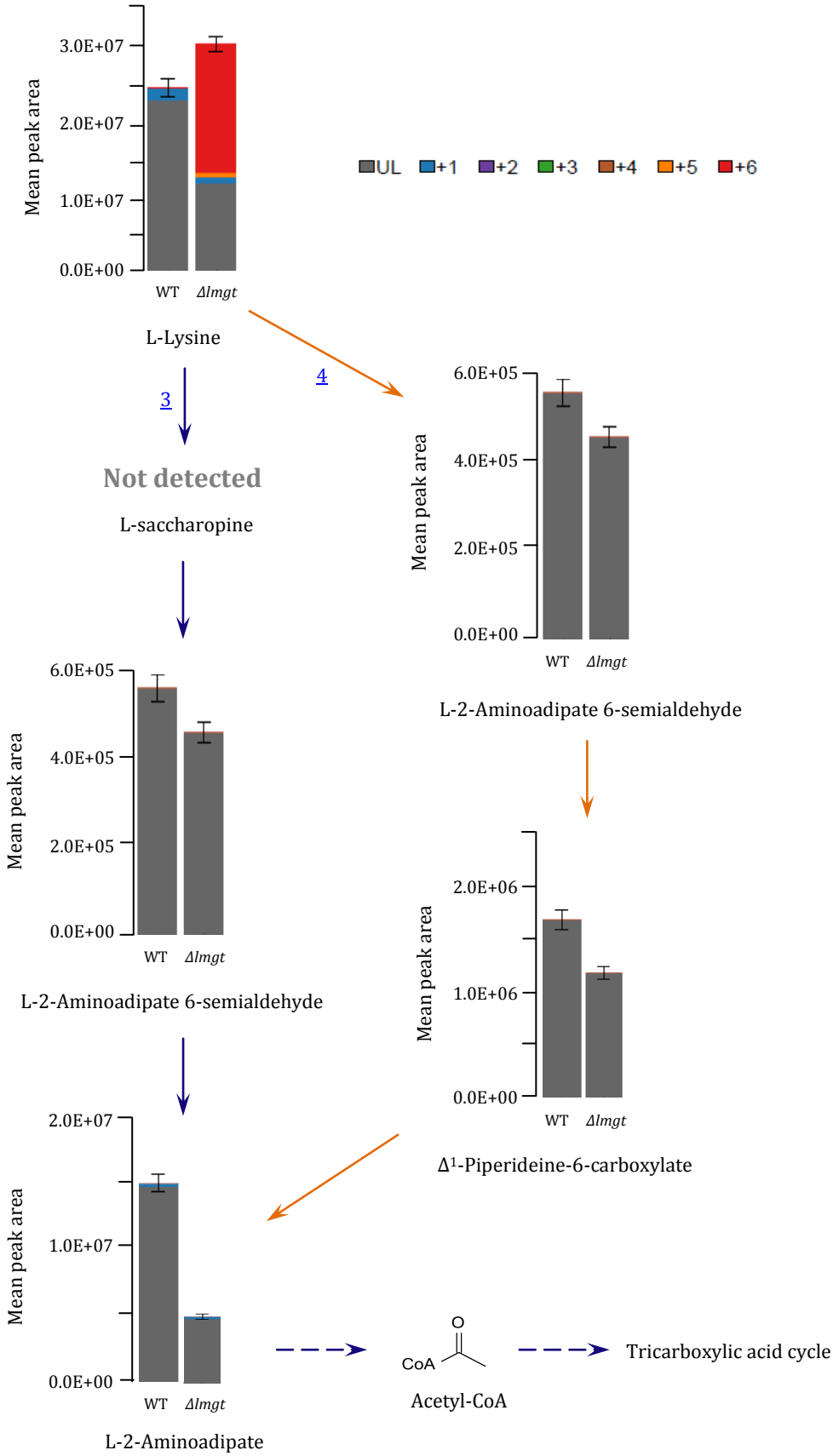

Supplemental figure V-4. Labelling profile of L-lysine degradation via L-2-aminoadipate 6-semialdehyde in the SILAC-labelled wild type and *Δlmgt* promastigotes. Abbreviations: WT – wild type promastigotes, *Δlmgt* - *Δlmgt* promastigotes, UL- unlabelled carbon, +1 - 1-^{13}C-labelled carbon, +2 - 2-^{13}C-labelled carbon, +3 - 3-^{13}C-labelled carbon, +4 - 4-^{13}C-labelled carbon, +5 - 5-^{13}C-labelled carbon, +6 - 6-^{13}C-labelled carbon. Dashed lines indicate indirect enzymatic reaction. Adapted from KEGG and MetaCyc.

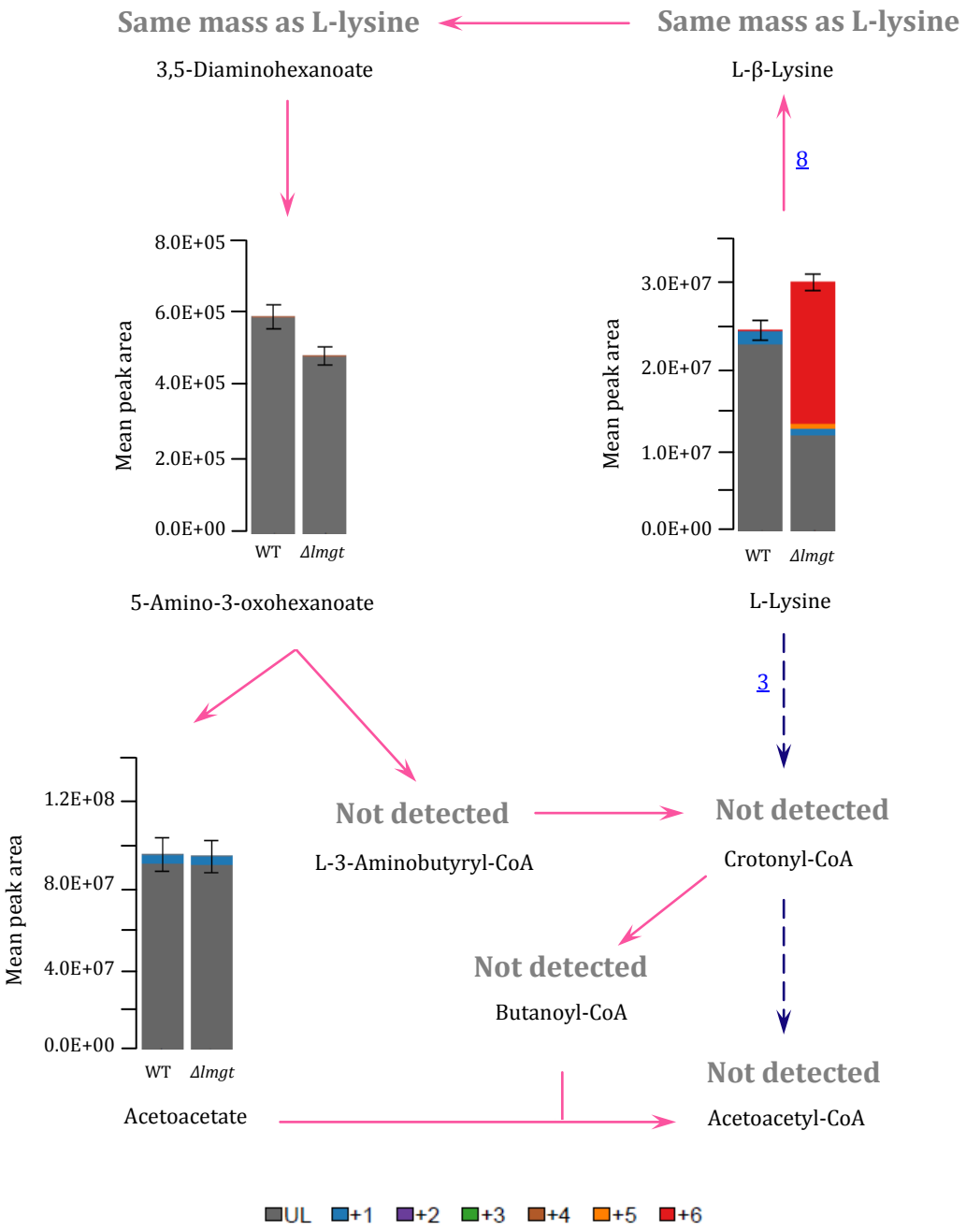

Supplemental figure V-5. Labelling profile of L-lysine degradation via L-β-lysine in the SILAC-labelled wild type and *Δlmgt* promastigotes. Abbreviations: WT – wild type promastigotes, *Δlmgt* - *Δlmgt* promastigotes, UL- unlabelled carbon, +1 - 1-^{13}C-labelled carbon, +2 - 2-^{13}C-labelled carbon, +3 - 3-^{13}C-labelled carbon, +4 - 4-^{13}C-labelled carbon, +5 - 5-^{13}C-labelled carbon, +6 - 6-^{13}C-labelled carbon. Dashed lines indicate indirect enzymatic reaction.
Adapted from KEGG and MetaCyc.

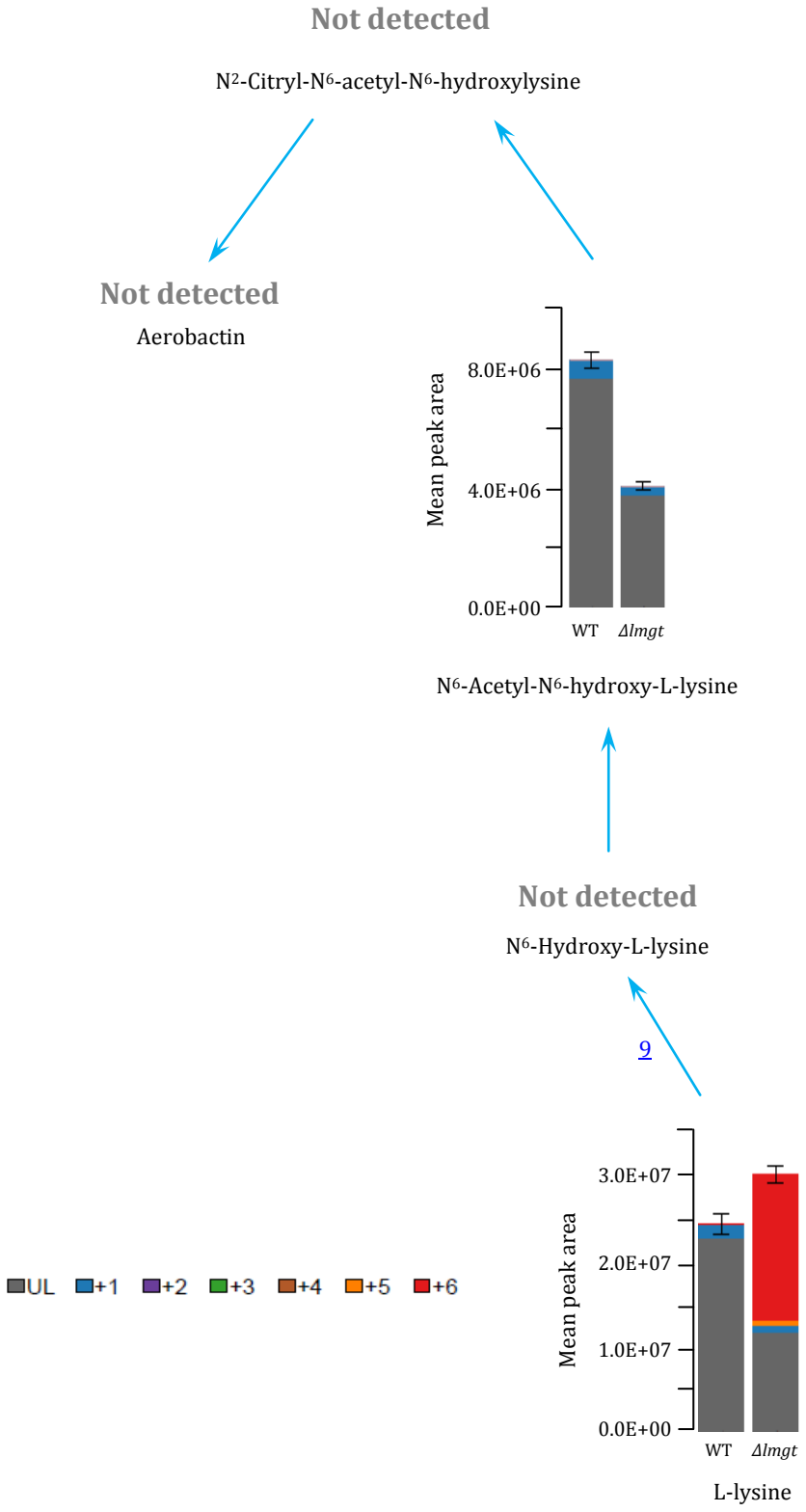

Supplemental figure V-6. Labelling pattern of L-lysine degradation via N^6-hydroxy-L-lysine in the wild type and *Δlmgt* promastigotes. Abbreviations: WT – wild type promastigotes, *Δlmgt* - *Δlmgt* promastigotes, UL- unlabelled carbon, +1 - 1-^{13}C-labelled carbon, +2 - 2-^{13}C-labelled carbon, +3 - 3-^{13}C-labelled carbon, +4 - 4-^{13}C-labelled carbon, +5 - 5-^{13}C-labelled carbon, +6 - 6-^{13}C-labelled carbon.
Adapted from KEGG and MetaCyc.